Planar Chiral Oxazolines Based on [2.2]Paracyclophane: A New Toolbox for Asymmetric Synthesis

A thesis presented in partial fulfilment of the requirements for the degree of

Doctor of Philosophy
in
Chemistry

at Massey University, Manawatū, New Zealand

Shashank Tewari

2023

Dedications

In loving memory of my Father

&

My Family

Contents

Acknowledgement

It is my great pleasure to take this opportunity to thank the people who have contributed to my Ph.D. research work and thesis.

I would like to take this opportunity to extend my deepest appreciation and gratitude to my supervisor, A/Prof. Gareth J. Rowlands for his invaluable guidance, unwavering support, and encouragement throughout my Ph.D. journey. His dedication to my research and his insightful feedback has been instrumental in shaping this thesis. I would like to acknowledge the patience and understanding shown by Gareth during the inevitable moments of struggle and self-doubt that arise during the course of a Ph.D. His belief in my abilities, even when I doubted myself, has been a source of motivation that I will carry with me throughout my career.

I would also like to thank my co-supervisors, Prof. Paul Plieger and Assoc. Prof. Vyacheslav Filichev for their much-valued insights and constructive feedback, which greatly enriched the quality of this thesis. I am thankful to them for allowing me to share the resources from their lab during my research.

I would also like to thank other members of the school, notably Prof. Shane Telfer, and Prof. David Harding for sharing their time and laboratory resources.

I also thank Leonie Etheridge, Maulik Mungalpara, Suraj Patel, Sam, Aaron Whitehead for scientific discussions and sharing common precursors. I also thank Becky Severinsen, Jenna Buchanan, Tyson Dais, Sidney Woodhouse, Hossein Etemadi, Harikrishnan Kurup, Bruce Chilton, Joel Cornelio, Adil Alkaş, and other members of Plieger's group, Telfer's group and Filichev's group.

I also thank the staff of Chemstore, Mechanical workshop, and Electronic workshop for their constant support throughout my research.

I would like to acknowledge the financial support from the School of Natural Sciences, formerly, School of Fundamental Sciences (SFS), SFS fee remission over four years for looking after my finances, so that helped me to carry out my research without any financial crux.

I am also thankful to the administrative staff of School of Natural Sciences, Ann, Debbie, Catherine, Cynthia for their assistance and guidance in the hour of need.

I am thankful to GRS for believing in me and supporting my research.

Last but the least, I would like to express my heartfelt gratitude to my loving family for their unwavering support and encouragement during the entire course of my Ph.D. Without their love, understanding, and belief in my abilities, this academic endeavor would not have been possible. I am thankful to my mother, for her constant encouragement, sacrifices, and unwavering belief in my potential have been the driving force behind my accomplishments. I am thankful to my sister, who stood by me through all my ups and down during my Ph.D. journey. I am thankful to my brother and sister-in-law for their valuable feedback and words of encouragement. Their belief in me, even during challenging times, has been a reminder of the strength of our familial bond. I am thankful to my wife for her support throughout this Ph.D. journey, her love and encouragement have been my anchor during both the triumphs and the setbacks.

Finally, I want to acknowledge that none of this would have been possible without the love and grace of a higher power, whatever form it may take for each individual. I humbly express my gratitude for the blessings that have guided me on this path.

Thank you, from the bottom of my heart.

Contributions

All the research work in the thesis was completed by Shashank Tewari Except:

- All HRMS data were obtained by David Lun.
- 2D NMRs on 700 MHz were recorded by Pat.
- All Crystal Data obtained by Suraj Patel and Tyson Dais
- Maulik Mungalpara shared [2.2]paracyclophane precursors.

Abbreviations

Ac	Acetyl
BQ	1,4-Benzoquinone
Cy	Cyclohexyl
dba	Dibenzylidineacetone
DCM	Dichloromethane
de	Diastereomeric excess
DME	Dimethoxyethane
DMF	*N*,*N*-Dimethylformamide
DMS	Dimethyl sulfide
dppf	[1,1′-Bis(diphenylphsophino)ferrocene]
dr	Diastereomeric ratio
ee	Enantiomeric excess
eq.	Equivalent
er	Enantiomeric ratio
ESI-MS	Electrospray Ionisation Mass Spectrometry
HASPO	Heteroatom-substituted secondary phosphine oxide
HFIP	Hexafluoroisopropanol
HRMS	High Resolution Mass Spectrometry
h	Hours
i-Pr	Isopropyl
min.	Minutes
m/z	Mass to charge ratio

n.d.	Not detected
NMR	Nuclear Magnetic Resonance
P	Product
SM	Starting material
SPO	Secondary phosphine oxide
rt	Room temperature
t-Bu	tert-Butyl
TDG	Transient directing group
TEA	Triethylamine
THF	Tetrahydrofuran
TIPS	Triisopropyl silane
TLC	Thin layer chromatography
TS	Transition state
Ts	(4-Methylphenyl)sulfonyl

Abstract

Planar Chiral Oxazolines Based on [2.2]Paracyclophane:

A New Toolbox for Asymmetric Synthesis

This thesis contains total 7 chapters, dealing with the synthesis of planar chiral Oxazolines Based on [2.2]paracyclophane, enantiopure products obtained from their resolution, synthesis of metal-based chiral complexes, studies on C-H activation field, namely selective remote β-C-H activation of cyclic amines, and future ideas towards the goal.

As the main focus of this thesis is on the development of novel planar chiral [2.2]paracyclophane derivatives, Chapter 1 starts with a brief description of [2.2]paracyclophane chemistry. A short introduction about the synthesis of key enantioenriched [2.2]paracyclophane derivatives is given. Finally, a short introduction of the recent applications of [2.2]paracyclophane-based ligands in asymmetric catalysis is also mentioned.

Chapter 2 outlines a brief overview of the role of 2-oxazolines. 2-Oxazolines have been utilized in the field of asymmetric catalysis as ligands and chiral auxiliaries. The chapter briefly discusses the synthesis and highlights some of the uses of 2-oxazolines as chiral ligands.

Chapter 3 describes the concise synthesis of planar chiral oxazolines based on [2.2]paracyclophanes. Various oxazoline-based compounds that were synthesized are all discussed in Chapter 3. The synthesis of mono-oxazolines coupled to [2.2]paracyclophanes, based on the methodology developed in our lab was accomplished. The next were the synthesis of bis-oxazolines and tetra-oxazolines coupled to [2.2]paracyclophane. The chapter mentions all the details and substrate scope generated with oxazolines.

Chapter 4 focuses on the resolution of [2.2]paracycoplane by the hydrolysis of the oxazolines. The enantiopure products like planar chiral mono-acids, bis-acids, and partial acids were obtained by hydrolysis of the oxazolines. Apart from them, a section in the chapter describes the decarboxylative phosphorylation that was achieved through our planar chiral acids. Synthesis of planar chiral diamines via Curtius rearrangement of the diacids is also described in the chapter, followed by phanol synthesis.

A part of the above chapter describes about the rhodium paddle-wheel complex formed by partial chiral acids. An attempt to make dinuclear gold complexes was made that was also

successful. Overall, chapter four is the highlight of the thesis, where a lot of pure chiral products are made and their utility is explained in the field of asymmetric catalysis.

Chapter 5 describes the remote β-C-H activation of cyclic amines. Attempts were made to accomplish the functionalization through the directing group strategy. The directing groups based on heterocyclic piperidine and cyclic amines were synthesized successfully. These pre-made directing groups were used for the C-H bond functionalization but the functionalization possessed many challenges that made the functionalization difficult.

Chapter 6 explains the future scope of the research work mentioned in this thesis.

Finally, Chapter 7 describes the experimental procedures and characterization of the synthesized compounds mentioned in Chapters 3 to 5.

Chapter 1:

An Overview of the Role of Enantioenriched [2.2]Paracylophane Derivatives in Asymmetric Synthesis

1.1 Introduction to Asymmetric Synthesis

The synthesis of novel molecules leads the way to healthy living and sustainability of society in this modern era. Asymmetric synthesis has emerged as a powerful route to synthesize these novel molecules and chemical entities in enantiomerically pure chiral form. Of all the strategies for asymmetric synthesis, enantioselective catalysis is the most attractive.[1]

Chirality or handedness is an intrinsic feature of life. Many organic molecules exist as pairs of enantiomers, non-identical mirror images that only differ as our left and right hands are unlike. Biology can amplify this disparity with trivial repercussions, such as altering taste, or with profound consequences such as the thalidomide disaster.

There is a large market for single-handed compounds. The synthesis of single-handed molecules is hard. One of the most important advances in asymmetric synthesis is the use of a chiral catalyst formed from a metal and a ligand. Catalysis allows a small quantity of chiral material to be amplified producing large amounts of single-handed molecules. Asymmetric catalysis constitutes the most efficient route to such molecules.

Chemists colloquially characterize the chirality of a molecule based on the stereogenic element that breaks symmetry. The most common are "centre" of chirality, the classic tetrahedral atom with four different substituents.[3] Axial and planar chirality were introduced in the middle of the last century and are found in an increasing number of chiral compounds devoid of a tetrahedral stereocentre.[4] Some of the commonly used ligands (**Figure 1.1**) possessing non-traditional chirality are axially chiral binaphthalene derivatives,[5] planar chiral ferrocene derivatives,[6,7]and planar chiral arene transition metal complexes.[8,9] Recently, planar chiral cyclophanes have also attracted considerable interest due to their unusual structural and electronic properties.[10,11] Cyclophanes offer a well-defined, three-dimensional structure suited for chiral induction and these characteristics are being harnessed in the formation of planar chiral functional materials.[12,13]

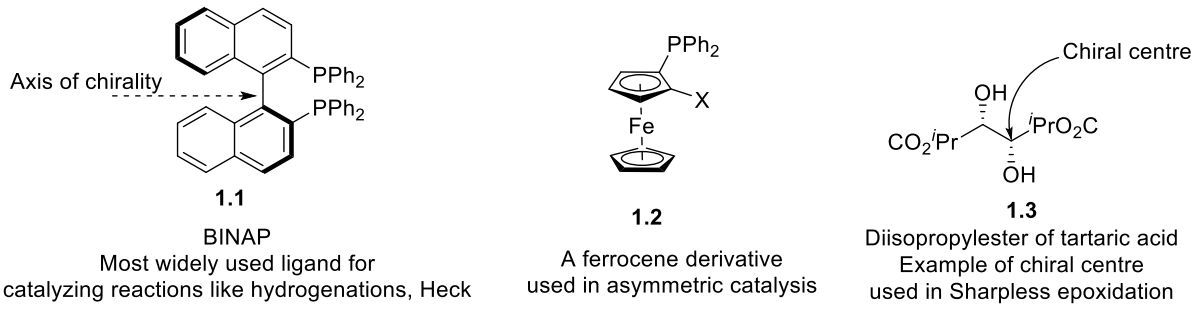

Figure 1.1: Commonly used ligands with different types of chirality

1.2 [2.2]Paracyclophane

[2.2]Paracyclophane was discovered from high temperature pyrolysis of *p*-xylene and is a member of the cyclophane family, is a distinctive molecule owing to its unique structure. [2.2]Paracyclophane has been called "the archetypical layered organic compound" and its structure described as "bent & battered" by Cram.[4] It consists of two co-facially stacked, strongly interacting benzene rings. These are held together at an average distance of 3.09 Å by two ethylene bridges at the *para* carbon atoms. At their closest, the rings are only 2.78 Å apart leading to deformation of rings into a shallow boat-like shape (**Figure 1.2**).

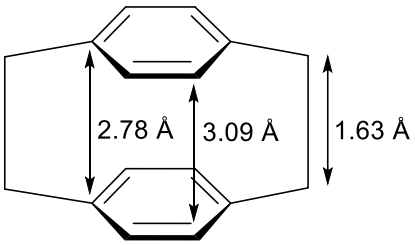

1.4

Figure 1.2: [2.2]Paracyclophane

[2.2]Paracyclophane derivatives are generally robust, crystalline, stable towards light, mild acids, bases, and thermally stable up to 160-180 ˚C. The distortion of [2.2]paracyclophane rings, along with electronic interactions, increases the nucleophilicity of the aromatic ring and it undergoes electrophilic substitution more rapidly than analogous aryl systems. It also has the ability to form π-complexes. The [2.2]paracyclophane framework acts as a bulky shield and planar chirality can be introduced by the addition of single substituents. With the appropriate steric bulk, the chiral environment can be properly modulated on the [2.2]paracyclophane framework for catalysis.[14,15]

1.3 Transannular Effect

The phrase "transannular effect" was coined by Cram & Singer, and it describes the electronic effect of a substituent on one ring and the reactivity of the other ring. It revealed that the transannular effect plays a role in the formation of π-complexes with [2.2]paracyclophane.[16] According to the studies, the complexes formed between [2.2]paracyclophane and tetracyanoethylene (TCNE) are more stable than the analogous aryl complexes (**Figure 1.3**).

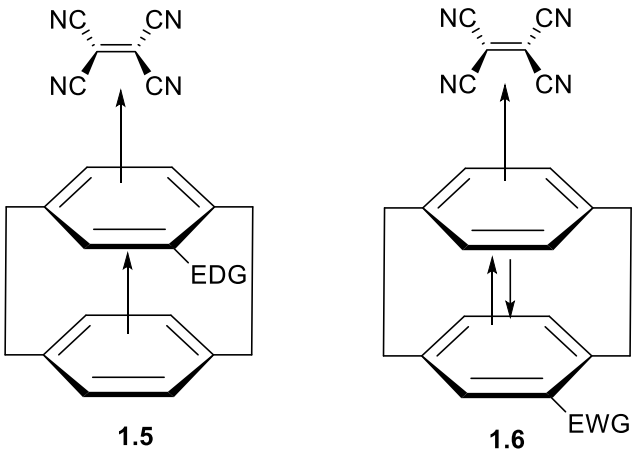

Figure 1.3: π-π Complexes between TCNE and [2.2]paracyclophane with electron-donating group (EDG) and electron withdrawing group (EWG) .

Derivatives with electron-donating substituents, EDG (**1.5**) are found to be more stable than those with electron-withdrawing groups. Due to this, π-cloud system present in [2.2]paracyclophane, reactions taking place on one aromatic ring can be influenced by electronic effects exerted by the substituents on the second aromatic ring. This is defined as the 'transannular effect'.

Described below is an important example that shows the transannular electronic effects of the substituent on the *pseudo-ortho*-substituted [2.2]paracyclophanyl-NHC having significant influence on the catalytic performances (**Scheme 1.1**).[17]

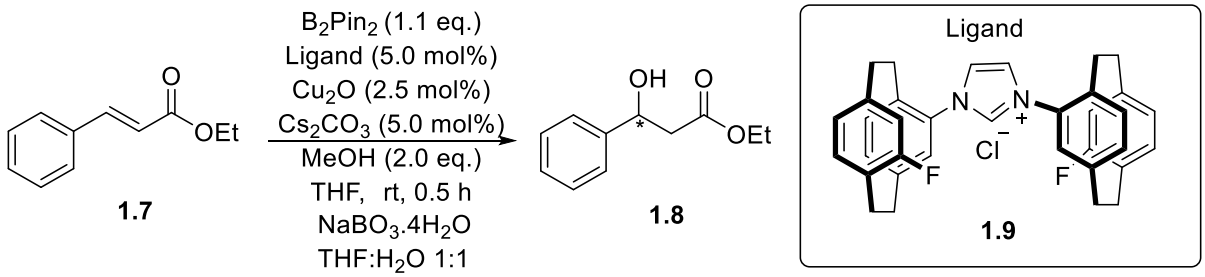

Scheme 1.1: Investigation of the transannular electronic effects.

Moreover, NHC–copper complexes with more electron deficient ligands (having fluoro, **1.9**) gave higher yield of 87% and 80% *ee* as compared to, methoxyl-substituted ligand that gave 65% yield and 22% *ee*.

1.4 Stereochemical Notation of [2.2]Paracyclophane:

The planar chirality of [2.2]paracyclophane derivatives can be assigned the stereochemical descriptor R_p or S_p. The first step in assigning a descriptor is to determine which plane

contains the groups or atoms that break the plane of symmetry.[18] For a monosubstituted [2.2]paracyclophane, the benzene ring that contains the substitution is considered as the chiral plane. After identification of the plane, a pilot atom is chosen. This is the first atom outside the chiral plane and closest to the atom of higher priority as chosen according to the Cahn–Ingold–Prelog (CIP) system of stereochemical assignment (**Figure 1.4**).

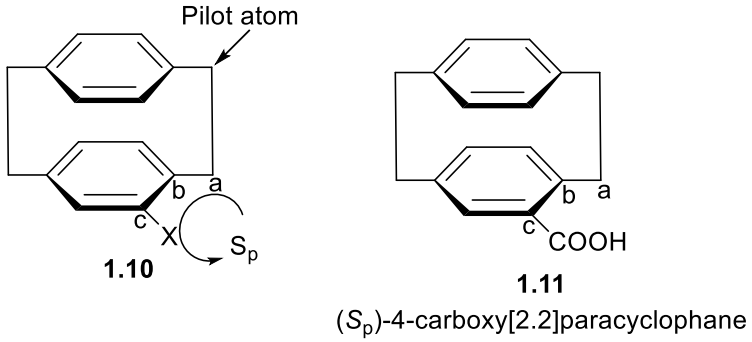

Figure 1.4: Assignment of [2.2]paracyclophane configuration

When viewed from the pilot atom, if atoms a, b, and c are in a clockwise array, the descriptor is R_p and if the array is counter-clockwise, the descriptor is S_p, where subscript p($_p$) denotes planar chirality. For example, the carboxy[2.2]paracyclophane shown in figure **1.4** is S_p.

1.5 [2.2]Paracyclophane Derivatives

In recent years, studies on the reactivity and optoelectronic properties and various substitution patterns of [2.2]paracyclophane have been conducted.[19] The structure of [2.2]paracyclophane permits a number of isomers, just differing by the relative position of substituents, to be prepared. Some of these are chiral regardless of the substituents, while others require different groups or else they will have an element of symmetry (**Figure 1.5**).

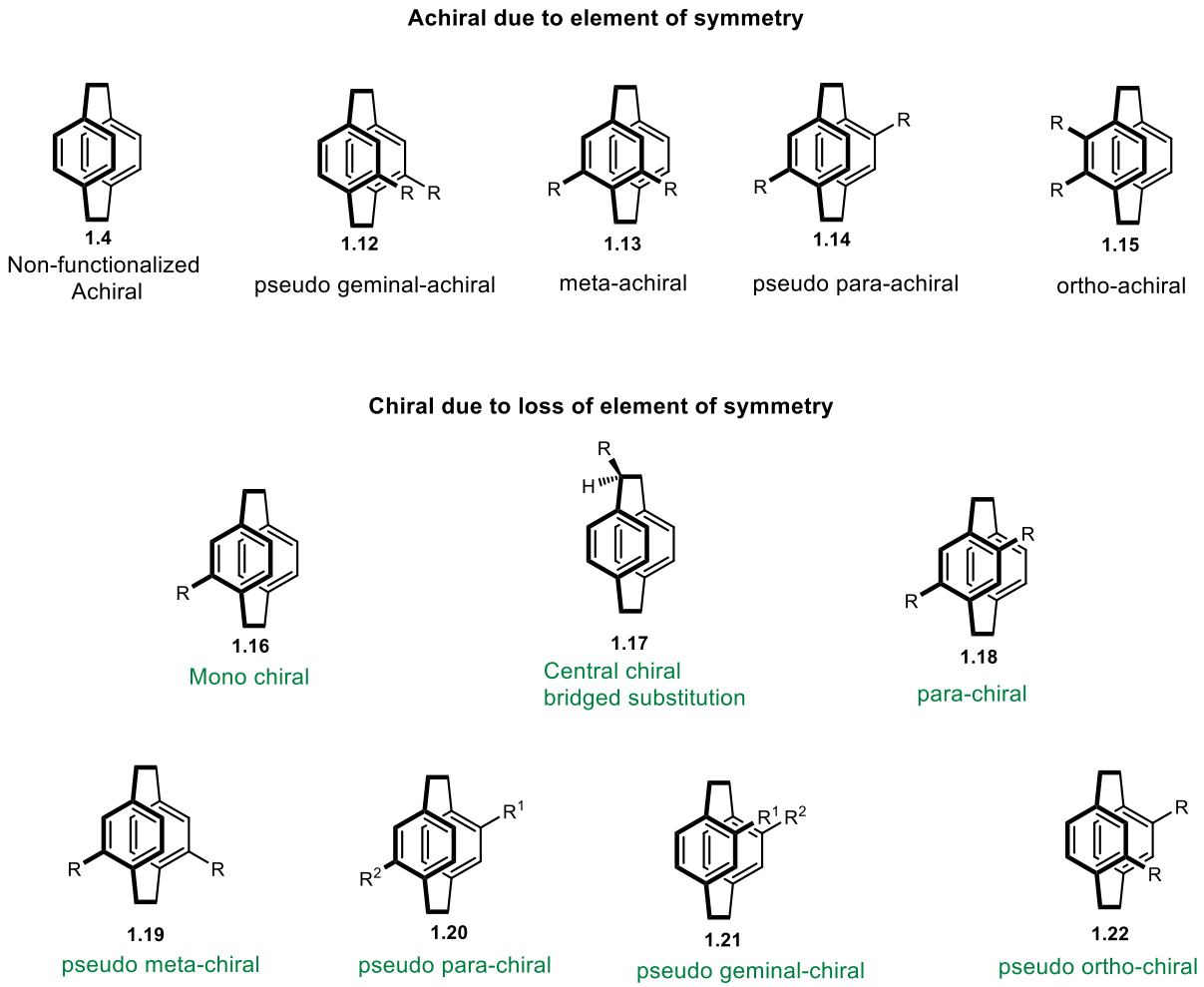

Figure 1.5: Common substitution patterns in mono- and di-substituted [2.2]paracyclophanes with stereochemical description (in green are chiral derivatives)

To be useful, it is necessary to have methods to resolve the planar chirality of these derivatives. There can be two general ways of obtaining enantiopure compounds, the first is by separation of one enantiomer from the racemic mixture and the second is by the synthesis of the single enantiomer.[19]

1.6 Enantioenriched [2.2]Paracyclophanes

Planar chiral monosubstituted [2.2]paracyclophane derivatives have been employed in asymmetric synthesis or catalytic reactions. Synthesis of enantiopure mono-substituted [2.2]paracyclophanes (**Figure 1.6**) is challenging as the majority of routes are still based on the classical resolution of mixtures. There are different approaches to resolve these key compounds into pure enantiomers. Some of them are explained below:

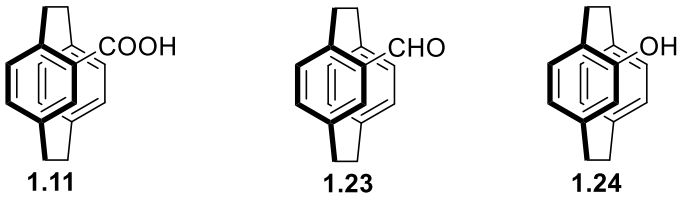

Figure 1.6: Substituted [2.2]paracyclophanes

1.6.1 Resolution of 4-Carboxy[2.2]paracyclophane

The method to resolve racemic [2.2]paracyclophane carboxylic acid **(±)-1.11** was established by Rozenberg and Belokon' (**Scheme 1.2**).[20]

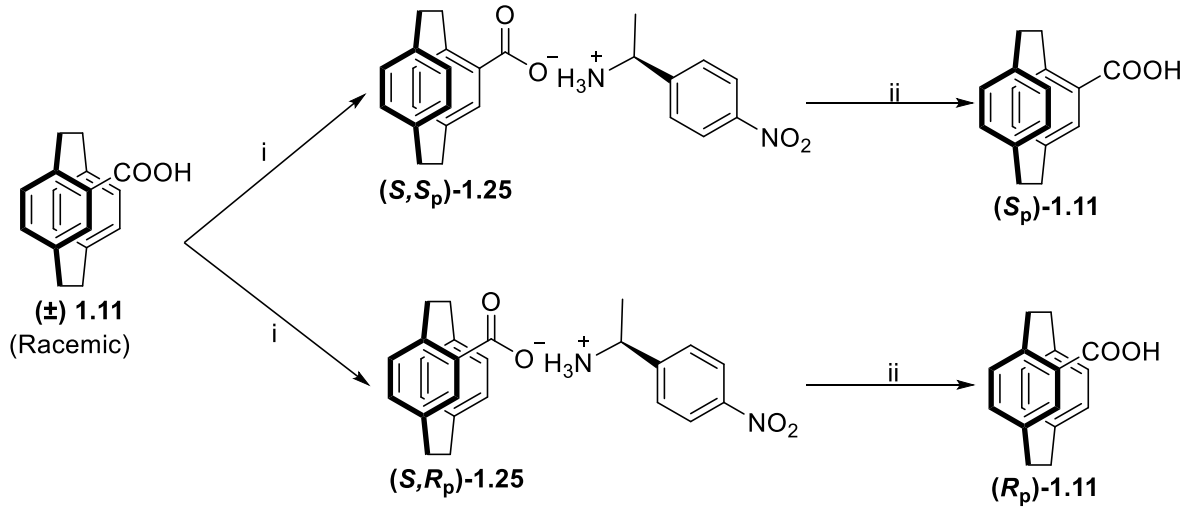

Scheme 1.2: Resolution of 4-carboxy[2.2]paracyclophane, i) (*S*)-(+)-α-(*p*-nitrophenyl)ethylamine, ii) HCl

It involves the formation of diastereoisomeric salts with (*S*)-(+)-α-(*p*-nitrophenyl)ethylamine. The less soluble (***S,S*p-1.25**) salt was crystallized from chloroform at —5 ˚C and is subsequently hydrolyzed with hydrochloric acid, to give (S_p)-(+)-4-carboxy[2.2]paracyclophane **1.11** in 89% *ee* (32% yield). The mother liquor from the crystallization was concentrated to yield (***S,R*p-1.25**) diastereoisomeric salt which was further hydrolyzed to give (R_p)-(–)-4-carboxy[2.2]paracyclophane **1.11** in 84% *ee* (24% yield). However, due to multiple recrystallizations being performed in multiple stages, much of the desired material was lost, as evidenced by the yields.

1.6.2 Resolution of Racemic 4-Formyl[2.2]paracyclophane

Qunici *et al*. developed a method for the resolution of racemic 4-formyl[2.2]paracyclophane **1.23**.[21] A racemic aldehyde was reacted with (*R*)-(+)-α-methylbenzylamine to form diastereoisomeric imines (**Scheme 1.3**).

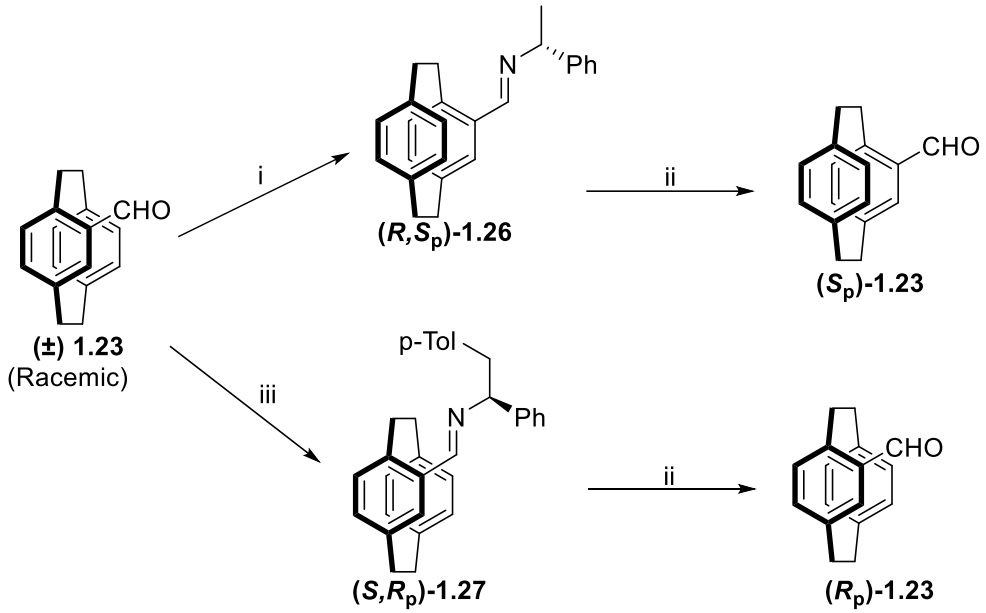

Scheme 1.3: Resolution of 4-formyl[2.2]paracyclophane. i) (*R*)-(+)-α-methylbenzylamine, ii) hydrolysis iii) (*S*)-(+)-1-phenyl-2-(*p*-tolyl)ethylamine

A single recrystallization of the crude product yielded crystals enriched in the (***R,S*$_p$-1.26**) diastereoisomer. Pure (***R,S*$_p$-1.26**) diastereoisomer was obtained by the second crystallization with this material in ≥ 98% *de*. Hydrolysis on silica gel during column chromatography gave (S_p)-(+)-4-formyl[2.2]paracyclophane **1.23** in ≥ 98% *ee* and 20% isolated yield. The enantiomer (R_p)-(–)-4-formyl[2.2]paracyclophane **1.23** was obtained by an alternative method. Racemic 4-formyl[2.2]paracyclophane **1.23** was reacted with (+)-1-phenyl-2-(*p*-tolyl)ethylamine to give **1.27** and repeated crystallization of the diastereoisomeric imine followed by hydrolysis, afforded (R_p)-(–)-4-formyl[2.2]paracyclophane **1.23** in ≥ 98% *ee* and 26% isolated yield.

The resolution was not economical by this method, as it required two different chiral amines and repetitive recrystallization, that resulted in the loss of the yield.

1.6.3 Kinetic Resolution of Racemic 4-Formyl[2.2]paracyclophane

In addition to the conventional resolution methods, described above, aldehydes and ketones derived from [2.2]paracyclophane can be obtained in their enantiopure form using different kinetic resolution approaches. Asymmetric hydrogenation of racemic carbonyl compound (±)-**1.23** using RuCl (*p*-cymene)[(*R,R*)-Ts-DPEN] also known as Noyori's catalyst and *t*-BuOK in a 1:1 *i*-PrOH-MeCN mixture at –10 ˚C yields optically active 4-formyl[2.2]paracyclophane **1.23 (*R*$_p$)-1.23** and reduced alcohol **(*S*$_p$)-1.28** 99% ee and 68% ee, respectively, at 56% conversion (**Scheme 1.4**).[22]

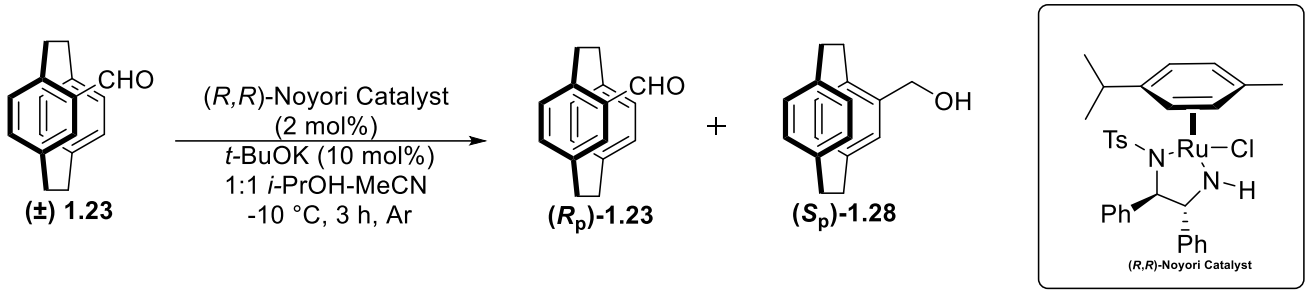

Scheme 1.4 Kinetic resolution of racemic 4-formyl[2.2]paracyclophane

1.6.4 Kinetic Resolution of Racemic 4-Acetyl[2.2]paracyclophane

The kinetic resolution of racemic 4-acetyl[2.2]paracyclophane **1.29** can be achieved through asymmetric reduction using Corey–Bakshi–Shibata oxazaborolidine catalyst (*S*)-CBS and boranes as the stoichiometric reductant (**Scheme 1.5**).[22]

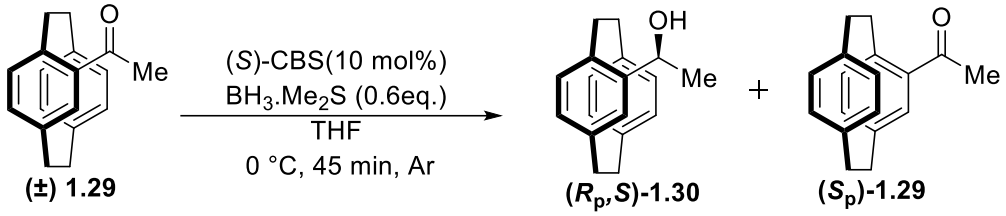

Scheme 1.5: Kinetic resolution of racemic 4-acetyl[2.2]paracyclophane

The ee obtained of the reduced benzylic alcohol **(R_p,*S*)-1.30** is > 61%, whereas of methyl ketone **(S_p)-1.29** was > 99%.

1.6.5 Resolution of Racemic 4-Hydroxy[2.2]paracyclophane

The resolution of racemic 4-hydroxy[2.2]paracyclophane **1.24** was achieved by ester formation with (1*S*)-(–)-camphanoyl chloride (**Scheme 1.6**).[23] First recrystallization from ethyl acetate gives **(*S*,R_p)-1.31** diastereoisomer with *de* >95%. The **(*S*,S_p)-1.31** diastereoisomer can be obtained after multiple crystallizations from the mother liquor in ≥99% de. The diastereoisomeric esters can then be cleaved by reduction with lithium aluminium hydride, to afford enantiopure (R_p)-(+)-4-hydroxy[2.2]paracyclophane **1.24** and (S_p)-(–)-4-hydroxy[2.2]paracyclophane **1.24** in 10-11% isolated yield and >99% *ee*.

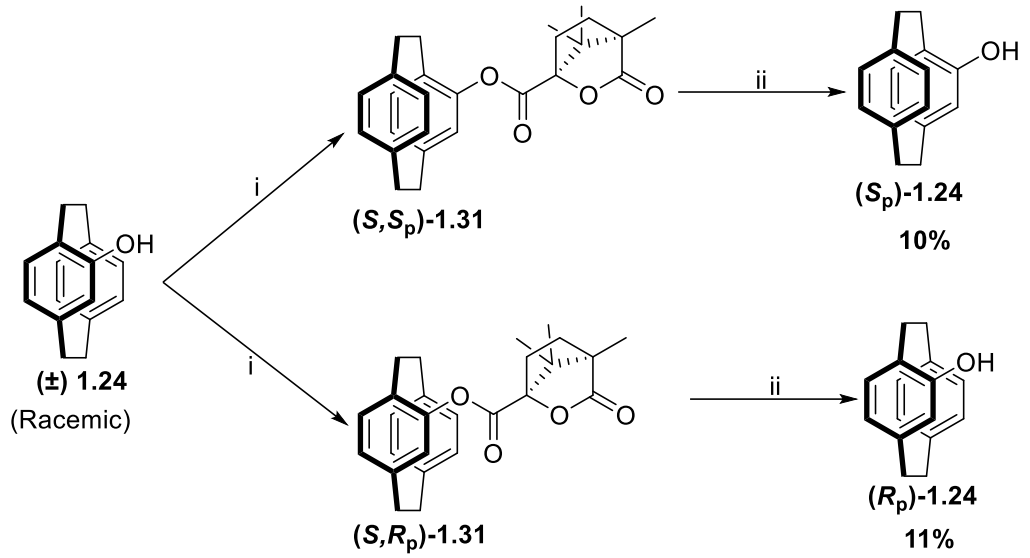

Scheme 1.6: Resolution of 4-hydroxy[2.2]paracyclophane. i) (1*S*)-(–)-camphanoyl chloride, ii) $LiAlH_4$

The shortcoming of the above method is the multiple recrystallization, that resulted in the loss of the pure enantiomeric product, ultimately leading to the loss of the yield.

1.7 [2.2]Paracyclophane-based Chiral Auxiliaries

Another method for the formation of enantiomerically pure [2.2]paracyclophane derivatives is to incorporate a second stereogenic element into the molecule and then resolve the resulting diastereoisomers. The hydroxy imine ligands (**Figure 1.7**) of Bräse and co-workers,[24,25] can be prepared in such a manner. Similarly, oxazoline-based [2.2]paracyclophane derivatives (**Figure 1.7**), are invariably synthesized from the racemic carboxylic acid and only resolved after the formation of diastereoisomeric oxazolines.[26,27]

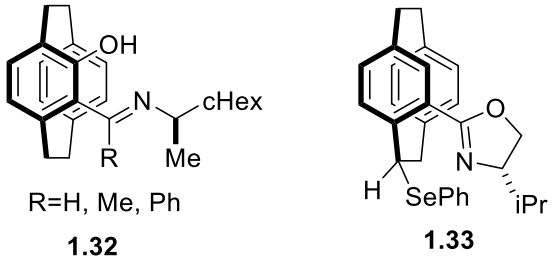

Figure 1.7: Enantioselective substituted [2.2]paracyclophanes chiral auxiliaries

The application of the above planar chiral *N,Se*-ligands can be seen in the asymmetric synthesis of the palladium-catalyzed allylic alkylation, resulted in the formation of the desired product with 98% yield and 94% *ee* (**Scheme 1.7**).[27]

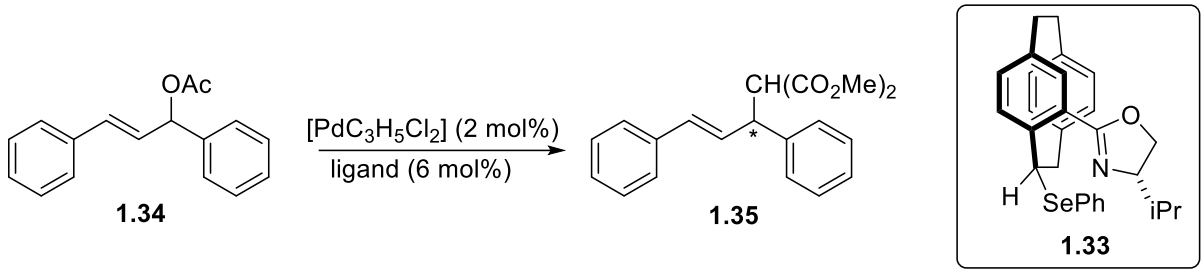

Scheme 1.7 Planar chiral *N*,*Se*-ligands catalyzing allylic alkylation

Hopefully, it is clear that the majority of enantiomerically pure derivatives are either prepared from a small pool of resolved starting materials or that each new compound requires its resolution protocol. This can be a tedious endeavor, especially when larger quantities of enantiomerically pure [2.2]paracyclophanes are needed. Moreover, conventional resolution methods require stoichiometric amounts of enantiopure derivatizing agents or chiral auxiliaries, are a tedious process, and often give moderate yields.[28]

1.8 Applications of [2.2]Paracyclophane in Asymmetric Synthesis

The planar chirality of [2.2]paracyclophane **1.4** has been known since 1955, yet it was not until the 1990s that this chirality was exploited in the field of asymmetric catalysis. [2.2]Paracyclophane derivatives are utilized as chiral auxiliaries, catalysts, pre-ligands in enantioselective synthesis. There has been several reviews on [2.2]paracyclophane derivatives in enantioselective catalysis.[1b,15,29]

1.8.1 Enantioselective hydrogenation by Phanephos

Phanephos **1.35** was synthesized by Pye *et al.* in 1997. It is based upon the same principles as the chiral diphosphine ligand BINAP, which has also been extensively employed as an enantioselective catalyst for enantioselective transformations (**Figure 1.8**).[29]

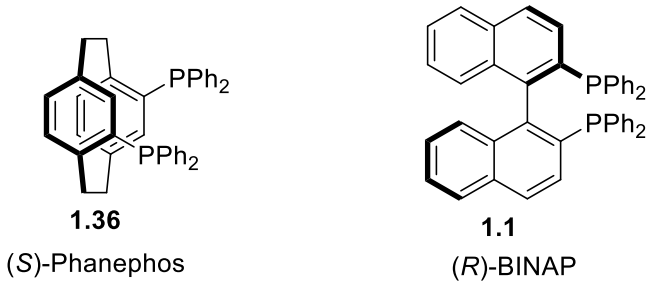

Figure 1.8: Structure of (*S*)-Phanephos and (*R*)-BINAP

One such example is where Phanephos was applied in the enantioselective hydrogenation of dehydroamino acid methyl ester by forming the triflate salt with rhodium(I) under extremely mild conditions like using 2 mol% of the catalyst, hydrogen gas at ambient temperature to give 99.6% *ee* and >99% yield (**Scheme 1.8**).[10]

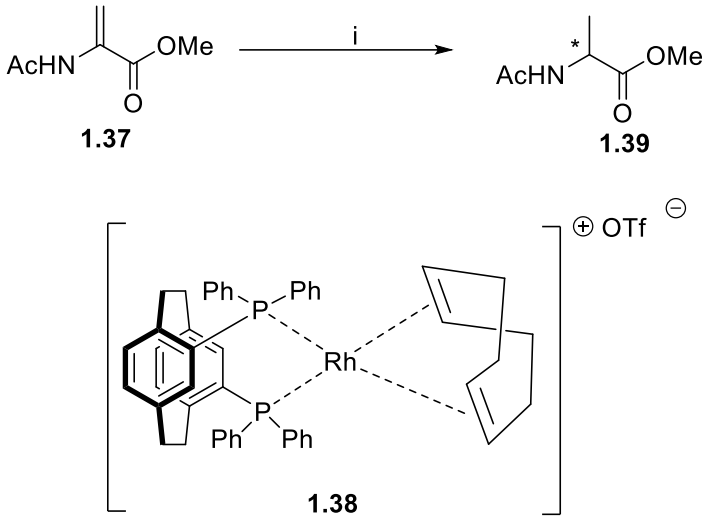

Scheme 1.8: Enantioselective hydrogenation of dehydroamino acid methyl ester. (i = 2 mol% catalyst 1,5-cyclooctadiene, H_2 (5.5 atm) at 23 ˚C in MeOH)

1.8.2 Planar-Chiral Oxazole–Pyridine *N,N*-Ligands

A recent report on the synthesis of a class of [2.2]paracyclophane-based planar-chiral oxazole–pyridine *N,N*-ligands have been reported by Yu *et al*. These ligands were utilized in the enantioselective palladium-catalyzed asymmetric acetoxylative cyclization of alkyne-tethered cyclohexadienones, providing the chiral *cis*-hydrobenzofurans with upto 91% yield and upto 96% *ee* (**Scheme 1.9**).[30]

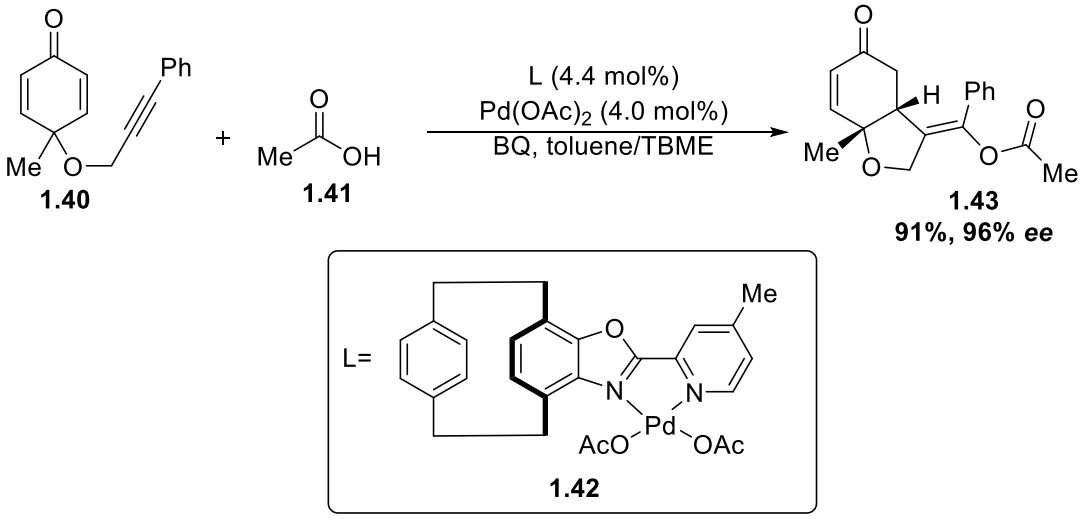

Scheme 1.9: Enantioselective palladium-catalyzed asymmetric acetoxylative cyclization

1.8.3 Enantioselective [3+2] Cycloaddition of Azomethine Ylides using Planar Chiral [2.2]Paracyclophane-imidazoline *N,O*-ligands

Sundarvel *et al.*, have designed and synthesized a series of new planar chiral imidazolinyl-paracyclophanol *N,O*-ligand (UCD-Imphanol).[31] This novel class of ligand has an extra advantage over chiral oxazoline-containing ligands. These imidazoline-based ligands, possess an additional nitrogen atom compared to an oxazoline, that affords the opportunity for fine-tuning the ligand electronic and conformational properties by choice of the substituent in the non-ligating nitrogen atom. They demonstrated excellent efficiency in the enantioselective Zn(II)-catalyzed [3+2] azomethine ylide cycloaddition, furnishing the corresponding cycloadducts in excellent diastereo- and enantioselectivities, 86% yield and 99.3% *ee* (**Scheme 1.10**).

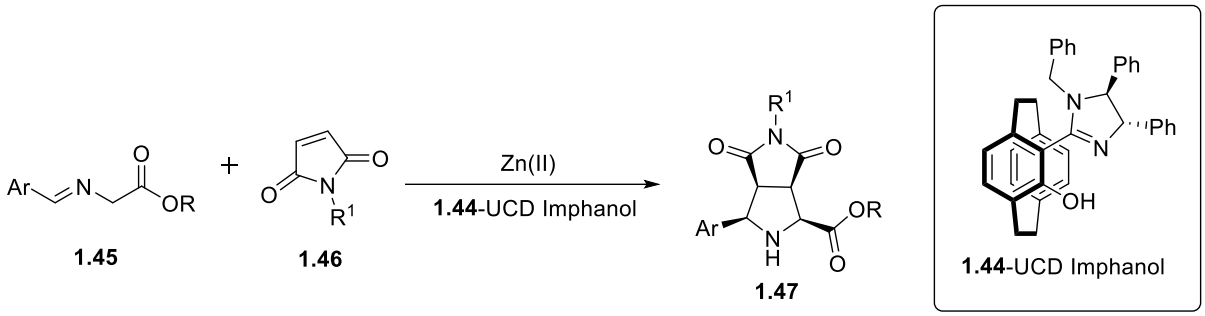

Scheme 1.10: Zinc-Catalyzed Enantioselective [3+2] Cycloaddition of Azomethine Ylides Using Planar Chiral [2.2]Paracyclophane-Imidazoline *N,O*-ligands

1.8.4 Planar Chiral [2.2]Paracyclophane-derived *N*-Heterocyclic Carbene Ligands

Bolm *et al.* reported the first carbene precursors derived from the [2.2]paracyclophane framework.[32]

Since then many reports on the generation of the carbene ligands derived from paracyclophane have been published including the fluorine-substituted [2.2]paracyclophane-based carbene precursor (R,R_p)-**1.9** discussed earlier. Another fluorine derivative that was reported by Wang *et al.* (**Scheme 1.11**).[33] The role and effect of a fluorinated [2.2]paracyclophane backbone and the corresponding stereoelectronic effect on catalytic activity was postulated and shown. The copper-catalysed asymmetric β-boration of α,β-unsaturated ketones **1.49** to form chiral β-boryl ketones **1.50** was selected as a model reaction. Some of the findings are discussed below:

It was observed that fluorination of the planar chiral carbene has a significant effect on the catalytic performance of the NHC-copper complex.

Moreover, the planar and centrally chiral 1,2,4-triazolium salt (R,R_p)-**1.48** exhibited a significantly better catalytic performance compared to the planar chiral imidazolium salts enantioselectivity (up to 99% *ee*).

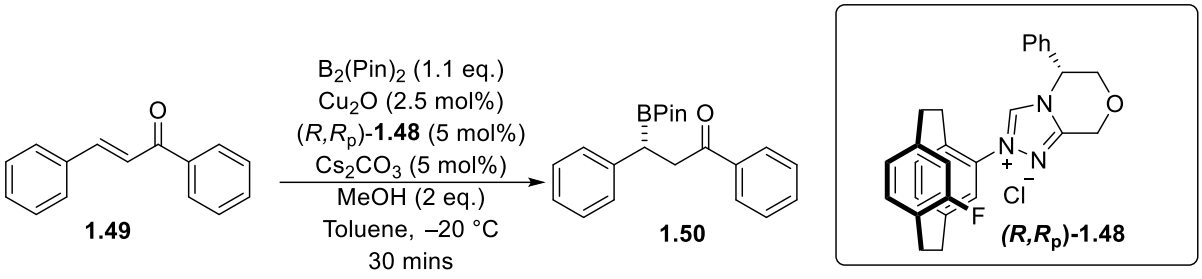

Scheme 1.11: Planar chiral [2.2]paracyclophane-derived *N*-heterocyclic carbene ligands

1.8.5 Planar Chiral [2.2]Paracyclophane-derived *N,O*-Chelating Ligands

A recent example of the utilization of [2.2]paracyclophane-containing mono- and tethered bis-amide ligands have been shown (**Figure 1.9**) by Bräse and Schafer et al.[34]

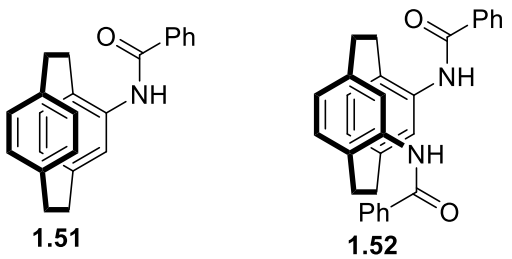

Figure 1.9: Mono- and bis-amide *N,O*-chelating ligands

These amides act as potent chelating ligands for titanium- and zirconium-catalyzed hydroamination of aminoalkenes. The translation of planar chirality of the starting material (S_p)-**1.51** and (S_p)-**1.52** was converted to central chirality by the formation of a hydroamination product (**Scheme 1.12**).[34] The substrate **1.53** produced the hydroamination product **1.54** with hydroaminoalkylation by-product **1.55** (from C-H activation). The bis-amide ligand (S_p)-**1.52** with $Zr(NMe_2)_4$ proved superior for enantioselectivity (68% *ee*) and chemoselectivity (**1.52** vs. **1.51**: 36% vs. 6%) as compared to mono-amide **1.51.** It is predicted that in the case of zirconium metal as it is less affected and sterically shielded by the tethered ligand as compared to the titanium metal tethering.

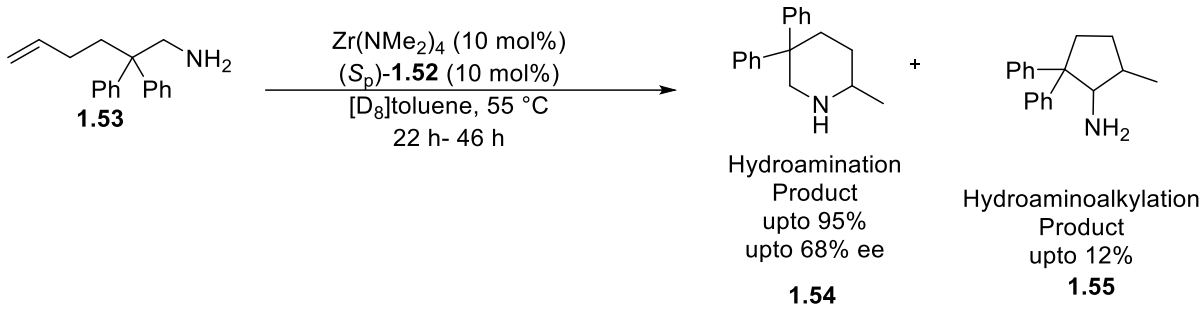

Scheme 1.12 Hydroamination of aminoalkenes

1.9 Conclusion:

The general introduction above provides a brief overview of [2.2]paracyclophane derivatives and their potential in the stereoselective synthesis. Despite the recent advancements in [2.2]paracyclophane chemistry, the main limitation is the lack of elegant methods to sythesize the enantiomerically pure planar chiral derivatives.

There are still many opportunities to explore before [2.2]paracyclophane derivatives show their full potential in asymmetric catalysis. These chiral compounds have great potential and can be useful in many ways. This research project aims at providing new methodologies and routes to synthesize chiral [2.2]paracyclophanes.

We have seen in examples above that the [2.2]paracyclophane needs a substituent to introduce planar chirality. The next chapter will focus on the brief overview of one of coupling partner, i.e., oxazolines.

1.10 References

1. J. T. Mohr, Natural products as inspiration for the development of asymmetric catalysis, *Nature*, **2008**, 7211, 323-332. b) S. Felder, S. Wu, J. Brom, L. Micouin and E. Benedetti, Enantiopure planar chiral [2.2]paracyclophanes: Synthesis and applications in asymmetric organocatalysis, *Chirality*, **2021**, *33*, 506-527.
2. T. Etsuko, Y. Takeshi, I. Emi, S. Norio, Understanding the Thalidomide Chirality in Biological Processes by the Self-disproportionation of Enantiomers, S*cientific Reports*, 2018, 8, Article number: 17131.
3. P. G. Mezey, A global approach to molecular chirality, *New Developments in Molecular Chirality*, 1991, 257-289.
4. H. Hopf, Guest Editorial: [2.2]Paracyclophane-After 60 Years, Stronger Than Ever, *Isr. J. Chem.*, 2012, *52*, 18-19.
5. K. Schlögl, Stereochemistry of metallocenes: 20 Years of progress and recent advances, *J. Organomet. Chem.*, 1986, *300*, 219-248.
6. R. Noyori, & T. Ohkuma, Asymmetric Catalysis by Architectural and Functional Molecular Engineering: Practical Chemo- and Stereoselective Hydrogenation of Ketones, *Angew. Chem. Int. Ed.*, 2001, *40*, 40-73.
7. M. Keith, The preparation of ferrocene-containing phosphinamine ligands possessing central and planar chirality and their application in palladium-catalysed allylic substitution, *Tetrahedron*, 2021, *90*, 132088-132101.
8. C. Bolm, K. Muñiz, Planar chiral arene chromium(0) complexes: potential ligands for asymmetric catalysis, *Chem. Soc. Rev.* **1999**, *28*, 51-59.
9. M. Rosillo, G. Domínguez,; Chromium arene complexes in organic synthesis, *Chem. Soc. Rev.* **2007**, 36, 1589-1604.
10. Rozenberg, V.; Sergeeva, E.; Hopf, H., Cyclophanes as templates in stereoselective synthesis, *Modern Cyclophane Chemistry*, **2004**, 435-437.
11. K. Tanaka,, Catalytic Enantioselective Synthesis of Planar Chiral Cyclophanes, *Bull. Chem. Soc. Jpn.* **2017**, *91*, 187-194.
12. Z. Liu, S. K. M. Nalluri, J. F. Stoddart, Surveying macrocyclic chemistry: from flexible crown ethers to rigid cyclophanes, *Chem. Soc. Rev.*, **2017**, *46*, 2459-2478.
13. T. Friščić, L. R. Macgillivray, Cyclophanes and Ladderanes: Molecular Targets for Supramolecular Chemists, *Supramol. Chem.*, **2005**, *17*, 47-51.
14. G. J. Rowlands, Planar Chiral Phosphines Derived from [2.2]Paracyclophane, *Isr. J. Chem*. **2012**, *52*, 60-75.

15. J. Paradies, [2.2]Paracyclophane derivatives: synthesis and application in catalysis, *Synthesis*, **2011**, 3749-3766.
16. Z. Hassan,; E. Spuling,; D. M. Knoll,; J. Lahann,; S. Bräse, Regioselective Functionalization of [2.2]Paracyclophanes: Recent Synthetic Progress and Perspectives, *Angew. Chem. Int. Ed.*, **2020**, *58*, 2156-2170.
17. C. Jianqiang, D. Wenzeng, C. Zhen, M. Manyuan, S. Chun, M. Yudao, [2.2]Paracyclophane-based carbene–copper catalyst tuned by transannular electronic effects for asymmetric boration, *RSC Adv*., **2016**, *6*, 75144-75151.
18. S. E. Gibson, J. D. Knight, [2.2]Paracyclophane derivatives in asymmetric catalysis, *Org. Biomol. Chem.*, **2003**, *1*, 1256 -1269.
19. Z. Hassan,; E. Spuling, D. M. Knoll, J. Lahann, S. Bräse, Planar chiral [2.2]paracyclophanes: from synthetic curiosity to applications in asymmetric synthesis and materials, *Chem. Soc. Rev.* **2018**, *47*, 6947-6963.
20. V. Rozenberg, N. Dubrovina, E. Sergeeva, D. Antonov, Y. Belokon', An improved synthesis of (*S*)-(+)- and (*R*)-(−)-[2.2]paracyclophane-4-carboxylic acid, *Tetrahedron: Asymmetry*, **1998**, *9*, 653-656.
21. S. Banfi, A. Manfredi, F. Montanari, G. Pozzi; S. Qunici, Synthesis of chiral Mn(III)-meso-tetrakis-[2.2]paracyclophanyl-porphyrin: a new catalyst for enantioselective epoxidation, *J. Mol. Catal., B. Chem.*, **1996**, *113*, 77-86.
22. C. Zippel, Z. Hassan, A. Q. Parsa, J. Hohmann, S. Bräse, Multigram-Scale Kinetic Resolution of 4-Acetyl[2.2]Paracyclophane *via* Ru-Catalyzed Enantioselective Hydrogenation: Accessing [2.2]Paracyclophanes with Planar and Central Chirality, *Adv.Synth. Catal.*, **2021**, 363, 2861-2865.
23. V. Rozenberg, T. Danilova, E. Sergeeva, E. Vorontsov, Z. Starikova, A. Korlyukov, H. Hopf, Resolution and Novel Reactions of 4-Hydroxy[2.2]paracyclophane, *Eur. J. Org. Chem.*, **2002**, 468-477.
24. F. Lauterwasser, J. Gall, S. Hofener, S. Bräse,, Second-Generation N, O-[2.2]Paracyclophane Ketimine Ligands for the Alkenylzinc Addition to Aliphatic and Aromatic Aldehydes: Scope and Limitations, *Adv. Syn. & Cat.*, 2006, *348*, 2068-2074; M. Kreis, Nieger, M.; S. Bräse, Synthesis of novel planar-chiral [2.2] paracyclophane derivatives as potential ligands for asymmetric catalysis, *J. Organomet. Chem.*, **2006**, *691*, 2171-2181; F. Lauterwasser, S. Vanderheiden, S. Bräse, Planar- and Central-Chiral N,O-[2.2]Paracyclophane Ligands: Non-Linear-Like Effects and Activity, *Adv. Syn. Cat.*, **2006**, 348, 443-448; F. Lauterwasser, M. Nieger, H. Mansikkamaki, K. Nattinen, S. Bräse, Structurally Diverse Second-Generation [2.2]Paracyclophane

Ketimines with Planar and Central Chirality: Syntheses, Structural Determination, and Evaluation for Asymmetric Catalysis, *Chem.-A Eur. J.* **2005**, *11*, 4509-4525; S. Bräse, S. Dahmen, S. Hofener, F. Lauterwasser, M. Kreis,; R. E. Ziegert, Planar and central chiral [2.2]paracyclophanes as powerful catalysts for asymmetric 1,2-addition reactions, *Synlett* **2004**, 2647-2669; S. Dahmen, S. Bräse, [2,2]Paracyclophane-Based *N,O*-Ligands in Alkenylzinc Additions to Aldehydes, *Org. Lett.*, **2001**, *3*, 4119-4122.

25. M. Kreis,; C. J. Friedmann,; S. Bräse,, *Chem. Eur. J.*, **2005**, *11*, 7387-7394.
26. X. W. Wu, T. Z. Zhang, K. Yuan, X. L. Hou, Regulation of the flexibility of planar chiral [2.2]paracyclophane ligands and its significant impact on enantioselectivity in asymmetric reactions of diethylzinc with carbonyl compounds, *Tetrahedron: Asymmetry*, 2004, *15*, 2357-2365.
27. X.-L. Hou, X.-W. Wu, L.X. Dai, B.X. Cao, J. Sun, Novel *N,S*- and *N,Se*-planar chiral [2,2]paracyclophane ligands: synthesis and application in Pd-catalyzed allylic alkylation, *Chem. Comm.*, **2000**, 1195-1196.
28. G. J. Rowlands, The synthesis of enantiomerically pure [2.2] paracyclophane derivatives, *Org. Biomol. Chem.*, **2008**, *6*, 1527-1534.
29. P. J. Pye, K. Rossen, R. A. Reamer, N. N. Tsou, R. P. Volante, P. J. Reider, A New Planar Chiral Bisphosphine Ligand for Asymmetric Catalysis: Highly Enantioselective Hydrogenations under Mild Conditions, *J. Am. Chem. Soc.*, **1997**, *119*, 6207-6208.
30. Q. B. Yu, W. Xin, B. W. Wang, Q. Xiao, R. Z. Wang, M. L. Liao, G. Z. Yong, Design and Synthesis of Planar-Chiral Oxazole–Pyridine *N,N*-Ligands: Application in Palladium-Catalyzed Asymmetric Acetoxylative Cyclization, *ACS Catal.* **2023**, *13*, 9829-9838.
31. V. K. Sundarvel, J. G. Patrick, Zinc-Catalyzed Enantioselective [3+2] Cycloaddition of Azomethine Ylides Using Planar Chiral [2.2]Paracyclophane-Imidazoline N,O-ligands, *Angew. Chem. Int. Ed.*, **2022**, *134*, 5516-5524.
32. T. Focken, G. Raabe, C. Bolm, Synthesis of iridium complexes with new planar chiral chelating phosphinyl-imidazolylidene ligands and their application in asymmetric hydrogenation, *Tetrahedron: Asymmetry*, **2004**, *15*, 1693-1706.
33. L. Wang, M. Ye, L. Wang, W. Duan, C. Song, Y. Ma, Synthesis of fluorine-substituted [2.2]paracyclophane-based carbene precursors for copper-catalyzed enantioselective boration of α,β-unsaturated ketones, *Tetrahedron: Asymmetry*, **2017**, *28*, 54-61.
34. C. Braun, S. Bräse, L. L. Schafer, Planar-Chiral [2.2]Paracyclophane-Based Amides as Proligands for Titanium- and Zirconium-Catalyzed Hydroamination, *Eur. J. Org. Chem.*, **2017**, 1760-1764.

Chapter 2:

Chiral Oxazolines and their Role in Stereoselective Transformations

2.1 Introduction

Oxazoline derivatives are an important class of heterocyclic compounds found in nature as well as synthetic compounds.[1,2] The five-membered ring contains one oxygen and one nitrogen atom and is partially saturated (**Figure 2.1**). The nitrogen of oxazoline is a good σ-donor for metal coordination.

2.1

Figure 2.1: Oxazoline

According to the position of the double bond in the structure, oxazoline can be classified into three different types: 2-oxazoline, 3-oxazoline, and 4-oxazoline (**Figure 2.2**). Among them, 2-oxazoline compounds are the most abundant and most widely used due to their unique chemical properties and stability. The 3- and 4-oxazolines are mainly used up for laboratory research.[3,4,5]

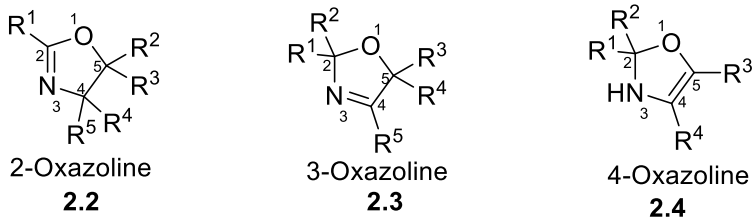

Figure 2.2: Different classes of oxazolines

Oxazolines are chemically robust and have been studied in many fields. There are a large number of biologically active oxazolines and they are found in applications such as the agriculture industry, pharmaceutical, food industry, natural product, medicine, polymers, and various other industries.[2] But the most important use of oxazolines is as ligands and auxiliaries for stereoselective synthesis.

Ligands containing chiral oxazoline are widely recognized as one of the most successful and versatile classes of ligands in asymmetric catalysis. They are commonly used due to their easy accessibility, modular nature, and ability to be applied in a broad range of metal-catalyzed reactions.[6]

Some useful compounds that utilize 2-oxazoline moiety are shown in **Figure 2.3** below.

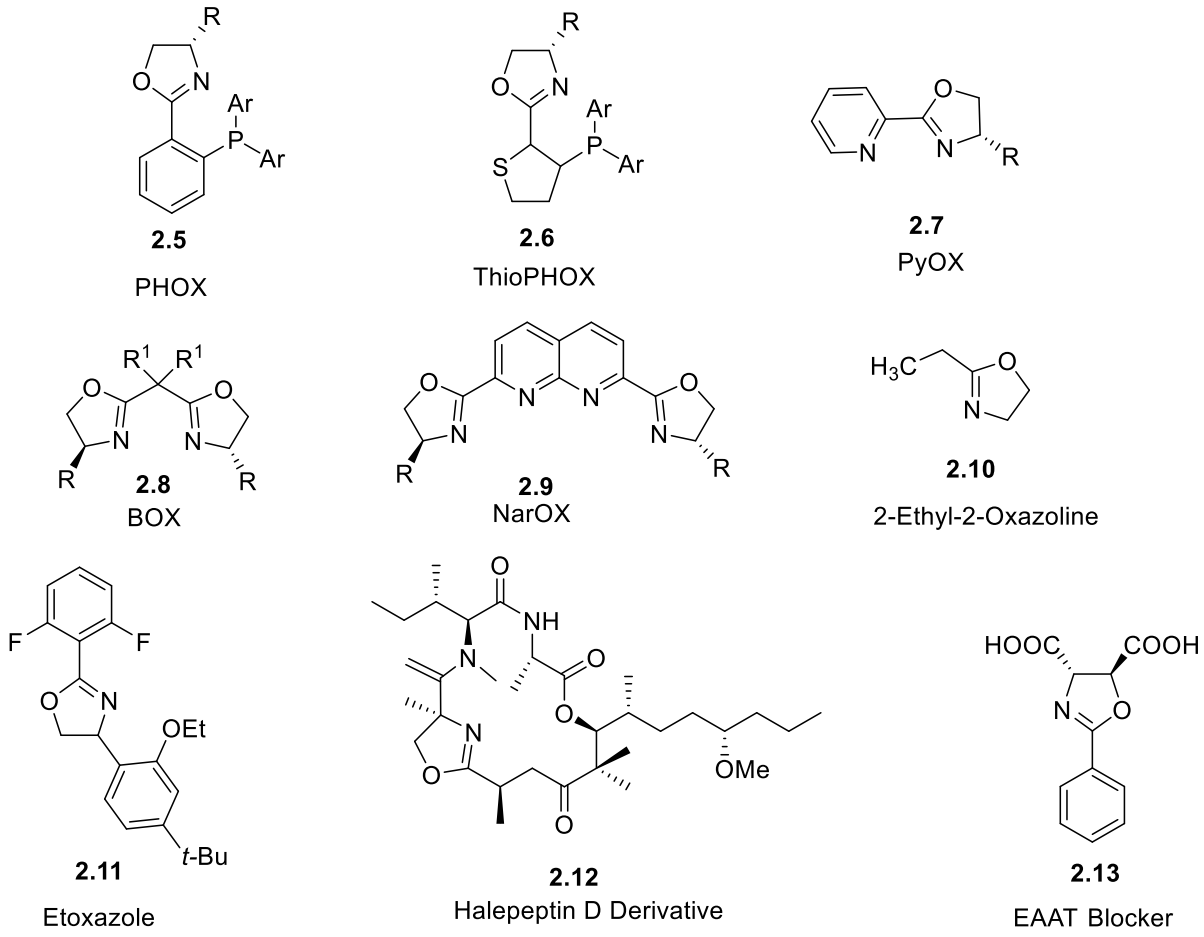

Figure 2.3: Some useful examples containing 2-oxazoline moiety

The vast majority of these ligands are formed in short, high-yielding synthesis from readily available chiral β-amino alcohols. Therefore, the stereocenter controlling the enantioselectivity of the metal-catalyzed process resides α- to the oxazolinyl nitrogen donor and, as a result, is in close proximity to the metal active site to directly influence the asymmetry induced in the reaction.

2.2 Synthesis of 2-Oxazolines

The majority of these ligands can be synthesized quickly and efficiently from readily available chiral β-amino alcohols, resulting in high yields. Consequently, the stereocenter that governs the enantioselectivity of the metal-catalyzed process is located α- to the oxazolinyl nitrogen donor. This proximity to the metal active site allows it to directly influence the asymmetry induced in the reaction.

The classical way to synthesize 2-oxazolines from amino alcohol (**Scheme 2.1**). The condensation between the acyl chloride and amino alcohol yields **2.16** or **2.17**. This then undergoes cyclization to yield oxazolines **2.17**. There are lot a of new reports available in the literature that yields 2-oxazolines in an efficient way using different approaches.

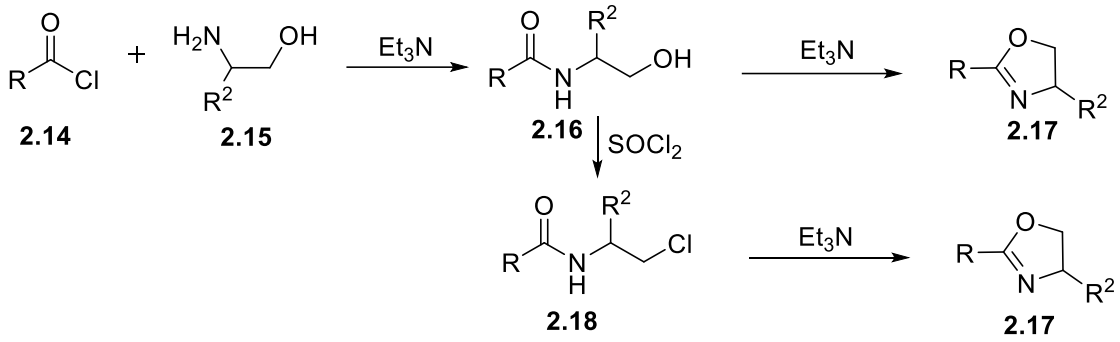

Scheme 2.1: Synthesis of oxazolines from amino alcohols

There are many more ways by which we can synthesize 2-oxazolines.[7]

2.2a 2-Oxazolines from nitriles

This approach to synthesizing 2-oxazolines is shown by Garg et al., where the synthesis of various 2-aryl/(hetero)aryloxazolines from nitriles and amino alcohols has been achieved without metals and catalysts in good to excellent yields (**Scheme 2.2. Table 2.1**). The reaction tolerates many functional groups and allows the introduction of many important biologically active motifs such as azoles, ring-fused azoles, saturated heterocyclics, and amines.[8]

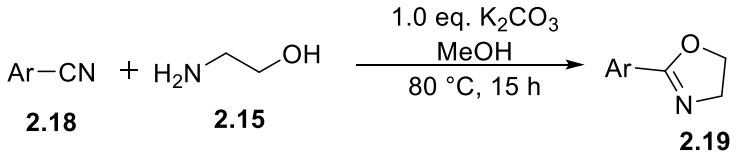

Scheme 2.2: Synthesis of various 2-aryl/(hetero)aryl oxazolines from nitriles

2.18	2.19	Yield
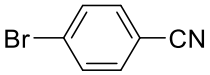 **2.18a**	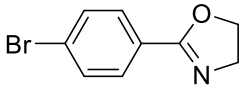 **2.19a**	89%
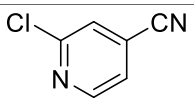 **2.18b**	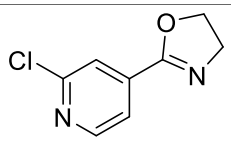 **2.19b**	97%

Table 2.1: Substrate scope of aromatic and hetero-aromatic 2-oxazolines

Proposed mechanism for the 2-oxazoline from nitriles:

Scheme 2.3 highlights the proposed mechanism for the formation of 2-oxazolines. The nucleophilic attack on the aryl nitrile **2.18**, followed by addition of amino alcohol **2.15** and intra-molecular cyclization lead to the formation of 2-oxazoline **2.19**.

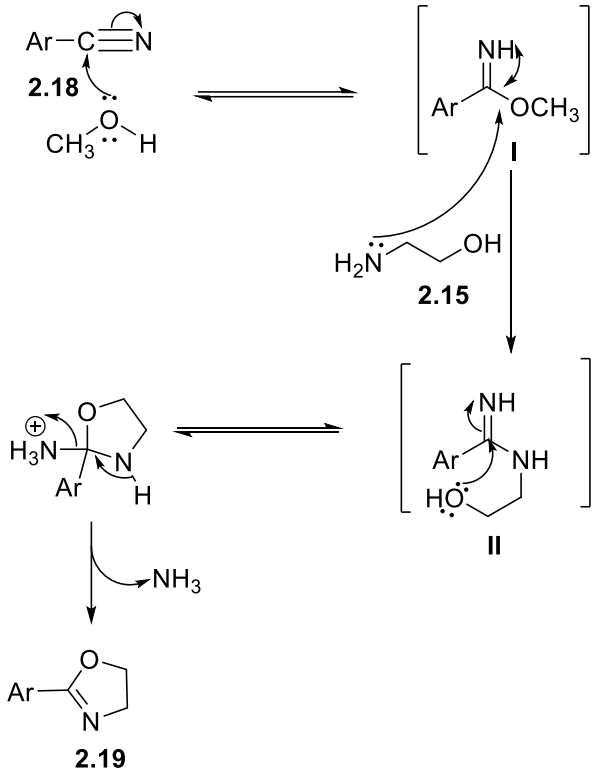

Scheme 2.3: Proposed mechanism for the 2-oxazoline from nitriles

2.2b Microwave-assisted synthesis of 2-Oxazolines

The synthesis of oxazolines has seen a recent advancement through the application of assisted microwave techniques. Deng *et al*., have developed a microwave-accelerated strategy to synthesize aminophenol-containing chiral oxazolines from aryl nitriles in a simpler and greener way with improved efficiency and reliability (**Scheme 2.4**).[9]

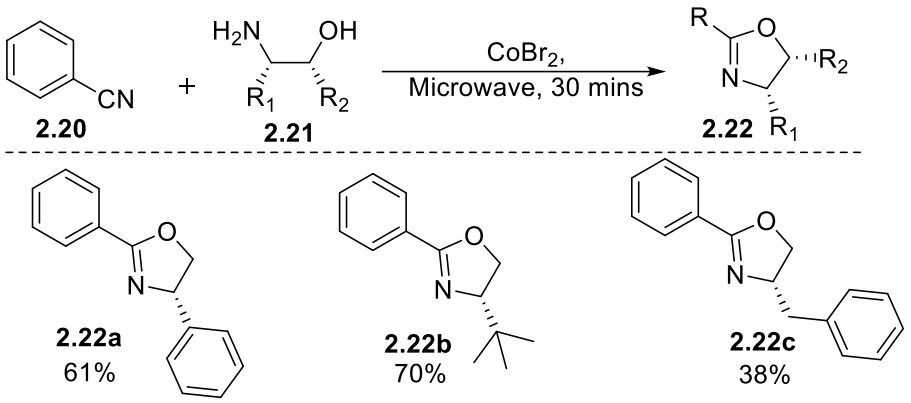

Scheme 2.4: Microwave assisted synthesis of 2-oxazolines

The reported method offers several advantages, including a wider range of compatible substrates, high yields, significantly reduced reaction time, the use of a recyclable catalyst, and either solvent-free conditions or reduced solvent usage. These characteristics align with the principles of green chemistry and enable efficient access to cost-effective chiral ligands. Consequently, this method holds the potential to expedite the discovery and application of new asymmetric reactions.

2.2c Synthesis of Oxazolines from *N*-Allyl Amides

A recent literature has shown that a chiral triazole-substituted iodoarene catalyzes an enantioselective oxidative cyclization of *N*-allyl carboxamides to provide highly enantioenriched oxazolines and oxazines. Quaternary stereocenters can be constructed and, besides *N*-allyl amides, the corresponding thioamides and imideamides are well tolerated as substrates (**Scheme 2.5**).[10]

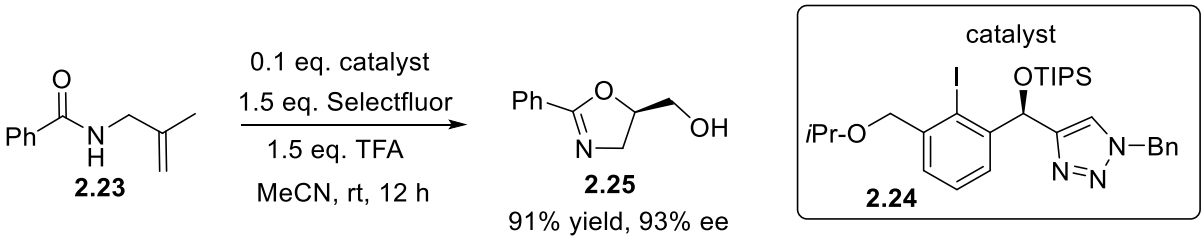

Scheme 2.5: Synthesis of oxazolines from *N*-allyl amides

A more general approach for the cyclization of *N*-allyl amides involves their treatment with a chiral hypervalent iodine compound. This induces an oxidative cyclization via a π-complexed iodane. Iodine(III) activates π-complexed NAA **2.23** to produce **II** through an intramolecular attack by the amide oxygen (**Scheme 2.6**). The emerging alkyl-substituted iodane then reacts rapidly with additives, usually added Brønsted acids HX, to form compound **2.26** under

reduction of the iodane to the iodoarene. Depending on the nature of **2.26**, rapid substitution often follows with external nucleophiles NuH, for example water or hydroxide anions, to generate the substituted oxazoline **2.25**.

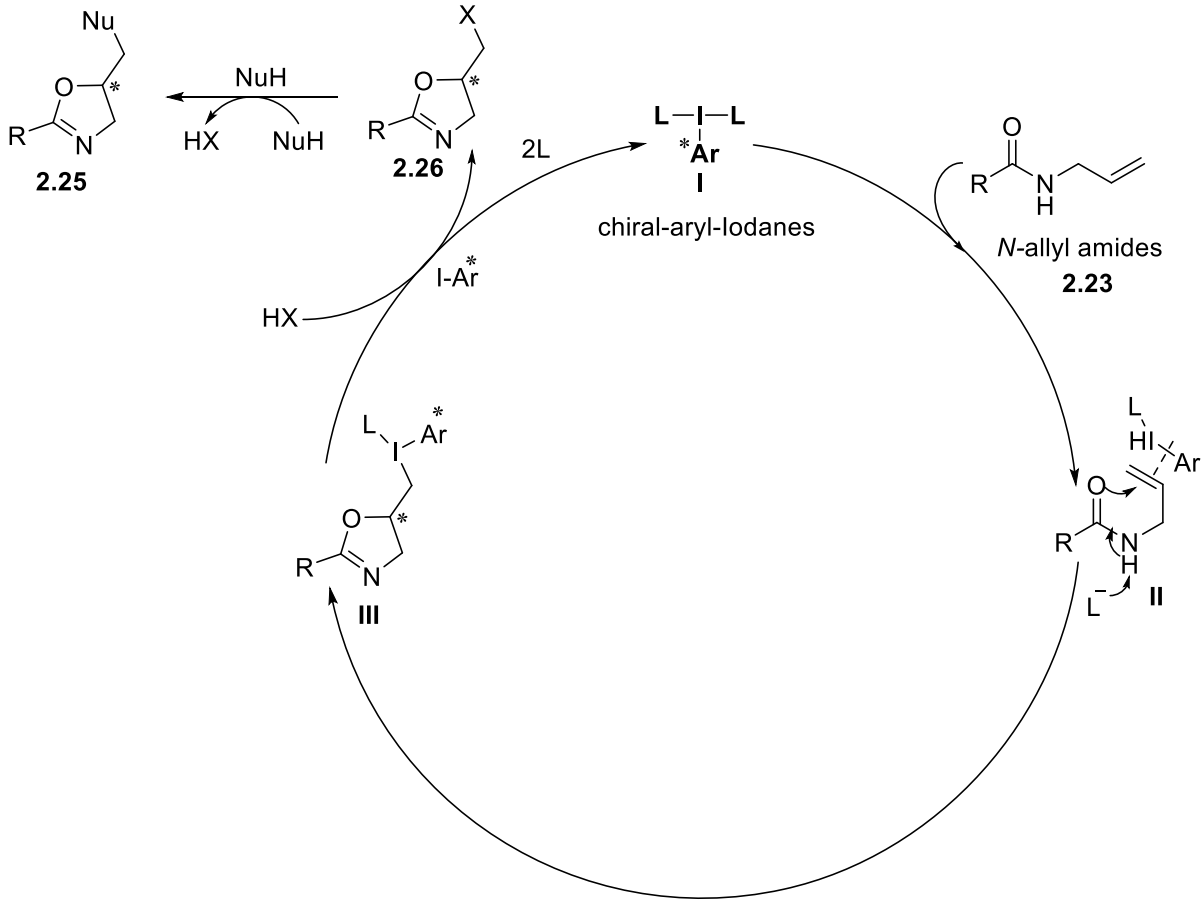

Scheme 2.6: General Mechanism for an Iodane-Mediated *N*-Oxidative Cyclization of *N*-allyl amides

2.3 Physical Properties of Oxazolines

The physical properties of the oxazolines depend significantly on the substitution that it bears, as they rarely oxazolines are found without any substituent. They have a very strong and characteristic odor, which may be pungent pyridine-like in some of them. The different substituents on 2-oxazoline are responsible for the variable boiling points of different oxazolines.

2.4 Chemical Properties of 2-Oxazolines:

Oxazolines have been widely employed for various purposes beyond their extensive use as chiral ligands or pre-ligands. Although these applications may not directly relate to my specific chemistry, they are worth mentioning to showcase the versatility of this remarkable

molecule. Here are a few examples of how oxazolines have been utilized for different purposes.

Adams and Leffler prepared a series of compounds based on 2-oxazolines **2.27** and characterized their activities as mild local anesthetics owing to the structure relationship with procaine **2.28**, a well-known local anesthetic (**Figure 2.4**).[11]

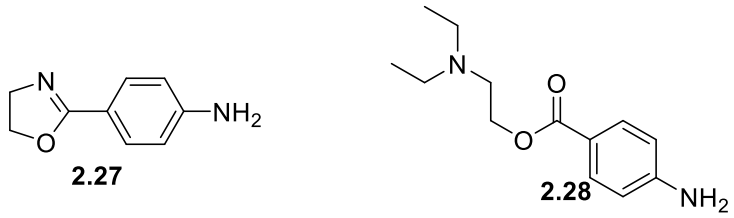

Figure 2.4: 2-Oxazolines as mild anesthetics

2.5 Oxazolines as Ligands in Aymmetric Catalysis

Oxazolines have been utilized as ligands in a wide range of applications. These versatile molecules exhibit excellent coordinating abilities and have found extensive use in coordination chemistry. As ligands, oxazolines can form complexes with metal ions, facilitating various catalytic processes. They have been employed in asymmetric catalysis, where their chiral nature helps induce stereochemical control in chemical reactions. Additionally, oxazoline ligands have been utilized in transition metal-catalyzed cross-coupling reactions, C-H activation, and other important transformations. Their unique structural features make oxazolines valuable tools for designing and fine-tuning catalytic systems in organic synthesis.

Here are a few examples, where oxazolines have been used as chiral ligands in catalysis.

2.5a *P,N*- Ligands in Asymmetric Catalysis

Many privileged chiral ligand classes, including BINAP, PyBox, and BINOL, often possess a C2 axis of symmetry.[12] However, an alternative approach to enhancing ligand functionality in the catalytic cycle involves desymmetrizing the ligand by adjusting each donor atom to serve a specific purpose. A highly successful method of achieving ligand desymmetrization is by incorporating different donor atoms, resulting in ligands with phosphorus and nitrogen as their donor atoms (referred to as *P,N* ligands).[13a] The π-acceptor properties of phosphorus enable the stabilization of a metal center in a low oxidation state, while the nitrogen's σ-donor ability enhances the metal's susceptibility to oxidative addition reactions. This unique

combination aids in stabilizing intermediate oxidation states that arise during a catalytic cycle.

Herein, an example of asymmetric catalysis is reported using a new class of *P,N* ligand, NeoPhox. Pfaltz *et al.* demonstrated the utility of these ligands when he applied them in the Ir-catalyzed hydrogenation of several stilbenes affording enantioselectivities of up to 99% (**Scheme 2.7**).[13b]

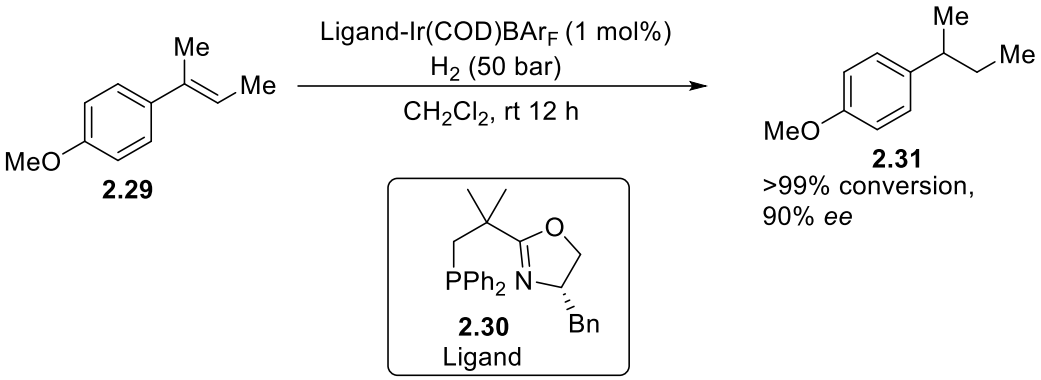

Scheme 2.7: Asymmetric catalysis using a new class of *P,N* ligand, NeoPhox

2.5b C_2-Symmetric Pyrazolate-Bridged Bis(oxazoline) Ligands (pyrbox)

Though oxazoline-based ligands have become very common, binucleating systems where a central bridging unit with appended oxazoline rings can host two metal centers have remained a point of interest for chemists around the world (**Figure 2.5**).[14]

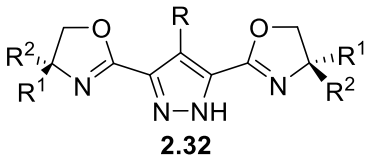

Figure 2.5: Pyrazole-bridged ligand

The generally adopted metal-metal separations are in the range of 3.4-4.5 Å and are thus suitable for exploiting cooperative reactivity toward substrate molecules. Further enhancement of preorganization of the two metal ions can be achieved by the attachment of chelating side arms to the 3,5-positions of the pyrazole heterocycle, and a variety of symmetrical and unsymmetrical 3,5-disubstituted ligands can be developed. To investigate the effect of steric and electronic modifications at both the bridging unit and the chelate arms, four different ligands were prepared, followed by their coordination with monocationic bis (methallypalladium) to yield 2.33a-d (**Scheme 2.8**).

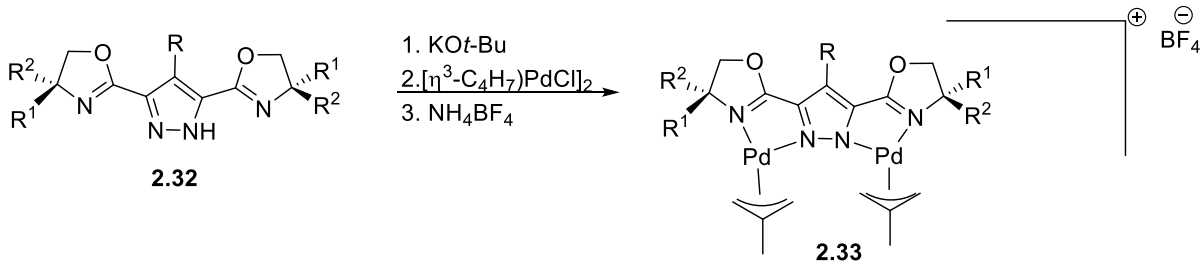

2.33a- R = H, R^1 = H, R^2 = Ph
2.33b- R = Ph, R^1 = H, R^2 = Ph
2.33c- R = H, R^1 = *i*-Pr, R^2 = H
2.33d- R = Ph, R^1 = *i*-Pr, R^2 = Ph

Scheme 2.8: Synthesis of pyrazole-bridged ligands

The catalytic activity of the bis(methallylpalladium) complexes was tested in the allylic alkylation of the model substrate rac-(*E*)-1,3-diphenylallyl acetate, using dimethyl malonate as a nucleophile under basic conditions, (**Scheme 2.9**).

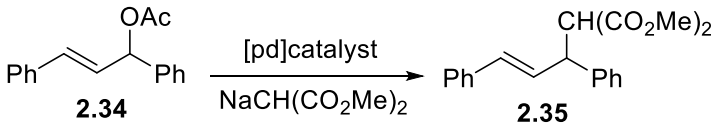

2.33a- 40%, 68% ee
2.33b- 53%, 23% ee
2.33c, 67%, 44% ee
2.33d- 54%, 5% ee

Scheme 2.9: Allylic alkylation of rac-(*E*)-1,3-diphenylallyl acetate with dimethyl malonate using C2-symmetric pyrazolate-bridged bis(oxazoline) ligands

2.5c Pincer Oxazolines

The first-of-its-kind studies on pincer bis-oxazolines (PBox) (**Figure 2.6**) were carried out independently by Denmark, Richards, and the group of Nishiyama and co-workers in 1997. Pincer oxazolines have been shown to be an important sub-class of the pincer ligands in both the general coordination chemistry sense and for applications in catalysis.[15]

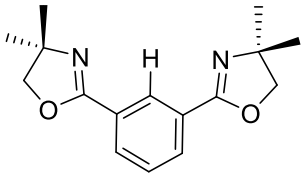

Figure 2.6: Pincer Oxazolines

It has been shown that the oxazoline-containing pincers are an interesting and diverse group of metal-binding agents.

2.5d Asymmetric synthesis of chiral chromanols

Yujie etal., synthesized Chiral chromanols and their derivatives via a RuPHOX–Ru catalyzed asymmetric hydrogenation of chromones (**Scheme 2.10**) in high yields, >20 : 1 drs and with up to 99.9% ee.[16]

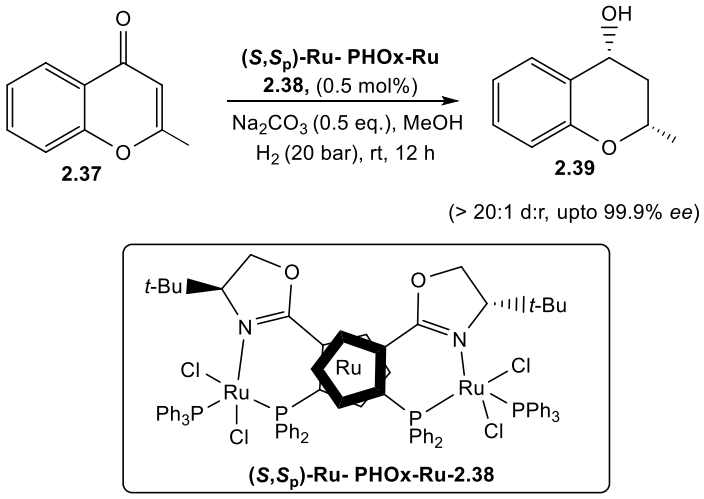

Scheme 2.10: Asymmetric synthesis of chiral chromanols

2.5e Asymmetric Heck-type reactions

In 2007, Jung reported an oxidative asymmetric intermolecular Heck-type reaction of electron-deficient alkenes by using a Pd-Pyox diacetate complex. In this reaction, a premade Pd-ligand complex afforded higher enantioselectivities than when the Pd-ligand catalytic system was generated *in situ* (**Scheme 2.11**).[17]

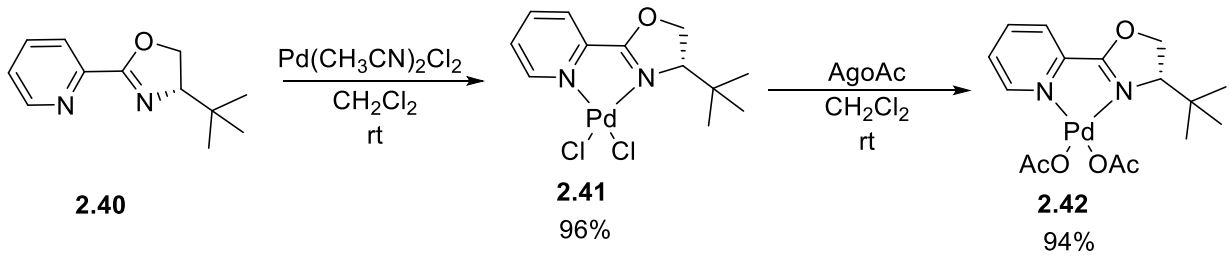

Scheme 2.11: Fresh preparation of the Pd-ligand catalytic system

The pyridine-oxazoline ligand showed higher enantioselectivity than the Box ligand. Substrates, including tiglic aldehyde and ester, were able to react with several electron-rich

aryl boronic acids to yield the corresponding arylation products in moderate yields and *ee* (**Scheme 2.12**).

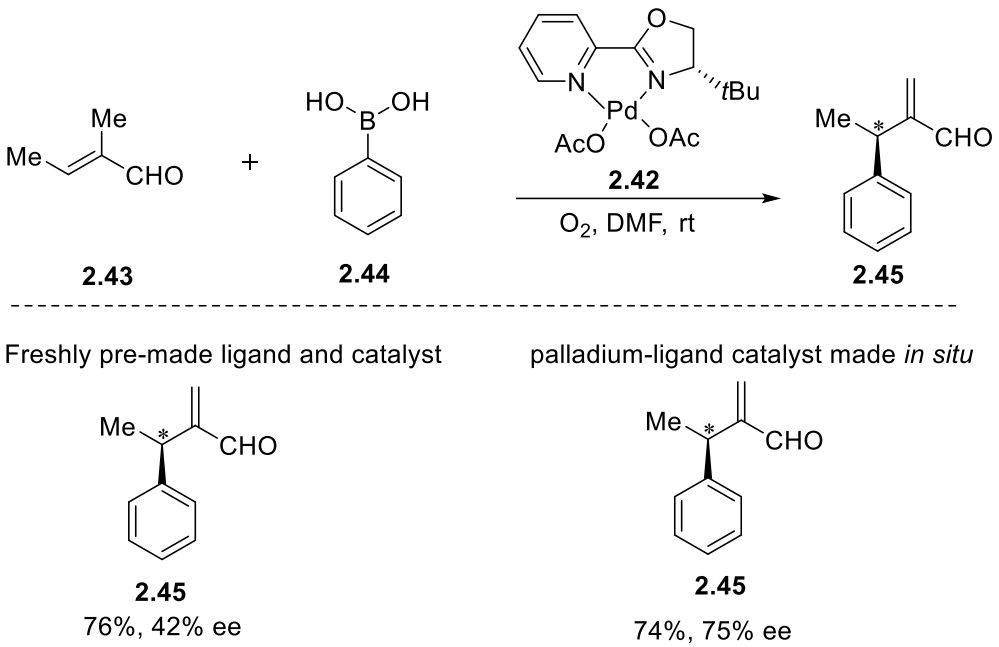

Scheme 2.12: Asymmetric Heck-type reaction

2.5f Oxazolines-catalyzed Asymmetric Cross-coupling Reactions

The Fu group developed a series of Ni-catalyzed achiral cross couplings of organometallic reagents with alkyl halides.[18] This group described the first catalytic enantioselective cross-couplings of secondary alkyl electrophiles, using primary alkyl zinc reagents and a *t*-Bu-iQuinox ligand with ortho steric repulsion towards the oxazoline ring could increase the yield and ee to an excellent level.

Scheme 2.13 shows the comparative analysis between the two ligands, where the difference in both yields and *ee* is evident while using *t*-Bu-iQuinox ligand.

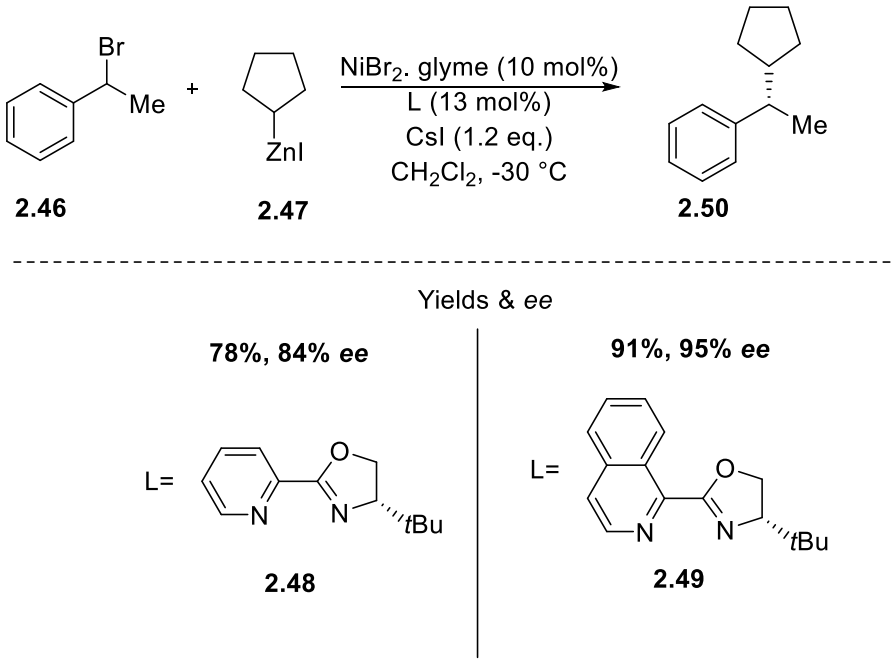

Scheme 2.13: Oxazolines-catalyzed Asymmetric Cross-coupling reactions

2.5g Oxazolines-catalyzed C-H Activation

In 2012, Shi and Hartwig reported the first Ir-catalyzed asymmetric C–H silylation employing a chiral tetrahdroquinoline-oxazoline ligand ((4H)Quinox).[19] These ligands are the hybrids of one tetrahydro-quinoline and one oxazoline unit. This catalytic system was employed for the enantioselective desymmetrization of symmetrical diaryl methanol derivatives, as well as their kinetic resolution with high enantioselectivities upto 92% ee, and high yields, 90% (**Scheme 2.14**).

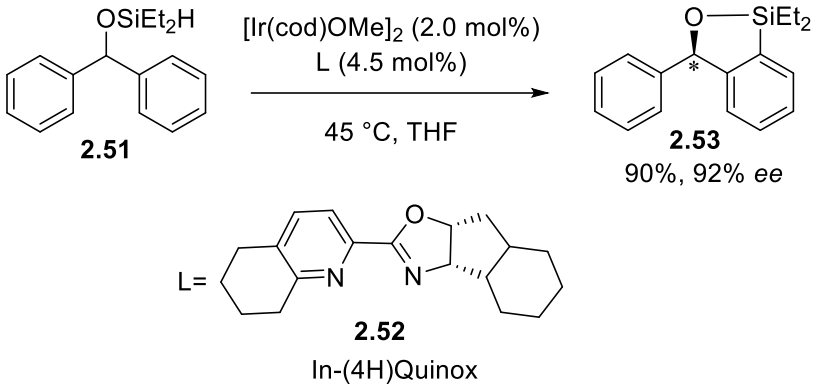

Scheme 2.14: Oxazolines-catalyzed C-H Activation

2.5h Rh-catalyzed hydrosilylation of Ketones using Pyox Ligands

Brunner *et al*., attempted the first successful rhodium-catalyzed hydrosilylation of ketones in the presence of oxazoline-based pyox ligands. the desired products were obtained with up to 91% *ee* using this ligand (**Scheme 2.15**).[20,21,22]

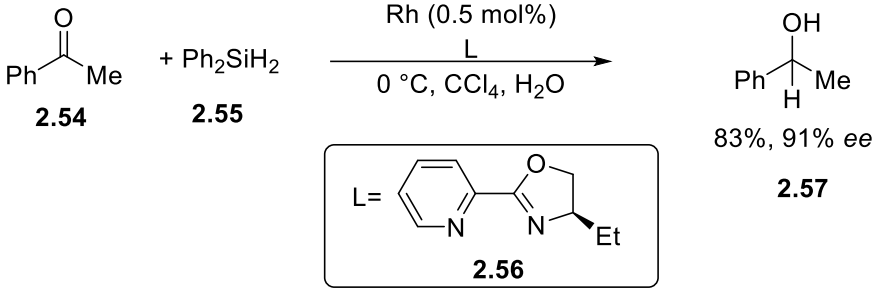

Scheme 2.15: Rh-catalyzed hydrosilylation of ketones using Pyox Ligands

2.6 Oxazolines as chiral Auxiliaries

2.6a Switchable and efficient conversion of 2-amidoaryl oxazolines to quinazolin-4(3H)-ones and N-(2-chloroethyl)benzamides.

Aryl oxazolines are very useful for functionalization reactions in organic synthesis as they can be utilized as complementary precursors for various heterocycles. An atom-economic and step-efficient, one-pot method was developed by Weiqiang *et al*., for the synthesis of quinazolin-4(*3H*)-ones. It was a switchable chemoselective conversion of 2-amido-aryl oxazolines to quinazolin-4(*3H*)-ones or *N*-(2-chloroethyl)benzamides that have been developed (**Scheme 2.16**).[23]

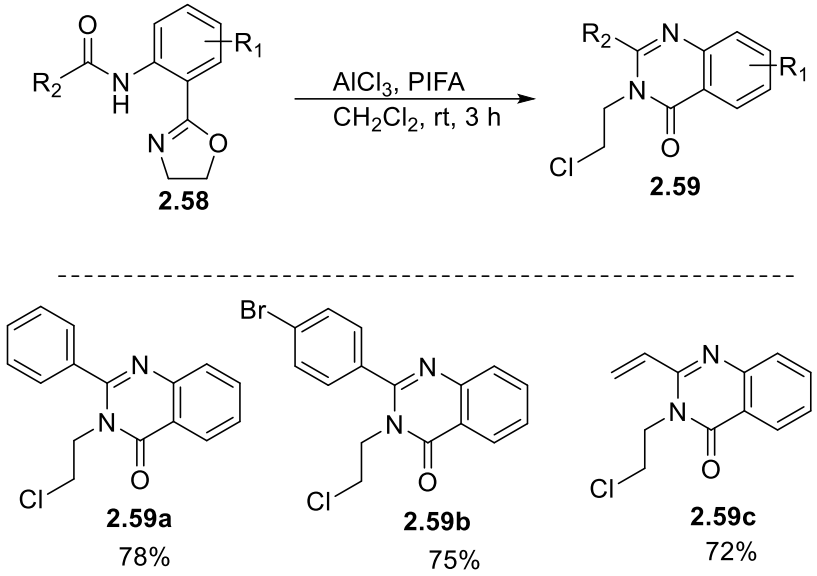

Scheme 2.16: Conversion of 2-amidoaryl oxazolines to quinazolin-4(3H)-ones

2.6b C_2-symmetric chiral tetrathiafulvalene-bis(oxazolines) (TTF-BOX) as precursors for electroactive metal complexes

Another use of oxazolines is highlighted here in this section (**Figure 2.7**), where they act as a precursor to form chiral conductors.[24] The unprecedented chiral C2-symmetric electroactive bis(oxazolines) containing a EDT-TTF backbone, are used as precursors for chiral multifunctional molecular materials and coordination metal complexes generally termed as chiral conductors. In these materials the chirality is expected to influence the conductivity either by the modulation of the structural disorder, the TTF-BOX present a C2-symmetry axis and a larger chiral space in the vicinity of the redox active core, besides their characteristic properties in coordination and catalysis, which make them of huge interest.

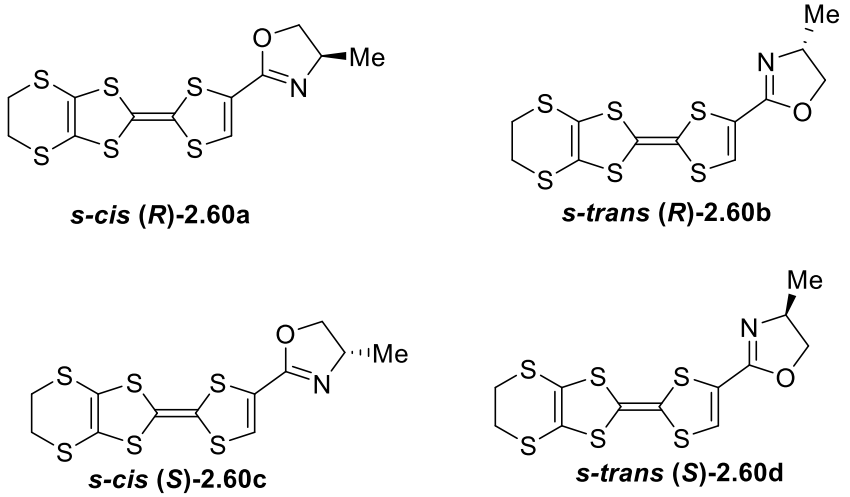

Figure 2.7: Chiral tetrathiafulvalene-bis(oxazolines) (TTF-BOX)

2.7 Hydrolysis of Oxazolines

The oxazoline ring is found to be stable under milder conditions of oxidation-reduction or even hydrolysis. But, under strong conditions, they are known to get cleaved and form open-chain counterparts. The oxazolines require harsh acidic and basic conditions[25] hydrolyze or to cleave the ring open forming amino alcohols. Acid hydrolysis of oxazoline starts with a protonation followed by the formation of the tetrahedral intermediate via water. This step is the rate determining step. The last step removes the carboxylic acid. Basic hydrolysis of oxazolines starts with the attack of the OH^-on the amide bond forming the tetrahedral intermediate. After protonation of the nitrogen, there is an irreversible release of the carboxylate (**Scheme 2.17**).

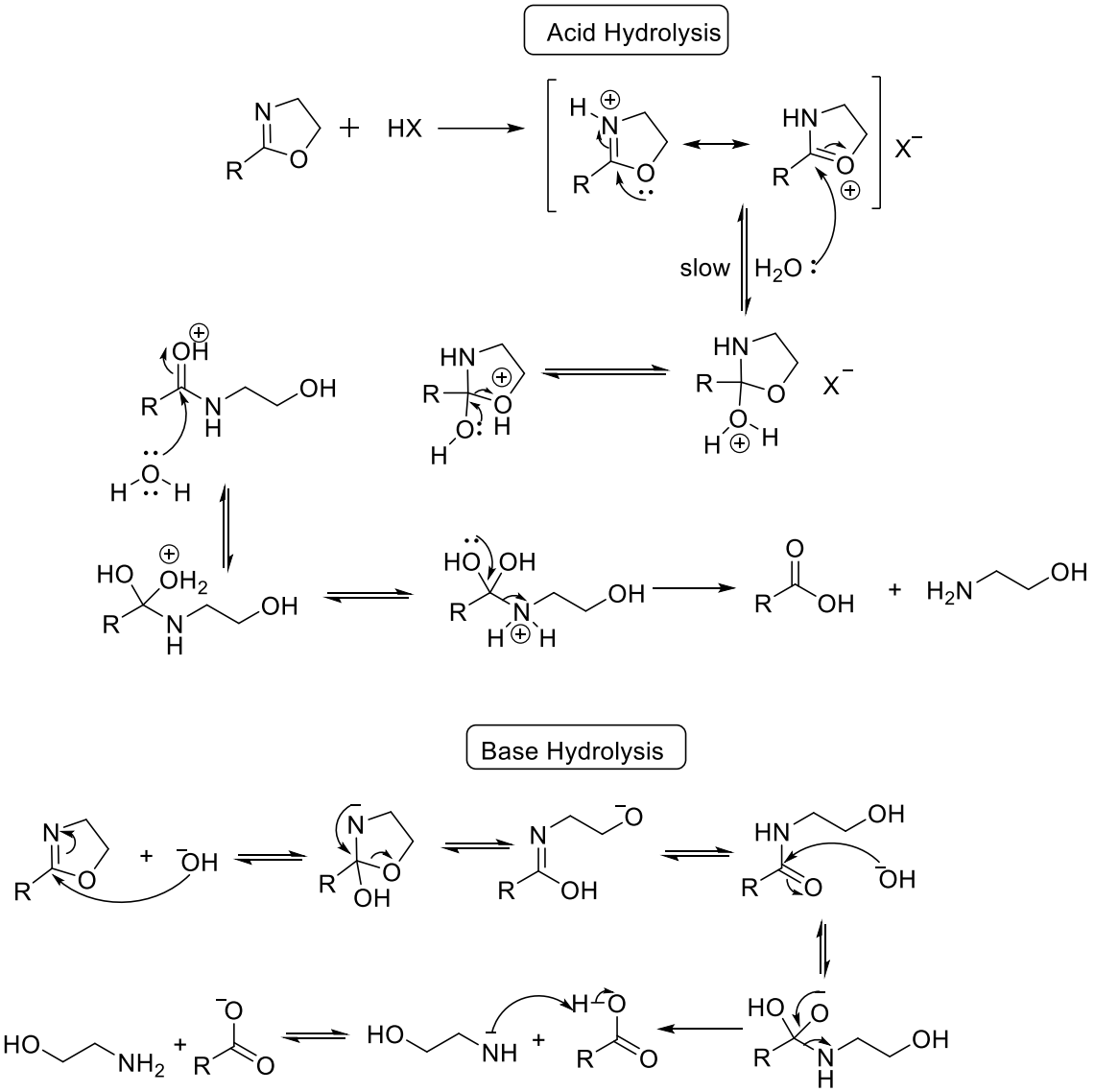

Scheme 2.17: Hydrolysis of Oxazolines

Hydrolysis becomes important inorder to convert pre-ligands to chiral ligands or simpler from diastereomers to enantiomers

Chiral oxazolines can be hydrolyzed to enantio-enriched acids under strong acidic conditions, which will be discussed in the upcoming chapters.

2.8 Conclusion

This chapter has highlighted some of the usefulness of 2-oxazolines like bis(oxazoline) (box), pyridine-2,6-bis(oxazoline) (pybox), and many more with 2-oxazoline core that have been used as chiral ligands with various metals. Due to their ease of synthesis, adaptable structure, and suitability for various metal-catalyzed reactions, chiral compounds incorporating an oxazoline ring have emerged as highly successful, versatile, and widely employed ligands in asymmetric catalysis.

The extensive applicability of this ligand class in catalytic asymmetric synthesis is evidenced by its ability to achieve exceptional enantioselectivity in a wide range of metal-catalyzed transformations. These transformations span various reactions, including oxidations, reductions, cycloadditions, and carbon-carbon bond-forming reactions.

The next chapter will focus on the coupling of the chiral oxazolines with [2.2]paracyclophane that will be resolved to give enantiopure products.

2.6 References

1. J. A. Frump, Oxazolines. Their preparation, reactions, and applications, *Chem. Rev.*, **1971**, *71*, 483-505.
2. K. C. Nicolaou, D. E. Lizos, D. W. Kim, D. Schlawe, R. G. D. Noronha, D. A. Longbottom, M. Rodriquez, M. Bucci and A. G. Cirino, Total Synthesis and Biological Evaluation of Halipeptins A and D and Analogues, *J. Am. Chem. Soc.*, **2006**, *128*, 4460-4470.
3. a. E. J. Alexy, H. Zhang and B. M. Stoltz, *J. Am. Chem. Soc.*, **2018**, *140*, 10109-10112. b. D. C. Duquette, A. Q. Cusumano, L. Lefoulon, J. T. Moore and B. M. Stoltz, Probing Trends in Enantioinduction via Substrate Design: Palladium-Catalyzed Decarboxylative Allylic Alkylation of α-Enaminones, *Org. Lett.*, **2020**, *22*, 4966-4969.
4. W. Shao, C. Besnard, L. Guenee and C. Mazet, Ni-Catalyzed Regiodivergent and Stereoselective Hydroalkylation of Acyclic Branched Dienes with Unstabilized C(sp^3) Nucleophiles, *J. Am. Chem. Soc.*, **2020**, *142*, 16486-16492.
5. M. P. Carroll and P. J. Guiry, *P,N* ligands in asymmetric catalysis, *Chem. Soc. Rev.*, **2014**, *43*, 819-833.
6. V. B. RocheBalaji, P. Rokade, J. Guiry, Further Developments and Applications of Oxazoline-Containing Ligands in Asymmetric Catalysis, *Chem. Rev.* **2021**, *121*, 6373−6521
7. S. Takahashi, H. Togo, An Efficient Oxidative Conversion of Aldehydes into 2-Substituted 2-Oxazolines Using 1, 3-Diiodo-5, 5-dimethylhydantoin, *Synthesis*, **2009**, 2329-2332.
8. P. Garg, S. Chaudhary, M. D. Milton, Synthesis of 2-aryl/heteroaryloxazolines from nitriles under metal-and catalyst-free conditions and evaluation of their antioxidant activities, *J. Org. Chem.*, **2014**, *79*, 8668-8677.
9. H. Deng, J. Wang, W. He, Y. Ye, R. Bai, X. Zhang, Xiang-Yang Ye, T. Xie, and Zi. Hui, Microwave-assisted rapid synthesis of chiral oxazolines, *Org. Biomol. Chem.*, **2023**, *21*, 2312-2319
10. A. H. Abazid, T.-N. Hollwedel, B. J. Nachtsheim, Stereoselective Oxidative Cyclization of *N*-Allyl Benzamides to Oxazolines *Org. Lett.*, 2021, *23*, 5076-5080.
11. M. T. Leffler, and R. Adams, Aminophenyl-2-oxazolines as Local Anesthetics, *J. Am. Chem. Soc.*, **1937**, *59*, 2252-2258.

12. Q. Zhou, Privileged Chiral Ligands and Catalysts, John Wiley & Sons Inc., New York, **2011**.
13. a. M. P. Carroll, P. J. Guiry, P, N ligands in asymmetric catalysis, *Chem. Soc. Rev.*, **2014**, *43*, 819-833. b. NeoPHOX- an easily accessible *P,N*-ligand for iridium-catalyzed asymmetric hydrogenation: preparation, scope and application in the synthesis of demethyl methoxycalamenene Marcus G. Schrems and Andreas Pfaltz *Chem. Commun.*, **2009**, 6210-6212.
14. A. Ficks, C. Sibbald, M. John, S. Dechert, and F. Meyer, Dinuclear Allylpalladium Complexes of C_2-Symmetric Pyrazolate-Bridged Bis(oxazoline) Ligands (pyrbox's): Structures, Dynamic Behavior, and Application in Asymmetric Allylic Alkylation *Organometallics*, **2010**, *29*, 1117-1126.
15. R. A. Gossage, Pincer oxazolines: emerging tools in coordination chemistry and catalysis – where to next?, *Dalton Trans.*, **2011**, *40*, 8755-8759.
16. Y. Ma, J. Li, J. Ye, D. Liu and W. Zhang, Synthesis of chiral chromanols *via* a RuPHOX-Ru catalyzed asymmetric hydrogenation of chromones, *Chem. Commun*., **2018**, *54*, 13571-13574.
17. K. S. Yoo, C. P. Park, C. H. Yoon, S. Sakaguchi, S., and K. W. Jung, Asymmetric Intermolecular Heck-Type Reaction of Acyclic Alkenes via Oxidative Palladium(II) Catalysis, *Org. Lett.*, **2007**, *9*, 3933-3935.
18. J.T. Binder, C. J. Cordier, and G. C. Fu, Catalytic Enantioselective Cross-Couplings of Secondary Alkyl Electrophiles with Secondary Alkylmetal Nucleophiles: Negishi Reactions of Racemic Benzylic Bromides with Achiral Alkylzinc Reagents *J. Am. Chem. Soc.*, **2012**, *134*, 17003-17006.
19. B. Su, T. G. Zhou, X. W. Li, X. R. Shao, P. L. Xu, W. L. Wu, J. F. Hartwig, Z. J. Shi, A Chiral Nitrogen Ligand for Enantioselective, Iridium-Catalyzed Silylation of Aromatic C−H Bonds *Angew. Chem. Int. Ed.*, **2017**, *56*, 1092-1096.
20. H. Brunner, and U. Obermann, Enantioselective Hydrosilylation of Ketones with (Rh(COD)Cl)2/Pyridinyloxazoline Catalysts., *Chem. Ber.*, **1989**, *122*, 499-507.
21. H. Brunner, and P. Brandl, Asymmetric catalysis: Enantioselective hydrosilylation of acetophenone with a rhodium/picolineoxazoline catalyst 1:1, *J. Organomet. Chem.*, **1990**, 81-83.
22. H. Brunner, and P. Brandl, Enantioselective catalysis 74.: Ligand excess and intermediates in the rhodium-catalyzed enantioselective hydrosilylation of acetophenone with pyridineoxazoline ligands, *Tetrahedron: Asymmetry*, **1991**, *2*, 919-930.

23. C. Weiqiang, L. Mei, L. Hui-Jing, and W. Yan-Chao, Switchable and efficient conversion of 2-amidoaryl oxazolines to quinazolin-4(3H)-ones and N-(2-chloroethyl)benzamides, *Org. Chem. Front.*, **2021**, 8, 584-590.
24. F. Riobé, N. Avarvari, C2-symmetric chiral tetrathiafulvalene-bis(oxazolines) (TTF-BOX): new precursors for organic materials and electroactive metal complexes, *Chem. Commun.*, **2009**, 3753-3755.
25. M. A. Mees and R. Hoogenboom, Full and partial hydrolysis of poly(2-oxazoline)s and the subsequent post-polymerization modification of the resulting polyethylenimine (co)polymers, *Polym. Chem.*, **2018**, *9*, 4968-4978

Chapter 3:

Scope of [2.2]Paracyclophane-Oxazoline Coupling

In the first chapter, our focus was on examining the unique properties of the [2.2]paracyclophane molecule. Specifically, we explored [2.2]paracyclophane, which is characterized by its fascinating "bent and battered rings". This compound has garnered notable attention as an organic analogue to ferrocene with each molecule capable of producing planar chiral ligands and catalysts.

The second chapter, we delved into the broad scope of oxazolines and their versatility in various stereoselective transformations. Oxazolines are one of the so-called privileged ligands that enable a range of asymmetric catalysis in various reactions. They can coordinate with transition metal catalysts and control the stereochemistry of the reaction, leading to the formation of an enantiomerically enriched product.[1]

3.1 Coupling between [2.2]paracyclophane halides and chiral oxazolines

Similar to the success of BOX ligands in asymmetric catalysis,[2-3] [2.2]paracyclophane-bisoxazolines could be explored as chiral ligands in various stereoselective transformations.[4,5,6] In the literature, [2.2]paracyclophane-oxazoline derivatives are synthesised from the corresponding carboxylic acid derivatives by a traditional route involving three steps (**Scheme 3.1**).[7-17] In the first step, carboxylic acid **3.1** is converted into an acyl chloride which subsequently reacts with an amino alcohol to form amide derivative **3.3**. Finally, Appel cyclization[18] of the amide derivative gives oxazoline derivative **3.4**.

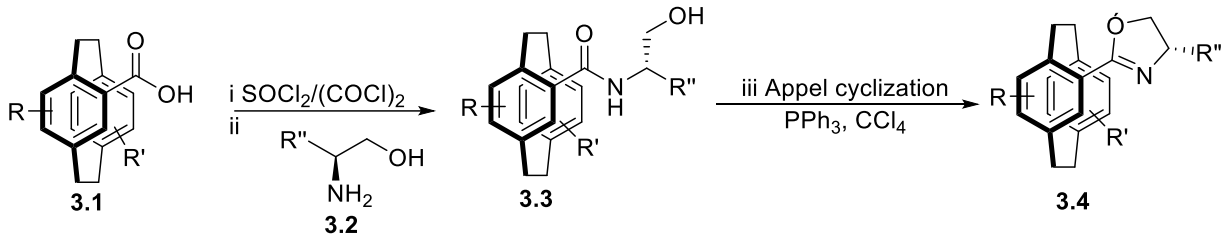

Scheme 3.1: Traditional route to synthesis [2.2]paracyclophane-oxazoline derivatives

It is worth mentioning that the synthesis of the [2.2]paracyclophane-carboxylic acid derivatives is not always straightforward. The synthesis of the monosubstituted carboxylic acid requires a minimum of two steps from [2.2]paracyclophane (**Scheme 3.2**).

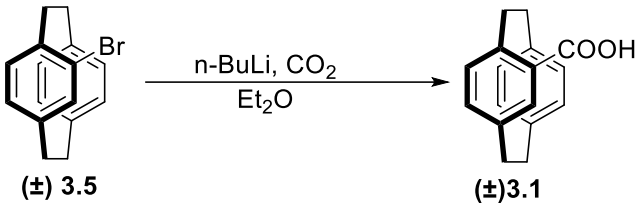

Scheme 3.2: Synthesis of racemic 4-carboxy[2.2]paracyclophane

The resolution of the racemic 4-carboxy[2.2]paracyclophane is discussed in the chapter 1.

Therefore, accessing enantioselective carboxylic acid derivatives takes more steps. Due to these challenges associated with the synthesis of [2.2]paracyclophane-oxazoline derivatives, there is always a need for a practical methodology that can access these valuable compounds.

Recently, Lu *et* al[19,20] and Ackermann *et al*[21] independently reported the direct C-H (hetero)arylation of oxazolines **3.9** at the 2-position (**Scheme 3.3**). The former group employed bidentate diphosphine ligands (dppe or dppp) while the latter group used a bulky SPO-based catalyst **3.8**. These protocols are good alternatives to the traditional methods for the synthesis of chiral oxazoline ligands.[1,2]

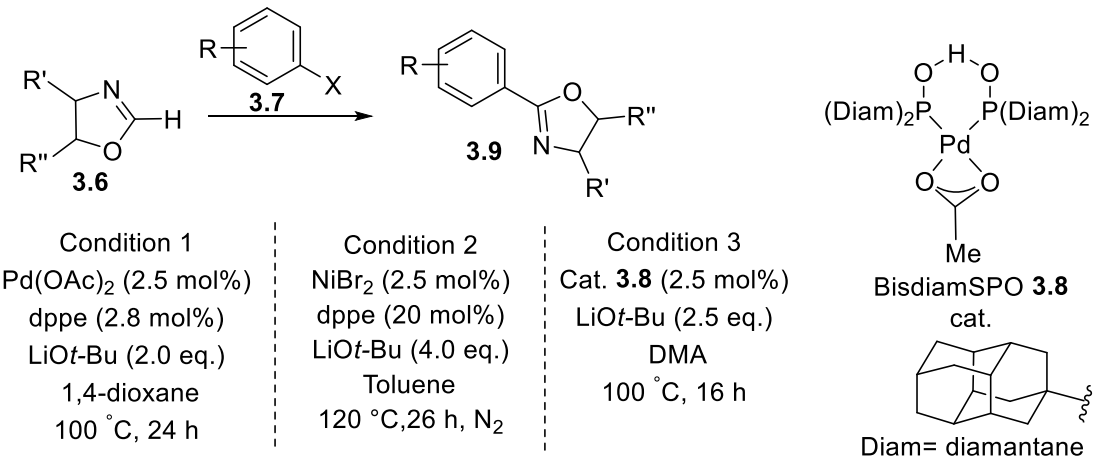

Scheme 3.3: Reported conditions for the C-H (hetero)arylation of oxazolines.

However, we were interested in the opposite approach from what is shown in Scheme 3.3. In order to eliminate the multi-step synthesis, as well as dissuade the use of hazardous chemicals, we were interested in the concise and economical synthesis of planar chiral oxazolines followed by their subsequent hydrolysis.

Adding the oxazoline first, using this moiety to resolve the planar chirality of [2.2]paracyclophane, and act as a precursor to the carboxylic acid or for the further functionalization of the backbone (**Scheme 3.4**). Such a strategy would permit a wider range of substituents, specifically those that were not compatible with halogen-metal exchange, to

be present in the molecule. Simpler, more rapid access to [2.2]paracyclophane derivatives would permit a wider variety of chemists to employ this fascinating molecule in their research.

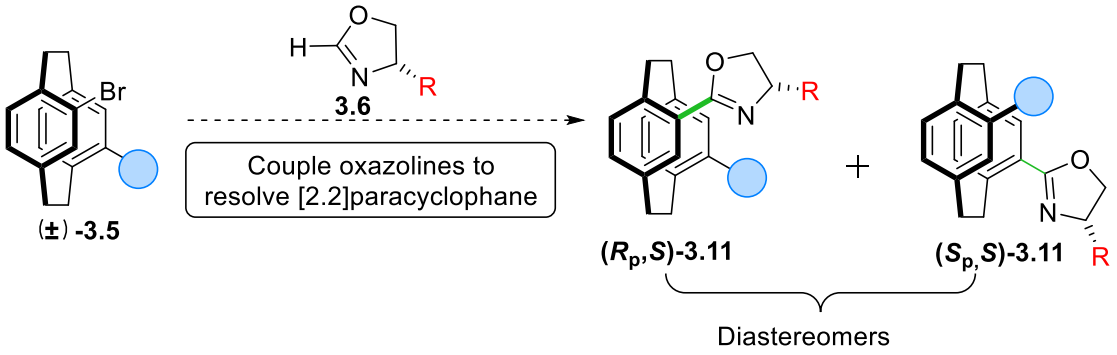

Scheme 3.4: Our strategy for the desired coupling

4.2 Scope of bromo[2.2]paracyclophane for oxazoline coupling

We conducted a screening of various secondary phosphine pre-ligands [(HA)SPO], including those substituted with heteroatoms. Among them, di-*tert*-butylphosphine oxide (*t*-Bu_2SPO) emerged as a catalyst that demonstrated complete conversion of simple [2.2]paracyclophane derivatives. After screening multiple conditions and numerous coupling partners (different oxazolines as well as different regioisomers of [2.2]paracyclophane), we found that a combination of $Pd(OAc)_2$ and di-*tert*-butyl SPO **3.10** coupled (4*S*)-substituted-oxazoline **3.6** to (±)-4-bromo[2.2]paracyclophane **3.5** (**Scheme 3.5**).

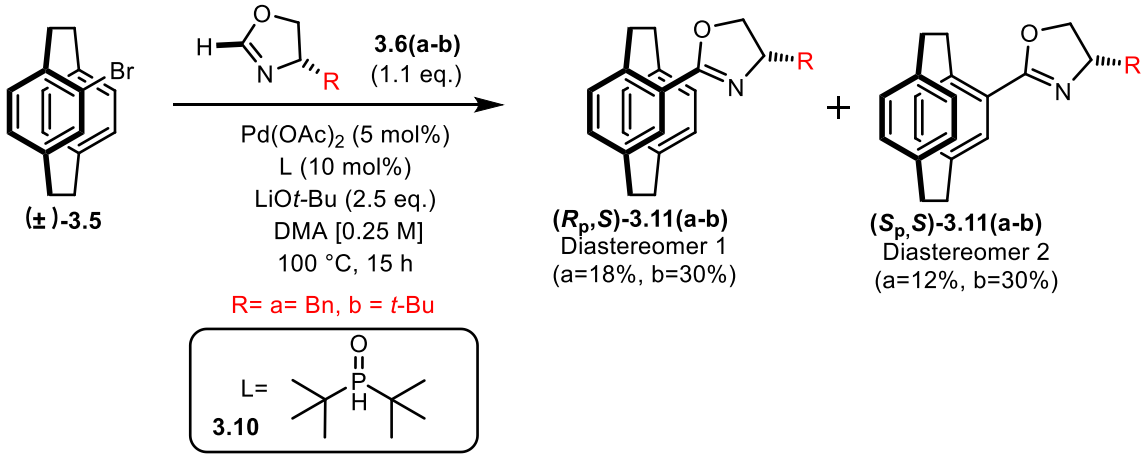

Scheme 3.5: Optimized conditions for the 4-bromo[2.2]paracyclophane for oxazoline coupling

The initial aim of the project was to determine the scope of the coupling with a range of [2.2]paracyclophane substrates and the two different oxazolines. We were successful in forming different desired coupled products. The following section will discuss the various coupled [2.2]paracyclophane-oxazoline products.

4.2.1 4-Bromo[2.2]paracyclophane with benzyl oxazoline coupling:

The coupling of 4-bromo[2.2]paracyclophane **3.5** with (4*S*)-substituted-oxazoline **3.6** under the optimized conditions using $Pd(OAc)_2$ and di-*tert*-butyl SPO **3.10** gave a mixture of diastereomers in 82% yield. Very careful chromatography allowed some of the pure **(R_p,*S*)-3.11a** (18%) and **(S_p,*S*)-3.11a** (12%) to be isolated, but the majority remained a mixture**(±)3.11a** (52%) (**Scheme 3.6**).

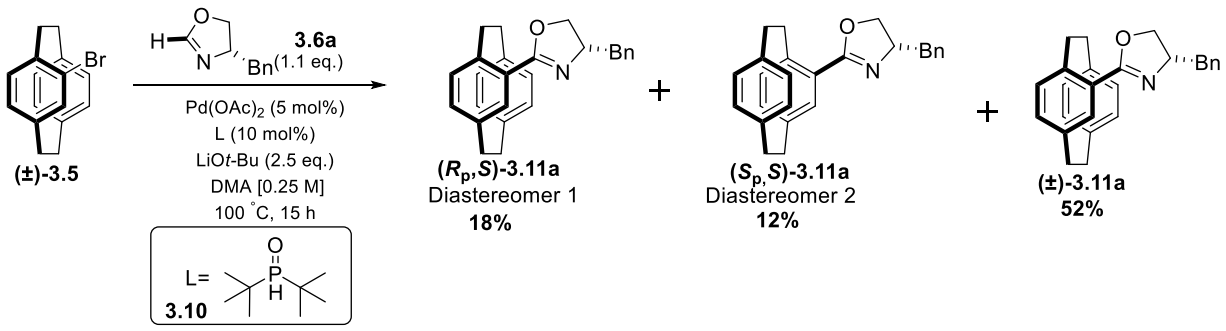

Scheme 3.6: Coupling of 4-Bromo[2.2]paracyclophane with benzyl oxazoline

A plausible mechanism for the coupling is based on the Pd^0/Pd^{II} pathway and is shown in **Figure 3.1**. The catalytic cycle is initiated by the oxidative addition of the ligated Pd^0 to the [2.2]paracyclophane-halide **I**. The oxazoline **3.6a** is deprotonated by the LiO*t*Bu to generate the lithium oxazoline intermediate, which subsequently undergoes transmetallation with the organopalladium to give the palladium-oxazoline **II**. Finally, reductive elimination produces coupled product **3.11a**, and simultaneously reducing the Pd^{II} back to Pd^0.

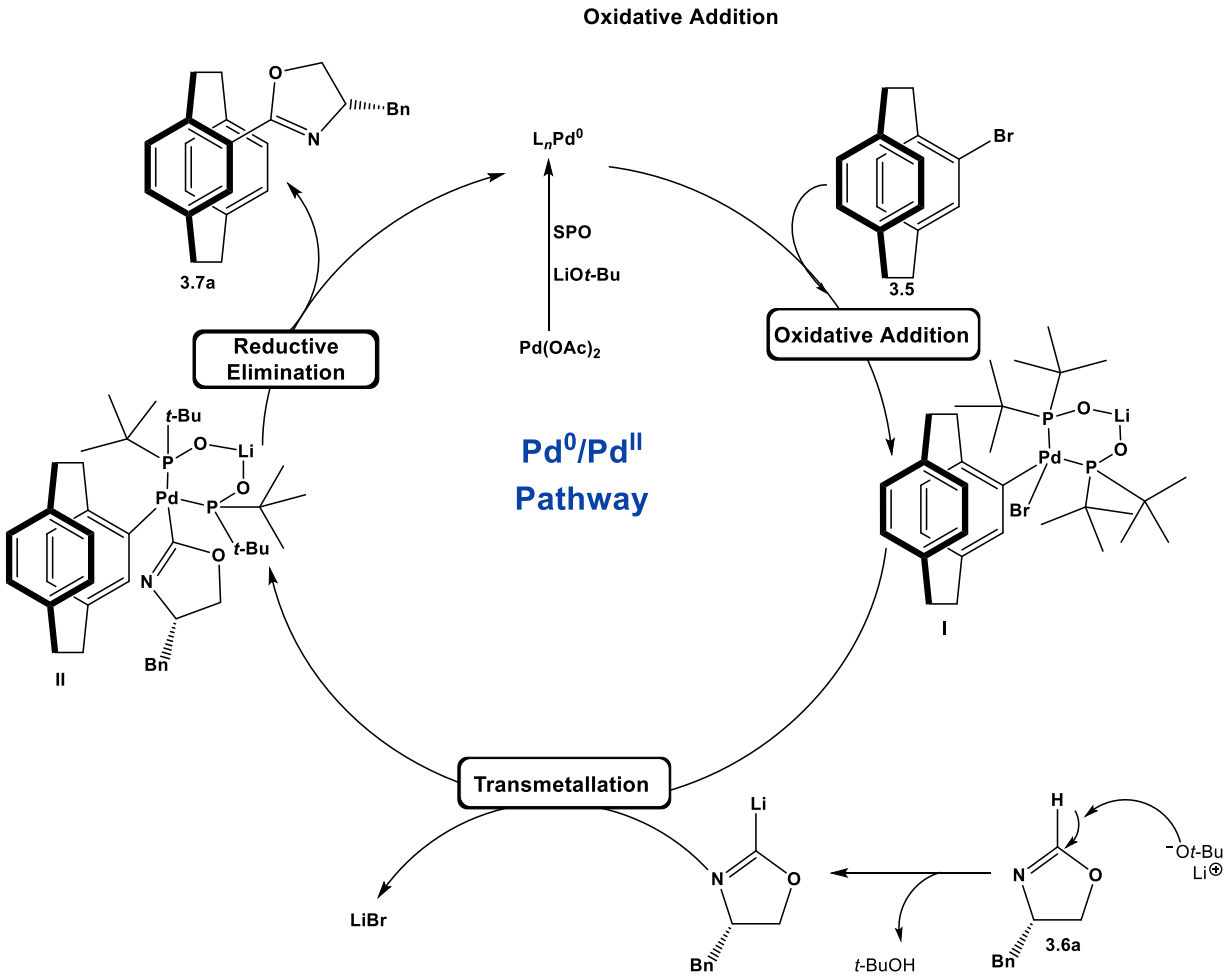

Figure 3.1: Proposed mechanism for [2.2]paracyclophane halide and oxazoline coupling.

As the separation was challenging, this was not an ideal method for resolution, especially if we wanted to scale up and so it was decided to investigate the coupling of bulkier oxazoline in the hope that this would increase the difference between diastereomers, making separation easier.

4.2.2. 4-Bromo[2.2]paracyclophane with *tert*-butyl oxazoline coupling:

Next we looked at the coupling of *tert*-butyl oxazoline **3.6b**. This bulkier group places a greater steric demand closer to the oxazoline as compared to the benzyl oxazoline, and might cause a bigger difference in the R_f of the diastereomers. The coupling gave unsatisfactory results with the *t*-Bu$_2$SPO **3.10** and we investigated the use of different SPOs. The diadamantyl SPO **3.12** gave a much better result. It is unclear why there was such a marked difference. The literature suggests that the adamantyl moiety is slightly larger than a *t*-Bu groups, but was not sure why this makes a difference. The literature also states that

adamantly groups exhibit a huge noncovalent contact area that maximizes attractive London dispersion interactions that might counteract the repulsive steric effects.[22]

So, changing just the ligand from *t*-Bu$_2$SPO **3.10** to Ad$_2$SPO **3.12**, and keeping all other conditions same as previous mono-coupling, the desired diastereomers were formed and readily separated by column chromatography to give 30% yield of each diastereomer (**Scheme 3.7**).

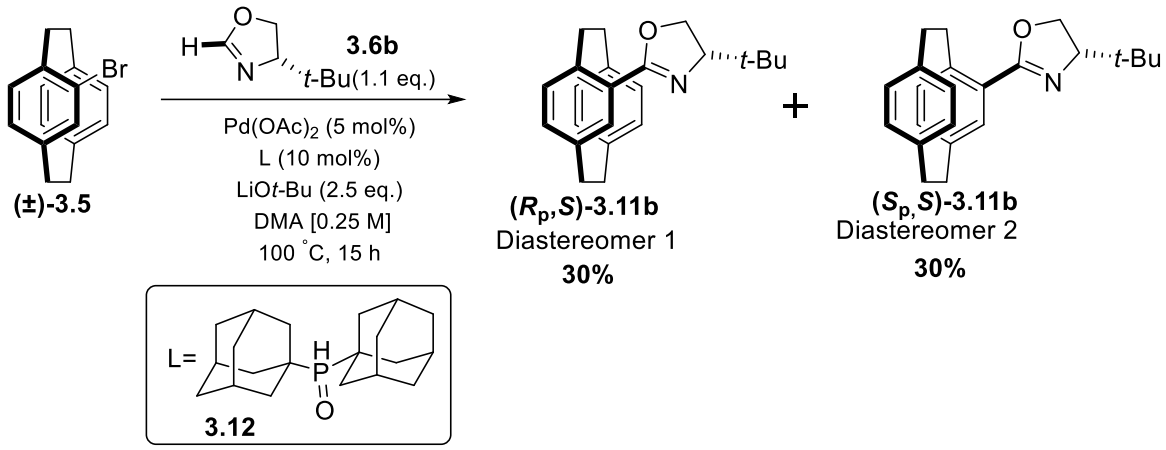

Scheme 3.7: Coupling of 4-Bromo[2.2]paracyclophane with *tert*-butyl oxazoline

So, the *tert*-butyl oxazoline proved a better coupling partner with Ad$_2$SPO ligand for mono-coupling.

The absolute configuration was assigned on the basis of the reported literature that showed the **(*R*$_p$,*S*)-3.11b** is always formed above the **(*S*$_p$,*S*)-3.11b**.[23] The first product that came off from the column out of the two isomers matched the *R*$_p$,*S* configuration of the product. This comparison was confirmed by the chemical shifts of the peaks in the proton and carbon NMR.

Figure 3.2 and **3.3** below shows the slight changes in the chemical shifts of the ^{1}H and ^{13}C NMR spectra of the two diastereomers **(*R*$_p$,*S*)-3.11b** and **(*S*$_p$,*S*)-3.11b** respectively. The blue spectrum is of **(*R*$_p$,*S*)-3.11b,** and the red one belongs to **(*S*$_p$,*S*)-3.11b**. The values correlate with the literature, and thus, the configuration is assigned.

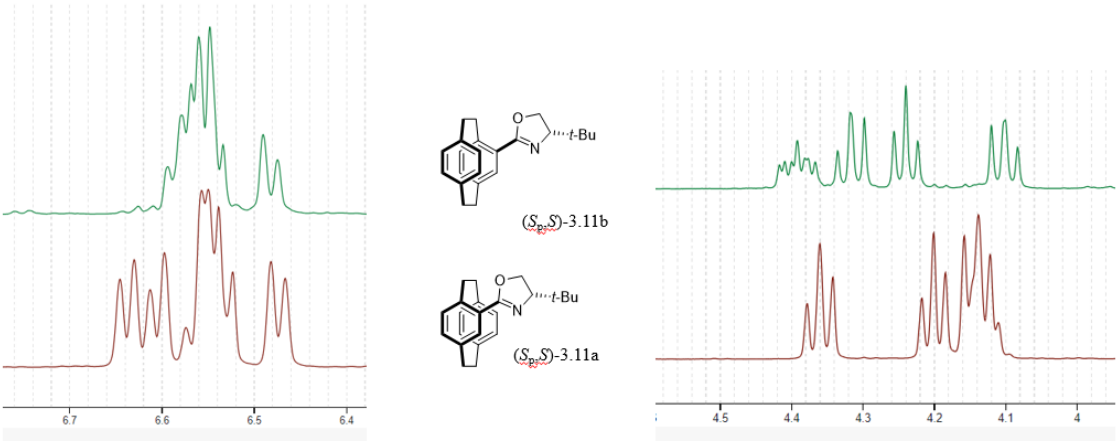

Figure 3.2: Comparison of ^{1}H NMR spectrum of two diastereomers to show the difference

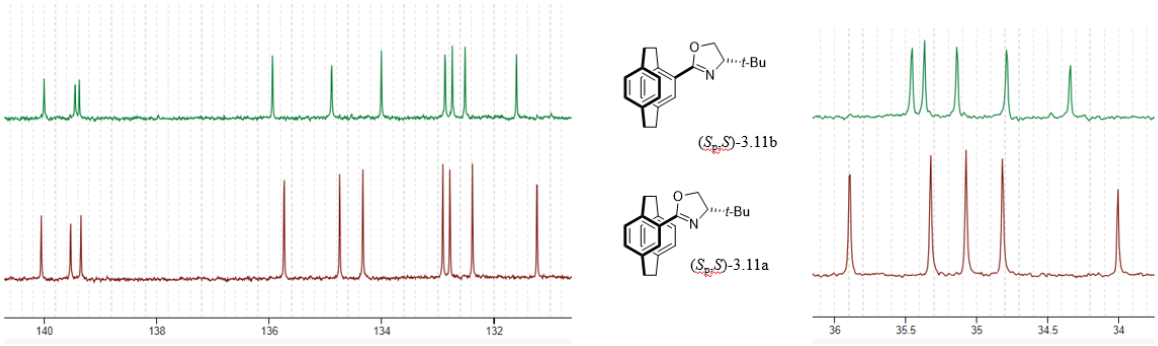

Figure 3.3: Comparison of ^{13}C NMR spectrum of two diastereomers to show the difference

Such slight difference was observed between our all pairs of diastereomers. We assumed that the ***R*p,*S*** isomer is always the first to come from the column for all the couplings that we performed.

4.2.3 4,12-Dibromo[2.2]paracyclophane derivatives for oxazoline coupling:

4.2.3a Coupling with Benzyl Oxazoline

Interestingly, the bis-coupling of pseudo-*ortho* dibromo[2.2]paracyclophane **(±)-3.13** and the two oxazolines showed the opposite result, with the benzyl oxazoline **3.6a** performing better. Doubling the stoichiometry of the reaction compared to the mono-coupling led to the desired coupling, i.e., the formation of 4,12-bis(4′-benzyloxazolin-2′-yl)[2.2]paracyclophane **3.14a** as the desired separable diastereomers **(*R*p,*S*)-3.14a** and **(*S*p,*S*)-3.14a**. The diastereomers were easily isolated through chromatographic techniques (30/25%).[8,13,24]

Along with the desired isomers of the di-coupled products, we also isolated two other pairs of diastereomers from the reaction mixture. They were the mono-bromo-mono-oxazoline diastereomers **(±)-3.15a** and the mono-oxazoline **(±)-3.11a** formed by the proto-

debromination. Additionally, we observed traces of pseudo-*para*-di-oxazoline. This is not shown in the scheme as it is attributed to the reaction of an impurity from the synthesis of pseudo-*ortho*-dibromo [2.2]paracyclophane **(±)-3.13** rather than isomerisation under the reaction conditions (**Scheme 3.8**).

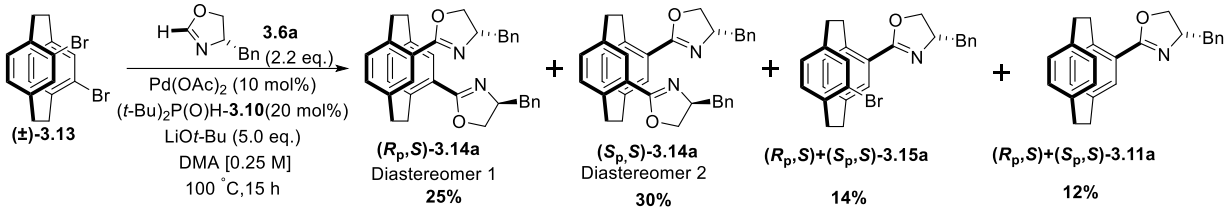

Scheme 3.8: Bis-oxazoline coupling with pseudo *ortho* dibromo paracyclophane

If we discuss about the R_f position of the isomers so formed on the TLC, the first pair of the isomers was proto-debromo coupled product, i.e., a mono-coupled product. As already discussed in the section above, the diastereomers were very close to each other which led to their separation difficult. Just below them, was formed the first isomer of bis-coupling, i.e., 4,12-bis(4′-benzyloxazolin-2′-yl)[2.2]paracyclophane **(*R*p,*S*)-3.14a** followed by (*S*p,*S*)-4,12-bis(4′-benzyloxazolin-2′-yl)[2.2]paracyclophane **(*S*p,*S*)-3.14a**. The difference between the R_f values of these two diastereomers was large and was easily separated by column chromatography.

Below them, was the mixture of one brome-one oxazoline diastereomers **(±)-3.15a** that were formed during the bis-coupling. The mixture was not separated during the column chromatography due to minimal difference in the R_f values of the two isomers. We then tried using recrystallization of the mixture. After multiple attempts using different solvents and their combinations, we were successful in separating the two isomers using 5% EtOAc in n-hexane (**Scheme 3.9**).

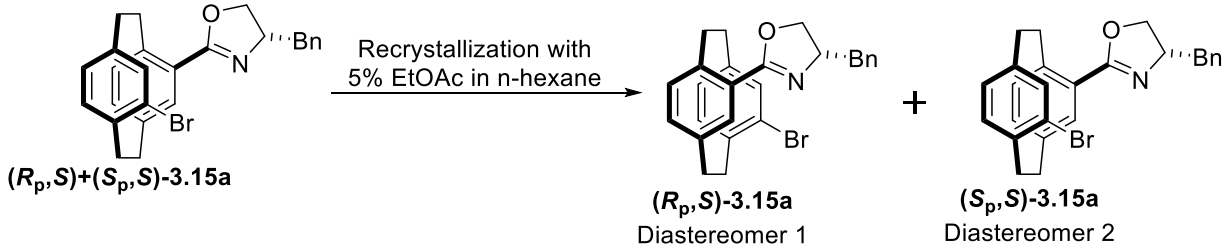

Scheme 3.9: Purification of mono-bromo-mono-oxazoline diastereomers

Isolating both the product of proto-debromination and partially reacted mono-bromo-mono-oxazoline is unusual but possibly reveals potential problems with this challenging di-coupling. Isolation of the mono-bromo-mono-oxazoline suggests insertion into the C-Br is hard. Arguably, insertion requires a transition state that has a Pd-C-Br three-membered ring (This would force the large bromo atom down towards the second ring of [2.2]paracyclophane and the oxazoline.

On the other hand, the formation of mono-oxazoline **(±)-3.15a** reveals C-Br insertion is possible but that either transmetallation or reductive elimination is problematic. Possibly, proto-debromination occurs prior to the first oxazoline coupling and **(±)-3.15a** is not formed from mono-bromo-mono-oxazoline. We never observed 4-bromo[2.2]paracyclophane **3.5** as a side product so this might rule this pathway out. Regardless, the isolation of these side products show that the reaction is not easy.

Alternatively, changing the stoichiometry and only using one equivalent of 2H-oxazoline **3.6a** did not have the expected result and we still obtained a mixture of bis-oxazoline and mono-bromo-mono-oxazoline products (**Scheme 3.10**).

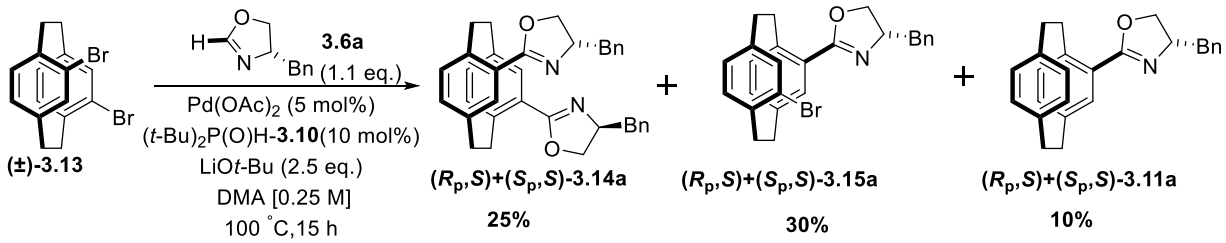

Scheme 3.10: Mono-bromo-mono-oxazoline coupling with pseudo *ortho* dibromo paracyclophane

4.2.3b Coupling with *Tert*-butyl Oxazoline

Anticipating that the bis(*t*-butyl)oxazoline **3.6b** would be easier to resolve, we attempted the double coupling under the same conditions that worked for the benzyl derivatives. Using the *t*-Bu_2SPO **3.10** as a ligand resulted in the failure and only starting material returned back. This is strange as we would at least expect the palladium to insert. We then used the di-1-adamantylphosphine oxide (Ad_2SPO) **3.12**, as this had worked with the mono oxazoline derivative **3.7b**.

Use of the new ligand successfully gave the coupling product. Unfortunately, separation proved very challenging. Only one diastereoisomer of the tert-butyl derivative **(S_p,*S*)-3.14b**

could be isolated in low yield (10%). The other diastereoisomer **(R_p,*S*)-3.14b** co-ran with the two diastereomers of the product of protodebromination **(±)-3.11b** (**Scheme 3.11**). The pattern on the TLC was quite similar as obtained in the case of benzyl oxazoline. The protodebromo isomers were non-polar and following them was the bis-coupled diastereomers. But the only difference was the closeness in the R_f values, that made the separation challenging.

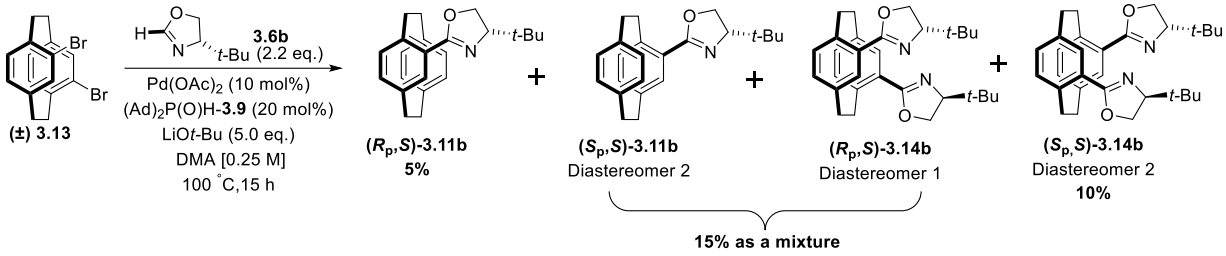

Scheme 3.11: Bis-oxazoline coupling with pseudo *ortho* dibromo paracyclophane

Despite our dissatisfaction with the outcomes with bis coupling using *tert*-butyl oxazoline, the mono-bromo oxazoline isomers were not formed. This tells us that the Ad_2SPO ligand **3.12** probably encourages palladium insertion into C-Br bond, but something is either preventing coordination of the oxazoline or reductive elimination. Moreover, we currently possess two distinct isomers resulting from mono-coupling, as well as an additional two from bis-coupling that can be taken up further for the formation of more useful products in the future.

4.2.4 Tetrabromo[2.2]paracyclophane derivatives for oxazoline coupling

Next, we extended the scope of the coupling reaction to tetra coupling with oxazolines. We thought having oxazolines at four positions will allow to increase the substrate scope and may be useful to obtain various enantiopure product after hydrolysis or other derivatizations.

We synthesised the 4,7,12,15-tetra(4′-benzyloxazolin-2′-yl)[2.2]paracyclophane **(±)-3.19** from tetrabromo[2.2]paracyclophane **(±)-3.17**. The synthesis of tetrabromo[2.2]paracyclophane was done using excess bromine in the presence of an iron with paracyclophane-**3.16** (**Scheme 3.12**). The reaction gave two products. Apart from the desired product, 4,7,12,15-tetrabromo[2.2]paracyclophane **(±)-3.17**, another product, i.e., 4,5,12,13-tetrabromo[2.2]paracyclophane **(±)-3.18** was also formed. After careful chromatographic separation due to closeness in R_f of the two products, the desired 4,7,12,15-tetrabromo[2.2]paracyclophane **(±)-3.17** was isolated with 83% yield.[27]

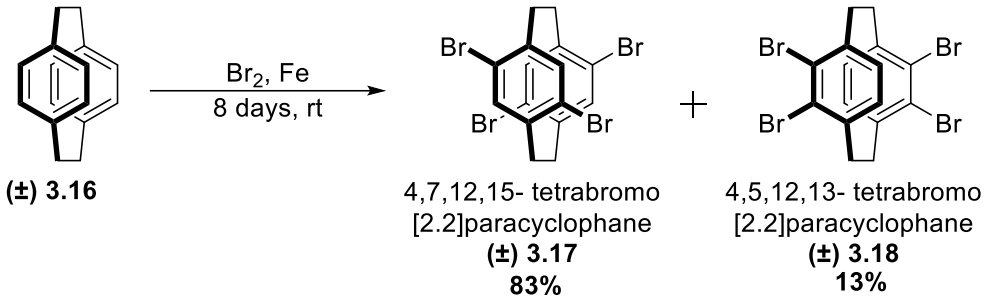

Scheme 3.12: Synthesis of tetra-bromo[2.2]paracyclophane

Initial reaction with the *t*-Bu$_2$SPO ligand **3.10** gave a complex mixture of regio- and stereoisomers. The resolved tetra(oxazoline) ligand **(*R*$_p$,*S*)-3.19** and **(*S*$_p$,*S*)-3.19** was isolated in 10%. In addition, the para-bis(oxazoline)-dibromo[2.2] paracyclophane **(*R*$_p$,*S*)-3.20** and **(*S*$_p$,*S*)-3.20** was isolated as separable diastereomers along with an unidentified regioisomer of the diastereomeric bis(oxazoline)-dibromo[2.2]paracyclophanes (not included in the yield). Finally, the two diastereomers of the protodebromo tris(oxazoline) were isolated as a mixture **(±)-3.21** (**Scheme 3.13**).

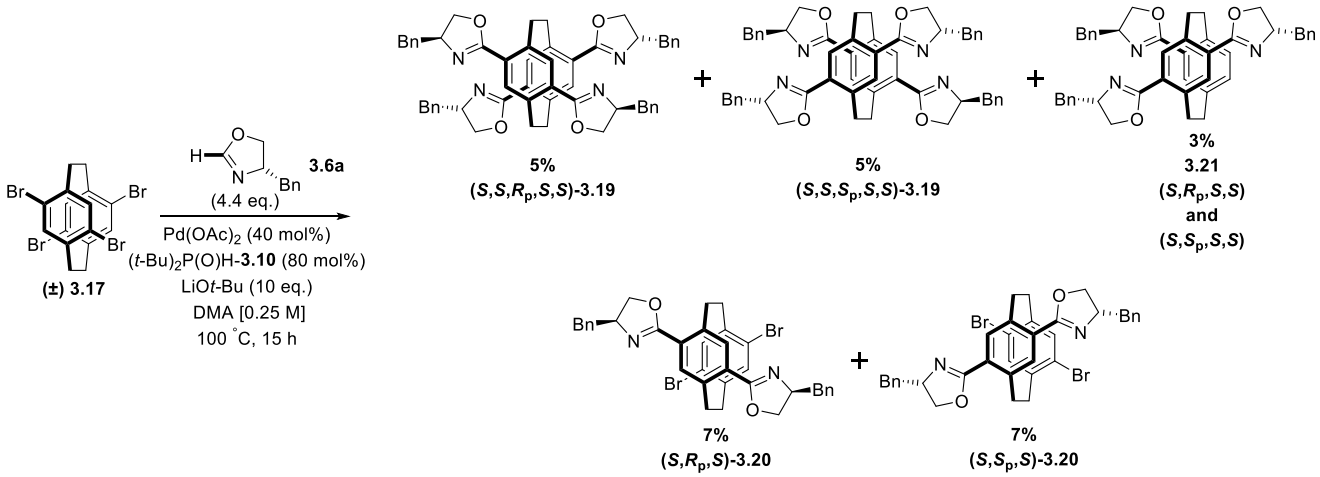

Scheme 3.13: Tetra-oxazoline coupling with tetra-bromo[2.2]paracyclophane

As the reaction mixture contained multiple spots due to the diastereomer formation of each compound. The initial challenge was to carefully isolate the different spots through gradient and slow purification.

Next challenge was to confirm and characterize the isolated spots. The confirmation of the desired 4,7,12,15-tetra(4′-benzyloxazolin-2′-yl)[2.2]paracyclophane-**3.19** was done by recording the mass spectrum and HRMS. The peak at 845.4052 corresponds with our desired

isomers. We had two spots that gave the same mass and labelled them as our desired **(R_p,*S*)-3.19** and **(S_p,*S*)-3.19**. Similarly, the other isolated spots were also characterized. The tris-compound was identified by the peak obtained at 685.0879 of one of the spots. It was labelled as **(±)-3.21** and that equals the protodebromo-three oxazolines attached to 4,7,12,15-tetrabromo[2.2]paracyclophane **3.17**. The two other spots showed the peaks at 684.0899, that corresponded to bis(oxazoline)-dibromo[2.2] paracyclophane **(R_p,*S*)-3.20** and **(S_p,*S*)-3.20**.

The confirmation was done through NMR spectra, where the integrations of the tetra-, tris- and bis- products were obtained in the multiples of 4, 3 and, 2 respectively while interpreting the NMR samples of the various products obtained through the reaction.

Now, the major challenge was to identify the correct regioselectivity of the bis-bromo-bis-oxazoline product. There were chances of the formation of the following product (**Figure 3.3**).

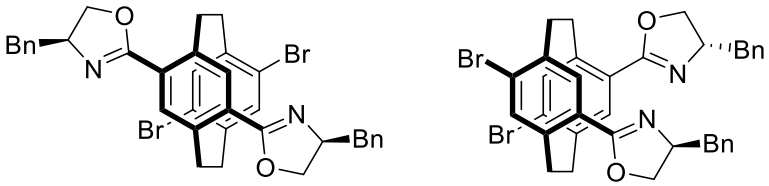

Figure 3.3: *para*-Dibromo-bis(oxazoline)[2.2]paracyclophane

To rule out the wrong isomers and identify the correct regioselectivity, we did 2D NMR study of the bis-bromo-bis-oxazoline samples, where COSY, NOESY, HMBC data were collected and analyzed.

The HMBC spectra revealed the correct structure of the compound and the correlation between the C-H is marked and shown in the **Figure 3.4** below.

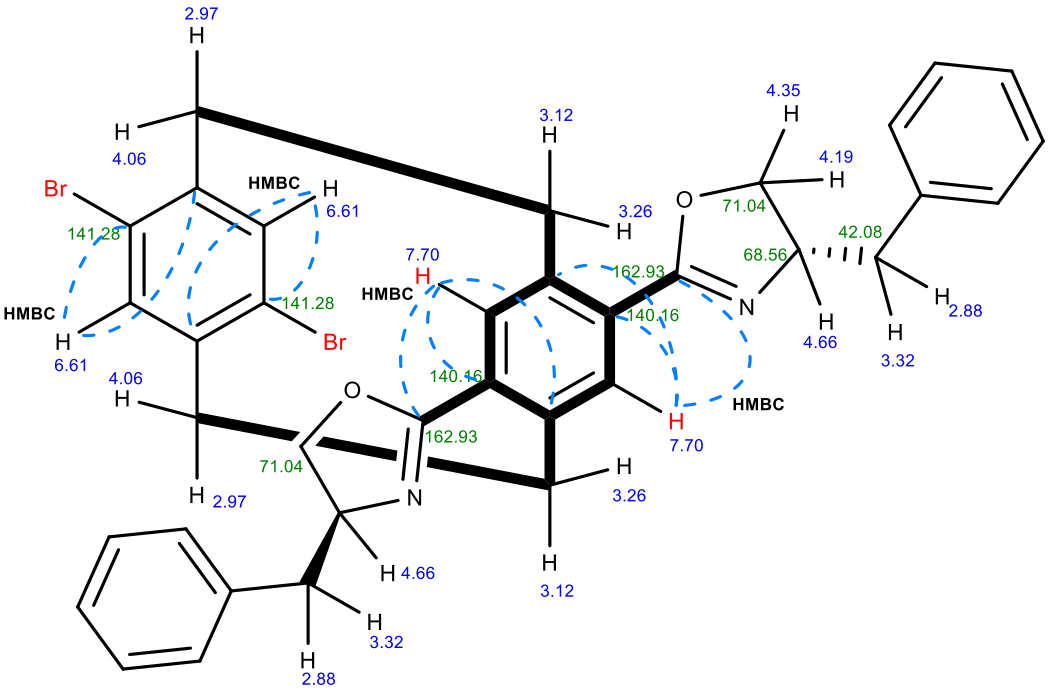

Figure 3.4: HMBC correlation of C and H to identify the correct regioselectivity of 3.19

To push the limits of this coupling, we altered the ligand to Ad_2SPO **3.12**, so as to see if ithe bulkier ligand makes any difference in the yield.

The Ad_2SPO **3.12,** did not much altered the yields of the desired isomers but simplified the mixture and gave just the desired tetra-coupled isomers, **(R_p,*S*)-3.19** and **(S_p,*S*)-3.19**.and tris(oxazoline) **(±)-3.21** (Scheme 3.14).

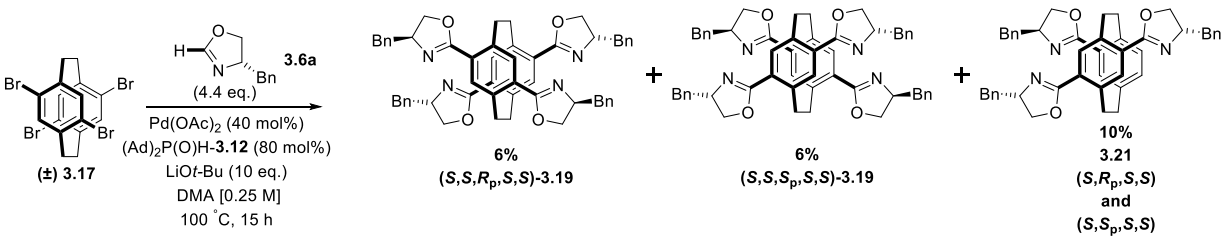

Scheme 3.14: Tetra-oxazoline coupling with tetra-bromo[2.2]paracyclophane

The yields that were obtained were not fascinating. Still, it has opened a new path to develop multi-oxazoline-[2.2]paracyclophane system.

4.3 Conclusion

Through our one-pot strategy, we offer a convenient approach to obtain [2.2]paracyclophane-oxazolines, which exhibit significant potential as planar chiral ligands in catalytic applications.

Some of the reactions yielded satisfactory results, but some did not work as per our plan. It is challenging as the methodology is still non-selective, yielding a range of products. That makes the separation difficult and makes our job tougher. A bit of optimization will definitely lead towards selectivity and will improve the yields of the desired diastereomers.

These oxazolines can be readily subjected to hydrolysis, resulting in the formation of a diverse range of planar chiral carboxylic acids. These acids, in turn, serve as valuable chiral building blocks. So, our next aim will focus on hydrolyzing these coupled oxazolines. The next chapter, i.e., chapter 4 will provide a comprehensive discussion of the process of hydrolysis and the subsequent formation of numerous valuable products.

4.4 References

1. G. Desimoni, G. Faita, P. Quadrelli, Pyridine-2,6-bis(oxazolines), Helpful Ligands for Asymmetric Catalysts, *Chem. Rev.* **2003**, *103*, 3119-3254.
2. C. Jönsson,; K. Hallman, H. Andersson, G. Stemme, M. Malkoch, E. Malmström, A. Hult, C. Moberg, Immobilized oxazoline-containing Ligands in asymmetric catalysis-a review, *Bioorg. Med. Chem. Lett.* **2002**, *12*, 1857-1861.
3. S. A. Babu, K. K. Krishnan, S. M. Ujwaldev, G. Anilkumar, Applications of pybox complexes in asymmetric catalysis, *Asian J. Org. Chem.*, **2018**, *7*, 1033-1053.
4. G. Desimoni, G. Faita, K. A., Jørgensen, C_2-Symmetric Chiral Bis(Oxazoline) Ligands in Asymmetric Catalysis, *Chem. Rev.*, **2006**, *106*, 3561-3651.
5. B. D. Ward, L. H. Gade, Rare earth metal oxazoline complexes in asymmetric catalysis, *Chem. Commun.*, **2012**, *48*, 10587-10599.
6. Y. Guoquiang, Z. Wanbin, Renaissance of pyridine-oxazolines as chiral ligands for asymmetric catalysis, *Chem. Soc. Rev.*, **2018**,1783-1810.
7. C. Braun, M. Nieger, W. R. Thiel, S. Bräse, [2.2]Paracyclophanes with N-Heterocycles as Ligands for Mono-and Dinuclear Ruthenium(II) Complexes, *Chem. Eur. J.*, **2017**, *23*, 15474-15483.
8. S. Kitagaki, K. Sugisaka, C. Mukai, Synthesis of planar chiral [2.2]paracyclophane-based bisoxazoline ligands bearing no central chirality and application to Cu-catalyzed asymmetric O–H insertion reaction, *Org. Biomol. Chem.*, **2015**, *13*, 4833-4836.
9. D. K. Whelligan, C. Bolm, Synthesis of Pseudo-*geminal*-, Pseudo-*ortho*-, and *ortho*-Phosphinyl-oxazolinyl-[2.2]paracyclophanes for Use as Ligands in Asymmetric Catalysis, *J. Org. Chem.*, **2006**, *71*, 4609-4618.
10. X.L. Hou, X.W. Wu, L.X. Dai, B.X. Cao, J. Sun, Novel *N,S*- and *N,Se*-planar chiral [2,2]paracyclophane ligands: synthesis and application in Pd-catalyzed allylic alkylation, *Chem. Comm.*, **2000**, 1195-1196.
11. A. Marchand, A. Maxwell, B. Mootoo, A. Pelter, A. Reid, Oxazoline mediated routes to a unique amino-acid, 4-amino-13-carboxy[2.2]paracyclophane, of planar chirality, *Tetrahedron*, **2000**, *56*, 7331-7338.
12. S. Kitagaki, S. Murata, K. Asaoka, K. Sugisaka, C. Mukai, N. Takenaga, K. Yoshida, Planar Chiral [2.2]Paracyclophane-Based Bisoxazoline Ligands: Design, Synthesis, and Use in Cu-Catalyzed Inter- and Intramolecular Asymmetric O–H Insertion Reactions, *Chem. Pharm. Bull.*, **2018**, *66*, 1006-1014.

13. C. Bolm, K. Wenz, G. Raabe, Regioselective palladation of 2-oxazolinyl[2.2] paracyclophanes.: Synthesis of planar-chiral phosphines, *J. Organomet. Chem.*, **2002**, *662*, 23-33.
14. X.W. Wu, T.Z. Zhang, K. Yuan, X.L. Hou, Regulation of the flexibility of planar chiral [2.2]paracyclophane ligands and its significant impact on enantioselectivity in asymmetric reactions of diethylzinc with carbonyl compounds, *Tetrahedron: Asymmetry*, **2004**, *15*, 2357-2365.
15. X. Wang, Z. Chen, W. Duan, C. Song, Y. Ma, Synthesis of [2.2]paracyclophane-based bidentate oxazoline–carbene ligands for the asymmetric 1, 2-silylation of N-tosylaldimines, *Tetrahedron: Asymmetry*, **2017**, *28*, 783-790.
16. A. Pelter, B. Mootoo, A. Maxwell, A. Reid, The synthesis of homochiral ligands based on [2.2] paracyclophane, *Tetrahedron Lett.*, **2001**, *42*, 8391-8394.
17. L. Ackermann, Air-and moisture-stable secondary phosphine oxides as pre-ligands in catalysis, *Synthesis*, **2006**, 1557-1571.
18. A. V. K. Henri, L. V. D. Floris, P. J. T. R. Floris, Catalytic Appel reactions, *Pure Appl. Chem.*, **2012**, *85*, 817-828.
19. T. Xi, Y. Mei, Z. Lu, Palladium-Catalyzed C-2 C–H Heteroarylation of Chiral Oxazolines: Diverse Synthesis of Chiral Oxazoline Ligands, *Org. Lett.*, **2015**, *17*, 5939-5941.
20. P. Lu, C. L. Ji, Z. Lu, Nickel-Catalyzed C-H Heteroarylation of Chiral Oxazolines *Asian J. Org. Chem.*, **2018**, *7*, 542-544.
21. D. Ghorai, V. Müller, H. Keil, D. Stalke, G. Zanoni, B. A. Tkachenko, B. P.R. Schreiner, L. Ackermann, Secondary Phosphine Oxide Pre-ligands for Palladium-Catalyzed C–H (Hetero) Arylations: Efficient Access to Pybox Ligands, *Adv. Synth. Catal.*, **2017**, *359*, 3137-3141.
22. M. Giordano, A. Iadonisi, Tin-Mediated Regioselective Benzylation and Allylation of Polyols: Applicability of a Catalytic Approach Under Solvent-Free Conditions, *J. Org. Chem.*, **2014**, *79*, 213-222.
23. S. Shamsuzzaman, B. Z. Ahmad, S. Khan, A convenient method for the synthesis of 3.beta.-hydroxy 4-en-6-one steroids *J. Org. Chem.* **1991**, *56*, 1936-1937.
24. D. M. Knoll, Y. Hu, Z. Hassan, M. Nieger, S. Brase, Planar Chiral [2.2]Paracyclophane-based BOX Ligands and Application in Cu-mediated N-H insertion reaction, *Molecules*, **2019**, 24, 4122-4136.

25. B. Hong, Y. Ma, L. Zhao, W. Duan, F. He and C. Song, Synthesis of planar chiral imidazo [1, 5-a] pyridinium salts based on [2.2] paracyclophane for asymmetric β-borylation of enones, *Tetrahedron: Asymmetry*, **2011**, *22*, 1055-1062.
26. R. Soren, B. Ciro, R. S. Peter, Sizing the role of London dispersion in the dissociation of all-*meta tert*-butyl hexaphenylethane, *Chem. Sci.*, **2017**, *8*, 405-410.
27. H. J. Reich and D. J. Cram, Macro rings. XXXVII. Multiple electrophilic substitution reactions of [2.2] paracyclophanes and interconversions of polysubstituted derivatives, *J. Am. Chem. Soc.*, **1969**, *91*, 3527-3533.

Chapter 4

The Elaboration of [2.2]Paracyclophane Oxazolines to Give Useful Planar Chiral Molecules

4.1 Introduction

Having shown that we could make a range of [2.2]paracyclophane-oxazoline and that these allowed the resolution of planar chirality, the next step was to explore the conversion of these into other valuable chiral products.

There are numerous reports describing the utility of [2.2]paracyclophane oxazolines. They have been used as preligands,[1-5] or have directed further functionalization of the [2.2]paracyclophane by either bromination[1,6] or metalation.[3,7] We believed that there was little to be gained by screening the oxazolines in other asymmetric reactions and were more interested in determining of the oxazolines could easily be converted to other pre-ligand structures that are hard to access in pure enantiopure form. The oxazolines should be converted to carboxylic acids which are useful pre-ligands and also precursors to a range of functional groups that we hope to make.

We believe straightforward elaboration of the acid functionality will deliver modular pre-ligands. In addition to the aforementioned approach, our objective is to resolve the [2.2]paracyclophane, followed by the hydrolysis of the oxazoline group and use thus, form useful enantiopure products. In this context, we present our preliminary findings on the hydrolysis and decarboxylative phosphorylation of oxazolines.

4.2 Preparation of Chiral Acids

Our first objective was to hydrolyze the oxazoline compounds in order to obtain enantiomerically pure planar chiral acids. Oxazolines possess high stability and necessitate severe conditions for hydrolysis. Previous studies in the literature indicated that successful hydrolysis could be achieved by employing strong acidic conditions, such as heating to reflux in 6M HCl.[2]

4.2.1 Preparation of Mono-Acids

4.2.1a Hydrolysis of Mono-Oxazolines using 6 M HCl

Therefore, we proceeded with our next phase of hydrolysis using 6M HCl. The hydrolysis of mono(benzyl oxazoline) **(R_p,*S*)-4.1** proceeded well and we were successful with an overall yield of > 95% (**Scheme 4.1**). Next, we applied the same 6M HCl conditions for the hydrolysis of mono-*t*-butyl oxazoline **(R_p,*S*)-4.3**. Unfortunately, this was unsuccessful. We made efforts to optimize the reaction using HCl, but it turned out that these hydrolysis conditions did not work for the *tert*-butyl oxazoline and only starting material was returned.

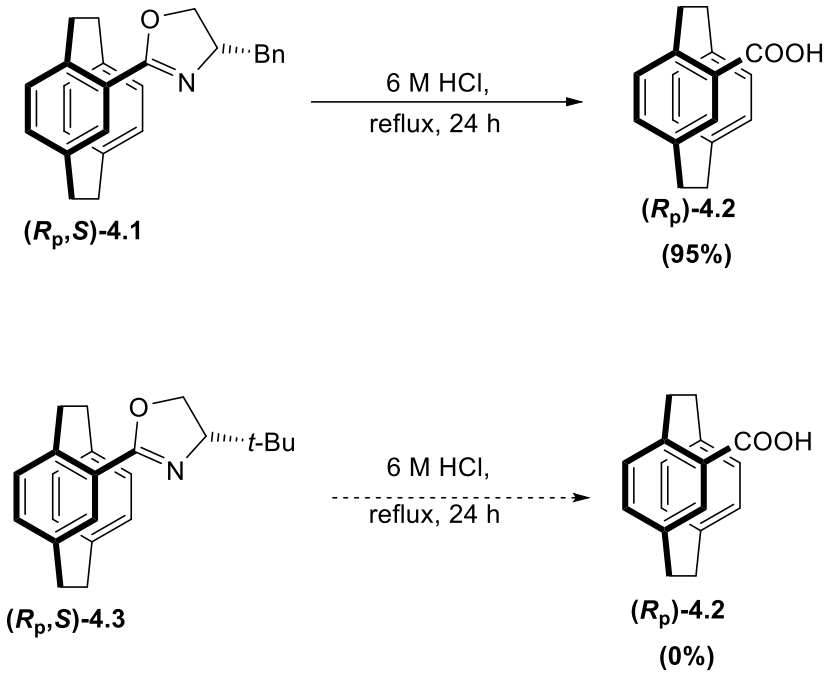

Scheme 4.1: Hydrolysis of mono-oxazolines using 6M HCl

4.2.1b Hydrolysis of Mono-Oxazolines using 3.6 M H_2SO_4

It was clear that these conditions were not harsh enough. Presumably, the bulk of the *tert*-butyl group protects the oxazoline possibly by preventing the water from approaching the C-2 carbon. We realized that more stringent conditions were necessary to hydrolyze the mono(*tert*-butyl oxazoline).

Initially, we attempted to use aqueous 3.6 M H_2SO_4, however, solubility became an issue with these new conditions, and the starting material remained unreacted. To overcome this challenge, we added a few drops of dioxane to aid the solubility of the starting material. Subsequently, we heated the mixture to reflux with aqueous 3.6 M H_2SO_4 (**Scheme 4.2**). The chiral acid precipitated out after the consumption of the starting material, and was readily filtered off. Purification by a simple methanol-DCM wash gave the product acid in good yields achieving an overall yield of 70% from the benzyl oxazoline and 62-64% from the *tert*-butyl oxazoline.

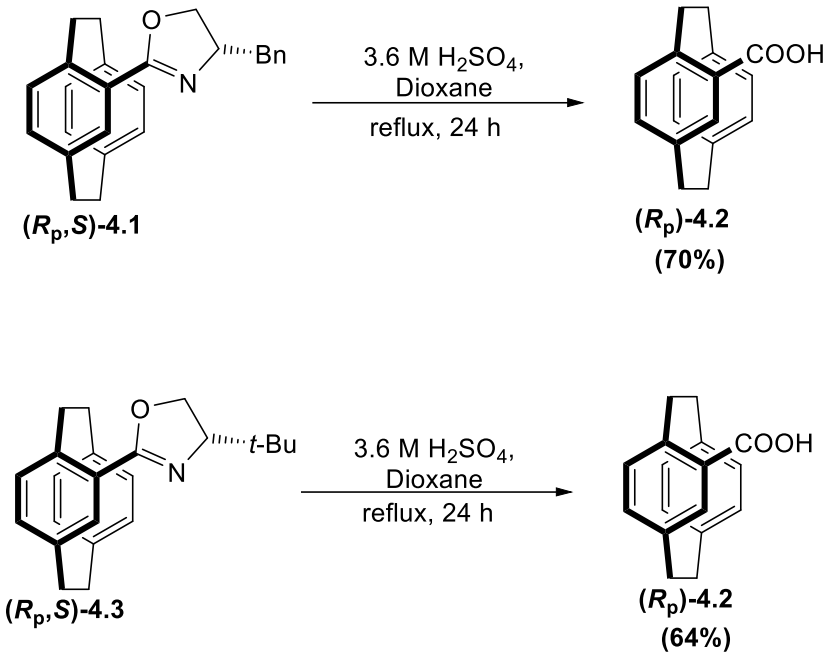

Scheme 4.2: Hydrolysis of oxazolines using 3.6 M H_2SO_4

The enantiomers were identified by measurement of the specific rotation using a polarimeter. The crystal structures of the pure enantiomers confirmed the formation of the desired chiral acids (**Figure 4.1**).

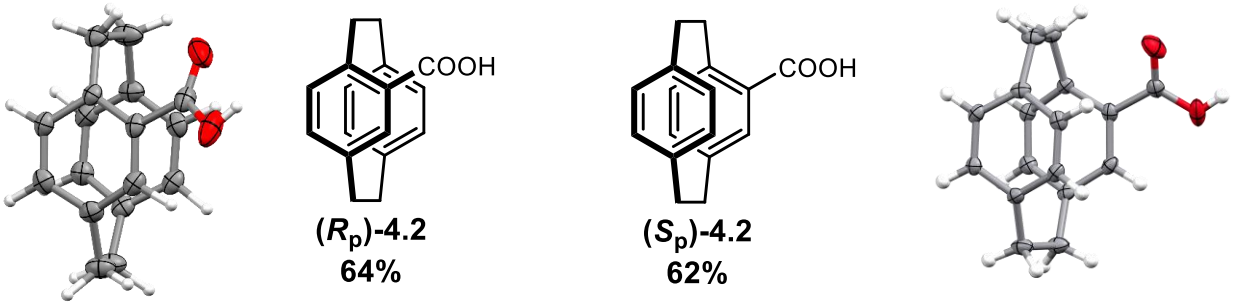

Figure 4.1: Crystal structures of formed planar chiral mono-acids

4.2.2 Preparation of Chiral Diacids

Our subsequent objective was to perform the hydrolysis of bis-oxazoline in order to obtain enantio-enriched chiral diacids. The role of diacids as precursors to chiral diamines is known as they can be readily converted to diamines via Curtius rearrangement, which then can be employed for generating chiral metal complexes. Employing the same hydrolysis conditions as before, we successfully produced the desired chiral diacids **(R_p)-4.5 or (S_p)-4.5** in significant yields 84% and 85% respectively. **Scheme 4.3** shows the formation of one enantiomer. The second isomer was also formed using the same conditions.

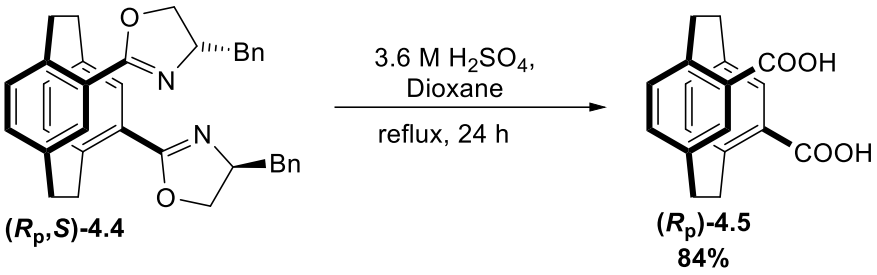

Scheme 4.3: Hydrolysis of bis-oxazolines using 3.6 M H_2SO_4

Figure 4.2 shows the crystal structure of the two enantiomers obtained, confirming the formation of the desired chiral diacids.

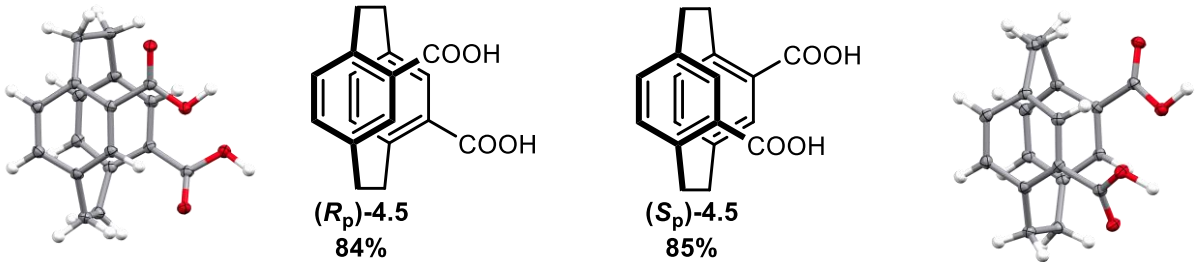

Figure 4.2: Crystal structures of formed planar chiral di-acids

4.2.3 Preparation of Mono-bromo-mono-acid

Any route that leads to two different functional groups that can be manipulated independently is useful and gives us a chance to make useful enantio-enriched materials. Having acquired the methodology, we were determined not to overlook any of the valuable side products generated during the coupling process. As a result, we utilized the hydrolysis technique on the bromo-mono oxazoline **(R_pS)-4.6**, which was obtained as a by-product during bis-coupling. Following successful separation through recrystallization, we conducted the hydrolysis, resulting in the successful production of bromo-planar chiral mono acid **(R_p)-4.7** with a yield of 68% (**Scheme 4.4**).

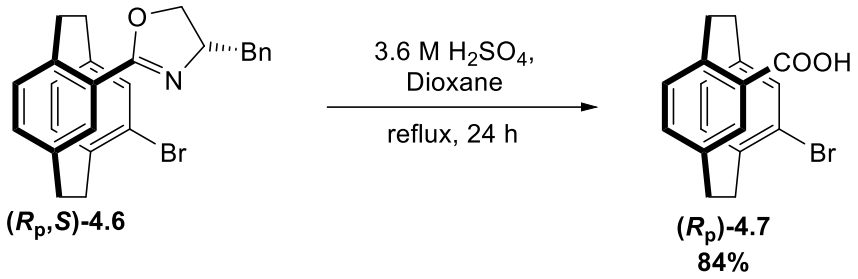

(*R*p,*S*)-4.6 **(*R*p)-4.7** **84%**

Scheme 4.4: Preparation of mono-bromo-mono-acid

4.2.4 Preparation of Partial Acids

As stated above, being able to differentiate two functional groups is useful, so, we explored the possibility of partial hydrolysis by reducing the hydrolysis time to half, specifically 12 hours instead of the usual 24 hours (**Scheme 4.5**).

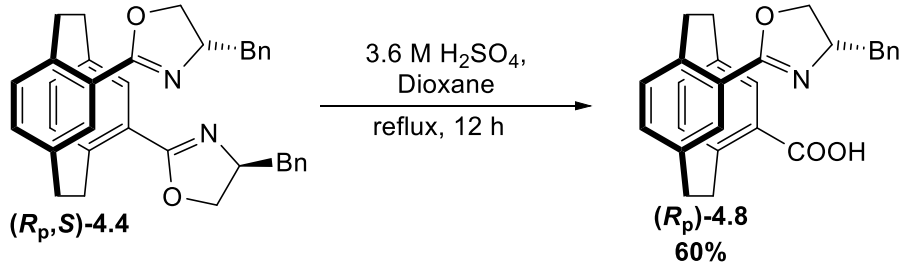

(*R*p,*S*)-4.4 **(*R*p)-4.8** **60%**

Scheme 4.5: Preparation of mono-oxazoline-mono-acid

We were successful in forming mono-oxazoline-mono-acid **(*R*p)-4.8** with 60% yield from the bis oxazoline-(***R*pS*)-4.4**. We also performed the hydrolysis on the other isomer (***S*pS*)-4.4** which yielded **(*S*p)-4.8** with 60% yield (**Figure 4.3**).

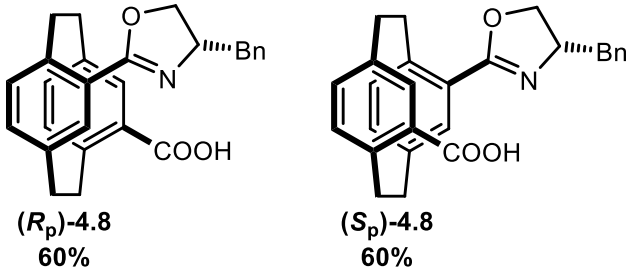

(*R*p)-4.8 **60%** **(*S*p)-4.8** **60%**

Figure 4.3: Both isomers of mono-oxazoline-mono-acid

4.3 Rhodium Paddle-Wheel Complex

Dirhodium(II) complexes are exceptional catalysts for a wide range of transformations, such as cyclopropanation, C–H functionalization and ylide formation.[8]

The dirhodium(II) paddlewheel complexes consist of a dinuclear core surrounded by four equatorial μ^2-ligands and two axial ligands.[9] The core is held together by a rhodium-rhodium single bond and each rhodium is considered to have octahedral geometry.

Utilizing the planar chirality of the [2.2]paracyclophane, Bräse and co-workers designed and synthesized planar chiral dirhodium(II) paddle-wheel complex $Rh_2(S_p\text{-PCP})_4$ bearing [2.2]paracyclophane carboxylate ligands and moreover, highlighted its catalytic applications in cyclopropanation reaction of vinyl arenes with α-methyl-α-diazoesters (**Scheme 4.6**). Thus, rhodium(II) paddlewheel complexes are highly potent catalysts with broad applications in metal-carbene transformations.[10]

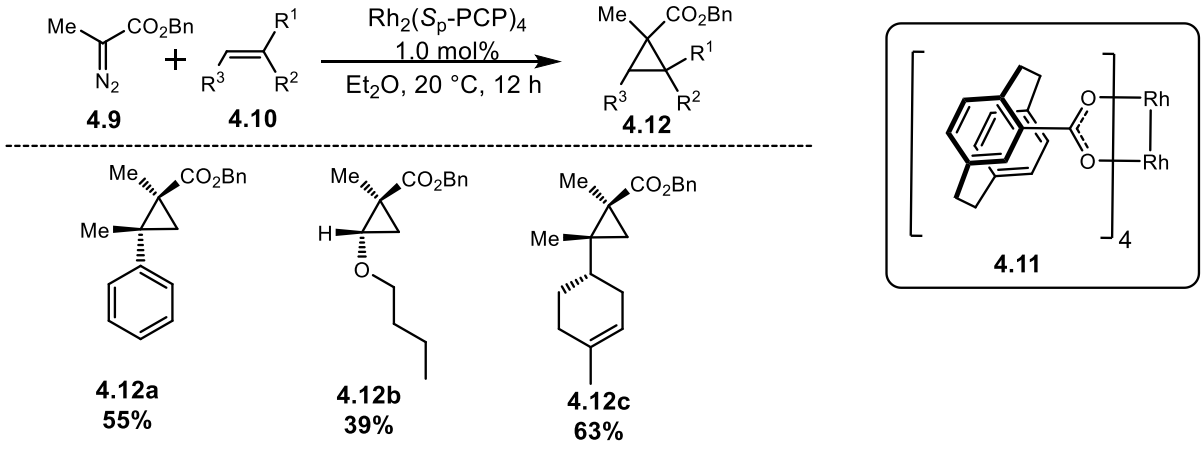

Scheme 4.6: Cyclopropanation using rhodium paddle-wheel

Our next target was to link rhodium metal to our chiral (R_p)-12-bromo-4-carboxy[2.2]paracyclophane **4.7**. But we had an advantage over Bräse's paddle-wheel. We had an extra bromo group that could be used to increase the bulk which can change the steric environment. It was even hoped that the bromine atom itself might have a beneficial effect. Further, the potency of the catalyst so formed will be tested for various transformations[11]

So, we developed a methodology to first link the rhodium to the carboxy group of (R_p)-12-bromo-4-carboxy[2.2]paracyclophane **4.7**, (**Scheme 4.7**). The green-colored Rh_2-PCP complex was obtained with 83% yield, which was confirmed by the crystal structure.

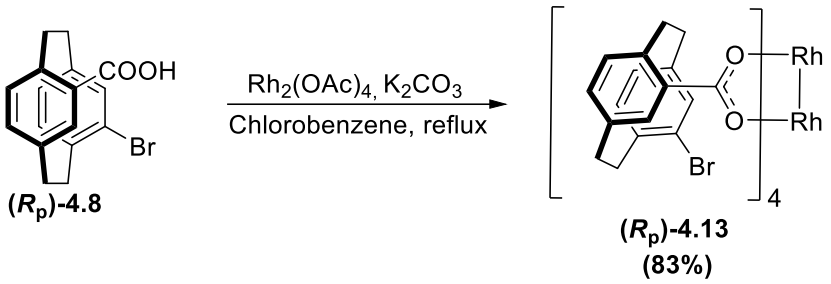

Scheme 4.7: Synthesis of the PCP-based planar-chiral dirhodium complex

Figure 4.4 shows the crystal structure of the complex (***R*p-4.13**) formed. The hydrogen atoms have been omitted so as to keep the structure clear.

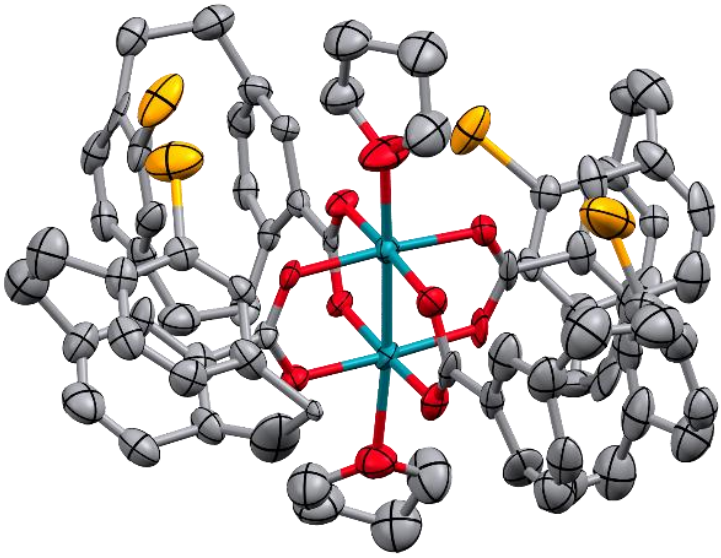

Figure 4.4: Crystal Structure of the Rh_2-Br-PCP complex

Ideally, we would like to make the paddle wheel with the bromo derivative. This would allow us to use a common precursor to create a range of different derivatives by the Suzuki coupling. This is more efficient than pre-forming different [2.2]paracyclophane acids and complexing each with $Rh_2(OAc)_4$. This strategy has successfully been applied by Huw Davies to make massive rhodium complexes.[12] Unfortunately, our preliminary results have not been promising (**Scheme 4.8**). Various attempts have led to a complex mixture from which we were unable to identify products. It is possible that the sterically demanding nature of *pseudo-ortho* substituted [2.2]paracyclophane derivatives has made the process challenging when compared to Davies systems.

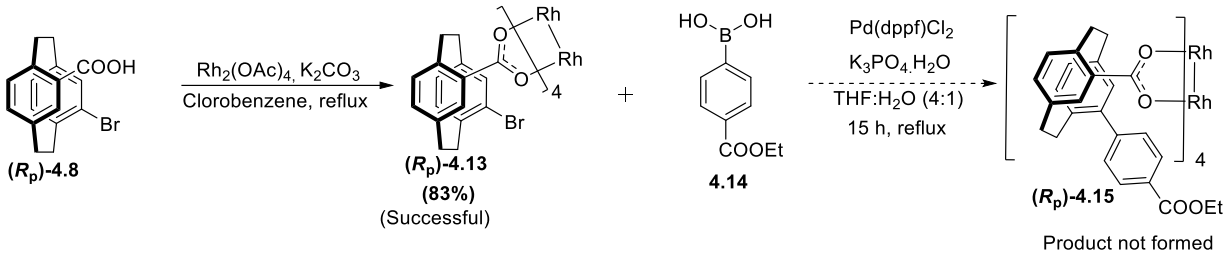

Scheme 4.8: Attempted Suzuki coupling on the rhodium complex

To simplify the problem, we attempted coupling prior to the complexation and studied coupling of (R_p)-12-bromo-4-carboxy[2.2]paracyclophane-**4.8** with boronic acids (**Scheme 4.9**). Suzuki reaction was successful, although only with moderate yields, which again suggests that the inherent bulk of [2.2]paracyclophane makes this reaction challenging. Disappointingly, complexation failed to deliver the desired paddle-wheel.

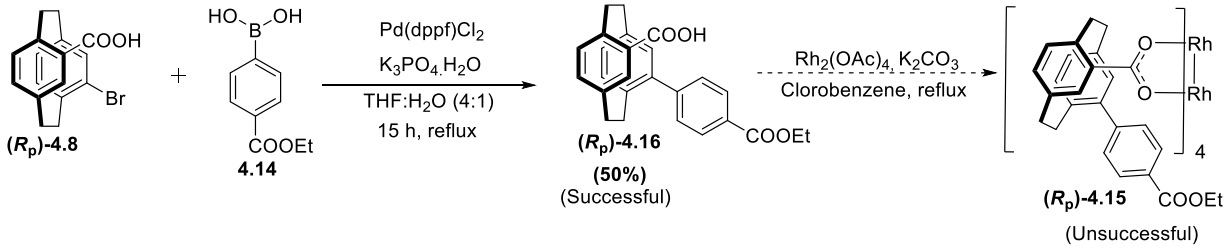

Scheme 4.9: Alternate route to synthesize rhodium paddle-wheel

We tried another methodology, where we performed Suzuki on the one-bromo-one-oxazoline **(R_pS)-4.6**. It was planned that after successful in achieving Suzuki coupling, we would go for hydrolysis before complexation with rhodium. But we suffered a setback during the hydrolysis step as it failed to give the desired product (**Scheme 4.10**).

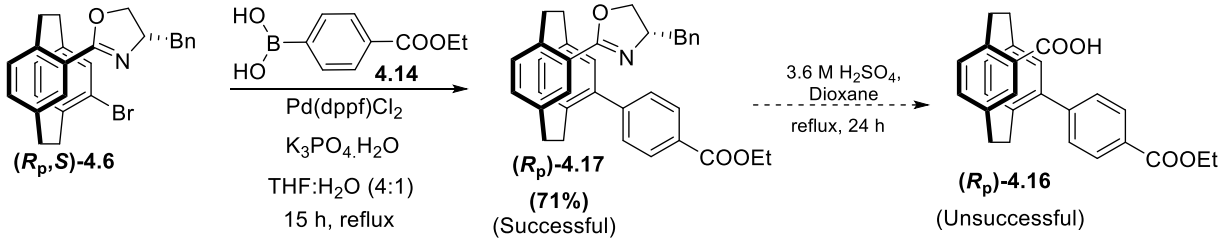

Scheme 4.10: Third attempted route to synthesize rhodium paddle-wheel

A summarized **Scheme 4.11** is shown below, showing the two routes followed to attempt the synthesis of the suzuki coupled rhodium-PCP paddle-wheel complex.

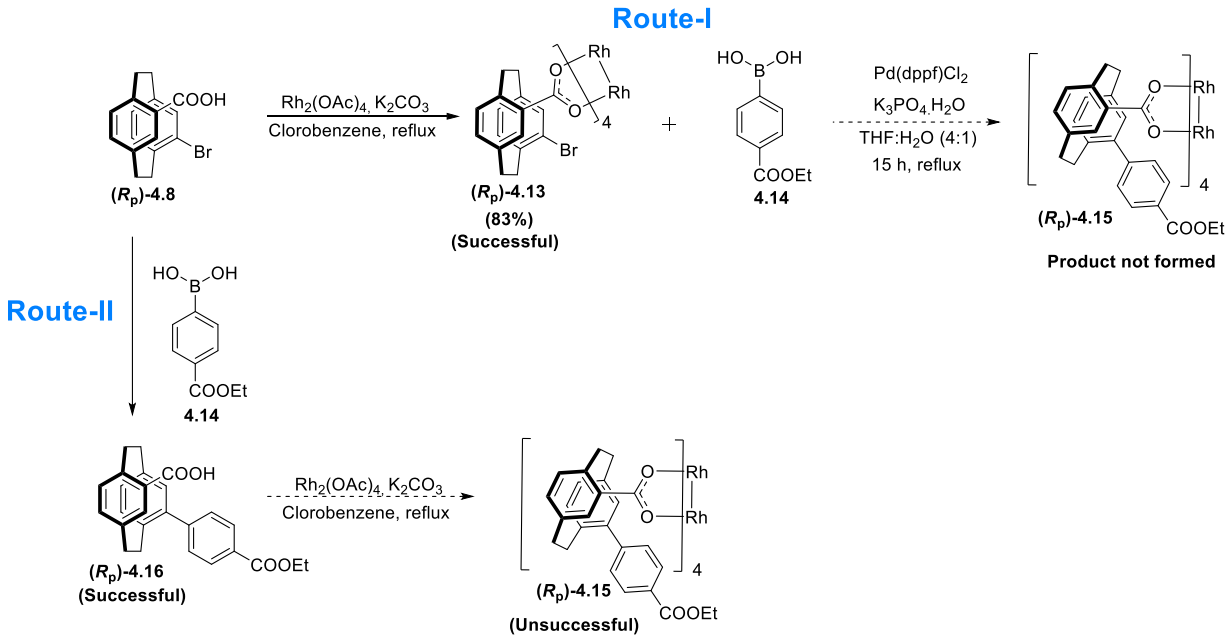

Scheme 4.11: Summarized attempted route to synthesize rhodium paddle-wheel

We thus evaluated the failure of introducing the bulk on our paddle-wheel. The crystal structure shows the orientation of the bromo groups facing each other, which be one of the problem, causing the failure of the Suzuki coupling.

The paddle-wheel was successful, yet the endeavor to attach a bulk remained an area that was unachievable.

4.4 Decarboxylative Phosphorylation

Having found the optimum hydrolysis conditions, the next stage was to look at the utility of the carboxylic acids. We investigated a range of reactions to demonstrate the scope. The most speculative, and interesting reaction was the potential to convert the acid into a phosphine through decarboxylative phosphorylation.

Organo-phosphorous compounds[13] are highly valuable chemicals due to their unique physical and chemical properties. These compounds find extensive applications in various fields, including medicinal chemistry,[14] catalysis,[15] organic synthesis,[16] coordination chemistry,[17] and material science.[18] The goal of this exploration was to develop an improved route to planar chiral phosphines such as Phanephos. The results so obtained did not show any loss of enantiopurity during the reaction, leading to the successful formation of phosphine oxide. (**Scheme 4.12**).[19]

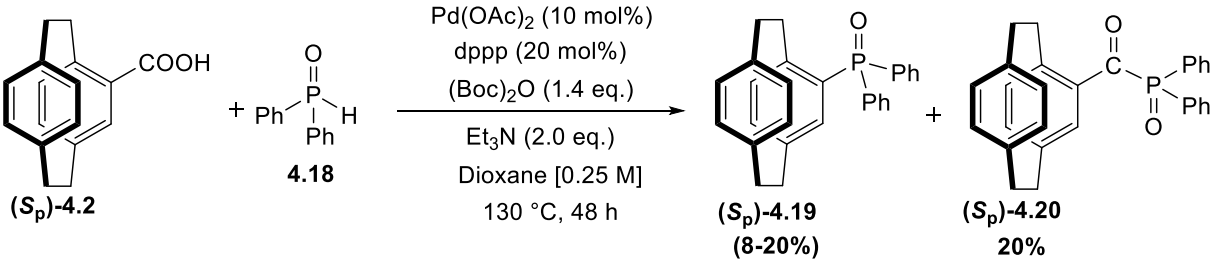

Scheme 4.12: Synthesis of planar chiral phosphine oxides

During the optimization of the reaction conditions, we tested different ligands and solvents. However, the conditions mentioned above yielded the best results. Although the yields obtained (8-20%) were not exceptionally high, with 50% of the starting material remaining unreacted, the outcomes were promising. These results have opened a new avenue or pathway for the synthesis of enantio-enriched phosphine oxides and their precursors. The R_f values of the desired product and carbonylated side products were close by, which made separation quite challenging and resulted in the loss of yields. The presence of extra carbonyl peak in IR and C-13 NMR helped us to differentiate the two compounds.

We attempted to convert the by-product **(S_p)-4.20** by heating in same reaction condition as mentioned in the scheme 4.12. The conversion to our desired phosphine oxide **(S_p)-4.19** was successful with 80% yield as shown in **Scheme 4.13**.

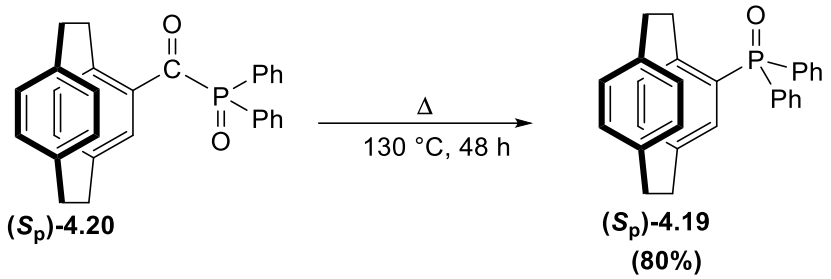

(S_p)-4.20 (S_p)-4.19 (80%)

Scheme 4.13: Synthesis of the chiral phosphine oxide from its carbonylated by-product

The other isomer of the phosphine oxide, i.e., **(R_p)-4.19** was also synthesized in the same way from the chiral mono-acid-**(R_p)-4.2**, using same methodology with 5-15% yields.

The range of yield is obtained while attempting multiple times the same reaction.

4.4.1 Proposed Mechanism for Decarboxylative Coupling

A possible mechanism for the decarboxylative phosphorylation is shown in the **Scheme 4.14** below. First, the acid reacts $(Boc)_2O$ to form a mixed anhydride. This acts as a dehydrating agent and activates the C-O bond to allow palladium insertion. The active palladium catalyst is formed by the reduction of $Pd(OAc)_2$ to Pd^0 by either phosphine or triethylamine base. The palladium undergoes oxidative addition and inserts into the C-O bond to give an acyl palladium species. Presumably, transmetallation occurs next. Either the OBoc group is substituted by the secondary phosphine oxide before decomposing to *tert*-butoxide and carbon dioxide or decomposition occurs first to give a vacant coordination site that allows SPO to complex the palladium. The resulting complex undergoes one of the two fates. Either there is reductive elimination to give the acyl phosphine oxide side product or undergoes thermal decarboxylation/ elimination to give the product.

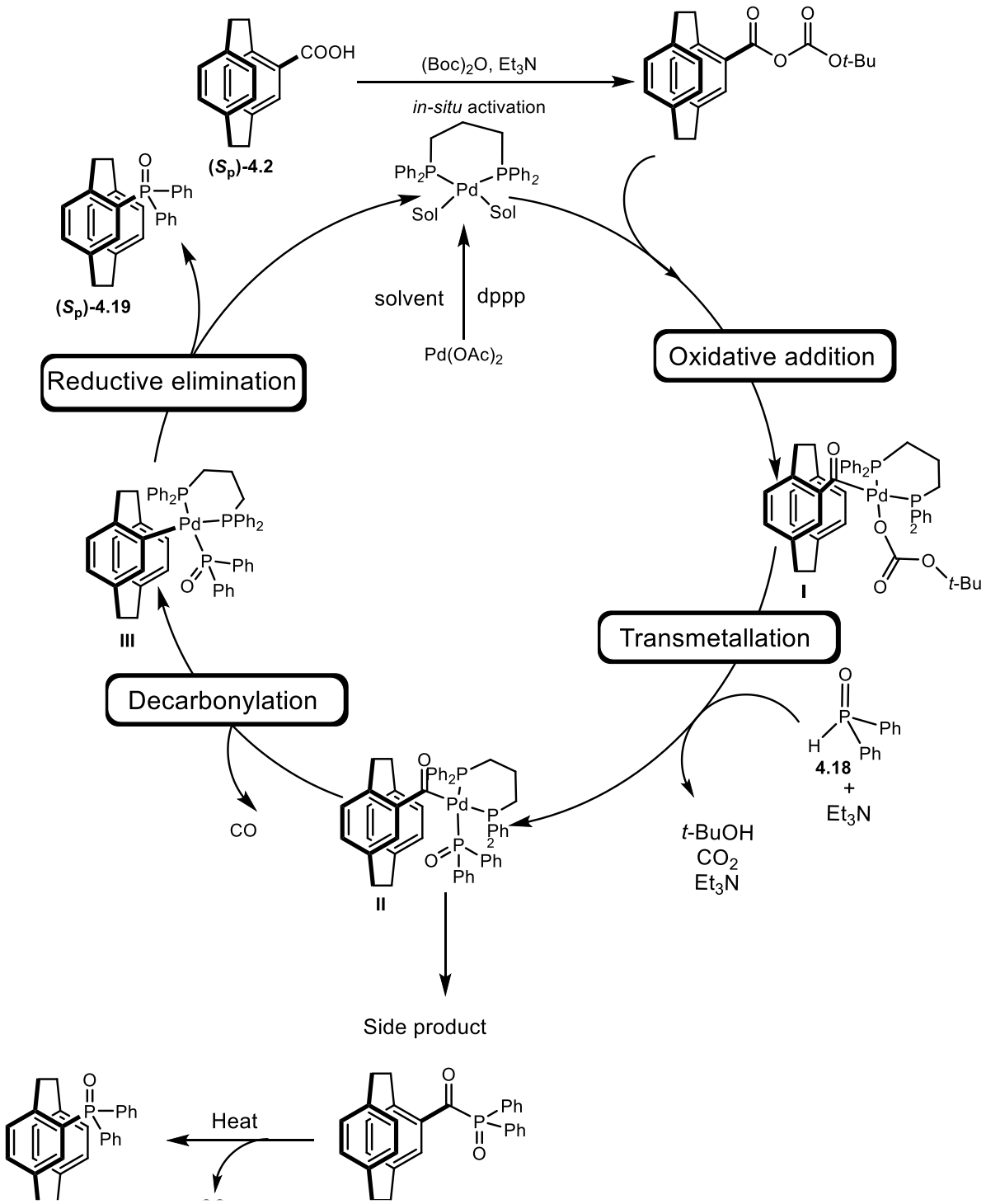

Scheme 4.14: Proposed Mechanism for Decarboxylative Coupling

4.5 Preparation of Planar Chiral Diamines

Planar chiral amines and diamines possess not only chirality but also provide a multitude of opportunities for subsequent transformations.

The transformation of chiral diacids into diamines was achieved through a four-step process,[20] as illustrated in **Scheme 4.15**. The process began with the conversion of (R_p)-4,12-dicarboxy[2.2]paracyclophane-**4.5** to (R_p)-4,12-bis(chlorocarbonyl)[2.2]paracyclophane-**4.21** by the use of oxalyl chloride. This acyl chloride was then coverted to (R_p)-4,12-bis(azido-carbonyl)[2.2]paracyclophane-**4.22**. Azides were then heated in toluene to yield isocyanate, (R_p)-4,12-diisocyanato[2.2]paracyclophane-**4.23,** which was readily converted into (R_p)-4,12-diamino[2.2]paracyclophane-**4.24** by Curtius rearrangement with 73% yield.

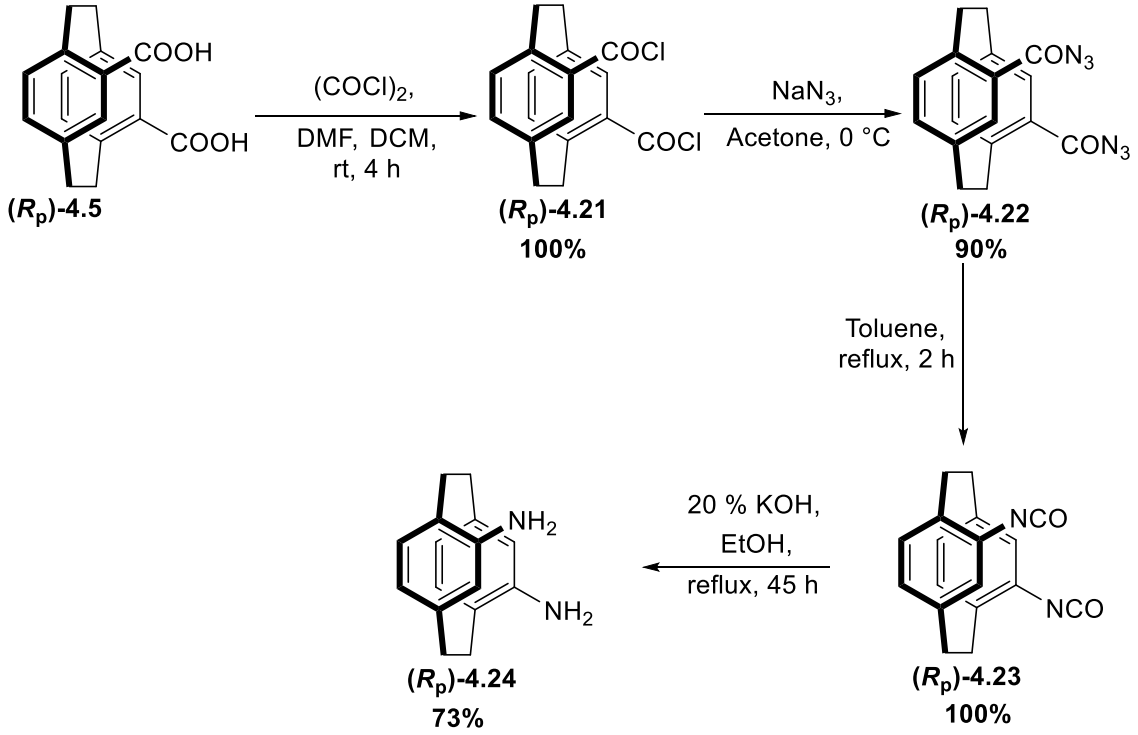

Scheme 4.15: Synthesis of chiral diamines

(S_p)-4,12-diamino[2.2]paracyclophane-**4.24** was prepared analogously to (R_p)-4,12-diamino[2.2]paracyclophane-**4.24** but employing (S_p)-(–)-4,12-dicarboxy[2.2]paracyclophane-**4.5** with 80% yield.

Full characterization was done and the CD data was recorded for both the isomers of the diamine-**4.24**.

Figure 4.5 shows the comparison between the two isomers through their CD spectra. The opposite orientation with the same concentration of both the isomers signifies the configuration of the two as opposite to each other.

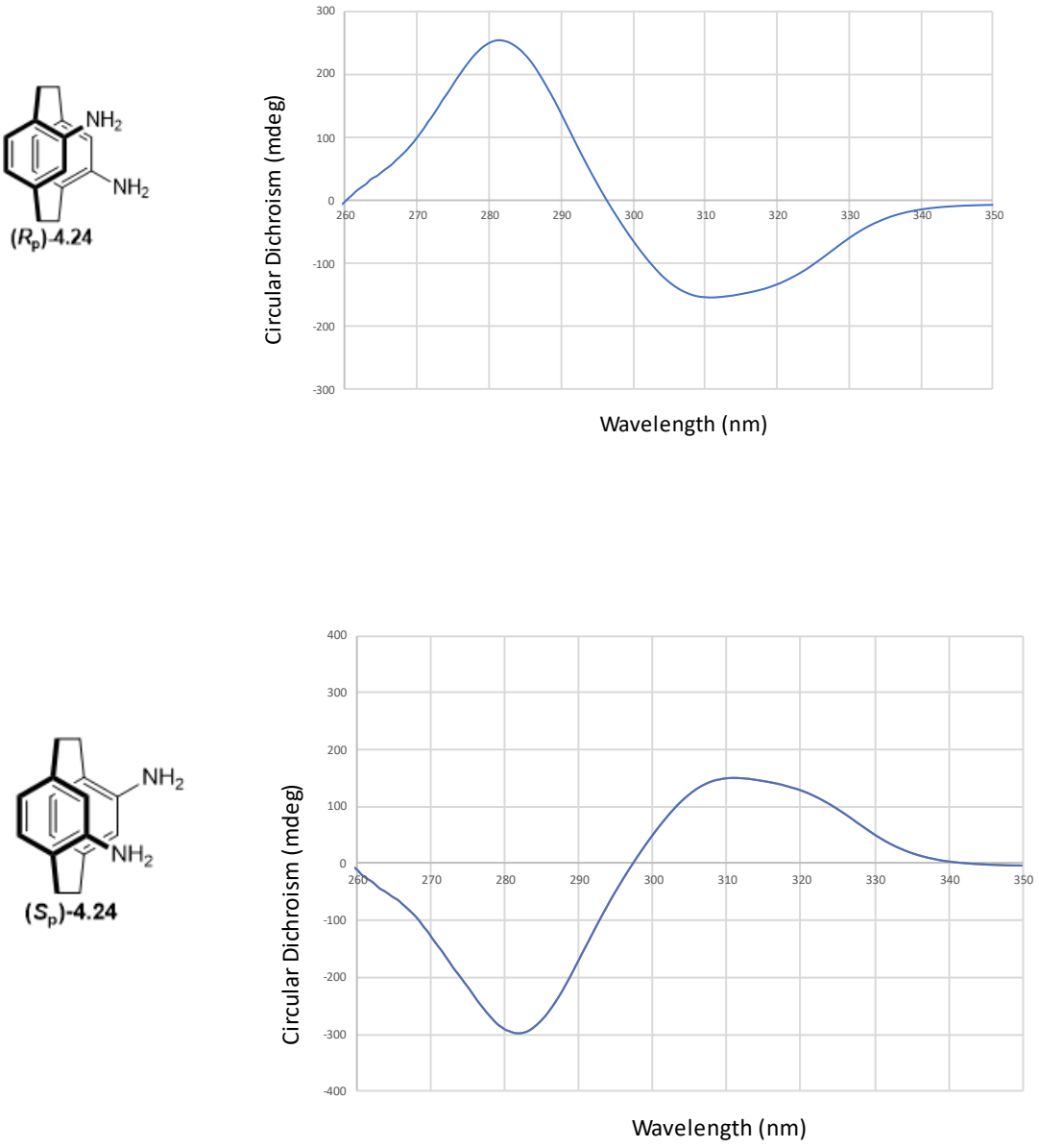

Figure 4.5: CD spectra of the two diamine enantiomers

4.6 Preparation of Chiral Phanol from Chiral Diamines

The previous report on the formation of chiral Phanol was reported by Braddock *et al*.[21]His group initially converted the dibromo [2.2]paracyclophanes to racemic Phanol by dilithiation-oxidation route. Later on, the kinetic resolution of the racemic Phanol using the commercially available lipase *Candida rugosa* as a hydrolase source. The method was long, multistep and uneconomical. In the **Scheme 4.16**, the racemic Phanol is converted to its acetate which upon action of *Candida rugosa* via enzymatic kinetic resolution.

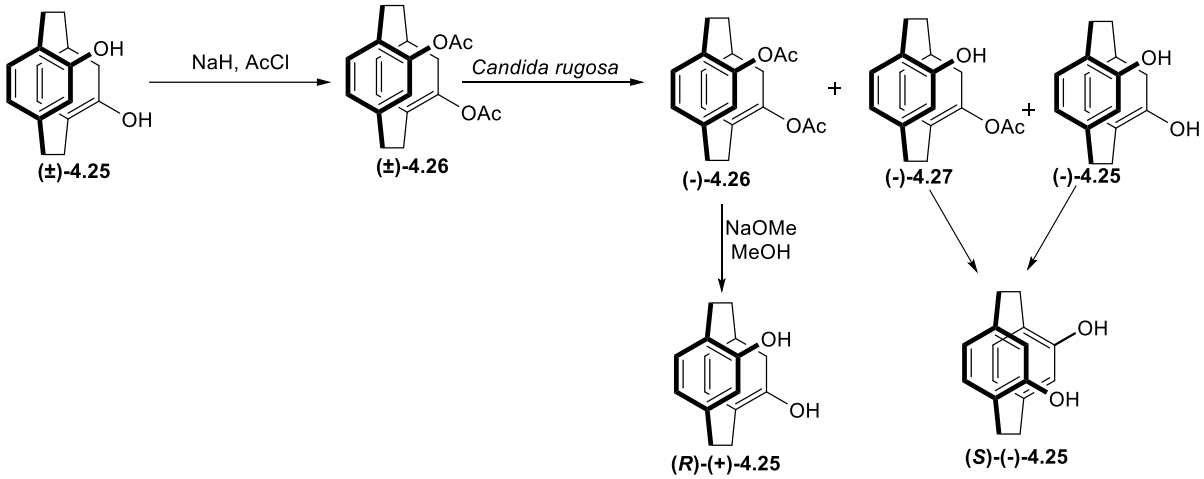

Scheme 4.16: Synthesis of chiral Phanol by *Candida rubosa*

As we had an efficient route to planar chiral diamines, we were interested in the conversion of this to chiral phanol or dihydroxy [2.2]paracyclophanes. This could be achieved in three steps (**Scheme 4.17**). The first step was amide formation achieved by mixing the diamine with acetic anhydride at room temperature. The amine was then converted to an ester by an elegant transformation.[22] his involved formation of a nitrosamide that thermally rearranges to the ester. Hydrolysis then gave phanol with 20% yield.

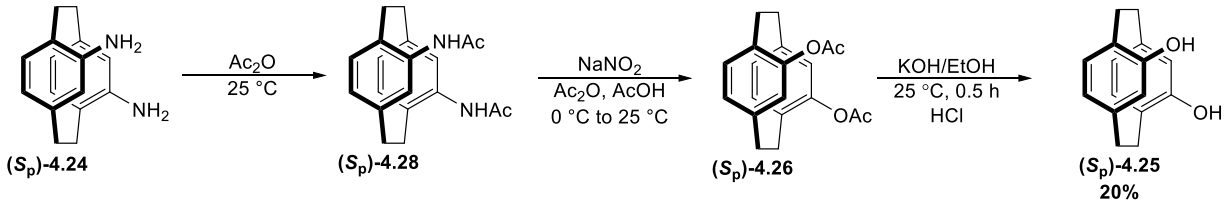

Scheme 4.17: Synthesis of chiral Phanol from diamine

The mechanism (**Scheme 4.18**) of the key rearrangement is thought to involve nitrosamide formation followed by either homolytic radical clevage and recombination.

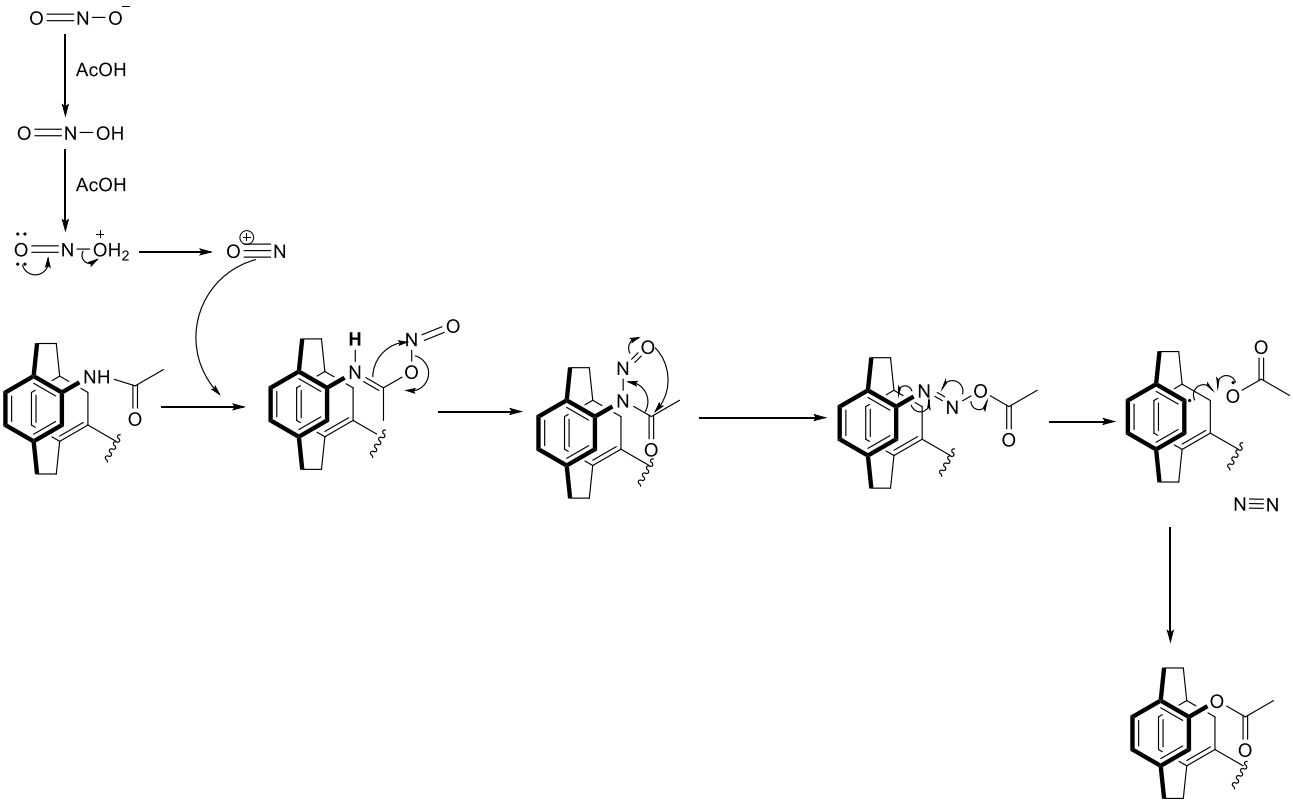

Scheme 4.18: Mechanism of the step 2

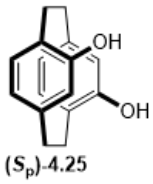

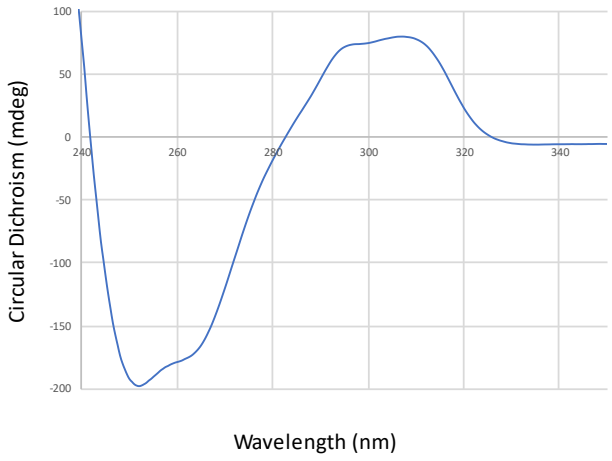

Figure 4.6: CD spectrum of Phanol

Still, this chiral Phanol offers new routes for the synthesis of various chiral pre-ligands that can be complexed with various metals like copper for catalytic asymmetric transformations.[23]

4.7 Planar Chiral Dinuclear Gold Complex

Gold catalysts have been known for decades and they catalyze a range of useful reactions.[24-27] A comprehensive review on Divergent Gold Catalysis (DGC), and its four categories has been done by Nitin *et al*.[27] The four categories, namely: (a) Metal-Dependent Divergent Gold Catalysis, (b) Ligand-Dependent Divergent Gold Catalysis, (c) Oxidation-State-Dependent Divergent Gold Catalysis, and (d) Counter-Anion Dependent Divergent Gold Catalysis. The four categories have shown the diverse range of catalysis that can be done with gold metal.[27]

Cationic gold complexes are considered the most powerful catalysts for the electrophilic activation of unactivated multiple carbon−carbon bonds (alkynes, allenes, alkenes) due to their unique π-affinity.[26]

Many studies have shown that there is a role of counterions and additives in the reaction outcomes such as kinetics and regioselectivity, when employed along with the gold catalyst.[28-30]

Dinuclear gold catalyst discussed in this review is defined as a single gold-complex with two gold centers linked by a bidentate ligand. Such catalyst possesses internal aurophilic interactions between the two atoms.[31] The mechanistic studies have revealed that the distance between two gold atoms should be between 2.5–3.5 Å, for such aurophilic interactions. aurophilic interaction between the two gold atoms which lowers the energy of the system. These interactions tend to decrease the limitations of this metal of requiring exogenously strong oxidants or counterions.

A classic example of comparative analysis of the catalytic activity of the mono-gold catalyst and di-gold catalyst is represented in **scheme 4.19** below.

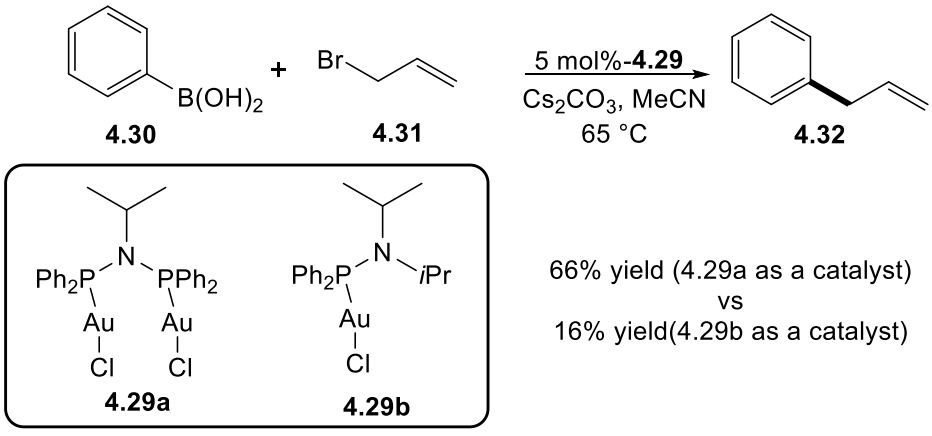

Scheme 4.19: A dinuclear gold-catalyzed cross-coupling reaction of Ar–$B(OH)_2$ and allyl bromides.

The cross-coupling reaction of Ar-B(OH)$_2$ and allyl bromides was achieved using two gold catalyst. Fascinated by this work, as our diamines possess the same potential to generate dinuclear gold catalyst, we focussed on developing new chiral dinuclear gold catalyst.

Our strategy was to convert the enantiomerically pure diamine into the isonitrile. The reaction of acetic anhydride and formic acid delivered the formamide **(R_p)-4.33**, which was purified by recrystallization from acetone/pentane. **(R_p)-4.33** delivered the isonitrile **(R_p)-4.34** when treated with phosphoryl trichloride and triethylamine in THF (**Scheme 4.20**).

It was then planned to synthesize the nitrogen acyclic carbene (NAC) complex **(R_p)-4.35** by reacting the simple (tht)-gold(I) chloride, isonitrile **(R_p)-4.34**, and a secondary amine which would directly lead to the desired gold complex **(R_p)-4.35**.

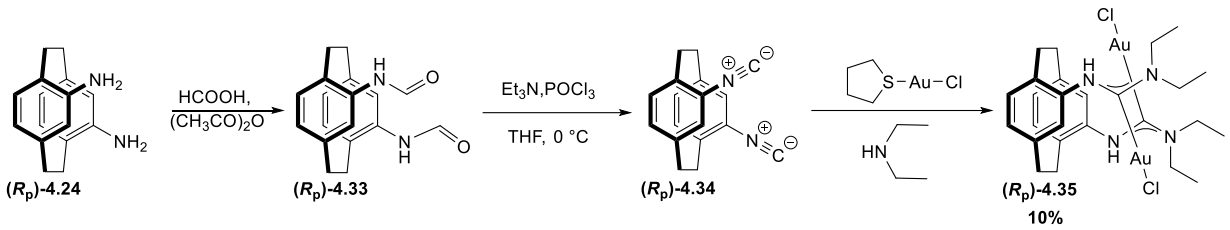

Scheme 4.20: Synthesis of dinuclear gold catalyst from chiral diamines

Despite employing an inert atmosphere and employing various purification methods such as washing with cold pentane, column chromatography, preparative TLC, the yields remained low as the major product underwent decomposition.

However, we were able to obtain the crystal structure of one of our compounds, confirming the success of the reaction (**Figure 4.7**). The crystal structure clearly shows that the two gold centres are oriented opposite to each other. The distance between the two centres is more than we desired. We wanted to form a gold complex where we can establish an aurophilic interaction between the two gold centres. Nevertheless, further optimization is necessary to achieve higher yields of the gold complex.

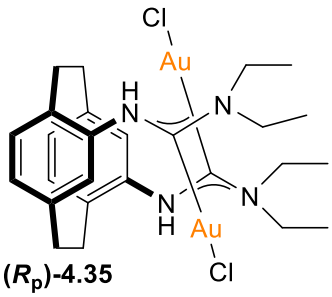

(R_p)-4.35

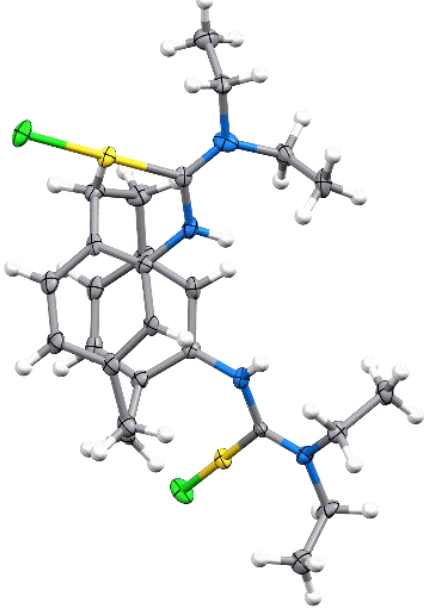

Figure 4.7: The crystal structure obtained of the desired gold catalyst

4.8 Conclusion

Various enantioselective products were obtained having a wide variety in terms to catalyze asymmetric transformations. We were successful in hydrolyzing the oxazolines coupled to [2.2]paracyclophane in good yields. The formation of various chiral acids like mono-acids, diacids, mono-bromo-monoacid, mono-oxazoline-mono-acid have opened up the diverse range of substrate, where these enantiopure compounds can be utilized.

We then attempted use of different chiral acids for various transformations like chiral diamines, chiral Phanol, decarboxylative coupling to yield precursors of Phanephos. All of these compounds could be utilized in asymmetric catalysis.

We also attempted the synthesis of various metal-PCP complexes using metals like rhodium and gold. Our aim is clear and straightforward where we want to employ our PCP-based chiral and enantiomerically pure compounds for various asymmetric transformations.

We have already crossed a halfway mark in our road to success to fulfill the above goal. Still, an insight is needed to utilize the complete potential of the formed catalysts. Also, optimization of the decarboxylative coupling will offer an exciting new route to enantiomerically enriched planar chiral molecules that are challenging to synthesize by conventional methods.

4.9 References

1. D. K. Whelligan and C. Bolm, Synthesis of Pseudo-geminal-, Pseudo-ortho-, and ortho-Phosphinyl-oxazolinyl-[2.2]paracyclophanes for Use as Ligands in Asymmetric Catalysis, *J. Org. Chem.,* **2006**, *71*, 4609-4618.
2. B. Hong, Y. Ma, L. Zhao, W. Duan, F. He and C. Song, Synthesis of planar chiral imidazo[1,5-*a*]pyridinium salts based on [2.2]paracyclophane for asymmetric β-borylation of enones, *Tetrahedron: Asymmetry*, **2011**, *22*, 1055–1062.
3. X.-L. Hou, X.-W. Wu, L.-X. Dai, B.-X. Cao and J. Sun, Novel *N,S*- and *N,Se*-planar chiral [2.2]paracyclophane ligands: synthesis and application in Pd-catalyzed allylic alkylation, *Chem. Commun.,* **2000**, 1195-1196.
4. D. M. Knoll, Y. Hu, Z. Hassan, M. Nieger and S. Brase, Planar Chiral [2.2]Paracyclophane-Based Bisoxazoline Ligands and Their Applications in Cu-Mediated N–H Insertion Reaction, *Molecules*, **2019**, *24*, 4122-4136.
5. S. Kitagaki, K. Sugisaka and C. Mukai, Synthesis of planar chiral [2.2]paracyclophane-based bisoxazoline ligands bearing no central chirality and application to Cu-catalyzed asymmetric O–H insertion reaction, *Org. Biomol. Chem.,* **2015**, *13*, 4833-4836.
6. A. Marchand, A. Maxwell, B. Mootoo, A. Pelter and A. Reid, Oxazoline Mediated Routes to a Unique Amino-acid, 4-Amino-13-carboxy[2.2]paracyclophane, of Planar Chirality, *Tetrahedron*, **2000**, *56*, 7331–7338.
7. C. Bolm, K. Wenz and G. Raabe, Regioselective palladation of 2-oxazolinyl-[2.2]paracyclophanes.: Synthesis of planar-chiral phosphines, *J. Organomet. Chem.,* **2002**, *662*, 23–33.
8. H. Lebel, C. Molinaro, A. B. Charette, Stereoselective Cyclopropanation Reactions, *Chem. Rev.* **2003**, 103 977-1050.
9. E. B. Boyar, S. D. Robinson, Rhodium(II) carboxylates, *Coord. Chem. Rev.*,**1989**, *50*, 109-208.
10. C. Zippel, Z. Hassan, M. Nieger, S. Bräse, Design and Synthesis of a [2.2]Paracyclophane-based Planar Chiral Dirhodium Catalyst and its Applications in Cyclopropanation Reaction of Vinylarenes with α-Methyl-α-Diazo Esters, *Adv. Synth.Catal.,* **2020**, *362*, 3431-3434.
11. H. M. L. Davies & J. R. Manning, Catalytic C–H functionalization by metal carbenoid and nitrenoid insertion, *Nature*, **2008**. *451*, 417-424.

12. J. Hansen, H. M. L. Davies, High symmetry dirhodium(II) paddle-wheel complexes as chiral catalysts *Coord. Chem. Rev.* **2008**, *252*, 545-555.
13. G. J. Rowlands, Planar Chiral Phosphines Derived from [2.2]Paracyclophane, *Isr. J. Chem.*, **2012**, *52*, 60-67.
14. W.-S. Huang, S. Liu, D. Zou, M. Thomas, Y. Wang, T. Zhou, J. Romero, A. Kohlmann, F. Li, J. Qi, L. Cai, T. A. Dwight, Y. Xu, R. Xu, R. Dodd, A. Toms, L. Parillon, X. Lu, R. Anjum, S. Zhang, F. Wang, J. Keats, S. D. Wardwell, Y. Ning, Q. Xu, L. E. Moran, Q. K. Mohemmad, H. G. Jang, T. Clackson, N. I. Narasimhan, V. M. Rivera, X. Zhu, D. Dalgarno, W. C. Shakespeare, Discovery of Brigatinib (AP26113), a Phosphine Oxide-Containing, Potent, Orally Active Inhibitor of Anaplastic Lymphoma Kinase, *J. Med. Chem.*, **2016**, *59*, 4948-4964; b) X. Chen, D. J. Kopecky, J. Mihalic, S. Jeffries, X. Min, J. Heath, J. Deignan, S. Lai, Z. Fu, C. Guimaraes, S. Shen, S. Li, S. Johnstone, S. Thibault, H. Xu, M. Cardozo, W. Shen, N. Walker, F. Kayser, Z. Wang, Structure-Guided Design, Synthesis, and Evaluation of Guanine-Derived Inhibitors of the eIF4E mRNA–Cap Interaction, *J. Med. Chem.*, **2012**, *55*, 3837-3851; c) Q. Dang, Y. Liu, D. K. Cashion, S. R. Kasibhatla, T. Jiang, F. Taplin, J. D. Jacintho, H. Li, Z. Sun, Y. Fan, J. DaRe, F. Tian, W. Li, T. Gibson, R. Lemus, P. D. van Poelje, S. C. Potter, M. D. Erion, Discovery of a Series of Phosphonic Acid-Containing Thiazoles and Orally Bioavailable Diamide Prodrugs That Lower Glucose in Diabetic Animals Through Inhibition of Fructose-1,6-Bisphosphatase, *J. Med. Chem.*, **2011**, *54*, 153-165.
15. H. Ni, W. L. Chan, Y. Lu**,** Phosphine-Catalyzed Asymmetric Organic Reactions, *Chem. Rev.*, **2018**, *118*, 9344-9411.
16. a) B.-G. Cai, J. Xuan, W.-J. Xiao, Visible light mediated C-P bond formation reactions, *Sci. Bull.*, **2019**, *64*, 337-350; b) J.-S. Zhang, L. Liu, T. Chen, L.-B. Han, Transition-Metal-Catalyzed Three-Component Difunctionalizations of Alkenes, *Chem. Asian J.* **2018**, *13*, 2277-2291.
17. For reviews on phosphorus compounds as ligands and directing groups, a) Y. N. Ma, S.-X. Li, S.-D. Yang, New Approaches for Biaryl-Based Phosphine Ligand Synthesis via P═O Directed C–H Functionalizations, *Acc. Chem. Res.* **2017**, *50*, 1480-1492 b) Z. Zhang, P. H. Dixneuf, J.-F. Soulé, Late-stage modifications of P-containing ligands using transition-metal-catalyzed C–H bond functionalization, *Chem. Commun.* **2018**, *54*, 7265-7280;
18. For selected reviews on P-containing materials, see: a) Organophosphorus π-Conjugated Materials, T. Baumgartner, R. Réau, *Chem. Rev.* **2006**, *106*, 4681-4727; b)

C. Queffelec, M. Petit, P. Janvier, D. A. Knight, B. Bujoli, Surface Modification Using Phosphonic Acids and Esters, *Chem. Rev.* **2012**, *112*, 3777-807; c) T. Baumgartner, Insights on the Design and Electron-Acceptor Properties of Conjugated Organophosphorus Materials, *Acc. Chem. Res.* **2014**, *47*, 1613-1622; d) R. Szucs, P. A. Bouit, L. Nyulaszi, M. Hissler, Phosphorus-Containing Polycyclic Aromatic Hydrocarbons, *ChemPhysChem* **2017**, *18*, 2618-2630.

19. S. Zhang, T. Chen,and Li-Biao Han, Palladium-Catalyzed Direct Decarbonylative Phosphorylation of Benzoic Acids with P(O)–H Compounds, *Eur. J. Org. Chem.* **2020**, 1148–1153.
20. H. Hopf, S. Narayanan, P. Jones, The preparation of new functionalized [2.2]paracyclophane derivatives with N-containing functional groups, *Beilstein J. Org. Chem.*, **2015**, *11*, 437-445.
21. D. C. Braddock, I. D. MacGilp, B. G. Perry, Improved Synthesis of (±)-4,12-Dihydroxy[2.2]paracyclophane and Its Enantiomeric Resolution by Enzymatic Methods: Planar Chiral (*R*)- and (*S*)-Phanol, *J. Org. Chem.*, **2002**, *67*, 8679-8681.
22. D. T. Glatzhofer, R. R. Roy, K. N. Cossey, Conversion of N-Aromatic Amides to O-Aromatic Esters, *Org. Lett.* **2002**, *14*, 2349-2352.
23. D. Xin, Y. Ma, F. He, Synthesis of new planar chiral [2.2]paracyclophane Schiff base ligands and their application in the asymmetric Henry reaction, *Tetrahedron Lett.*, **2010**, *21*, 333-338.
24. A. Collado, D. J. Nelson, S. P. Nolan, Optimizing Catalyst and Reaction Conditions in Gold(I) Catalysis–Ligand Development, *Chem. Rev.*, **2021**, *121*, 8559-8612.
25. J. Elzinga, M. Rosenblum, [2.2]Paracyclophane-iron(II) complexes-Synthesis and intramolecular charge-transfer interactions, *Organometallics*, **1983**, 1214-1219.
26. Z. Lu, T. Li, S. R. Mudshinge, B. Xu, G. B. Hammond, Optimization of Catalysts and Conditions in Gold(I) Catalysis Counterion and Additive Effects, *Chem. Rev.*, **2021**, *121*, 8452-8477.
27. C. C. Chintawar, A. K. Yadav, A. Kumar, S. P. Sancheti, N. T. Patil, Divergent Gold Catalysis: Unlocking Molecular Diversity through Catalyst Control, *Chem. Rev.*, **2021**, *121*, 8478-8558.
28. B.F.G. Johnson, C.M. Martin, P.J. Dyson, Ruthenium cluster-[2.2]paracyclophane complexes, *Coord. Chem. Rev.*, **1998**, *175*, 59-89.

29. M. Austeri, M. Enders, M. Nieger, S. Brase, [2.2]Paracyclophane–Triazolyl Monophosphane Ligands: Synthesis and Their Copper and Palladium Complexes, *Eur. J. Org. Chem.*, **2013**, 1667-1670.
30. A. Pradal, C.M. Chao, M. R. Vitale, P. Y. Toullec, V. Michelet, Asymmetric Au-catalyzed domino cyclization/nucleophile addition reactions of enynes in the presence of water, methanol, and electron-rich aromatic derivatives, *Tetrahedron*, **2011**, *67*, 4371-4377.
31. W. Wang, C. L. Ji, K. Liu, C.G. Zhao, W. Li, J. Xie, Dinuclear gold catalysis, *Chem. Soc. Rev.*, **2021**, *50,* 1874-1912.

Chapter 5

C-H Activation for the Remote Functionalization of Cyclic Amines.

5.1. An Overview of C-H Activation/Functionalization

Over the last few decades, chemists around the world have had tremendous success in transforming ubiquitous, but chemically inert, C-H bonds into synthetically useful products. This chemistry has revolutionized organic chemistry, streamlining synthesis and permitting new structural motifs to be prepared.[1a] Most isolated C-H bonds have low reactivity. This is due to the high strength of the bond (413 kJ/mol) and the similar electronegativities of carbon (2.5) and hydrogen (2.2), leading to a non-polar bond.[1b] There are several methods to achieve C-H activation, the one we are interested in involves the insertion of a transition metal into a C-H bond followed by functionalization (**Figure 5.1**).

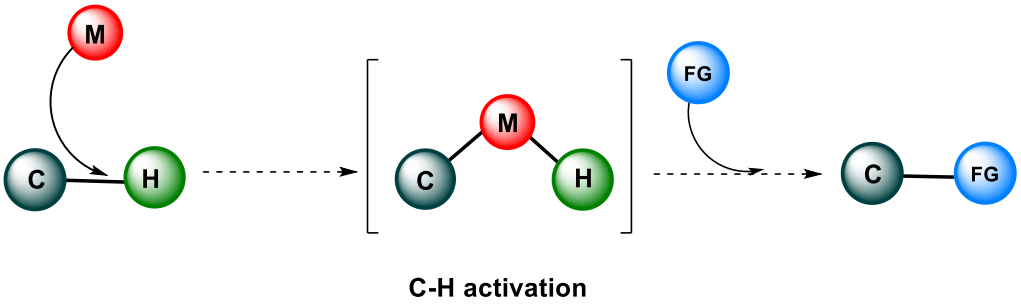

Figure 5.1: Generalized representation of transition metal-catalyzed C-H activation

Despite the successes, the selective activation and functionalization of C-H bonds still presents many opportunities as there are still limitations to current methods.[1c]

5.2. Role of Directing Groups in Selective C-H Activation/Functionalization

Directing groups allow the efficient and selective functionalization of unactivated C-H bonds by coordinating a metal and positioning it close to the desired C-H bond. Directing groups contain a Lewis basic functional group. The directing group facilitates C-H bond cleavage by inducing pre-association between the metal and the substrate (**Scheme 5.1**).[2a]

Scheme 5.1 gives an idealized pathway for directing group-mediated C-H activation. First, the directing group coordinates the metal, effectively intermolecularizing/internalizing the reaction. The position of the DG determines which C-H bond reacts by arranging the metal and bond in close proximity. This eases formation of the transition state & leads to the cyclometallation step. Functionalization can then occur. Finally, removal or elaboration of the DG leads to the desired compound.

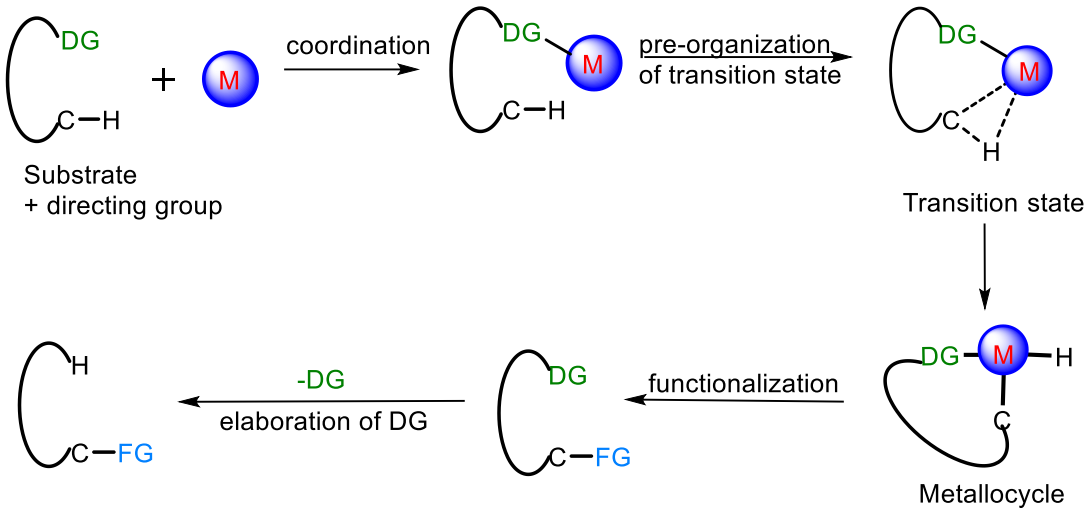

Scheme 5.1: Directing group-mediated C-H functionalization where DG = a directing group.

The directing group helps control site selectivity by positioning the metal close to the target C-H bond. It pre-organizes the reactants to facilitate metal insertion into the C-H bond.

5.3 Classification of Directing Groups

❖ 5.3.1 Monodentate Directing Groups

Monodentate directing groups can be categorized as X- and L-type donors (**Figure 5.2**). X are monoanionic, weak-directing groups that include polyfluoroanilides and hydroxamic acids.[3] L-Type monodentate auxiliaries or strong donors tend to be neutral nitrogen donors, such as pyridines, oxazolines, and thioamide based.[4]

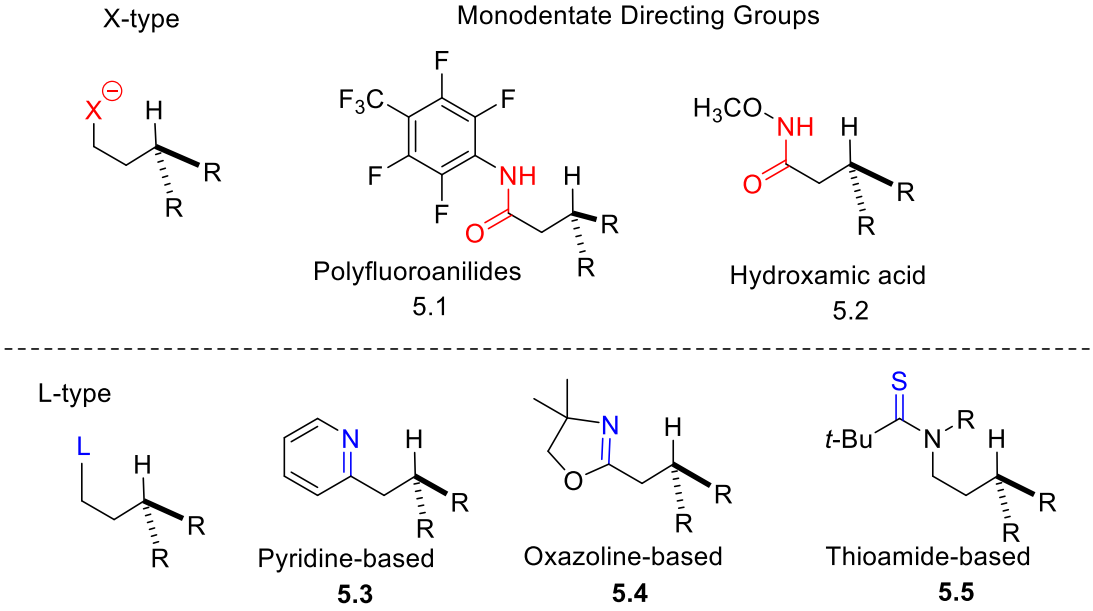

Figure 5.2: Monodentate directing groups

With few exceptions,[4c,5] monodentate groups allow functionalization of only primary unactivated sp^3 C-H bonds (**Scheme 5.2**). Secondary C-H bonds typically react only in the

presence of added ligands, and transformations often require high loadings of the palladium catalyst as well as more forcing conditions.

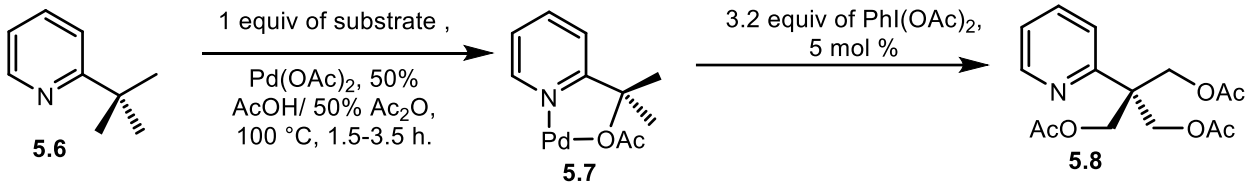

5.6 5.7 5.8

Scheme 5.2: Unactivated sp^3 C-H Bond Oxygenation using monodentate DG.

❖ **Bidentate Directing Groups:**

Bidentate directing groups are invariably strong donors comprising of a combination of both X- and L-type groups.[6a] Less common are those that contain only L-type donors (**Figure 5.3**). They are known to functionalize primary as well as secondary unactivated C-H bonds. In a limited number of examples, bidentate directing groups have permitted functionalization of tertiary C(sp^3)-H bonds.[6b]

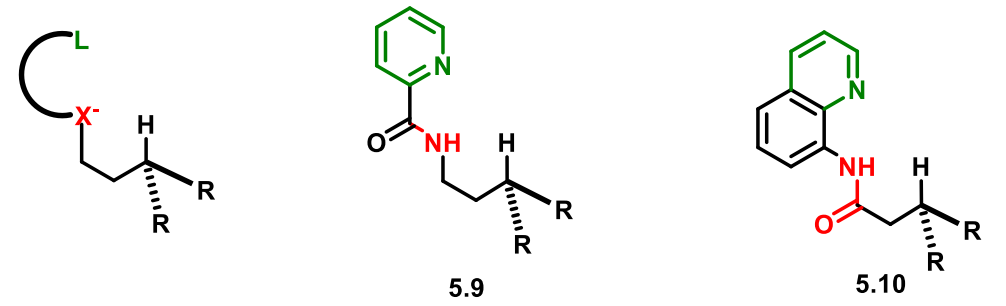

5.9 5.10

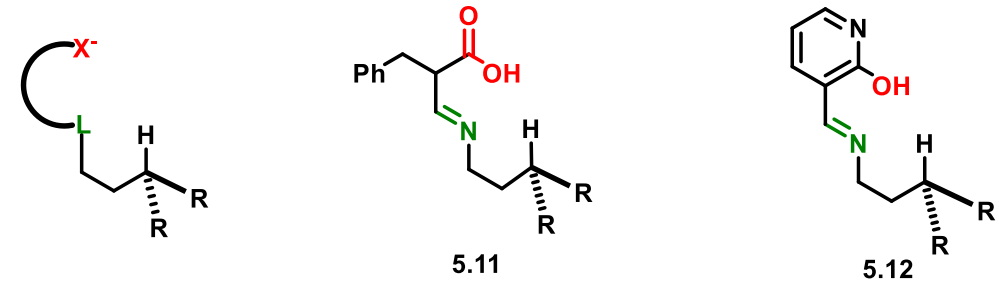

5.11 5.12

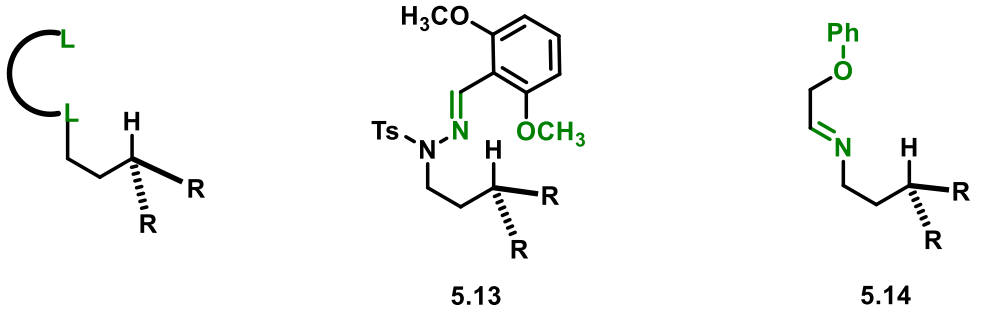

5.13 5.14

Figure 5.3: Bidentate directing groups

5.3 Concerted Metallation-Deprotonation (CMD)

Having identified the various types of directing groups, it is worth outlining the probable mechanism of functionalization. Palladium-catalyzed direct arylation is an emerging and efficient alternative to traditional metal-catalyzed cross-couplings in the construction of functionalized C-H bonds.[7-9] To predict substrate suitability and regioselectivity, however, will require a more complete understanding of the underlying physical parameters governing reactivity and selectivity across the broadest range of substrates possible. With palladium, several reaction pathways have been proposed including oxidative C-H insertion,[10] electrophilic aromatic substitutions (S_EAr),[11] Heck-like,[12] anionic cross-coupling, and concerted metallation-deprotonation (CMD).[13]

CMD involves a concerted six-membered transition state in which carboxylate, or another appropriate conjugate base transfers the proton while simultaneously facilitating the formation of palladacycle. The metallocycle is then free to undergo a variety of different transformations that result in the functionalized substrate (**Scheme 5.3**).

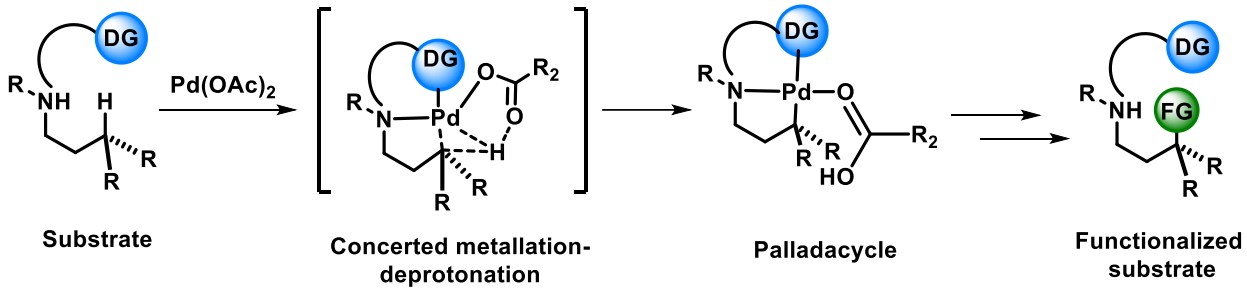

Scheme 5.3: Mechanism of concerted metallation-deprotonation

Formation of five-membered palladacycles is kinetically favored over the formation of the six-membered ring,[14] but the size of the chelate ring size can influence regioselectivity. The literature suggests that 5,5-bicyclic palladacycles are the most common. So, it will be helpful to understand the influence of chelate ring size to ensure regioselectivity with a different directing group that will have a 5,5-system and 6,5-system (**Figure 5.4**).

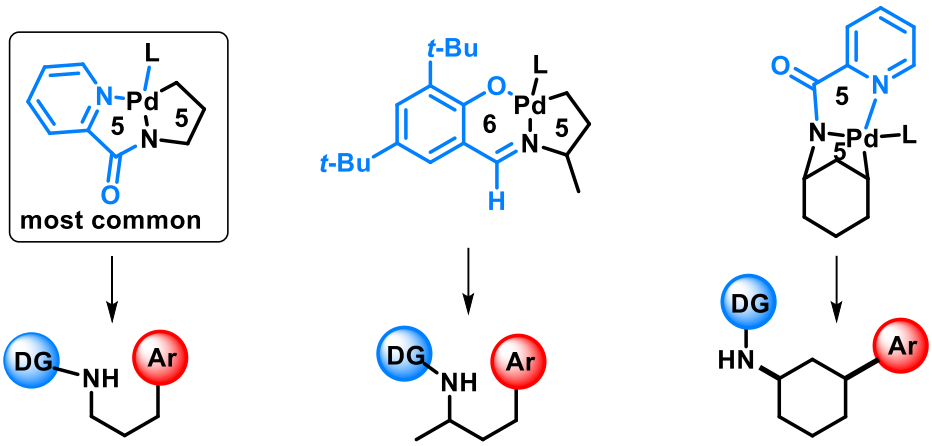

Figure 5.4: Influence of chelate ring on regioselectivity

5.4 Nitrogen Heterocycles - A key Structure in Pharmaceuticals

Nitrogen heterocycles are one of the most significant structural components present in the majority of pharmaceuticals.[15a] Among them, saturated cyclic amines are the most prevalent nitrogen ring system found in the majority of small drug molecules. They are present as a common building block in the active ingredients of various pharmaceuticals or agrochemicals. Some of the cyclic amines found in pharmaceuticals are shown below (**Figure 5.5**).[15b]

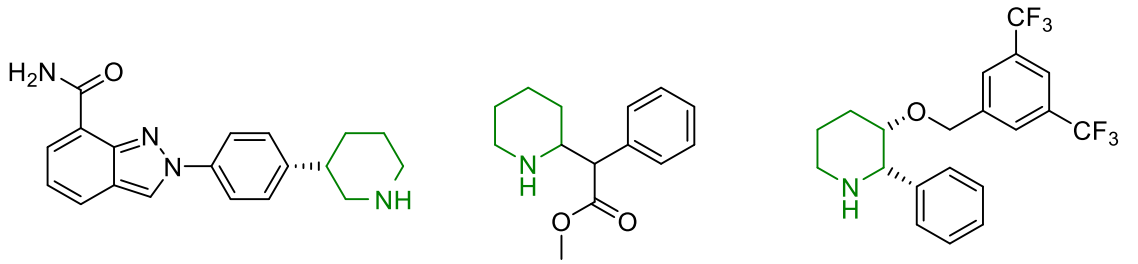

5.15
niraparib
(treats Ovarian cancer)

5.16
methyl phenidate
(treats ADHD)

5.17
L-733,060
(NK_1 receptor antagonist)

Figure 5.5: Saturated cyclic amines structures present in various pharmaceuticals with their applications

5.5. Review of Regioselective C-H Functionalization of Cyclic/Acyclic Amines

Based on the literature reviewed, it is found that the number of reports on the β- C-H bond activation/functionalization are very few as compared to α- and γ- C–H bond functionalization (**Figure 5.6**)

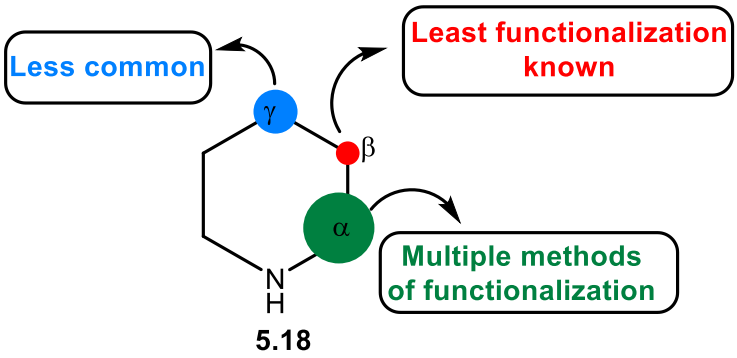

Figure 5.6: C-H Functionalization

5.5.1. α-C–H bond functionalization

This is the easiest site-selective functionalization observed. Seidel group[16] (**Scheme 5.4**) demonstrated the functionalization of the α-site of cyclic secondary amines through successive formation of lithiated amines, carbonyl agent-promoted hydride transfer, and imine trapping by organolithium nucleophiles. Presumably, in the process, an N-lithiated amine reduces the electron deficient ketone to form a lithium alkoxide and cyclic imine, via the transition state as shown in the **scheme 5.4**. The imine traps the organolithium reagent, providing an α-functionalized amine **5.22**.

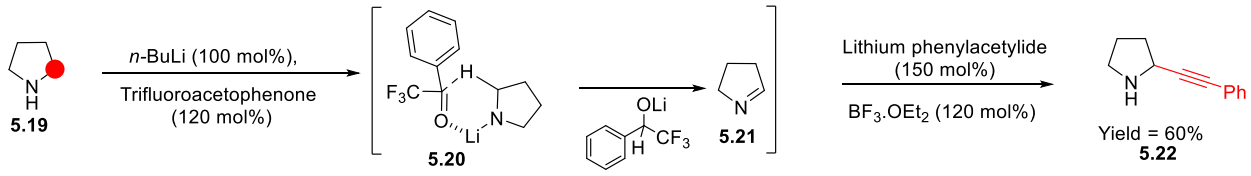

Scheme 5.4: α-C–H bond functionalization of secondary amines

Zhang *et al.*,[17] demonstrated a transition metal-catalyzed direct α-functionalization (**Scheme 5.5**) by employed iridium-catalyzed partial dehydrogenation as a substrate-activating strategy to achieve the α-C(sp^3)-H bond functionalization of the (hetero)aryl-fused cyclic secondary amines. As shown in Scheme 5.5, dehydrogenation of the piperidine-based amine-**5.23** formed imine by the action of iridium catalyst and oxidant. The imine then reacts with indole-**5.24** to form the desired product-**5.27**.

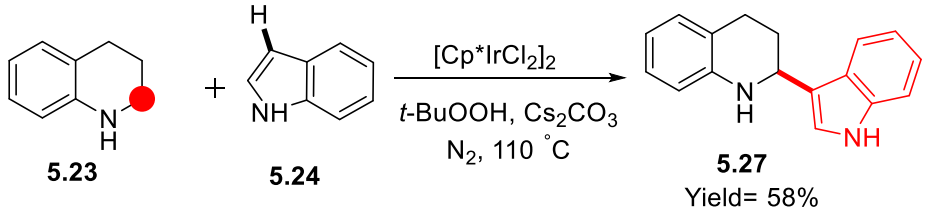

Scheme 5.5: Transition metal-catalyzed direct α-functionalization

Yu's group utilized directing group-assisted enantioselective α-C(sp^3)–H coupling of amines in the presence of a chiral phosphate anion, which permits the arylation of a diverse array of aliphatic amines through the use of a thioamide directing group (**Scheme 5.6**).[18]

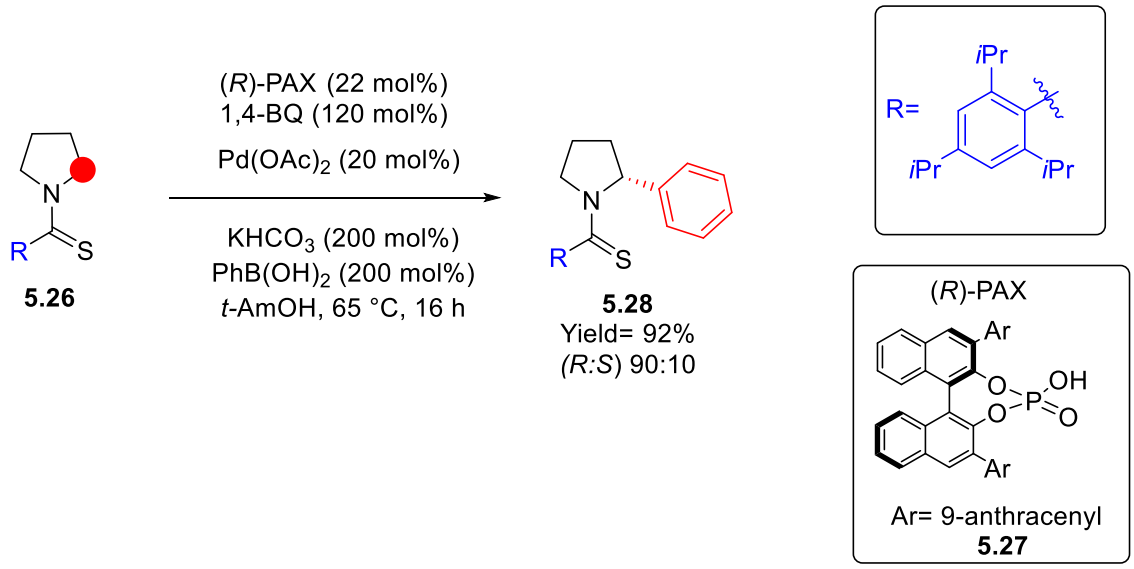

Scheme 5.6: Directing group-assisted enantioselective α-C(sp3)–H functionalization of amines

These examples show that there are many methods to functionalize α-C-H bonds.

5.5.2. β-C–H Bond Functionalization

Maes[19] (**Scheme 5.7**) reported regioselective C-H activation at the β-position by a directing group to an amine at C3.

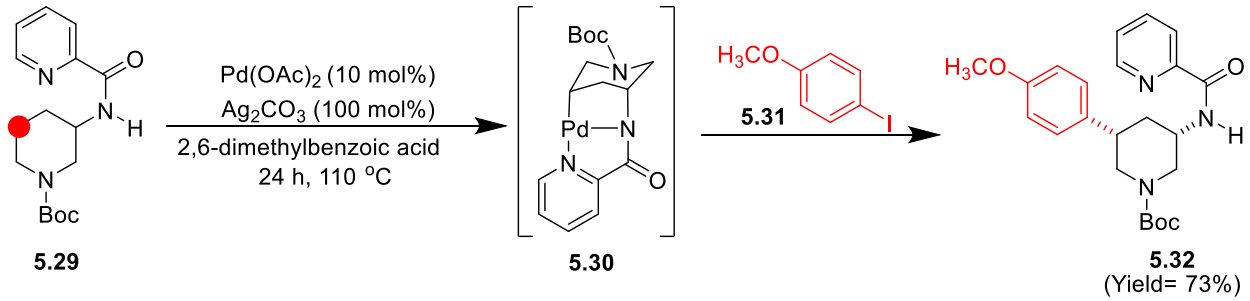

Scheme 5.7: β-C–H bond functionalization

This can be termed as indirect β-C-H bond activation as we need to first install a subsituent at C-3 position, which can then direct the functionalization at the β-position. The substrate scope with this methodology is limited as there must be a substituent at C3 to control functionalization at the β-position.

5.5.3. γ- & δ-C–H Bond Functionalization

The strong cooperative effect between the ligand and the transient directing group (TDG, made *in situ*) has led to the development of Pd(II)-catalyzed γ-methylene C(sp^3)–H heteroarylation and δ-C(sp^3)–H arylation of simple aliphatic amines with aryl iodides as the coupling partners (**Scheme 5.8**).[20] The choice of using substituted 2-pyridone as ligands was made as the ligand acts as an internal base to cleave the C–H bond. Also, the palladium-pyridone complex exhibit enhanced reactivity and broader heterocycle scope compared to palladium acetate.[20]

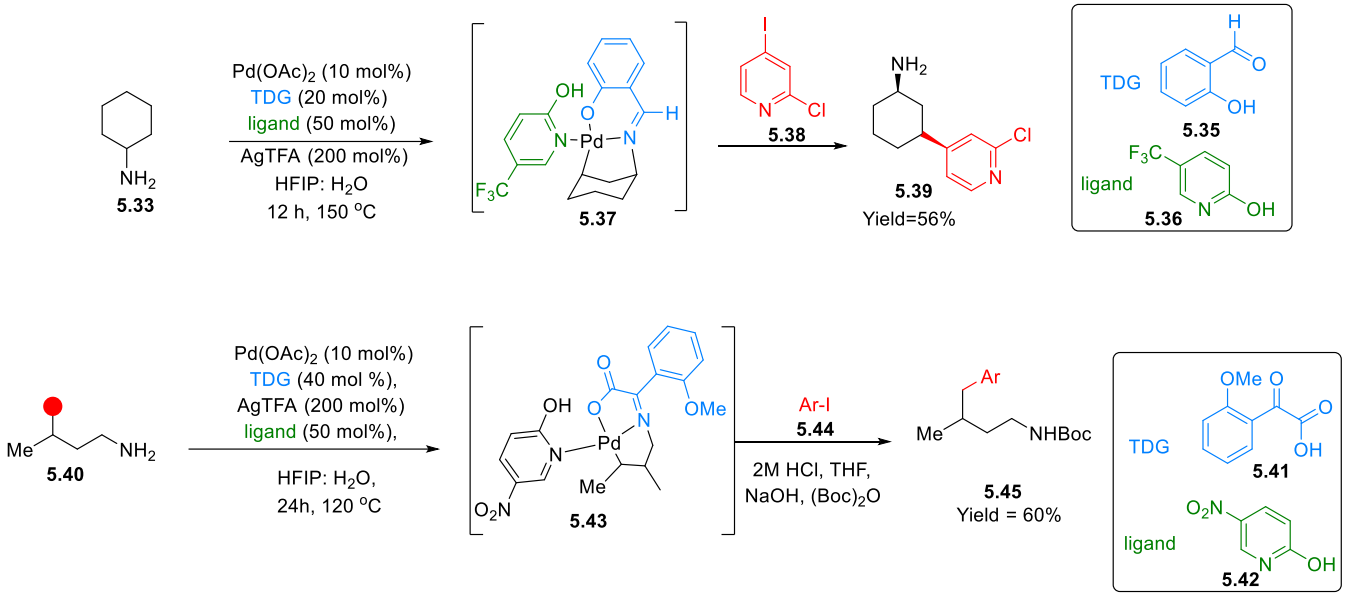

Scheme 5.8: γ- & δ-C–H bond functionalization

The literature clearly marks the gap for the direct activation of the remote β-C-H bond. Thus, this area offers a wider scope of research and development, but at the same time, can be challenging as none of the reports attempts direct functionalization.

5.6. Objective- C-H Activation of Cyclic Amines

Our objective was to selectively activate the remote β-C-H bond of nitrogen containing heterocycles. This would allow us to extend the substrate scope of these heterocycles. Piperidine is the most commonly used nitrogen heterocycle among U.S. FDA approved pharmaceuticals.[21] Therefore we started our work to activate and functionalize the β-C–H of piperidine (**Figure 5.7**).

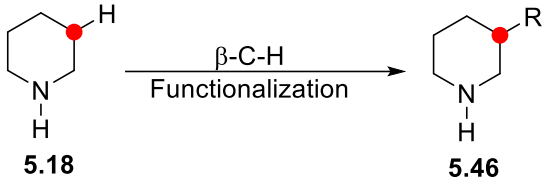

5.18 5.46

Figure 5.7: Our strategy to functionalize β-C-H bond of piperidine

Activation of β-C-H bond piperidine will be accomplished with the aid of directing group containing a donor atom directly attached to the ring nitrogen (**Figure 5.8**). This would allow forming the right-sized palladacycle, and will help in the easy removal of the DG after the bond activation.

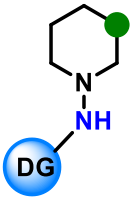

Figure 5.8: Selective remote β-C-H bond functionalization

So, the directing group should fulfill the following criteria in order to successfully functionalize the C-H bond with its help.

- We need a DG that would coordinate palladium and permit the formation of a 5-ring palladacycle.
- The DG should directly attach to the ring nitrogen of the heterocycle.
- Most importantly, the DG should be readily cleaved so that the desired products, without traces of the DG, could be isolated.

The literature reports have shown β-C-H bond activation of cyclohexylyamine. As a test control, a few directing groups will also be synthesized using cyclohexylamine as a substrate.[22] The use of two similar substrates with the only difference of one ring nitrogen will help us to compare the results and deduce the right inference regarding the role of that ring nitrogen. Following the synthesis of various directing groups, C-H activation and functionalization at the remote β-position will be performed using the different reaction conditions (**Scheme 5.9**).

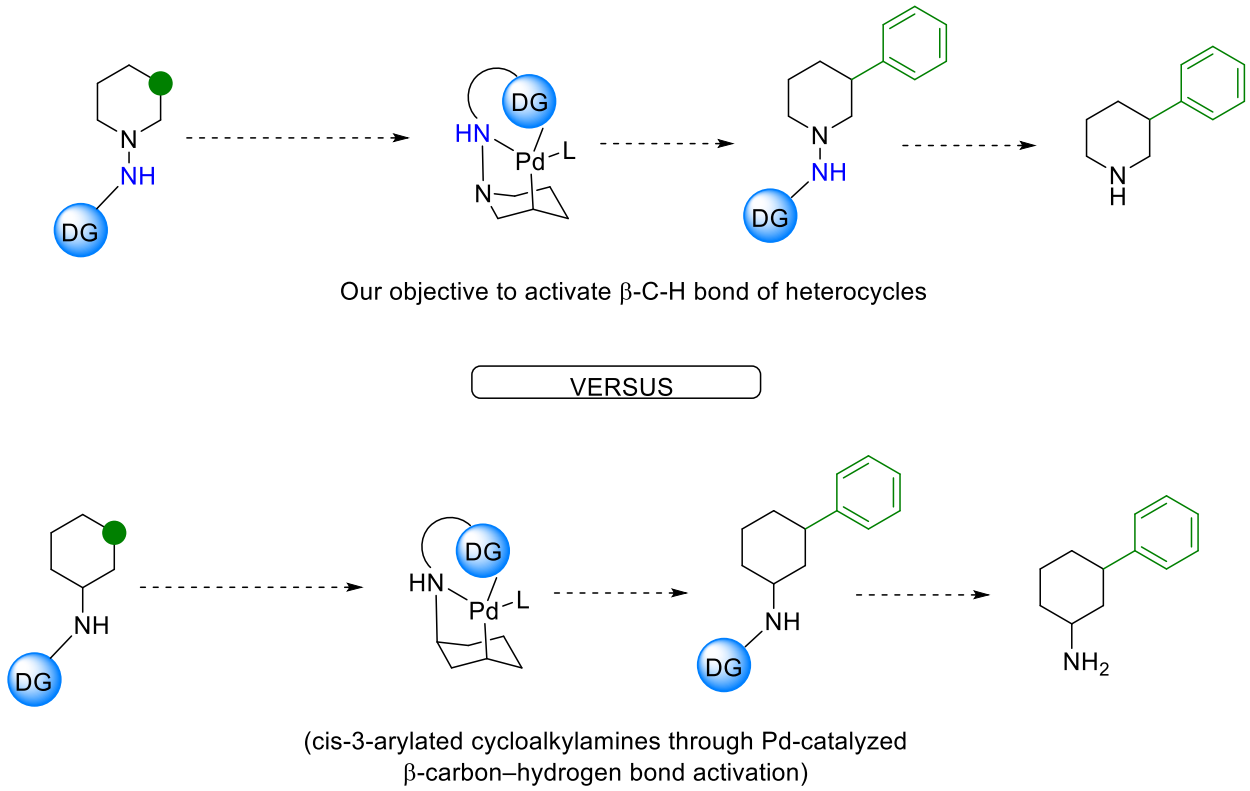

Scheme 5.9: Directing group strategy β-C-H bond functionalization

Hydrazines or hydrazones seem to fulfill these criteria. The second N coordinates the metal in the correct position while the weak N-N bond should allow easy removal of the DG. In addition, there has been an example of an acyclic hydrazone developed by Dong's group for the functionalization of unactivated primary β-C-H bonds of aliphatic amines (**Scheme 5.10**).[23] They sought to use an *in situ* formation and removal of the exo-type DG (with the π-bond of the DG outside the metallacycle) for the direct C-H activation of free primary amines.

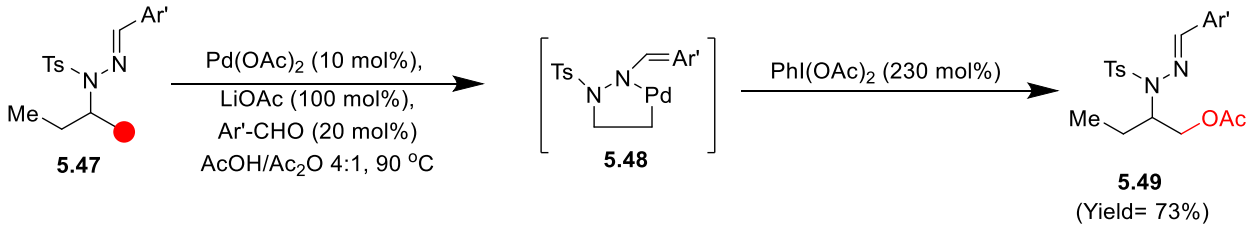

Scheme 5.10: β-C–H bond functionalization

5.7 Result & Discussion

5.7.1. Synthesis of Hydrazine-based Directing Groups

By adding a nitrogen atom to the piperidine nitrogen to form a hydrazine, we will place a directing group in such a position that it favors the formation of the 5-membered palladacycle with β-C–H bond as stated earlier. The directing group will be a hydrazide or hydrazone. There are different strategies to make the desired directing groups depending on their structure. These include the direct use of the commercially available saturated cyclic hydrazines 1-aminopiperidine followed by condensation with an acid derivative to furnish the hydrazide or hydrazine. The second route involves the building of rings on to existing hydrazine derivatives.

5.7.1a Synthesis of *N*-(piperidin-1-yl) Picolinamide

The picolinic acid auxiliary is a successful directing group for arylation of 3-position of cycloalkyl amines and other substrates as shown in our control experiment.[22] Therefore, our first target was to make a picolinamide-based directing group. Initially, we attempted the reaction of 1-aminopiperidine **5.50** with an acid chloride derivative of picolinic acid **5.51**. The reaction failed to give the desired hydrazide (**Scheme 5.11**).

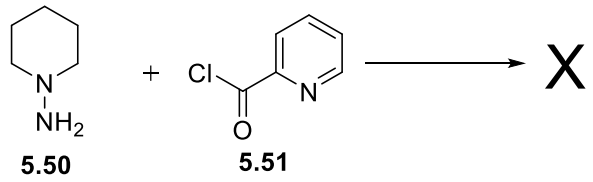

Scheme 5.11: Attempted synthesis of hydrazide DG

It is believed that the weak N-N bond of 1-aminopiperidine was cleaved before the desired condensation occured. Thus, we tried another route with milder conditions. Esterification of picolinic acid **5.52** with ethanol catalyzed with sulfuric acid followed by substitution with hydrazine hydrate. The resulting hydrazide **5.54** was treated with 1,5-dibromopentane **5.55** to furnish the desired hydrazide **5.56** (Scheme 5.12).[24, 25] The ^{1}H NMR peaks showing 4 aromatic peaks of two doublets and two triplets confirmed the pyridine moiety and 10 piperidine protons confirmed the formation, as well as the high resolution mass spectrum $[M+H]^{+}$ peak at 206.0713, confirmed the formation of the desired hydrazide.

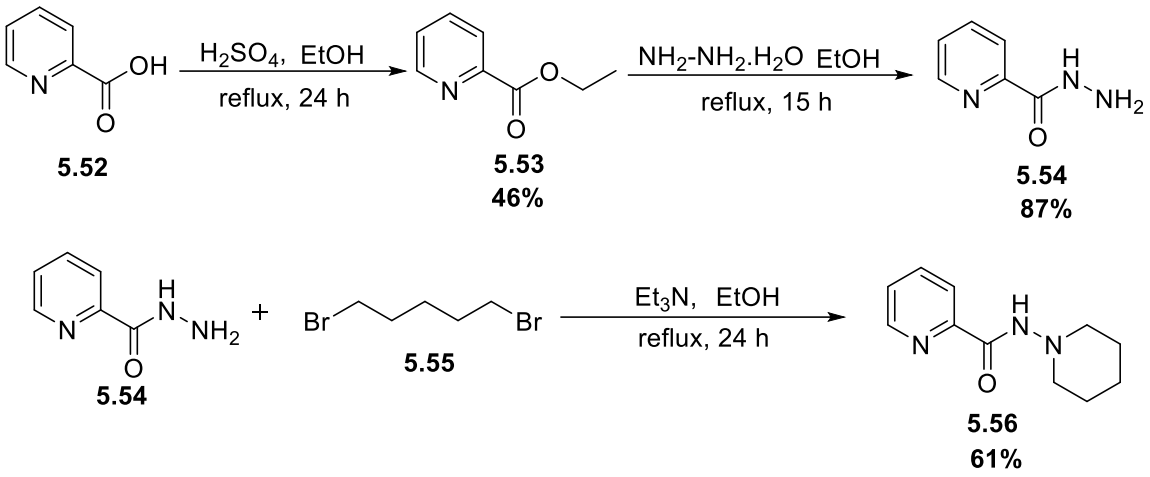

5.52 **5.53** 46% **5.54** 87%

5.54 **5.55** **5.56** 61%

Scheme 5.12: Synthesis of *N*-(piperidin-1-yl)picolinamide

5.7.1b Synthesis of (*E*)-2-(piperidin-1-ylimino)Acetic acid

The potential of carboxyl-directed C-H activation in developing C-C bond-forming reactions was demonstrated by Yu.[26] It involved a COOH directed Pd insertion into C-H bonds and subsequent oxidation. Encouraged by this, we decided to incorporate a carboxylic acid group in our hydrazine. The milder conditions were used to ensure that the N-N bond was not cleaved during the reaction. The condensation between 1-aminopiperidine and 2-oxoacetic acid gave the desired (*E*)-2-(piperidin-1-ylimino)acetic acid (**Scheme 5.13**).[27] The proton present next to imine was an easily identifiable one in proton NMR at 7.9 ppm apart from other piperidine protons. This helped us to confirm the formation of the desired proton. The (*E*)-conformation was assigned as (*E*)-selectivity is favored to avoid steric hindrance.

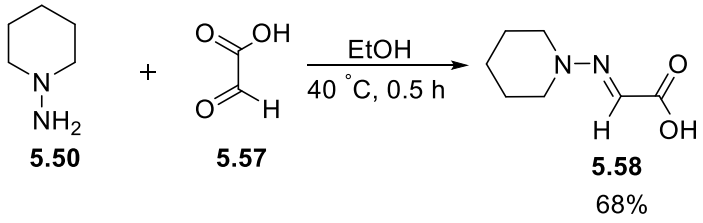

5.50 **5.57** **5.58** 68%

Scheme 5.13: Synthesis of (*E*)-2-(piperidin-1-ylimino)acetic acid

5.7.1c Synthesis of *(E)*-2-Phenyl-2-(piperidin-1-ylimino)acetic Acid

As stated before in section above, the potential of carboxyl-directed C-H activation, we thought to make another directing group having the carboxylic group and an additional phenyl ring instead of hydrogen. The incorporation of phenyl ring was done to increases the electron density of the system encouraging faster palladium insertion and also changes the steric environment. The two-step synthesis to yield desired directing group started with the

oxidation of acetophenone **5.59** with selenium dioxide to give 2-oxo-2-phenylacetic acid **5.60** which was further condensed with 1-aminopyridine **5.50** under milder conditions as used previously to give *(E)*-2-phenyl-2-(piperidin-1-ylimino)acetic acid **5.62** (**Scheme 5.14**).[27]

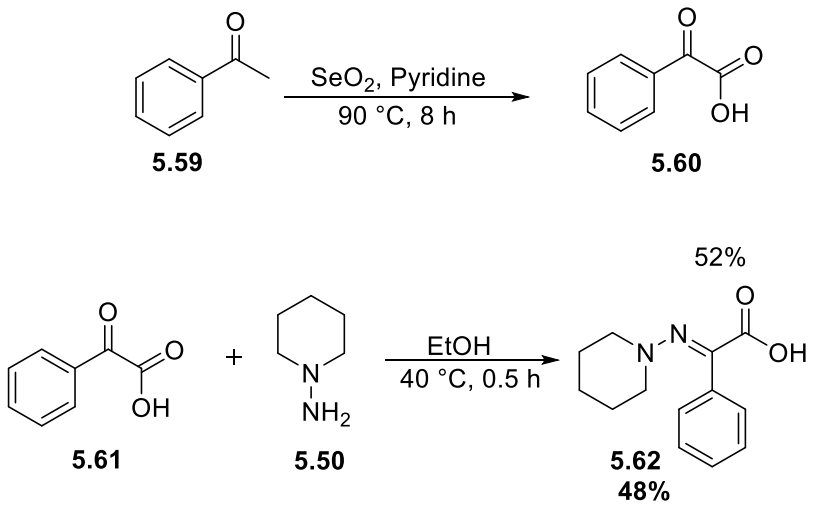

Scheme 5.14: Synthesis of *(E)*-2-phenyl-2-(piperidin-1-ylimino)acetic acid

5.7.1d Synthesis of (*E*)-2-((Piperidin-1-ylimino)methyl)phenol

Salicyaldehydes have been used as transient directing groups (TDG) for C-H functionalization.[13] Transient directing groups are formed in situ by a reversible reaction and allow a sub-stoichiometric quantity of directing group to functionalize suitable substrates. However, competitive binding interactions among multiple reaction components (TDG itself, substrate, and substrate-TDG adduct) with the palladium catalyst often lead to the formation of multiple unreactive complexes. It was decided to pre-form the hydrazone for two reasons: Firstly, it removes the complication of multiple reaction cycles occurring in our reaction, and secondly, we were unsure that a hydrazone would hydrolyze under the reaction conditions. As a result, we decided to make the hydrazone in a separate reaction by condensing the salicylaldehyde with hydrazine and used that group to direct the desired C-H functionalization. Keeping in mind the N-N bond, the milder experimental procedure was undertaken to avoid the N-N bond cleavage. The condensation between 1-aminopiperidine **5.50** and 2-hydroxybenzaldehyde **5.63** gave the desired (*E*)-2-((piperidin-1-ylimino)methyl)phenol **5.64** (**Scheme 5.15**).[27] The downfield proton next to imine nitrogen with δ value 7.69 as well as mass spectrum $[M+H]^+$ 205.2831 confirmed the formation of the desired product.

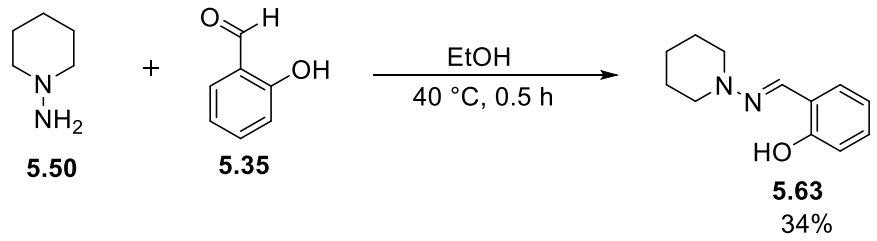

Scheme 5.15: Synthesis of (*E*)-2-((piperidin-1-ylimino)methyl)phenol

5.7.1e Synthesis of (*E*)-2,4-Di-*tert*-butyl-6-((piperidin-1-ylimino)methyl)phenol

Yada[40] reported that a bulky salicylaldehyde was key to the direct activation of C-H bond. The use of *tert*-butyl group provides a buttressing effect over simple salicyladehydes causing a sterically controlled reaction. We thought to use these bulky directing groups for our work apart from simple salicyaldehyde based hydrazones. The condensation between 1-aminopiperidine and 3,5-di-tert-butyl-2-hydroxybenzaldehyde gave the desired (*E*)-2,4-di-tert-butyl-6-((piperidin-1-ylimino)methyl)phenol (**Scheme 5.16**).[27] The desired product was confirmed by the NMR characterization. The peaks of two *t*-Bu groups proton were identified at 1.45 ppm and 1.31 ppm with the integration of nine each. Apart from this, singlet peak of proton adjacent to imine nitrogen at 7.75 ppm were observed apart from the phenyl peaks and piperidine peaks.

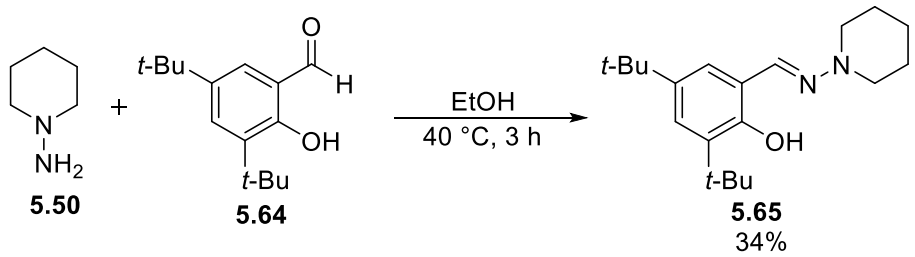

Scheme 5.16: Synthesis of (*E*)-2,4-di-*tert*-butyl-6-((piperidin-1-ylimino)methyl)phenol

5.7.1f Synthesis of (*Z*)-2-([2.2]Paracyclophane-4-yl)-2-(piperidin-1-ylimino)acetic acid

The rationale behind using substituted [2.2]paracyclophanes is the isolation of the enantiopure product at the end. The use of chiral auxiliary (substituted [2.2]paracyclophane) in this methodology, if made, will have the possibility of it being used as a chiral auxiliary that would yield a regioselective as well as the enantioselective functionalized product.

The two-step synthesis to yield the desired directing group started with oxidation of 4-acetyl[2.2]paracyclophane (synthesized previously by a co-worker in the lab) with selenium

dioxide to give 2-([2.2]paracyclophane-4-yl)-2-oxoacetic acid which was further condensed with 1-aminopiperidine to give 2-([2.2]paracyclophane-4-yl)-2-(piperidin-1-ylimino)acetic acid (**Scheme 5.17**).[27,28]

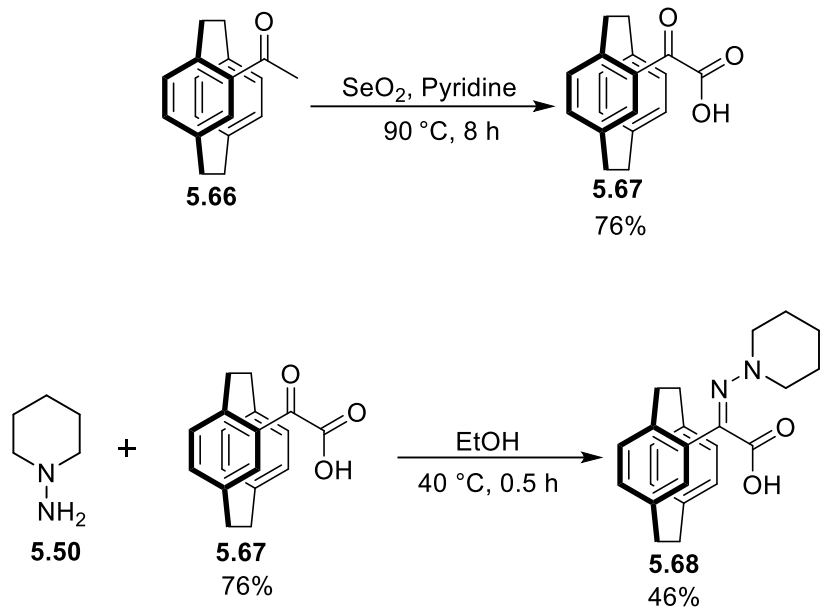

Scheme 5.17: Synthesis of (*Z*)-2-([2.2]paracyclophane-4-yl)-2-(piperidin-1-ylimino)acetic acid

5.7.2 Synthesis of Cyclohexyl Amine-Based Directing Groups

To understand the influence of the ring nitrogen in the hydrazine-based directing group, we synthesized several models that lacked the challenging hydrazine nitrogen. To achieve this, we used cyclohexylamine instead of 1-aminopiperidine. This would give some clue as to whether the directing group or the ring nitrogen was a problem under each set of reaction conditions.

The following **table 5.1** shows the synthesized hydrazine/hydrazone-based DGs and their cyclohexyl amine-based counterparts.

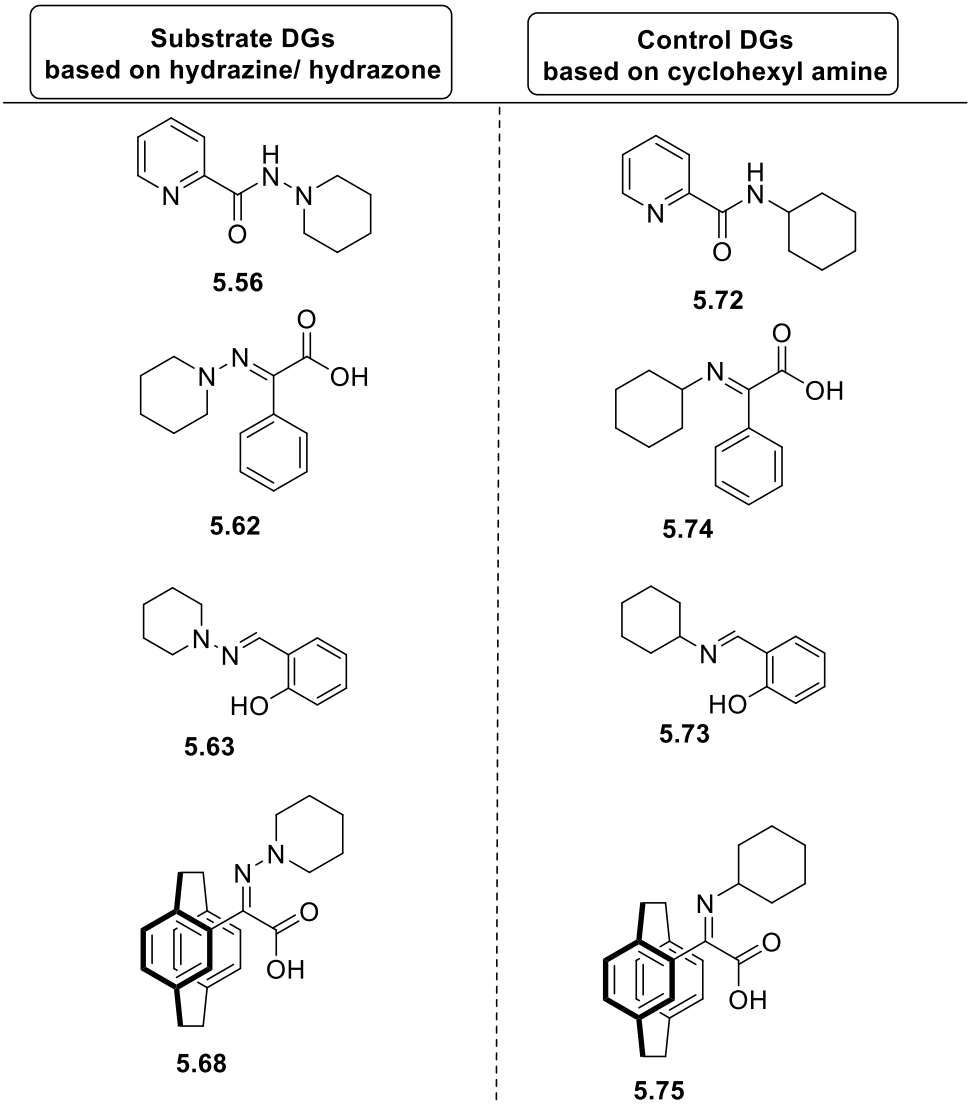

Table 5.1: Various synthesized DGs

5.7.2a Synthesis of *N*-(Piperidin-1-yl)benzamide

The first control substrate was made from the esterification of picolinic acid **5.52** with ethanol catalyzed with sulfuric acid followed by substitution with hydrazine hydrate. The resulting hydrazide **5.54** was treated with 1,5-dibromopentane **5.55** to furnish the desired hydrazide **5.56** (Scheme 5.12).[24, 25] The ^{1}H NMR peaks showing 5 aromatic peaks of two doublets and three triplets confirmed the pyridine moiety and 10 piperidine protons confirmed the formation, as well as the high resolution mass spectrum $[M+H]^{+}$ peak at 205.0878, confirmed the formation of the desired hydrazide.

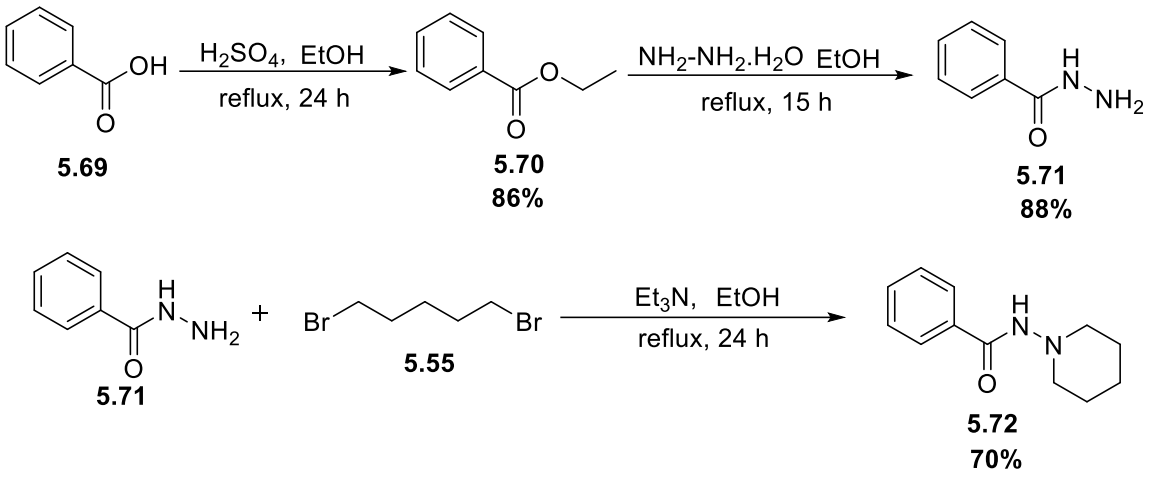

Scheme 5.18: Synthesis of *N*-(piperidin-1-yl)benzamide

5.7.2b Synthesis of (*E*)-2-((Cyclohexylimino)methyl)phenol

The next substrate was made from cyclohexylamine **5.33** and salicyladehyde **5.63**. The condensation between cyclohexylamine and 2-hydroxybenzaldehyde under the same reaction conditions as used with 3.1.3 gave the desired (*E*)-2-((piperidin-1-ylimino)methyl)phenol **5.75** (**Scheme 5.19**).[27] The crude product isolated was pure enough and did not need any further purification. The yield was 97% (crude yield). The characterization was based on comparison of the similar peaks observations made on ^{1}H-NMR of its hydrazone counterpart.

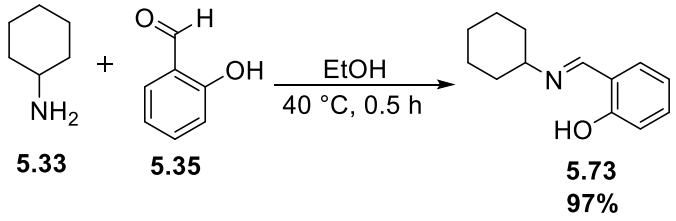

Scheme 5.19: Synthesis of (*E*)-2-((cyclohexylimino)methyl)phenol

5.7.2c Synthesis of (*E*)-2-(Cyclohexylimino)-2-phenylacetic Acid

The second control substrate was made from cyclohexylamine and 2-oxo-2-phenylacetic acid. The condensation between cyclohexylamine and 2-oxo-2-phenylacetic acid gave the desired (*E*)-2-(cyclohexylimino)-2-phenylacetic acid phenol (**Scheme 5.20**).[27,28]

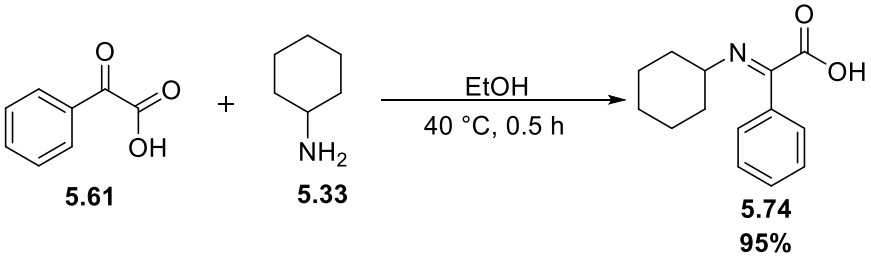

Scheme 5.20: Synthesis of (*E*)-2-(cyclohexylimino)-2-phenylacetic acid

The NOESY spectrum (**Figure 5.9**) confirmed the geometry of the structure as *E*-isomer as It was seen that H-14 had interaction with H-3, H-4 and H-8 aromatic protons. This is only possible if the configuration is *E*.

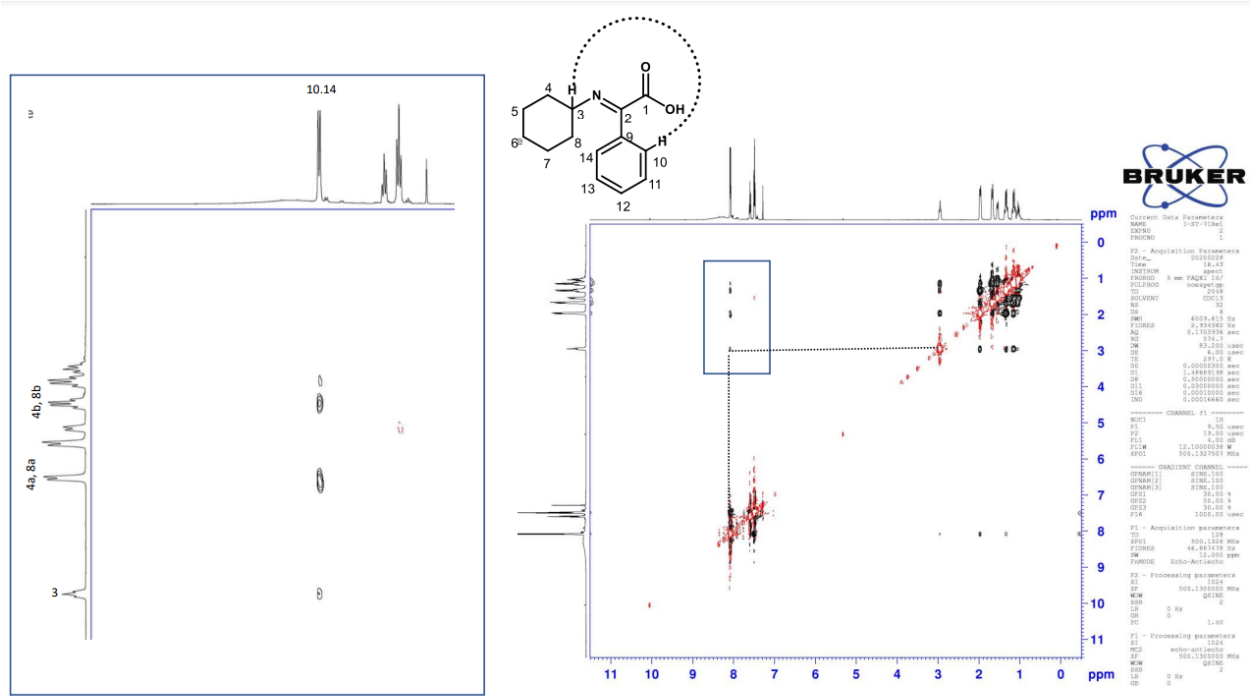

The NOESY correlation of H-14 with H-3, H-4 and H-8 confirms the geometry of structure as '*E*'-

Figure 5.9: NOESY correlation of 5.76

5.7.2d Synthesis of (*Z*)-2-([2.2]Paracyclophane-4-yl)-2-(cyclohexylimino)acetic Acid

This precursor was synthesized using cyclohexylamine-based substrate so that the results can be compared with the directing group synthesized in **5.7.1f**. The condensation between cyclohexylamine **5.33** and 2-([2.2]paracyclophane-4-yl)-2-oxoacetic acid **5.68** gave the desired synthesis of (*Z*)-2-([2.2]paracyclophane-4-yl)-2-(cyclohexylimino)acetic acid **5.77**. (**Scheme 5.21**).[27] The isolated yield of the product was 62% and was confirmed by ^{1}H-NMR. The downfielded peak at 6.91 ppm of the proton of [2.2]paracyclophane adjacent to the substitution is characteristic apart from other paracyclophane protons.

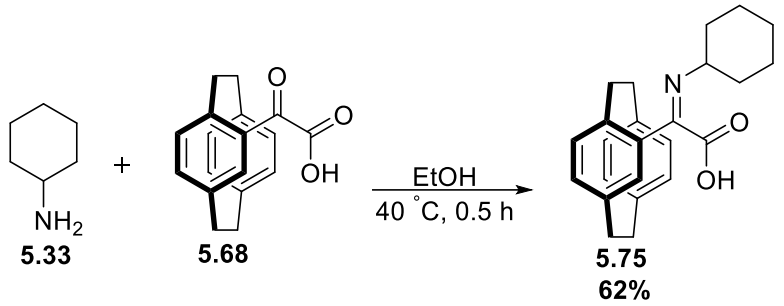

Scheme 5.21: Synthesis of (*Z*)-2-([2.2]paracyclophan-4-yl)-2-(cyclohexylimino)acetic acid

5.8 Model Study of Cyclohexyl Amine-Based Substrate with Picolinamide as a Directing Group

A model study with *N*-cyclohexylpicolinamide was carried out before testing our hydrazine-based directing groups. This study served two purposes, firstly it allowed us to confirm that literature C-H activation could be performed, and, secondly, it would also reveal any problems with the hydrazine-based systems. The starting material was consumed completely after 48 h (**Scheme 5.22**).[22]

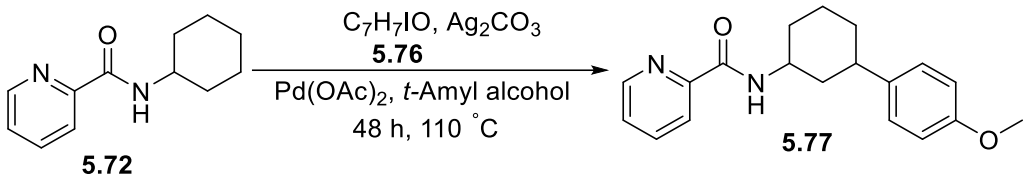

Scheme 5.22: Model study of cyclohexyl amine-based substrate with picolinamide as a directing group

The new spot observed on TLC was confirmed to be the desired product after comparison with the reference (already synthesized by one of the co-workers). The crude yield of the product was 70%. Additionally, the crude ^{1}H-NMR recorded has all the desired peaks that were present in the reference compound. These observations confirmed the usefulness of the conditions used for C-H activation. No further characterizations were done.

5.9 C-H Activation of Cyclic Amines Using Hydrazine-Based Directing Groups

Fascinated by the positive results obtained by the model study conducted with cyclohexylamine, we started our work on a hydrazine-based system for selective functionalization of the β- C-H.

Attempted studies and experiments that were performed are illustrated below.

5.9.1 Attempted Synthesis of *N*-(3-(4-Methoxyphenyl)piperidin-1-yl)picolinamide

We first tried the same reaction conditions used in our model study[22] as shown in **Scheme 5.23**.

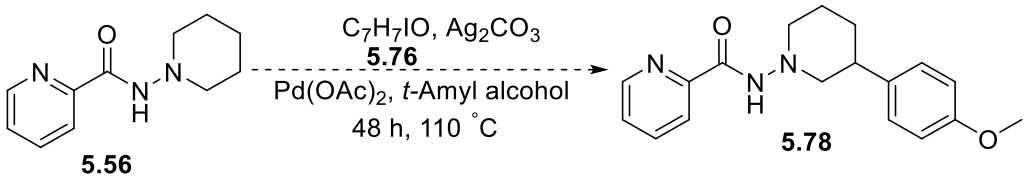

Scheme 5.23: Attempted synthesis of *N*-(3-(4-methoxyphenyl)piperidin-1-yl)picolinamide

However, the reaction failed to give the desired functionalization and the starting material decomposed during the reaction.

So, we looked for some milder conditions as well as use of oxidants and additives. Various reaction conditions[29a-g] using different combinations of additives/ligands, solvents, temperature and time were put to use for the successful formation of the desired product 5.80. (**Scheme 5.24**).

Different additives and oxidants are shown in the box below, that gave successful other C-H functionalization.

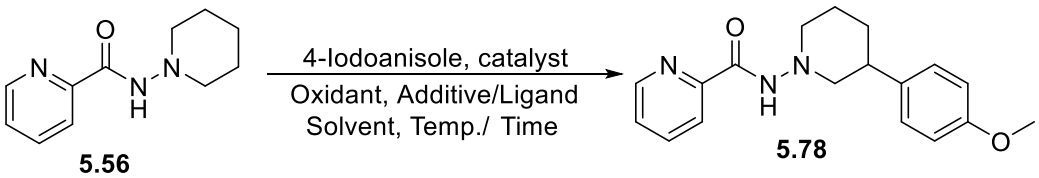

Scheme 5.24: Attempted synthesis of *N*-(3-(4-methoxyphenyl)piperidin-1-yl)picolinamide

Entry	4-Iodo anisole (mol%)	Base (mol%)	Oxidant (mol%)	Solvent	Additive/ Ligand (mol%)	Catalyst (mol%)	Temp/Time	Inference
1[a]	200		Ag_2CO_3 (150)	*t*-AmOH		$Pd(OAc)_2$ (20)	110 °C, 48 h	Decomposed
2[b]	150		Ag_2CO_3 (100)	*t*-BuOH	*o*-toluic acid	$Pd(OAc)_2$ (10)	110 °C, 24 h	SM returned.
3[c]	130		Ag_2CO_3 (150)	DCE	PivOH (50)	$Pd(OAc)_2$ (5)	100 °C, 24 h	SM returned.
4[d]	200		Ag_2CO_3 (150)	Toluene	N-Ac-leu (100)	$Pd(OAc)_2$ (10)	100 °C, 24 h	Decomposed
5[e]	400	CsOPiv (400)	$CuBr_2$ (10)	*t*-AmOH		$Pd(OAc)_2$ (10)	140 °C, 24 h	Decomposed
6	400	CsOPiv (110)	Ag_2CO_3 (150)	neat		$Pd(OAc)_2$ (5)	150 °C, 24 h	Decomposed
7[f]	150	K_2CO_3 (200)	Ag_2CO_3 (150)	Toluene	PivOH (30)	$Pd(OAc)_2$ (5)	130 °C, 24 h	Decomposed
8	130	CsOPiv (200)	Ag_2CO_3 (150)	DCE		$Pd(OAc)_2$ (5)	120 °C, 24 h	SM returned.
9	400	CsOPiv (130)	Ag_2CO_3 (200)	Toluene	PivOH (50)	$Pd_2(dba)_3$ (5)	140 °C, 24 h	Decomposed
10	130		Ag_2CO_3 (200)	Toluene	PivOH (50)	$Pd_2(dba)_3$ (5)	140 °C, 24 h	Decomposed
11	130		Ag_2CO_3 (200)	HFIP	PivOH (50)	$Pd(OAc)_2$ (5)	140 °C, 24 h	Decomposed
12	130		Ag_2CO_3 (200)	Toluene	PivOH (50)	$Pd(OAc)_2$ (5)	140 °C, 24 h	Decomposed
13[g]	200	KOAc (180)	TBAF (200)	AcOH		$Pd(OAc)_2$ (5)	120 °C, 24 h	SM returned.
14	200	KOAc (180)	TBAF (200)	*t*-AmOH		$Pd(OAc)_2$ (5)	120 °C, 24 h	SM returned.
15[h]	120		AgOAc (200)	AcOH		$Pd(OAc)_2$ (10)	120 °C, 24 h	SM returned.

Table 5.2: Various combinations used for the attempted synthesis of *N*-(3-(4-methoxyphenyl)piperidin-1-yl)picolinamide

In total, 15 different combinations were attempted with above reagents. Disappointingly, none of the conditions worked for our DG. In most of the cases, the reaction mixture was decomposed. The rest gave the starting material unreacted. This gave us idea that there is problem in palladium insertion, as we are getting the starting material back, or the reaction conditions are too harsh for our DG to survive the reaction.

After the failure to achieve desired C-H activation with the reaction conditions used in model study, we turned to different synthesized DGs We then thought to use the other synthesized directing groups to check their utility in accomplishing the desired selective functionalization of the β-C-H.

5.9.2 Attempted Synthesis of (*E*)-2-(((3-(4-Methoxyphenyl)piperidin-1-yl)imino)methyl) phenol

We then thought to use the other synthesized directing groups to check their utility in accomplishing the desired selective functionalization of the β-C-H.[22,30a,b]

Initial reaction conditions were same as that were used for the model study. This directing group also could not get success in forming the right product and reaction decomposed after 24 h of the reaction (**Scheme 5.25**).

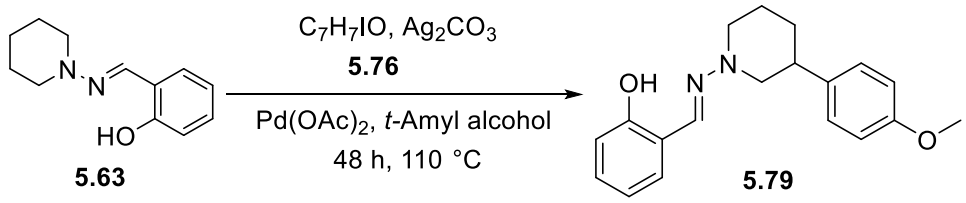

Scheme 5.25: Attempted synthesis of (*E*)-2-(((3-(4-methoxyphenyl)piperidin-1-yl)imino)methyl)phenol

Entry	4-Iodo anisole (mol%)	Base (mol%)	Oxidant (mol%)	Solvent	Additive/ Ligand (mol%)	Catalyst (mol%)	Temp/ Time	Inference
1[a]	200		AgTFA (200)	HFIP:H_2O	2-pyridone (50)	$Pd(OAc)_2$ (10)	150 °C, 24 h	No-reaction, SM returned.
2[b]	300	Na_2CO_3 (100)	Ag_2CO_3 (300)	AcOH	2-pyridone (20)	$Pd(OAc)_2$ (10)	100 °C, 24 h	No-reaction, SM returned.
3	130	Na_2CO_3 (150)	Ag_2CO_3 (300)	HFIP	2-pyridone (20)	$Pd(OAc)_2$ (5)	100 °C, 24 h	No-reaction, SM returned.

Table 5.3: Various combinations used for the attempted synthesis of (*E*)-2-(((3-(4-methoxyphenyl)piperidin-1-yl)imino)methyl)phenol

After this failure with our second DG, we tested other directing groups with hydrazine/hydrazone-based as well as the synthesized cyclohexylamine-based, to check if any one gave the desired β-C-H functionalization.

5.9.3 Attempted Synthesis of (*E*)-2-(((3-(4-Methoxyphenyl)piperidin-1-yl)imino)methyl) Phenol

The following **Scheme 5.26** shows the various DGs that were used for the functionalization.

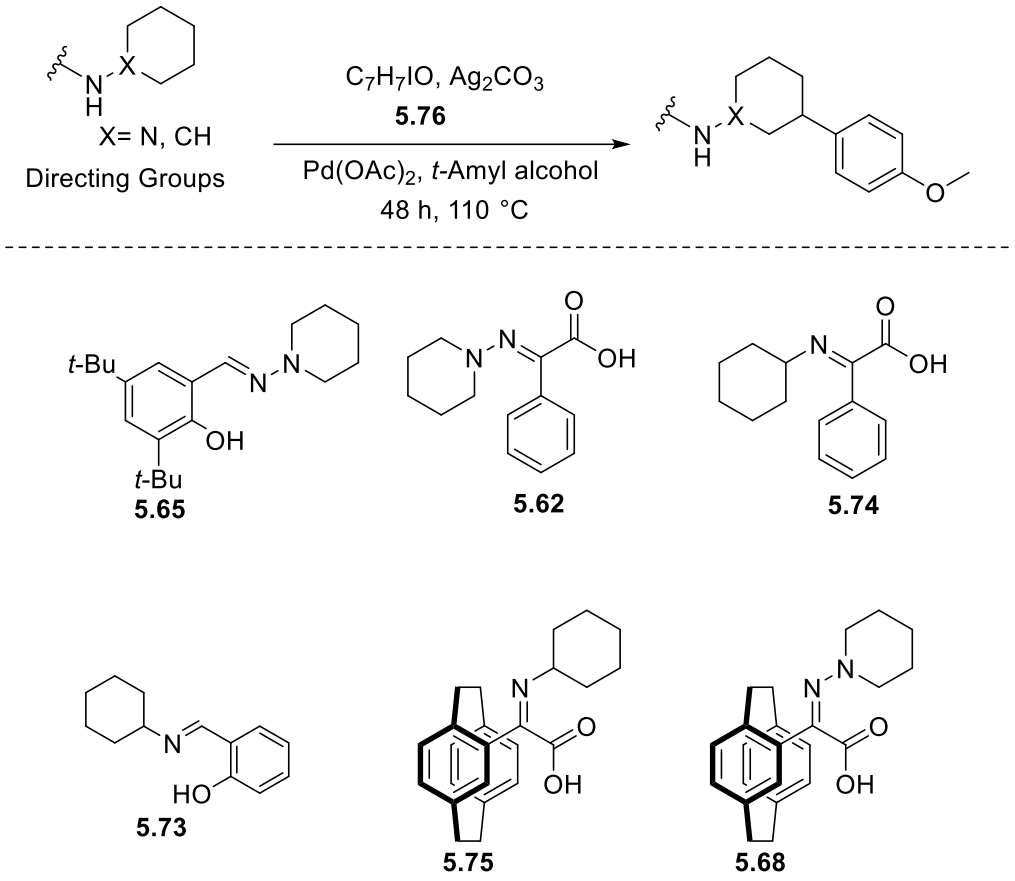

Scheme 5.26: Attempted synthesis with various synthesized DGs using model study conditions.

The results were disheartening and none of the above mentioned DGs worked successfully utilizing the same conditions that were used in the model study.

It is well clear by now, that the functionalization is unsuccessful for both the groups od DGs. Except for the model study, none of the reaction gave positive results.

The loss of the starting material through decomposition if we kept the reaction for the longer time, or the return of the starting material were the only two possibilities realized after utilizing multiple reaction conditions with various combinations of additives, oxidants, and solvents. This shows that how challenging and difficult this C-H activation actually is. The fact that only one set of reaction condition yielded the desired activation, shows the specificity of the reaction.

5.10 Transient Directing Group Strategy

Getting no positive results from the current strategy for the desired selective functionalization of the β-C-H, it was thought to use a different known strategy of using transient directing group.[30] The transient directing groups are advantageous for transition metal-catalyzed C-H activation due to non-installation and removal of exogenous directing groups. Control substrate, cyclohexylamine, was used to test the efficiency of this strategy (**Scheme 5.27**).[15] We decided to try known methodology from literature in our lab. Once that methodology was successful, next step was to apply this methodology on our challenging substrate.

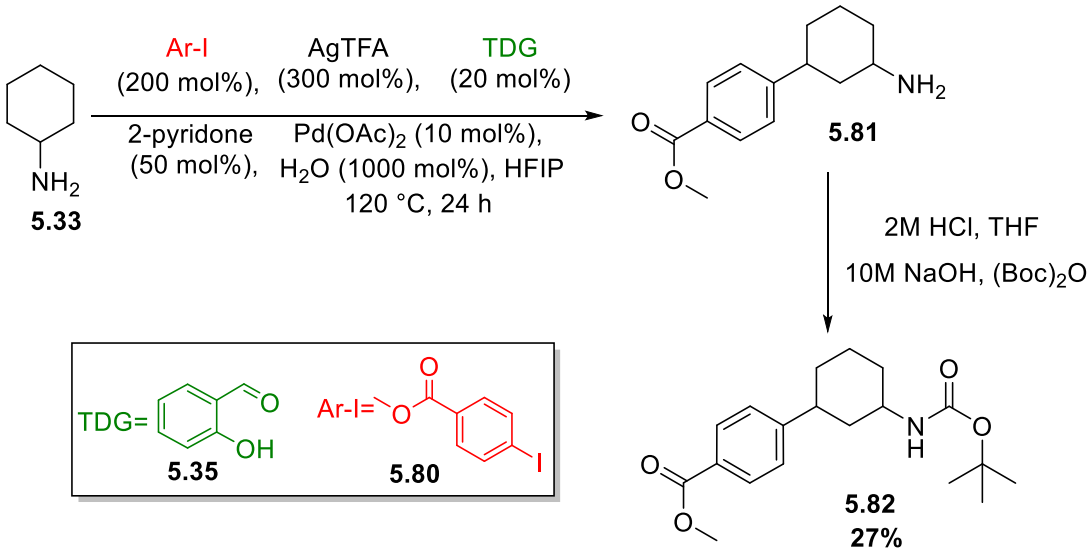

Scheme 5.27: Transient directing group strategy attempted with cyclohexylamine as a substrate

The yield obtained was 27% versus 39% reported in the literature using the same ligand but different aryl iodide. Though the conditions proved to work for this cyclohexylamine, we failed to reproduce the above conditions to work on our piperidine based system (**Scheme 5.28**).

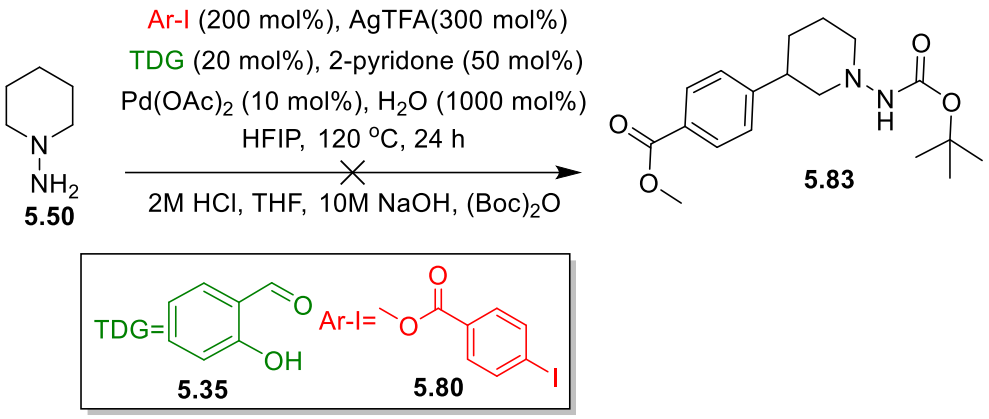

Scheme 5.28: Transient directing group strategy attempted with 1-amino piperidine as substrate

With the problems associated with the C-H activation of piperidine, it was decided to use C-H activation in the resolution of [2.2]paracyclophane derivatives, chemistry that our group is currently developing.

5.11 Conclusion

Taking hints from the literature, we started the first phase of our project. The synthesis of various directing groups with the piperidine-based substrate as well as control cyclohexyl amine-based substrates was achieved. The successful model study concluded the potential of the optimized reaction conditions. But the desired selective activation of the β- C-H bond of cyclic amine systems is not as easy as the literature revealed.

There can be some factors responsible for the failure encountered.

a) The basicity of the hydrazine/ring nitrogen.
b) The stability of the N-N bond.
c) Other variables (solvent, ligands/additives, temperature, etc.) need to be optimized to achieve the desired reaction.

We will start looking at the shortcomings and will work on improving the conditions to make project successful.

Apart from this, work on resolving substituted [2.2]paracyclophane has also started in order to develop new methodologies to develop regioselective and enantioselective pseudo-*ortho* [2.2]paracyclophane.

5.12 References

1. (a) J. He, M. Wasa, S. K. Chan, Q. Shao, J. Q. Yu, Palladium-Catalyzed Transformations of Alkyl C-H Bonds *Chem. Rev.*, **2017**, *117*, 8754-8786. (b) F. Roudesly, J. Oble, G. Poli, Metal-catalyzed C-H activation/functionalization: The fundamentals, *J. Mol. Catal. Chem.*, **2017**, *426*, 275-296.
2. (a) D. Gallego, E. A. Baquero, Recent Advances on Mechanistic Studies on C–H Activation Catalyzed by Base Metals, *Open Chemistry*, **2018**, *16*, 1001-1058. (b) M. Zhang, Y. Zhang, X. Jie, H. Zhao, G. Li, W. Su, Recent advances in directed C–H functionalizations using monodentate nitrogen-based directing groups, *Org. Chem. Front.*, **2014**, *1*, 843-896.
3. (a) R. Giri, N. Maugel, J. J. Li, D.-H. Wang, S. P. Breazzano, L. B. Saunders, J. Q. Yu, Palladium-catalyzed methylation and arylation of sp2 and sp3 C-H bonds in simple carboxylic acids, *J. Am. Chem. Soc*., **2007**, *129*, 3510-3511. (b) Kapoor, M.; Liu, D.; Young, M. C., Carbon Dioxide-Mediated C(sp^3)–H Arylation of Amine Substrates, *J. Am. Chem. Soc*., **2018**, *140*, 6818-6822. (c) D. H. Wang, M. Wasa, R. Giri, J. Q., Yu, Pd(II)-Catalyzed Cross-Coupling of sp^3 C−H Bonds with sp^2 and sp^3 Boronic Acids Using Air as the Oxidant, *J. Am. Chem. Soc*., **2008**, *130*, 7190-7191. (d) Wasa, M.; Engle, K. M.; Yu, J. Q., Pd(0)/PR_3-Catalyzed Intermolecular Arylation of sp^3 C−H Bonds, *J. Am. Chem. Soc*., **2009**, *131*, 9886-9887. (e) Z. Zhuang, C.-B. Yu, G. Chen, Q.-F. Wu, Y. Hsiao, C. L. Joe, J. X. Qiao, M. A. Poss, J. Q. Yu, Ligand-Enabled β-C(sp^3)-H Olefination of Free Carboxylic Acids, *J. Am. Chem. Soc*., **2018**, *140*, 10363-10367.
4. (a) J. Calleja, D. Pla, T. W. Gorman, V. Domingo, B. Haffemayer, M. J. Gaunt, A steric tethering approach enables palladium-catalysed C-H activation of primary amino alcohols, *Nature Chemistry*, **2015**, *7*, 1009-1016. (b) Chen, X. Chen, C.E. Goodhue J. Q., Palladium-Catalyzed Alkylation of sp^2 and sp^3 C−H Bonds with Methylboroxine and Alkylboronic Acids: Two Distinct C−H Activation Pathways *Journal of the American Chemical Society*, **2006**, *128*, 12634-12635. (c) L.V. Desai, K. L. Hull, M.S. Sanford, Palladium-Catalyzed Oxygenation of Unactivated sp^3 C−H Bonds, *Journal of the American Chemical* Society, **2004**, *126*, 9542-9543. (d) L.V. Desai, K. J. Stowers, M. S. Sanford, Insights into Directing Group Ability in Palladium-Catalyzed C−H Bond Functionalization *Journal of the American Chemical Society* **2008**, *130*, 13285-13293. (e) Giri, R.; Chen, X.; Yu, J. Q., *Angewandte Chemie International Edition* Palladium-Catalyzed Asymmetric Iodination of Unactivated C□H Bonds under Mild Conditions, **2005**, *44*, 2112-2115.

5. (a), J. R. Cabrera-Pardo; A. Trowbridge, M. Nappi, K. Ozaki, M. J. Gaunt, Selective Palladium (II)-Catalyzed Carbonylation of Methylene β-C− H Bonds in Aliphatic Amines, *Angew. Chem. Int. Ed.*, 2017, *56*, 11958-11962. (b) N. Gulia,; O. Daugulis,, Palladium-Catalyzed Pyrazole-Directed sp^3 C−H Bond Arylation for the Synthesis of β-Phenethylamines, *Angew. Chem. Int. Ed.*, **2017**, *56*, 3630-3634.
6. (a) G. Rouquet, N. Chatani, Catalytic Functionalization of C(sp^2)-H and C(sp^3)-H Bonds by Using Bidentate Directing Groups, *Angew. Chem. Int. Ed.*, **2013**, *52*, 11726-11743. (b) K.J. Stowers, x K.C. Stowers, M.S. Sanford, Aerobic Pd-Catalyzed sp^3 C−H Olefination: A Route to Both N-Heterocyclic Scaffolds and Alkenes, *J. Am. Chem. Soc.*, **2011**, *133*, 6541-6544. (c) N. Hoshiya, T. Kobayashi, M. Arisawa, S. Shuto, Direct Observation of C-H Cyclopalladation at Tertiary Positions Enabled by an Exo-Directing Group, *Org. Lett.*, **2013**, *15*, 6202-6205.
7. (a) F. Kakiuchi, N. Chatani, Catalytic methods for C-H bond functionalization: application in organic synthesis *Adv. Syn. Catal.*, **2003**, *345*, 1077-1101. (b) L. C. Campeau, D. R. Stuart, K. Fagnou, Palladium-catalyzed direct arylation of nitro-substituted aromatics with aryl halides, *Aldrichimica Acta*, **2007**, *40*, 35. (c) I. V. Seregin, V. Gevorgyan, Direct transition metal-catalyzed functionalization of heteroaromatic compounds, *Chem. Soc. Rev.*, **2007**, *36*, 1173-1193. (d) D. Alberico, M. E. Scott, M. Lautens, Aryl-aryl bond formation by transition-metal-catalyzed direct arylation, *Chem. Rev.*, **2007**, *107*, 174-238.
8. (a) N. R. Deprez, D. Kalyani, A. Krause, M. S. Sanford, Room temperature palladium-catalyzed 2-arylation of indoles, *J. Am. Chem. Soc.*, **2006**, *128*, 4972-4973. (b) D. Kalyani, N. R. Deprez, L. V. Desai, M. S. Sanford, Oxidative C− H activation/C− C bond forming reactions: synthetic scope and mechanistic insights, *J. Am. Chem. Soc.*, **2005**, *127*, 7330-7331. (c) B. B. Toure, B. S. Lane, D. Sames, Catalytic C− H arylation of SEM-protected azoles with palladium complexes of NHCs and phosphines, *Org. Lett.*, **2006**, *8*, 1979-1982.
9. (a) J. C. Lewis, A. M. Berman, R. G. Bergman, J. A. Ellman, Rh (I)-catalyzed arylation of heterocycles via C-H bond activation: expanded scope through mechanistic insight, *J. Am. Chem. Soc* **2008**, *130*, 2493-2500. (b) Wang, X.; Lane, B. S.; Sames, D., Direct C-arylation of free (NH)-indoles and pyrroles catalyzed by Ar-Rh (III) complexes assembled in situ, *J. Am. Chem. Soc.*, **2005**, *127*, 4996-4997.
10. T. Okazawa, T. Satoh, M. Miura, M. Nomura, Palladium-catalyzed multiple arylation of thiophenes, *J. Am. Chem. Soc.*, **2002**, *124*, 5286-5287.

11. (a) S. Pivsa-Art, T. Satoh, Y. Kawamura, M. Miura, M. Nomura, Palladium-Catalyzed Arylation of Azole Compounds with Aryl Halides in the Presence of Alkali Metal Carbonates and the Use of Copper Iodide in the Reaction, *Bulletin of the Chemical Society of Japan* **1998**, *71*, 467-473. (b) B. S. Lane, M. A. Brown, D. Sames, Direct palladium-catalyzed C-2 and C-3 arylation of indoles: a mechanistic rationale for regioselectivity, *J. Am. Chem. Soc.*, **2005**, *127*, 8050-8057. (c) C.-H. Park, V.; I. V. Seregin, A. W. Sromek, V. Gevorgyan, Palladium-catalyzed arylation and heteroarylation of indolizines, *Org. Lett.*, **2004**, *6*, 1159-1162.
12. B. Glover, K. A. Harvey, B. Liu, M. J. Sharp, M. Tymoschenko, Regioselective palladium-catalyzed arylation of 3-carboalkoxy furan and thiophene, *Org. Lett.*, **2003**, *5*, 301-304.
13. (a) Garcia-Cuadrado, D.; de Mendoza, P.; Braga, A. A. C.; Maseras, F.; Echavarren, A. M., *Journal of the American Chemical Society* 2007, *129*, 6880-6886. (b) Ozdemir, I.; Demir, S.; Cetinkaya, B.; Gourlauoen, C.; Maseras, F.; Bruneau, C.; Dixneuf, P. H., *Journal of the American Chemical Society* 2008, *130*, 1156-1157. (c) Ackermann, L.; Vicente, R.; Althammer, A., *Organic Letters 2008*, *10*, 2299-2302. (d) Davies, D. L.; Donald, S. M. A.; Al-Duaij, O.; Macgregor, S. A.; Polleth, M., *Journal of the American Chemical Society* 2006, *128*, 4210-4211.
14. Y. Q. Chen, Z. Wang, Y. Wu, S. R. Wisniewski, J. X. Qiao, W. R. Ewing, M. D. Eastgate, J. Q. Yu, Overcoming the Limitations of γ-and δ-C–H Arylation of Amines through Ligand Development, *J. Am. Chem. Soc.*, **2018**, *140*, 17884-17894.
15. S. D. Roughley, A. M. Jordan, The medicinal chemist's toolbox: an analysis of reactions used in the pursuit of drug candidates *J.Med. Chem.*, 2011, *54*, 3451-3479.
16. A. Paul, D. Seidel, α-Functionalization of cyclic secondary amines: Lewis acid promoted addition of organometallics to transient imines, *J. Am. Chem. Soc.*, **2019**, *141*, 8778-8782.
17. X. Chen, H. Zhao; C. Chen, H. Jiang, M. Zhang, Iridium-Catalyzed Dehydrogenative α-Functionalization of (Hetero)aryl-Fused Cyclic Secondary Amines with Indoles, *Org. Lett.*, **2018**, *20*, 1171-1174.
18. P. Jain, P. Verma, G. Xia, J. Q. Yu, Enantioselective amine α-functionalization via palladium-catalysed C–H arylation of thioamides, *Nature Chem.*, **2017**, 140-144.
19. B. F. V. Steijvoort, N. Kaval, A. A. Kulago, B. U. W. Maes, Remote Functionalization: Palladium-Catalyzed C5(sp^3)-H Arylation of 1-Boc-3-aminopiperidine through the Use of a Bidentate Directing Group, *ACS Catal.* **2016**, *6*, 4486-4490.

20. P. Wang, P. Verma, G. Xia, J. Shi, J. X. Qiao,; S. Tao, P. T. W. Cheng, M. A. Poss, Farmer, M. E.; Yeung, K. S.; Yu, J. Q., Ligand-accelerated non-directed C–H functionalization of arenes, *Nature*, **2017**, *551*, 489-493.
21. E. Vitaku, D. T. Smith, J. T. Njardarson, Analysis of the Structural Diversity, Substitution Patterns, and Frequency of Nitrogen Heterocycles among U.S. FDA Approved Pharmaceuticals, *J. Med. Chem.*, **2014**, *57*, 10257-10274.
22. S. Atsushi, T. Yoshiaki, M. Toshiaki, Synthesis of *cis*-3-arylated cycloalkylamines through palladium-catalyzed methylene sp^3 carbon–hydrogen bond activation, *Tetrahedron Lett.*, **2014**, *55*, 2838-2841.
23. Z. Huang, C. Wang, G. Dong, A Hydrazone-Based *exo*-Directing-Group Strategy for β C−H Oxidation of Aliphatic Amines, *Ang. Chem. Int. Ed.*, **2016**, *55*, 5299-5303.
24. Y.-F. Zhou, S.-P. Zhang, Z. Feng, X. Shen, D.-R. Zhu, Syntheses, Crystal Structures, and Spectral Characterization of Six Novel Benzimidazolyl Substituted Triaryltriazoles, *J. Het. Chem.*, **2017**, *54*, 2773-2780.
25. M. Ilisson, K. Tomson, A. Selyutina, S. Türk, U. Mäeorg, Synthesis of Novel Saccharide Hydrazones, *Syn. Comm.*2015, *45*, 1367-1373.
26. R. Giri, N. Maugel, J. J. Li, D. H. Wang, S. P. Breazzano, L. B. Saunders, J. Q. Yu, Palladium-Catalyzed Methylation and Arylation of sp^2 and sp^3 C−H Bonds in Simple Carboxylic Acids, *J. Am. Chem. Soc.* **2007**, *129*, 3510-3511.
27. T. Setierin, W. Supp, G. Manninger, Umsetzungen mit Monohydrazonen von Dicarbonylverbindungen, IX. Neue Wege zur Darstellung von 3-Alkoxypyrrolen und Pyrrolin-3-onen, *Chem. Ber.* **1979**, *112*, 3013-3022.
28. L. Chengwei, J. Chong-Lei, Palladium-Catalyzed Decarbonylative Borylation of Carboxylic Acids: Tuning Reaction Selectivity by Computation *Angew. Chem. Int. Ed.*, **2018**, *57*, 16721-16726.
29. (a) Dr. G. He, G. Chen, A Practical Strategy for the Structural Diversification of Aliphatic Scaffolds through the Palladium-Catalyzed Picolinamide-Directed Remote Functionalization of Unactivated C(sp^3)-H Bond, *Angew. Chem. Int. Ed.*, **2011**, *50*, 5192 -5196, (b) P. X. Ling, S. L. Fang, X.-S. Yin, K. Chen, B.-Z. Sun, B. F. Shi, Palladium-Catalyzed Arylation of Unactivated γ-Methylene C(sp^3)-H and δ-C-H Bonds with an Oxazoline-Carboxylate Auxiliary, *Chem. Eur. J.*, **2015**, *21*, 17503-17507, (d) D. Munz, M. W. Gardiner, R. Fu, T. Strassner, W. A. Goddard, Proton or Metal? The H/D Exchange of Arenes in Acidic Solvents, *ACS Catal.* **2015**, 5, 769-75, (e) E. T. Nadres, D. Shabashov, O. Daugulis,, Scope and Limitations of Auxiliary-Assisted, Palladium-Catalyzed Arylation and Alkylation of sp^2 and sp^3 C–H Bonds, *J. Org. Chem.*, **2013**, *78*,

9689-9714, (f) D. S. Roman, A. B. Charette, C–H Functionalization of Cyclopropanes: A Practical Approach Employing a Picolinamide Auxiliary, *Org. Lett.*, **2013**, *15*, 4394-4397, (g)- M. Fei,, L. Min, Lihong, Acetohydrazone: A Transient Directing Group for Arylation of Unactivated C(sp^3)–H Bonds, *Org. Lett.*, **2016**, *18*, 2708-2711.

30. A) C. Y. Qiao, W. Zhen, W. Yongwei, R. W. Steven, X. Q. Jennifer, W. R. Ewing,, M. D. Eastgate, Y. Quan, Overcoming the Limitations of γ- and δ-C-H Arylation of Amines through Ligand Development, *J. Am. Chem. Soc*. 2018, 140, 17884-17894, (b) S. Guin, P. Dolui, X. Zhang, S. Paul, V. K. Singh, Iterative Arylation of Amino Acids and Aliphatic Amines via δ-C(sp^3)-H Activation: Experimental and Computational Exploration, *Angew. Chem. Int. Ed.* **2019**, *58*, 5633-5638.
31. A. Yada, W. Liao, Y. Sato, M. Murakami, Buttressing Salicylaldehydes: A Multipurpose Directing Group for C (sp^3)-H Bond Activation, *Angew. Chem. Int. Ed.*, **2017**, *56*, 1073-1076.

32. M. Fei, L. Min, H. Lihong, Palladium-Catalyzed Unactivated C(sp^3)–H Bond Activation and Intramolecular Amination of Carboxamides: A New Approach to β-Lactams, *Org. Lett.*, **2016**, *18*, 2708-2711.

Chapter 6

Future Goals

6.1. Expanding the Scope of Bromo[2.2]paracyclophane Derivatives for Oxazoline Coupling

We have developed a protocol to couple chiral oxazolines with bromo[2.2]paracyclophane derivatives (Chapter 3). This methodology has provided exciting results. In most cases, the resolution of diastereomers was possible. It would be intriguing to elaborate on the scope of bromo[2.2]paracyclophane derivatives. Our lab has synthesised two new bromo[2.2]paracyclophane precursors, (±)-4-(tert-butylamino)-7-bromo[2.2]paracyclophane carbamate and (±)-4-(tert-butylamino)-8-bromo[2.2]paracyclophane carbamate (Scheme 6.1). With the oxazoline coupling, different amino[2.2]paracyclophane-oxazoline derivatives can be synthesized, which could be hydrolyzed to provide planar chiral amino acids

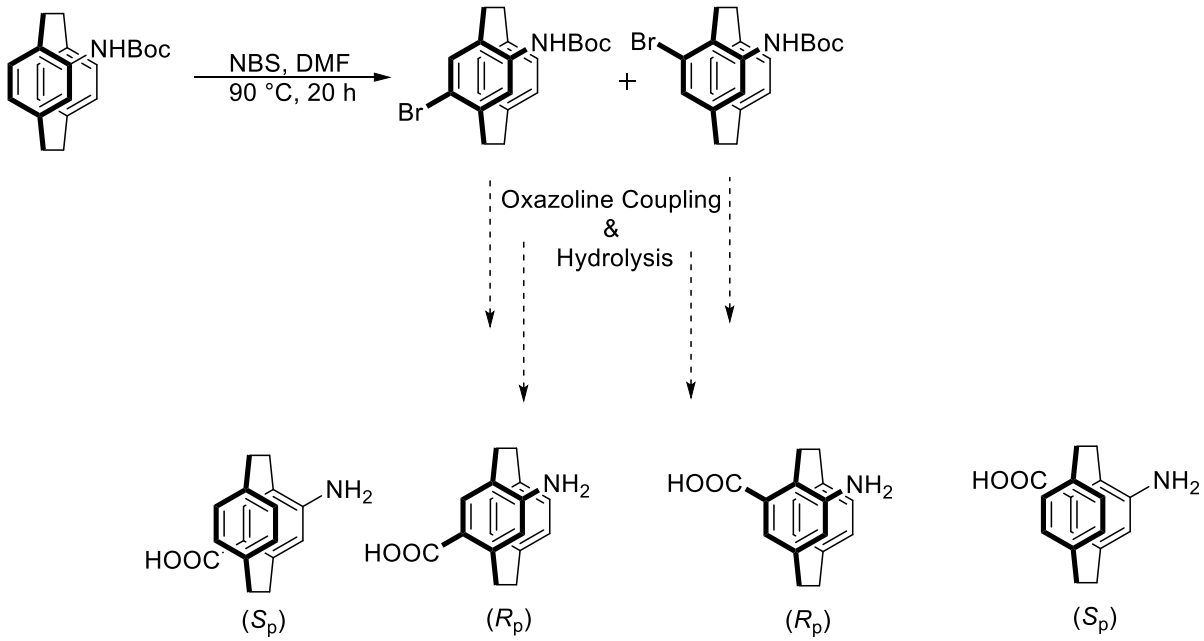

Scheme 6.1: Synthesis of planar chiral amino acids

Planar chiral [2.2]paracyclophane amino acids (pseudo amino acids) provide a unique opportunity to prepare planar chiral pseudopeptides. They can be promising supramolecular organic frameworks. With these fascinating properties, planar chiral pseudopeptides can be applied in asymmetric catalysis, the biomedical field, and the development of new materials.

6.2. Optimization of Reaction Conditions of Decarboxylative Phosphorylation:

In chapter 4, we have seen the potential to convert the chiral acid into a phosphine through decarboxylative phosphorylation. These results have opened a new avenue or pathway for the synthesis of enantio-enriched phosphine oxides and their precursors.

The optimization of reaction conditions and elaboration of the scope of the decarboxylative phosphorylation will be done with diacids (Scheme 6.2).

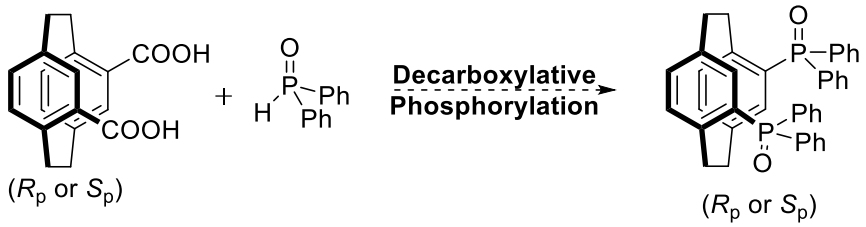

Scheme 6.2: Decarboxylative phosphorylation with chiral diacids

The product formed from the above coupling will be a precursor to Phanephos. Thus, a new route to synthesize such useful ligands and their precursors will help chemists around the globe.

6.3. Scope of Rhodium Paddle-Wheel in Asymmetric Catalysis: (C-H Amination Reaction):

The C-H insertion reaction using metal nitrenes can be catalyzed using rhodium catalyst for both inter- as well as intra-molecular insertion reactions.[1] We can employ the rhodium paddle-wheel complex for catalyzing such reactions, (Scheme 6.3).

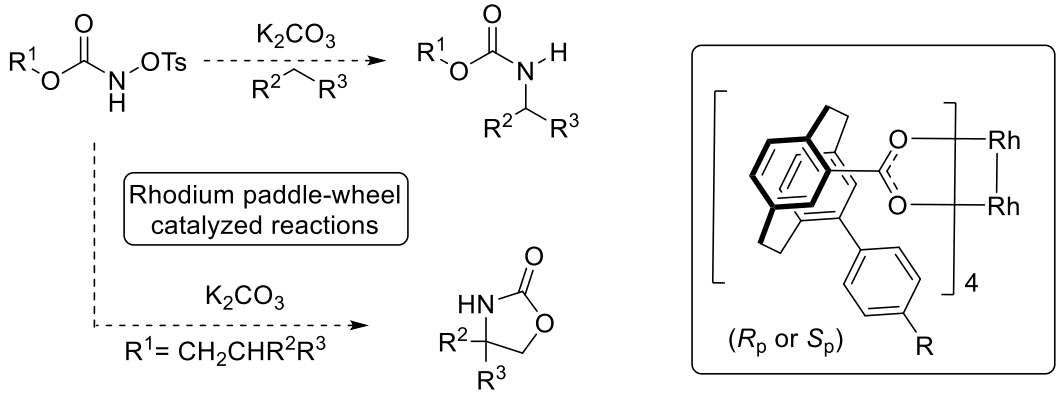

Scheme 6.3: Scope of Rhodium paddle-wheel in Asymmetric Catalysis: (C-H Amination Reaction)

6.4. Elaboration of Chiral PCP-Gold Complexes:

After having optimized conditions, we can elaborate on the scope of our gold catalysts by changing the amine partners (Scheme 6.4). N-heterocyclic carbenes (NHCs) have become one of the most important ligand classes in homogeneous transition metal catalysis.[2]

The use of cyclic and heterocyclic amines may alter the steric as well as can increase the bulk of the catalyst, which can help in increasing *ee* of the enantioselective products formed through asymmetric catalysis.

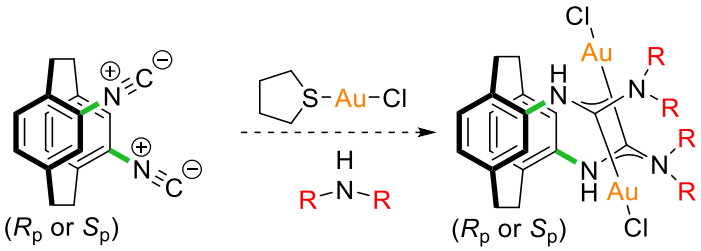

Scheme 6.4: Synthesis of gold complex

Scope of various amine partners that can be used to form the gold complex are shown below in the fig. 6.1.

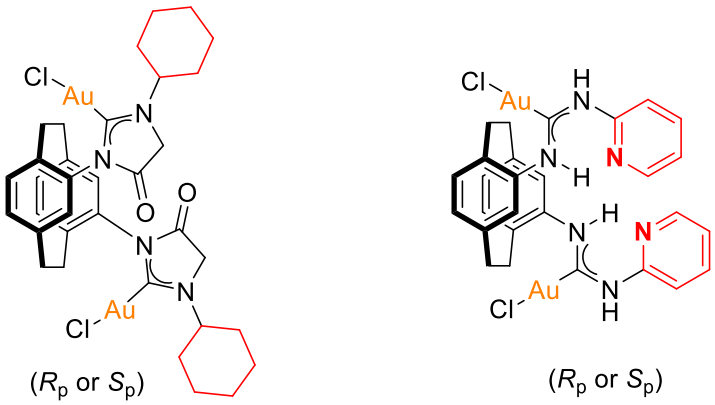

Fig. 6.1: Substrate scope of gold complexes

6.5. Alkylation of Ring Nitrogen:

The failure to selectively functionalize β-C-H bond of the heterocyclic amines, has pointed out some of the challenges that might be the root cause and can be looked on to make the selective β-C-H bond functionalization facile.

The first challenge is the basicity of the ring nitrogen that needs to be controlled as there are chances that it could coordinate with palladium preventing the C-H insertion. Protection of nitrogen by alkylation can be one solution that can help to form the desired product (Scheme 6.5).

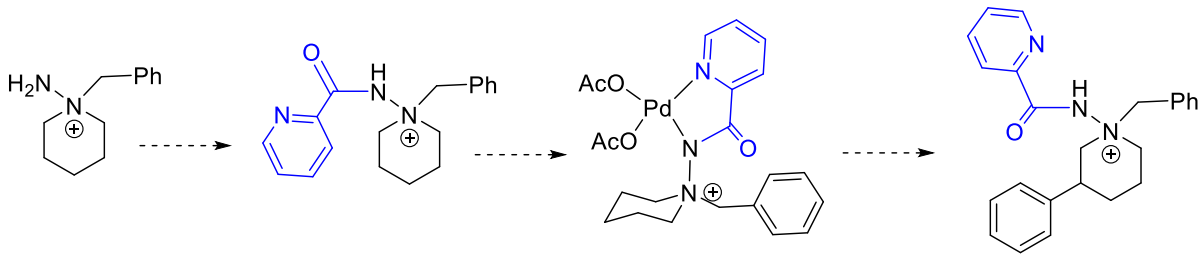

Scheme 6.5: Protection of the nitrogen by alkylation

Employing a quaternary ammonium center in palladium-mediated C–H activation could be detrimental to stability,[3] although it should be noted that ammonium salts have been used in ion-pair directed iridium-mediated C–H activation,[4] and a 1-aminopyridinium ylide has been used as a directing group in palladium chemistry.[5] The precursor for such chemistry, 1-amino-1-benzylpiperidinium chloride[6] is known and might offer an added advantage by promoting the necessary axial hydrazine conformation.

6.6. Optimization of Reaction Conditions:

Once the desired activation is achieved, the second goal will aim at optimizing the different variables such as solvents, temperature, and use of different ligands and additives to get the best yields. There are numerous reports on various reaction conditions that can yield C-H bond functionalization. We will aim to increase the yields of the reaction by trying different combinations after establishing the mechanistic cycle of the β-C-H bond functionalization

6.7. β-C-H Functionalization of Other Cyclic Amine Systems:

Apart from piperidine, other cyclic amine systems are useful feedstocks for pharmaceuticals and agrochemicals. As the desired C-H activation of β-C-H of piperidine is successfully achieved, the next goal will focus on other substituted cyclic amines as shown in Figure XX.

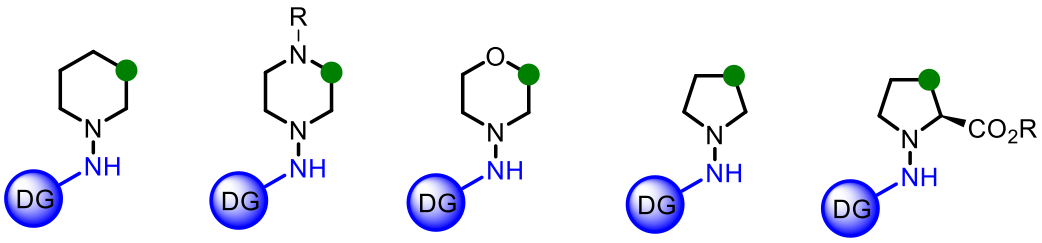

Figure 6.2: Different substituted cyclic amines

6.8. References:

1. K. Huard, H. Lebel, N-Tosyloxycarbamates as Reagents in Rhodium-Catalyzed C-H Amination Reactions, *Chem. Eur. J.*, **2008**, *14*, 6222-6230.
2. A. Hashmi, K. Stephen, C. Lothschütz, K. Graf; T. Häffner, A. Schuster, F. Rominger, Sterically Demanding AgI and CuI N-Heterocyclic Carbene Complexes: Synthesis, Structures, Steric Parameters, and Catalytic Activity *Adv. Synth. Catal.*, **2011**, *353*, 1407-1412.
3. M. Spettel, R. Pollice, M. Schnürch, Quaternary Ammonium Salts as Alkylating Reagents in C–H Activation Chemistry, *Org. Lett.*, **2017**, *19*, 4287-4290.
4. M. T. Mihai, Davis, H. J. Davis, G. R. Genov; R. J. Phipps, Ion Pair-Directed C–H Activation on Flexible Ammonium Salts: meta-Selective Borylation of Quaternized Phenethylamines and Phenylpropylamines, *ACS Catal.*, **2018**, *8*, 3764-3769.
5. K.K.A., Le, H. Nguyen, O. Dauglis, 1-Aminopyridinium Ylides as Monodentate Directing Groups for sp^3 C–H Bond Functionalization, *J. Am. Chem. Soc.*, **2019**, *141*, 14728-14735.
6. K. Nagarajan; C. L. Kulkarni, R. K. Shah, Novel dealkylating and deaminating reactions of 2-chlorobenzoxazole, 2-chloropyridine, and methyl 2-chloro-5-nitrobenzoate with N-amino compounds, *Indian J. Chem.*, **1971**, *9*, 748-754.

Chapter 7:
Experimental Section

Experimental Section Chapter 3

General Information

All reactions were performed in scintillation vials, round bottom flasks (RBFs), or pressure tubes under an inert atmosphere of dry argon unless otherwise noted. Moisture-sensitive reactions were carried out using standard syringe septum techniques. Reaction solvent tetrahydrofuran (Fisher, HPLC grade) was dried by distillation from sodium-benzophenone radical ketyl. 1,4-Dioxane (Fisher, HPLC grade) was dried by distillation over calcium hydride. DMA (Sigma-Aldrich, ≥ 99.5% GC) was stored over 4Å molecular sieves. Solvents for filtration, transfers, and chromatography were certified ACS grade. Evaporation of solvents was carried out under reduced pressure on the rotary evaporator below 42 °C. Palladium catalysts and phosphine ligands were purchased from Sigma-Aldrich, Strem, and Apollo Scientific. Other reagents were purchased from Sigma-Aldrich, Alfa Aesar, and Acros Organics. Purification of the reaction mixture was performed by Bruker flash chromatography, column chromatography, or preparative TLC. The stationary phase for chromatography was silica gel 40-63 UM 60A, or 230-400 mesh. Preparative TLC was performed on MERCK precoated silica gel 60-F254 (0.5-mm) aluminium plates. Solvents for purification were purchased from LabServe. TLC visualisation was carried out using ultraviolet light (254 nm) and different staining reagents such as potassium permanganate.

Analytical Instruments

Optical rotation was recorded on a Perkin Elmer 241 polarimeter with the sodium lamp emitting at 589 nm (D = 589 nm). All samples were measured in chloroform unless otherwise noted in a 10 cm cell and an average of 3 readings was taken.

Circular Dichroism spectrum was recorded using a Chirascan CD spectrophotometer (150 W Xe arc) from Applied Photophysics. CD spectra (average of at least 2 scans) were recorded between 220 and 350 nm with 1 nm intervals, 120 nm/min scan rate, and 10 mm path length followed by subtraction of a background spectrum (solvent).

Infrared spectroscopy was carried out on ThermoScientific Nicolet iS5 iD7 ATR.

NMR spectroscopy was performed on Bruker 400 MHz, Bruker 500 MHz, or Bruker 700 MHz. Chemical shifts are reported in parts per million (ppm). All spectra were run in $CDCl_3$ unless otherwise stated. Spin multiplicities are described as s (singlet), bs (broad singlet), d

(doublet), dd (doublet of doublets), ddd (doublet of doublet of doublets), dddd (doublet of doublet of doublet of doublets), t (triplet), td (triplet of doublets), q (quartet), quint (quintet), m (multiplet), dt (doublet of triplet), ddt (doublet of doublet of triplets), dtd (doublet of triplet of doublets), dq (doublet of quartets). Coupling constants are reported in Hertz (Hz).

HRMS data were recorded on ThermoScientific Q Exactive Focus Hybrid Quadrupole-orbitrap

MS data were recorded on ThermoScientific MSQ plus. Samples were injected via Dionex Ultimate 3000 HPLC system running at 0.1 mL/min, in MeOH.

General procedures for the synthesis of oxazolines

Method I

A solution of amino alcohol (1.0 eq.), triethyl orthoformate (1.5 eq.), and catalytic glacial AcOH (10 mol%) in dry DCE (10 mL) (dried over P_2O_5) was heated to reflux overnight. The solution was cooled down and the volatiles were removed under reduced pressure. The oxazoline was purified by either Kugelrohr distillation or flash chromatography as specified in the respective compound procedure.

Method II

An amino alcohol (1.0 eq.) and DMF-DMA (1.2 eq.) was heated to reflux at 85 °C for 24 hrs. Then *p*-toluenesulfonic acid monohydrate (0.1 eq.) and hexane (10 mL) were added. An addition funnel containing approximately 4 mL of activated 4 Å molecular sieves was placed on top of the flask, along with a condenser. The solution was heated to 90 °C for 24 hrs, allowing the distillate to condense over the sieves. The reaction mixture was washed with saturated aqueous $NaHCO_3$ solution and brine (10 mL). The aqueous layers were combined and back-extracted with Et_2O (3 × 20 mL). The combined organic layers were dried over Na_2SO_4 and filtered. The concentration of the filtrate gave the desired oxazoline.

(4*S*)-4-Benzyl-2-oxazoline 3.6a

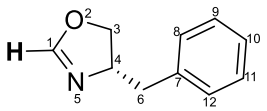

4-Benzyl-2-oxazoline-**3.6a**

DMF-DMA (1.0 mL, 7.93 mmol, 1.2 eq.) was added to L-phenylalaninol (1.0 g, 6.61 mmol, 1.0 eq.). This mixture was allowed to reflux at 75 °C for 24 h. The volatiles were removed

under reduced pressure, and the mixture was triturated with hexane (4 × 30 mL). Then *p*-toluenesulfonic acid monohydrate (2 mg, 0.01 mmol) and hexane (10 mL) were added. An addition funnel containing approximately 4 mL of activated 4 Å molecular sieves was placed on top of the flask, and a condenser was placed on top of the addition funnel. The solution was heated at 90 °C for 24 h, and the condensed liquid was washed over the sieves as the reaction proceeded. The reaction mixture was washed with saturated aqueous $NaHCO_3$ solution (10 mL) and then with brine (10 mL). The aqueous layers were combined and back extracted with diethyl ether (6 × 15 mL), and then the organic extracts were combined with the organic layer, dried over Na_2SO_4 overnight, and filtered. The concentration of the filtrate gave 4-benzyl-2-oxazoline-**3.6a** as a clear colorless oil (0.72 g, 4.47 mmol, 68%).

^{1}H NMR ($CDCl_3$, 400 MHz): δ 7.35-7.28 (2H, m), 7.27-7.19 (3H, m), 6.82 (1H, d, J = 1.5 Hz), 4.39 (1H, ddt, J = 7.8, 5.6, 2.0 Hz), 4.18 (1H, t, J = 9.1 Hz), 3.94 (1H, t, J = 8.2 Hz), 3.10 (1H, dd, J = 8.1, 5.8 Hz), 2.69 (1H, dd, J = 8.6, 5.6 Hz).

Data are comparable to that reported in the literature.[1]

(4*S*)-*tert*-Butyl-2-oxazoline 3.6b

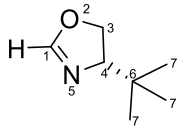

4-*tert*-butyl-2-oxazoline-**3.6b**

DMF-DMA (1.2 mL, 10.23 mmol, 1.2 eq.), L-*tert*-leucinol (1.0 g, 8.53 mmol, 1.0 eq.), *p*-toluenesulfonic acid monohydrate (1.6 mg, 0.08 mmol) were used following the above-mentioned method II. The concentration of the filtrate gave 4-*tert*-butyl--2-oxazoline-**3.6b** as a clear colorless oil (75%).

^{1}H NMR ($CDCl_3$, 400 MHz): 6.83 (1H, s, H-1), 4.15 (1H, t, J = 9.5 Hz, H-4), 4.02 (1H, t, J = 8.6 Hz, H-3a), 4.02 (1H, t, J = 9.3 Hz, H-3b), 0.93 (9H, s, H-7).

Data are comparable to that reported in the literature.[1]

General Conditions A: Mono-coupling of oxazoline with 4-bromo[2.2]paracyclophane

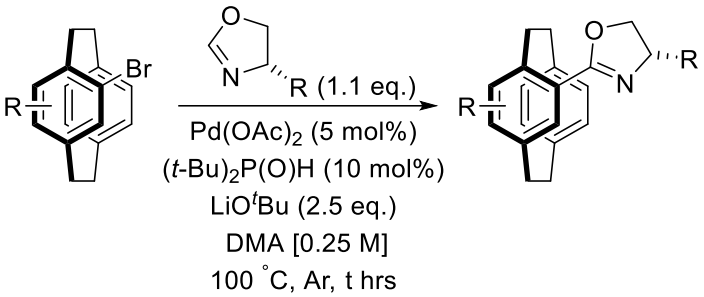

A 4 ml scintillation vial was charged with bromo[2.2]paracyclophane (1.0 eq.), oxazoline (1.1 eq.), LiO*t*Bu (2.5 eq.), (*t*-Bu)$_2$P(O)H (0.1 eq.), and Pd(OAc)$_2$ (0.05 eq.). The vial was purged and degassed with argon three times. Degassed DMA (0.25 M) was introduced by syringe and the reaction was heated to 100 °C for the time specified. The reaction mixture was cooled and diluted with CH_2Cl_2/MeOH (1:1) before passing through Celite®. The filtrate was concentrated under reduced pressure and the crude material was purified by chromatography as specified.

General conditions B: Bis-coupling of oxazoline with dibromo[2.2]paracyclophane

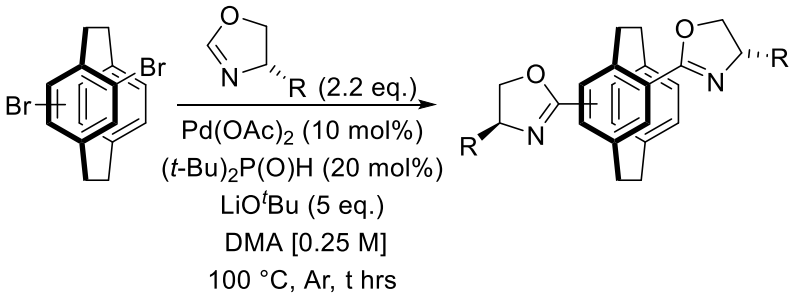

A 4 ml scintillation vial was charged with dibromo[2.2]paracyclophane (1.0 eq.), oxazoline (2.2 eq.), LiO*t*Bu (5 eq.), (*t*-Bu)$_2$P(O)H (0.2 eq.), and Pd(OAc)$_2$ (0.1 eq.). The vial was purged and degassed with argon three times. Degassed DMA (0.25 M) was introduced by syringe and the reaction heated to 100 °C for the time specified. The reaction mixture was cooled and diluted with CH_2Cl_2/MeOH (1:1) before filtering through Celite®. The filtrate was concentrated under reduced pressure and the crude material was purified by chromatography as described.

General conditions C: Tetra-coupling of oxazoline with tetrabromo[2.2]paracyclophane

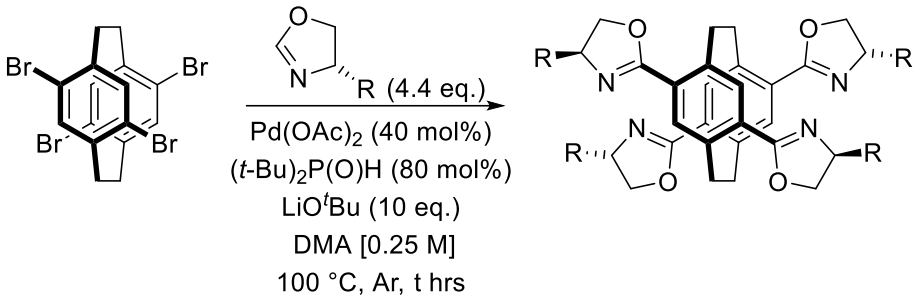

A 4 ml scintillation vial was charged with tetrabromo[2.2]paracyclophane (1.0 eq.), oxazoline (4.4 eq.), LiO^{t}Bu (10.0 eq.), (t-Bu)$_2$P(O)H (0.8 eq.), and Pd(OAc)$_2$ (0.4 eq.). The vial was purged and degassed with argon three times. Degassed DMA (0.25 M) was introduced by syringe and heated to 100 °C for the specified time. The reaction mixture was cooled and diluted with CH_2Cl_2/MeOH (1:1) before passing through a pad of Celite®. The filtrate was concentrated under reduced pressure and the crude material was purified by chromatography as described.

General Conditions D: Mono-coupling of oxazoline with bromo[2.2]paracyclophane

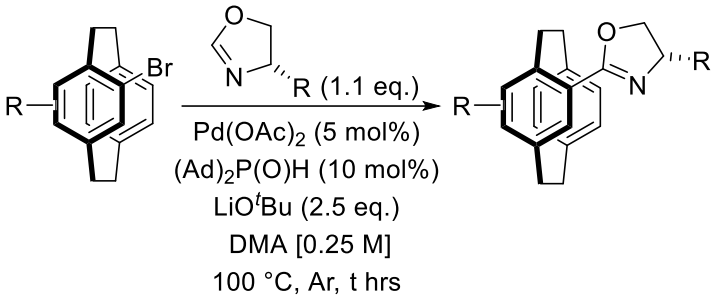

A 4 ml scintillation vial was charged with bromo[2.2]paracyclophane (1.0 eq.), oxazoline (1.1 eq.), LiO^{t}Bu (2.5 eq.), (Ad)$_2$P(O)H (0.1 eq.), and Pd(OAc)$_2$ (0.05 eq.). The vial was purged and degassed with argon three times. Degassed DMA (0.25 M) was introduced by syringe and the reaction heated to 100 °C. The reaction mixture was cooled and diluted with CH_2Cl_2/MeOH (1:1) filtering through Celite®. The filtrate was concentrated under reduced pressure and the crude material was purified by chromatography as described.

General conditions E: Tetra-coupling of oxazoline with tetrabromo[2.2]paracyclophane

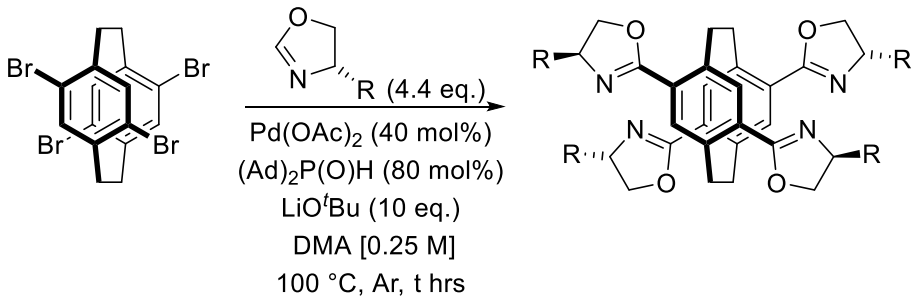

A 4 ml scintillation vial was charged with tetrabromo[2.2]paracyclophane (1.0 eq.), oxazoline (4.4 eq.), LiO^{t}Bu (10.0 eq.), $(Ad)_2P(O)H$ (0.8 eq.), and $Pd(OAc)_2$ (0.4 eq.). The vial was purged and degassed with argon three times. Degassed DMA (0.25 M) was introduced by syringe and heated to 100 °C for the specified time. The reaction mixture was cooled and diluted with CH_2Cl_2/MeOH (1:1) before passing through a pad of Celite®. The filtrate was concentrated under reduced pressure and the crude material was purified by chromatography as described.

General conditions F: Bis-coupling of oxazoline with dibromo[2.2]paracyclophane

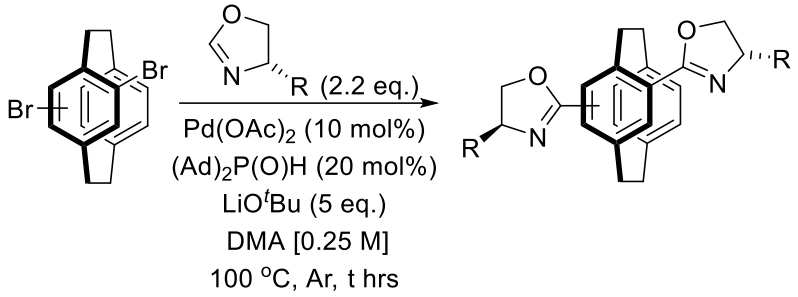

A 4 ml scintillation vial was charged with dibromo[2.2]paracyclophane (1.0 eq.), oxazoline (2.2 eq.), LiO^{t}Bu (5 eq.), $(Ad)_2P(O)H$ (0.2 eq.), and $Pd(OAc)_2$ (0.1 eq.). The vial was purged and degassed with argon three times. Degassed DMA (0.25 M) was introduced by syringe and the reaction heated to 100 °C. The reaction mixture was cooled and diluted with CH_2Cl_2/MeOH (1:1) filtering through Celite®. The filtrate was concentrated under reduced pressure and the crude material was purified by chromatography as described.

(R_p,*S*)-4-(4′-Benzyloxazolin-2′-yl)[2.2]paracyclophane and (S_p,*S*)-4-(4′-benzyloxazolin-2′- yl)[2.2]paracyclophane 3.11a

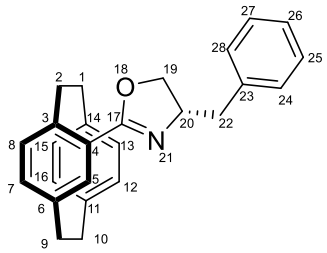

(R_p,*S*) 3.11a
Diastereomer 1

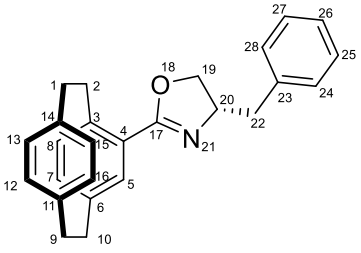

(S_p,*S*) 3.11a
Diastereomer 2

General procedure **A** was followed using (±)-4-bromo-[2.2]paracyclophane (70 mg, 0.24 mmol, 1.0 eq.), (4*S*)-4-benzyl-oxazoline (43 mg, 0.27 mmol, 1.1 eq.), LiO*t*Bu (49 mg, 0.61 mmol, 2.5 eq.), (*t*-Bu)$_2$P(O)H (4 mg, 0.025 mmol, 10 mol%), Pd(OAc)$_2$ (4 mg, 0.012 mmol, 5 mol%), DMA (0.98 ml) for 15 h.

Purification: Isocratic column chromatography [SiO_2, EtOAc:Hexanes (05:95)] to obtain the title compound **(R_p,*S*)-3.11a** (72 mg, 0.2 mmol, 82%) as diastereomer 1, , off-white solid (16 mg, 0.04 mmol, 18%), mixture of diastereomers (46 mg, 0.13 mmol, 52%), and diastereomer 2, **(S_p,*S*)-3.11a**, off-white solid (10 mg, 0.03 mmol, 12%).

R_f : EtOAc:Hexanes (05:95): 0.5

Diastereomer 1 **(R_p,*S*)-3.11a**

IR: ν_{max} 2925, 2852, 2121, 1896, 1712, 1634, 1497 cm^{-1}.

$[\alpha]_D^{20}$: -22 (*c* 1, CH_2Cl_2).

^{1}H NMR ($CDCl_3$, 500 MHz): δ 7.35-7.34 (4H, m, H-28, H-27, H-25, H-24), 7.27-7.24 (1H, H-26), 7.01 (1H, d, *J* = 19.4 Hz, H-5), 6.65-6.63 (1H, m, H-8), 6.57-6.50 (3H, m, H-7, H-13, H-12), 6.48-6.46 (1H, m, H-16), 6.42 (1H, s, H-15), 4.66-4.58 (1H, m, H-20), 4.45 (1H, q, *J* = 17.7, 8.7 Hz, H-19a), 4.28-4.22 (1H, m, H-19b), 4.04-3.89 (1H, m, H-22a), 3.19-2.82 (9H, m, H-22b, H-2a, H-2b, H-9a, H-9b, H-1a, H-1b, H-10a, H-10b).

^{13}C NMR ($CDCl_3$, 125 MHz): ^{13}C NMR ($MeOD_4$, 125 MHz): δ 165.93 (C-17), 140.87 (C-14), 139.75 (C-11), 139.48 (C-3), 139.27 (C-23), 137.99 (C-4), 135.81 (C-6), 135.23 (C-7), 133.91 (C-15), 132.73 (C-16), 132.50 (C-13), 132.06 (C-5), 131.18 (C-27), 129.34 (C-25), 129.19 (C-28), 128.20 (C-8, C-7), 127.80 (C-24), 126.24 (C-26), 71.2 (C-20), 66.85 (C-19), 41.30 (C-22), 40.84 (C-22), 35.27 (C-2), 35.12 (C-9), 34.80 (C-1), 34.57 (C-10).

HRMS (ESI-TOF) m/z: $[M + H]^+$ Calcd $C_{26}H_{26}NO$ for 368.2009; Found 368.2003.

Diastereomer 2 **(S_p,*S*)-3.11a**

IR: ν_{max} 2925, 1631, 1475, 1328, 1273, 1045 cm^{-1}.

$[\alpha]_D^{20}$: +12 (*c* 1, CH_2Cl_2).

^1H NMR ($CDCl_3$, 500 MHz): ^1H NMR (CDCl3, 500 MHz): δ 7.41-7.33 (4H, m, H-28, H-27, H-25, H-24), 7.31-7.25 (1H, m, H-26), 7.13 (1H, s), 6.63 (1H, d, J = 7.7 Hz, H-5), 6.59-6.49 (5H, m, H-7, H-13, H-8, H-15, H-16), 4.73-4.66 (1H, m, H-20), 4.41 (1H, t, J = 8.7 Hz, H-19a), 4.18 (1H, t, J = 7.9 Hz, H-19b), 4.12 (1H, t, J = 11.5 Hz, H-22a), 3.33 (1H, dd, J = 13.7, 5.0 Hz, H-22b), 3.19-3.11 (3H, m. H-2b, H-1a, H-1b), 3.09- 2.98 (3H m, H-9a, H-9b, H-2a), 2.92-2.83 (2H, m, H-10a, H-10b).

^{13}C NMR ($CDCl_3$, 125 MHz): δ 165.93 (C-17), 141.08 (C-14), 139.80 (C-11), 139.71 (C-3), 139.42 (C-23), 135.91 (C-4), 135.21 (C-6), 134.47 (C-7), 132.93 (C-15), 132.79 (C-16), 132.73 (C-13), 132.40 (C-5), 131.32 (C-27), 129.45 (C-25), 129.36 (C-28), 128.85 (C-8, C-7), 128.62 (C-24), 126.60 (C-26), 71.32 (C-20), 41.72 (C-19), 35.93(C-22), 35.33 (C-2), 35.09 (C-9), 34.98 (C-1), 29.72 (C-10).

HRMS (ESI-TOF) m/z: [M + H]+ Calcd. for $C_{26}H_{26}NO$ 368.2009; found 368.2005.

Data comparable to that reported in literature.[2]

(R_p,*S*)-4-(4′-tert-Butyloxazolin-2′-yl)[2.2]paracyclophane and (S_p,*S*)-4-(4′-tertbutyloxazolin-2′-yl)[2.2]paracyclophane-3.11b

General procedure **D** was followed using (±)-4-bromo-[2.2]paracyclophane (100 mg, 0.35 mmol, 1.0 eq.), (4*S*)-4-tert-butyl-2-oxazoline (49 mg, 0.38 mmol, 1.1 eq.), LiO*t*Bu (70 mg, 0.87 mmol, 2.5 eq.). $(Ad)_2P(O)H$ (11 mg, 0.035 mmol, 10 mol%), $Pd(OAc)_2$ (4 mg, 0.017 mmol, 5 mol%), DMA (1.3 mL) for 15 hrs.

Purification: isocratic column chromatography [SiO_2, EtOAc: Hexane (05:95)] to obtain the title compound as an off-white solid (70 mg, 0.21 mmol, 60% yield, diastereomer 1 **(R_p,*S*)-3.11b**, off-white solid (35 mg, 0.1 mmol, 30%), and diastereomer 2 **(S_p,*S*)- 3.11b**, off-white solid (35 mg, 0.1 mmol, 30%).

Rf: EtOAc: Hexane (05:95):0.4

Diastereomer 1 **(R_p,*S*)-3.11b**

IR- ν_{max} 3355, 2933, 1666, 1608, 1506, 1399, 1249, 1032 cm^{-1}.

$[\alpha]_D^{20}$: -141.16 (*c* 1, CH_2Cl_2), (Lit. $[\alpha]_D^{20}$ -128 (*c* 1, CH_2Cl_2)).[3]

^{1}H NMR ($CDCl_3$, 400 MHz): δ 7.03 (1H, d, *J*= 1.9 Hz, H-5), 6.64-6.50 (5H, m, H-7, H-12, H-13, H-15, H-16), 6.47 (1H, d, *J* = 7.8 Hz, H-8), 4.34 (1H, dd, *J* = 8.2, 8.3Hz, H-20), 4.22-4.08 (3H, m, H-19a, H-19b, H-2a), 4.12-4.05 (1H, m, H-19b), 3.22-2.97 (6H, m, H-9a, 9b, 10a, 10b, H-1a, 1b), 2.90-2.80 (m, 1H, H-2b), 1.04 (s, 9H, H-23)

^{13}C NMR ($CDCl_3$, 125 MHz): δ 163.48 (C-17), 140.86 (C-14), 140.05 (C-11), 139.53 (C-3), 139.35 (C-4), 139.73 (C-6), 134.74 (C-12), 134.33 (C-13), 132.91 (C-15), 132.78 (C-16), 132.38 (C-5), 131.24 (C-8), 128.49 (C-7), 76.64 (C-19), 68.00 (C-20), 35.89 (C-1), 35.32 (C-9), 35.07 (C-10), 34.81 (C-2), 34.00 (C-22), 26.09 (C-23).

HRMS (ESI-TOF) m/z: $[M + H]^+$ Calcd $C_{23}H_{28}NO$ for 334.2093; Found 334.2105.

Diastereomer 2 **(S_p,*S*)-3.11b**

$[\alpha]_D^{20}$: +40.03(*c* 1, CH_2Cl_2), (Lit. $[\alpha]_D^{20}$ +56.5 (*c* 1, CH_2Cl_2)).[3]

^{1}H NMR ($CDCl_3$, 400 MHz): δ 7.03 (1H, d, *J*= 1.3 Hz, H-5), 6.60-6.49 (5H, m, H-7, H-12, H-13, H-15, H-16), 6.47 (1H, d, *J* = 7.8 Hz, H-8), 4.42-4.34 (1H, m, H-20), 4.34-4.26 (1H, m, H-19a), 4.22 (1H, t, *J* = 8.7 Hz, H-2a), 4.12-4.05 (1H, m, H-19b), 3.22-3.07 (4H, m, H-9a, 9b, 10a, 10b), 3.07-2.96 (2H, m, H-1a, 1b), 2.95-2.83 (1H, m, H-2b), 1.09 (9H, s, H-23).

^{13}C NMR ($CDCl_3$, 125 MHz): δ 163.01 (C-17), 141.03 (C-14), 140.00 (C-11), 139.45 (C-3), 139.37 (C-4), 135.94 (C-6), 134.88 (C-12), 134.00 (C-13), 132.87 (C-15), 132.74 (C-16), 132.52 (C-5), 131.60 (C-8), 128.38 (C-7), 76.83 (C-19), 67.63 (C-20), 35.46 (C-1), 35.37 (C-9), 35.14 (C-10), 34.79 (C-2), 34.34 (C-22), 26.31 (C-23).

HRMS (ESI-TOF) m/z: $[M + H]^+$ Calcd $C_{23}H_{28}NO$ for 334.2093; Found 334.2109.

Data comparable to that reported in literature.[3]

(R_p,*S*)-4,12-Bis(4′-benzyloxazolin-2′-yl)[2.2]paracyclophane-3.14a and (S_p,*S*)-4,12-bis-(4′-benzyloxazolin-2′-yl)[2.2]paracyclophane-3.14a

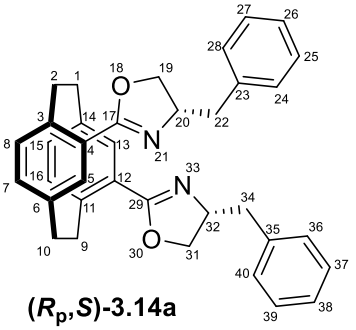

(R_p,*S*)-3.14a
Diastereomer 1

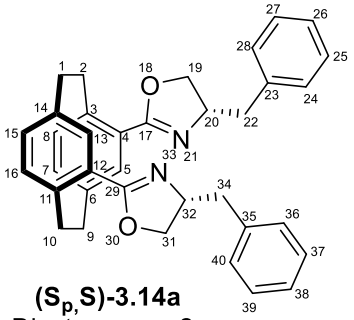

(S_p,S)-3.14a
Diastereomer 2

General procedure B was followed using (±)-4,12dibromo[2.2]paracyclophane (60 mg, 0.16 mmol, 1.0 eq.), (4*S*)-4-benzyl-oxazoline (58 mg, 0.36 mmol, 2.2 eq.), Li*O*tBu (66 mg, 0.82 mmol, 5 eq.), (tBu)$_2$P(O)H (5 mg, 0.032 mmol, 20 mol%), Pd(OAc)$_2$ (4 mg, 0.016 mmol, 10 mol%), DMA (0.66 ml)

Purification: isocratic column chromatography [SiO_2, EtOAc: Hexane (05:95)] to obtain the title the separate diastereomer 1 **(R_p,*S*)-3.14a**, pale yellowish semisolid (30 mg, 0.057 mmol, 34% yield) and diastereomer 2 **(S_p,*S*)-3.14a,** pale yellowish semisolid (31 mg, 0.068 mmol, 36% yield).

R_f : EtOAc: Hexane (05:95):0.3

Diastereomer 1 **(R_p,*S*)-3.14a**

IR: ν_{max} 3627, 2955, 2919, 1639, 1601, 1590, 1452 cm^{-1}.

$[\alpha]_D^{20}$: –61.70 (c = 0.47, CHCl3), (Lit. $[\alpha]_D^{20}$ –68.5 (c = 0.47, $CHCl_3$)).[4]

^{1}H NMR ($CDCl_3$, 500 MHz): δ 7.36-7.30 (8H, m, H-24, H-25, H-28, H-27, H-36, H-37, H-40, H-39), 7.28-7.25 (2H, m, H-26, H-38), 7.17 (2H, s, H-5, H-13), 6.69 (2H, d, *J* = 7.6 Hz, H-8, H-15), 6.60 (2H, d, *J* = 7.7 Hz, H-7, H-16), 4.71-4.65 (2H, m, H-20, H-32), 4.33-4.26 (4H, m, H-19a, H-19b, H-31a, H-31b), 4.08-4.05 (2H, t, *J* = 7.5 Hz, H-2a, H-9a), 3.29 (2H, dd, *J* = 13.7, 4.8 Hz, H-1a, H-10a), 3.18-3.15 (4H, m, H-22a, H-22b, H-34a, H-34b), 2.88-2.82 (2H, m, H-2b, H-9b), 2.73-2.68 (2H, dd, *J* = 13.4, 9.4 Hz, H-1b, H-10b).

^{13}C NMR ($CDCl_3$, 125 MHz): δ 163.69 (C-29, C-17), 141.02 (C-35, C-23), 140.10 (C-11, C-3), 138.44 (C-12, C-4), 135.75 (C-14, C-6), 134.87 (C-27, C-25), 132.57 (C-39, C-37), 129.25 (C-40, C-36, C-28, C-24), 128.55 (C-16, C-13, C-8, C-5), 127.98 (C-15, C-7), 126.43 (C-38, C-26), 70.73 (C-32, C-20), 68.43 (C-31, C-19), 41.97 (C-34, C-22), 36.04 (C-9, C-1), 34.02 (C-11, C-2).

HRMS (ESI-TOF) m/z: $[M + H]^+$ Calcd $C_{36}H_{34}N_2O_2$ 527.2693 for; Found 527.2690.

Diastereomer 1 **(S_p,*S*)-3.14a**

IR: ν_{max} 3674, 2925, 1634, 1590, 1495, 1352 cm^{-1}.

$[\alpha]_D^{20}$: +23.61(c = 0.72, CHCl3), (Lit. $[\alpha]_D^{20}$ +13.9 (c = 0.72, $CHCl_3$)).[4]

^{1}H NMR ($CDCl_3$, 500 MHz): δ 7.39-7.38 (8H, m, H-24, H-25, H-28, H-27, H-36, H-37, H-40, H-39), 7.32-7.29 (2H, m, H-26, H-38), 7.20 (2H, s, H-5, H-13), 6.68 (2H, d, *J* = 7.7 Hz, H-8, H-15), 6.59 (2H, d, *J* = 7.8 Hz, H-7, H-16), 4.67-4.61 (2H, m, H-20, H-32), 4.35-4.30 (4H, m, H-19a, H-19b, H-31a, H-31b), 4.11 (2H, t, *J* = 7.7 Hz, H-2a, H-9a), 3.41 (2H, dd, *J* = 13.8, 5.9 Hz, H-1a, H-10a), 3.26-3.20 (2H, m, H-22a, H-34a), 3.16 (2H, t, *J* = 10.5 Hz, H-2b, H-9b), 2.93 (2H, dd, *J* = 13.8, 8.5 Hz, H-1b, H-10b), 2.87-2.83 (2H, m, H-22b, H-34b).

^{13}C NMR ($CDCl_3$, 125 MHz): δ 163.51 (C-29, C-17), 141.10 (C-35, C-23), 140.14 (C-11, C-3), 138.64 (C-12, C-4), 135.95 (C-14, C-6), 135.00 (C-27, C-25), 132.11 (C-39, C-37), 129.28 (C-40, C-36, C-28, C-24), 128.65 (C-16, C-13, C-8, C-5), 128.00 (C-15, C-7), 126.50 (C-38, C-26), 70.71 (C-32, C-20), 68.74 (C-31, C-19), 42.27 (C-34, C-22), 35.66 (C-9, C-1), 33.72 (C-11, C-2).

HRMS (ESI-TOF) m/z: $[M + H]^+$ Calcd $C_{36}H_{34}N_2O_2$ 527.2693 for; Found 527.2690.
Data comparable to that reported in literature.[4]

(R_p,*S*)-4,12-Bis-(4′-*tert*-butyloxazolin-2′-yl)[2.2]paracyclophane-3.14b and (S_p,*S*)-4,12-bis-(4′-*tert*-butyl-oxazolin-2′-yl)[2.2]paracyclophane 3.14b

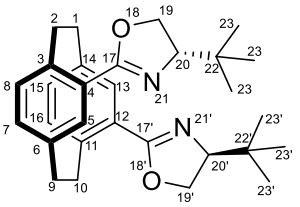

(R_p,*S*)-3.11b
Diastereomer 1

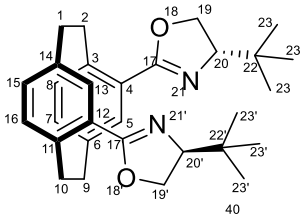

(S_p,*S*)-3.11b
Diastereomer 2

General conditions **F** were followed using (±)-4,12-dibromo[2.2]paracyclophane **3.13** (100 mg, 0.27 mmol, 1.0 eq.), (4*S*)-4-*tert*-butyl-2-oxazoline **3.6b** (77 mg, 0.60 mmol, 2.2 eq.), LiO^tBu (110 mg, 1.37 mmol, 5.0 eq.), $(Ad)_2P(O)H$ (18 mg, 0.027 mmol, 20 mol%), $Pd(OAc)_2$ (6 mg, 0.055 mmol, 10 mol%), DMA (1.1 ml) for 12 hrs .

Purification: Isocratic column chromatography [SiO_2, EtOAc: Hexanes (05:95)] to obtain the title compound **(R_p,*S*)-3.14b**, an off-white solid (10 mg), impure (1:1) with diastereomer **(S_p, *S*)-3.11b**, (refer to ^{1}H NMR data of **(S_p, *S*)-3.11b**) for cross-reference), mixture of diastereomers (4 mg, 0.008 mmol, 3%), and a separate diastereomer **(S_p,*S*)-3.14b**, off-white solid (12 mg, 0.026 mmol, 10%).

(R_p,*S*)-3.14b (Impure with (S_p,*S*)-3.11b)

R_f : EtOAc: Hexane (05:95):0.3

^{1}H NMR ($CDCl_3$, 400 MHz): δ 7.10 (2H, d, J = 1.6 Hz), 7.02 (1H, d, J = 1.7 Hz), 6.63 (2H, dd, J = 5.96, 1.7 Hz), 6.59-6.50 (7H, m), 6.46 (1H, d, J = 7.9 Hz), 4.49-4.19 (7H, m), 4.02-4.14 (5H, m), 3.27-3.07 (8H, m), 3.07-2.97 (2H, m), 2.95-2.80 (3H, m), 1.11 (18H, s), 1.09 (9H, s).

HRMS (ESI-TOF) m/z: $[M + H]^+$ Calcd $C_{30}H_{39}N_2O_2$ for 459.6428; Found 459.6434.

Diastereomer 2 **(S_p,*S*)-3.14b**,

R_f : EtOAc: Hexane (05:95):0.3

IR: ν_{max} 2954, 1640, 1477, 1259, 1048 cm^{-1}.

$[\alpha]_D^{24}$: -50.1 (c = 0.9, $CHCl_3$)

^{1}H NMR ($CDCl_3$, 400 MHz): δ 7.03 (d, J= 1.8 Hz, 2H, H-5, H-13), 6.64 (d, J= 8.0 Hz, 2H, H-15, H-16), 6.55 (d, J= 8.0 Hz, 2H, H-7, H-8), 4.34-4.07 (m, 8H, H-1a, H-1b, H-2a, H-2b,

H-19a, H-19a', H-19b, H-19b'), 3.22-3.07 (m, 4H, H-9a, H-9b, H-20a, H-20a'), 3.07-2.96 (m, 2H, H-1a, 1b), 2.84-2.73 (m, 2H, H-10a, H-10b), 1.02 (s, 18H, H-23, H-23').

^{13}C NMR ($CDCl_3$, 125 MHz): δ 162.70 (2C, C-17, C-17'), 140.87 (2C, C-3, C11), 140.14 (2C, C-4, C-12), 135.49 (C-14), 134.53 (C-6), 132.08 (4C, C-5, C-8, C-13, C-16), 127.99 (2C, C-7, C-15), 76.90 (2C, C-19, C-19'), 67.58 (2C, C-20, C-20'), 36.10 (2C, C-1, C-9), 33.96 (2C, C-22, C-22'), 33.91 (2C, C-2, C-10), 26.03 (2C, C-23. C-23').

MS (ESI-TOF) m/z: $[M + H]^+$ Calcd. for $C_{30}H_{39}N_2O_2$ 459.6428; found 459.6437.

4-Bromo-12-(4-benzyl-oxazoline-2-yl)[2.2]paracyclophane 3.15a

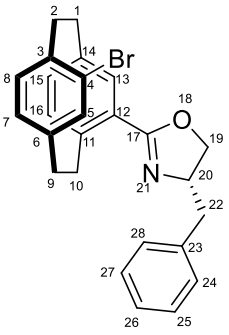

(R_p,*S*)-3.15a
Diastereomer 1

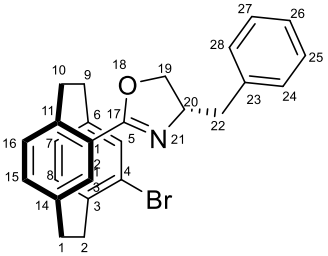

(S_p,*S*)-3.15a
Diastereomer 2

General procedure A was followed using (±)-4,12-dibromo-[2.2]paracyclophane **3.13** (50 mg, 0.14 mmol, 1.0 eq.), (4*S*)-4-benzyl-oxazoline- **3.6a** (24 mg, 0.15 mmol, 1.1 eq.), LiO*t*Bu (27 mg, 0.34 mmol, 2.5 eq.), (tBu)$_2$P(O)H (2 mg, 0.013 mmol, 10 mol%), $Pd(OAc)_2$ (2 mg, 0.006 mmol, 5 mol%), DMA (0.55 ml).

Purification: flash chromatography [SiO_2, EtOAc: Hexane (3:7)] to obtain the title compound **(S_p,*S*)-3.12a** as white semisolid (19 mg, 0.042 mmol, 31% yield).

R_f : EtOAc: Hexane (3:7):0.5

Diastereomer 2 **(S_p,*S*)-3.15a**

^{1}H NMR ($CDCl_3$, 500 MHz): δ 7.70 (1H, d, J = 8.5 Hz, H-13), 7.40-7.35 (4H, m, H-28, H-24, H-27, H-25), 7.31-7.26 (1H, m, H-26), 6.66-6.58 (4H, m, H-16, H-15, H-8, H-7), 6.52 (1H, d, J = 7.7 Hz, H-5), 4.68 (1H, quint, J = 7.0Hz, H-20), 4.40 (1H, t, J = 8.6 Hz, H-22a), 4.34 (1H, t, J = 8.6 Hz, H-22b), 4.28-4.12 (2H, m, H-19a, H-19b), 3.51 (2H, t, J = 10.2 Hz, H-22a, H-22b), 3.37 (1H, dd, J = 13.8, 5.6 Hz, H-10a), 3.30 (1H, dd, J = 13.7, 5.4 Hz, H-

10b), 3.24-3.19 (2H, m, H-10a, H-10b), 3.16-3.03 (2H, m, H-9a, H-9b), 2.98-2.89 (1H, m, H-1a), 2.88-2.76 (3H, m, H-1b, H-2a, H-2b).

^{13}C NMR ($CDCl_3$, 125 MHz): δ 163.92 (C-17), 142.16 (C-6), 140.58 (C-11), 139.25 (C-23), 138.86 (C-3), 138.39 (C-12), 135.67 (C-16, C-15), 135.16 (C-14), 134.97 (C-5), 131.36 (C-27), 130.44 (C-25), 129.40 (C-28), 129.30 (C-24), 128.63 (C-8), 128.54 (C-7), 128.07 (C-26), 126.63 (C-13), 126.46 (C-4), 71.10 (C-20), 68.29 (C-19), 42.03 (C-22), 36.06 (C-10), 35.79 (C-9), 33.95 (C-1), 32.60 (C-2).

HRMS (ESI-TOF) m/z: $[M + H]^+$ Calcd for $C_{26}H_{25}Br^{79}NO$ 445.1036; Found 446.1111; $C_{26}H_{25}Br^{81}NO$ 448.1099; Found 448.1088.

(*S*,*S*,*R*$_p$,*S*,*S*)-4,7,12,15-Tetra(4′-benzyl-oxazolin-2′-yl)[2.2]paracyclophane-3.19 and (*S*,*S*,*S*$_p$,*S*,*S*)-4,7,12,15-tetra(4′-benzyl-oxazolin-2′-yl)[2.2]paracyclophane-3.19

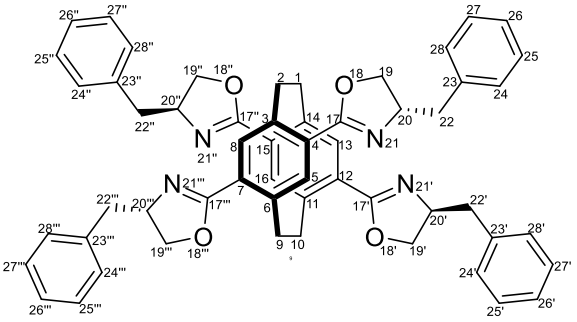

(*S*,*S*,*R*$_p$,*S*,*S*)-3.19

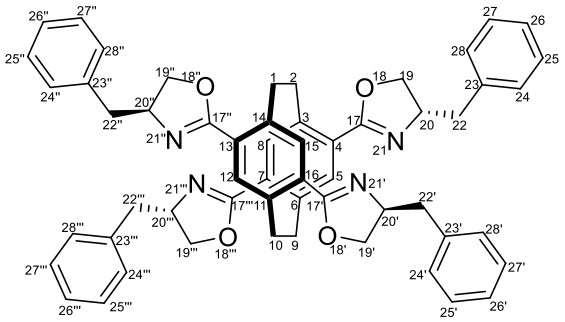

(*S*,*S*,*S*$_p$,*S*,*S*)-3.19

General conditions C was followed using (±)-4,7,12,15-tetrabromo[2.2]paracyclophane **3.14** (100 mg, 0.19 mmol, 1.0 eq.), (4S)-4-benzyl-2-oxazoline **3.6a** (136 mg, 0.85 mmol, 4.4 eq.), LiOtBu (154 mg, 1.92 mmol, 10.0 eq.), (*t*-Bu)$_2$P(O)H (12.4 mg, 0.077 mmol, 40 mol%), $Pd(OAc)_2$ (9 mg, 0.038 mmol, 20 mol%), DMA (1.1 ml) for 15 hrs.

Purification: Isocratic column chromatography [SiO2, EtOAc:Hexanes (20:80)] to obtain the title compound **3.19** as two diastereomers, **(*S*,*S*,*R*$_p$,*S*,*S*)-3.19**, as an off-white solid (9 mg, 0.010 mmol, 5% yield), and the second diastereomer **(*S*,*S*,*S*$_p$,*S*,*S*)-3.19**, as an off-white solid (9 mg, 0.010 mmol, 5% yield), along with two separable diastereomers of para-dibromo-para-bis(oxazoline)-**(*S*,*R*$_p$,*S*)-3.20** (10 mg, 0.015 mmol, 8%) and 2 diastereomer-**(*S*,*S*$_p$,*S*)-3.20** (9 mg, 0.013 mmol, 7%), as well as an inseparable mixture of diastereomers of debromo-tris(oxazoline) **(±)-3.21** (4 mg, 0.006 mmol, 3%).

General conditions E was followed using (±)-4,7,12,15-tetrabromo[2.2]paracyclophane **3.17** (100 mg, 0.19 mmol, 1.0 eq.), (4S)-4-benzyl-2-oxazoline **3.6a** (136 mg, 0.85 mmol, 4.4 eq.), LiO*t*Bu (154 mg, 1.92 mmol, 10.0 eq.), $(Ad)_2P(O)H$ (24 mg, 0.077 mmol, 40 mol%), $Pd(OAc)_2$ (9 mg, 0.038 mmol, 20 mol%), DMA (1.1 ml) for 15 hrs.

Purification: Isocratic column chromatography [SiO2, EtOAc:Hexanes (20:80)] to obtain the title compound 11o (20 mg, 0.22 mmol, 12% yield) as a separate diastereomer 1, **(*S*,*S*,*R*$_p$,*S*,*S*)-3.19**, an off-white solid (10 mg, 0.012 mmol, 6% yield), and a separate diastereomer 2 **(*S*,*S*,*S*$_p$,*S*,*S*)-3.19**, an off-white solid (10 mg, 0.012 mmol, 6% yield) along with an inseparable mixture of **(±)-3.21** (13 mg, 0.019 mmol, 10%).

R_f : EtOAc: Hexane (20:80):0.3

Diastereomer 1 **(*S*,*S*,*R*$_p$,*S*,*S*)-3.19**

IR- ν_{max} 2928, 1628, 1470, 1354, 1275, 1068 cm^{-1}

^1H NMR ($CDCl_3$, 500 MHz): δ 7.41-7.35 (15H, m, H-24, H-24', H-24'', H-24''', H-25, H-25', H-25'', H-25''', H-27, H-27', H-27'', H-27''', H-28, H-28', H-28''), 7.31-7.27 (5H, m, H-26, H-26', H-26'', H-26''', H-28'''), 7.24 (4H, s, H-5, H-8, H-13, H-16), 4.66 (4H, q, *J* = 7.7 Hz, H-20, H-20', H-20'', H-20'''), 4.35 (4H, t, *J* = 8.7 Hz, H-19a, H-19a', -19a'', H-19a'''), 4.18-4.09 (8H, m, H-1a, H-1b, H-2a, H-2b, H-19b, H-19b', H-19b'', H-19b'''), 3.39 (4H, dd, *J* = 7.8 Hz, 6.0 Hz, H-22a, H-22a', H-22a'', H-22a'''), 3.16-3.07 (4H, m, H-9a, H-9b, H-10a, H-10b), 2.93 (dd, *J* = 8.5 Hz, 5.4 Hz, 4H, H-22b, H-22b', H-22b'', H-22b'''),

^{13}C NMR ($CDCl_3$, 125 MHz): δ 162.91 (4C, C-17, C-17', C-17'', C-17'''), 141.45 (2C, C-4, C-15), 138.44 (2C, C-7, C-12), 134.32 (4C, C-23, C-23', C-23'', C-23'''), 130.23 (4C, C-3, C-6, C-11, C-14), 129.25 (12C, C-5, C-8, C-13, C-16, C-24, C-24', C-24'', C-24''', C-28, C-28', C-28'', C-28'''), 128.66 (8C, C-25, C-25', C-25'', C-25''', C-27, C-27', C-27'', C-

27’’’), 126.54 (4C, C-26, C-26’, C-26’’, C-26’’’), 70.87 (4C, C-20, C-20’, C-20’’, C-20’’’), 68.82 (4C, C-19, C-19’, C-19’’, C-19’’’), 42.18 (4C, C-22, C-22’, C-22’’, C-22’’’), 33.87 (4C, C-1, C-2, C-9, C-10).

HRMS (ESI-TOF) m/z: $[M + H]^+$ Calcd $C_{56}H_{53}N_4O_4$ for 854.4061; Found 845.4056.

CD-2 mg/ml sample is prepared in $CDCl_3$.

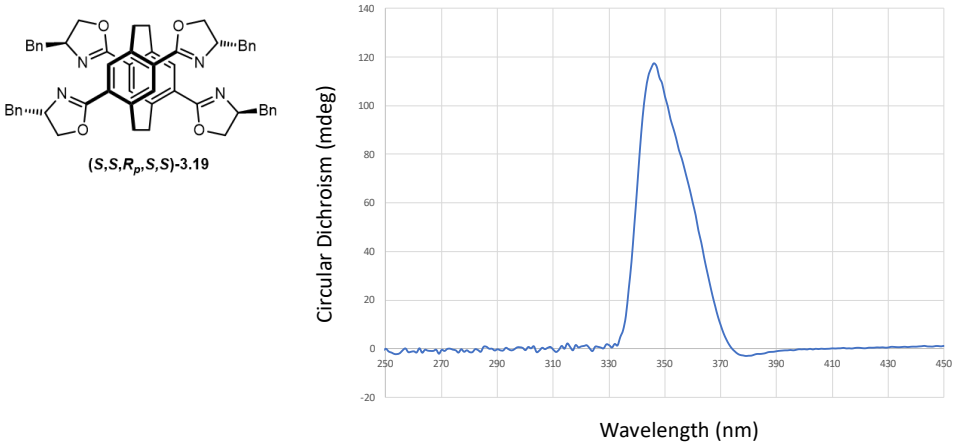

Figure 1: CD spectrum of Diastereomer 1 **(*S*,*S*,*R*$_p$,*S*,*S*)-3.19**.

Diastereomer 2 **(*S*,*S*,*S*$_p$,*S*,*S*)-3.19**

IR- ν_{max} 2923, 1631, 1497, 1349, 1273, 1056 cm^{-1}

^{1}H NMR ($CDCl_3$, 500 MHz): δ 7.40-7.23 (20H, m, H-24, H-24’,H-24’’, H-24’’’, H-25, H-25’, H-25’’, H-25’’’, H-26, H-26’, H-26’’, H-26’’’, H-27, H-27’, H-27’’, H-27’’’, H-28, H-28’, H-28’’, H-28’’’), 7.21 (4H, s, H-5, H-8, H-13, H-16), 4.69 (4H, q, *J* = 7.6 Hz, H-20, H-20’, H-20’’, H-20’’’), 4.28 (4H, t, *J* = 8.7 Hz, H-19a, H-19a’, -19a’’, H-19a’’’), 4.20-4.11 (4H, m, H-1a, H-1b, H-2a, H-2b), 4.08 (4H, t, *J* = 8.6 Hz, H-19b, H-19b’, H-19b’’, H-19b’’’), 3.28 (4H, dd, *J* = 9.0 Hz, 5.3 Hz, H-22a, H-22a’, H-22a’’, H-22a’’’), 3.12-3.01 (4H, m, H-9a, H-9b, H-10a, H-10b), 2.71 (4H, dd, *J* = 9.3 Hz, 4.5 Hz, H-22b, H-22b’, H-22b’’, H-22b’’’),

^{13}C NMR ($CDCl_3$, 125 MHz): δ 162.10 (4C, C-17, C-17’, C-17’’, C-17’’’), 141.34 (2C, C-4, C-15), 138.27 (2C, C-7, C-12), 134.67 (4C, C-23, C-23’, C-23’’, C-23’’’), 130.22 (4C, C-3, C-6, C-11, C-14), 130.22 (12C, C-5, C-8, C-13, C-16, C-24, C-24’, C-24’’, C-24’’’, C-28, C-28’, C-28’’, C-28’’’), 128.57 (8C, C-25, C-25’, C-25’’, C-25’’’, C-27, C-27’, C-27’’, C-27’’’), 126.48 (4C, C-26, C-26’, C-26’’, C-26’’’), 70.89 (4C, C-20, C-20’, C-20’’, C-20’’’),

68.53 (4C, C-19, C-19', C-19'', C-19'''), 41.87 (4C, C-22, C-22', C-22'', C-22'''), 34.52 (4C, C-1, C-2, C-9, C-10).

HRMS (ESI-TOF) m/z: $[M + H]^+$ Calcd $C_{56}H_{53}N_4O_4$ for 854.4061; Found 845.4052.

CD-2 mg/ml sample is prepared in $CDCl_3$.

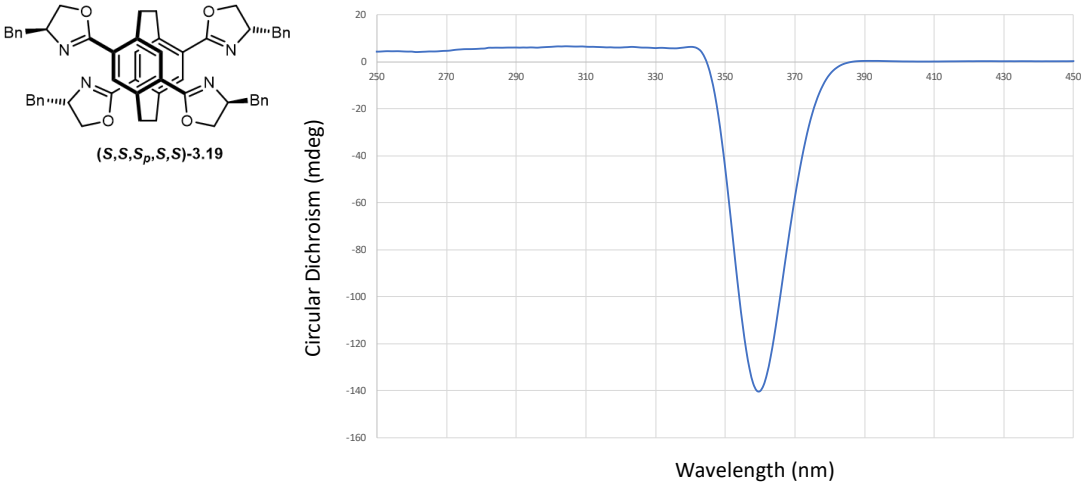

Figure 2: CD spectrum of Diastereomer 2 **(*S*,*S*,*S*$_p$,*S*,*S*)-3.19**.

(*S*,*R*$_p$,*S*)-4,7-dibromo-12,15-bis-(4′-benzyloxazolin-2′-yl)[2.2]paracyclophane and (*S*,*S*$_p$,*S*)-4,7-dibromo-12,15-bis-(4′-benzyloxazolin-2′-yl)[2.2]paracyclophane 3.20

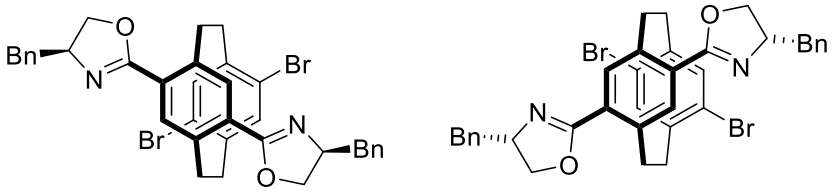

(*S*,*R*$_p$,*S*)-3.20 **(*S*,*S*$_p$,*S*)-3.20**

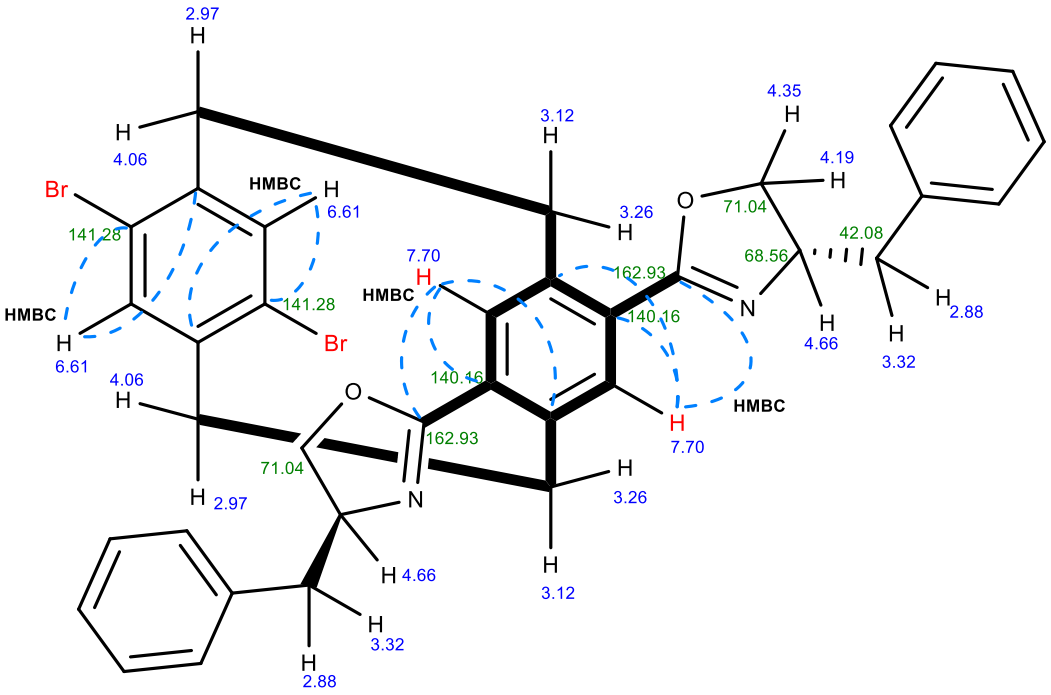

Figure 3: Structure elucidation of 3.20 (The indicated values are the ppm values obtained in ^{1}H & ^{13}C NMR spectrum and blue dotted lines denote the HMBC correlation).

(*S*,*R*$_p$,*S*)-4,7-dibromo-12,15-bis-(4′-benzyloxazolin-2′-yl)[2.2]paracyclophane-3.20

The small quantity of this by product made it impossible to get full data.

R_f : 0.5 (EtOAc:Hexanes 20:80)

^{1}H NMR ($CDCl_3$, 700 MHz): δ 7.70 (2H, s), 7.38-7.34 (8H, m), 7.29-7.26 (2H, m), 6.61 (2H, s), 4.66 (2H, quint, *J* = 15.7, 8.6 Hz), 4.35 (2H, t, *J* = 8.5 Hz), 4.19 (2H, t, *J* = 7.7 Hz), 4.06 (2H, dd, *J* = 12.4, 10.2 Hz), 3.32 (2H, dd, *J* = 13.9, 5.5 Hz), 3.26 (2H, dd, *J* = 13.3, 9.7 Hz), 3.12 (2H, dt, *J* = 12.7, 7.7 Hz), 2.97 (2H, ddd, *J* = 12.9, 13.9, 9.6, 7.6 Hz), 2.88 (2H, dd, *J* = 13.9, 8.4 Hz).

^{13}C NMR ($CDCl_3$, 176 MHz): δ 162.93, 141.28, 140.16, 138.10, 135.81, 132.80, 130.22, 129.25, 128.88, 128.64, 126.57, 125.31, 71.04, 68.56, 42.08, 33.94, 32.58.

HRMS (ESI-TOF) m/z: $[M + H]^+$ Calcd. for $C_{36}H_{33}Br_2N_2O_2$ 685.0883; found 685.0879.

(*S*,*S*$_p$,*S*)-4,7-dibromo-12,15-bis-(4′-benzyloxazolin-2′-yl)[2.2]paracyclophane 3.20

The small quantity of this by product made it impossible to get full data.

R_f : EtOAc:Hexanes (20:80) : 0.4

^{1}H NMR ($CDCl_3$, 400 MHz): δ 7.75 (2H, s), 7.40-7.31 (8H, m), 7.30-7.24 (2H, m), 6.60 (2H, s), 4.70 (2H, q, *J*= 7.5 Hz), 4.41 (2H, t, *J*=9.0 Hz), 4.17 (2H, t, *J*= 8.0 Hz), 4.01 (2H, dd, *J*= 9.8 Hz, 2.4 Hz), 3.31-3.22 (4H, m), 3.20-3.09 (2H, m), 2.89-2.77 (4H, m).

(*S*,*R*$_p$,*S*,*S*)-4,7,12-tris-(4′-benzyloxazolin-2′-yl)[2.2]paracyclophane and

(*S*,*S*$_p$,*S*,*S*)-4,7,12-tris-(4′-benzyloxazolin-2′-yl)[2.2]paracyclophane-3.21

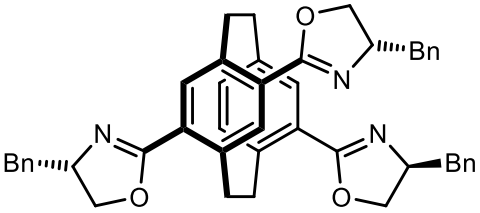

(*S*,*R*$_p$,*S*,*S*)-3.21

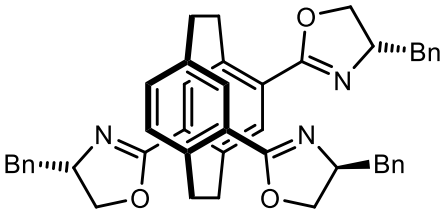

(*S*,*S*$_p$,*S*,*S*)-3.21

R_f: EtOAc:Hexane (20:80): 0.2

IR: ν_{max} 3059, 2925, 1716, 1634, 1495, 1453, 1261, 1082, 976, 700 cm^{-1}.

^{1}H NMR ($CDCl_3$, 500 MHz): δ 7.40-7.22 (15H, m), 7.17 (3H, d, *J* = 10.2 Hz), 6.69-6.55 (2H, m), 4.75-4.62 (3H, m), 4.42 (1H, t, *J* = 8.8 Hz), 4.30 (3H, dd, *J* = 17.5, 8.8 Hz), 4.19 (2H, dd, *J* = 16.2, 7.9 Hz), 4.09 (2H, dd, *J* = 13.8, 7.0 Hz), 4.03 (1H, dd, *J* = 12.3, 9.6 Hz), 3.35 (1H, dd, *J* = 13.7, 5.0 Hz), 3.28 (2H, dd, *J* = 13.7, 4.0 Hz), 3.20 (2H, m), 3.06 (1H, dt, *J* = 12.3, 8.9 Hz), 2.92-2.79 (3H, m), 2.73 (2H, dt, *J* = 13.7, 8.5 Hz).

^{13}C NMR ($CDCl_3$, 126 MHz): δ 163.84, 163.62, 163.07, 141.29, 141.25, 140.86, 139.99, 138.39, 138.28, 138.01, 136.63, 134.89, 134.56, 133.72, 132.25, 130.59, 129.97, 129.41, 129.24, 128.61, 128.55, 128.13, 126.60, 126.60, 126.47, 126.44, 71.36, 70.85, 70.77, 68.54, 68.40, 68.15, 41.94, 41.88, 41.82, 35.62, 35.44, 34.50, 33.81.

HRMS (ESI-TOF) m/z: $[M + H]^+$ Calcd. for $C_{46}H_{44}N_3O_3$ 686.3377; found 686.3357.

References

1. W. R. Leonard, J. L.Romine, A. I. Meyers, A rapid and efficient synthesis of chiral 2-hydro-2-oxazolines, *J. Org. Chem.*, **1991**, *56*, 1961-1963.
2. S. Shamsuzzaman, B. Z. Ahmad, S. Khan,, A convenient method for the synthesis of 3.beta.-hydroxy 4-en-6-one steroids, *J. Org. Chem.*,**1991**, *56*, 1936-1937.
3. C. Bolm, K. Wenz, G. Raabe, Regioselective palladation of 2-oxazolinyl [2.2] paracyclophanes.: Synthesis of planar-chiral phosphines, *J.Org. met. Chem.*, **2002**, *662*, 23- 33.

4. S. Kitagaki, S. Murata, K. Asaoka, K. Sugisaka, C. Mukai, N. Takenaga, K. Yoshida, Planar Chiral [2.2]Paracyclophane-Based Bisoxazoline Ligands: Design, Synthesis, and Use in Cu-Catalyzed Inter- and Intramolecular Asymmetric O–H Insertion Reactions, *Chem. Pharm. Bull.*, **2018**, *66*, 1006-1014.

Experimental Section for Chapter 4

General Information

All reactions were performed in scintillation vials, round bottom flasks (RBFs), or pressure tubes under an inert atmosphere of dry argon unless otherwise noted. Moisture-sensitive reactions were carried out using standard syringe septum techniques. Reaction solvent tetrahydrofuran (Fisher, HPLC grade) was dried by distillation from sodium-benzophenone radical ketyl. 1,4-Dioxane (Fisher, HPLC grade) was dried by distillation over calcium hydride. DMA (Sigma-Aldrich, ≥ 99.5% GC) was stored over 4Å molecular sieves. Solvents for filtration, transfers, and chromatography were certified ACS grade. Evaporation of solvents was carried out under reduced pressure on the rotary evaporator below 42 °C. Palladium catalysts and phosphine ligands were purchased from Sigma-Aldrich, Strem, and Apollo Scientific. Other reagents were purchased from Sigma-Aldrich, Alfa Aesar, and Acros Organics. Purification of the reaction mixture was performed by Bruker flash chromatography, column chromatography, or preparative TLC. The stationary phase for chromatography was silica gel 40-63 UM 60 Å, or 230-400 mesh. Preparative TLC was performed on MERCK precoated silica gel 60-F254 (0.5-mm) aluminium plates. Solvents for purification were purchased from LabServe. TLC visualisation was carried out using ultraviolet light (254 nm) and different staining reagents such as potassium permanganate.

Analytical Instruments

Optical rotation was recorded on a Perkin Elmer 241 polarimeter with the sodium lamp emitting at 589 nm (D = 589 nm). All samples were measured in chloroform unless otherwise noted in a 10 cm cell and an average of 3 readings was taken.

Circular Dichroism spectrum was recorded using a Chirascan CD spectrophotometer (150 W Xe arc) from Applied Photophysics. CD spectra (average of at least 2 scans) were recorded between 220 and 350 nm with 1 nm intervals, 120 nm/min scan rate, and 10 mm path length followed by subtraction of a background spectrum (solvent).

Infrared spectroscopy was carried out on ThermoScientific Nicolet iS5 iD7 ATR.

NMR spectroscopy was performed on Bruker 400 MHz, Bruker 500 MHz, or Bruker 700 MHz. Chemical shifts are reported in parts per million (ppm). All spectra were run in $CDCl_3$ unless otherwise stated. Spin multiplicities are described as s (singlet), bs (broad singlet), d (doublet), dd (doublet of doublets), ddd (doublet of doublet of doublets), dddd (doublet of doublet of doublet of doublets), t (triplet), td (triplet of doublets), q (quartet), quint (quintet),

m (multiplet), dt (doublet of triplet), ddt (doublet of doublet of triplets), dtd (doublet of triplet of doublets), dq (doublet of quartets). Coupling constants are reported in Hertz (Hz).

HRMS data were recorded on ThermoScientific Q Exactive Focus Hybrid Quadrupole-orbitrap

MS data were recorded on ThermoScientific MSQ plus. Samples were injected via Dionex Ultimate 3000 HPLC system running at 0.1 mL/min, in MeOH.

General procedures for the Hydrolysis of oxazolines

Conditions A: Aqueous HCl (6M) was added dropwise to a flask containing [2.2]paracyclophane-oxazoline. The resulting mixture was heated to reflux before cooling to room temperature. A solution of aqueous NaOH (40%) was added till the pH of the reaction mixture dropped to 5. The aqueous layer was extracted with CH_2Cl_2 (3 x 10 mL), combined organic layers dried over anhydrous $MgSO_4$, and concentrated under vacuum to afford pure compound.

Conditions B: A pressure tube was charged with [2.2] paracyclophane-oxazoline, with a few drops of 1,4-dioxane, H_2SO_4 (3.6 M) and heated at 100 °C for the specified time to control the mono- or bis-hydrolysis. After the completion of the reaction, 10 mL of distilled water was added to the reaction mixture. The diacid by-product was filtered as an off-white product using a Buchner funnel. The filtrate was extracted with CH_2Cl_2 (3 x 30 mL), and the combined organic layers were dried over anhydrous $MgSO_4$, and concentrated under a vacuum to afford pure compound.

(R_p)-(–)-4-Carboxy[2.2]paracyclophane 4.2

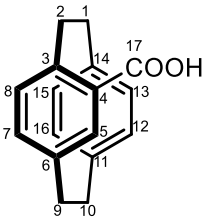

(R_p)-4.2

General condition B was followed using (R_p,*S*)-4-(4′-*tert*-butyloxazolin-2′-yl)[2.2]paracyclophane **4.1** (100 mg, 0.19mmol, 1.0 eq.), H_2SO_4 (3.6 M, 5 mL), few drops of 1,4-doxane, and heated at 100 °C for 12 hrs. After the completion of the reaction, (TLC monitored), 10 mL of distilled water was added to the reaction mixture. The aqueous layer was extracted with CH_2Cl_2 (3 x 30 mL), combined organic layers dried over anhydrous

$MgSO_4$, and concentrated under vacuum before keeping under high vacuum to afford the pure title compound **(R_p)-(–)-4.2**, white solid (48 mg, 0.190 mmol, 64%).
R_f: EtOAc:Hexane (20:80): 0.3

IR: ν_{max} 2923, 2852, 1674, 1422, 1300 cm^{-1}.

$[\alpha]_D^{20}$: –146 (*c* = 0.5, $CHCl_3$) (lit $[\alpha]_D^{23}$ –151.1 (*c* = 0.5, $CHCl_3$)][1]

^1H NMR ($CDCl_3$, 500 MHz): δ 7.32 (1H, s, H-5), 6.75 (1H, d, *J* = 7.7 Hz, H-15), 6.66-6.59 (3H, m, H-16, H-7, H-8), 6.55 (2H, d, *J* = 7.8 Hz, H-12, H-13), 4.24 (1H, t, *J* = 10.9 Hz, H-10a), 3.28-3.17 (4H, m, H-10b, H-9a, H-1a, H-1b), 3.13-3.03 (2H, m, H-2b, H-9b), 2.97-2.89 (m, 1H, H-2a).

^{13}C NMR ($CDCl_3$, 126 MHz): δ 171.99 (C-17), 143.74 (C-4), 140.08 (C-5), 140.04 (C-12), 139.46 (C-13), 137.38 (C-16), 136.39 (C-15), 136.17 (C-7), 133.15 (C-8), 132.79 (C-3), 132.33 (C-3), 131.78 (C-14), 129.61 (C-11), 36.29 (C-2), 35.27 (C-1), 35.11 (C-10), 34.95 (C-9).

HRMS (ESI-TOF) m/z: $[M - H]^+$ Calcd $C_{17}H_{15}O_2$ for 251.1067; Found 251.1075.

Data are comparable to that reported in the literature.[1]

(S_p)-(+)-4-Carboxy[2.2]paracyclophane 4.2

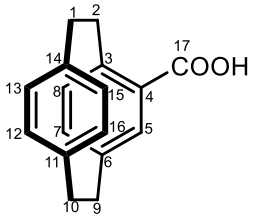

(S_p)-4.2

Prepared analogously to (R_p)-(–)-4-carboxy[2.2]paracyclophane **4.2** (100 mg, 0.189 mmol, 1.0 eq.) but employing (S_p,*S*)-4-(4′-benzyl-oxazolin-2′-yl)[2.2]paracyclophane **4.1**, H_2SO_4 (3.6 M, 5 mL), and heated at 100 °C for 12 hrs to afford the pure title compound **(S_p)-(+)-4.2**, white solid (48 mg, 0.19 mmol, 64 %).

$[\alpha]_D^{20}$: +155.1 (*c* = 0.5, $CHCl_3$) (lit $[\alpha]_D^{23}$ +161 (*c* = 0.943, $CHCl_3$)[1]

Data comparable to that reported in literature. [1]

(R_p)-(–)-[2.2]Paracyclophane-4,12-dicarboxylic acid 4.5

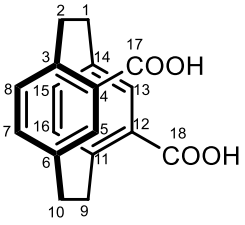

(R_p)-4.5

General procedure **B** was followed using (R_p,*S*)-(–)-4,12-bis(4′-benzyloxazolin-2′-yl)[2.2]paracyclophane **4.4** (100 mg, 0.189 mmol, 1.0 eq.), H_2SO_4 (3.6 M, 5 mL) for 24 hours to obtain the title compound **(R_p)-(–)-4.4** as an off-white product (30 mg, 0.101 mmol, 55 %).

R_f: EtOAc:Hexane (50:50): 0.2

$[\alpha]_D^{20}$: –152 (*c* = 0.25, EtOH) [Lit. $[\alpha]_D^{20}$: –156 (*c* = 0.25, EtOH)][2]

IR: ν_{max} 2954, 2658, 1674, 1652, 1422, 1276 cm^{-1}.

^{1}H NMR (MeOD-d_4, 500 MHz): δ 7.22 (2H, s, H-5, H-13), 6.80 (2H, d, *J* = 7.4 Hz, H-8, H-15), 6.63 (2H, d, *J* = 7.8 Hz, H-7, H-16), 4.14 (2H, t, *J* = 11.9 Hz, H-2a, H-9a), 3.23-3.17 (2H, m, H-2b, H-9b), 3.17-3.10 (2H, m, H-1a, H-10a), 2.88 (2H, d, *J* = 10.4, 7.5 Hz, H-1b, H-10b).

^{13}C NMR (MeOD-d_4, 126 MHz): δ 168.94 (C-17, C-18), 142.45 (C-11, C-3), 140.18 (C-12, C-4), 136.20 (C-14, C-6), 135.90, 133.56 (C-8, C-5), (C-16, C-13), 130.52 (C-15, C-7), 35.41 (C-9, C-1), 33.69 (C-10, C-2).

HRMS (ESI-TOF) m/z: $[M - H]^+$ Calcd $C_{18}H_{15}O_4$ for 295.0965; Found 295.0971.

Data comparable to that reported in literature.[2]

(S_p)-(+)-[2.2]Paracyclophane-4,12-dicarboxylic acid 4.5

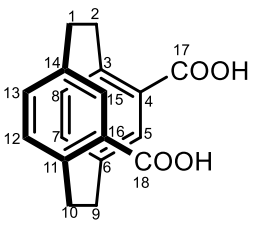

(S_p)-4.5

General procedure **B** was followed using (S_p,*S*)-(+)-4,12-bis(4′-benzyloxazolin-2′-yl)[2.2]paracyclophane **4.4** (100 mg, 0.189 mmol, 1.0 eq.), H_2SO_4 (3.6 M, 5 mL) for 24 hours to obtain the title compound **(S_p)-(+)-4.5** as an off-white product (30 mg, 0.101 mmol, 55 %).

R_f: EtOAc:Hexane (50:50): 0.2

$[\alpha]_D^{20}$: +155.1 (*c* = 0.098, EtOH) [Lit. $[\alpha]_D^{20}$: +150 (*c* = 0.09, EtOH)].[2]

Other data were the same as the other enantiomer.

Data comparable to that reported in literature.[2]

(R_p,*S*)-(–)-12-Bromo-4-carboxy-[2.2]paracyclophane 4.7

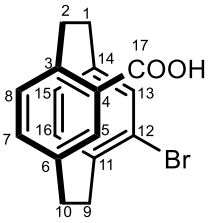

(R_p)-4.7

General procedure **B** was followed using (R_p,*S*)-(–)-12-bromo,4-benzyloxazolin-2′-yl)[2.2]paracyclophane **4.6** (100 mg, 0.189 mmol, 1.0 eq.), H_2SO_4 (3.6 M, 5 mL) for 24 hours to obtain the title compound **(R_p)-(–)-4.7** as an off-white product (50 mg, 0.101 mmol, 68 %).

R_f: EtOAc: Hexane (20:80): 0.3

$[\alpha]_D^{20}$: –50.1 (*c* = 0.9, $CHCl_3$)

IR: ν_{max} 2928, 1672, 1422, 1269, 1200, 1033, 708 cm^{-1}.

^1H NMR ($CDCl_3$, 500 MHz): δ 7.96 (1H, s, H-5), 6.74 (1H, d, *J* =7.9 Hz, H-7), 6.71-6.65 (2H, m, H-8, H-13), 6.64 (1H, d, *J* =8.0 Hz, 1H, H-15), 6.53 (1H, d, *J* =7.7 Hz, H-16), 4.21 (1H, t, *J* = 11.5 Hz, 1H, H-10a), 3.53 (1H, t, J = 11.4 Hz), 3.33-3.25 (1H, m, H-1b), 3.23-3.05 (3H, m, H-9a, H-9b, H-1a), 2.94-2.79 (2H, m, H-2a, H-2b).

^{13}C NMR ($CDCl_3$, 126 MHz): *δ* 171.58 (C-17), 143.10 (C-4), 142.09 (C-5), 139.72 (C-12), 138.98 (C-13), 137.71 (C-16), 136.19 (C-15), 135.82 (C-7), 135.00 (C-8), 131.89 (C-3), 131.17 (C-3), 129.26 (C-14), 126.80 (C-11), 36.24 (C-2), 35.78 (C-1), 34.09 (C-10), 32.51 (C-9).

HRMS (ESI-TOF) m/z: $[M - H]^+$ Calcd $C_{17}H_{14}BrO_2$ for 329.0172; Found 329.0197.

(S_p,*S*)-(+)-12-Carboxy-4-(4′-benzyloxazolin-2′-yl)[2.2]paracyclophane XX

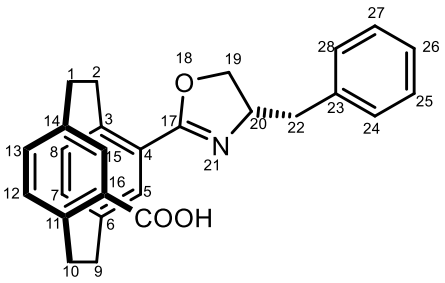

(S_p,*S*)-(+)-4.8

An Ace pressure tube was charged with (R_p,*S*)-(–)-4,12-bis-(4′-benzyl-oxazolin-2′-yl)[2.2]paracyclophane **4.4** (100 mg, 0.189 mmol, 1.0 eq.), H_2SO_4 (3.6 M, 5 mL) and heated at 100 °C. The reaction was purposely stopped at 12 hrs. After cooling, 10 mL of distilled water was added to the reaction mixture. The diacid by-product was filtered as an off-white product using Buchner funnel. The filtrate was extracted with CH_2Cl_2 (3x30 mL), combined organic layers dried over anhydrous $MgSO_4$, and concentrated under vacuum before performing the column chromatography.

Purification: Isocratic column chromatography [SiO_2, EtOAc:Hexanes (20:80)] to obtain the title compound **(S_p,*S*)-(+)-4.8** as an off-white solid (40 mg, 0.09 mmol, 51%).

R_f: EtOAc:Hexane (20:80): 0.3

$[\alpha]_D^{20}$: +21.83 (*c* = 1.2, $CHCl_3$)

IR: ν_{max} 2920, 2357, 1651, 1495, 1289, 1255, 1017 cm^{-1}.

^{1}H NMR ($CDCl_3$, 500 MHz): δ 7.37-7.32 (2H, m, H-24, H-25), 7.31-7.24 (3H, m, H-28, H-27, H-26), 7.12 (1H, s, H-13), 6.92 (1H, s, H-5), 6.82 (1H, d, *J* = 7.5 Hz, H-8), 6.67-6.56 (3H, m, H-15, H-7, H-16), 4.85 (1H, dtd, *J* = 14.8, 8.9, 4.5 Hz, H-20), 4.55 (1H, t, *J* = 9.0 Hz, H-19a), 4.38 (1H, t, *J* = 8.0 Hz, H-19b), 4.02 (1H, dd, *J* = 13.0, 2.5 Hz, H-2a,), 3.70 (1H, t, *J* =

11.4 Hz, H-9a), 3.30 (1H, dd, *J* = 13.7, 4.2 Hz, H-1a), 3.22-3.06 (3H, m, H-10a, H-22a, H-22b), 3.05-2.97 (1H, m, H-2b), 2.93-2.83 (2H, m, H-1b, H-9b), 2.83-2.75 (1H, m, H-10b).

^{13}C NMR ($CDCl_3$, 126 MHz): δ 169.29 (C-29), 168.86 (C-17), 140.92 (C-23), 140.69 (C-12), 139.95 (C-4), 138.91 (C-14), 136.46 (C-6), 135.94 (C-27), 135.85 (C-25), 135.59 (C-28), 135.49 (C-24), 135.25 (C-16), 133.04 (C-13), 129.50 (C-8), 128.78 (C-5), 128.72 (C-15), 127.82 (C-7), 126.93 (C-26), 72.75 (C-20), 65.51 (C-19), 41.02 (C-22), 34.71 (C-9), 34.48 (C-1), 34.33 (C-10), 33.82 (C-2).

HRMS (ESI-TOF) m/z: $[M - H]^+$ Calcd. for $C_{27}H_{24}NO_3$ 410.1751; found 410.1761.

(*R*$_p$,*S*)-(–)-12-Carboxy-4-(4′-benzyloxazolin-2′-yl)[2.2]paracyclophane 4.8

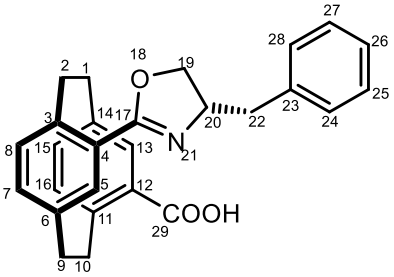

(*R*$_p$,*S*)-(-)-4.8

Prepared analogously to (*S*$_p$,*S*)-(–)-4-carboxy-12-(4′-benzyloxazolin-2′-yl)-[2.2]paracyclophane **4.8** but employing (*S*$_p$,*S*)-(+)-4,12-bis(4′-benzyloxazolin-2′-yl)[2.2]paracyclophane **4.4** (100 mg, 0.189 mmol, 1.0 eq.) and H_2SO_4 (3.6 M, 5 mL).

Purification: Isocratic column chromatography [SiO_2, EtOAc: Hexane (20:80)] to obtain the title compound as an off-white solid (43 mg, 0.10 mmol, 56%).

R_f: EtOAc:Hexane (20:80): 0.3

$[\alpha]_D^{20}$: –22 (*c* = 1, $CHCl_3$).

IR: ν_{max} 2927, 1696, 1628, 1452, 1260, 1238, 1189 cm^{-1}.

^{1}H NMR ($CDCl_3$, 500 MHz): δ 7.42-7.30 (4H, m, H-24, H-25, H-26, H-27, H-28), 7.15 (1H, s, H-13), 6.91 (1H, s, H-5), 6.81 (1H, d, *J* = 7.5 Hz, H-8), 6.66-6.59 (3H, m, H-15, H-7, H-16), 4.64 (1H, dtd, *J* = 13.3, 9.3, 4.2 Hz, H-20), 4.53 (1H, t, *J* = 9.0 Hz, H-19a), 4.36 (1H, t, *J* = 8.6 Hz, H-19b), 3.99 (1H, t, *J* = 10.9 Hz, H-2a), 3.68 (1H, t, *J* = 12.2 Hz, H-9a), 3.59 (1H, dd, *J* = 13.8, 3.9 Hz, H-1a), 3.22-3.11 (2H, m, H-10a, H-22a), 3.10-3.05 (1H, m, H-22b), 3.04-2.95 (2H, m, H-1b, H-2b), 2.93-2.86 (1H, m, H-9b), 2.79-2.69 (1H, m, H-10b).

^{13}C NMR ($CDCl_3$, 126 MHz): δ 169.16 (C-29), 168.98 (C-17), 140.97 (C-23), 140.76 (C-12), 139.70 (C-4), 138.88 (C-14), 136.79 (C-6), 135.97 (C-27), 135.87 (C-25), 135.59 (C-28), 135.54 (C-24), 135.17 (C-16), 132.97 (C-13), 129.26 (C-8), 128.96 (C-5), 128.88 (C-15), 127.85 (C-7), 127.06 (C-26), 73.26 (C-20), 66.42 (C-19), 41.03 (C-22), 34.71 (C-9), 34.45 (C-1), 34.30 (C-10), 33.90 (C-2).

HRMS (ESI-TOF) m/z: $[M - H]^+$ Calcd. for $C_{27}H_{24}NO_3$ 410.1751; found 410.1762.

General procedures for the synthesis of Rhodium Paddle-wheel 4.13

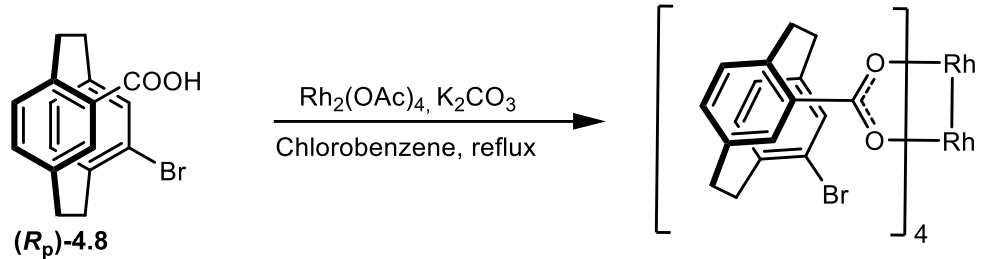

(R_p)-4.8 **(R_p)-4.13** **(83%)**

Rhodium (II) acetate (22 mg, 0.05 mmol, 1.00 eq.) and (R_p)-12-bromo-4-carboxy[2.2]paracyclophane **4.7** (100 mg, 0.3 mmol, 6.00 eq.) in anhydrous chlorobenzene (25 mL) was heated to reflux under argon atmosphere in a Soxhlet extraction apparatus. The extraction thimble was charged with potassium carbonate that had been dried at 155 °C for 24 h. A new thimble containing potassium carbonate was introduced every 24 h. After 72 h, the solvent was removed under reduced pressure.

Purification: The crude mixture was purified by column chromatography (silica, n-pentane /CH_2Cl_2/THF, 4:4:1), yielding the product as a green crystalline solid (70 mg, 83% yield).

R_f: n-pentane/CH_2Cl_2/THF (4:4:1): 0.7

$[\alpha]_D^{20}$: –28 (c = 0.5, $CHCl_3$).

IR: ν_{max} 2928, 2853, 1568, 1409, 1372, 1198, 1032, 707 cm^{-1}.

^{1}H NMR ($CDCl_3$, 500 MHz): δ 7.80 (4H, d, *J* =10.9 Hz), 6.50-6.36 (12H, m), 6.35-6.28 (4H, m), 6.1 (3H, s), 4.20 (8H, s), 4.10-3.99 (4H, m), 3.41-3.32 (4H, m), 3.18-3.08 (4H, m), 2.98 (4H, t, J =11.5 Hz), 2.89 (4H, t, *J* =9.9 Hz), 2.75-2.58 (12H, m), 2.09 (8H, s).

The carbon spectrum was quite complex.

HRMS (ESI-TOF) m/z: $[M - H]^-$Calcd. for $C_{68}H_{55}Br_4O_8Rh_2$ 1560.6091; found 1560.8559.

(R_p)-(–)-Diphenyl([2.2]paracyclophane-4-yl)phosphine oxide 4.19

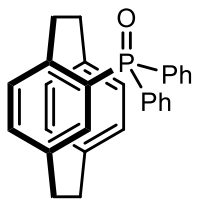

(R_p)-(-)-4.19

A pressure tube was charged with (R_p)-(–)-4-carboxy[2.2]paracyclophane **4.2** (40 mg, 0.16 mmol, 1.0 eq.), diphenylphosphine oxide (32 mg, 0.13 mmol, 0.8 eq.), triethylamine (44 µL, 0.32 mmol, 2.0 eq.), $(Boc)_2O$ (48 mg, 0.22 mmol, 1.4 eq.) under argon. In a separate 4 ml scintillation vial, Dppp (13 mg, 0.032 mmol, 0.2 eq.), $Pd(OAc)_2$ (4 mg, 0.016 mmol, 0.1 eq.) were dissolved in 1,4-dioxane (1.0 mL) and transferred to the pressure tube under argon. The reaction mixture was heated at 130 °C for 48 hrs. After cooling, the reaction mixture was diluted with CH_2Cl_2: MeOH (1:1) and filtered. The filtrate was concentrated under reduced pressure and purified using column chromatography.

Purification: Isocratic column chromatography [SiO_2, EtOAc:Hexanes (20:80)] to obtain the title compound **(R_p)-(–)-4.19** as an off-white solid (4-10 mg, 6.3-15.6% in 5 experiments).

R_f: EtOAc:Hexane (20:80): 0.3

$[\alpha]_D^{20}$: –45 (c = 0.2, $CHCl_3$) [Lit. $[\alpha]_D^{32}$: –68.3 (c =1.88, $CHCl_3$)][3]

IR: ν_{max} 2954, 2658, 1674, 1652, 1422, 1276 cm^{-1}.

^{1}H NMR ($CDCl_3$, 500 MHz): δ 7.73 (2H, d, J = 10.6, 7.1 Hz), 7.62-7.53 (3H, m, H), 7.53-7.44 (3H, m), 7.43-7.35 (2H, m), 7.20 (1H, d, J = 7.9 Hz), 6.65 (1H, d, J = 7.6 Hz), 6.62-6.50 (3H, m), 6.32-6.24 (2H, m), 3.60-3.48 (2H, m), 3.17-3.07 (2H, m), 3.05 (1H, d, J = 9.7 Hz), 2.99 (1H, ddd, J = 14.2, 11.3, 5.7 Hz, H-), 2.90 (1H, td, J = 12.8, 3.7 Hz), 2.80 (1H, ddd, J = 13.5, 10.9, 7. 1Hz).

^{31}P NMR ($CDCl_3$, 200 MHz) δ_P 27.08.

HRMS (ESI-TOF) m/z: $[M + H]^+$ Calcd $C_{28}H_{26}OP$ for 409.1716; Found 409.1709.

Data are comparable to that reported in the literature.[3]

(S_p)-(+)-Diphenyl([2.2]paracyclophane-4-yl)phosphine oxide 4.19

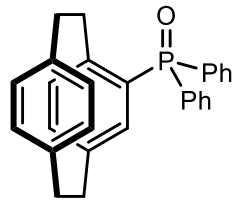

(S_p)-(-)-4.19

Prepared analogously to (R_p)-(–)-diphenyl([2.2]paracyclophane-4-yl)phosphine oxide **XX** but employing (S_p)-(+)-4-carboxy[2.2]paracyclophane **XX** (40 mg, 0.16 mmol, 1.0 eq.), diphenylphosphineoxide (32 mg, 0.13 mmol, 0.8 eq.), triethylamine (44 µL, 0.32 mmol, 2.0 eq.), $(Boc)_2O$ (48 mg, 0.22 mmol, 1.4 eq.) Dppp (13 mg, 0.032 mmol, 0.2 eq.), $Pd(OAc)_2$ (4 mg, 0.016 mmol, 0.1 eq.), 1,4-dioxane (1.0 mL) for 48 hrs.

$[\alpha]_D^{20}$: +18.75 (c = 0.16, $CHCl_3$).

Other data were same as the other enantiomer.

General procedures for the synthesis of (R_p)-(–)-4,12-Diamino[2.2]paracyclophane XX:

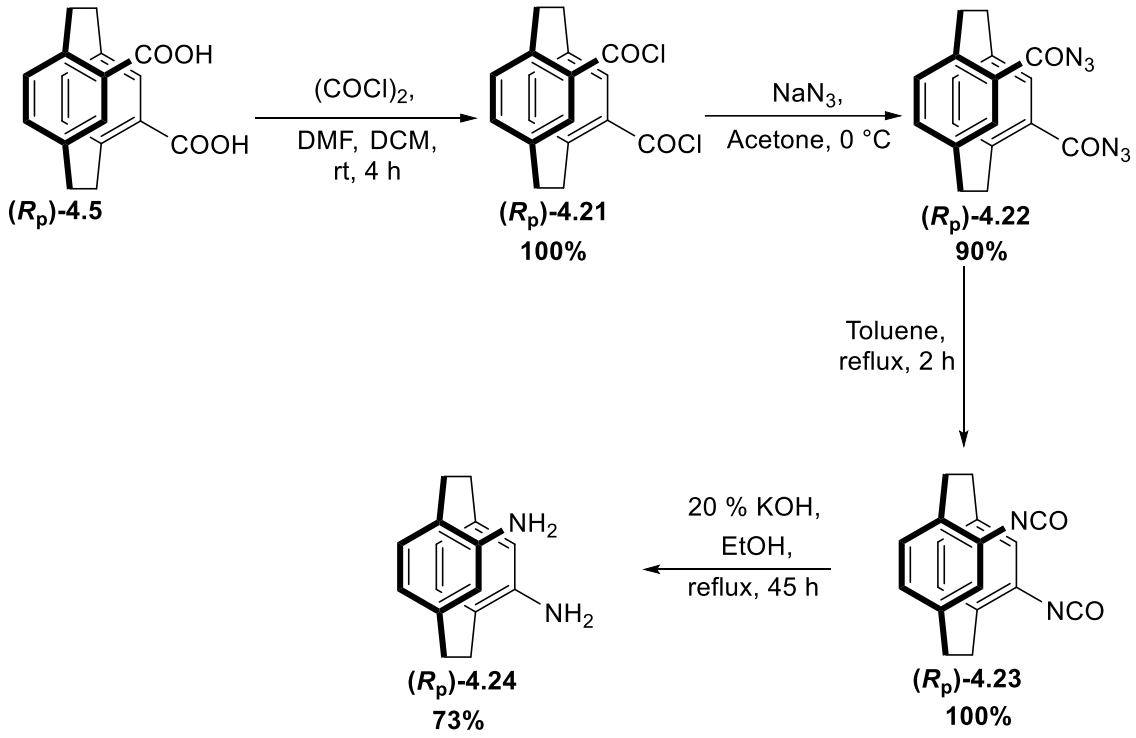

Step 1:

(R_p)-4,12-Bis(chlorocarbonyl)[2.2]paracyclophane 4.21:

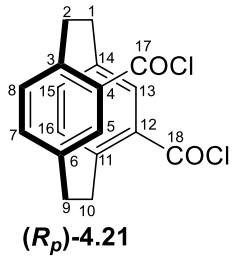

To a suspension of (R_p)-4,12-dicarboxy[2.2]paracyclophane **4.5** (6 mg, 0.202 mmol) in anhydrous CH_2Cl_2 (8 mL) was added oxalylchloride (174 µL) and three drops of a 10% mixture of CH_2Cl_2/DMF (v/v) at room temp. The reaction mixture was stirred at room temp. for 3 h until it became clear. Then benzene (10 mL) was added, and the solvents were evaporated under reduced pressure. The crude product (67 mg, 100% yield) was used for further synthesis.

Step 2:

(R_p)-4,12- bis(azido-carbonyl)[2.2]paracyclophane 4.22:

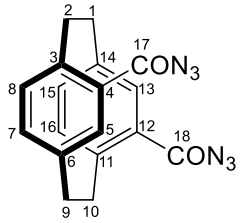

(R_p)-4.22

To a suspension of the crude (R_p)-4,12-bis(chlorocarbonyl)[2.2]paracyclophane **4.21** (67 mg, 0.201 mmol) in acetone (15 mL) was added dropwise at 0 °C, an aqueous solution of NaN_3 (131 mg, 2.01 mmol) in water (10 mL), and the mixture was stirred at the same temp. for 1 h. Then ice-cold water (50 mL) was added and the precipitate was filtered off; the residue was washed several times with ice-cold water and allowed to air dry. The crude pale yellow amorphous solid (62 mg) was obtained in 90% yield.

R_f: EtOAc: n-hexane (1:1): 0.3

$[\alpha]_D^{20}$: –82.4 (c = 0.1, $CHCl_3$).

IR: ν_{max} 2931, 2269, 2138, 1679, 1652, 1422, 1246 cm^{-1}.

^{1}H NMR ($CDCl_3$, 500 MHz): δ 7.18 (2H, s, H-5, H-15), 6.80 (2H, d, J = 6.21 Hz, H-7, H-13), 6.62 (2H, d, J = 6.21 Hz, H-8, H-12), 4.20 (2H, t, J = 12.0 Hz, H-2a, H-10a), 3.34-3.09 (4H, m, H-9a, H-9b, H-1a, H-1b), 2.97-2.80 (2H, m, H-2b, H-10b).

Data are comparable to that reported in the literature.[4]

Step 3:

(R_p)-(–)-4,12-Diisocyanato[2.2]paracyclophane 4.23

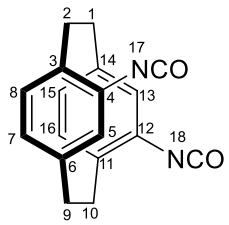

(R_p)-4.23

The crude (R_p)-4,12-bis- (azidocarbonyl)[2.2]paracyclophane **4.22** (60 mg, 0.732 mmol) was taken up in dry toluene (50 mL) under N_2 and the mixture refluxed for 30 min. The solvent was evaporated in vacuo and the crude residue was column chromatographed on silica gel with CH_2Cl_2/pentane (1:4, v/v) to yield the (R_p)-4,12diisocyanato-[2.2]paracyclophane (52 mg, 100%) as a colorless solid.

R_f: CH_2Cl_2:pentane (25:75): 0.3

^{1}H NMR ($CDCl_3$, 500 MHz): δ 6.58-6.50 (4H, m, H-5, H-8, H-12, H-15), 6.47-6.41 (2H, m, H-7, H-13), 3.34 (2H, t, J = 12.0 Hz, H-2a, H-10a), 3.15-2.98 (4H, m, H-9a, H-9b, H-1a, H-1b), 2.71-2.82 (2H, m, H-2b, H-10b).

Only proton NMR was recorded and the product proceeded to the next step.

HRMS (ESI-TOF) m/z: $[M+H]^+$ ($C_{18}H_{15}N_2O_2$) calcd.: 291.1055, found: 291.10542

Data are comparable to that reported in the literature.[4]

(R_p)-4,12-Diamino[2.2]paracyclophane 4.24

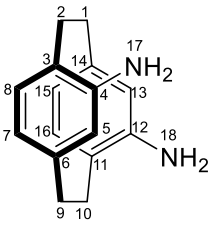

(R_p)-4.24

(R_p)-(–)-4,12-Diisocyanato[2.2]- paracyclophane (50 mg, 0.172 mmol) was taken up in ethanol (10 mL) and the mixture was refluxed for 2 h. To this solution was added 20% aq. KOH solution (5 mL) and the mixture was refluxed for 45 h with stirring. To the cooled reaction mixture was added 20% aq. KOH solution (30 mL), and the mixture was stirred for 5 min. The precipitate was removed by filtration, washed several times with water, and dried (Na_2SO_4), yielding the (R_p)-(–)-4,12-diamino[2.2]paracyclophane (30 mg, 73%) as a pale brown solid.

R_f: EtOAc:Hexane (20:80): 0.3

IR: ν_{max} 3368, 2923, 1608, 981, 784 cm^{-1}

^{1}H NMR ($CDCl_3$, 500 MHz): δ 6.33-6.38 (m, 2H, H-8, H-12), 6.20 (br s, 2H, H-5, H-15), 6.07-6.06 (m, 2H, H-7, H-13), 3.60-3.20 (m, 2H, H-17, H-18), 3.23-2.75 (m, 6H, H-9a, H-9b, H-1a, H-1b, H-2a, H-10a), 2.75-2.55 (2H, m, H-2b, H-10b).

^{13}C NMR ($CDCl_3$, 125 MHz): δ 144.58(C-4, C-16), 141.12 (C-6, C-14), 135.15 (C-8, C-12), 124.09 (C-3, C-11), 123.09 (C-7, C-13), 116.33 (C-5, C-15), 32.74 (C-9, C-1), 32.04 (C-10, C-2).

HRMS (ESI-TOF) m/z: $[M+H]^+$ ($C_{16}H_{19}N_2$) calcd.: 239.1469, found: 239.1470

CD was recorded in $CHCl_3$.

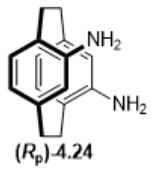

(R_p)-4.24

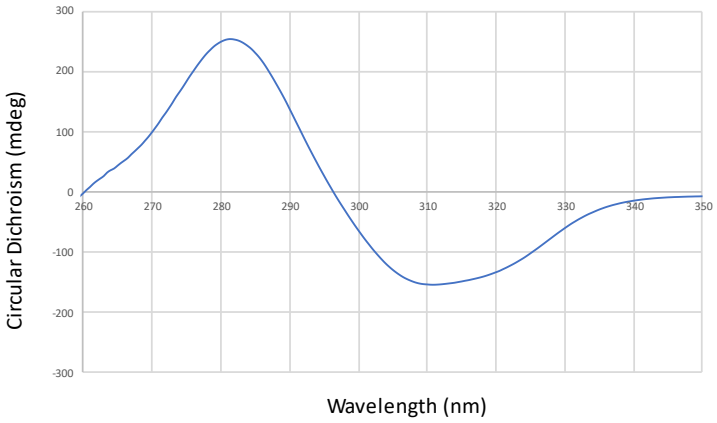

Data comparable to that reported in literature.[4]

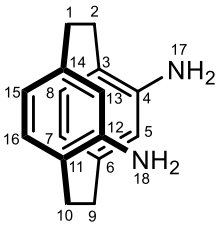

(S_p)-4.24

Prepared analogously to **(R_p)-4,12-Diamino[2.2]paracyclophane XX** but employing (S_p)-(–)-4,12-dicarboxy[2.2]paracyclophane **XX** (500 mg).

Yield, 320 mg, 80%.

CD was recorded in $CHCl_3$.

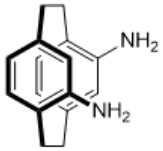

(S_p)-4.24

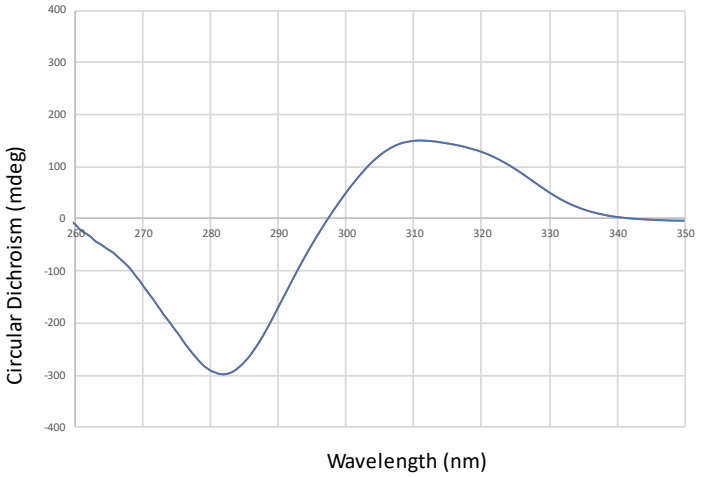

Other data were same as the other enantiomer.

General procedures for the synthesis of (S_p)-(+)-4,12-Dihydroxy[2.2]paracyclophane XX:

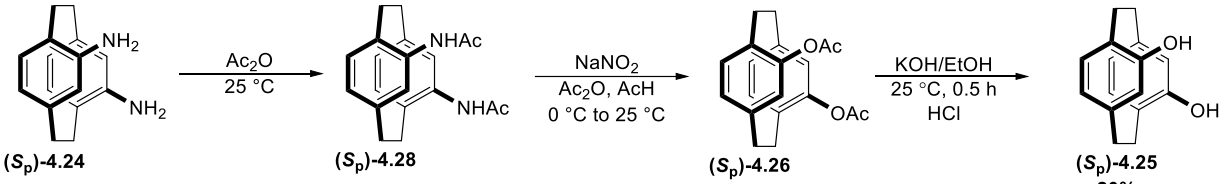

(S_p)-4.24 (S_p)-4.28 (S_p)-4.26 (S_p)-4.25 20%

An oven-dried flask was charged with **(S_p)-4,12-Diamino[2.2]paracyclophane 4.24** (50 mg, 0.210 mmol), acetic anhydride (0.5 mL), and one drop of pyridine. The mixture was stirred at room temperature followed by TLC. After the starting material was consumed (24 h), acetic anhydride (0.5 mL) and acetic acid (0.5 mL) were added. After the reaction mixture was cooled to 0 °C, $NaNO_2$ powder (90 mg, 1.68 mmol, 8 eq.) was added in equal portions over 2 h, followed by TLC, and stirred at room temperature for 12 h. The white precipitate formed was filtered and washed with CH_2Cl_2 (3 × 2.0 mL). The filtered solution was combined with CH_2Cl_2 phase and the solvent was removed. The residue was washed with water (3 × 2.0 mL), dried in vacuum, and purified by chromatography on silica gel (petroleum

ether/CH_2Cl_2 = 2:1) to give **(S_p)-4,12-Dihydroxy[2.2]paracyclophane 4.25** as a white solid (10 mg, 20%).

R_f: petroleum ether/CH_2Cl_2 (2:1): 0.3

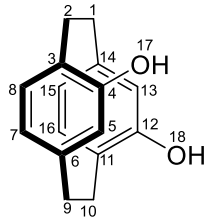

(S_p)-(+)-4.25

IR: ν_{max} 3303, 2926, 2853, 2489, 2396, 1600, 1560, 1415, 1252, 1142 cm^{-1}

^1H NMR ($CDCl_3$, 500 MHz): δ 6.38-6.32 (2H, m, H-8, H-12), 6.21-6.14 (2H, m, H-5, H-15), 6.10-6.01 (2H, m, H-7, H-13), 3.36-3.26 (4H, m, H-17, H-18), 2.93-2.85 (6H, m, H-9a, H-9b, H-1a, H-1b, H-2a, H-10a), 2.57-2.45 (2H, m, H-2b, H-10b).

^{13}C NMR ($CDCl_3$, 125 MHz): δ 154.83(C-4, C-16), 142.09 (C-6, C-14), 135.09 (C-8, C-12), 124.65 (C-3, C-11), 123.75 (C-7, C-13), 117.26 (C-5, C-15), 33.01 (C-9, C-1), 30.66 (C-10, C-2).

CD was recorded in $CHCl_3$.

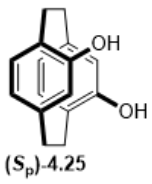

(S_p)-4.25

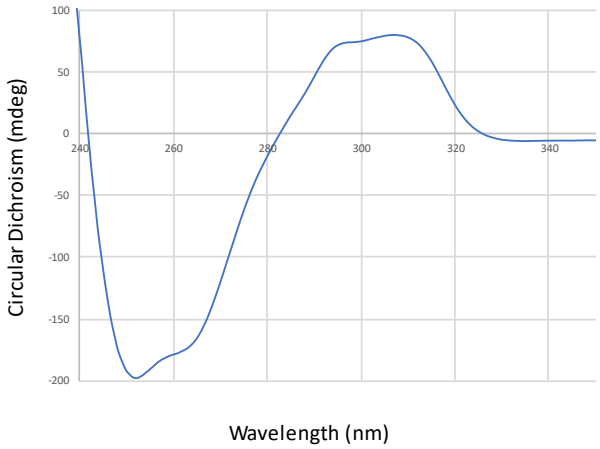

General procedures for the synthesis of Chiral Gold Catalyst:

Step 1: Synthesis of (R_p)-[2.2]Paracylophane isonitrile 4.34

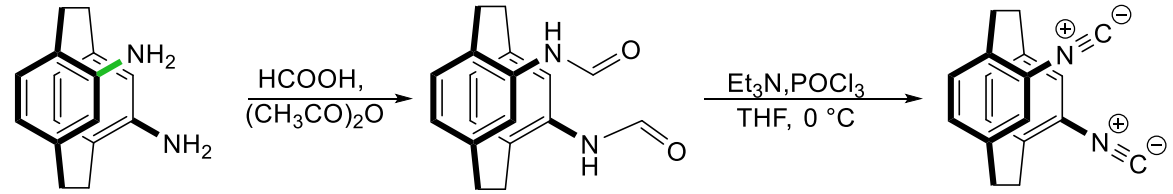

(R_p)-4.24 (R_p)-4.33 (R_p)-4.34

The enantiomerically pure amine (R_p)-4,12-Diamino[2.2]paracyclophane **4.24** was converted into the isonitrile. The reaction of the amine with ethyl formate at reflux temperature delivered the formamide 4.33, which was purified by recrystallization from acetone/pentane. The formamide, then delivered the **(R_p)-[2.2]Paracylophane isonitrile 4.34** (60 mg, 56%), when treated with phosphoryl chloride and triethylamine in THF.

(R_p)-[2.2]Paracylophane isonitrile 4.34

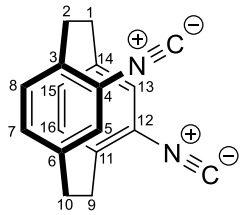

(R_p)-4.34

The isonitrile is very unstable, so it is always preferred to use it as it is formed. We proceeded to the next step and tried characterization with 10 mg of the isonitrile. Complete characterization was not achieved due to the degradation of the isonitrile.

$[\alpha]_D^{20}$: –11.4 (c = 0.5, $CHCl_3$).

^{1}H NMR ($CDCl_3$, 500 MHz): δ 6.98 (2H, s, H-8, H-12), 6.67-6.61 (4H, m, H-5, H-7, H-13, H-15), 3.36-3.26 (2H, m, H-9a, H-9b), 3.28-3.19 (2H, m, H-2a, H-10a), 3.08-3.17 (2H, m, H-1a, H-1b), 2.93-2.82 (2H, m, H-2b, H-10b).

^{13}C NMR ($CDCl_3$, 125 MHz): δ 141.38(C-4, C-12), 136.61 (C-3, C-6, C-11, C-14), 134.80 (C-8, C-16), 134.03 (C-7, C-13), 127.49 (C-5, C-15), 32.74 (C-9, C-1), 32.04 (C-10, C-2).

Dept-135 ($CDCl_3$, 500 MHz): 134.80 (C-8, C-16), 134.03 (C-7, C-13), 127.49 (C-5, C-15), 32.74 (C-9, C-1), 32.04 (C-10, C-2).

Step 2:

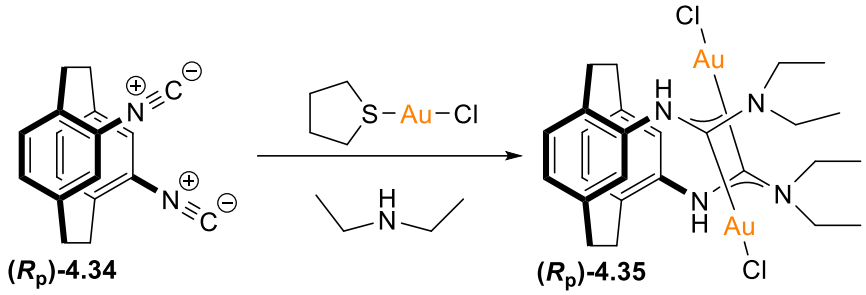

(R_p)-4.34 (R_p)-4.35

Method A:

Under an atmosphere of nitrogen (tht)AuCl (2.0 eq.) was dissolved in absolute DCM (0.10 M) at RT. The isonitrile (1.0 eq.) was added and the solution was stirred for 15 min. After this, the amine (4.0 eq.) was added and stirring was continued for 2 h. The solvent was removed under reduced pressure and the resulting crude product was washed with cold pentane five times. The product was dried under reduced pressure.

Method B:

Under an atmosphere of nitrogen (tht)AuCl (2.0 eq.) was dissolved in absolute DCM (0.10 M) at RT. The isonitrile (1.0 eq.) was added and the solution was stirred for 2 h. After this, the amine (4.0 eq.) was added and stirring was continued for 12 h. The solvent was removed under reduced pressure and the resulting crude product was washed with cold pentane five times. The product was dried under reduced pressure.

Method C:

Under an atmosphere of nitrogen (tht)AuCl (2.0 eq.) was dissolved in absolute DCM (0.10 M) at RT. The isonitrile (1.0 eq.) was added and the solution was stirred for 2 h. The solid was filtered off on the Buchner funnel and dried.

Under an atmosphere of nitrogen, the amine (4.0 eq.) was added to the above filtered isonitrile-gold complex, and stirring was continued for 12 h. The solvent was removed under reduced pressure and the resulting crude product was washed with cold pentane five times. The product was dried under reduced pressure.

Alternatively, the compounds can be purified by column chromatography using MeOH: DCM (05:95) as eluent on basic alumina.

(R_p)-Gold complex with diethyl amine 4.35

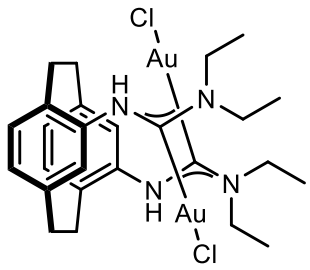

(R_p)-4.35

General method C was employed for the synthesis of **(R_p)-4.35** from **(R_p)-(2.2]Paracylophane isonitrile 4.34.** Under an atmosphere of nitrogen (tht)AuCl (120 mg, 0.387 mmol) was dissolved in absolute DCM (0.10 M) at RT. The isonitrile (50 mg, 0.194 mmol) was added and the solution was stirred for 2 h. The solid was filtered off on the Buchner funnel and dried. Under an atmosphere of nitrogen, the amine (80 µL, 0.775 mmol) was added to the above filtered isonitrile-gold complex, and stirring was continued for 12 h. The solvent was removed under reduced pressure and the resulting crude product was washed with cold pentane five times. The product was dried under reduced pressure.

Purification: the crude mixture was purified by column chromatography using MeOH: DCM (05:95) as eluent on basic alumina to give **(R_p)-Gold complex with diethyl amine 4.35** as a white solid (10 mg, 6%).

R_f: MeOH: DCM (05:95):0.5

HRMS (ESI-TOF) m/z: $[M+Na]^+$ ($C_{26}H_{38}Au_2Cl_2N_4$) calcd.: 893.1702, found: 893.1697.

Due to poor yield, most of the characterization could not be accomplished. Still, we were successful in getting the crystal structure of our desired compound.

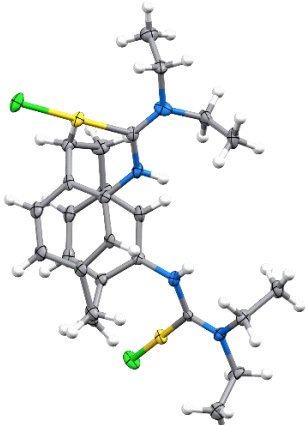

References

1. D. J. Cram, N. L. Allinger, Macro Rings. XII. Stereochemical Consequences of Steric Compression in the Smallest Paracyclophane, *J. Am. Chem. Soc.*, **1955**, *77*, 6289-6294.
2. B. Jiang, X. L. Zhao, X. Y. Xu, Resolution of (±)-[2.2] paracyclophane-4, 12-dicarboxylic acid, *Tetrahedron: Asymmetry*, **2005**, *16*, 1071-1074.
3. R. Parmar, M. P. Coles, P. B. Hitchcock, G. J. Rowlands, Towards a flexible strategy for the synthesis of enantiomerically pure [2.2] paracyclophane derivatives: the chemistry of 4-tolylsulfinyl [2.2] paracyclophane, *Synthesis*, **2010**, *24*, 4177-4187.
4. H. Hopf, S. Narayanan, P. Jones, The preparation of new functionalized [2.2] paracyclophane derivatives with N-containing functional groups, *Beilstein J. Org. Chem.*, **2015**, *11*, 437-445.

Experimental Section Chapter 5

General:

All reactions were performed in oven and/or flame-dried glassware under an atmosphere of dry argon unless otherwise noted. Moisture-sensitive reactions were carried out using standard syringe septum techniques. All solvents and reagents were purified by standard techniques unless otherwise noted. Solvents for filtration, transfers, and chromatography were certified ACS grade. Evaporation of solvents was carried out under reduced pressure on a rotary evaporator below 40 ˚C. Brine refers to a saturated solution of sodium chloride in water.

TLC visualisation was carried out using ultraviolet light (254 nm) and different staining reagents such as potassium permanganate.

^{1}H, ^{13}C NMR spectra were recorded on Bruker 400, 500 MHz spectrometers using tetramethylsilane (TMS) asan internal standard. Chemical shifts are reported in parts per million(ppm) downfield from tetramethylsilane. Spin multiplicities are described as s (singlet), bs (broad singlet), d (doublet), dd (double of doublet), ddd (doublet of doublet of doublet), t (triplet), td (triplet of doublet), q (quartet), m (multiplet). Coupling constants are reported in Hertz (Hz). Analytical thin layer chromatography(TLC) was performed on MERCK precoated silicagel 60-F254 (0.5mm) aluminium plates. Visualization of the spots was achieved either by exposure to UV light or by dipping the plates into $KMnO_4$ and heating with heat gun. Column chromatography was performed using silicagel 60-120 and 100-200 mesh. The names of all the compounds given in the experimental section were taken from ChemDraw Professional 15.0.

HRMS data were recorded by David Lun using a ThermoScientific Q Exactive Focus Hybrid Quadrupole-orbitrap Mass Spectrometer. Sample(s) were injected via Dionex Ultimate 3000 HPLC system running at 0.1 mL/min CH_3OH.

***N*-(Piperidin-1-yl)picolinamide-5.56**

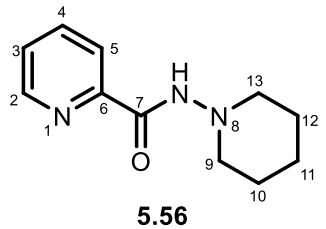

5.56

Ninety-eight percent concentrated sulfuric acid (2.59 mL, 48.78 mmol) was added dropwise to a solution of 2-picolinic acid (6 g, 48.78 mmol) in anhydrous ethanol (40 mL) surrounded by an ice-water bath. The mixture was refluxed for 24 h. Upon cooling to ambient temperature, the product was poured into 20 mL ice water. The resulting solution was neutralized to pH = 7-8 with a solution of potassium carbonate. The precipitate was filtered, and the filtrate was extracted with ether (3 × 100 mL). After drying over magnesium sulfate, the organic phases were evaporated to dryness under reduced pressure. The unpurified ester can be used for next hydrazinolysis without any further purification. A mixture of above ester, 80% hydrazine hydrate (1 mL), and ethanol (30 mL) was refluxed for 12 h. Then, the solution was evaporated to dryness and the resulting white solid (1.0 g, 7.30 mmol) was dissolved in ethanol (10 mL). It was used for the next step, without any further purification. Triethylamine (1.3 mL, 8.76 mmol) was added and the reaction mixture was refluxed. 1,5-dibromo pentane (1.2 mL, 8.75 mmol) was added to the refluxed reaction mixture. It was further refluxed for 24 h. The reaction mixture was concentrated on rota vapor under reduced pressure and the resulting mixture was purified by flash column chromatography using EtOAc: n-hexane (4:6) to give a white solid (0.9 g, 61%).

R_f: EtOAc: n-hexane (4:6): 0.3

^{1}H NMR ($CDCl_3$, 500 MHz) δ 8.70 (1H, s, NH), 8.54 (1H, d, *J*=4.74 Hz, H-2), 8.23 (1H, d, *J*=8.2 Hz, H-5), 7.85 (1H, t, *J*= 8.2 Hz, H-4), 7.44 (1H, t, *J*= 5.6 Hz, H-3), 2.90 (4H, s, H-9a, H-9b, H-13a, H-13b), 1.80 (4H, quint, *J*= 5.7Hz, H-11a, H-11b, H-13a, H-13b), 1.48-1.38 (2H, m, H-12a, H-12b).

^{13}C NMR ($CDCl_3$, 125 MHz) δ 160.93 (C-7), 150.05 (C-2), 147.89 (C-7), 137.31 (C-3, C-5), 126.20 (C-4), 122.53 (C-9, C-13), 57.10 (C-12), 25.25 (C-10), 23.35 (C-11).

HRMS (ESI-TOF) m/z: $[M+H]^+$ calcd for $C_{11}H_{15}N_3O$ 206.1317; Found 206.1409.

(*E*)-2-(Piperidin-1-ylimino)acetic acid – 5.58

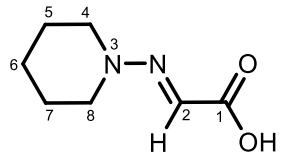

5.58

Glyoxylic acid (74 mg, 0.998 mmol) was dissolved in anhydrous ethanol (1mL). 1-aminopiperidine (100 mg, 0.998 mmol) was added to it. The reaction mixture was then heated to 40 ˚C for 0.5 h. It was then concentrated under reduced pressure and was purified by flash column chromatography using EtOAc: n-hexane (4:6) to give off white solid (70 mg, 45%).

R_f: MeOH: DCM (02:98): 0.3

^{1}H NMR ($CDCl_3$, 400 MHz): δ 12.79 (1H, s, H-1), 7.65 (1H, s, H-2), 6.90-6.80 (2H, m, H-2, H-5), 3.35-3.22 (4H, m, H-5a, H-5b, H-8a, H-8b),1.78-1.45 (4H, m, H-5a, H-5b, H-7a, H-7b), 1.59-1.53 (2H, m, H-6a, H-6b).

The ^{13}C spectrum was not recorded.

HRMS (ESI-TOF) m/z: $[M-H]^+$ calcd for $C_7H_{12}N_2O_2$ 156.0899; Found 156.0954.

***(E)*-2-Phenyl-2-(piperidin-1-ylimino)acetic acid-5.62**

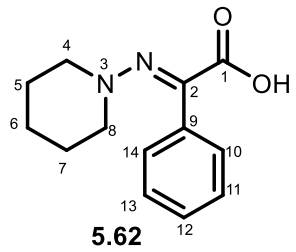

5.62

2-Oxo-2-phenylacetic acid (500 mg, 3.33 mmol) was dissolved in anhydrous ethanol (1 mL). 1-Aminopiperidine (334 mg, 3.33 mmol) was added to it. The reaction mixture was then heated to 40 ˚C for 0.5 h. It was then concentrated under reduced pressure and the resulting mixture was purified by flash column chromatography using MeOH: DCM (02:98) to give off a white solid **5.62** (370 mg, 48%).

R_f: MeOH: DCM (02:98): 0.3

^{1}H NMR ($CDCl_3$, 500 MHz): δ 7.90 (2H, d, *J*= 7.27 Hz, H-10, H-14), 7.50 (1H, t, *J*= 7.72 Hz, H-12), 7.44 (2H, t, *J*= 7.72 Hz, H-11, H-13), 3.19 (4H, t, *J*=5.78 Hz, H-4a, H-4b, H- 8a, H-8b), 2.00 (4H, quint, *J*= 5.70 Hz, H-5a, H-5b, H-7a, H-7b), 1.12 (2H, quint, *J*= 5.30 Hz, H- 6a, H- 6b).

The ^{13}C spectrum was not recorded.

HRMS (ESI-TOF) m/z: $[M-H]^+$ calcd for $C_{13}H_{16}N_2O_2$ 231.1123; Found 231.0707.

(*E*)-2-((piperidin-1-ylimino)methyl)phenol-5.63

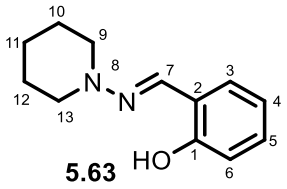

5.63

2-hydroxybenzaldehyde (122 mg, 0.998 mmol) was dissolved in anhydrous ethanol (1 mL). 1-aminopiperidine (100 mg, 0.998 mmol) was added to it. The reaction mixture was then heated to 40 ˚C for 0.5 h. It was then concentrated under reduced pressure and the resulting mixture was purified by flash column chromatography using EtOAc: n-hexane (05:95) to give off white solid (70 mg, 34%).

R_f: EtOAc: n-hexane (05:95): 0.3

^{1}H NMR ($CDCl_3$, 400 MHz): δ 11.79 (1H, s, OH), 7.69 (1H, s, H-7), 6.98-6.84 (2H, m, H-2, H-5), 3.15-3.12 (4H, m, H-10a, H-10b, H-13a, H-13b),1.78 (4H, quint, *J*= 5.7Hz, H-11a, H-11b, H-12a, H-12b), 1.59-1.53 (2H, m, H-11a, H-11b).

The ^{13}C spectrum was not recorded.

HRMS (ESI-TOF) m/z: $[M+H]^+$ calcd for $C_{12}H_{16}N_2O$ 205.1323; Found 205.1317.

(*E*)-2, 4-di-tert-butyl-6-((piperidin-1-ylimino)methyl)phenol-5.65

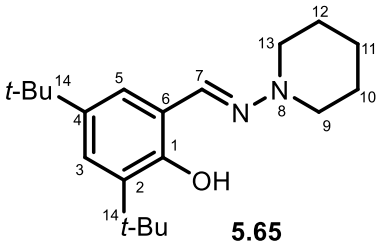

5.65

3,5-di-tert-butyl-2-hydroxybenzaldehyde (210 mg, 0.898 mmol) was dissolved in anhydrous ethanol (1 mL). 1-aminopiperidine (100 mg, 0.998 mmol) was added to it. The reaction

mixture was then heated to 40 ˚C for 3 h. It was then concentrated under reduced pressure and the resulting mixture was purified by flash column chromatography using EtOAc: n-hexane (07:93) to give white solid (100 mg, 32%).

R_f: EtOAc: n-hexane (07:93): 0.3

^{1}H NMR ($CDCl_3$, 500 MHz): δ 12.14 (1H, s, 1H, OH), 7.75 (s, 1H, H-7), 7.26 (1H, d, *J*= 2.38 Hz, H-3), 7.00 (1H, d, *J*= 2.22 Hz, H-5), 3.13 (4H, t, *J*= 5.78 Hz, H-10a, H-10b, H-13a, H-13b),1.77 (4H, quint, *J*= 5.7Hz, H-11a, H-11b, H-12a, H-12b), 1.61-1.53 (2H, m, H-11a, H-11b), 1.45 (9H, s, -C(CH_3)$_3$), 1.31 (9H, s, -C(CH_3)$_3$).
The ^{13}C spectrum was not recorded.
HRMS (ESI-TOF) m/z: $[M+H]^+$ calcd for $C_{20}H_{32}N_2O$ 317.2605; Found 317.2589.

(*Z*)-2-([2.2]paracyclophane-4-yl)-2-(piperidin-1-ylimino)aceticacid-5.68

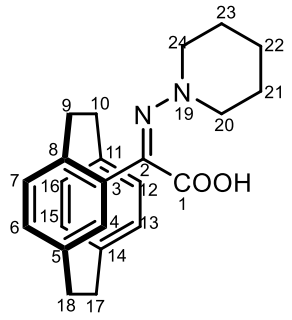

5.68

2-([2.2]Paracyclophane-4-yl)-2-oxoacetic acid (170 mg, 0.599 mmol) was dissolved in anhydrous ethanol (1 mL). 1-aminopiperidine (60 mg, 0.599 mmol) was added to it. The reaction mixture was then heated to 40 ˚C for 0.5 h. It was then concentrated under reduced pressure and the resulting mixture was purified by flash column chromatography using MeOH: DCM (10:90) to give a yellow solid (100 mg, 46%).

R_f: MeOH: DCM (10:90): 0.3

^{1}H NMR ($CDCl_3$, 400 MHz): δ 7.13 (1H, s, H-4), 6.66-6.63 (2H, m, H-7, H-6), 6.56-6.45 (4H, m, H-12, H-13, H-15, H-16), 4.07 (1H, t, *J*= 11.2 Hz, 1H, H- 9a), 3.17-3.09 (4H, m, H-9b, H-10a, H-10b), 3.04-2.94 (2H, m, H-18a, H-18b), 2.90-2.83 (m, 2H, H-17a, H-17b) 1.97 (4H,

4H, H-20a, H-20b, H- 24a, H- 24b), 1.67 (4H, quint, *J*= 5.30 Hz, H-21a, H-21b, H-23a, H-23b), 1.44 (2H, m, H- 22a, H- 22b).

The ^{13}C spectrum was not recorded.

HRMS (ESI-TOF) m/z: $[M+H]^+$ calcd for $C_{12}H_{16}N_2O$ 363.2113; Found 363.2135.

(*E*)-2-((cyclohexylimino)methyl)phenol-5.73

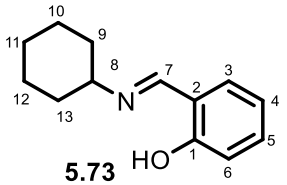

5.73

2-Hydroxybenzaldehyde (612 mg, 5.041 mmol) was dissolved in anhydrous ethanol (1mL). cyclohexylamine (500 mg, 5.041 mmol) was added to it. The reaction mixture was then heated to 40 ˚C for 3 h. It was then concentrated under reduced pressure to give off white solid (1.2 g, 97% crude yield).

R_f: EtOAc:n-hexane(07:93):0.3

^1H NMR ($CDCl_3$, 400 MHz): δ 13.85 (1H, s, OH), 7.32-7.23 (2H, m, H-3, H-6), 6.96 (1H, d, *J*=8.34 Hz, H-4), 6.86 (1H, t, *J*= 7.5 Hz, H-5), 3.27-3.22 (1H, m), 1.84-1.82 (3H, m), 1.68-1.52 (3H, m), 1.44-1.27(3H, m).

The ^{13}C spectrum was not recorded.

HRMS (ESI-TOF) m/z: $[M+H]^+$ calcd for $C_{13}H_{18}NO$ 204.1388; Found 204.1401.

(*E*)-2-(cyclohexylimino)-2-phenylacetic acid-5.74

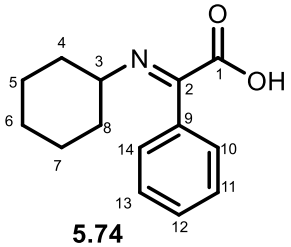

5.74

2-Oxo-2-phenylacetic acid (500mg, 3.367 mmol) was dissolved in anhydrous ethanol (1mL). cyclohexylamine (334 mg, 3.367 mmol) was added to it. The reaction mixture was then heated to 40 ˚C for 0.5 h. It was then concentrated under reduced pressure to give off a white solid (740 mg, 95%).

The ^{13}C spectrum was not recorded.

R_f: MeOH: DCM (10:90): 0.3

^1H NMR ($CDCl_3$, 500 MHz): δ 8.08 (2H, d, *J*= 7.65 Hz, H-10, H-14), 7.60 (1H, t, J= 7.28 Hz, H-12), 7.49 (2H, t, *J*= 7.28 Hz, H-11, H-13), 2.90 (1H, t, *J*= 11.21 Hz, 1H, H-3), 1.96 (1H, d, *J*= 11.20 Hz, H-4a, H-8a), 1.67 (2H, d, *J*= 13.71 Hz, 2H, H-5a, H-7a), 1.55 (1H, d, *J*= 12.46 Hz, 1H, H-6a), 1.38-1.26 (2H, m, H-4b, H-8b), 1.18-1.10 (2H, m, H-5b, H-7b), 1.06-0.98 (1H, m, H-6b).

The ^{13}C spectum was not recorded.

HRMS (ESI-TOF) m/z: $[M+H]^+$ calcd for $C_{14}H_{18}NO_2$ 232.1338; Found 232.1325.

(*Z*)-2-([2.2]paracyclophane-4-yl)-2-(cyclohexylimino)acetic acid

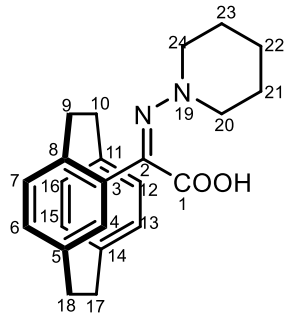

5.75

2-([2.2]Paracyclophane-4-yl)-2-oxoacetic acid (226 mg, 0.801 mmol) was dissolved in anhydrous ethanol (1 mL). Cyclohexylamine (80 mg, 0.801 mmol) was added to it. The reaction mixture was then heated to 40 ˚C for 0.5 h. It was then concentrated under reduced pressure and the resulting mixture was purified by flash column chromatography using MeOH: DCM (10:90) to give a white solid (180 mg, 62%).

The ^{13}C spectrumwas not recorded.

R_f: MeOH: DCM (10:90): 0.3

^1H NMR ($CDCl_3$, 400 MHz): δ 6.91 (1H, s, H-4), 6.84 (1H, d, *J*= 8.28 Hz, 1H, H-7), 6.69 (1H, d, *J*= 8.29 Hz, H-6), 6.58-6.51 (2H, m, H-12, H-13), 6.39-6.35 (2H, m, H-15, H-16), 3.89-3.83 (1H, m, H-9a), 3.17-2.90 (8H, m, H-9a, H-9b, H-10a, H-10b, H-17a, H-17b, H-18a, H-18b), 1.90 (2H, d, *J*= 11.19 Hz, H-21a, H-21b), 1.69 (2H, d, *J*=13.71 Hz, H-20a, H-20b), 1.55 (1H, d, *J*= 12.46 Hz, H-24a), 1.32-1.18 (4H, m, H-22a, H-22b, H-23a, H-23b), 1.10-1.05 (1H, m, H-24b).

The ^{13}C spectrum was not recorded.

HRMS (ESI-TOF) m/z: $[M+H]^+$ calcd for $C_{24}H_{28}NO_2$ 362.2120; Found 362.2135.

5.77 Methyl 4-(3-((tert-butoxycarbonyl)amino)cyclohexyl)benzoate

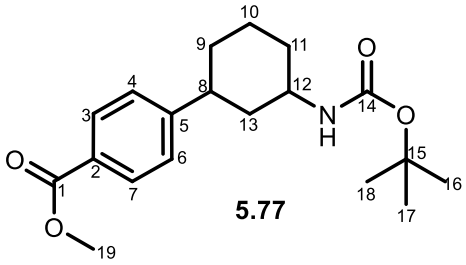

To a flame dried schlenk tube (5 mL) equipped with a magnetic stir bar was added $Pd(OAc)_2$ (8.9 mg, 0.04 mmol), transient directing group (salicyladehyde, 10 mg, 0.08 mmol), ligand (2-pyridone, 19 mg, 0.20 mmol), ArI (211 mg , 0.80 mmol), AgTFA (267 mg, 1.21 mmol) and solvent (HFIP 1.0 mL), followed by the free amine substrate (40 mg, 0.4 mmol), and H_2O (73 μL). The tube was capped and covered with a safety shield. The mixture was then stirred at room temperature for 10 mins before heating to 120 ˚C for 24 h under vigorous stirring. Upon completion, the reaction mixture was cooled to room temperature, and the dark brown suspension was passed through a pad of celite and washed with CH_2Cl_2 (3 x 1.0 mL). The combined CH_2Cl_2 solutions were concentrated under reduced pressure. THF (1.0 mL) and HCl (2 M, 0.8 mL) were added to the residue and the mixture was stirred at room temperature for 1 h. The mixture was subsequently basified with NaOH (10 M, 0.4 mL) (Checked with pH paper) and $(Boc)_2O$ (4.0 eq.) was added. The brown solution was then vigorously stirred at room temperature for 4 h. Ethyl Acetate (2.0 mL) was added and well mixed. The top organic layer was separated and passed through a pad of Silica (3 cm). The remaining aqueous layer was further extracted with ethyl acetate (3 x 2.0 mL). Every time the organic extract was passed through the above pad of Silica. All the organic extracts were collected, combined in a vial and evaporated under reduced pressure and the resulting mixture was purified by flash column chromatography using EtOAc: n-Hexane (10:90) to give a white solid (36 mg, 27%).

R_f: EtOAc: n-Hexane (10:90): 0.3

^{1}H NMR ($CDCl_3$, 500 MHz): δ 7.97 (2H, d, *J*= 8.39 Hz, H-3, H-7), 7.27 (2H, d, *J*= 8.01 Hz, 2H, H4, H-6), 4.47 (1H, br s, N-H), 3.91 (3H, s, -OCH_3), 3.61 (1H, br s, H-12), 2.70 (1H, t, *J*=

12.07 Hz, H-8), 2.22 (1H, d, *J*= 11.90 Hz), 2.07 (1H, d, *J*= 11.90 Hz), 1.95- 1.86 (2H, m), 1.54-1.51 (1H, m), 1.45 (9H, s, *t*-Bu-H-16, H-17, H-18), 1.41-1.33 (1H, m), 1.26 (1H, q, *J*= 12.12 Hz), 1.18- 1.09 (1H, m).

The ^{13}C spectrum was not recorded.

HRMS (ESI-TOF) m/z: $[M+Na]^+$ calcd for $C_{19}H_{27}NO_4$ 356.1845; Found 356.1887.

Planar chiral Oxazolines Based on [2.2]paracyclophane: A New Toolbox for Asymmetric Synthesis

This document contains electronic appendices for the Ph.D. thesis of Shashank Tewari

Table of Contents

Electronic appendix for Chapter 3

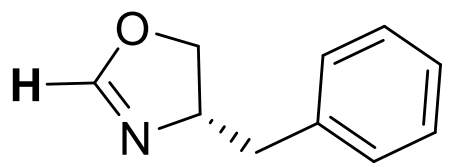

4-Benzyl-2-oxazoline-**3.6a**

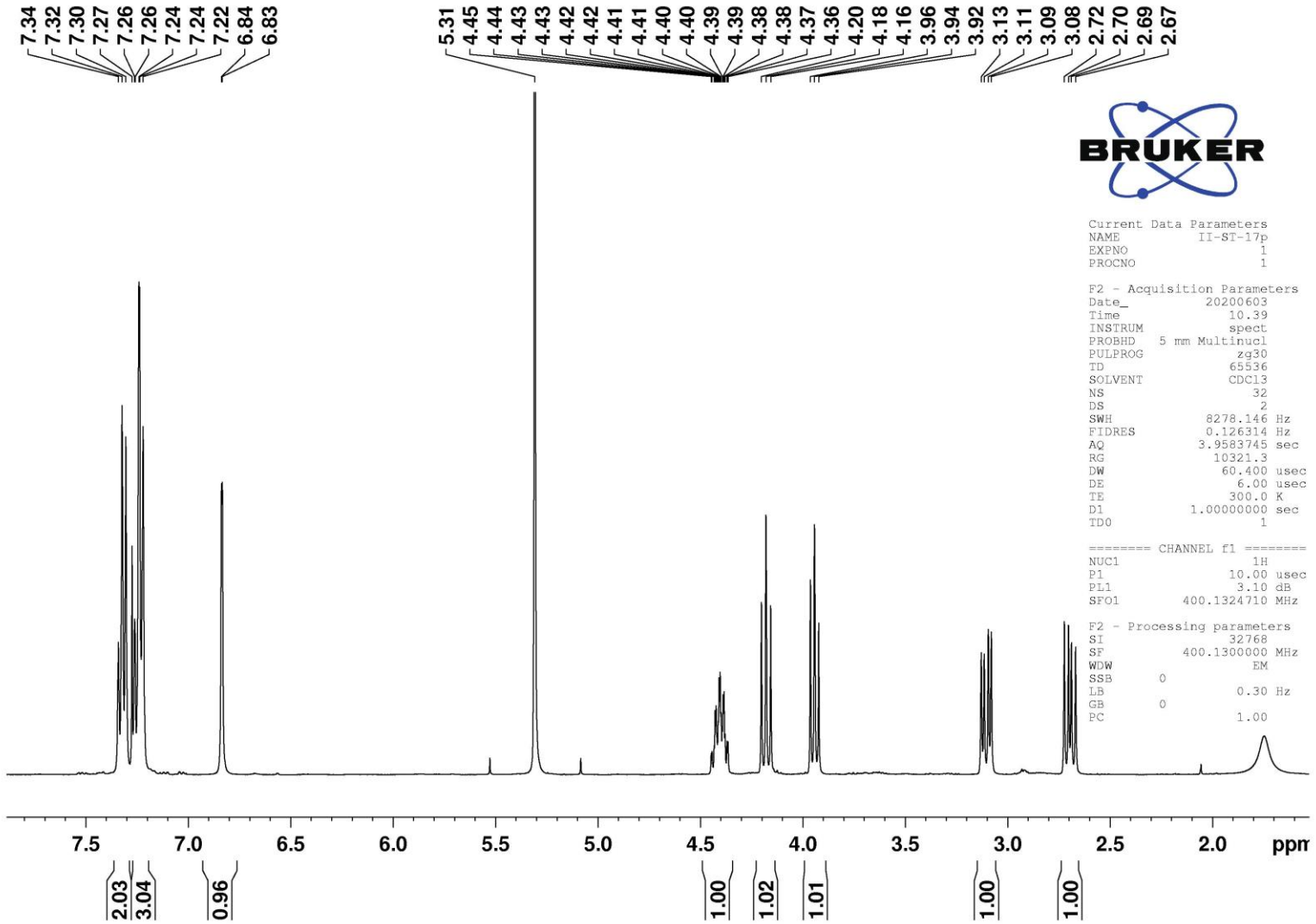

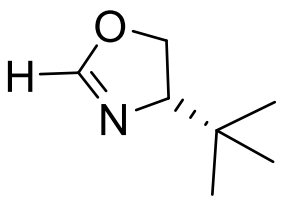

4-*tert*-butyl-2-oxazoline-**3.6b**

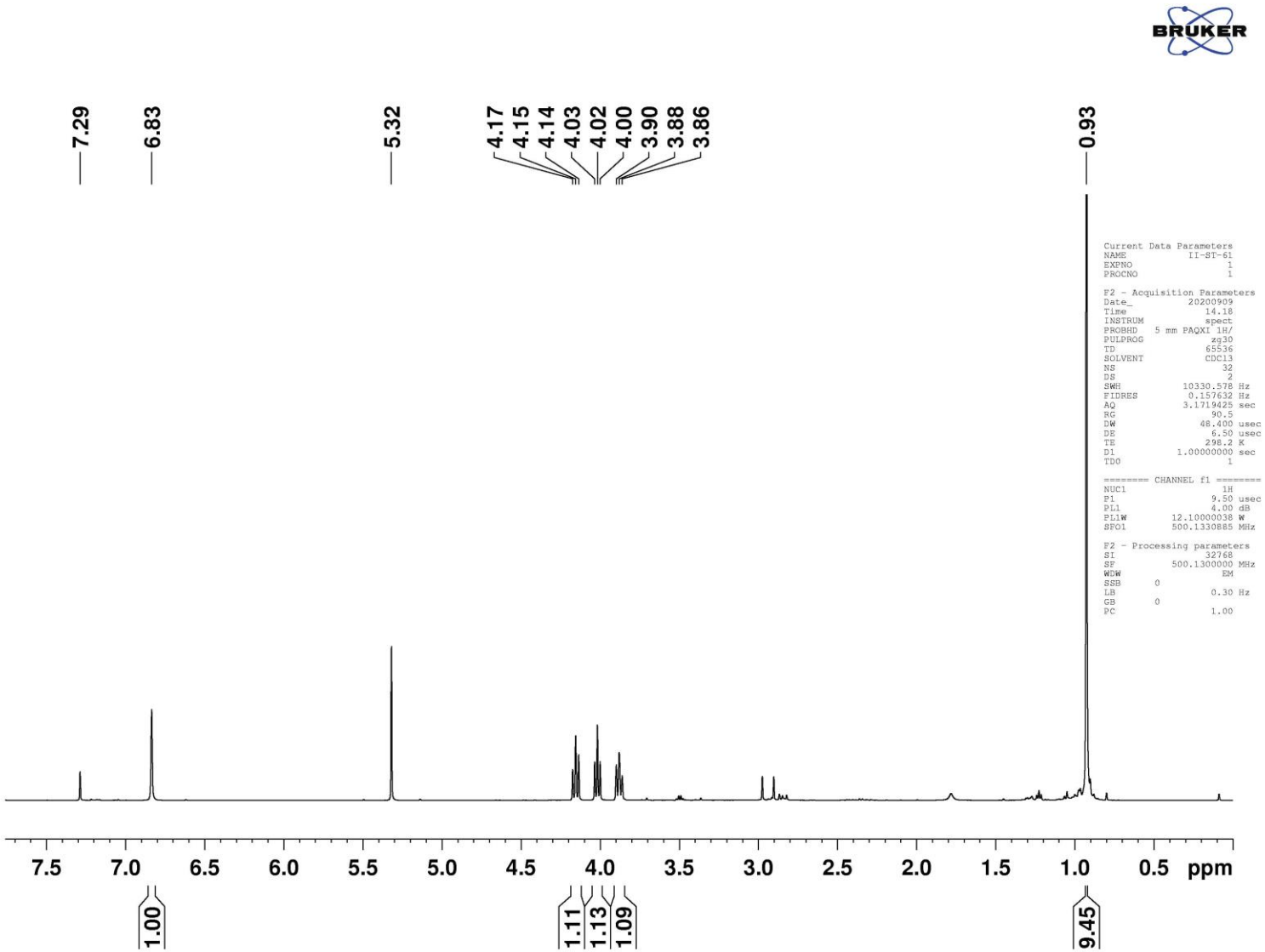

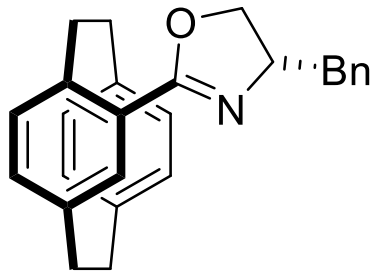

(R_p,*S*) 3.7a
Diastereomer 1

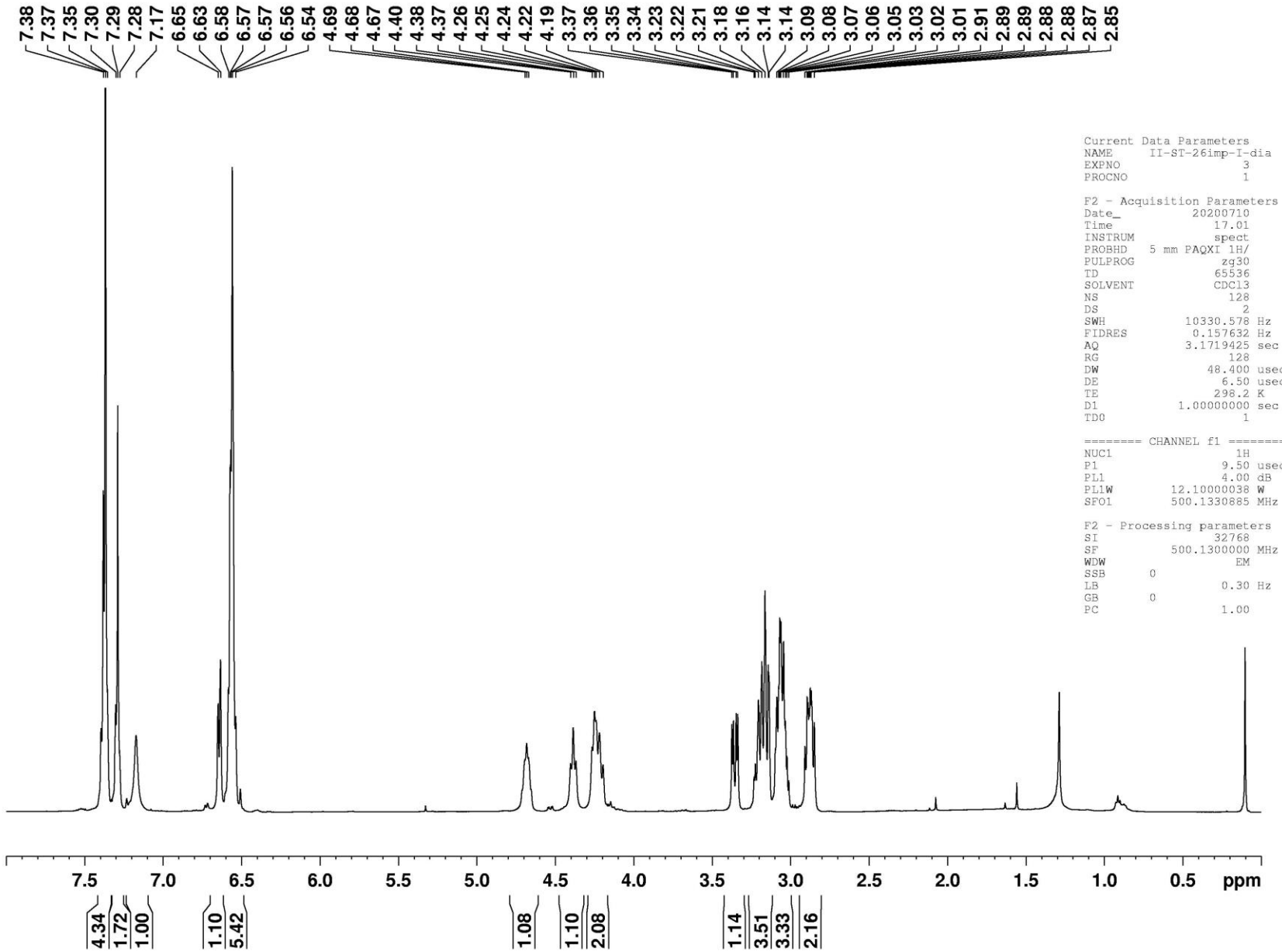

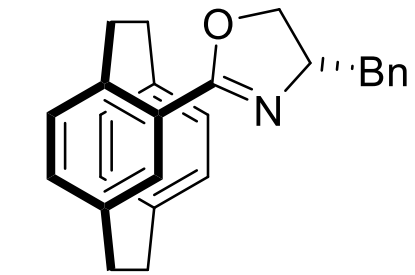

(R_p,*S*) 3.7a
Diastereomer 1

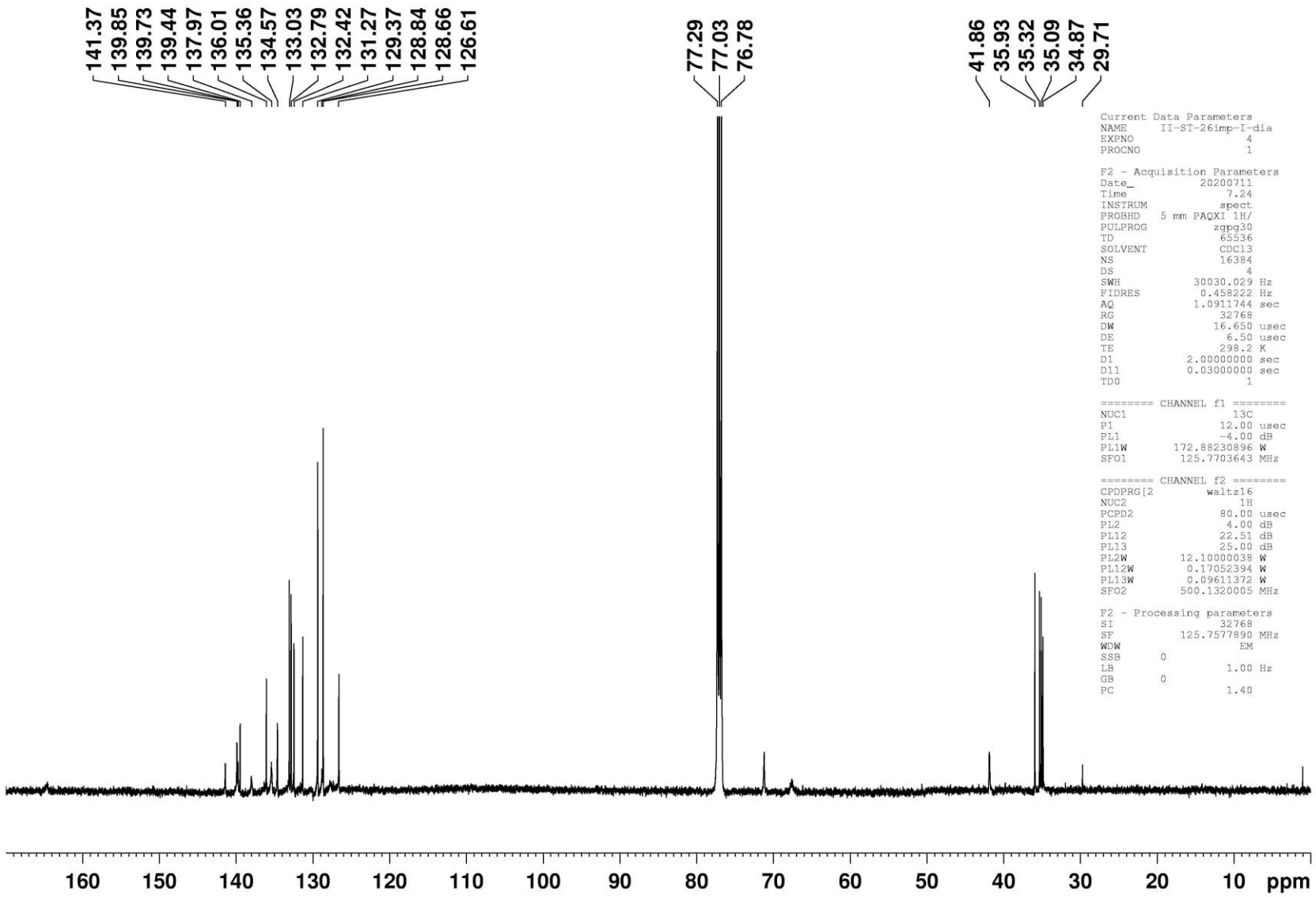


```
Current Data Parameters
NAME      II-ST-26imp-I-dia
EXPNO                     4
PROCNO                    1

F2 - Acquisition Parameters
Date_              20200711
Time                   7.24
INSTRUM               spect
PROBHD   5 mm PAQXI 1H/
PULPROG              zgpg30
TD                    65536
SOLVENT               CDCl3
NS                    16384
DS                        4
SWH               30030.029 Hz
FIDRES             0.458222 Hz
AQ                1.0911744 sec
RG                    32768
DW                 16.650 usec
DE                  6.50 usec
TE                  298.2 K
D1              2.00000000 sec
D11             0.03000000 sec
TD0                       1

======== CHANNEL f1 ========
NUC1                    13C
P1                   12.00 usec
PL1                  -4.00 dB
PL1W          172.88230896 W
SFO1           125.7703643 MHz

======== CHANNEL f2 ========
CPDPRG[2             waltz16
NUC2                     1H
PCPD2                80.00 usec
PL2                   4.00 dB
PL12                 22.51 dB
PL13                 25.00 dB
PL2W          12.10000038 W
PL12W          0.17052394 W
PL13W          0.09611372 W
SFO2          500.1320005 MHz

F2 - Processing parameters
SI                    32768
SF            125.7577890 MHz
WDW                      EM
SSB       0
LB                    1.00 Hz
GB        0
PC                    1.40
```

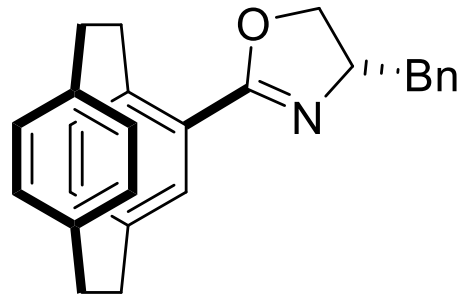

(S_p,S) 3.7a
Diastereomer 2

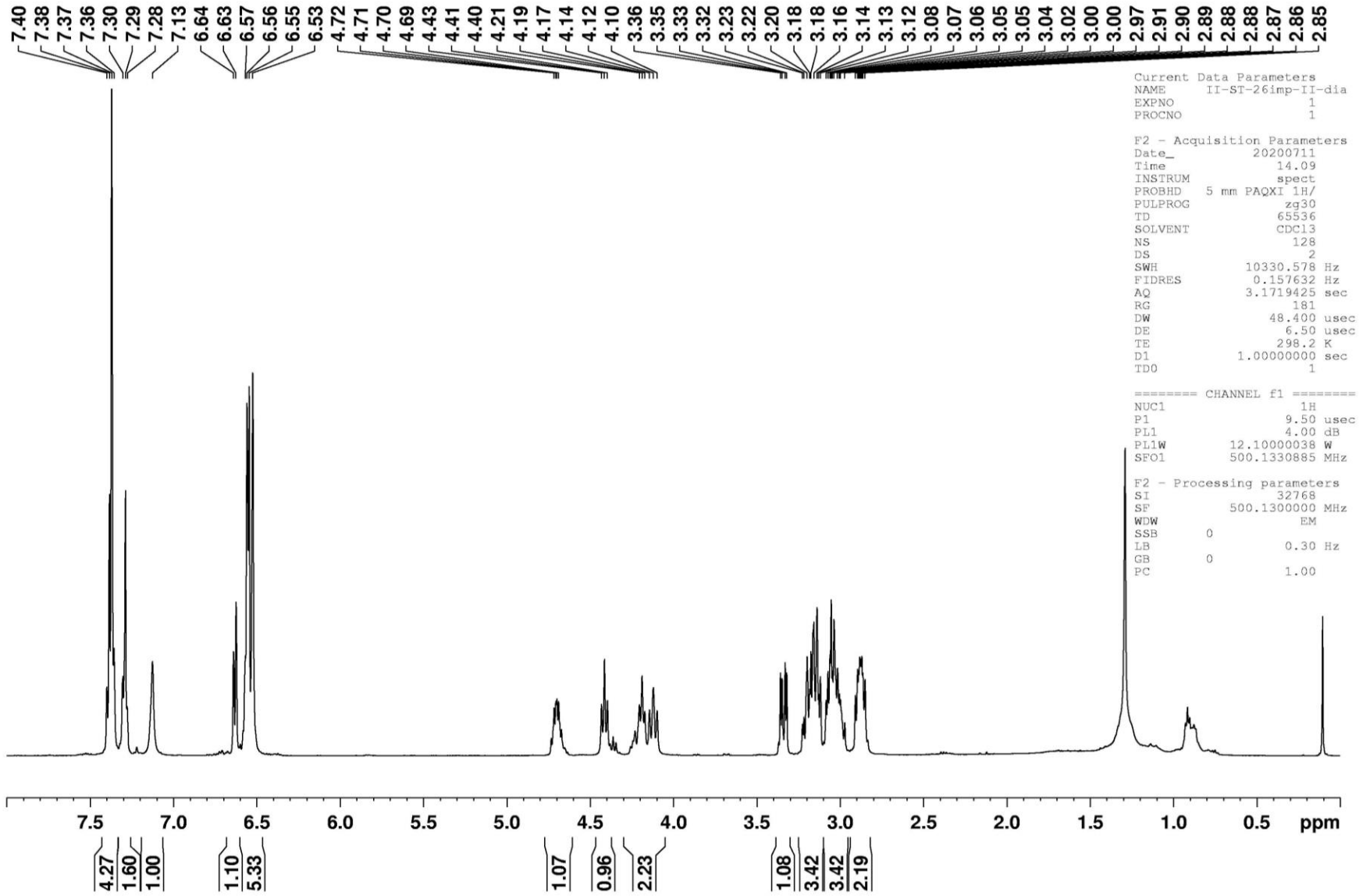

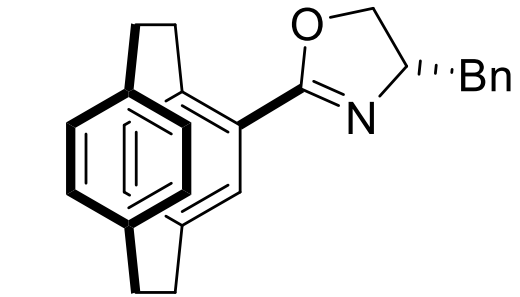

(S_p,S) 3.7a
Diastereomer 2

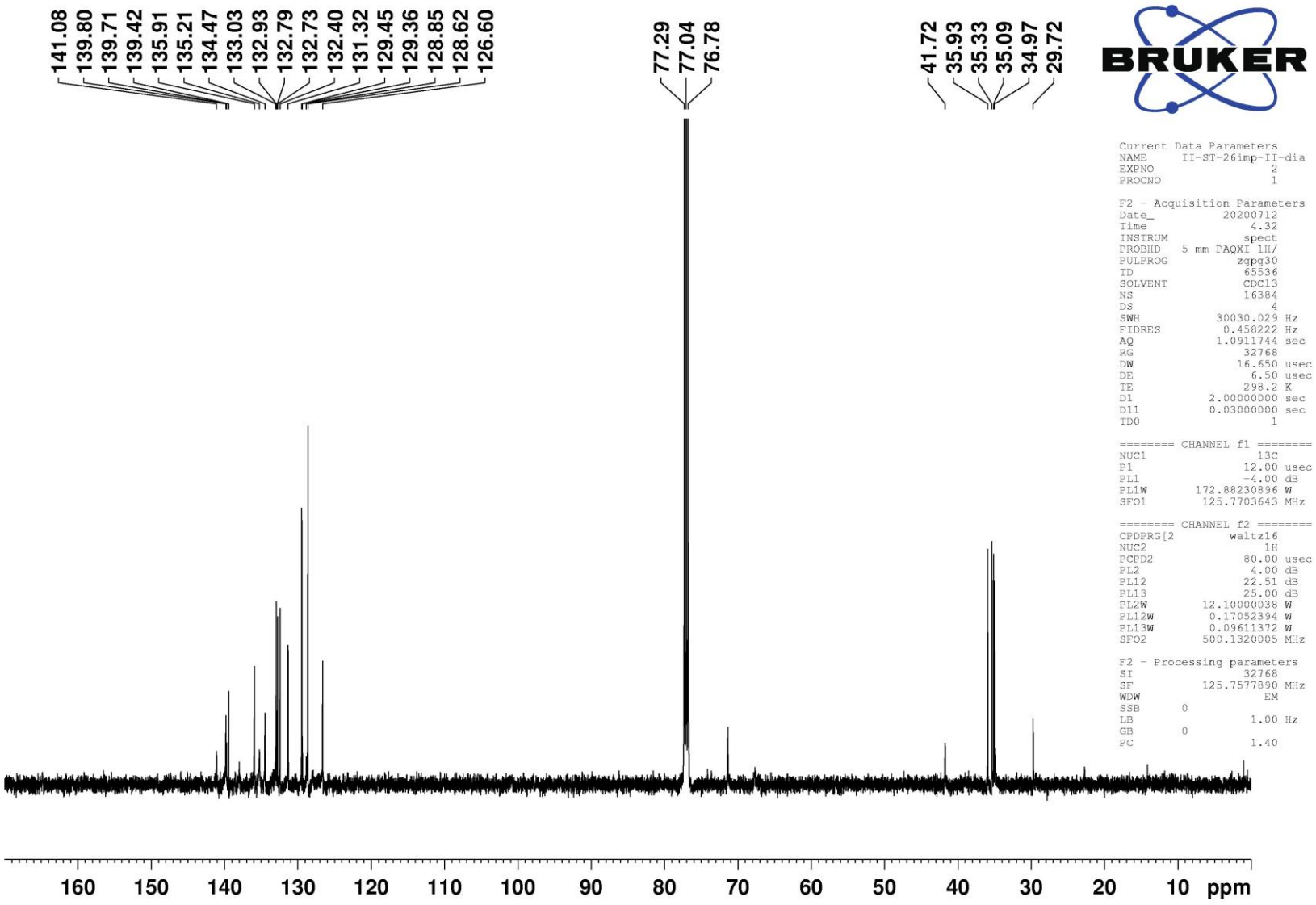

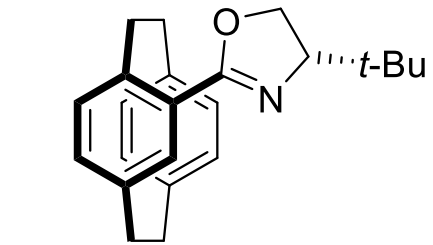

(R_p,*S*) 3.7b
Diastereomer 1

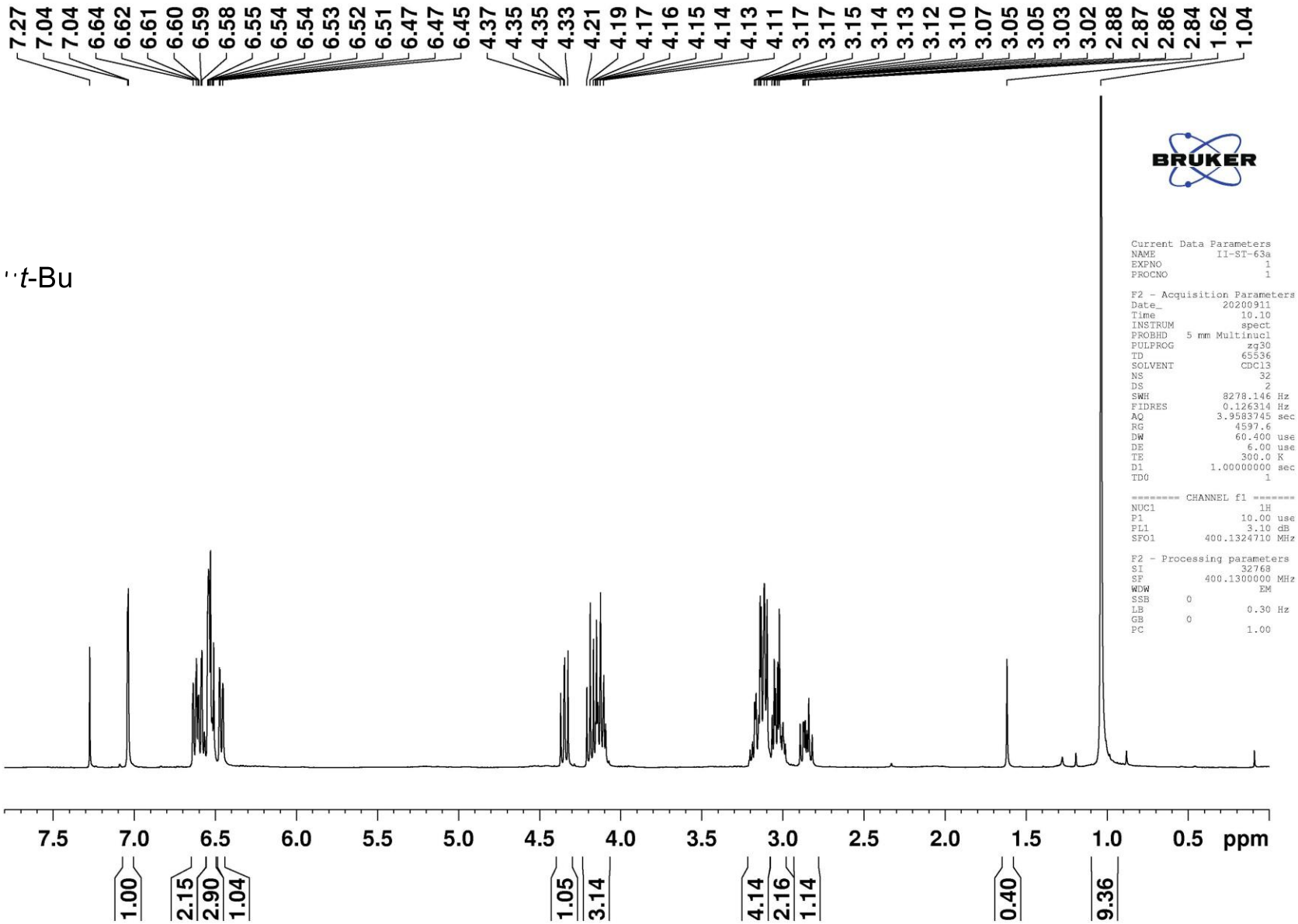

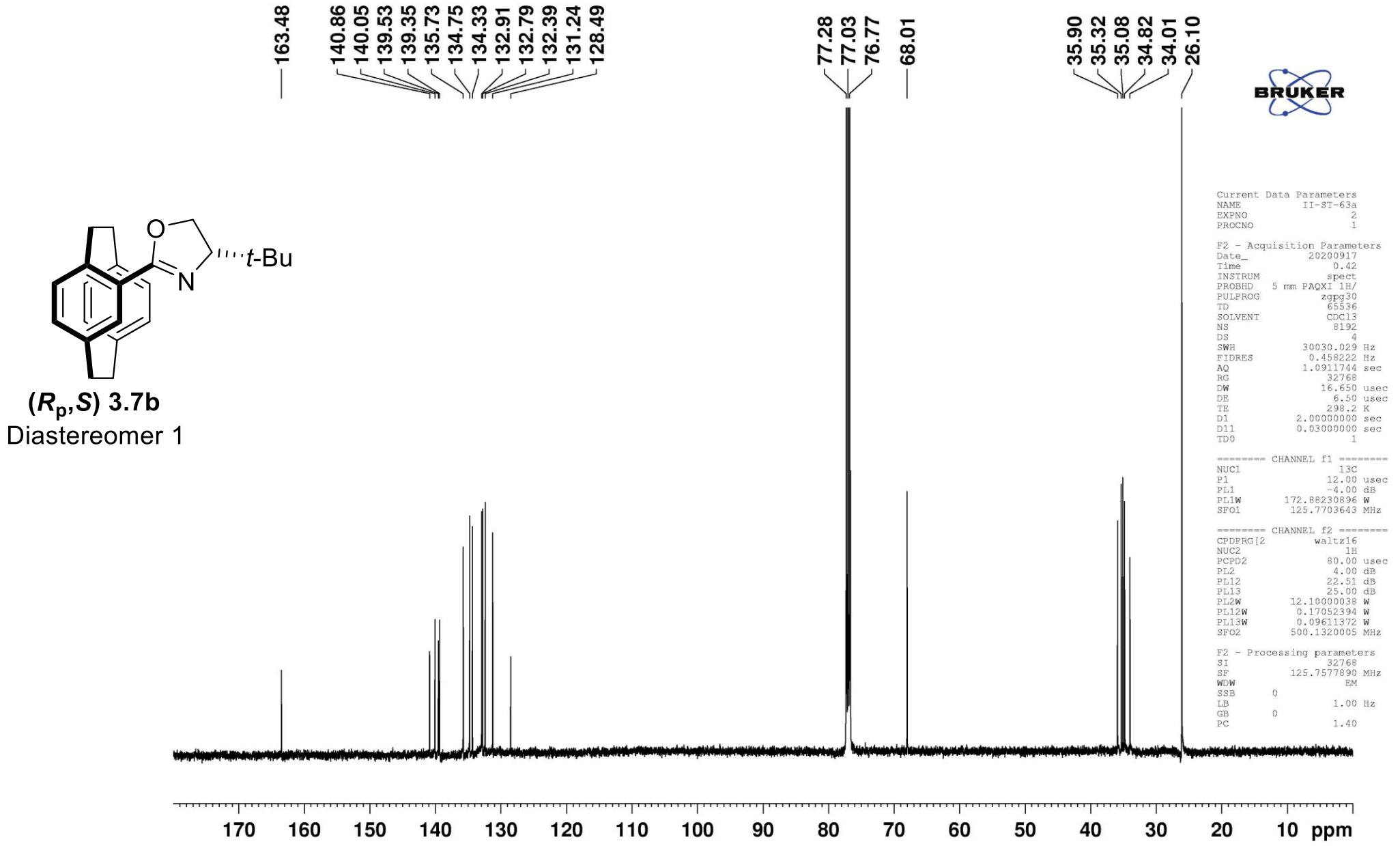
163.48
140.86
140.05
139.53
139.35
135.73
134.75
134.33
132.91
132.79
132.39
131.24
128.49
77.28
77.03
76.77
68.01
35.90
35.32
35.08
34.82
34.01
26.10
BRUKER
O
N
t-Bu
(Rp,S) 3.7b
Diastereomer 1
Current Data Parameters
NAME II-ST-63a
EXPNO 2
PROCNO 1
F2 - Acquisition Parameters
Date_ 20200917
Time 0.42
INSTRUM spect
PROBHD 5 mm PAQXI 1H/
PULPROG zgpg30
TD 65536
SOLVENT CDCl3
NS 8192
DS 4
SWH 30030.029 Hz
FIDRES 0.458222 Hz
AQ 1.0911744 sec
RG 32768
DW 16.650 usec
DE 6.50 usec
TE 298.2 K
D1 2.00000000 sec
D11 0.03000000 sec
TD0 1
======== CHANNEL f1 ========
NUC1 13C
P1 12.00 usec
PL1 -4.00 dB
PL1W 172.88230896 W
SFO1 125.7703643 MHz
======== CHANNEL f2 ========
CPDPRG[2 waltz16
NUC2 1H
PCPD2 80.00 usec
PL2 4.00 dB
PL12 22.51 dB
PL13 25.00 dB
PL2W 12.10000038 W
PL12W 0.17052394 W
PL13W 0.09611372 W
SFO2 500.1320005 MHz
F2 - Processing parameters
SI 32768
SF 125.7577890 MHz
WDW EM
SSB 0
LB 1.00 Hz
GB 0
PC 1.40
170 160 150 140 130 120 110 100 90 80 70 60 50 40 30 20 10 ppm

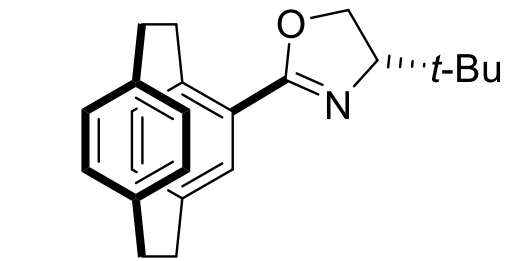

(S_p,S) 3.7b
Diastereomer 2

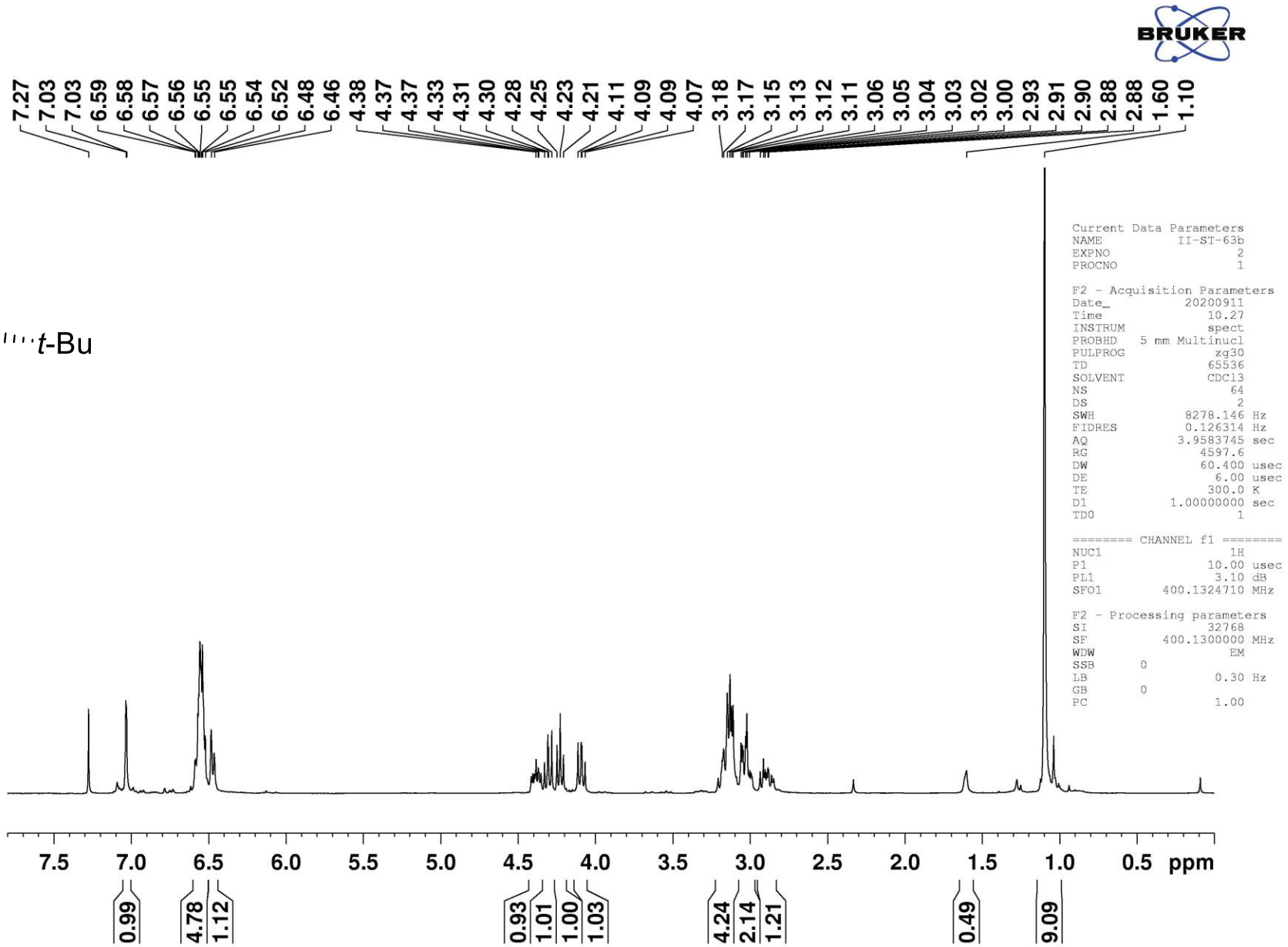

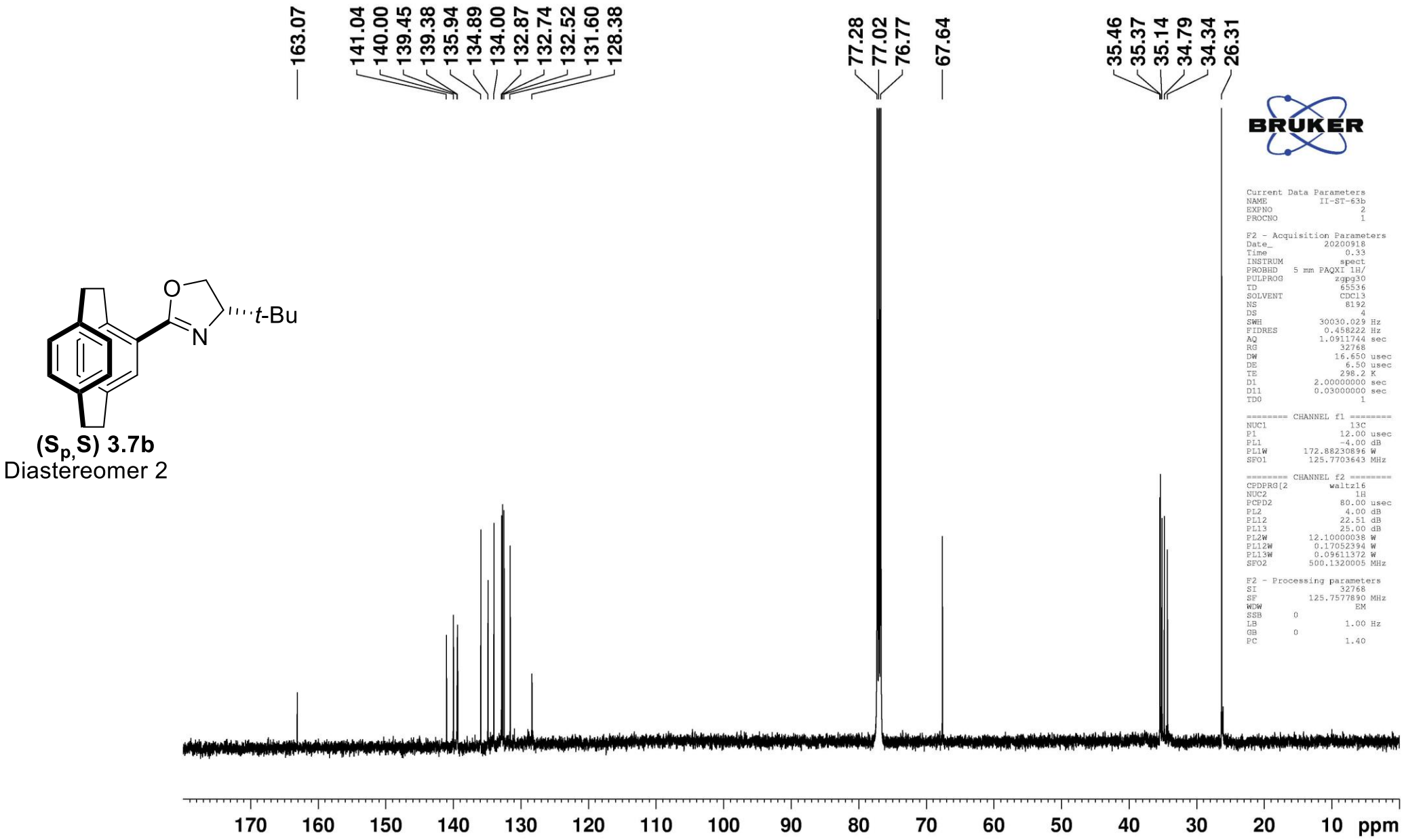
163.07
141.04
140.00
139.45
139.38
135.94
134.89
134.00
132.87
132.74
132.52
131.60
128.38
77.28
77.02
76.77
67.64
35.46
35.37
35.14
34.79
34.34
26.31
O
N
t-Bu
(Sp,S) 3.7b
Diastereomer 2
BRUKER
Current Data Parameters
NAME II-ST-63b
EXPNO 2
PROCNO 1
F2 - Acquisition Parameters
Date_ 20200918
Time 0.33
INSTRUM spect
PROBHD 5 mm PAQXI 1H/
PULPROG zgpg30
TD 65536
SOLVENT CDCl3
NS 8192
DS 4
SWH 30030.029 Hz
FIDRES 0.458222 Hz
AQ 1.0911744 sec
RG 32768
DW 16.650 usec
DE 6.50 usec
TE 298.2 K
D1 2.00000000 sec
D11 0.03000000 sec
TD0 1
======== CHANNEL f1 ========
NUC1 13C
P1 12.00 usec
PL1 -4.00 dB
PL1W 172.88230896 W
SFO1 125.7703643 MHz
======== CHANNEL f2 ========
CPDPRG[2 waltz16
NUC2 1H
PCPD2 80.00 usec
PL2 4.00 dB
PL12 22.51 dB
PL13 25.00 dB
PL2W 12.10000038 W
PL12W 0.17052394 W
PL13W 0.09611372 W
SFO2 500.1320005 MHz
F2 - Processing parameters
SI 32768
SF 125.7577890 MHz
WDW EM
SSB 0
LB 1.00 Hz
GB 0
PC 1.40
170 160 150 140 130 120 110 100 90 80 70 60 50 40 30 20 10 ppm

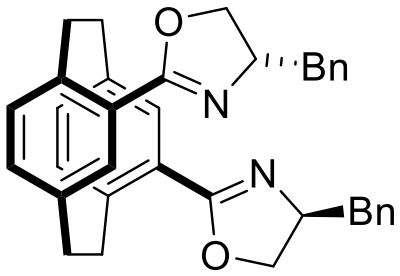

(R_p,*S*)-3.11a

Diastereomer 1

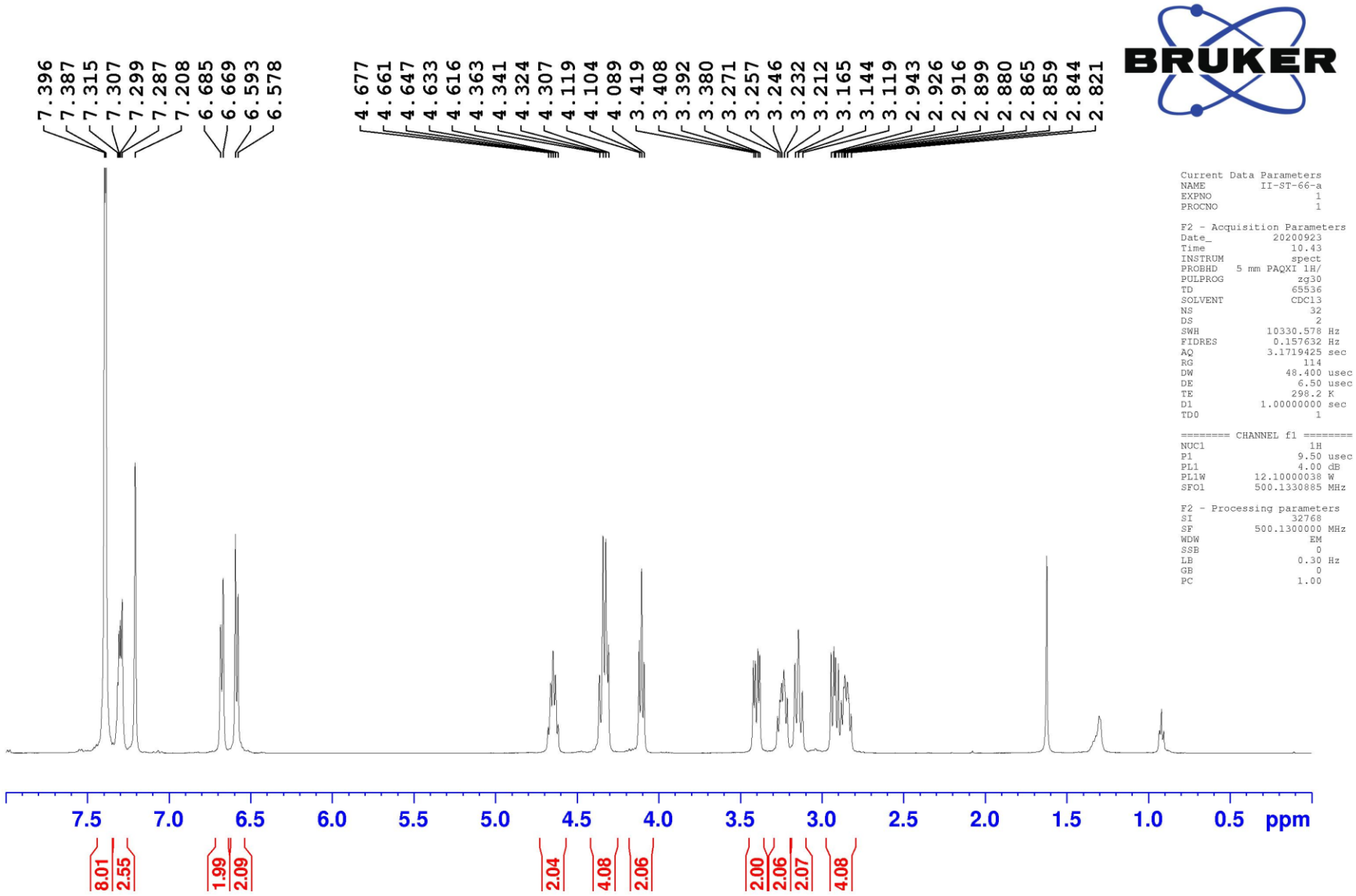


```
Current Data Parameters
NAME          II-ST-66-a
EXPNO                  1
PROCNO                 1

F2 - Acquisition Parameters
Date_           20200923
Time              10.43
INSTRUM           spect
PROBHD   5 mm PAQXI 1H/
PULPROG           zg30
TD               65536
SOLVENT          CDCl3
NS                  32
DS                   2
SWH          10330.578 Hz
FIDRES        0.157632 Hz
AQ            3.1719425 sec
RG                 114
DW              48.400 usec
DE               6.50 usec
TE              298.2 K
D1          1.00000000 sec
TD0                  1

======== CHANNEL f1 ========
NUC1                1H
P1               9.50 usec
PL1              4.00 dB
PL1W       12.10000038 W
SFO1       500.1330885 MHz

F2 - Processing parameters
SI                32768
SF        500.1300000 MHz
WDW                EM
SSB                 0
LB               0.30 Hz
GB                  0
PC               1.00
```

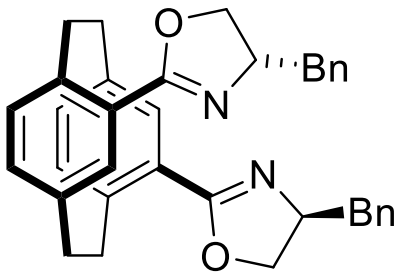

(R_p,*S*)-3.11a

Diastereomer 1

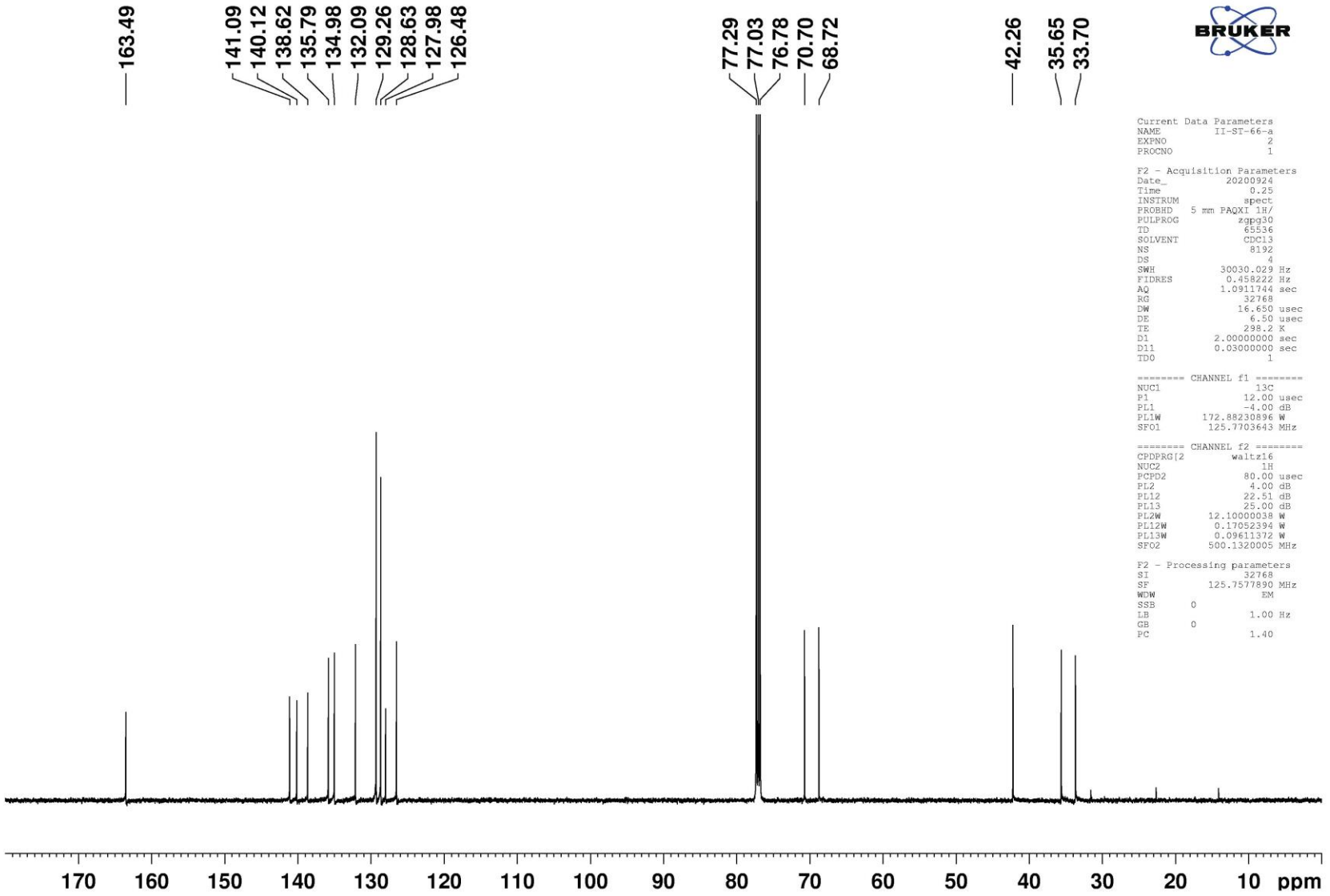

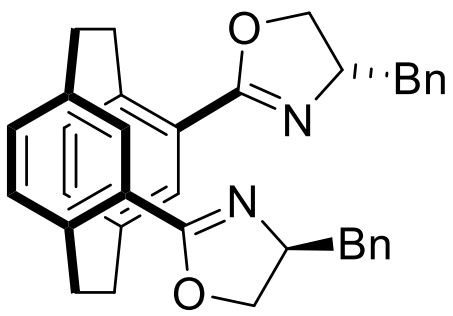

(S_p,S)-3.11a
Diastereomer 2

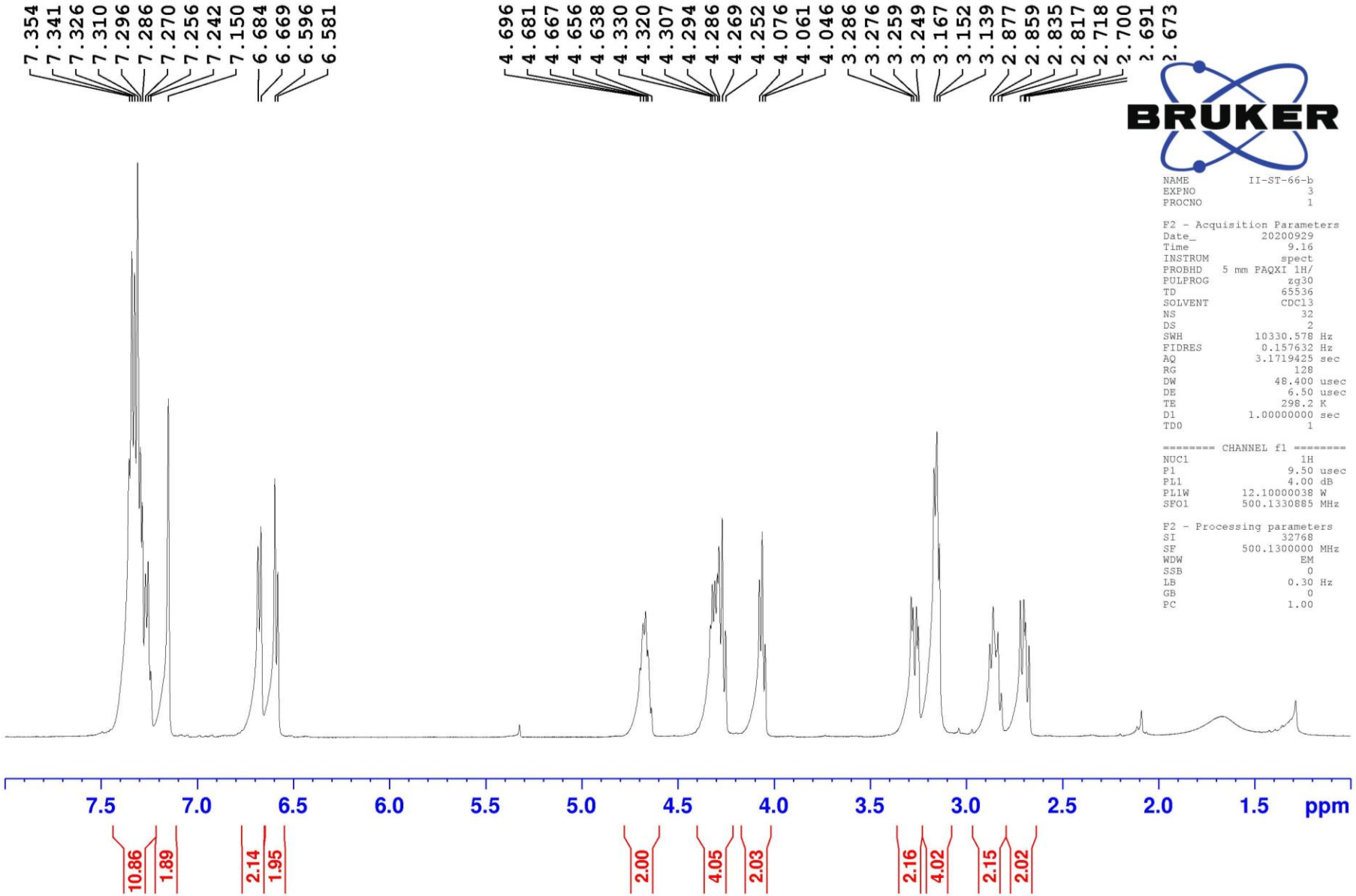

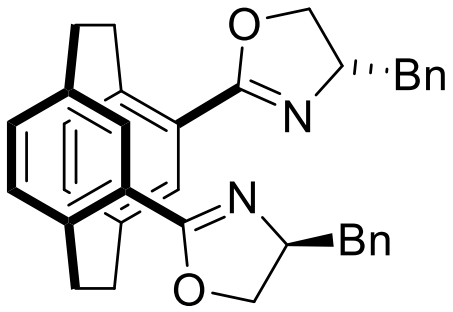

(S_p,S)-3.11a
Diastereomer 2

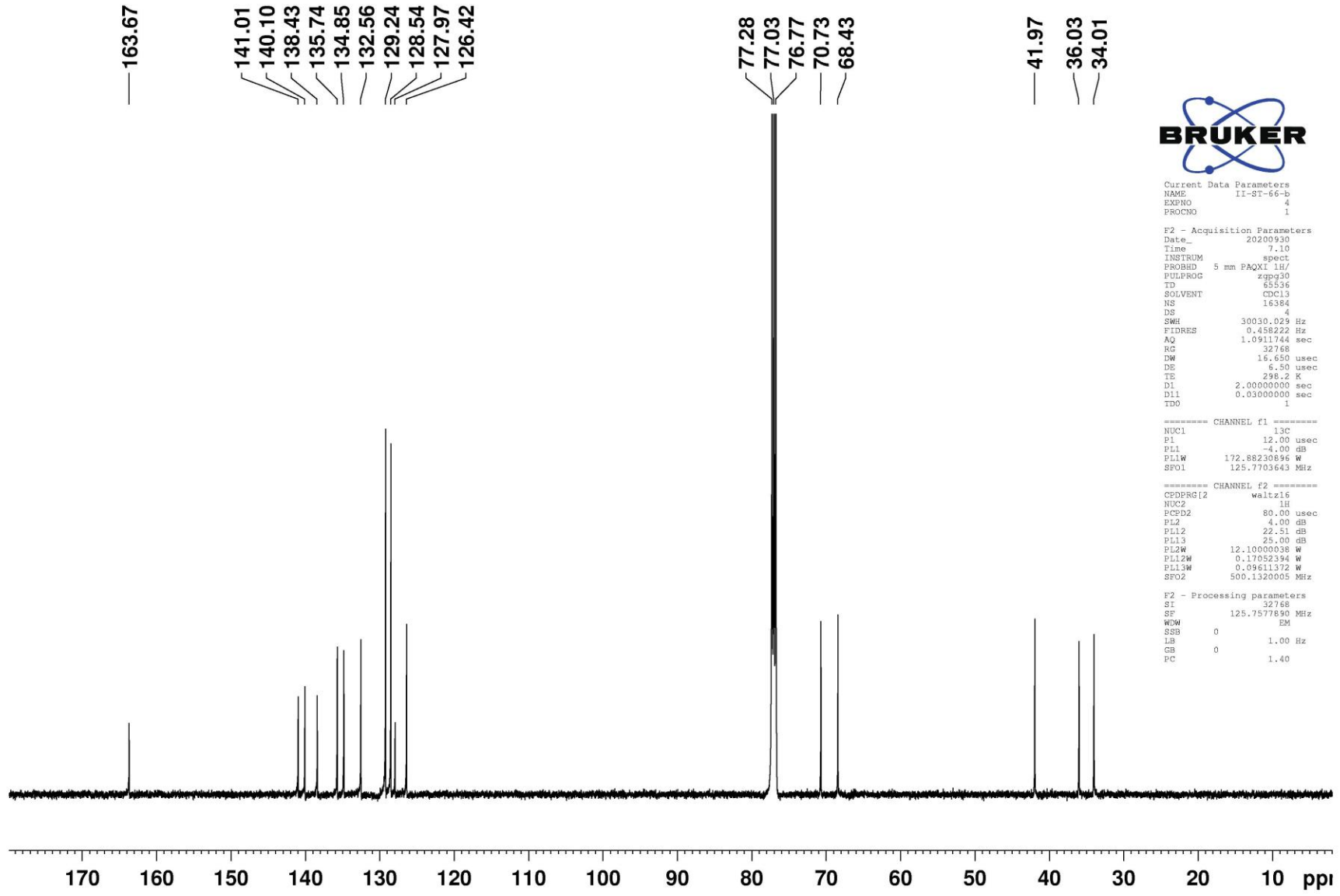

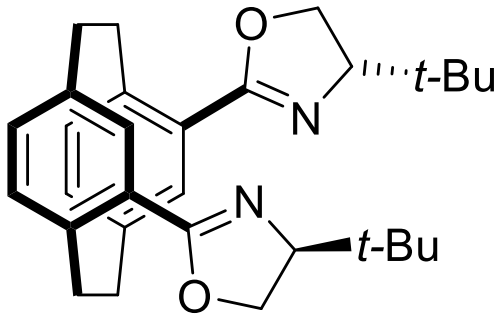

(S_p,S)-3.11b
Diastereomer 2

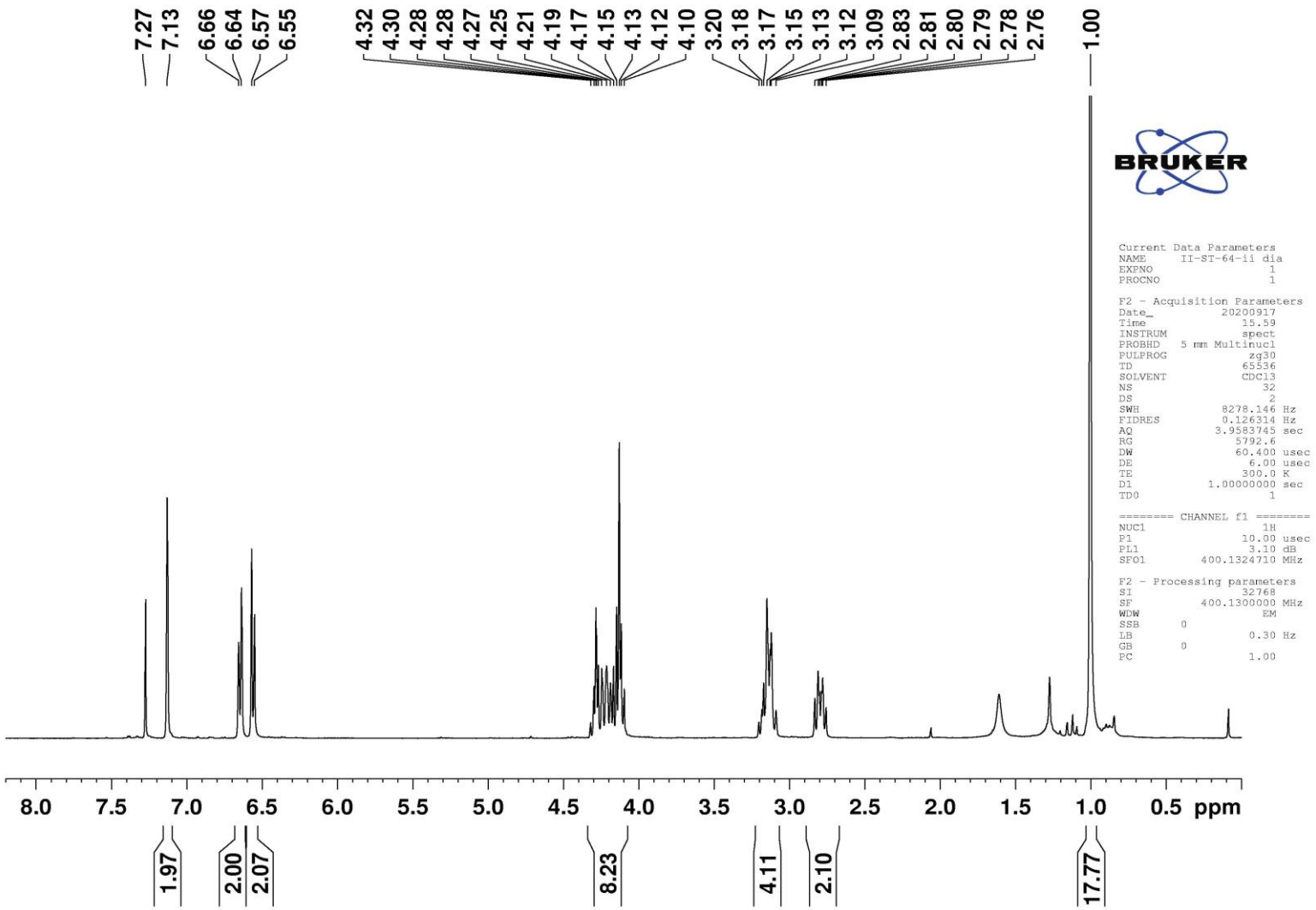

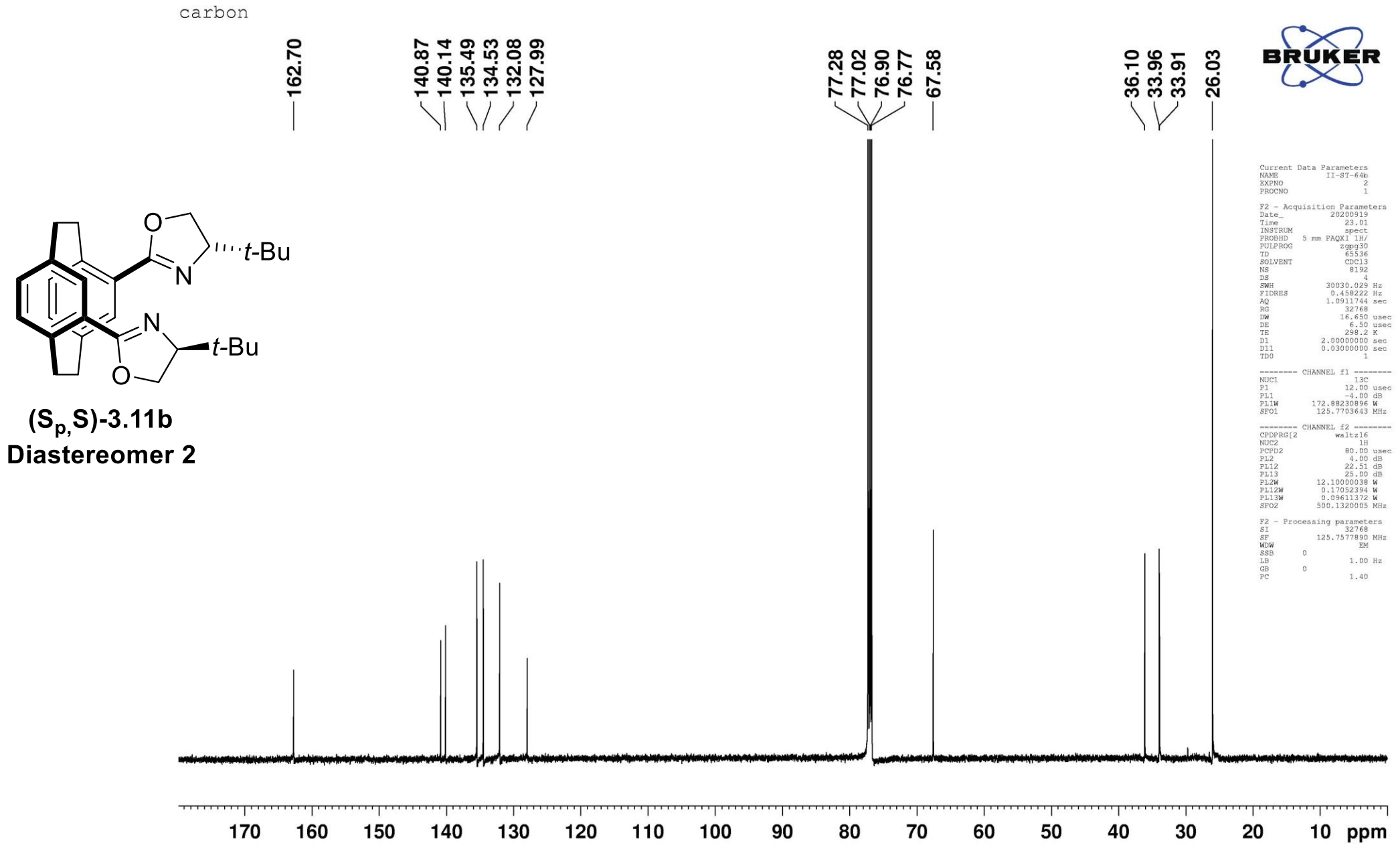

(S_p,S)-3.11b
Diastereomer 2

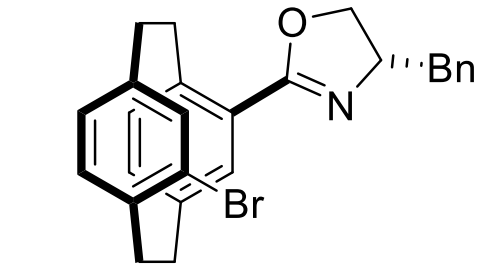

(S_p,*S*)-3.12a
Diastereomer 2

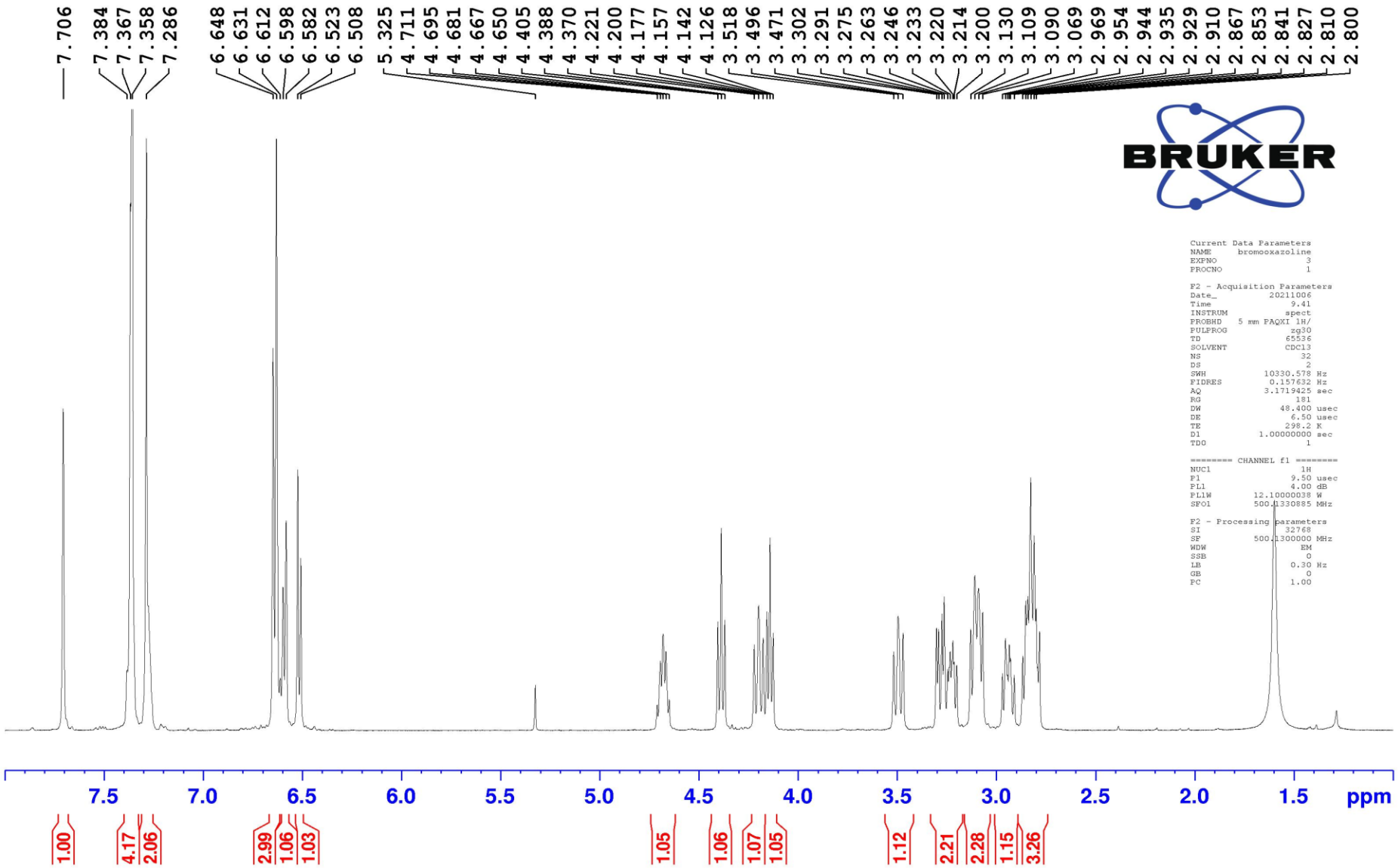

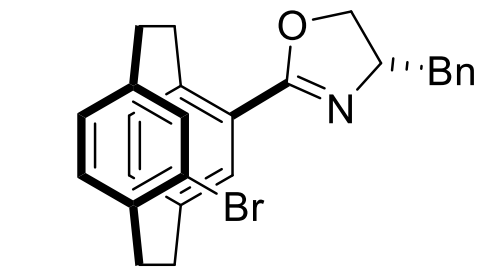

(S_p,*S*)-3.12a
Diastereomer 2

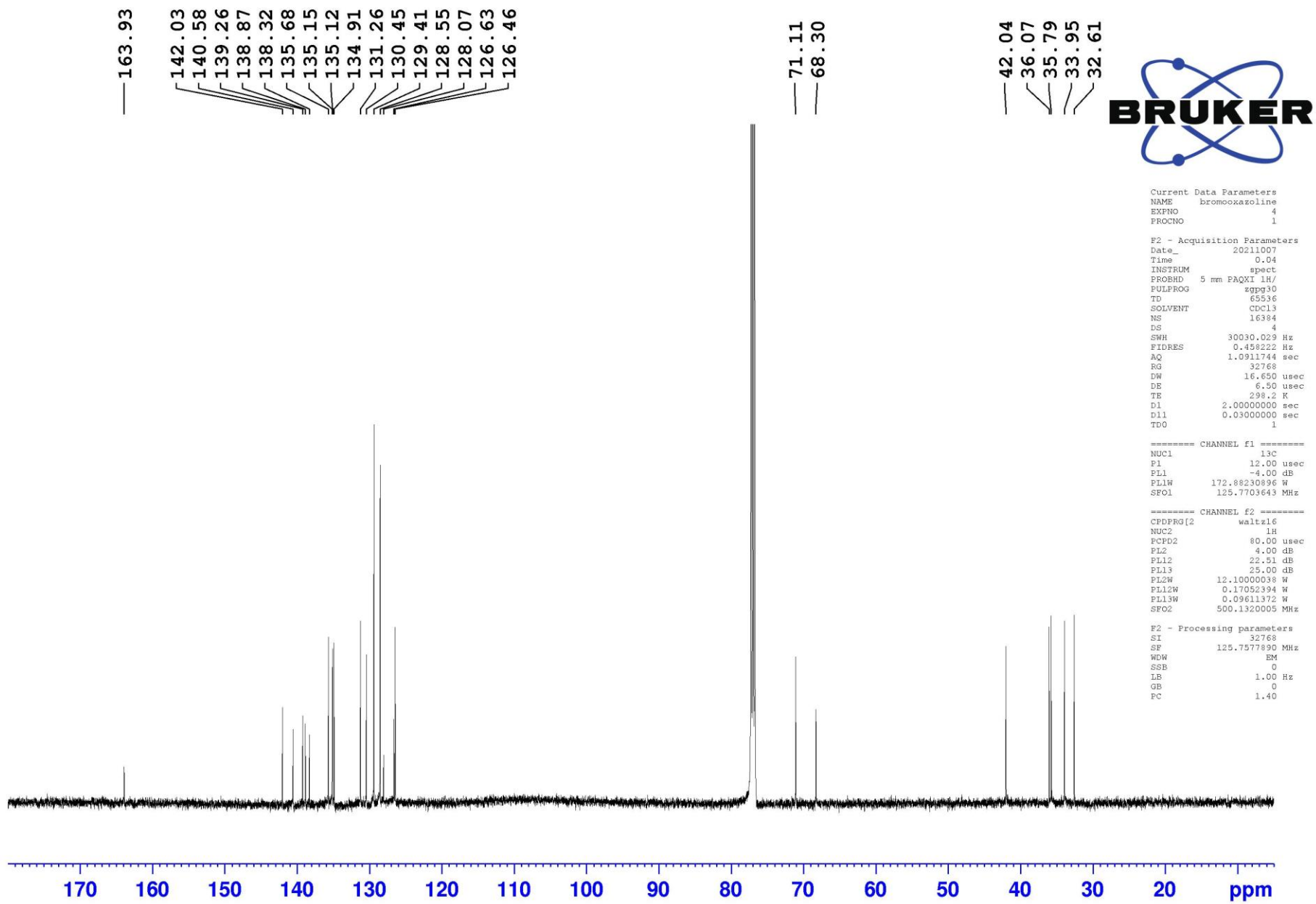

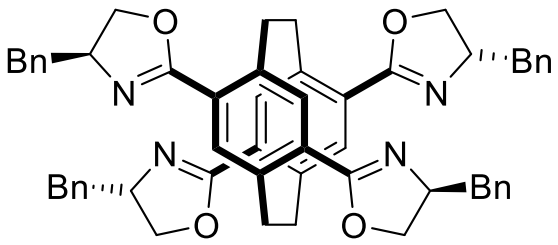
Bn
Bn
Bn
Bn
O
O
O
O
N
N
N
N

(*S*,*S*,*R*$_p$,*S*,*S*)-3.16

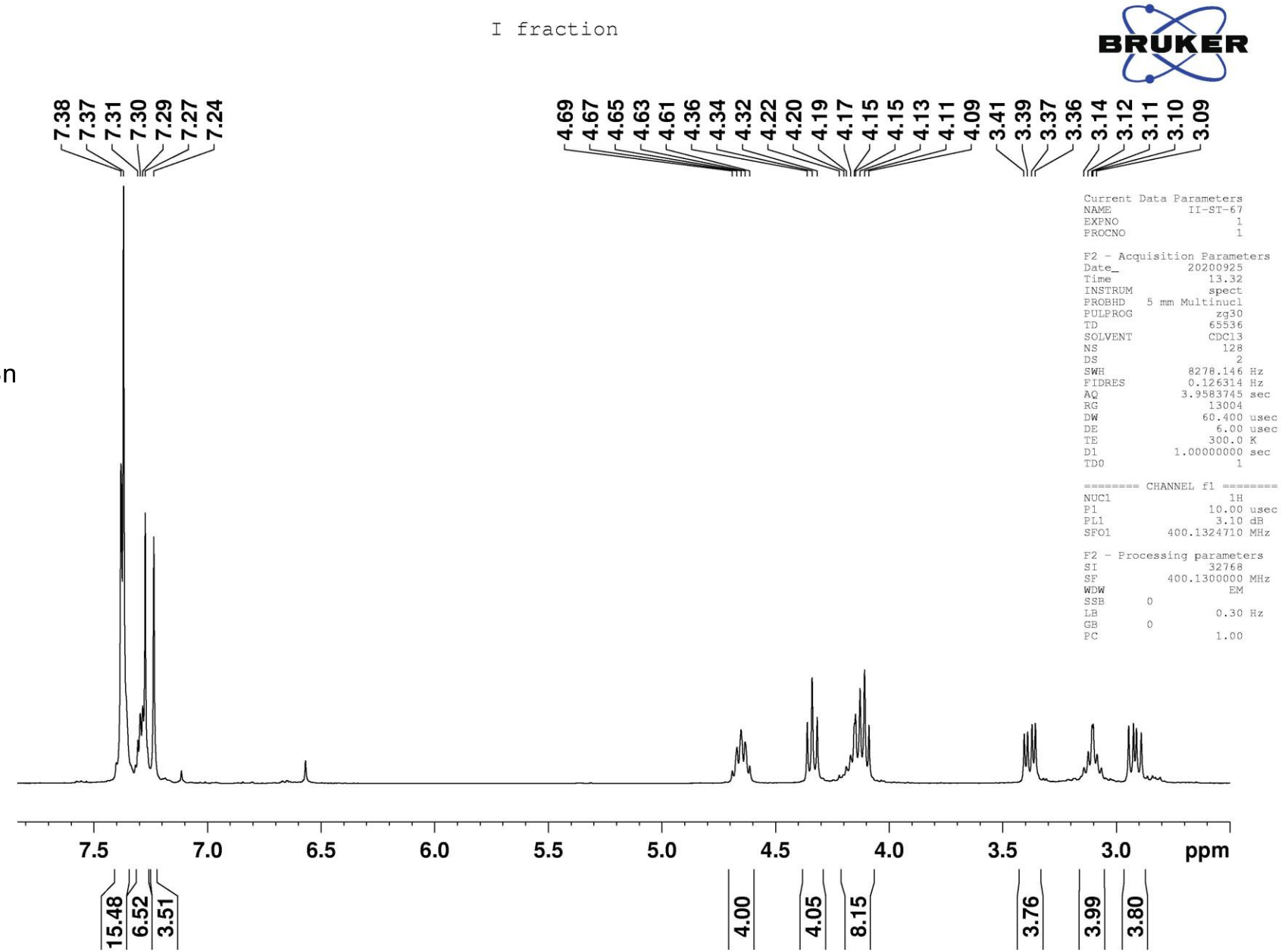
I fraction
BRUKER
7.38 7.37 7.31 7.30 7.29 7.27 7.24
4.69 4.67 4.65 4.63 4.61 4.36 4.34 4.32 4.22 4.20 4.19 4.17 4.15 4.15 4.13 4.11 4.09
3.41 3.39 3.37 3.36 3.14 3.12 3.11 3.10 3.09
Current Data Parameters
NAME II-ST-67
EXPNO 1
PROCNO 1
F2 - Acquisition Parameters
Date_ 20200925
Time 13.32
INSTRUM spect
PROBHD 5 mm Multinucl
PULPROG zg30
TD 65536
SOLVENT CDCl3
NS 128
DS 2
SWH 8278.146 Hz
FIDRES 0.126314 Hz
AQ 3.9583745 sec
RG 13004
DW 60.400 usec
DE 6.00 usec
TE 300.0 K
D1 1.00000000 sec
TD0 1
======== CHANNEL f1 ========
NUC1 1H
P1 10.00 usec
PL1 3.10 dB
SFO1 400.1324710 MHz
F2 - Processing parameters
SI 32768
SF 400.1300000 MHz
WDW EM
SSB 0
LB 0.30 Hz
GB 0
PC 1.00
7.5 7.0 6.5 6.0 5.5 5.0 4.5 4.0 3.5 3.0 ppm
15.48 6.52 3.51 4.00 4.05 8.15 3.76 3.99 3.80

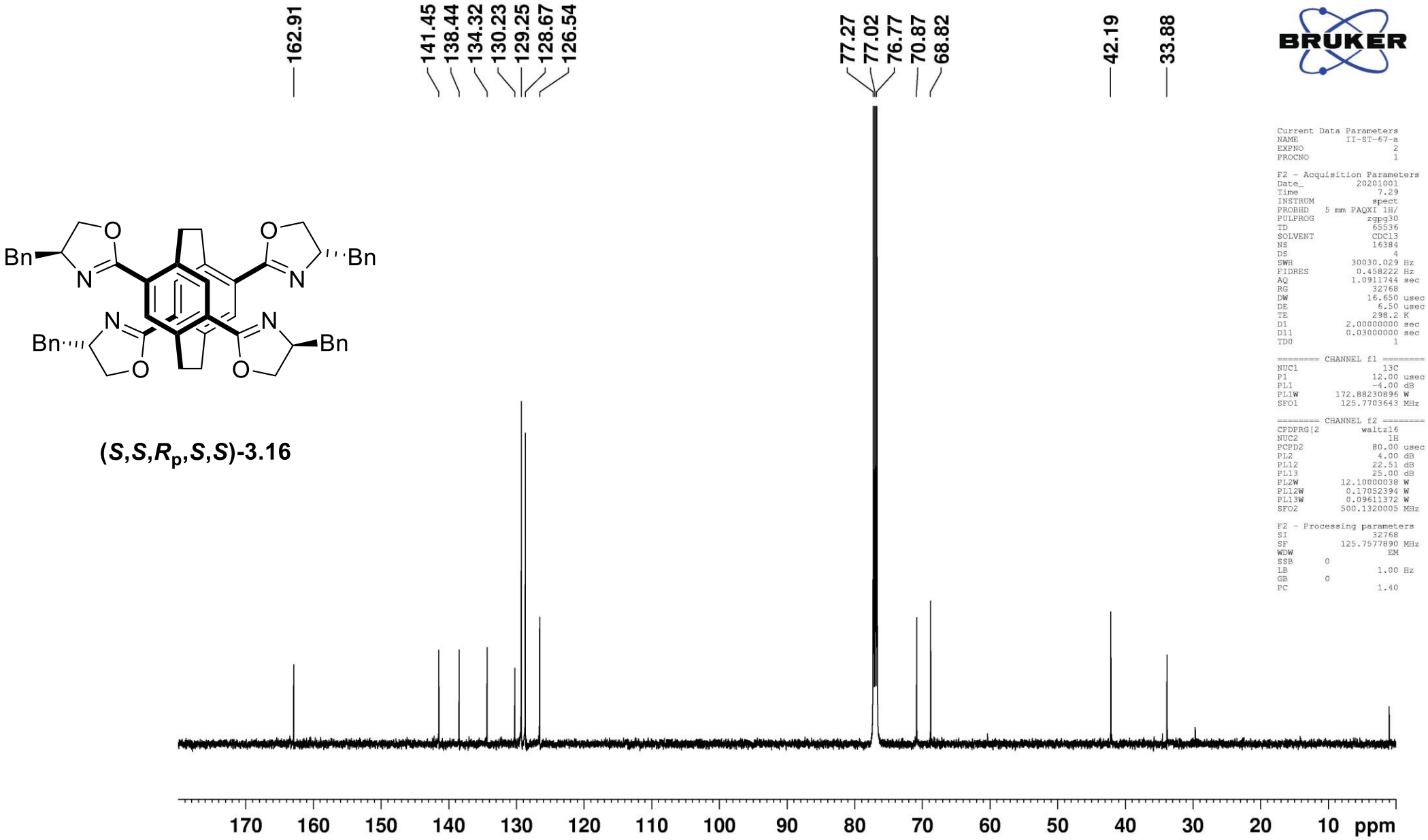
162.91
141.45
138.44
134.32
130.23
129.25
128.67
126.54
77.27
77.02
76.77
70.87
68.82
42.19
33.88
BRUKER
Current Data Parameters
NAME II-ST-67-a
EXPNO 2
PROCNO 1
F2 - Acquisition Parameters
Date_ 20201001
Time 7.29
INSTRUM spect
PROBHD 5 mm PAQXI 1H/
PULPROG zgpg30
TD 65536
SOLVENT CDCl3
NS 16384
DS 4
SWH 30030.029 Hz
FIDRES 0.458222 Hz
AQ 1.0911744 sec
RG 32768
DW 16.650 usec
DE 6.50 usec
TE 298.2 K
D1 2.00000000 sec
D11 0.03000000 sec
TD0 1
======== CHANNEL f1 ========
NUC1 13C
P1 12.00 usec
PL1 -4.00 dB
PL1W 172.88230896 W
SFO1 125.7703643 MHz
======== CHANNEL f2 ========
CPDPRG[2 waltz16
NUC2 1H
PCPD2 80.00 usec
PL2 4.00 dB
PL12 22.51 dB
PL13 25.00 dB
PL2W 12.10000038 W
PL12W 0.17052394 W
PL13W 0.09611372 W
SFO2 500.1320005 MHz
F2 - Processing parameters
SI 32768
SF 125.7577890 MHz
WDW EM
SSB 0
LB 1.00 Hz
GB 0
PC 1.40
Bn
Bn
Bn
Bn
O
O
O
O
N
N
N
N
(S,S,Rp,S,S)-3.16
170
160
150
140
130
120
110
100
90
80
70
60
50
40
30
20
10
ppm

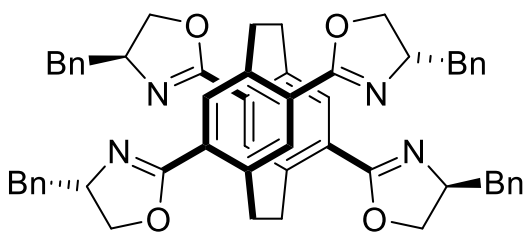
Bn
Bn
Bn
Bn
N
N
N
N
O
O
O
O

(*S*,*S*,*S*$_p$,*S*,*S*)-3.16

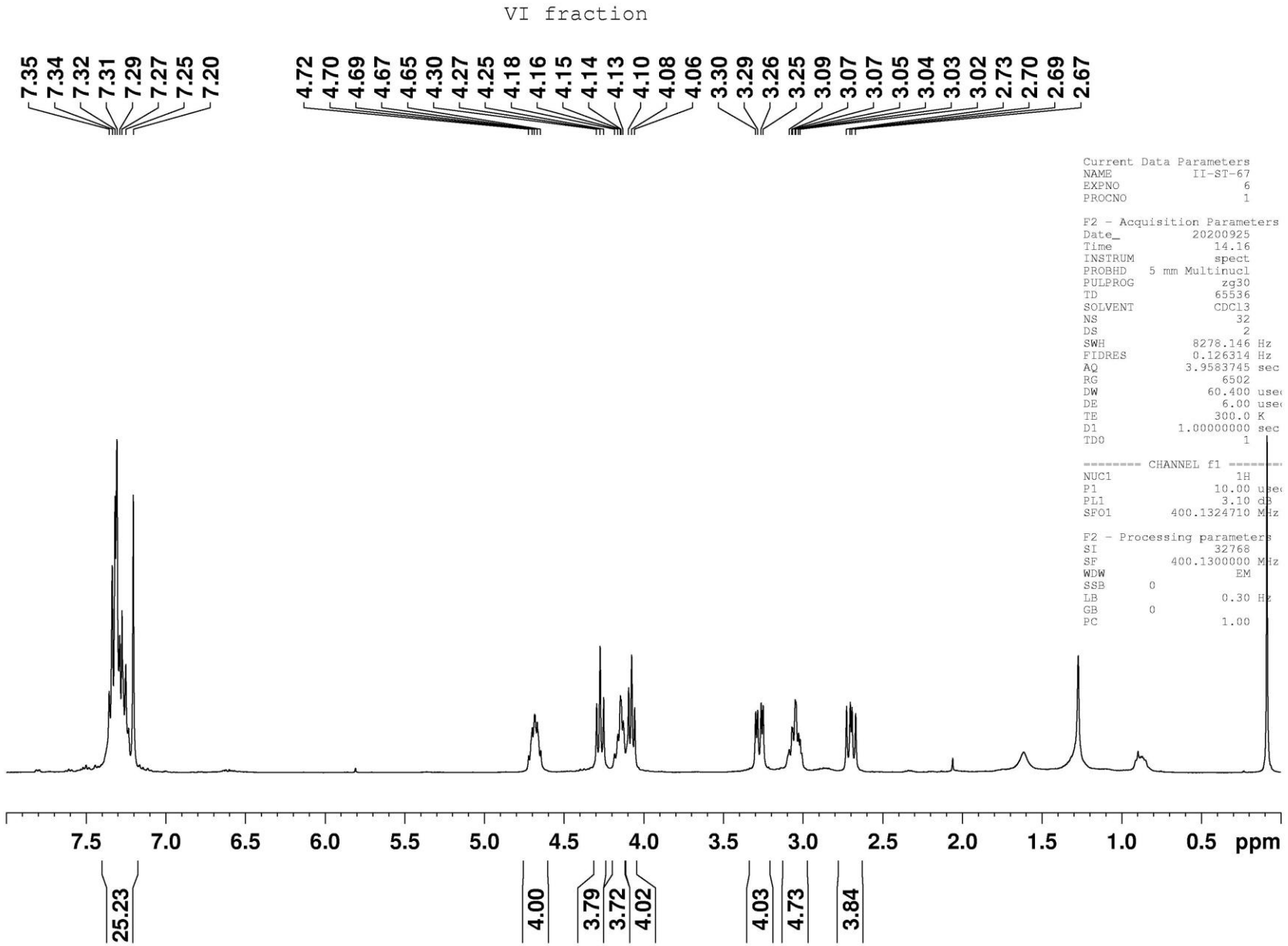
VI fraction
7.35 7.34 7.32 7.31 7.29 7.27 7.25 7.20
4.72 4.70 4.69 4.67 4.65 4.30 4.27 4.25 4.18 4.16 4.15 4.14 4.13 4.10 4.08 4.06
3.30 3.29 3.26 3.25 3.09 3.07 3.07 3.05 3.04 3.03 3.02 2.73 2.70 2.69 2.67
Current Data Parameters
NAME II-ST-67
EXPNO 6
PROCNO 1
F2 - Acquisition Parameters
Date_ 20200925
Time 14.16
INSTRUM spect
PROBHD 5 mm Multinucl
PULPROG zg30
TD 65536
SOLVENT CDCl3
NS 32
DS 2
SWH 8278.146 Hz
FIDRES 0.126314 Hz
AQ 3.9583745 sec
RG 6502
DW 60.400 use
DE 6.00 use
TE 300.0 K
D1 1.00000000 sec
TD0 1
======== CHANNEL f1 ========
NUC1 1H
P1 10.00 use
PL1 3.10 dB
SFO1 400.1324710 MHz
F2 - Processing parameters
SI 32768
SF 400.1300000 MHz
WDW EM
SSB 0
LB 0.30 Hz
GB 0
PC 1.00
7.5 7.0 6.5 6.0 5.5 5.0 4.5 4.0 3.5 3.0 2.5 2.0 1.5 1.0 0.5 ppm
25.23
4.00
3.79
3.72
4.02
4.03
4.73
3.84

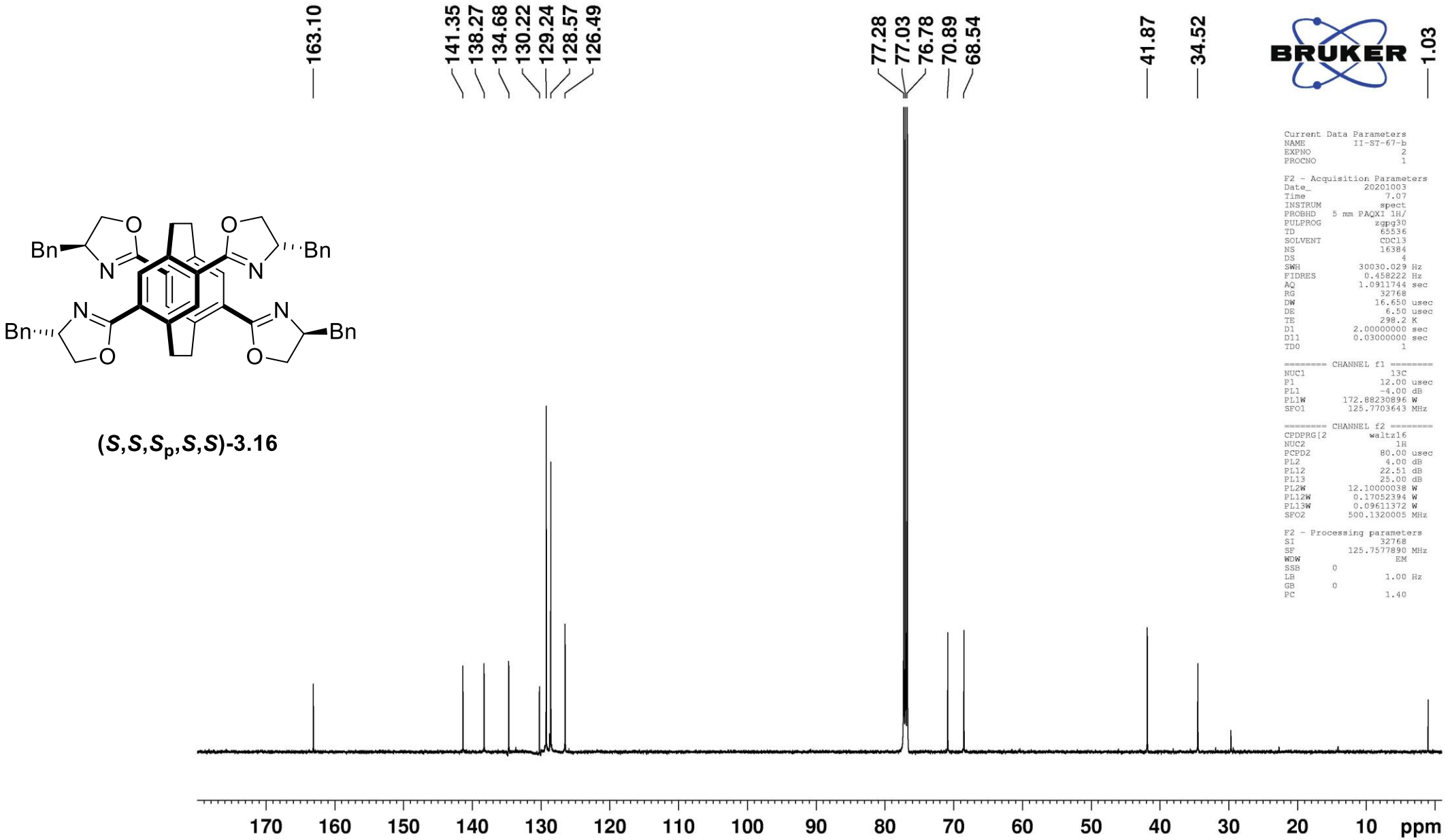
163.10
141.35
138.27
134.68
130.22
129.24
128.57
126.49
77.28
77.03
76.78
70.89
68.54
41.87
34.52
1.03
BRUKER
Bn
Bn
Bn
Bn
Current Data Parameters
NAME II-ST-67-b
EXPNO 2
PROCNO 1
F2 - Acquisition Parameters
Date_ 20201003
Time 7.07
INSTRUM spect
PROBHD 5 mm PAQXI 1H/
PULPROG zgpg30
TD 65536
SOLVENT CDCl3
NS 16384
DS 4
SWH 30030.029 Hz
FIDRES 0.458222 Hz
AQ 1.0911744 sec
RG 32768
DW 16.650 usec
DE 6.50 usec
TE 298.2 K
D1 2.00000000 sec
D11 0.03000000 sec
TD0 1
======== CHANNEL f1 ========
NUC1 13C
P1 12.00 usec
PL1 -4.00 dB
PL1W 172.88230896 W
SFO1 125.7703643 MHz
======== CHANNEL f2 ========
CPDPRG[2 waltz16
NUC2 1H
PCPD2 80.00 usec
PL2 4.00 dB
PL12 22.51 dB
PL13 25.00 dB
PL2W 12.10000038 W
PL12W 0.17052394 W
PL13W 0.09611372 W
SFO2 500.1320005 MHz
F2 - Processing parameters
SI 32768
SF 125.7577890 MHz
WDW EM
SSB 0
LB 1.00 Hz
GB 0
PC 1.40
170
160
150
140
130
120
110
100
90
80
70
60
50
40
30
20
10
ppm

(*S*,*S*,*S*$_p$,*S*,*S*)-3.16

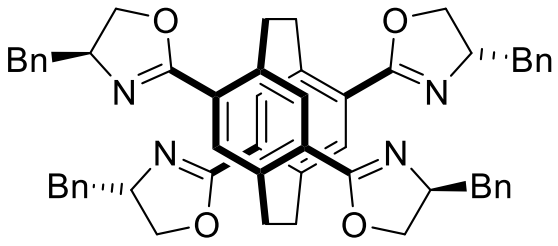
Bn
O
N
Bn
N
O
Bn
N
O
Bn
O
N

(*S*,*S*,*R*$_p$,*S*,*S*)-3.16

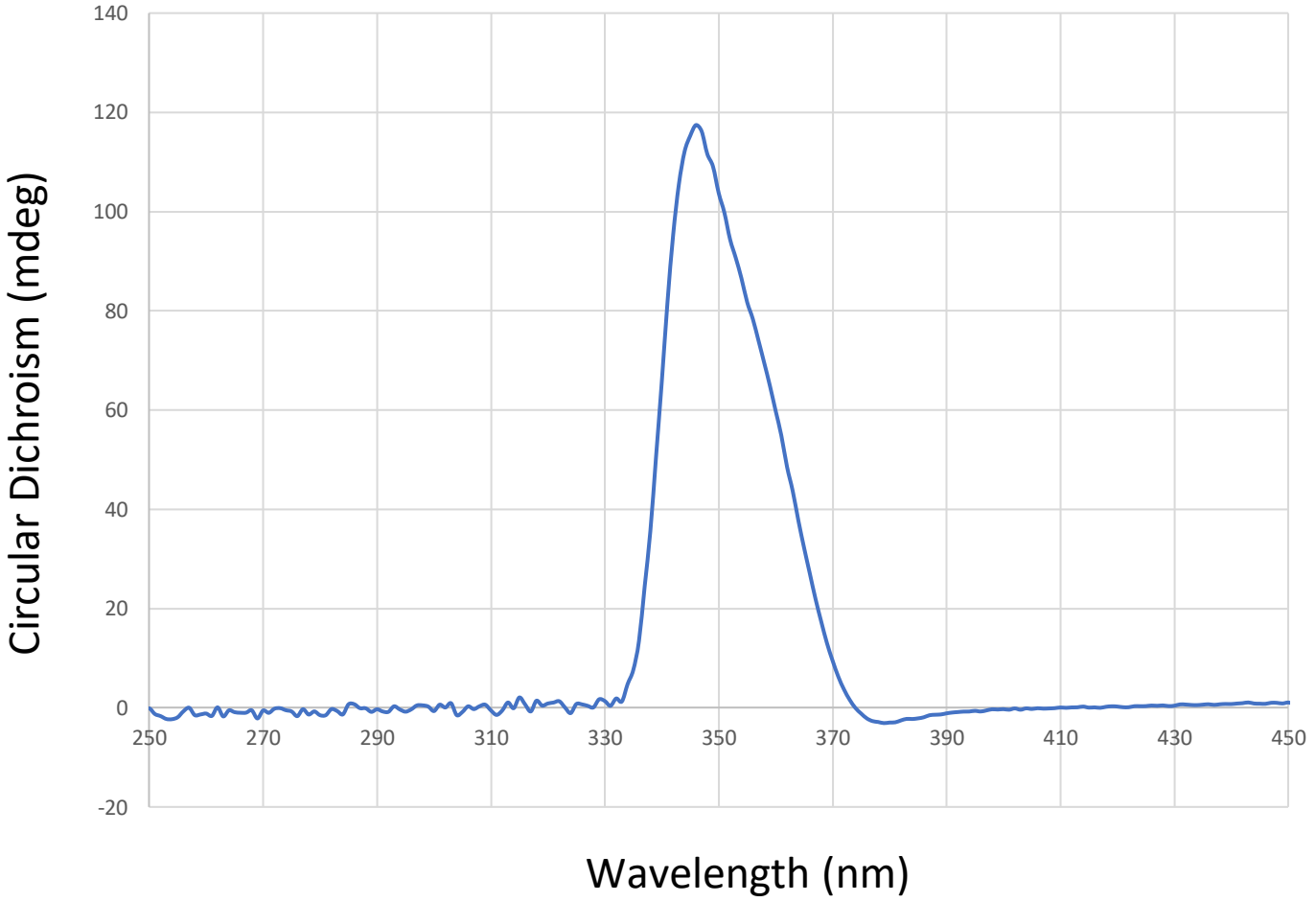
Circular Dichroism (mdeg)
140
120
100
80
60
40
20
0
-20
250
270
290
310
330
350
370
390
410
430
450
Wavelength (nm)

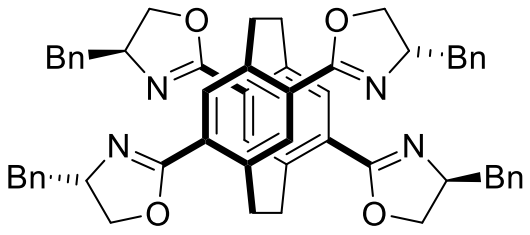
Bn
O
N
Bn
Bn
N
O
Bn
N
O

(*S*,*S*,*S*$_p$,*S*,*S*)-3.16

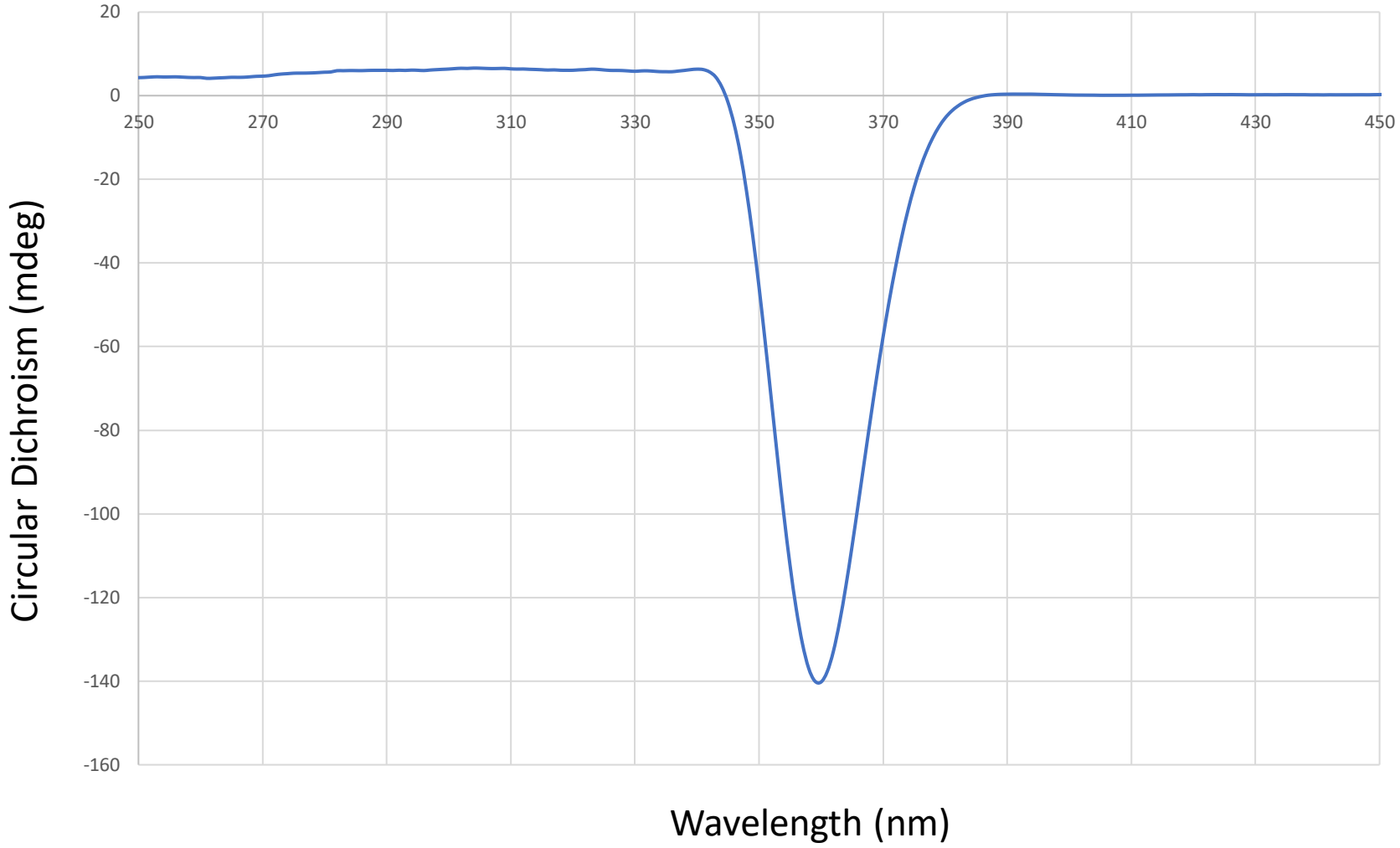
Circular Dichroism (mdeg)
20
0
-20
-40
-60
-80
-100
-120
-140
-160
250
270
290
310
330
350
370
390
410
430
450
Wavelength (nm)

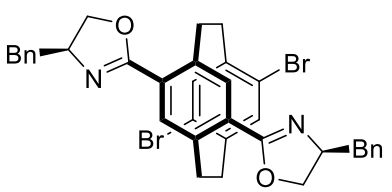

OR

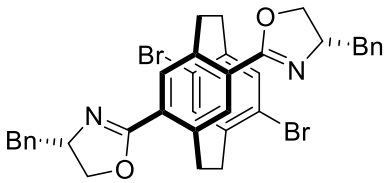

(*S*,*R*$_p$,*S*)-3.18 **(*S*,*S*$_p$,*S*)-3.18**

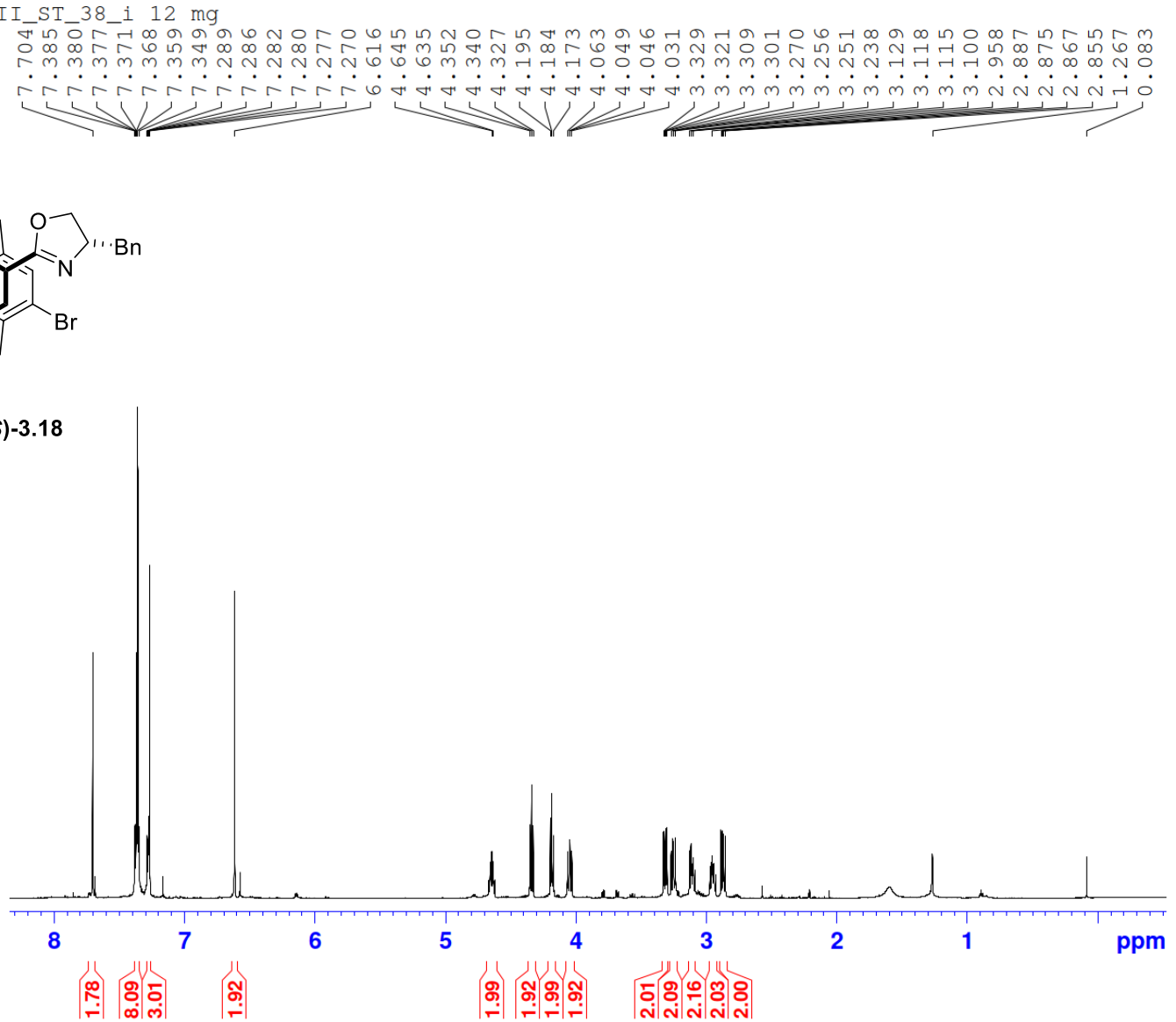

BRUKER

```
Current Data Parameters
NAME                  11pa
EXPNO                    1
PROCNO                   1

F2 - Acquisition Parameters
Date_              20200806
Time                 16.39
INSTRUM              spect
PROBHD    5 mm CPTCI 1H-
PULPROG              zg30
TD                  65536
SOLVENT             CDCl3
NS                       4
DS                       2
SWH             14492.754 Hz
FIDRES              0.221142 Hz
AQ                2.2609921 sec
RG                    35.9
DW                  34.500 usec
DE                   6.50 usec
TE                  298.0 K
D1             1.00000000 sec
TD0                      1

======== CHANNEL f1 ========
NUC1                    1H
P1                  10.00 usec
PL1                  6.90 dB
PL1W          10.71880245 W
SFO1          700.1343236 MHz

F2 - Processing parameters
SI                   32768
SF            700.1300133 MHz
WDW                     EM
SSB       0
LB                   0.30 Hz
GB        0
PC                   1.00
```

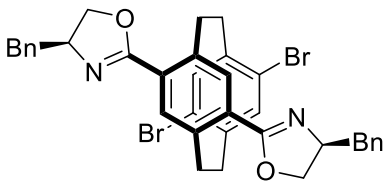

OR

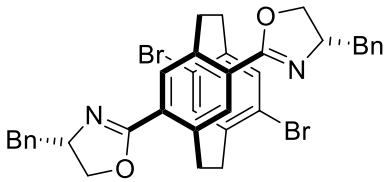

(*S*,*R*$_p$,*S*)-3.18 **(*S*,*S*$_p$,*S*)-3.18**


```
Current Data Parameters
NAME                  11pa
EXPNO                    6
PROCNO                   1

F2 - Acquisition Parameters
Date_              20200807
Time                   2.15
INSTRUM               spect
PROBHD    5 mm CPTCI 1H-
PULPROG              zgpg30
TD                    65536
SOLVENT               CDCl3
NS                     8192
DS                        4
SWH               42016.809 Hz
FIDRES             0.641126 Hz
AQ                 0.7798784 sec
RG                    32768
DW                   11.900 usec
DE                    6.50 usec
TE                   298.0 K
D1              2.00000000 sec
D11             0.03000000 sec
TD0                       2

======== CHANNEL f1 ========
NUC1                    13C
P1                    13.00 usec
PL1                   -2.60 dB
PL1W          164.55174255 W
SFO1           176.0654333 MHz

======== CHANNEL f2 ========
CPDPRG[2            waltz16
NUC2                    1H
PCPD2                80.00 usec
PL2                   6.90 dB
PL12                 24.96 dB
PL13                 19.50 dB
PL2W          10.71880245 W
PL12W          0.16755076 W
PL13W          0.58904201 W
SFO2           700.1328005 MHz

F2 - Processing parameters
SI                    32768
SF              176.0478348 MHz
WDW                      EM
SSB         0
LB                    1.00 Hz
GB          0
PC                    1.40
```

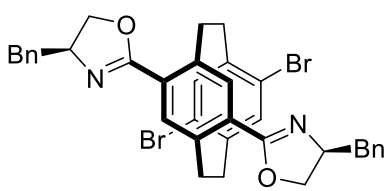

OR

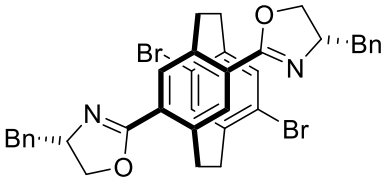

(*S*,*R*$_p$,*S*)-3.18 **(*S*,*S*$_p$,*S*)-3.18**

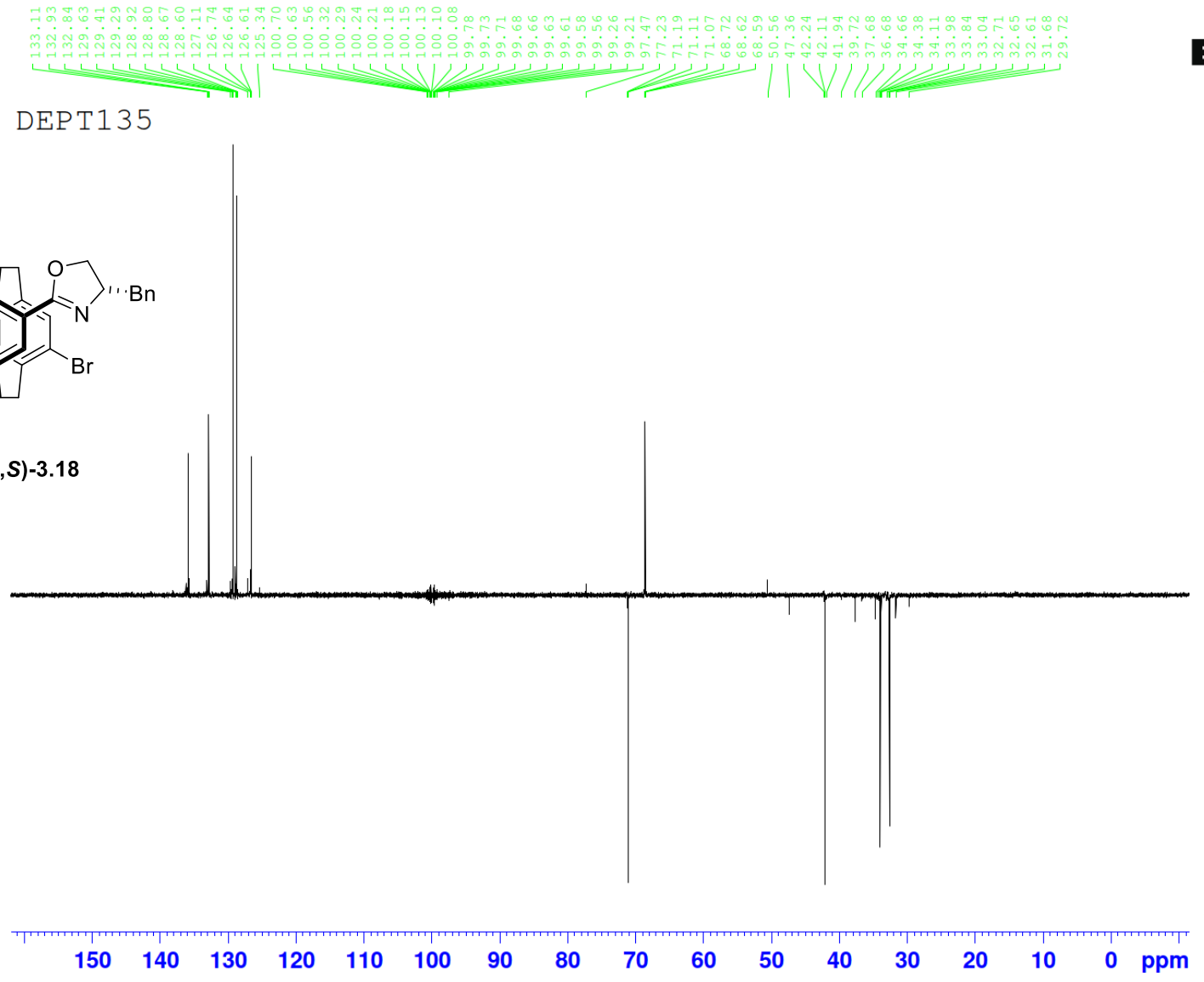


```
Current Data Parameters
NAME                  11pa
EXPNO                    7
PROCNO                   1

F2 - Acquisition Parameters
Date_              20200807
Time                   6.18
INSTRUM               spect
PROBHD    5 mm CPTCI 1H-
PULPROG          deptsp135
TD                   65536
SOLVENT              CDCl3
NS                    1024
DS                       4
SWH               42016.809 Hz
FIDRES             0.641126 Hz
AQ                 0.7798784 sec
RG                   16384
DW                  11.900 usec
DE                   6.50 usec
TE                  298.0 K
CNST2           145.0000000
D1                2.00000000 sec
D2                0.00344828 sec
D12               0.00002000 sec
TD0                      1

======== CHANNEL f1 ========
NUC1                   13C
P1                  13.00 usec
P12               2000.00 usec
PL0                 120.00 dB
PL1                  -2.60 dB
PL0W       0 W
PL1W         164.55174255 W
SFO1          176.0654333 MHz
SP2                  2.03 dB
SPNAM[2]      Crp80comp.4
SPOAL2               0.500
SPOFFS2   0 Hz

======== CHANNEL f2 ========
CPDPRG[2           waltz16
NUC2                   1H
P3                  10.00 usec
P4                  20.00 usec
PCPD2               80.00 usec
PL2                  6.90 dB
PL12                24.96 dB
PL2W           10.71880245 W
PL12W           0.16755076 W
SFO2           700.1328005 MHz

F2 - Processing parameters
SI                   32768
SF            176.0478290 MHz
WDW                    EM
SSB       0
LB                   1.00 Hz
GB        0
PC                   1.40
```

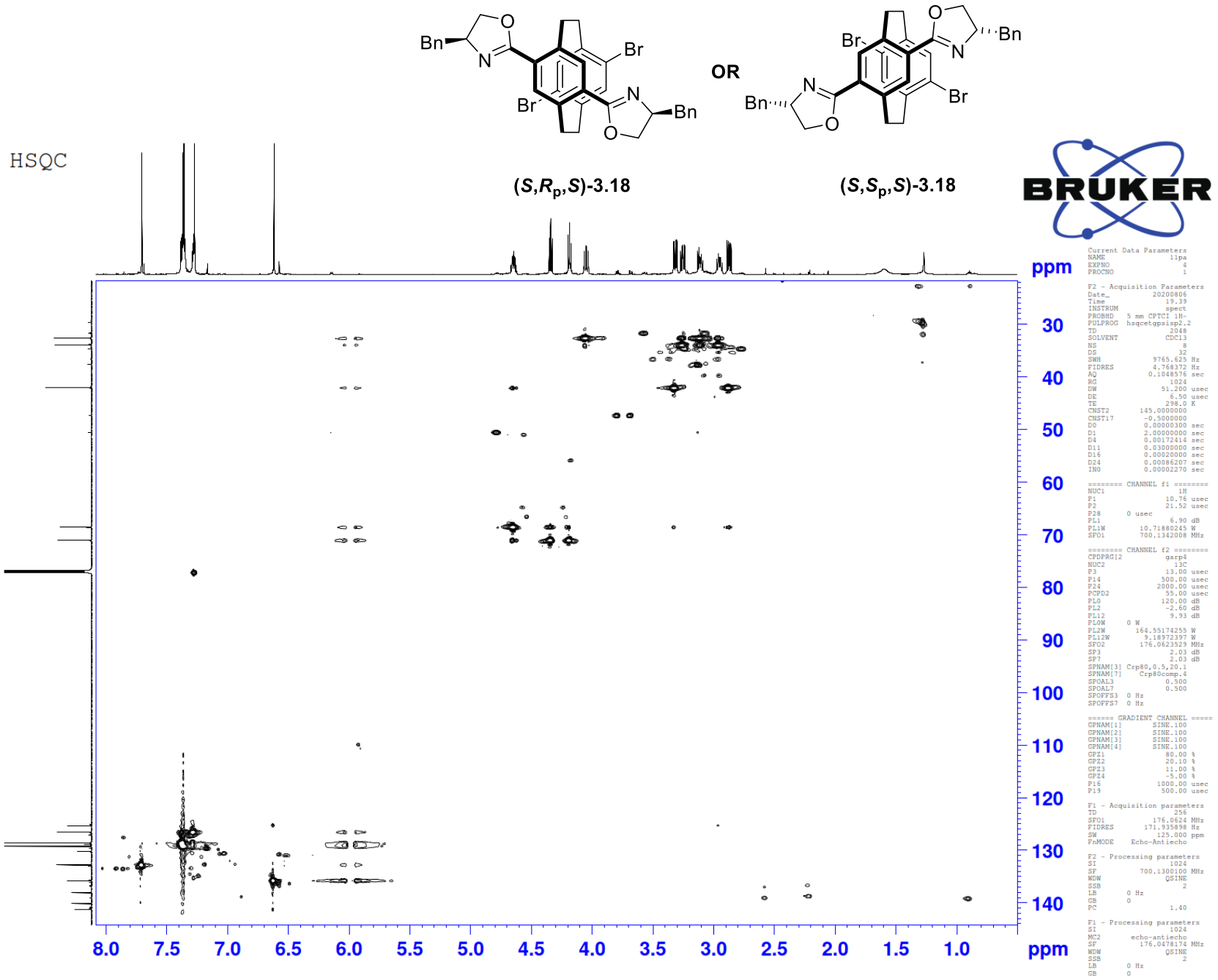
HSQC
OR
(S,Rp,S)-3.18
(S,Sp,S)-3.18
BRUKER
ppm
8.0
7.5
7.0
6.5
6.0
5.5
5.0
4.5
4.0
3.5
3.0
2.5
2.0
1.5
1.0
30
40
50
60
70
80
90
100
110
120
130
140

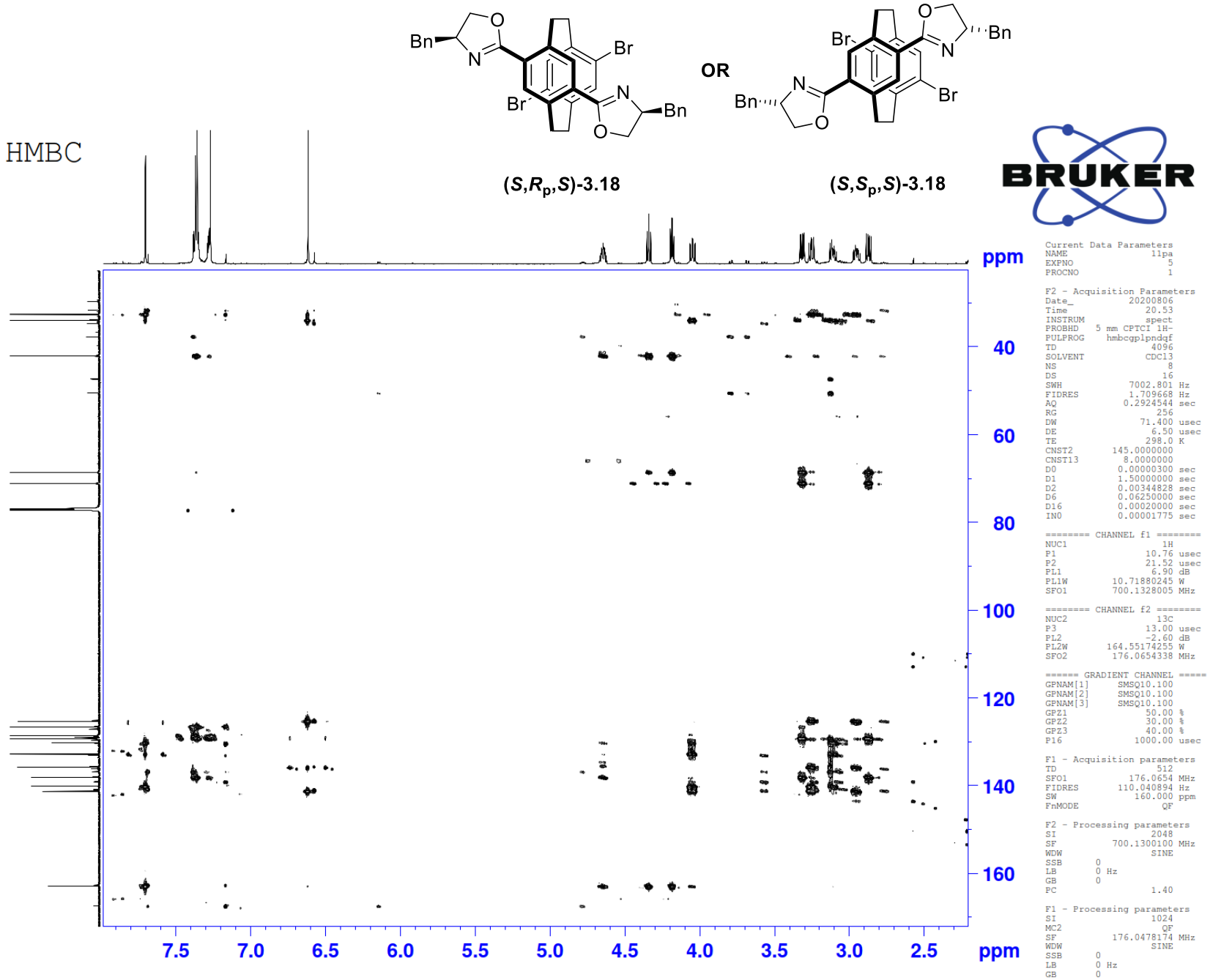
HMBC
OR
(S,Rp,S)-3.18
(S,Sp,S)-3.18
BRUKER
ppm
40
60
80
100
120
140
160
7.5
7.0
6.5
6.0
5.5
5.0
4.5
4.0
3.5
3.0
2.5
ppm
Current Data Parameters
NAME 11pa
EXPNO 5
PROCNO 1
F2 - Acquisition Parameters
Date_ 20200806
Time 20.53
INSTRUM spect
PROBHD 5 mm CPTCI 1H-
PULPROG hmbcgplpndqf
TD 4096
SOLVENT CDCl3
NS 8
DS 16
SWH 7002.801 Hz
FIDRES 1.709668 Hz
AQ 0.2924544 sec
RG 256
DW 71.400 usec
DE 6.50 usec
TE 298.0 K
CNST2 145.0000000
CNST13 8.0000000
D0 0.00000300 sec
D1 1.50000000 sec
D2 0.00344828 sec
D6 0.06250000 sec
D16 0.00020000 sec
IN0 0.00001775 sec
======== CHANNEL f1 ========
NUC1 1H
P1 10.76 usec
P2 21.52 usec
PL1 6.90 dB
PL1W 10.71880245 W
SFO1 700.1328005 MHz
======== CHANNEL f2 ========
NUC2 13C
P3 13.00 usec
PL2 -2.60 dB
PL2W 164.55174255 W
SFO2 176.0654338 MHz
====== GRADIENT CHANNEL =====
GPNAM[1] SMSQ10.100
GPNAM[2] SMSQ10.100
GPNAM[3] SMSQ10.100
GPZ1 50.00 %
GPZ2 30.00 %
GPZ3 40.00 %
P16 1000.00 usec
F1 - Acquisition parameters
TD 512
SFO1 176.0654 MHz
FIDRES 110.040894 Hz
SW 160.000 ppm
FnMODE QF
F2 - Processing parameters
SI 2048
SF 700.1300100 MHz
WDW SINE
SSB 0
LB 0 Hz
GB 0
PC 1.40
F1 - Processing parameters
SI 1024
MC2 QF
SF 176.0478174 MHz
WDW SINE
SSB 0
LB 0 Hz
GB 0

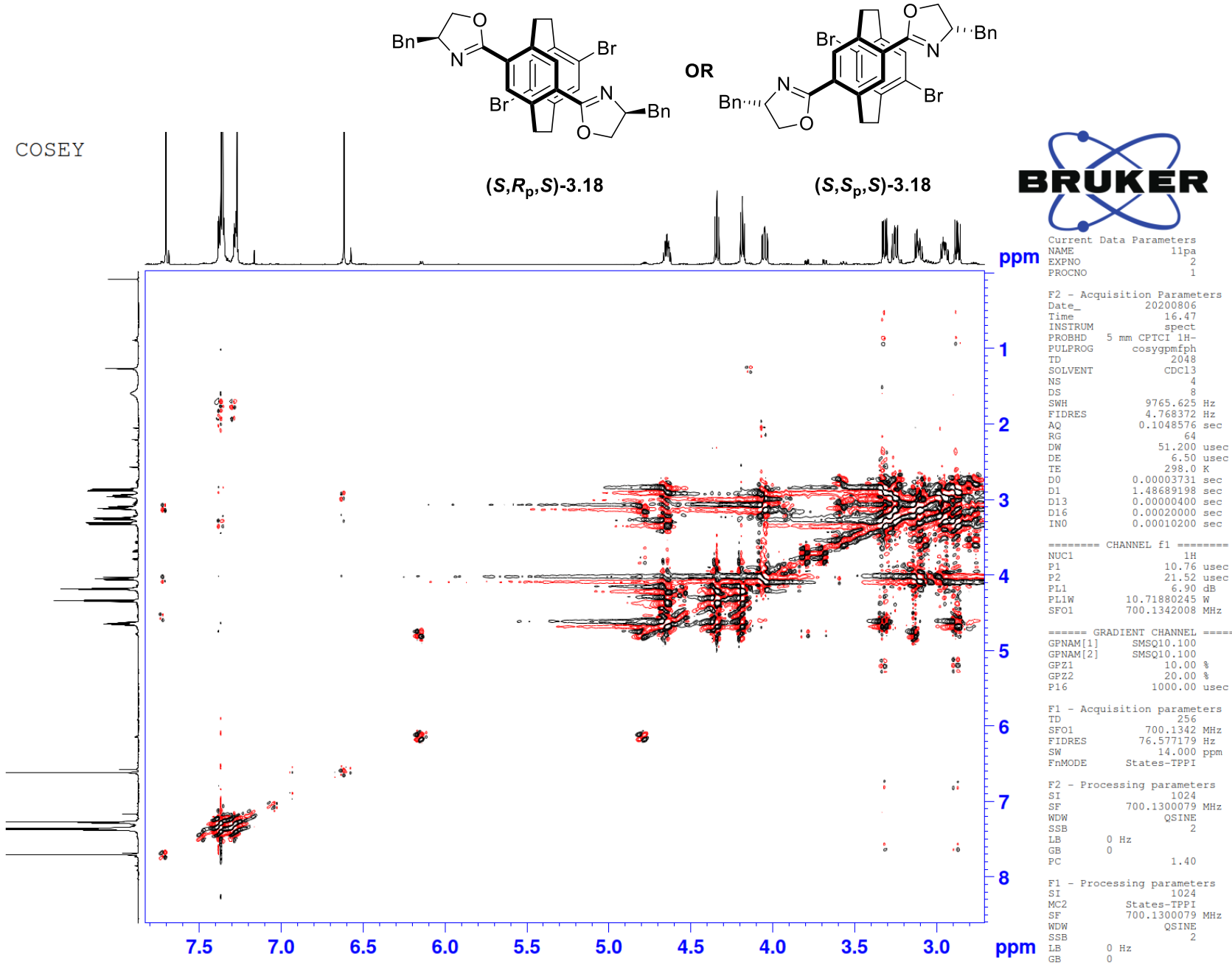
COSEY
OR
(S,Rp,S)-3.18
(S,Sp,S)-3.18
BRUKER
ppm
7.5
7.0
6.5
6.0
5.5
5.0
4.5
4.0
3.5
3.0
ppm
1
2
3
4
5
6
7
8
Current Data Parameters
NAME 11pa
EXPNO 2
PROCNO 1
F2 - Acquisition Parameters
Date_ 20200806
Time 16.47
INSTRUM spect
PROBHD 5 mm CPTCI 1H-
PULPROG cosygpmfph
TD 2048
SOLVENT CDCl3
NS 4
DS 8
SWH 9765.625 Hz
FIDRES 4.768372 Hz
AQ 0.1048576 sec
RG 64
DW 51.200 usec
DE 6.50 usec
TE 298.0 K
D0 0.00003731 sec
D1 1.48689198 sec
D13 0.00000400 sec
D16 0.00020000 sec
IN0 0.00010200 sec
======== CHANNEL f1 ========
NUC1 1H
P1 10.76 usec
P2 21.52 usec
PL1 6.90 dB
PL1W 10.71880245 W
SFO1 700.1342008 MHz
====== GRADIENT CHANNEL =====
GPNAM[1] SMSQ10.100
GPNAM[2] SMSQ10.100
GPZ1 10.00 %
GPZ2 20.00 %
P16 1000.00 usec
F1 - Acquisition parameters
TD 256
SFO1 700.1342 MHz
FIDRES 76.577179 Hz
SW 14.000 ppm
FnMODE States-TPPI
F2 - Processing parameters
SI 1024
SF 700.1300079 MHz
WDW QSINE
SSB 2
LB 0 Hz
GB 0
PC 1.40
F1 - Processing parameters
SI 1024
MC2 States-TPPI
SF 700.1300079 MHz
WDW QSINE
SSB 2
LB 0 Hz
GB 0

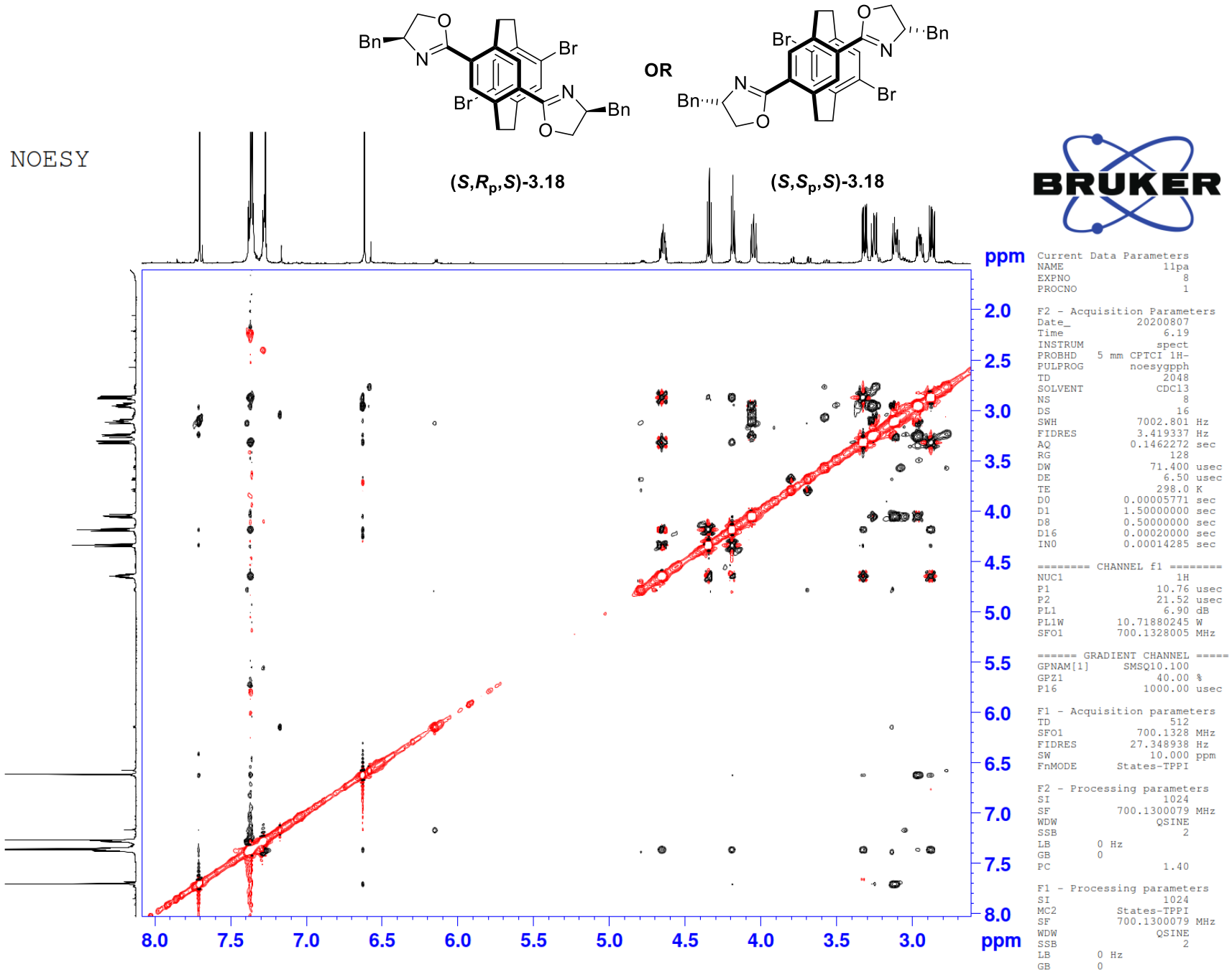
NOESY
OR
(S,Rp,S)-3.18
(S,Sp,S)-3.18
ppm
8.0
7.5
7.0
6.5
6.0
5.5
5.0
4.5
4.0
3.5
3.0
2.0
2.5
3.0
3.5
4.0
4.5
5.0
5.5
6.0
6.5
7.0
7.5
8.0
Current Data Parameters
NAME 11pa
EXPNO 8
PROCNO 1
F2 - Acquisition Parameters
Date_ 20200807
Time 6.19
INSTRUM spect
PROBHD 5 mm CPTCI 1H-
PULPROG noesygpph
TD 2048
SOLVENT CDCl3
NS 8
DS 16
SWH 7002.801 Hz
FIDRES 3.419337 Hz
AQ 0.1462272 sec
RG 128
DW 71.400 usec
DE 6.50 usec
TE 298.0 K
D0 0.00005771 sec
D1 1.50000000 sec
D8 0.50000000 sec
D16 0.00020000 sec
IN0 0.00014285 sec
======== CHANNEL f1 ========
NUC1 1H
P1 10.76 usec
P2 21.52 usec
PL1 6.90 dB
PL1W 10.71880245 W
SFO1 700.1328005 MHz
====== GRADIENT CHANNEL =====
GPNAM[1] SMSQ10.100
GPZ1 40.00 %
P16 1000.00 usec
F1 - Acquisition parameters
TD 512
SFO1 700.1328 MHz
FIDRES 27.348938 Hz
SW 10.000 ppm
FnMODE States-TPPI
F2 - Processing parameters
SI 1024
SF 700.1300079 MHz
WDW QSINE
SSB 2
LB 0 Hz
GB 0
PC 1.40
F1 - Processing parameters
SI 1024
MC2 States-TPPI
SF 700.1300079 MHz
WDW QSINE
SSB 2
LB 0 Hz
GB 0

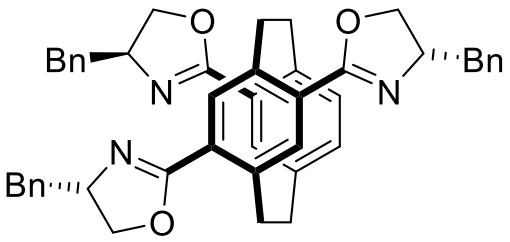

3.17
(*S*,*R*$_p$,*S*,*S*)
and
(*S*,*S*$_p$,*S*,*S*)

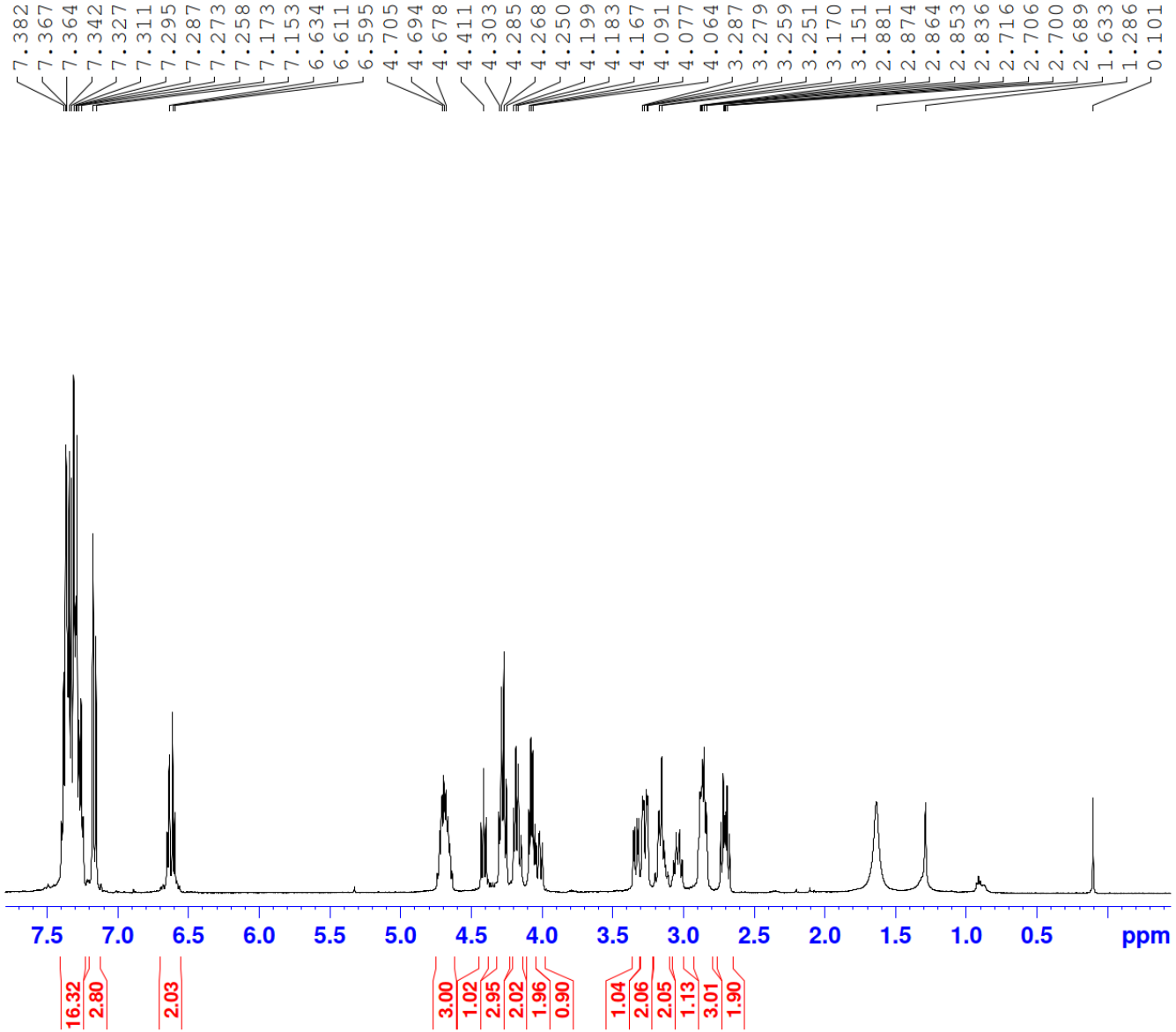


```
Current Data Parameters
NAME                  11q
EXPNO                   1
PROCNO                  1

F2 - Acquisition Parameters
Date_            20201020
Time                17.24
INSTRUM             spect
PROBHD    5 mm PAQXI 1H/
PULPROG              zg30
TD                  65536
SOLVENT             CDCl3
NS                     32
DS                      2
SWH            10330.578 Hz
FIDRES          0.157632 Hz
AQ             3.1719425 sec
RG                    128
DW                48.400 usec
DE                 6.50 usec
TE                298.2 K
D1           1.00000000 sec
TD0                     1

======== CHANNEL f1 ========
NUC1                   1H
P1                  9.50 usec
PL1                 4.00 dB
PL1W        12.10000038 W
SFO1        500.1330885 MHz

F2 - Processing parameters
SI                  32768
SF          500.1300000 MHz
WDW                    EM
SSB       0
LB                  0.30 Hz
GB        0
PC                  1.00
```

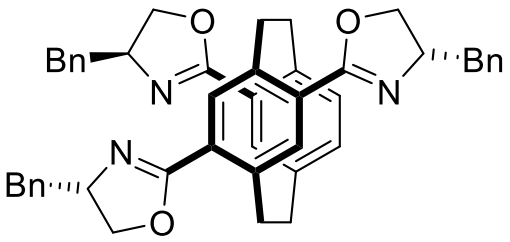

3.17
(*S*,R_p,*S*,*S*)
and
(*S*,S_p,*S*,*S*)

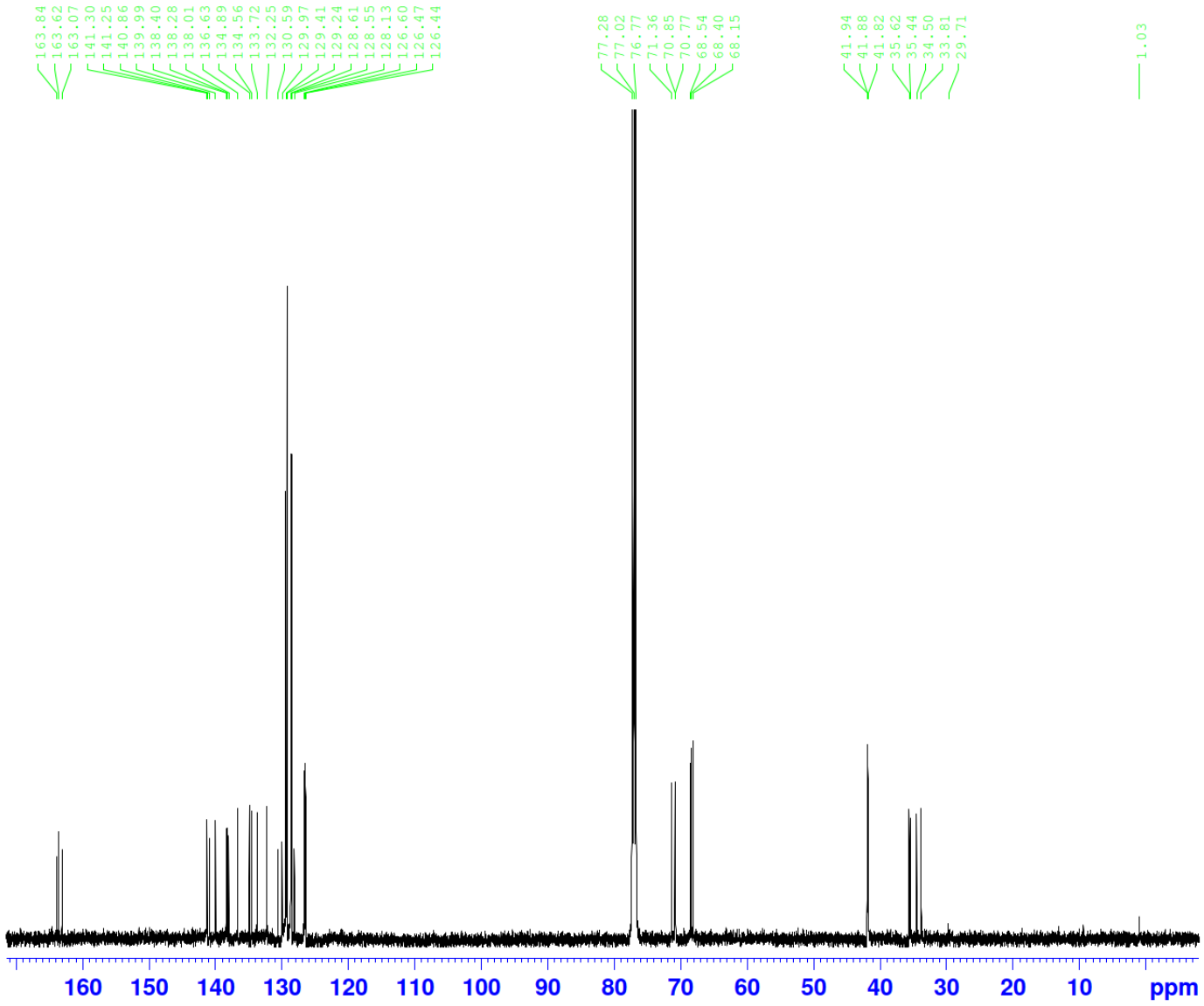

BRUKER

```
Current Data Parameters
NAME                  11q
EXPNO                   2
PROCNO                  1

F2 - Acquisition Parameters
Date_            20201021
Time                7.48
INSTRUM            spect
PROBHD   5 mm PAQXI 1H/
PULPROG           zgpg30
TD                 65536
SOLVENT            CDCl3
NS                 16384
DS                     4
SWH           30030.029 Hz
FIDRES         0.458222 Hz
AQ            1.0911744 sec
RG                 32768
DW               16.650 usec
DE                6.50 usec
TE                298.2 K
D1           2.00000000 sec
D11          0.03000000 sec
TD0                    1

======== CHANNEL f1 ========
NUC1                 13C
P1                12.00 usec
PL1               -4.00 dB
PL1W       172.88230896 W
SFO1        125.7703643 MHz

======== CHANNEL f2 ========
CPDPRG[2         waltz16
NUC2                 1H
PCPD2             80.00 usec
PL2                4.00 dB
PL12              22.51 dB
PL13              25.00 dB
PL2W       12.10000038 W
PL12W       0.17052394 W
PL13W       0.09611372 W
SFO2        500.1320005 MHz

F2 - Processing parameters
SI                 32768
SF          125.7577890 MHz
WDW                   EM
SSB       0
LB                 1.00 Hz
GB        0
PC                 1.40
```

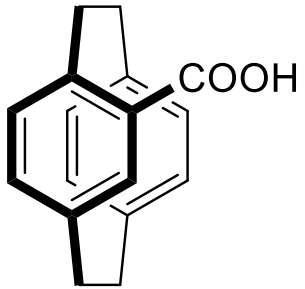
COOH

(R_p)-4.2

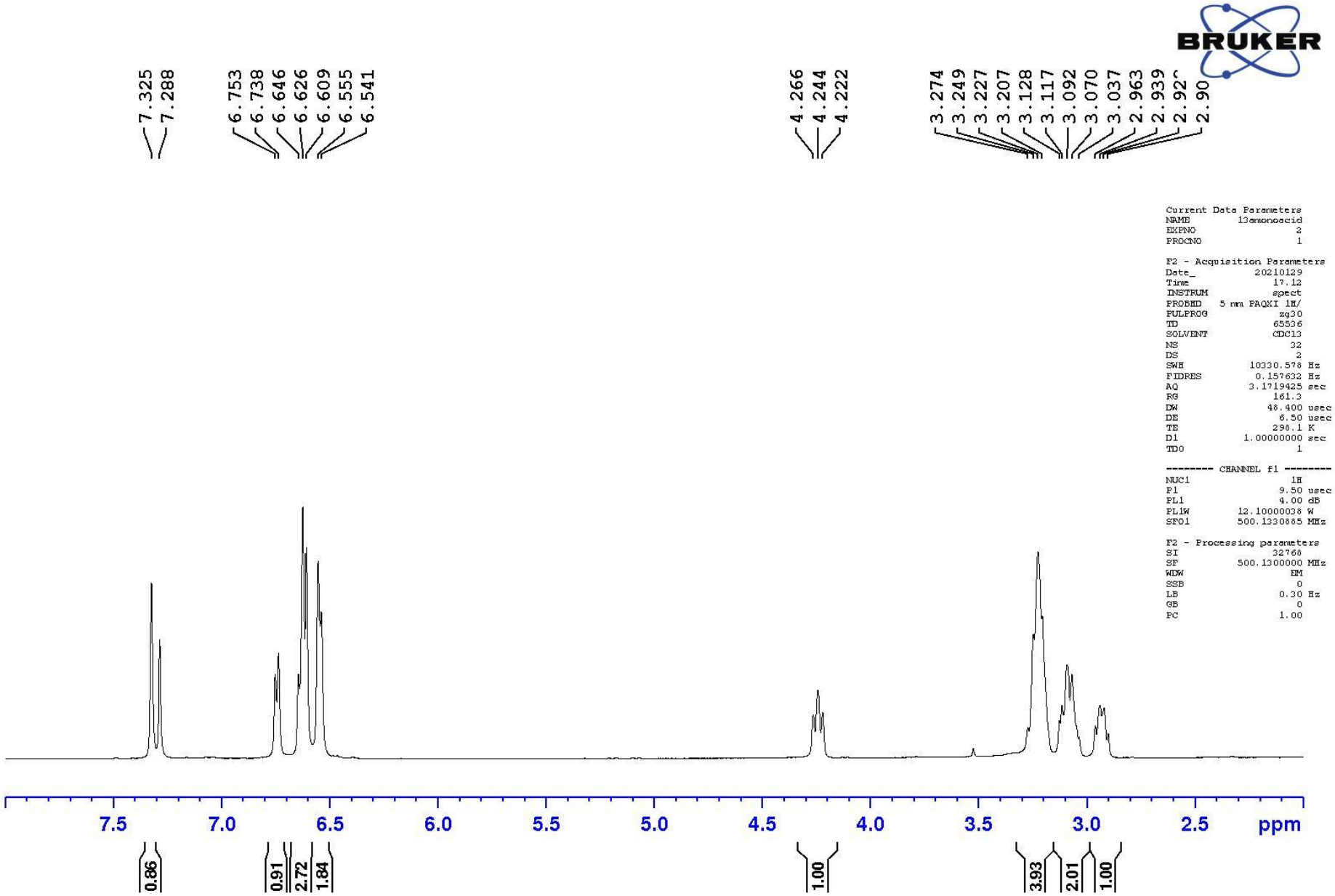
7.325
7.288
6.753
6.738
6.646
6.626
6.609
6.555
6.541
4.266
4.244
4.222
3.274
3.249
3.227
3.207
3.128
3.117
3.092
3.070
3.037
2.963
2.939
2.90
Current Data Parameters
NAME 13amonoacid
EXPNO 2
PROCNO 1
F2 - Acquisition Parameters
Date_ 20210129
Time 17.12
INSTRUM spect
PROBHD 5 mm PAQXI 1H/
PULPROG zg30
TD 65536
SOLVENT CDCl3
NS 32
DS 2
SWH 10330.578 Hz
FIDRES 0.157632 Hz
AQ 3.1719425 sec
RG 161.3
DW 48.400 usec
DE 6.50 usec
TE 298.1 K
D1 1.00000000 sec
TD0 1
CHANNEL f1
NUC1 1H
P1 9.50 usec
PL1 4.00 dB
PL1W 12.10000038 W
SFO1 500.1330885 MHz
F2 - Processing parameters
SI 32768
SF 500.1300000 MHz
WDW EM
SSB 0
LB 0.30 Hz
GB 0
PC 1.00
7.5
7.0
6.5
6.0
5.5
5.0
4.5
4.0
3.5
3.0
2.5
ppm
0.86
0.91
2.72
1.84
1.00
3.93
2.01
1.00

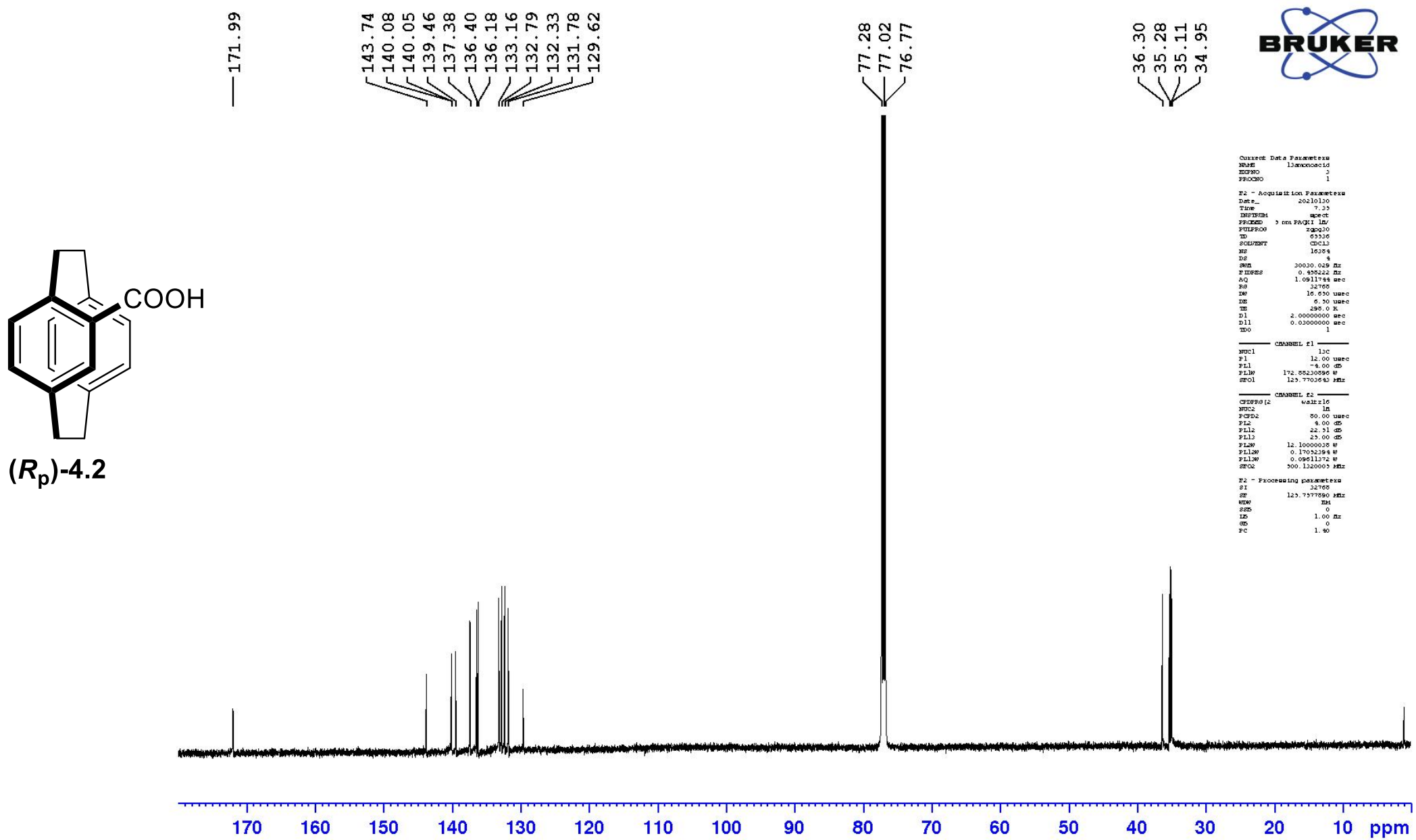
171.99
143.74
140.08
140.05
139.46
137.38
136.40
136.18
133.16
132.79
132.33
131.78
129.62
77.28
77.02
76.77
36.30
35.28
35.11
34.95
BRUKER
COOH
(Rp)-4.2
Current Data Parameters
NAME 13amcnoacid
EXPNO 3
PROCNO 1
F2 - Acquisition Parameters
Date_ 20210130
Time 7.35
INSTRUM spect
PROBHD 5 mm PABBO BB/
PULPROG zgpg30
TD 65536
SOLVENT CDCl3
NS 1638
DS 4
SWH 30030.029 Hz
FIDRES 0.458222 Hz
AQ 1.0911744 sec
RG 32768
DW 16.650 usec
DE 6.50 usec
TE 298.0 K
D1 2.00000000 sec
D11 0.03000000 sec
TD0 1
CHANNEL f1
NUC1 13C
P1 12.00 usec
PL1 -4.00 dB
PL1W 172.88230896 W
SFO1 125.7703643 MHz
CHANNEL f2
CPDPRG[2 waltz16
NUC2 1H
PCPD2 50.00 usec
PL2 4.00 dB
PL12 22.51 dB
PL13 23.00 dB
PL2W 12.10000038 W
PL12W 0.17052394 W
PL13W 0.09611372 W
SFO2 500.1320005 MHz
F2 - Processing parameters
SI 32768
SF 125.7577890 MHz
WDW EM
SSB 0
LB 1.00 Hz
GB 0
PC 1.40
170
160
150
140
130
120
110
100
90
80
70
60
50
40
30
20
10
ppm

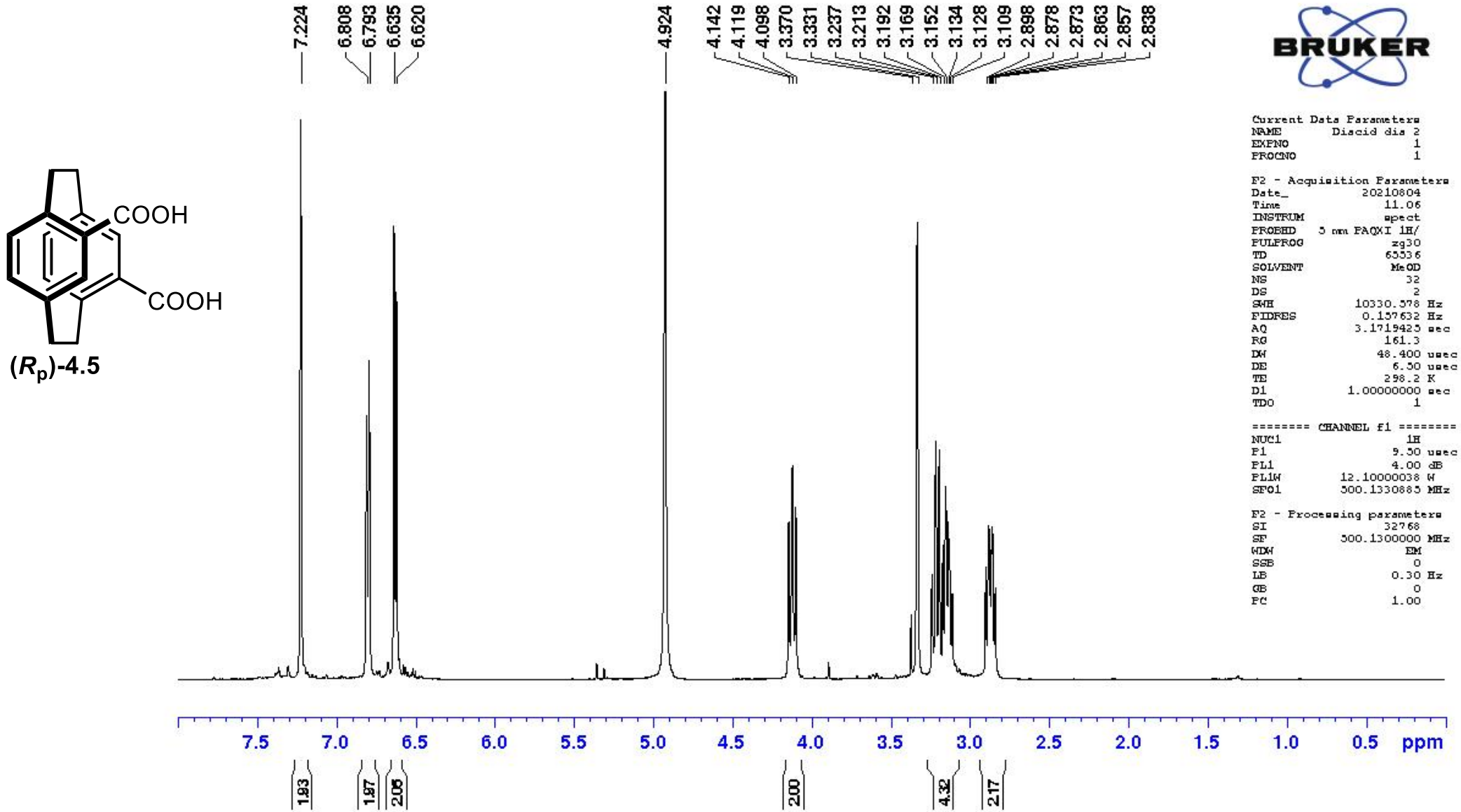
COOH
COOH
(Rp)-4.5
7.224
6.808
6.793
6.635
6.620
4.924
4.142
4.119
4.098
3.370
3.331
3.237
3.213
3.192
3.169
3.152
3.134
3.128
3.109
2.898
2.878
2.873
2.863
2.857
2.838
BRUKER
Current Data Parameters
NAME Diacid dia 2
EXPNO 1
PROCNO 1
F2 - Acquisition Parameters
Date_ 20210804
Time 11.06
INSTRUM spect
PROBHD 5 mm PAQXI 1H/
PULPROG zg30
TD 65536
SOLVENT MeOD
NS 32
DS 2
SWH 10330.578 Hz
FIDRES 0.157632 Hz
AQ 3.1719423 sec
RG 161.3
DW 48.400 usec
DE 6.50 usec
TE 298.2 K
D1 1.00000000 sec
TD0 1
======== CHANNEL f1 ========
NUC1 1H
P1 9.50 usec
PL1 4.00 dB
PL1W 12.10000038 W
SFO1 500.1330885 MHz
F2 - Processing parameters
SI 32768
SF 500.1300000 MHz
WDW EM
SSB 0
LB 0.30 Hz
GB 0
PC 1.00
7.5
7.0
6.5
6.0
5.5
5.0
4.5
4.0
3.5
3.0
2.5
2.0
1.5
1.0
0.5
ppm
1.93
1.97
2.05
2.00
4.32
2.17

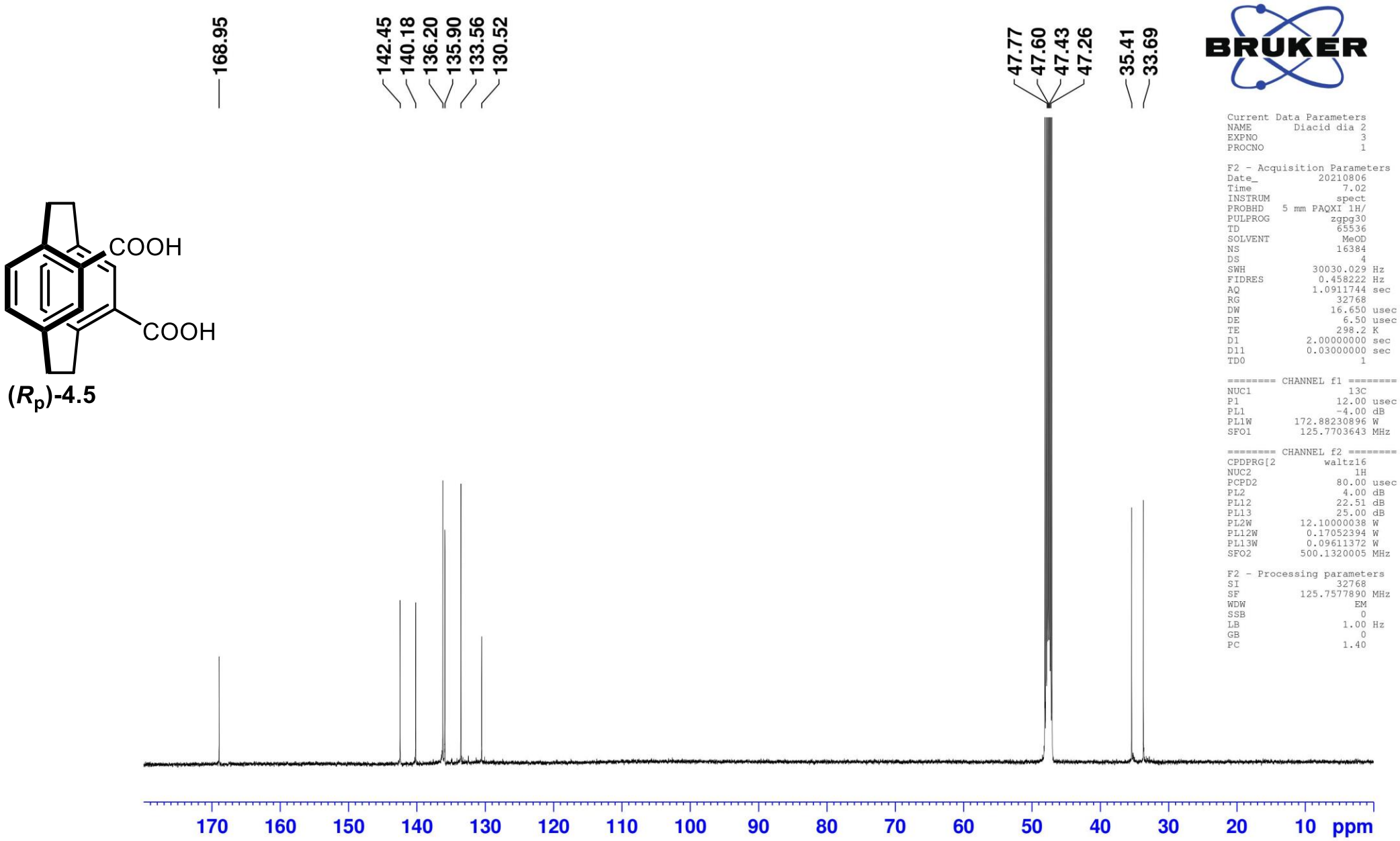
168.95
142.45
140.18
136.20
135.90
133.56
130.52
47.77
47.60
47.43
47.26
35.41
33.69
COOH
COOH
(Rp)-4.5
BRUKER
Current Data Parameters
NAME Diacid dia 2
EXPNO 3
PROCNO 1
F2 - Acquisition Parameters
Date_ 20210806
Time 7.02
INSTRUM spect
PROBHD 5 mm PAQXI 1H/
PULPROG zgpg30
TD 65536
SOLVENT MeOD
NS 16384
DS 4
SWH 30030.029 Hz
FIDRES 0.458222 Hz
AQ 1.0911744 sec
RG 32768
DW 16.650 usec
DE 6.50 usec
TE 298.2 K
D1 2.00000000 sec
D11 0.03000000 sec
TD0 1
======== CHANNEL f1 ========
NUC1 13C
P1 12.00 usec
PL1 -4.00 dB
PL1W 172.88230896 W
SFO1 125.7703643 MHz
======== CHANNEL f2 ========
CPDPRG[2 waltz16
NUC2 1H
PCPD2 80.00 usec
PL2 4.00 dB
PL12 22.51 dB
PL13 25.00 dB
PL2W 12.10000038 W
PL12W 0.17052394 W
PL13W 0.09611372 W
SFO2 500.1320005 MHz
F2 - Processing parameters
SI 32768
SF 125.7577890 MHz
WDW EM
SSB 0
LB 1.00 Hz
GB 0
PC 1.40
170 160 150 140 130 120 110 100 90 80 70 60 50 40 30 20 10 ppm

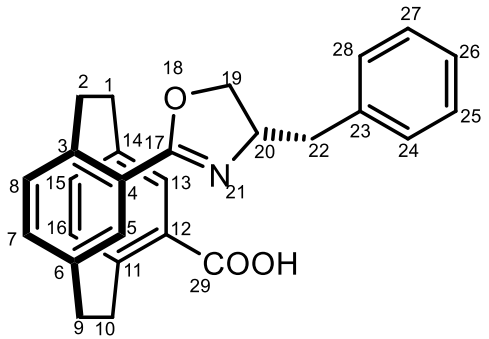
27
28
26
25
18
19
2
1
O
23
24
3
14
17
20
22
N
21
8
15
4
13
7
16
5
12
COOH
6
11
29
9
10

(R_p,*S*)-(-)-4.8

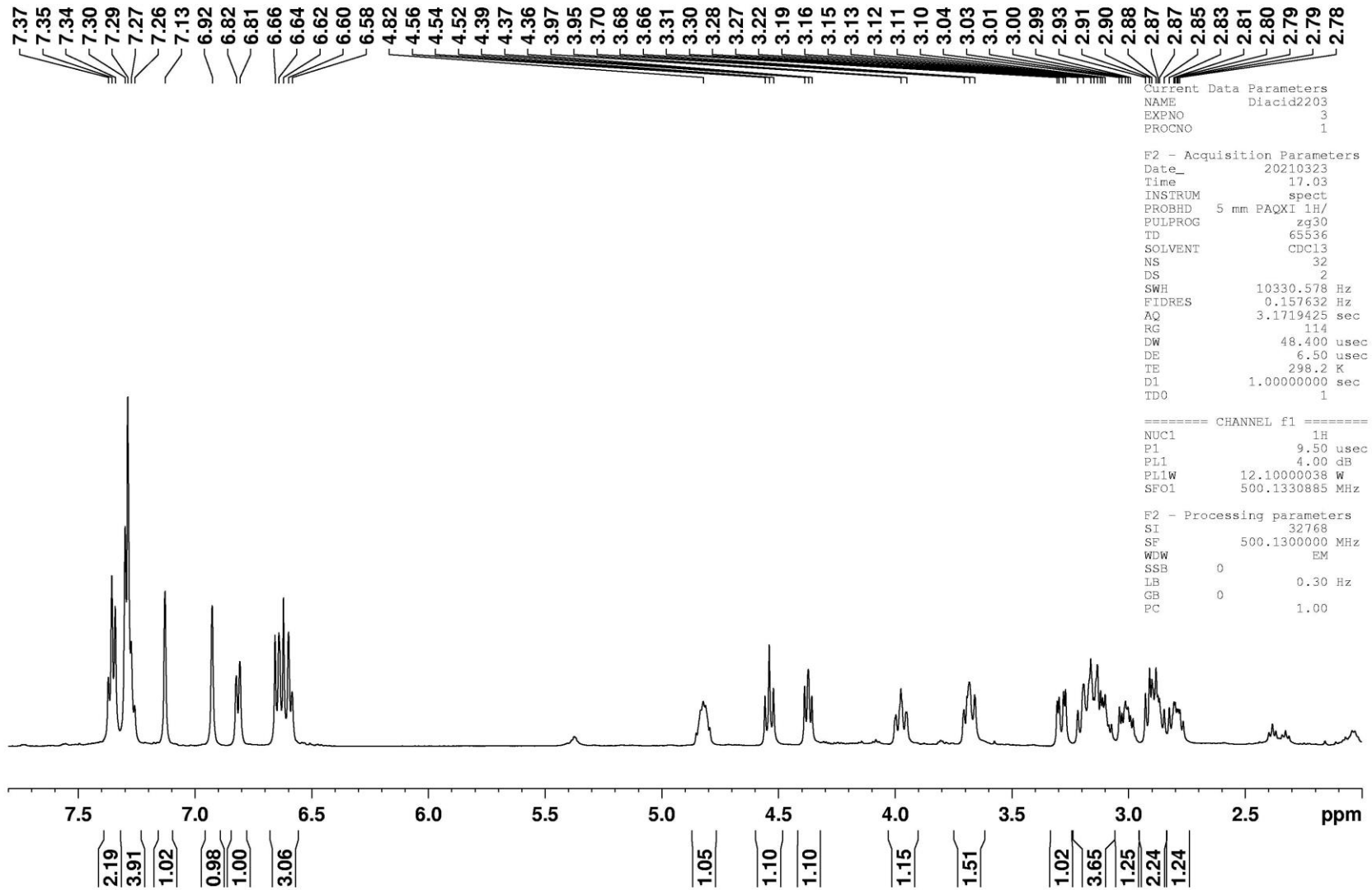
7.37 7.35 7.34 7.30 7.29 7.27 7.26 7.13 6.92 6.82 6.81 6.66 6.64 6.62 6.60 6.58 4.82 4.56 4.54 4.52 4.39 4.37 4.36 3.97 3.95 3.70 3.68 3.66 3.31 3.30 3.28 3.27 3.22 3.19 3.16 3.15 3.13 3.12 3.11 3.10 3.04 3.03 3.01 3.00 2.99 2.93 2.91 2.90 2.88 2.87 2.87 2.85 2.83 2.81 2.80 2.79 2.79 2.78
Current Data Parameters
NAME Diacid2203
EXPNO 3
PROCNO 1
F2 - Acquisition Parameters
Date_ 20210323
Time 17.03
INSTRUM spect
PROBHD 5 mm PAQXI 1H/
PULPROG zg30
TD 65536
SOLVENT CDCl3
NS 32
DS 2
SWH 10330.578 Hz
FIDRES 0.157632 Hz
AQ 3.1719425 sec
RG 114
DW 48.400 usec
DE 6.50 usec
TE 298.2 K
D1 1.00000000 sec
TD0 1
======== CHANNEL f1 ========
NUC1 1H
P1 9.50 usec
PL1 4.00 dB
PL1W 12.10000038 W
SFO1 500.1330885 MHz
F2 - Processing parameters
SI 32768
SF 500.1300000 MHz
WDW EM
SSB 0
LB 0.30 Hz
GB 0
PC 1.00
7.5 7.0 6.5 6.0 5.5 5.0 4.5 4.0 3.5 3.0 2.5 ppm
2.19 3.91 1.02 0.98 1.00 3.06 1.05 1.10 1.10 1.15 1.51 1.02 3.65 1.25 2.24 1.24

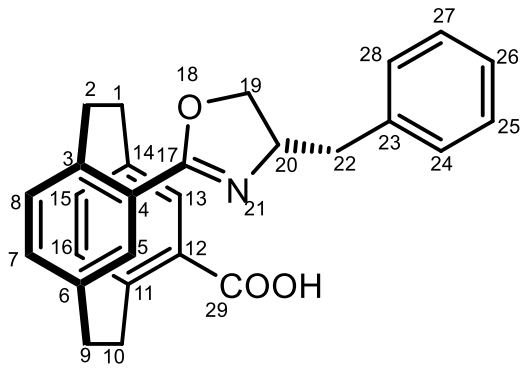
1
2
3
4
5
6
7
8
9
10
11
12
13
14
15
16
17
18
19
20
21
22
23
24
25
26
27
28
COOH
29

(R_p,*S*)-(-)-4.8

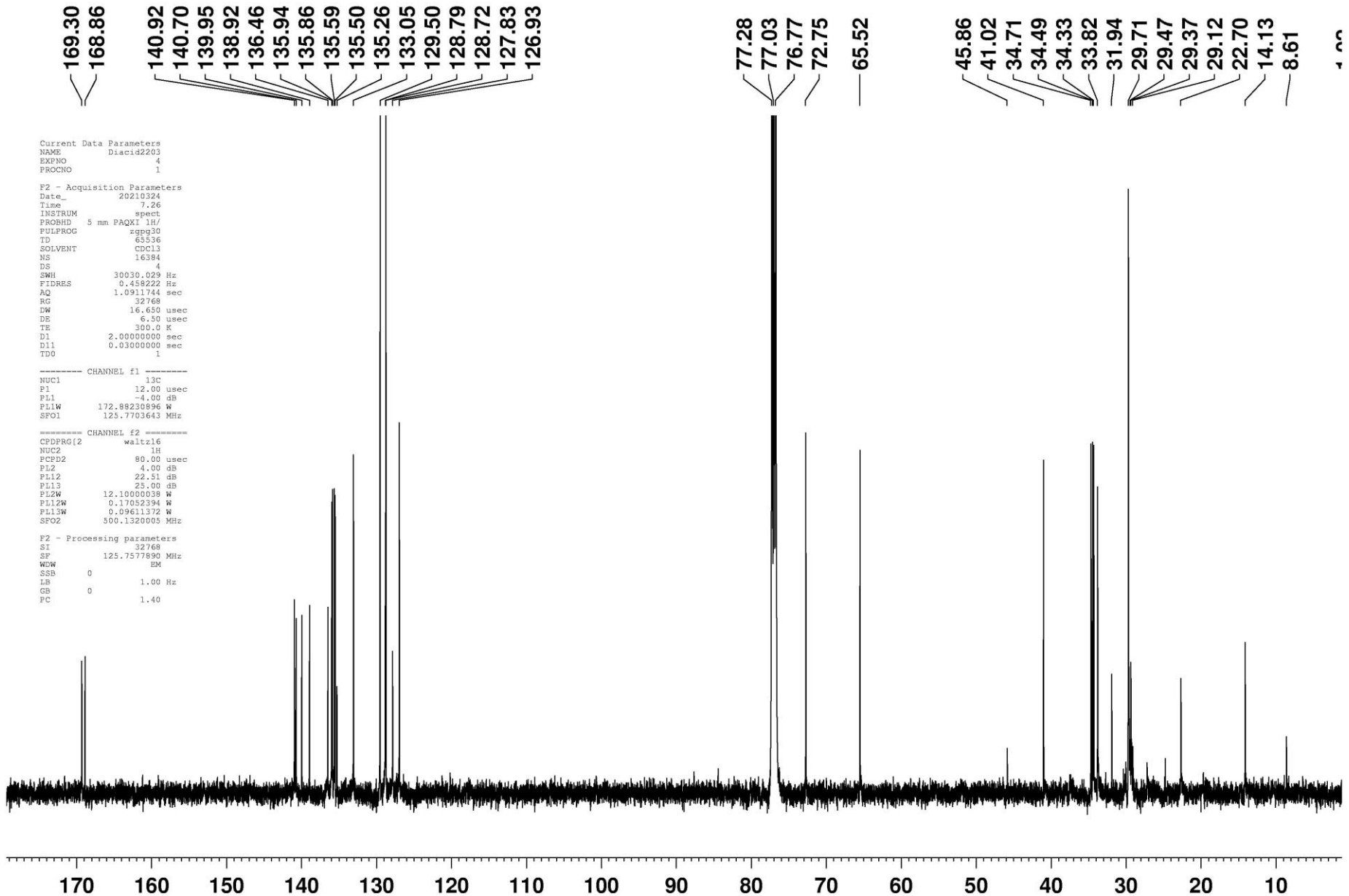
169.30
168.86
140.92
140.70
139.95
138.92
136.46
135.94
135.86
135.59
135.50
135.26
133.05
129.50
128.79
128.72
127.83
126.93
77.28
77.03
76.77
72.75
65.52
45.86
41.02
34.71
34.49
34.33
33.82
31.94
29.71
29.47
29.37
29.12
22.70
14.13
8.61
Current Data Parameters
NAME Diacid2203
EXPNO 4
PROCNO 1
F2 - Acquisition Parameters
Date_ 20210324
Time 7.26
INSTRUM spect
PROBHD 5 mm PAQXI 1H/
PULPROG zgpg30
TD 65536
SOLVENT CDCl3
NS 16384
DS 4
SWH 30030.029 Hz
FIDRES 0.458222 Hz
AQ 1.0911744 sec
RG 32768
DW 16.650 usec
DE 6.50 usec
TE 300.0 K
D1 2.00000000 sec
D11 0.03000000 sec
TD0 1
======== CHANNEL f1 ========
NUC1 13C
P1 12.00 usec
PL1 -4.00 dB
PL1W 172.88230896 W
SFO1 125.7703643 MHz
======== CHANNEL f2 ========
CPDPRG[2 waltz16
NUC2 1H
PCPD2 80.00 usec
PL2 4.00 dB
PL12 22.51 dB
PL13 25.00 dB
PL2W 12.10000038 W
PL12W 0.17052394 W
PL13W 0.09611372 W
SFO2 500.1320005 MHz
F2 - Processing parameters
SI 32768
SF 125.7577890 MHz
WDW EM
SSB 0
LB 1.00 Hz
GB 0
PC 1.40
170
160
150
140
130
120
110
100
90
80
70
60
50
40
30
20
10

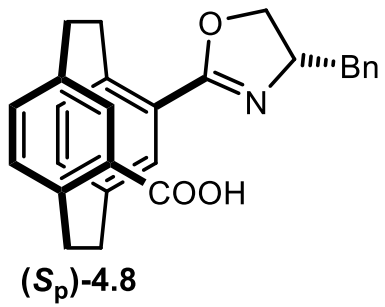
O
Bn
N
COOH

(S_p)-4.8

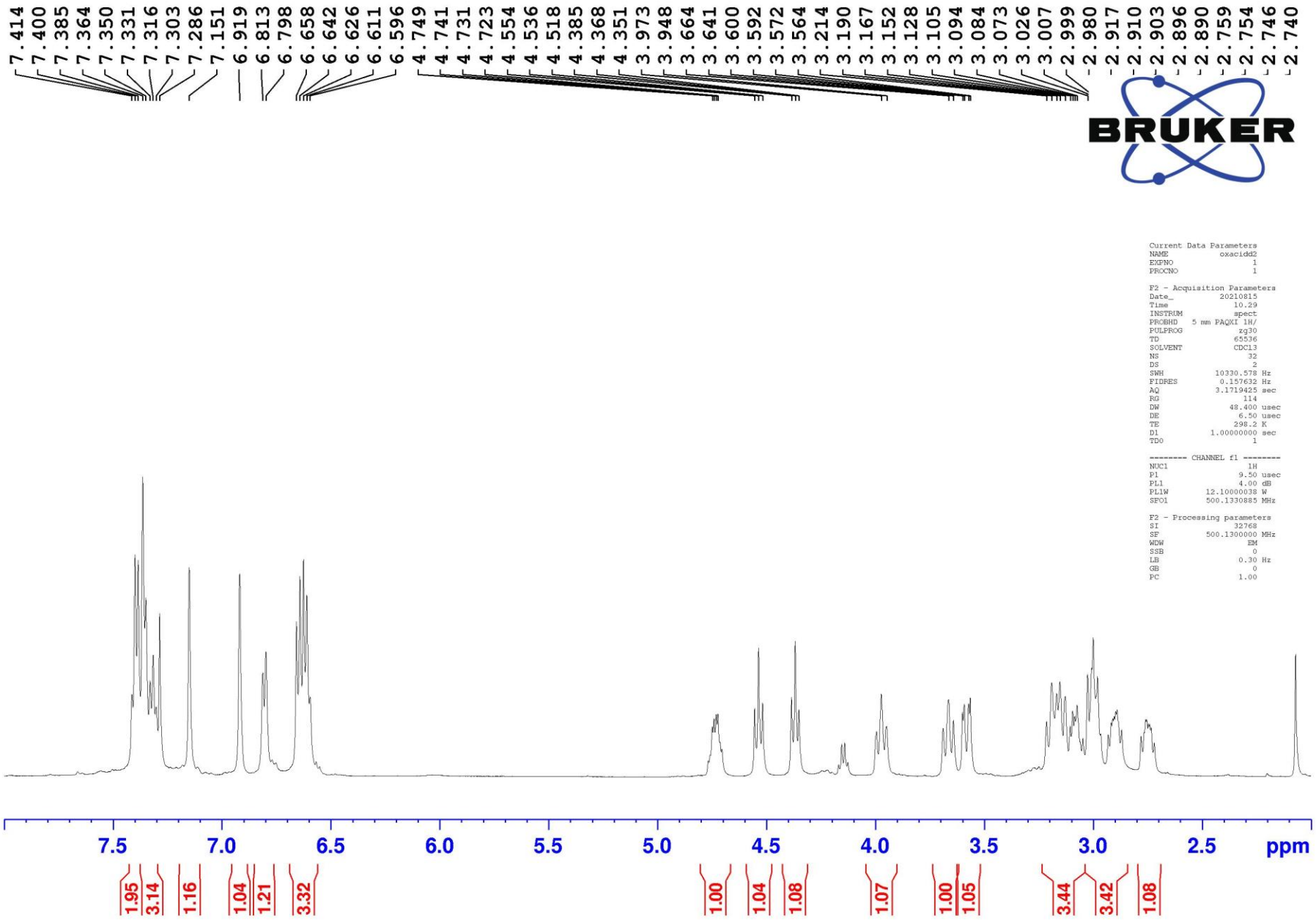
7.414 7.400 7.385 7.364 7.350 7.331 7.316 7.303 7.286 7.151 6.919 6.813 6.798 6.658 6.642 6.626 6.611 6.596 4.749 4.741 4.731 4.723 4.554 4.536 4.518 4.385 4.368 4.351 3.973 3.948 3.664 3.641 3.600 3.592 3.572 3.564 3.214 3.190 3.167 3.152 3.128 3.105 3.094 3.084 3.073 3.026 3.007 2.999 2.980 2.917 2.910 2.903 2.896 2.890 2.759 2.754 2.746 2.740
BRUKER
Current Data Parameters
NAME oxacidd2
EXPNO 1
PROCNO 1
F2 - Acquisition Parameters
Date_ 20210815
Time 10.29
INSTRUM spect
PROBHD 5 mm PAQXI 1H/
PULPROG zg30
TD 65536
SOLVENT CDCl3
NS 32
DS 2
SWH 10330.578 Hz
FIDRES 0.157632 Hz
AQ 3.1719425 sec
RG 114
DW 48.400 usec
DE 6.50 usec
TE 298.2 K
D1 1.00000000 sec
TD0 1
-------- CHANNEL f1 --------
NUC1 1H
P1 9.50 usec
PL1 4.00 dB
PL1W 12.10000038 W
SFO1 500.1330885 MHz
F2 - Processing parameters
SI 32768
SF 500.1300000 MHz
WDW EM
SSB 0
LB 0.30 Hz
GB 0
PC 1.00
7.5 7.0 6.5 6.0 5.5 5.0 4.5 4.0 3.5 3.0 2.5 ppm
1.95 3.14 1.16 1.04 1.21 3.32 1.00 1.04 1.08 1.07 1.00 1.05 3.44 3.42 1.08

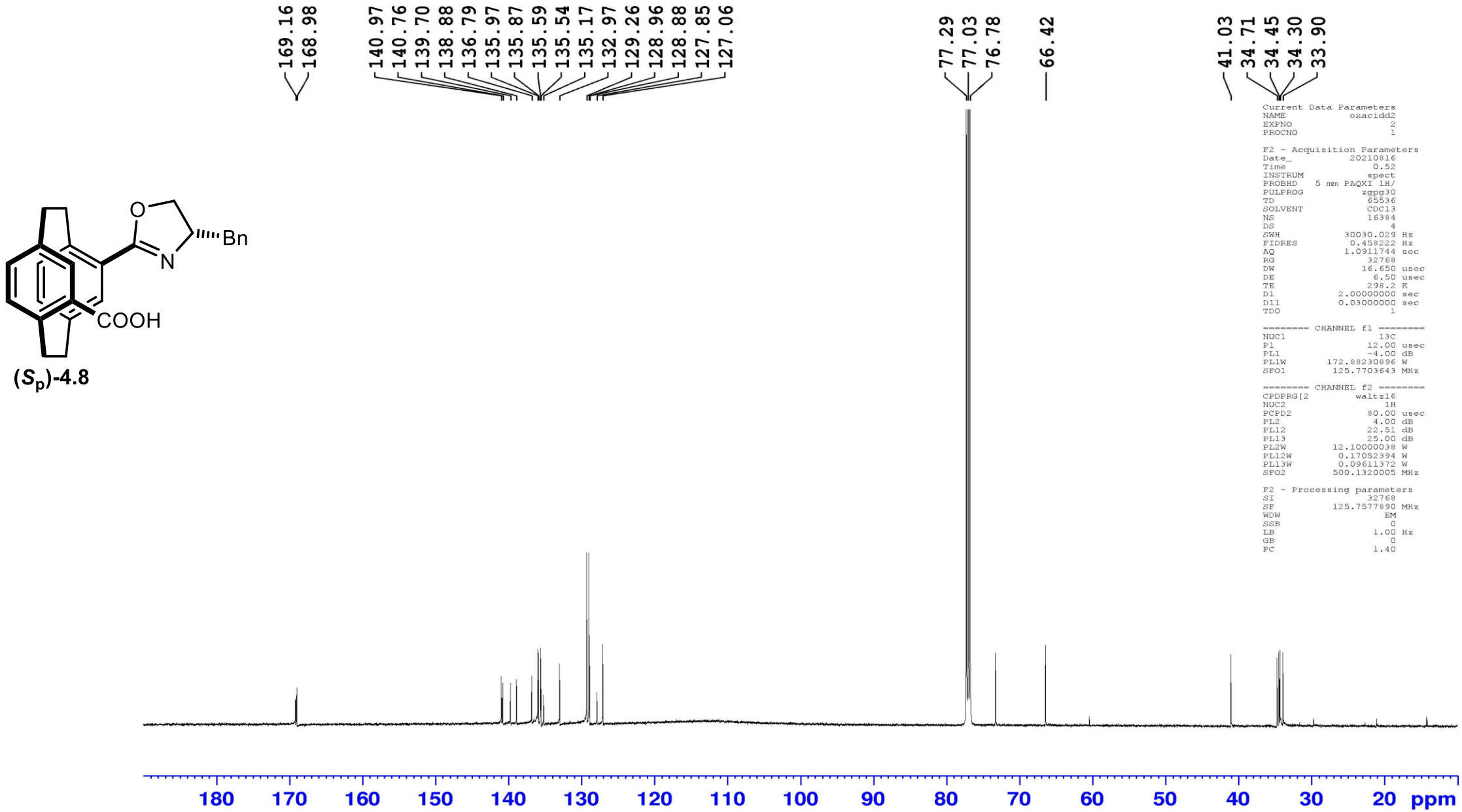
169.16
168.98
140.97
140.76
139.70
138.88
136.79
135.97
135.87
135.59
135.54
135.17
132.97
129.26
128.96
128.88
127.85
127.06
77.29
77.03
76.78
66.42
41.03
34.71
34.45
34.30
33.90
O
N
Bn
COOH
(Sp)-4.8
Current Data Parameters
NAME oxacidd2
EXPNO 2
PROCNO 1
F2 - Acquisition Parameters
Date_ 20210816
Time 0.52
INSTRUM spect
PROBHD 5 mm PAQXI 1H/
PULPROG zgpg30
TD 65536
SOLVENT CDCl3
NS 16384
DS 4
SWH 30030.029 Hz
FIDRES 0.458222 Hz
AQ 1.0911744 sec
RG 32768
DW 16.650 usec
DE 6.50 usec
TE 298.2 K
D1 2.00000000 sec
D11 0.03000000 sec
TD0 1
======== CHANNEL f1 ========
NUC1 13C
P1 12.00 usec
PL1 -4.00 dB
PL1W 172.88230896 W
SFO1 125.7703643 MHz
======== CHANNEL f2 ========
CPDPRG[2 waltz16
NUC2 1H
PCPD2 80.00 usec
PL2 4.00 dB
PL12 22.51 dB
PL13 25.00 dB
PL2W 12.10000038 W
PL12W 0.17052394 W
PL13W 0.09611372 W
SFO2 500.1320005 MHz
F2 - Processing parameters
SI 32768
SF 125.7577890 MHz
WDW EM
SSB 0
LB 1.00 Hz
GB 0
PC 1.40
180
170
160
150
140
130
120
110
100
90
80
70
60
50
40
30
20
ppm

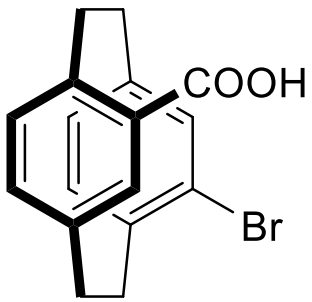
COOH
Br

(R_p)-4.7

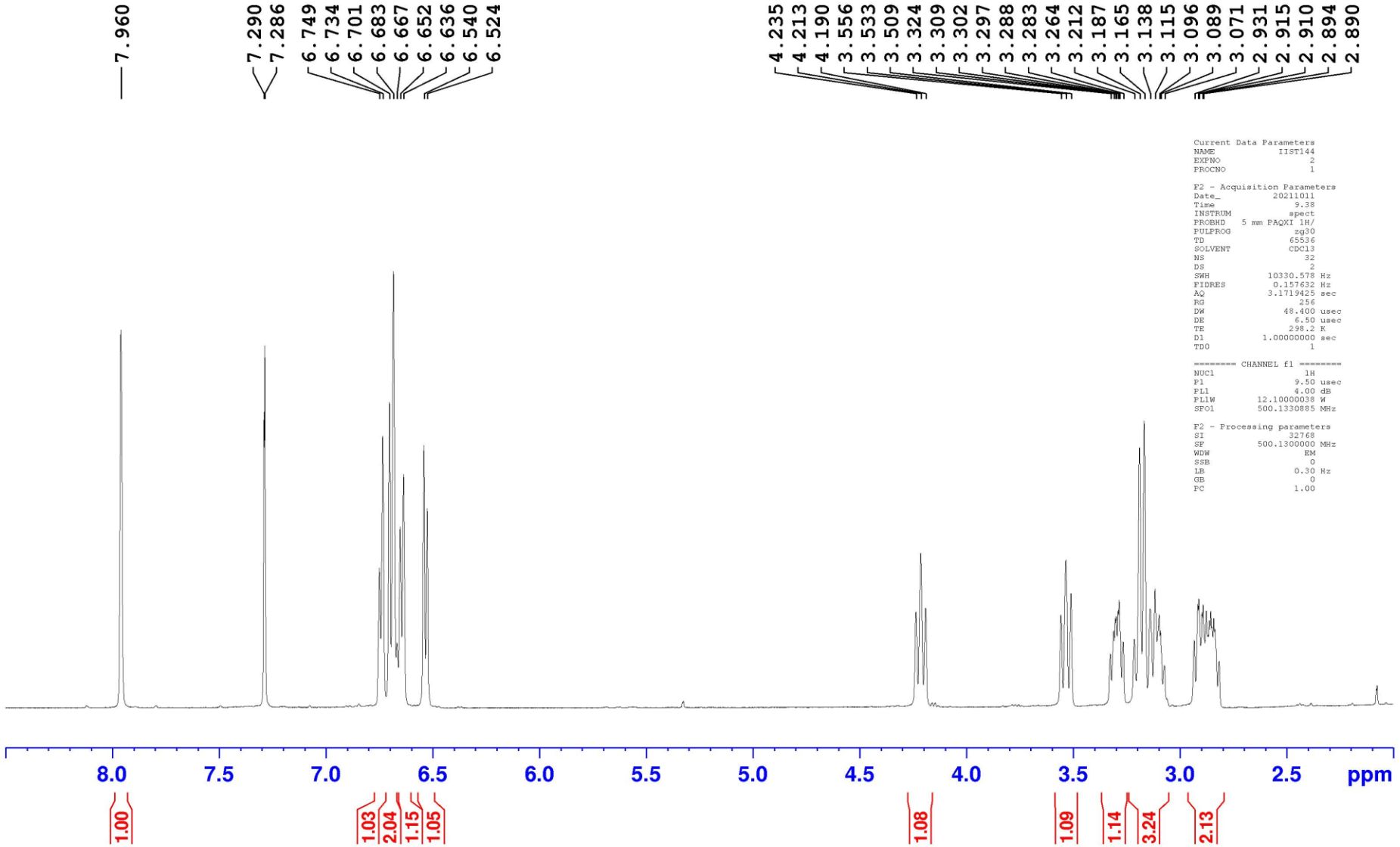
7.960
7.290
7.286
6.749
6.734
6.701
6.683
6.667
6.652
6.636
6.540
6.524
4.235
4.213
4.190
3.556
3.533
3.509
3.324
3.309
3.302
3.297
3.288
3.283
3.264
3.212
3.187
3.165
3.138
3.115
3.096
3.089
3.071
2.931
2.915
2.910
2.894
2.890
Current Data Parameters
NAME IIST144
EXPNO 2
PROCNO 1
F2 - Acquisition Parameters
Date_ 20211011
Time 9.38
INSTRUM spect
PROBHD 5 mm PAQXI 1H/
PULPROG zg30
TD 65536
SOLVENT CDCl3
NS 32
DS 2
SWH 10330.578 Hz
FIDRES 0.157632 Hz
AQ 3.1719425 sec
RG 256
DW 48.400 usec
DE 6.50 usec
TE 298.2 K
D1 1.00000000 sec
TD0 1
======== CHANNEL f1 ========
NUC1 1H
P1 9.50 usec
PL1 4.00 dB
PL1W 12.10000038 W
SFO1 500.1330885 MHz
F2 - Processing parameters
SI 32768
SF 500.1300000 MHz
WDW EM
SSB 0
LB 0.30 Hz
GB 0
PC 1.00
8.0
7.5
7.0
6.5
6.0
5.5
5.0
4.5
4.0
3.5
3.0
2.5
ppm
1.00
1.03
2.04
1.15
1.05
1.08
1.09
1.14
3.24
2.13

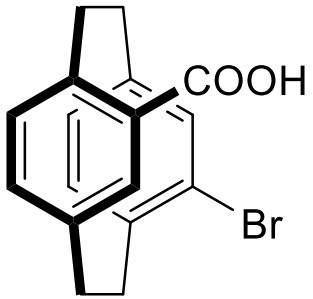

(R_p)-4.7

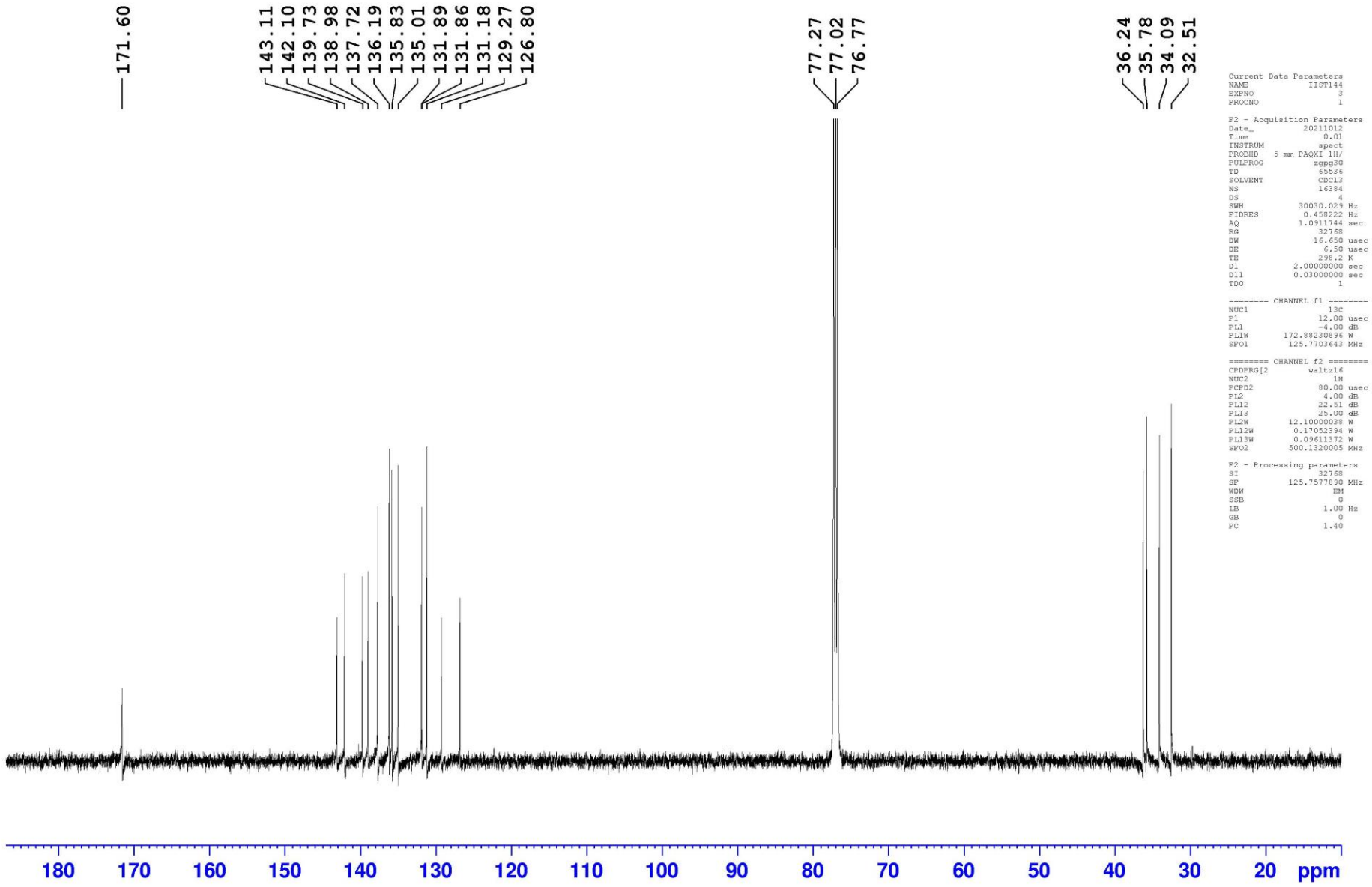

Current Data Parameters
NAME IIST144
EXPNO 3
PROCNO 1

F2 - Acquisition Parameters
Date_ 20211012
Time 0.01
INSTRUM spect
PROBHD 5 mm PAQXI 1H/
PULPROG zgpg30
TD 65536
SOLVENT CDCl3
NS 16384
DS 4
SWH 30030.029 Hz
FIDRES 0.458222 Hz
AQ 1.0911744 sec
RG 32768
DW 16.650 usec
DE 6.50 usec
TE 298.2 K
D1 2.00000000 sec
D11 0.03000000 sec
TD0 1

======== CHANNEL f1 ========
NUC1 13C
P1 12.00 usec
PL1 -4.00 dB
PL1W 172.88230896 W
SFO1 125.7703643 MHz

======== CHANNEL f2 ========
CPDPRG[2 waltz16
NUC2 1H
PCPD2 80.00 usec
PL2 4.00 dB
PL12 22.51 dB
PL13 25.00 dB
PL2W 12.10000038 W
PL12W 0.17052394 W
PL13W 0.09611372 W
SFO2 500.1320005 MHz

F2 - Processing parameters
SI 32768
SF 125.7577890 MHz
WDW EM
SSB 0
LB 1.00 Hz
GB 0
PC 1.40

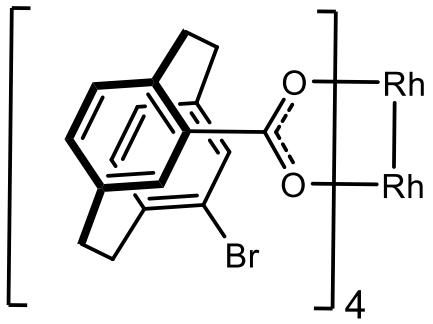

a

```
Current Data Parameters
NAME                  IIST149
EXPNO                       4
PROCNO                      1

F2 - Acquisition Parameters
Date_               20211021
Time                   10.05
INSTRUM                spect
PROBHD   5 mm PAQXI 1H/
PULPROG                zg30
TD                    65536
SOLVENT               CDCl3
NS                       32
DS                        2
SWH               10330.578 Hz
FIDRES             0.157632 Hz
AQ                3.1719425 sec
RG                      256
DW                   48.400 usec
DE                    6.50 usec
TE                   298.2 K
D1              1.00000000 sec
TD0                       1

======== CHANNEL f1 ========
NUC1                     1H
P1                    9.50 usec
PL1                   4.00 dB
PL1W           12.10000038 W
SFO1           500.1330885 MHz

F2 - Processing parameters
SI                    32768
SF             500.1300000 MHz
WDW                      EM
SSB                       0
LB                     0.30 Hz
GB                        0
PC                     1.00
```

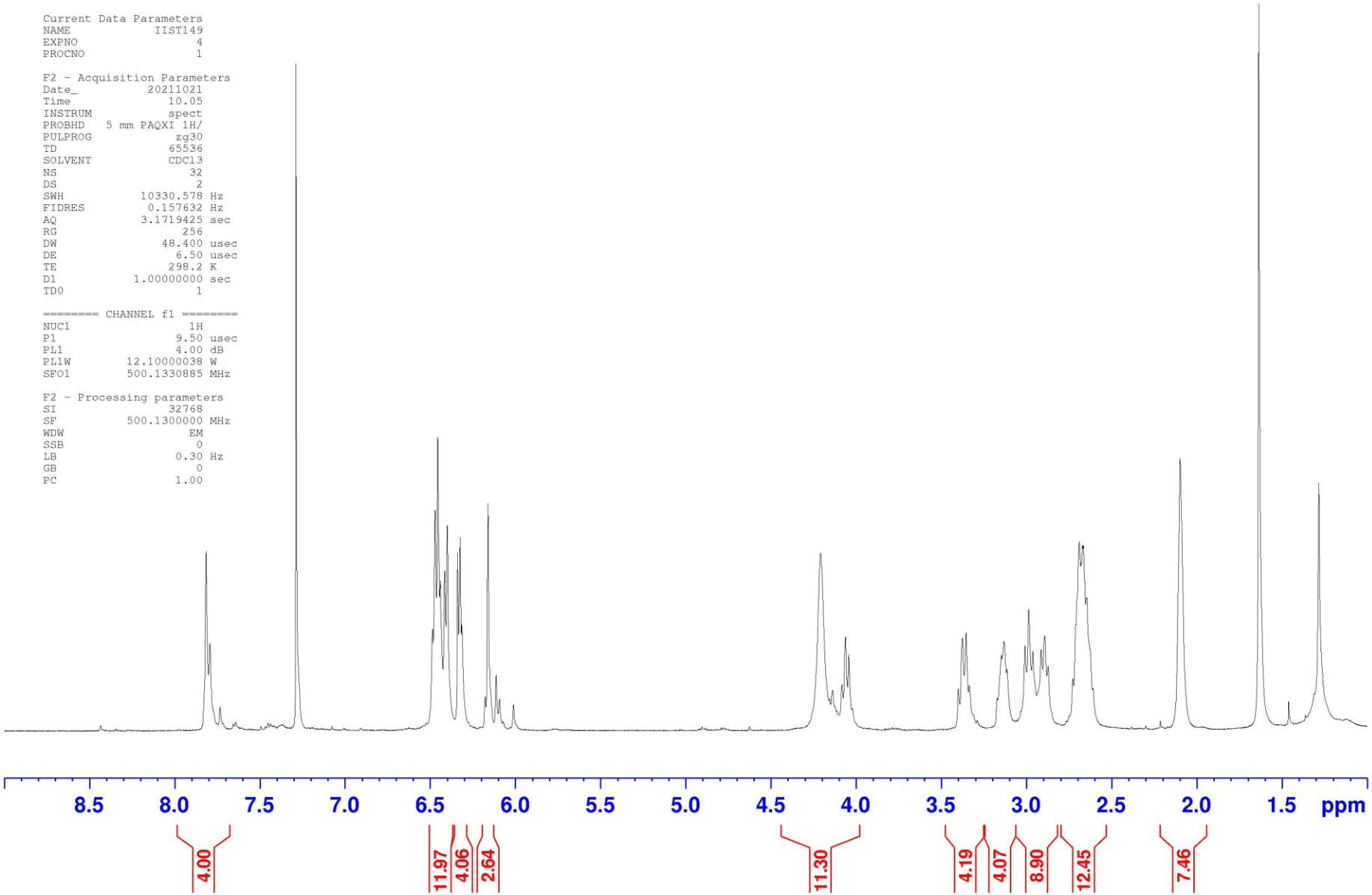

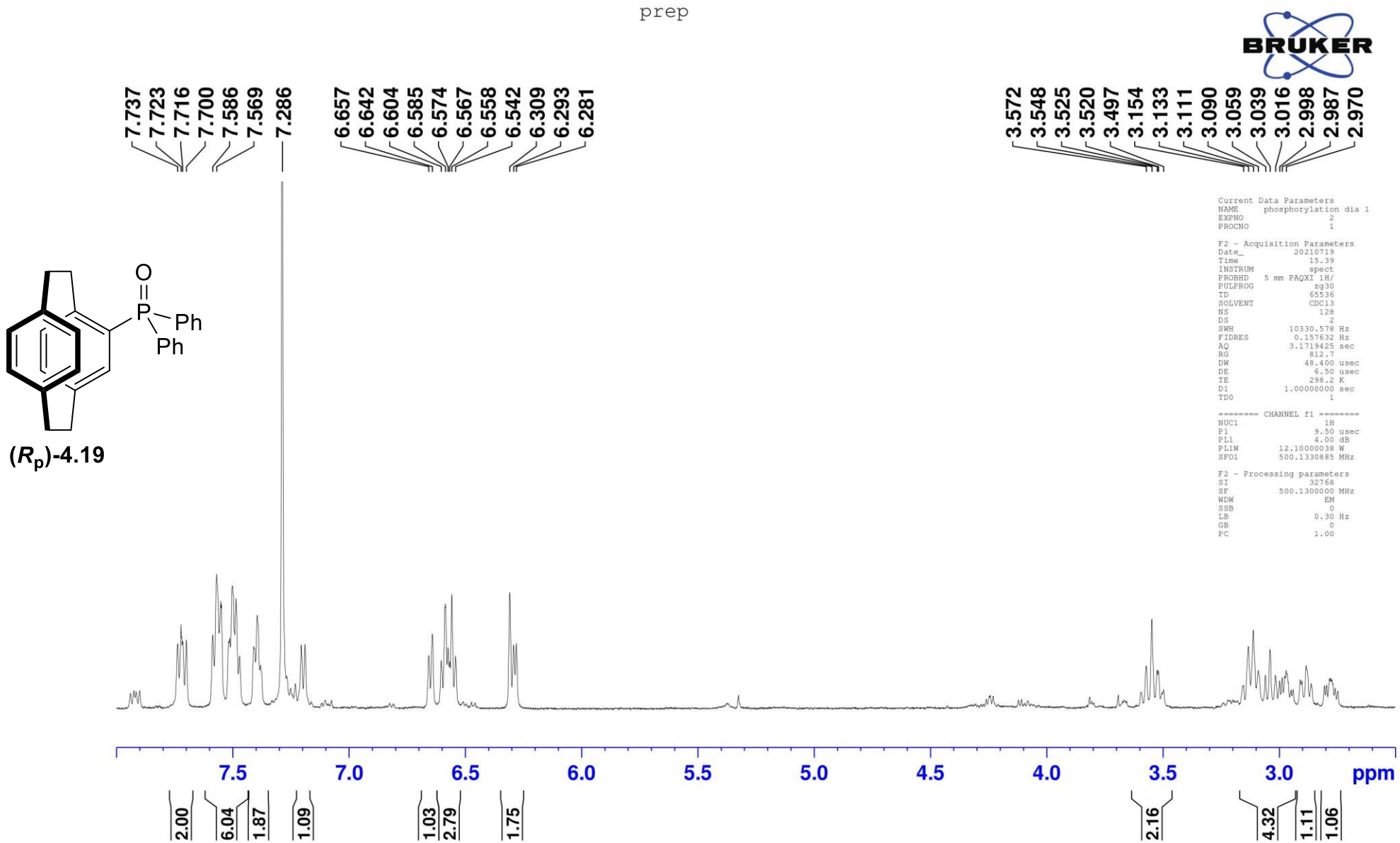
prep
BRUKER
7.737
7.723
7.716
7.700
7.586
7.569
7.286
6.657
6.642
6.604
6.585
6.574
6.567
6.558
6.542
6.309
6.293
6.281
3.572
3.548
3.525
3.520
3.497
3.154
3.133
3.111
3.090
3.059
3.039
3.016
2.998
2.987
2.970
O
P
Ph
Ph
(Rp)-4.19
Current Data Parameters
NAME phosphorylation dia 1
EXPNO 2
PROCNO 1
F2 - Acquisition Parameters
Date_ 20210719
Time 15.39
INSTRUM spect
PROBHD 5 mm PAQXI 1H/
PULPROG zg30
TD 65536
SOLVENT CDCl3
NS 128
DS 2
SWH 10330.578 Hz
FIDRES 0.157632 Hz
AQ 3.1719425 sec
RG 812.7
DW 48.400 usec
DE 6.50 usec
TE 298.2 K
D1 1.00000000 sec
TD0 1
======== CHANNEL f1 ========
NUC1 1H
P1 9.50 usec
PL1 4.00 dB
PL1W 12.10000038 W
SFO1 500.1330885 MHz
F2 - Processing parameters
SI 32768
SF 500.1300000 MHz
WDW EM
SSB 0
LB 0.30 Hz
GB 0
PC 1.00
7.5
7.0
6.5
6.0
5.5
5.0
4.5
4.0
3.5
3.0
ppm
2.00
6.04
1.87
1.09
1.03
2.79
1.75
2.16
4.32
1.11
1.06

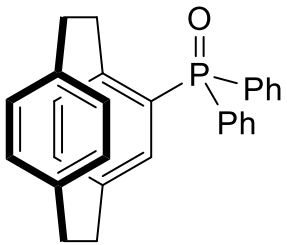

(R_p)-4.19

27.09

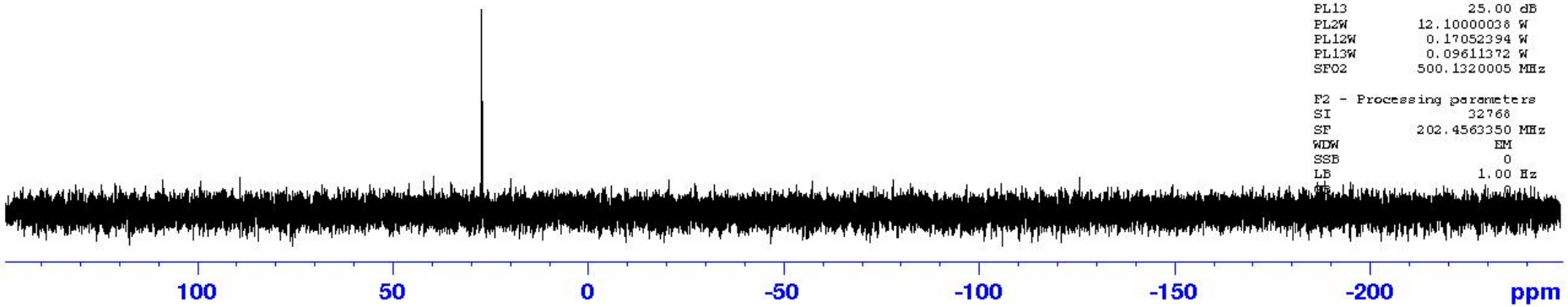


```
Current Data Parameters
NAME      II-ST-124-dia 1
EXPNO                   5
PROCNO                  1

F2 - Acquisition Parameters
Date_           20210622
Time              12.35
INSTRUM           spect
PROBHD   5 mm PAQXI 1H/
PULPROG         zgpg30
TD               65536
SOLVENT          CDCl3
NS                  16
DS                   4
SWH           80645.164 Hz
FIDRES         1.230548 Hz
AQ            0.4063232 sec
RG              20642.5
DW                6.200 usec
DE                6.50 usec
TE              298.2 K
D1           2.00000000 sec
D11          0.03000000 sec
TD0                  1

-------- CHANNEL f1 --------
NUC1                31P
P1                20.00 usec
PL1               -2.40 dB
PL1W       131.39126587 W
SFO1        202.4462121 MHz

-------- CHANNEL f2 --------
CPDPRG[2        waltz16
NUC2                1H
PCPD2             80.00 usec
PL2               4.00 dB
PL12              22.51 dB
PL13              25.00 dB
PL2W       12.10000038 W
PL12W       0.17052394 W
PL13W       0.09611372 W
SFO2        500.1320005 MHz

F2 - Processing parameters
SI                32768
SF          202.4563350 MHz
WDW                EM
SSB                0
LB                1.00 Hz
GB                 0
```

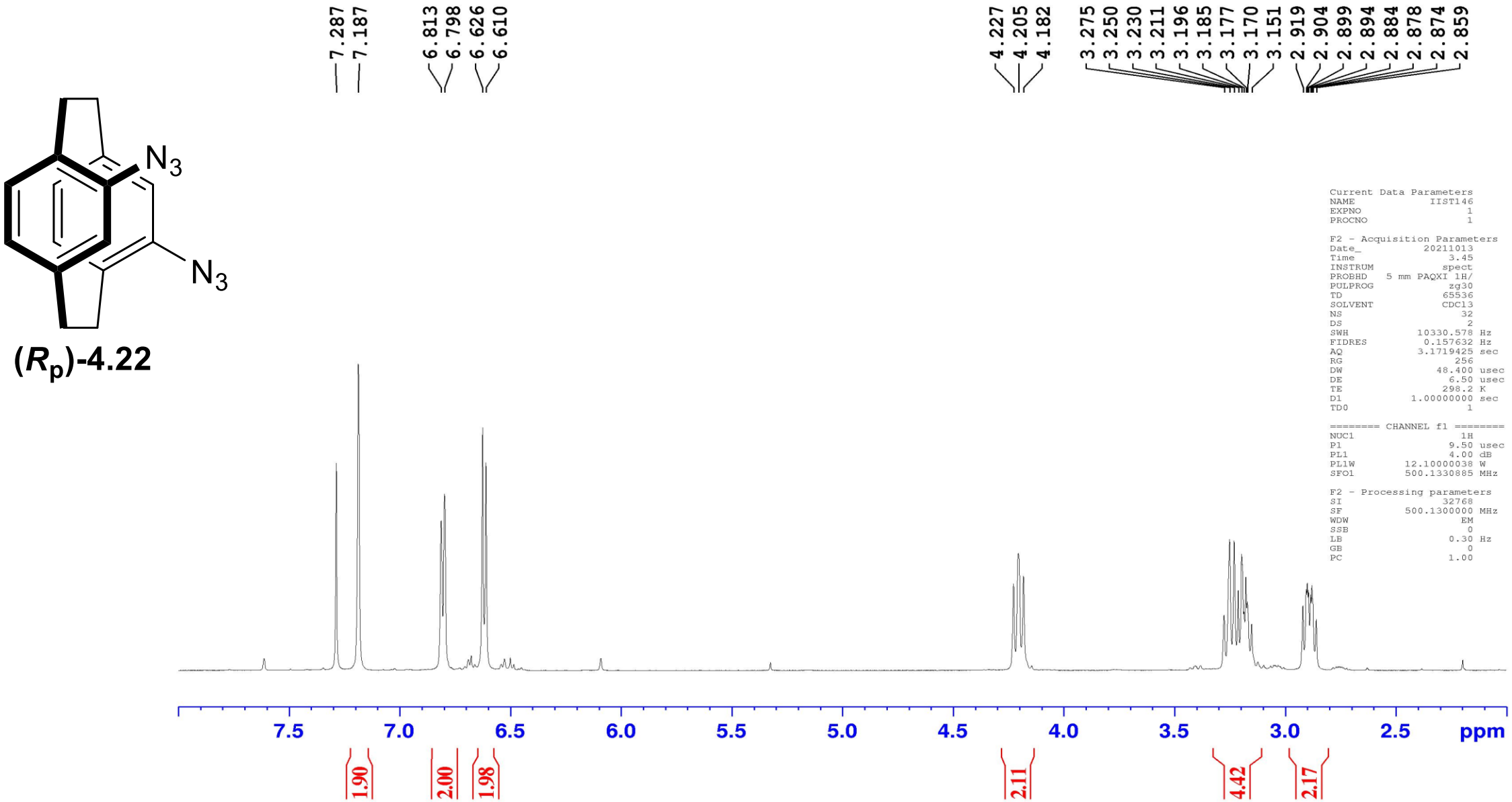
7.287
7.187
6.813
6.798
6.626
6.610
4.227
4.205
4.182
3.275
3.250
3.230
3.211
3.196
3.185
3.177
3.170
3.151
2.919
2.904
2.899
2.894
2.884
2.878
2.874
2.859
N3
N3
(Rp)-4.22
Current Data Parameters
NAME IIST146
EXPNO 1
PROCNO 1
F2 - Acquisition Parameters
Date_ 20211013
Time 3.45
INSTRUM spect
PROBHD 5 mm PAQXI 1H/
PULPROG zg30
TD 65536
SOLVENT CDCl3
NS 32
DS 2
SWH 10330.578 Hz
FIDRES 0.157632 Hz
AQ 3.1719425 sec
RG 256
DW 48.400 usec
DE 6.50 usec
TE 298.2 K
D1 1.00000000 sec
TD0 1
======== CHANNEL f1 ========
NUC1 1H
P1 9.50 usec
PL1 4.00 dB
PL1W 12.10000038 W
SFO1 500.1330885 MHz
F2 - Processing parameters
SI 32768
SF 500.1300000 MHz
WDW EM
SSB 0
LB 0.30 Hz
GB 0
PC 1.00
7.5
7.0
6.5
6.0
5.5
5.0
4.5
4.0
3.5
3.0
2.5
ppm
1.90
2.00
1.98
2.11
4.42
2.17

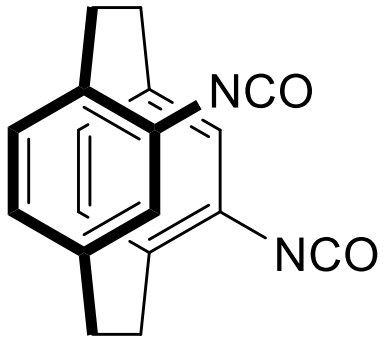
NCO
NCO

(R_p)-4.23

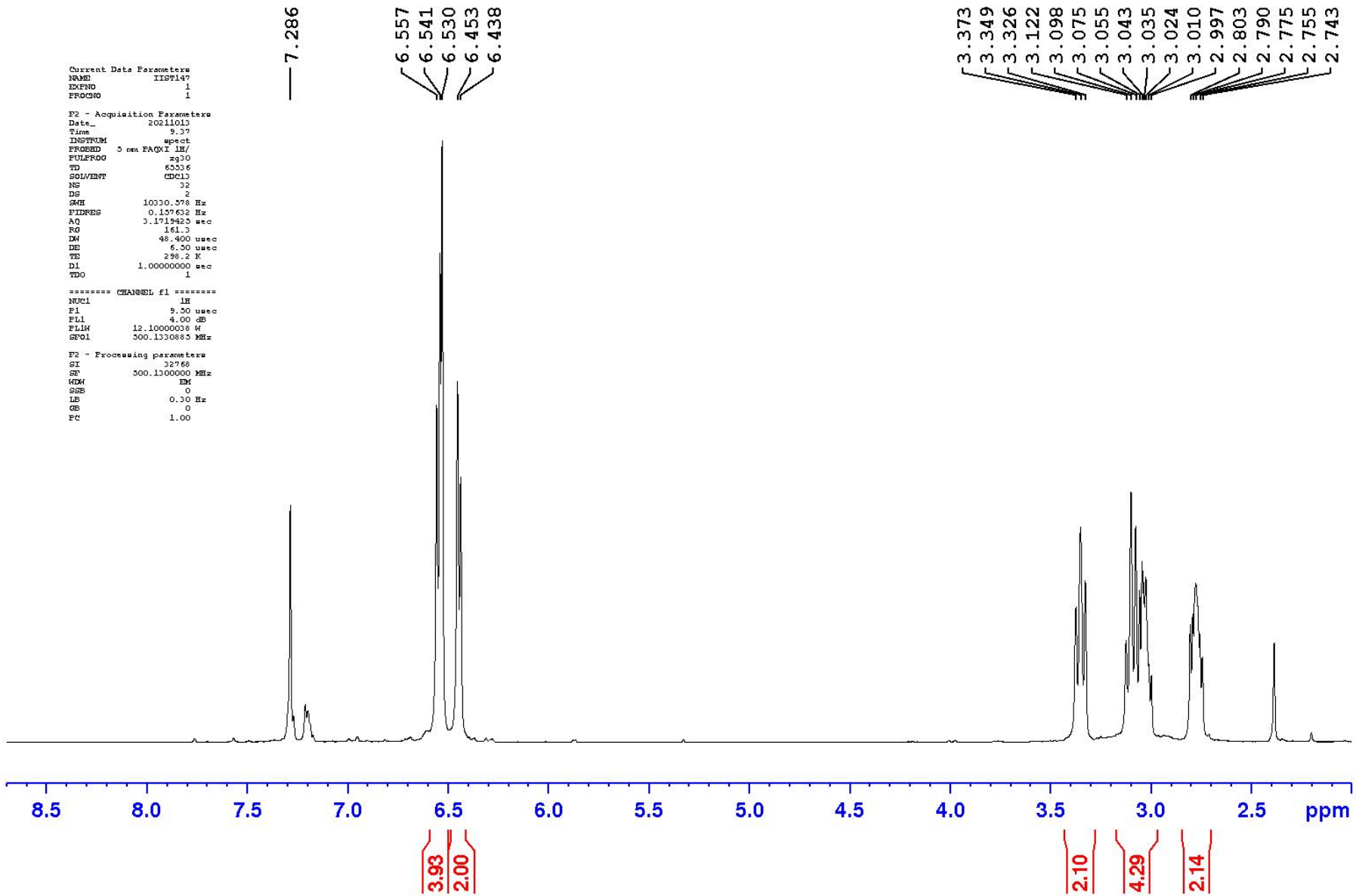
7.286
6.557
6.541
6.530
6.453
6.438
3.373
3.349
3.326
3.122
3.098
3.075
3.055
3.043
3.035
3.024
3.010
2.997
2.803
2.790
2.775
2.755
2.743
Current Data Parameters
NAME IIST147
EXPNO 1
PROCNO 1
F2 - Acquisition Parameters
Date_ 20211013
Time 9.37
INSTRUM spect
PROBHD 5 mm PAQXI 1H/
PULPROG zg30
TD 65536
SOLVENT CDCl3
NS 32
DS 2
SWH 10330.578 Hz
FIDRES 0.157632 Hz
AQ 3.1719423 sec
RG 161.3
DW 48.400 usec
DE 6.50 usec
TE 298.2 K
D1 1.00000000 sec
TD0 1
======== CHANNEL f1 ========
NUC1 1H
P1 9.50 usec
PL1 4.00 dB
PL1W 12.10000038 W
SFO1 300.1330885 MHz
F2 - Processing parameters
SI 32768
SF 300.1300000 MHz
WDW EM
SSB 0
LB 0.30 Hz
GB 0
PC 1.00
8.5
8.0
7.5
7.0
6.5
6.0
5.5
5.0
4.5
4.0
3.5
3.0
2.5
ppm
3.93
2.00
2.10
4.29
2.14

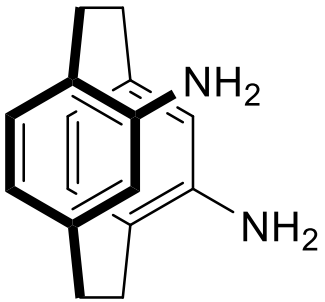

(R_p)-4.24

diamine1 fraction

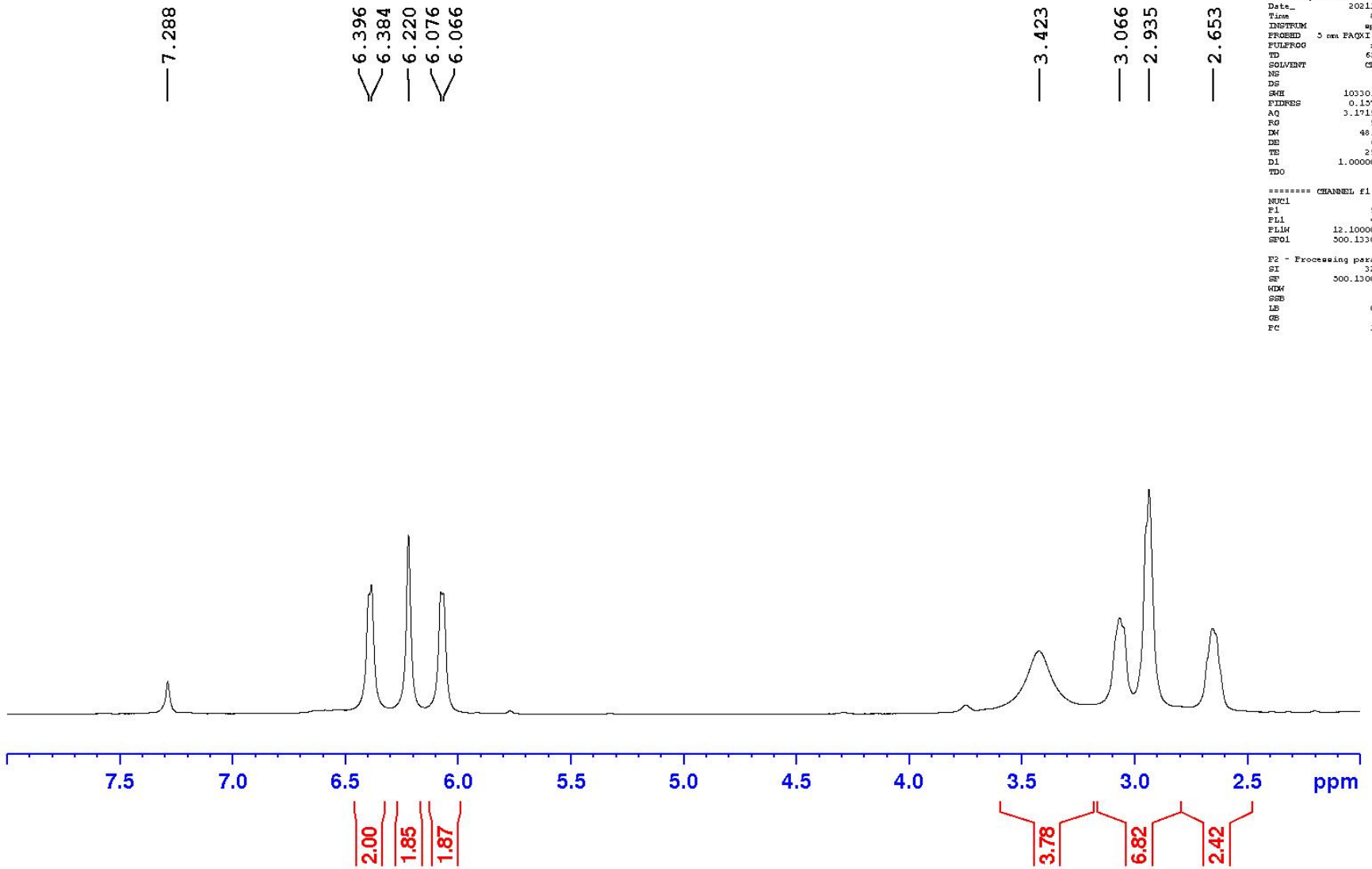

Current Data Parameters
NAME IIST148
EXPNO 4
PROCNO 1

F2 - Acquisition Parameters
Date_ 20211017
Time 8.30
INSTRUM spect
PROBHD 5 mm PABBI 1H/
PULPROG zg30
TD 65536
SOLVENT CDCl3
NS 64
DS 2
SWH 10330.578 Hz
FIDRES 0.157632 Hz
AQ 3.1719425 sec
RG 90.5
DW 48.400 usec
DE 6.50 usec
TE 298.2 K
D1 1.00000000 sec
TD0 1

======== CHANNEL f1 ========
NUC1 1H
P1 9.50 usec
PL1 4.00 dB
PL1W 12.10000038 W
SFO1 500.1330885 MHz

F2 - Processing parameters
SI 32768
SF 500.1300000 MHz
WDW EM
SSB 0
LB 0.30 Hz
GB 0
PC 1.00

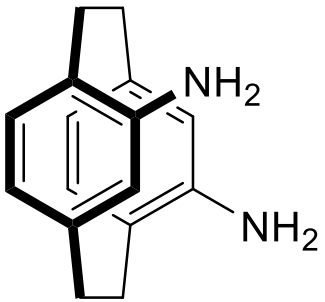
NH2
NH2

(R_p)-4.24

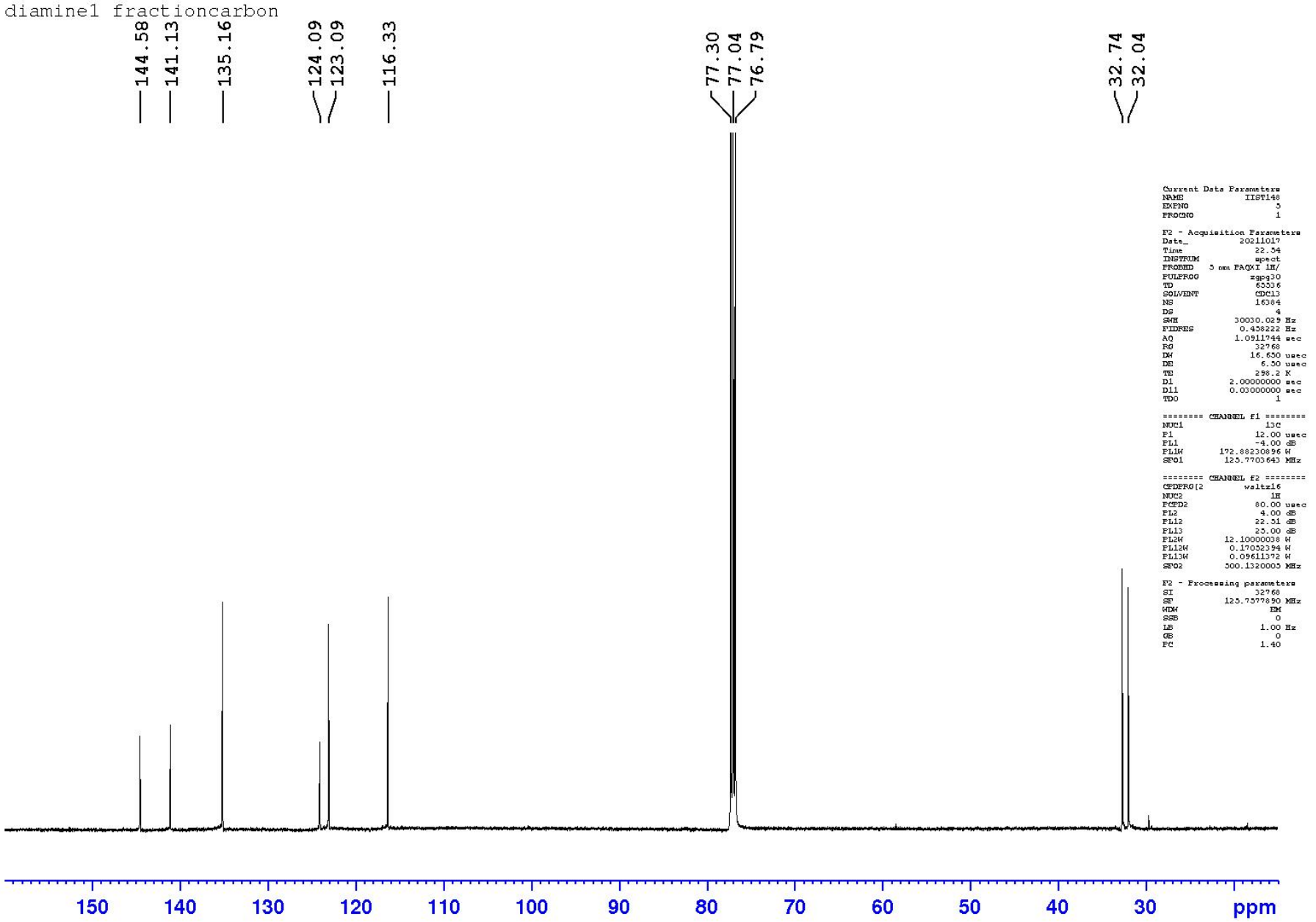
diamine1 fractioncarbon
144.58
141.13
135.16
124.09
123.09
116.33
77.30
77.04
76.79
32.74
32.04
150
140
130
120
110
100
90
80
70
60
50
40
30
ppm

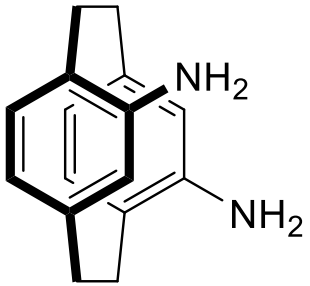
NH2
NH2

(R_p)-4.24

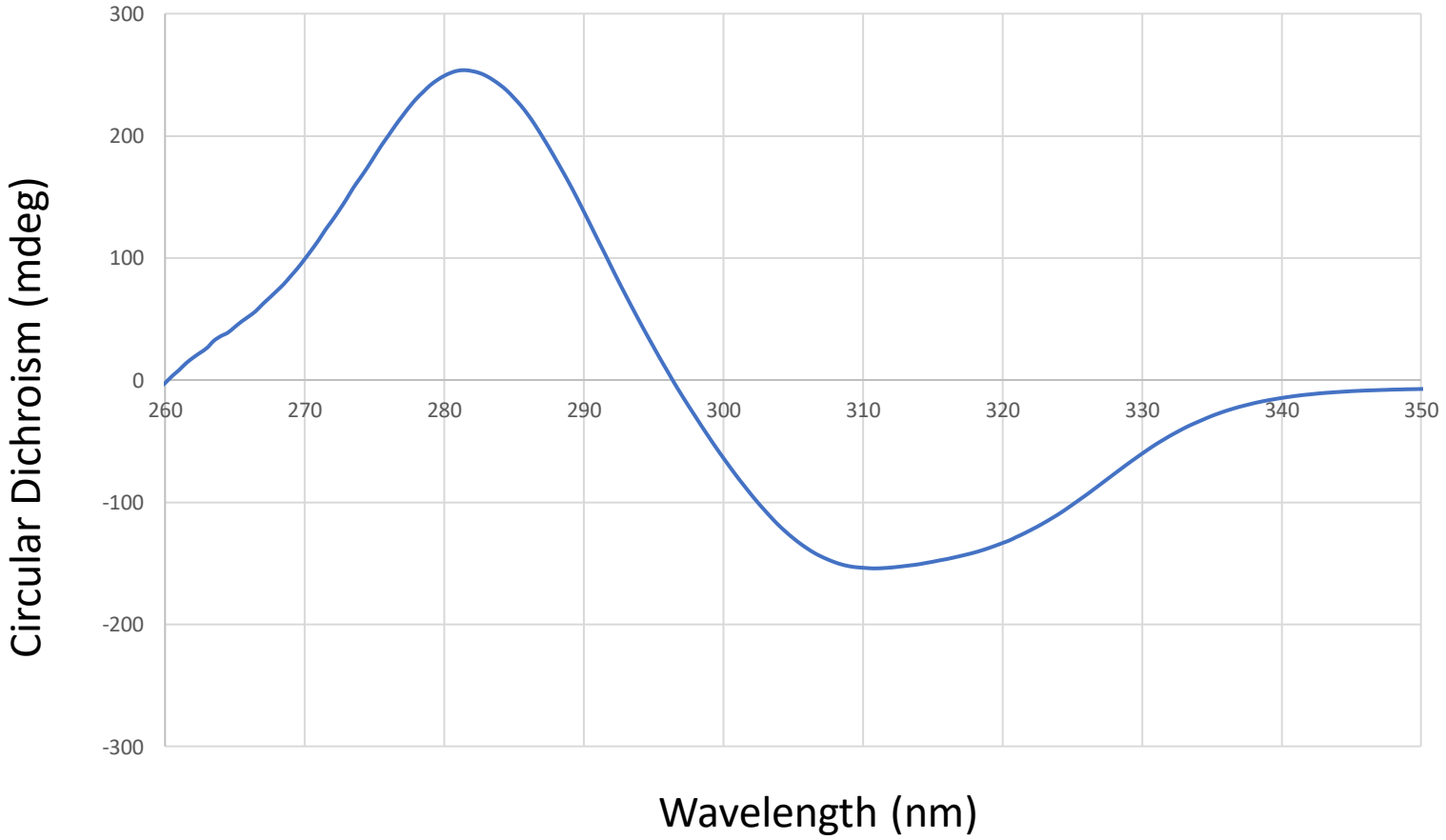
Circular Dichroism (mdeg)
300
200
100
0
-100
-200
-300
260
270
280
290
300
310
320
330
340
350
Wavelength (nm)

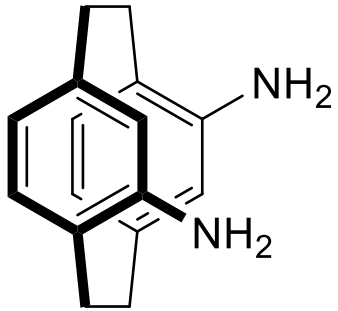
NH2
NH2

(S_p)-4.24

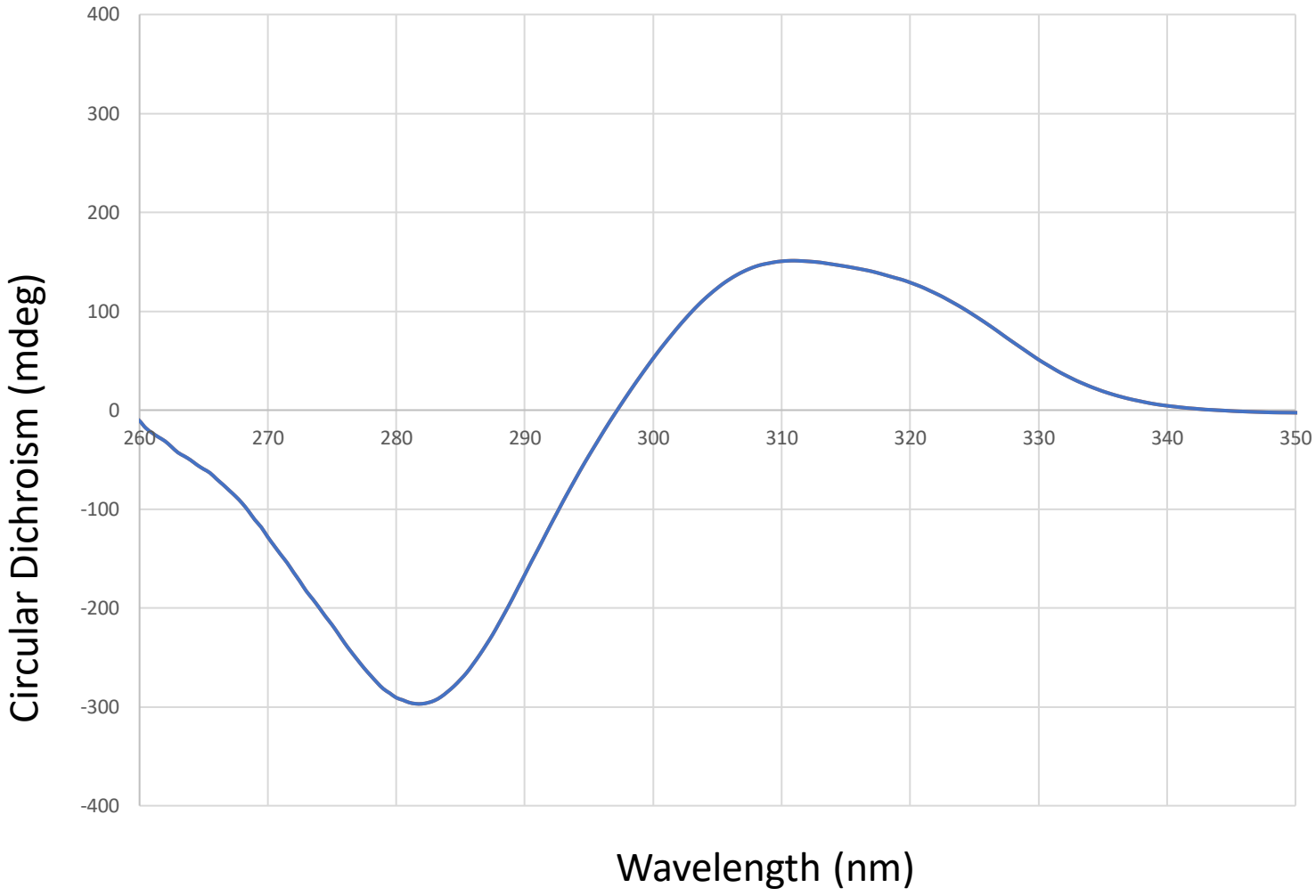
400
300
200
100
0
-100
-200
-300
-400
260
270
280
290
300
310
320
330
340
350
Circular Dichroism (mdeg)
Wavelength (nm)

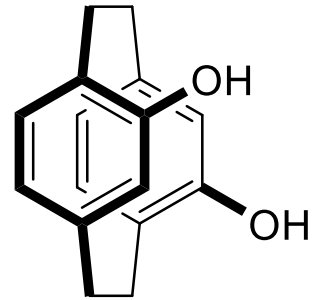
OH
OH

(S_p)-4.25

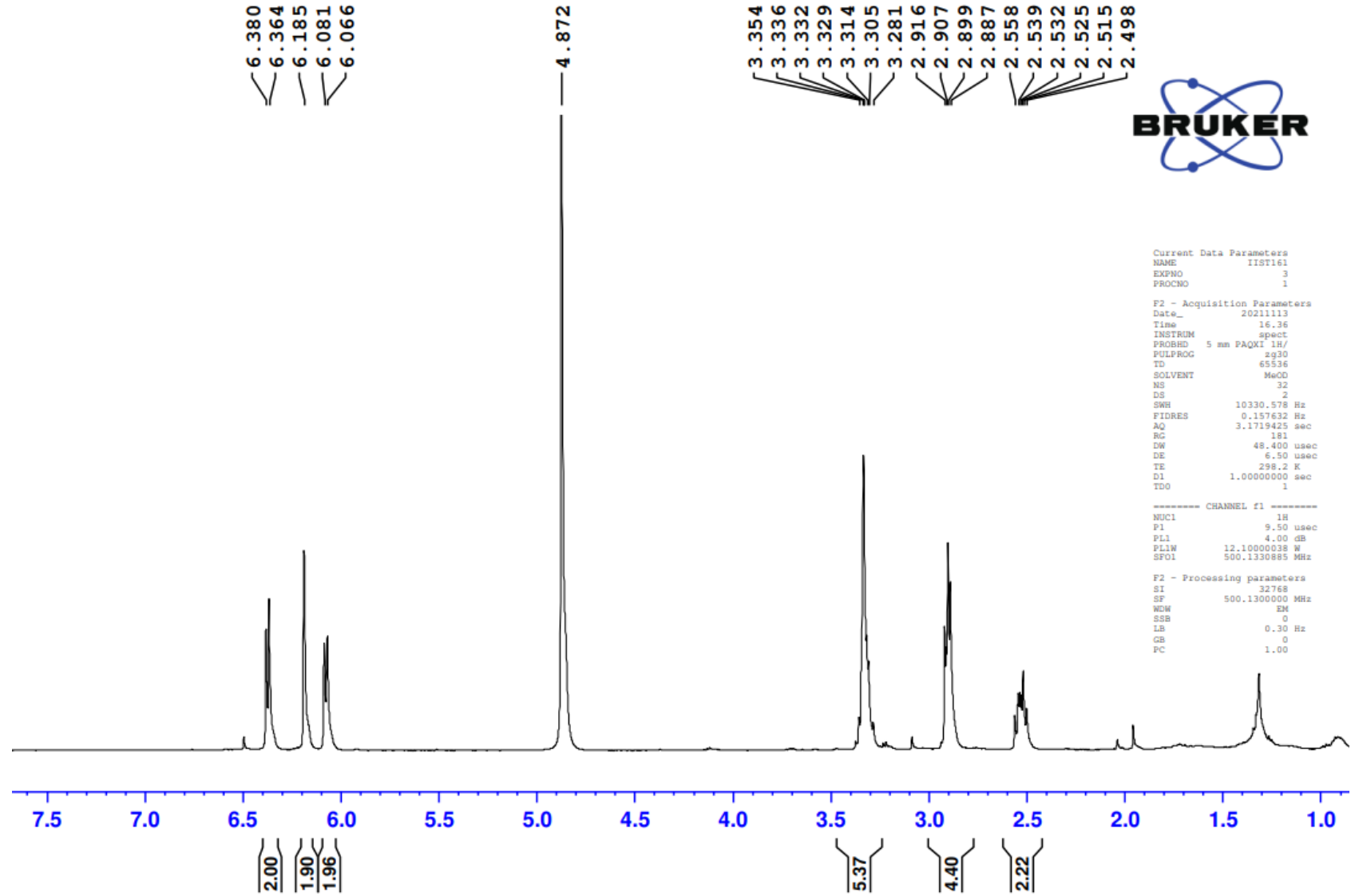
6.380
6.364
6.185
6.081
6.066
4.872
3.354
3.336
3.332
3.329
3.314
3.305
3.281
2.916
2.907
2.899
2.887
2.558
2.539
2.532
2.525
2.515
2.498
BRUKER
Current Data Parameters
NAME IIST161
EXPNO 3
PROCNO 1
F2 - Acquisition Parameters
Date_ 20211113
Time 16.36
INSTRUM spect
PROBHD 5 mm PAQXI 1H/
PULPROG zg30
TD 65536
SOLVENT MeOD
NS 32
DS 2
SWH 10330.578 Hz
FIDRES 0.157632 Hz
AQ 3.1719425 sec
RG 181
DW 48.400 usec
DE 6.50 usec
TE 298.2 K
D1 1.00000000 sec
TD0 1
======== CHANNEL f1 ========
NUC1 1H
P1 9.50 usec
PL1 4.00 dB
PL1W 12.10000038 W
SFO1 500.1330885 MHz
F2 - Processing parameters
SI 32768
SF 500.1300000 MHz
WDW EM
SSB 0
LB 0.30 Hz
GB 0
PC 1.00
7.5
7.0
6.5
6.0
5.5
5.0
4.5
4.0
3.5
3.0
2.5
2.0
1.5
1.0
2.00
1.90
1.96
5.37
4.40
2.22

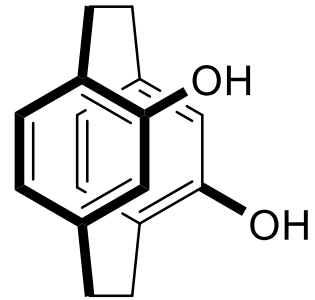
OH
OH

(S_p)-4.25

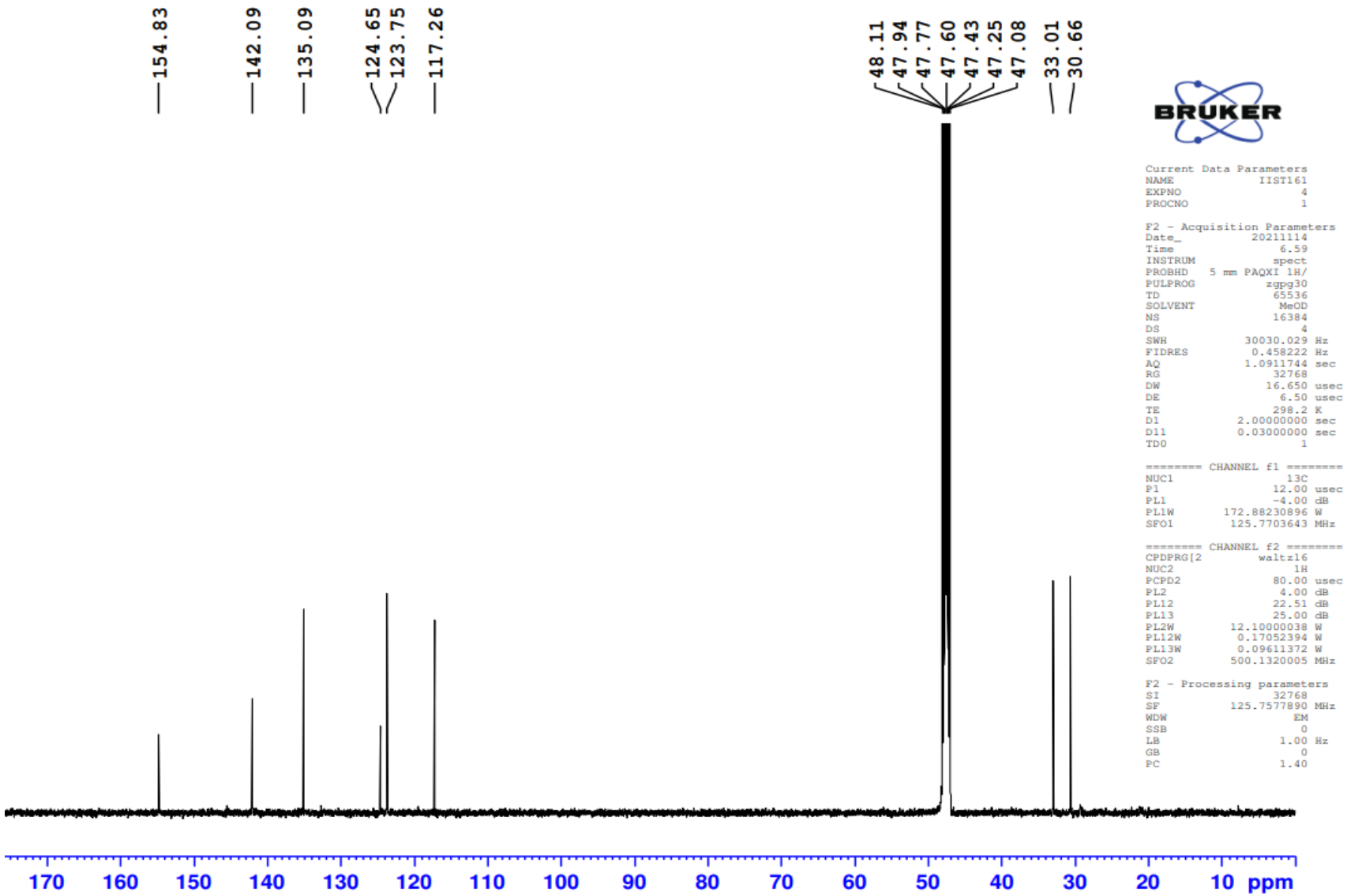
154.83
142.09
135.09
124.65
123.75
117.26
48.11
47.94
47.77
47.60
47.43
47.25
47.08
33.01
30.66
BRUKER
Current Data Parameters
NAME IIST161
EXPNO 4
PROCNO 1
F2 - Acquisition Parameters
Date_ 20211114
Time 6.59
INSTRUM spect
PROBHD 5 mm PAQXI 1H/
PULPROG zgpg30
TD 65536
SOLVENT MeOD
NS 16384
DS 4
SWH 30030.029 Hz
FIDRES 0.458222 Hz
AQ 1.0911744 sec
RG 32768
DW 16.650 usec
DE 6.50 usec
TE 298.2 K
D1 2.00000000 sec
D11 0.03000000 sec
TD0 1
======== CHANNEL f1 ========
NUC1 13C
P1 12.00 usec
PL1 -4.00 dB
PL1W 172.88230896 W
SFO1 125.7703643 MHz
======== CHANNEL f2 ========
CPDPRG[2 waltz16
NUC2 1H
PCPD2 80.00 usec
PL2 4.00 dB
PL12 22.51 dB
PL13 25.00 dB
PL2W 12.10000038 W
PL12W 0.17052394 W
PL13W 0.09611372 W
SFO2 500.1320005 MHz
F2 - Processing parameters
SI 32768
SF 125.7577890 MHz
WDW EM
SSB 0
LB 1.00 Hz
GB 0
PC 1.40
170 160 150 140 130 120 110 100 90 80 70 60 50 40 30 20 10 ppm

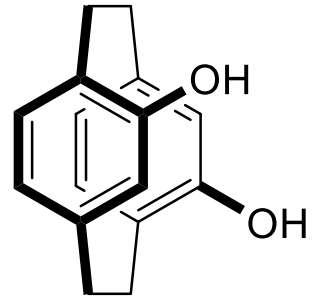
OH
OH

(S_p)-4.25

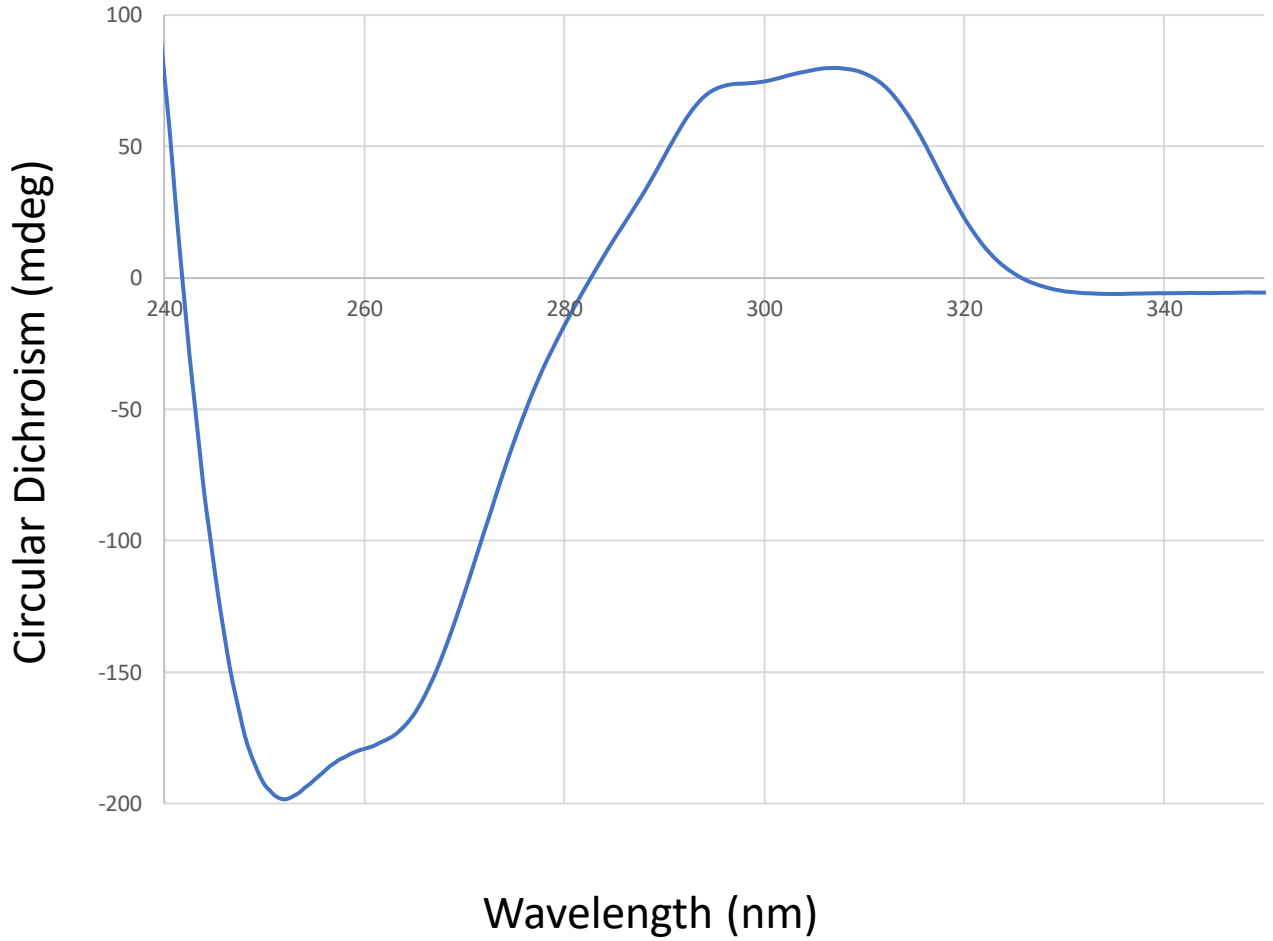
100
50
0
-50
-100
-150
-200
240
260
280
300
320
340
Circular Dichroism (mdeg)
Wavelength (nm)

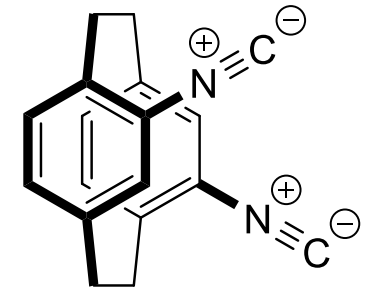

(R_p)-4.34

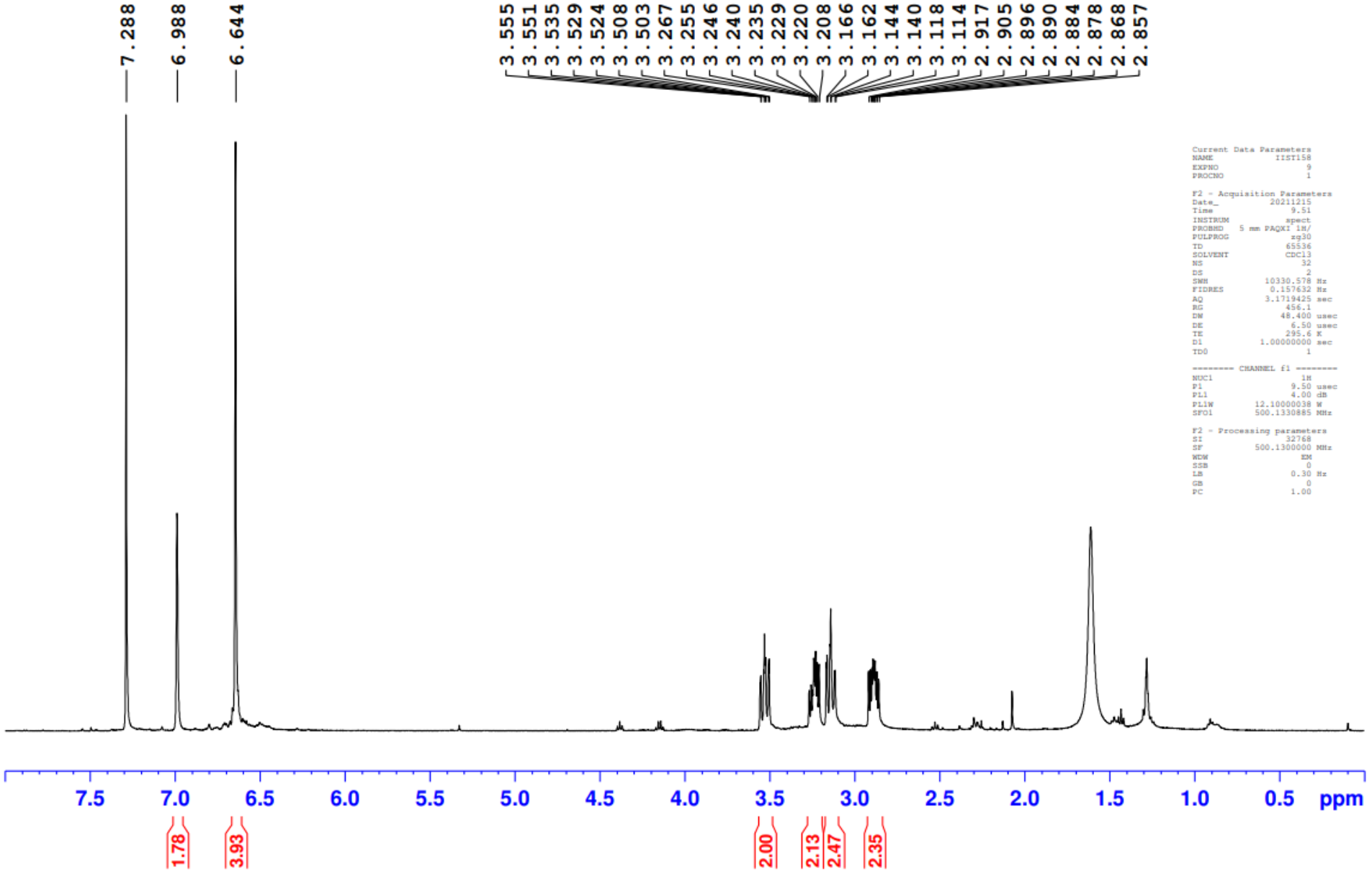
7.288
6.988
6.644
3.555
3.551
3.535
3.529
3.524
3.508
3.503
3.267
3.255
3.246
3.240
3.235
3.229
3.220
3.208
3.166
3.162
3.144
3.140
3.118
3.114
2.917
2.905
2.896
2.890
2.884
2.878
2.868
2.857
Current Data Parameters
NAME IIST158
EXPNO 9
PROCNO 1
F2 - Acquisition Parameters
Date_ 20211215
Time 9.51
INSTRUM spect
PROBHD 5 mm PAQXI 1H/
PULPROG zg30
TD 65536
SOLVENT CDCl3
NS 32
DS 2
SWH 10330.578 Hz
FIDRES 0.157632 Hz
AQ 3.1719425 sec
RG 456.1
DW 48.400 usec
DE 6.50 usec
TE 295.6 K
D1 1.00000000 sec
TD0 1
======== CHANNEL f1 ========
NUC1 1H
P1 9.50 usec
PL1 4.00 dB
PL1W 12.10000038 W
SFO1 500.1330885 MHz
F2 - Processing parameters
SI 32768
SF 500.1300000 MHz
WDW EM
SSB 0
LB 0.30 Hz
GB 0
PC 1.00
7.5
7.0
6.5
6.0
5.5
5.0
4.5
4.0
3.5
3.0
2.5
2.0
1.5
1.0
0.5
ppm
1.78
3.93
2.00
2.13
2.47
2.35

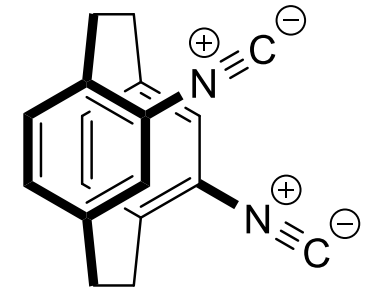

(R_p)-4.34

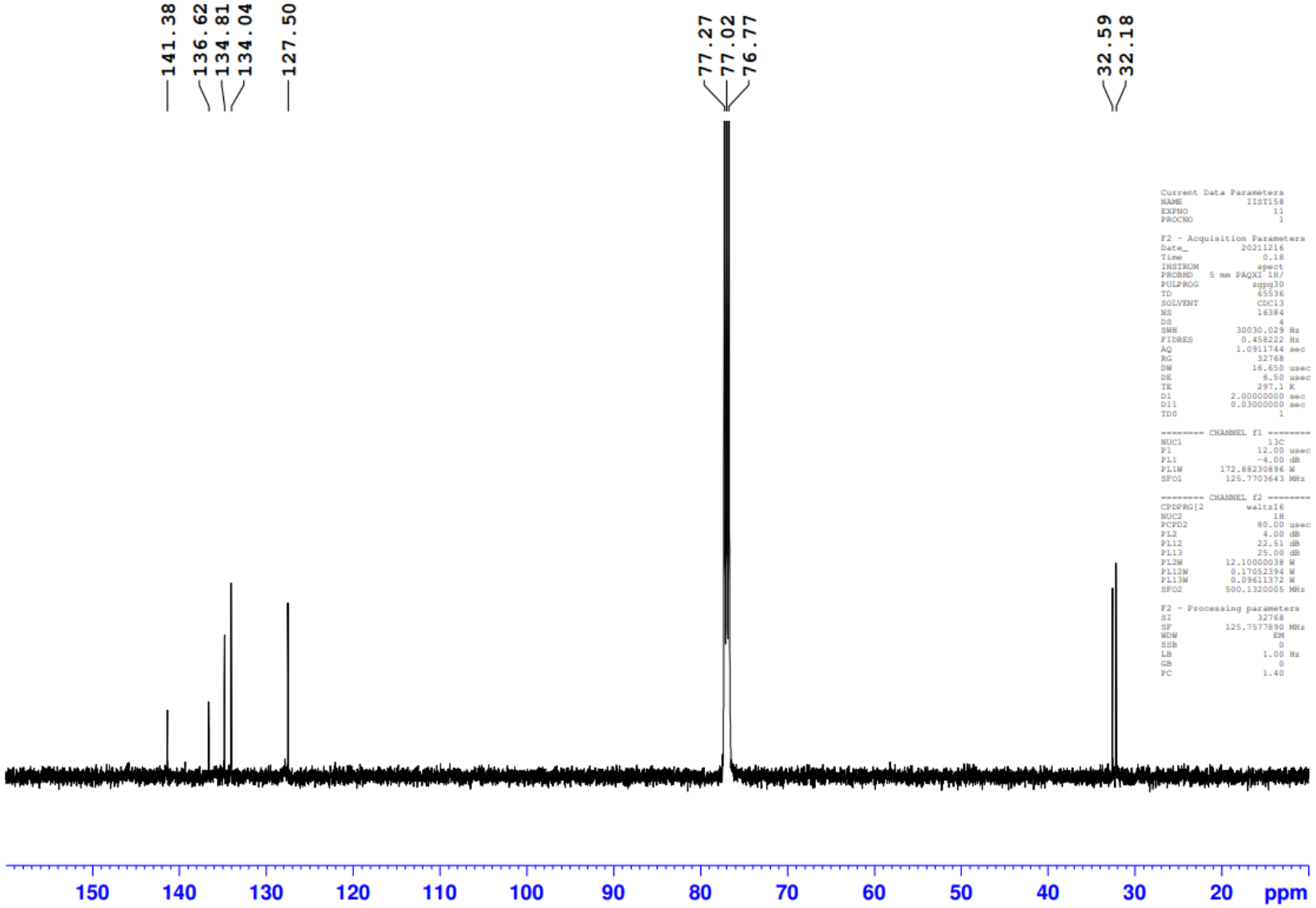
141.38
136.62
134.81
134.04
127.50
77.27
77.02
76.77
32.59
32.18
150
140
130
120
110
100
90
80
70
60
50
40
30
20
ppm

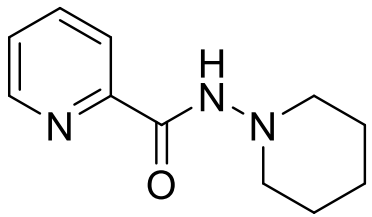

5.56

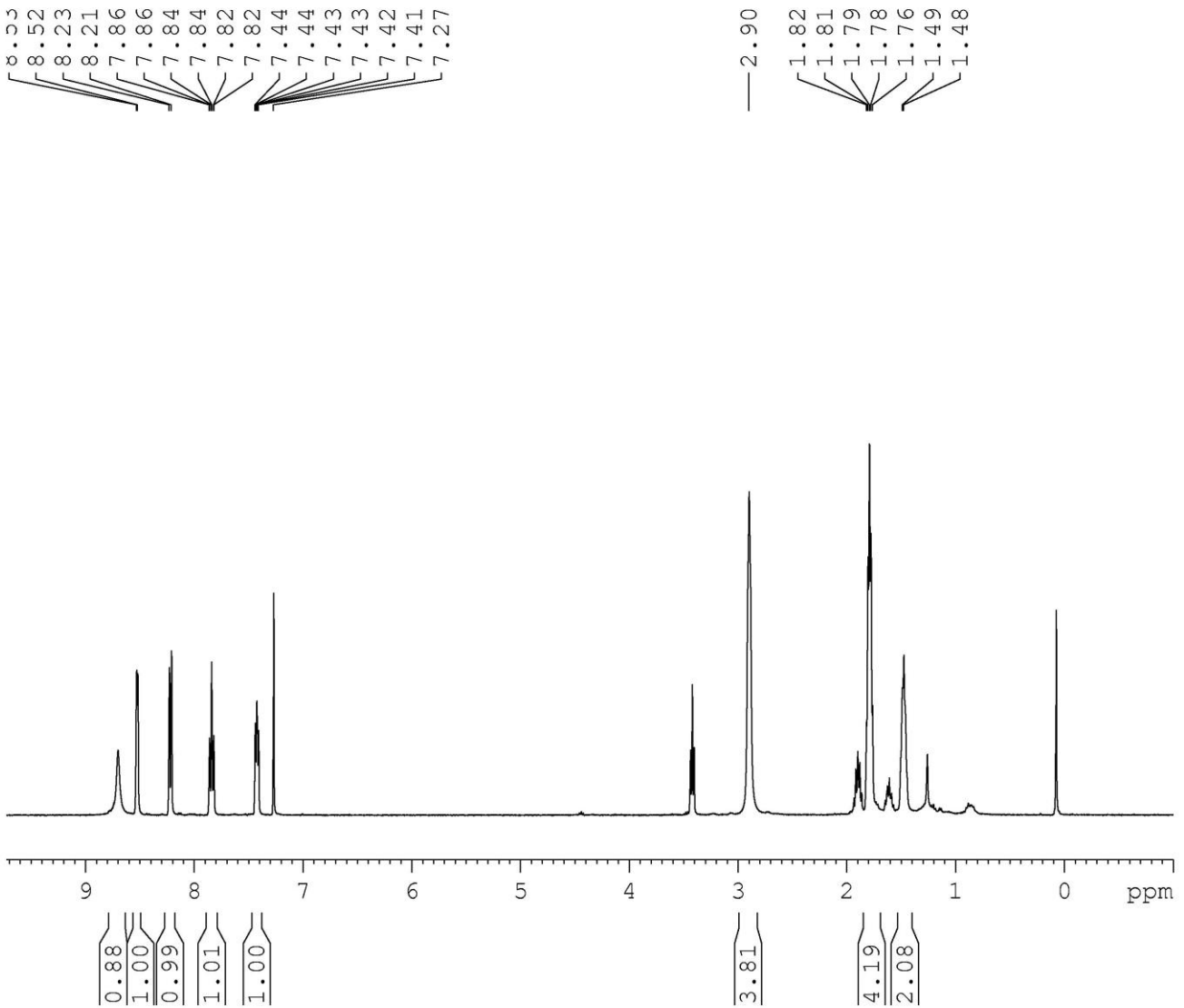


```
Current Data Parameters
NAME                  I-ST-31
EXPNO                       1
PROCNO                      1

F2 - Acquisition Parameters
Date_              20190207
Time                    9.33
INSTRUM                spect
PROBHD    5 mm Multinucl
PULPROG                 zg30
TD                     65536
SOLVENT                CDCl3
NS                        32
DS                         2
SWH                 8278.146 Hz
FIDRES              0.126314 Hz
AQ                3.9583745 sec
RG                     812.7
DW                    60.400 usec
DE                     6.00 usec
TE                     300.0 K
D1                1.00000000 sec
TD0                        1

======== CHANNEL f1 ========
NUC1                      1H
P1                     10.00 usec
PL1                     3.80 dB
SFO1             400.1324710 MHz

F2 - Processing parameters
SI                     32768
SF               400.1300000 MHz
WDW                       EM
SSB          0
LB                     0.30 Hz
GB           0
PC                     1.00
```

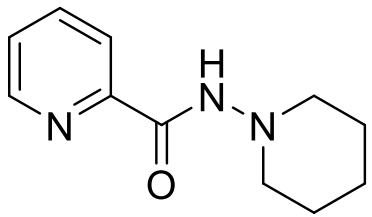

5.56

C13 - 1,5-dibromopentane withe hydrazide

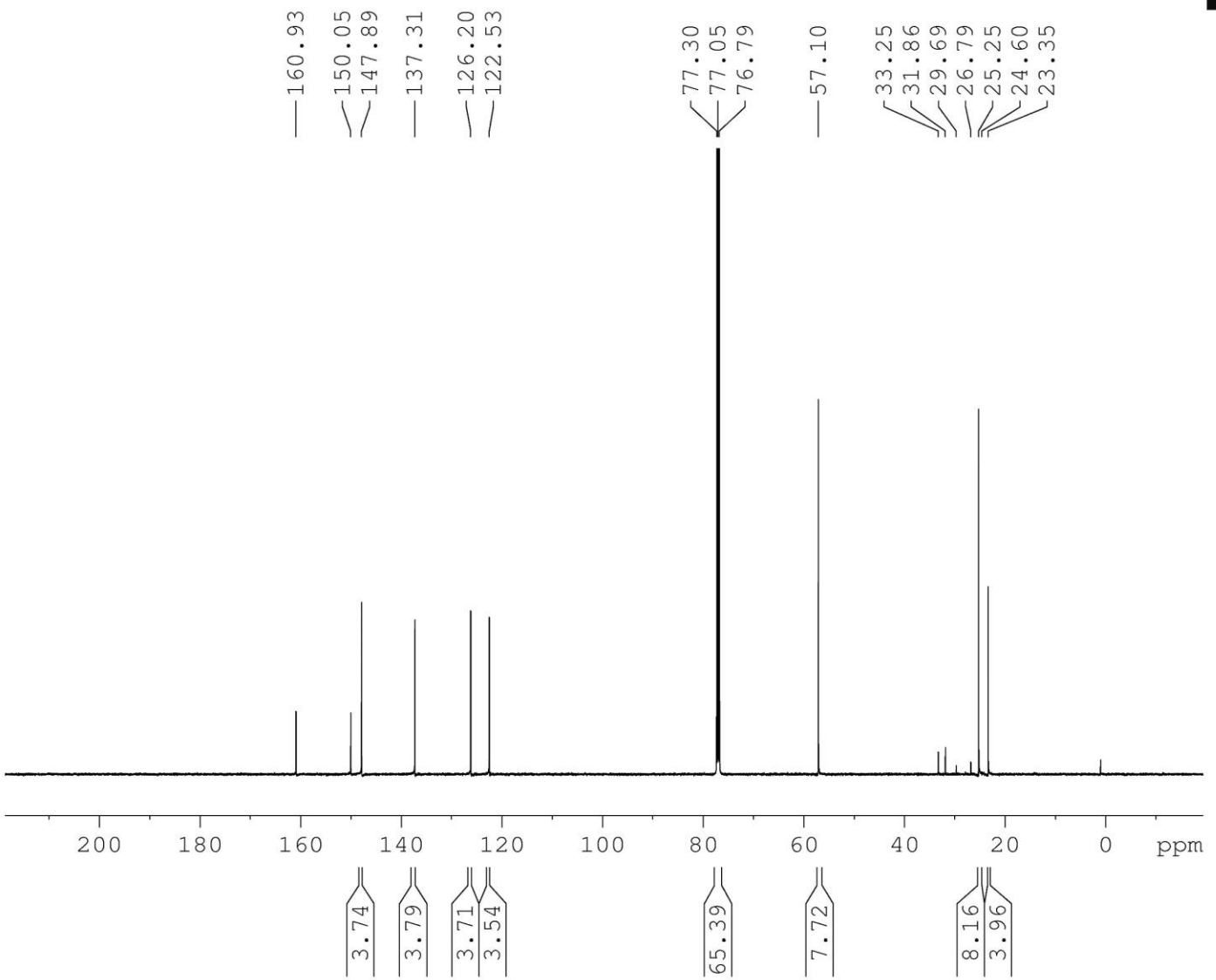


```
Current Data Parameters
NAME                  I-ST-31
EXPNO                       2
PROCNO                      1

F2 - Acquisition Parameter
Date_                20190216
Time                     7.57
INSTRUM                 spect
PROBHD    5 mm PAQXI 1H/
PULPROG                zgpg30
TD                      65536
SOLVENT                 CDCl3
NS                      16384
DS                          4
SWH                30030.029 Hz
FIDRES             0.458222 Hz
AQ                 1.0911744 se
RG                      32768
DW                    16.650 us
DE                     6.50 us
TE                     298.2 K
D1                2.00000000 se
D11               0.03000000 se
TD0                         1

======== CHANNEL f1 ======
NUC1                      13C
P1                      12.00 us
PL1                     -4.00 dB
PL1W            172.88230896 W
SFO1             125.7703643 MH

======== CHANNEL f2 ======
CPDPRG[2               waltz16
NUC2                       1H
PCPD2                   80.00 us
PL2                      4.00 dB
PL12                    22.51 dB
PL13                    25.00 dB
PL2W            12.10000038 W
PL12W            0.17052394 W
PL13W            0.09611372 W
SFO2            500.1320005 MH

F2 - Processing parameters
SI                      32768
SF                125.7577890 MH
WDW                        EM
SSB          0
LB                      1.00 Hz
GB           0
PC                      1.40
```

glyoxylic acid and 1-aminopiperidine

Crude NMR

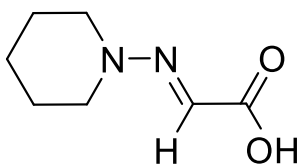

5.58

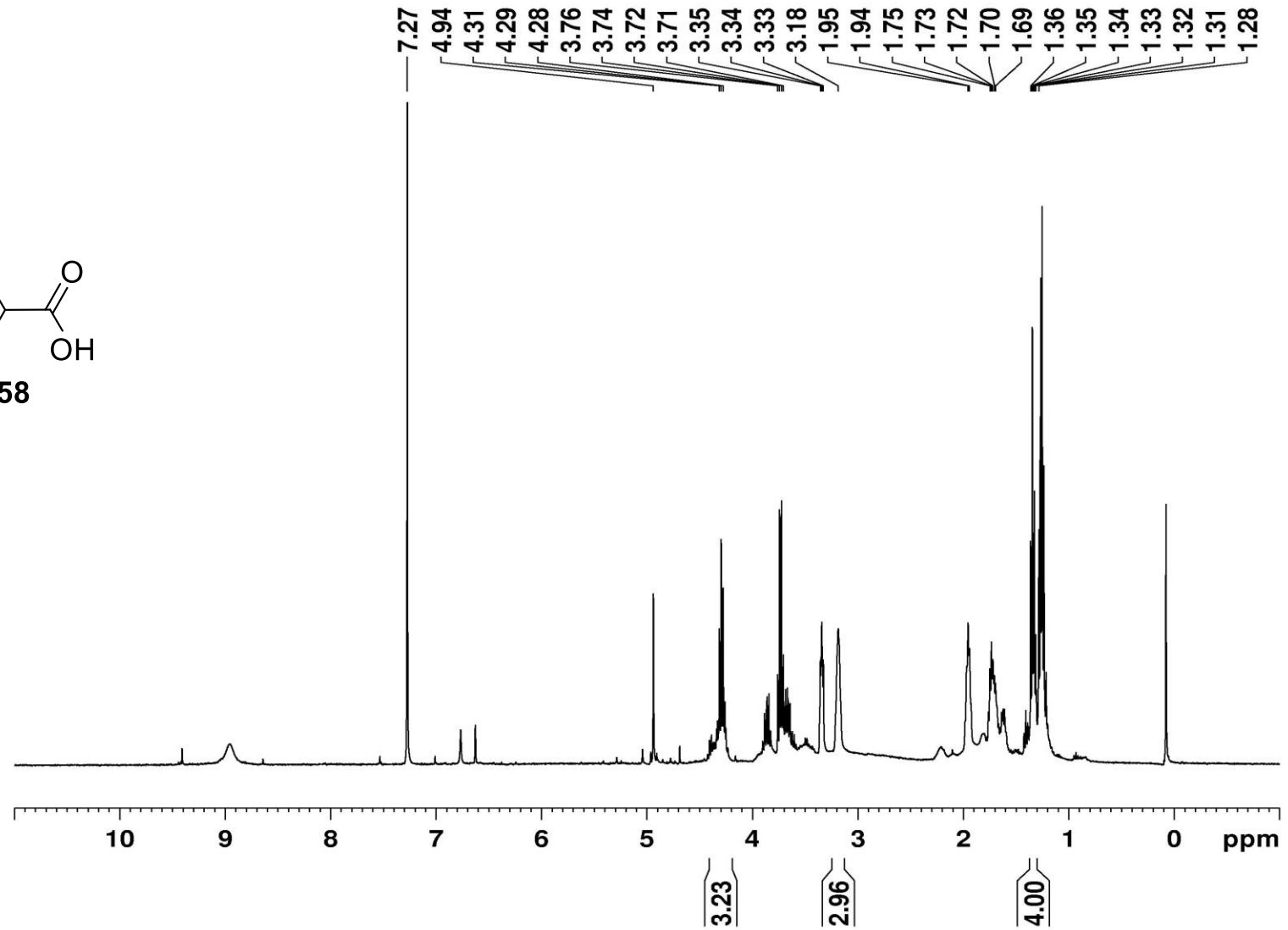


```
Current Data Paramete
NAME                 I-ST-
EXPNO
PROCNO

F2 - Acquisition Para
Date_              201902
Time                 15.
INSTRUM               spe
PROBHD    5 mm Multinu
PULPROG                zg
TD                   655
SOLVENT              CDC
NS                     1
DS                     2
SWH               8278.1
FIDRES            0.1263
AQ                3.9583
RG                     5
DW                60.4
DE                 6.
TE                   300
D1             1.000000
TD0                    1

======== CHANNEL f1 ==
NUC1                   1
P1                  10.
PL1                  3.
SFO1          400.13247

F2 - Processing param
SI                   327
SF            400.13000
WDW                    1
SSB        0
LB                  0.
GB         0
PC                  1.
```

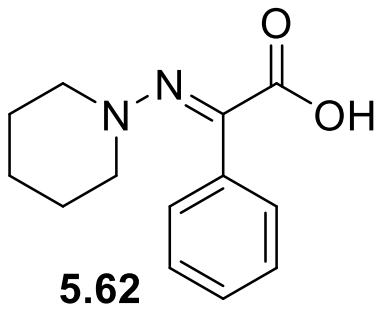

5.62

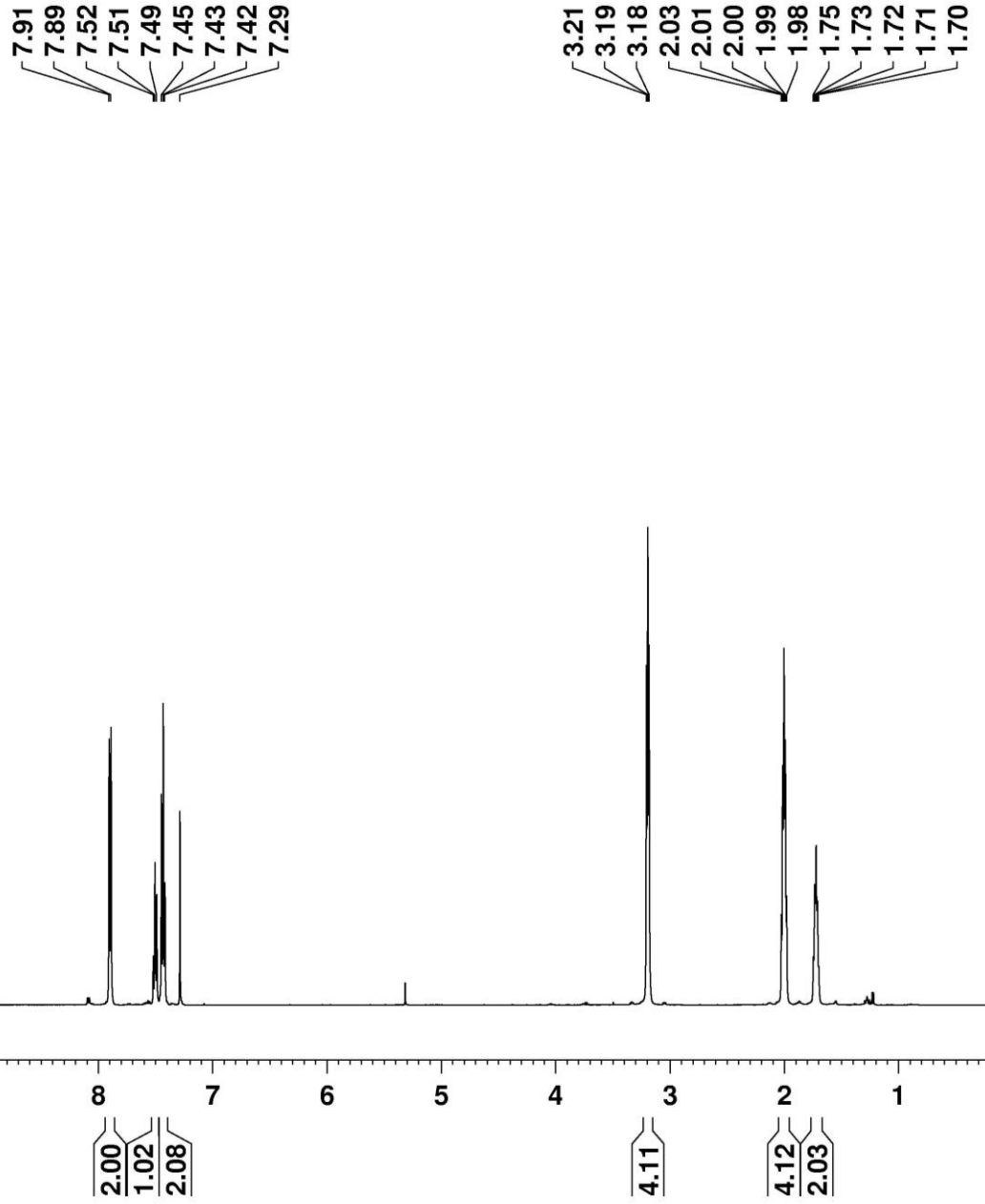


```
Current Data Parameters
NAME                  I-ST-70
EXPNO                       1
PROCNO                      1

F2 - Acquisition Paramete
Date_                20190401
Time                    15.02
INSTRUM                 spect
PROBHD   5 mm PAQXI 1H/
PULPROG                 zg30
TD                     65536
SOLVENT                CDCl3
NS                        16
DS                         2
SWH                10330.578 H
FIDRES              0.157632 H
AQ                  3.1719425 s
RG                        114
DW                     48.400 u
DE                      6.50 u
TE                     300.0 K
D1                 1.00000000 s
TD0                         1

======== CHANNEL f1 =====
NUC1                       1H
P1                       9.50 u
PL1                      4.00 d
PL1W            12.10000038 W
SFO1            500.1330885 M

F2 - Processing parameter
SI                      32768
SF              500.1300000 M
WDW                        EM
SSB          0
LB                       0.30 H
GB           0
PC                       1.00
```

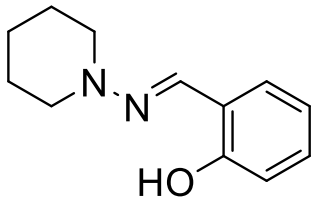

5.63

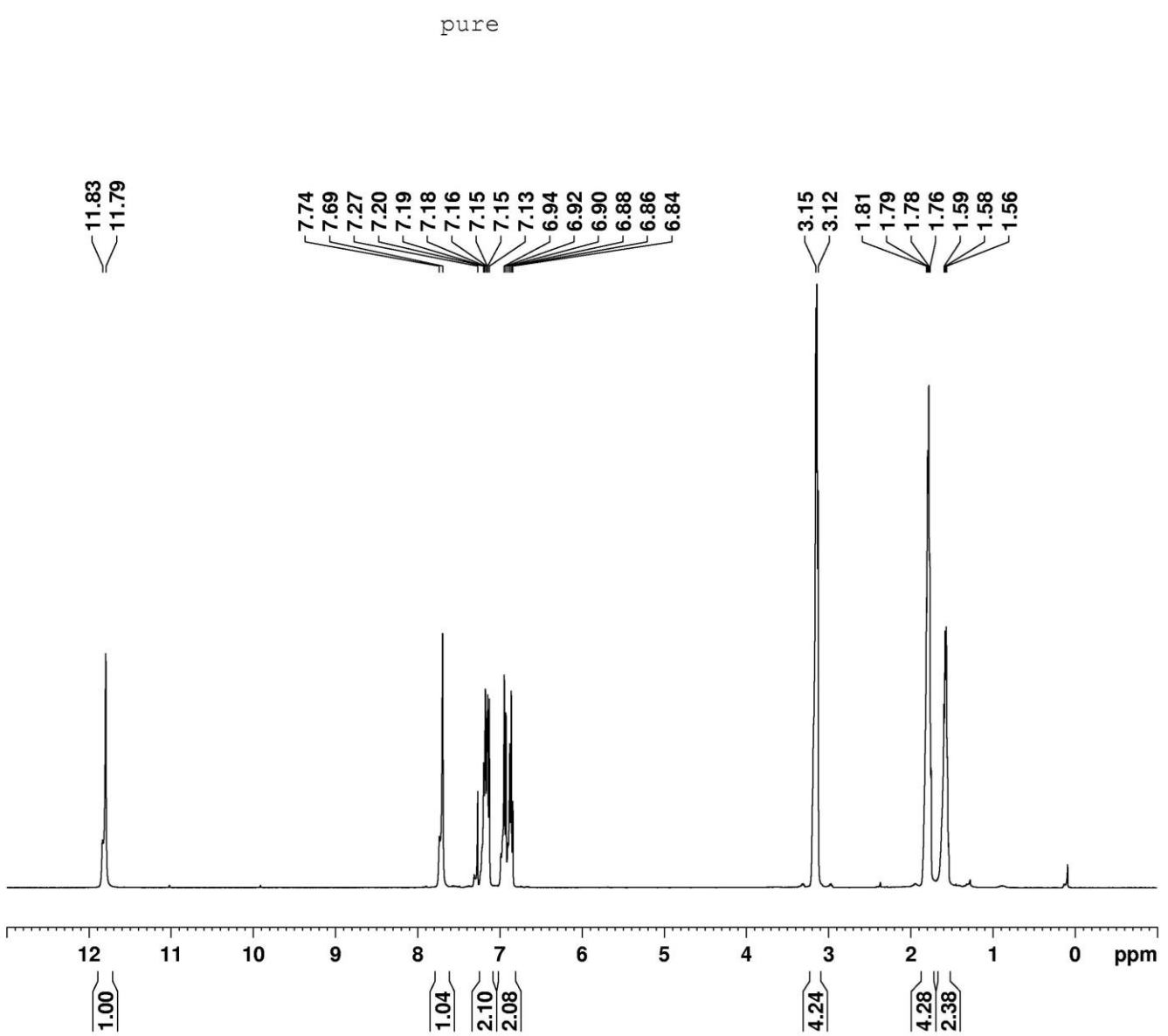

```
Current Data Parame
NAME            I-ST-
EXPNO
PROCNO

F2 - Acquisition Pa
Date_             201
Time
INSTRUM              s
PROBHD    5 mm Multi
PULPROG
TD                   6
SOLVENT              C
NS
DS
SWH               827
FIDRES            0.1
AQ                3.95
RG
DW                  6C
DE
TE                   3
D1             1.000C
TD0

======== CHANNEL f1
NUC1
P1                   1
PL1
SFO1          400.13

F2 - Processing par
SI                   3
SF            400.13C
WDW
SSB       0
LB
GB        0
PC
```

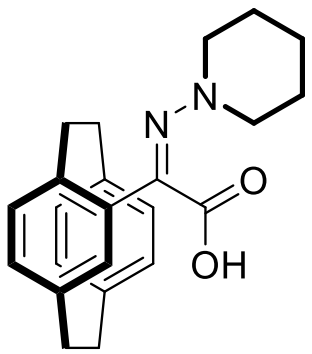

5.68

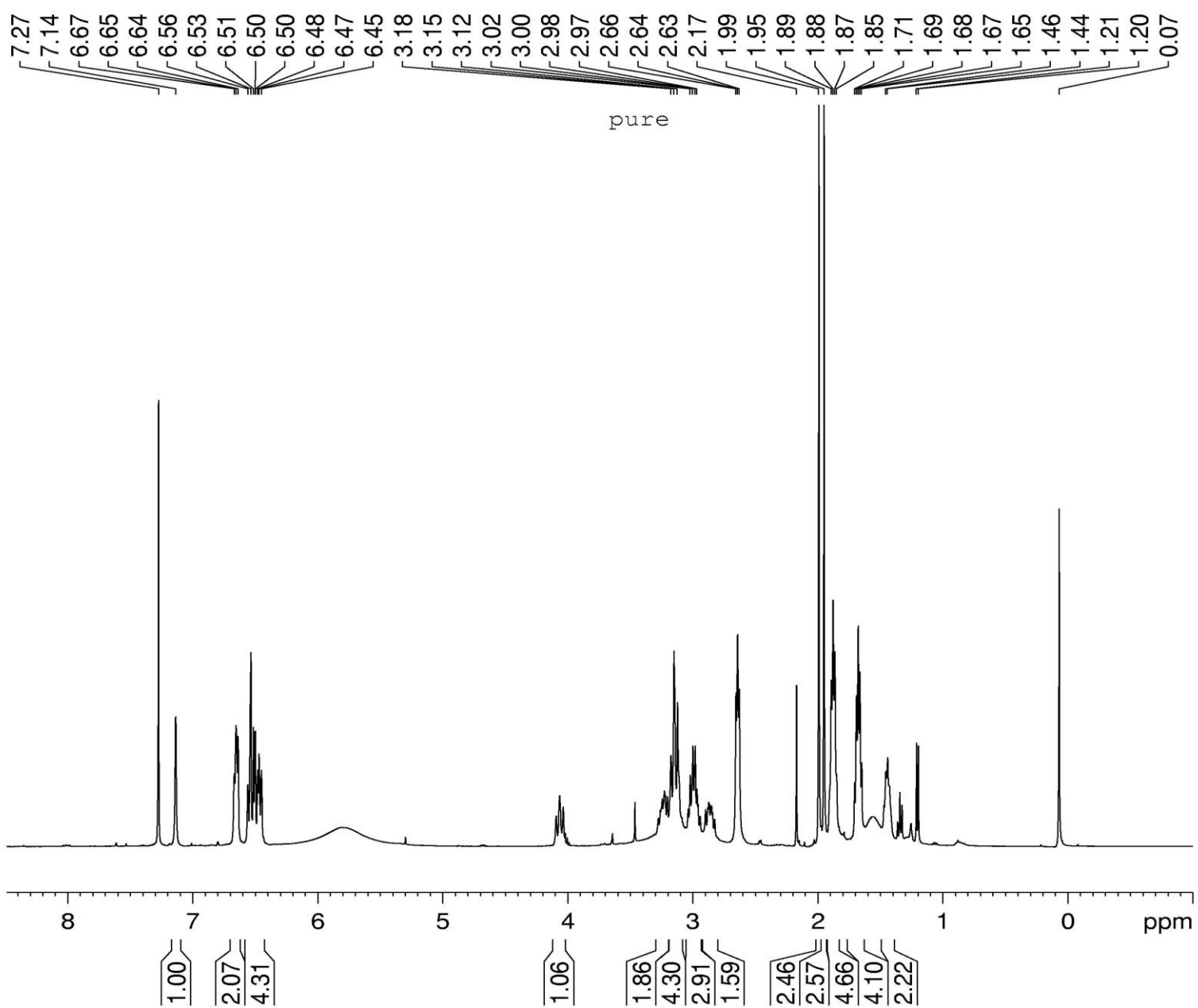


```
Current Data Parameters
NAME                  I-ST-88p
EXPNO                        1
PROCNO                       1

F2 - Acquisition Parameters
Date_                 20190504
Time                     13.34
INSTRUM                  spect
PROBHD    5 mm Multinucl
PULPROG                  zg30
TD                      65536
SOLVENT                 CDCl3
NS                         32
DS                          2
SWH                  8278.146 Hz
FIDRES               0.126314 Hz
AQ                   3.9583745 sec
RG                        80.6
DW                      60.400 use
DE                       6.00 use
TE                      300.0 K
D1                1.00000000 sec
TD0                          1

======== CHANNEL f1 ========
NUC1                        1H
P1                       10.00 use
PL1                       3.80 dB
SFO1             400.1324710 MHz

F2 - Processing parameters
SI                       32768
SF               400.1300000 MHz
WDW                         EM
SSB          0
LB                       0.30 Hz
GB           0
PC                       1.00
```

Pure

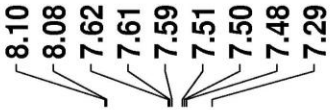

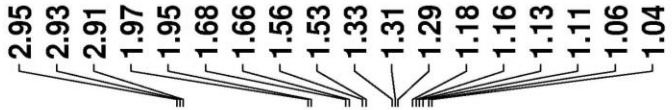

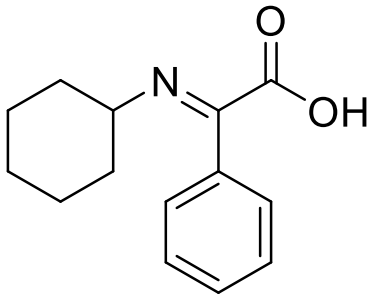

5.74

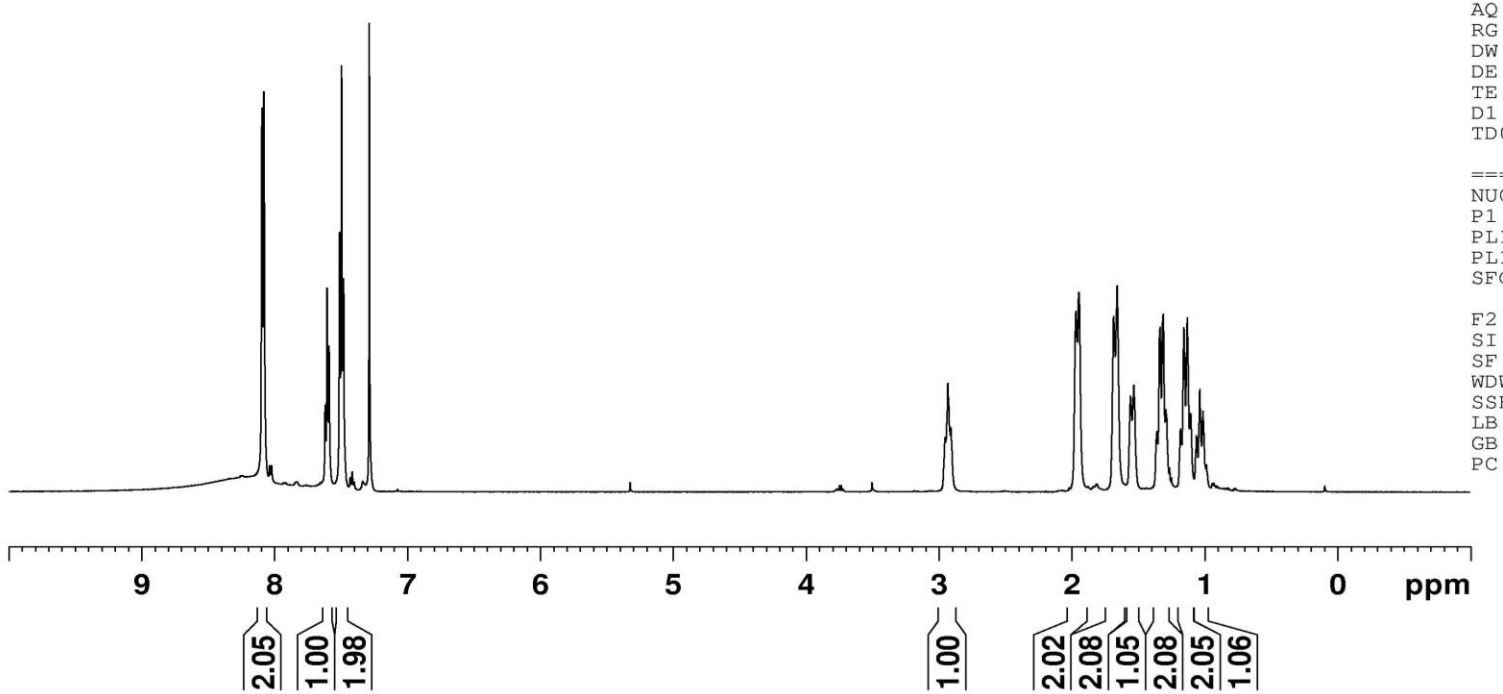


```
Current Data Parameters
NAME                  I-ST-71
EXPNO                       1
PROCNO                      1

F2 - Acquisition Paramete
Date_                20190404
Time                    10.45
INSTRUM                 spect
PROBHD    5 mm PAQXI 1H/
PULPROG                  zg30
TD                      65536
SOLVENT                 CDCl3
NS                         16
DS                          2
SWH                 10330.578 H
FIDRES                0.157632 H
AQ                  3.1719425 s
RG                        128
DW                     48.400 u
DE                      6.50 u
TE                     296.8 K
D1                 1.00000000 s
TD0                         1

======== CHANNEL f1 =====
NUC1                       1H
P1                       9.50 u
PL1                      4.00 d
PL1W            12.10000038 W
SFO1            500.1330885 M

F2 - Processing parameter
SI                      32768
SF              500.1300000 M
WDW                        EM
SSB          0
LB                       0.30 H
GB           0
PC                       1.00
```

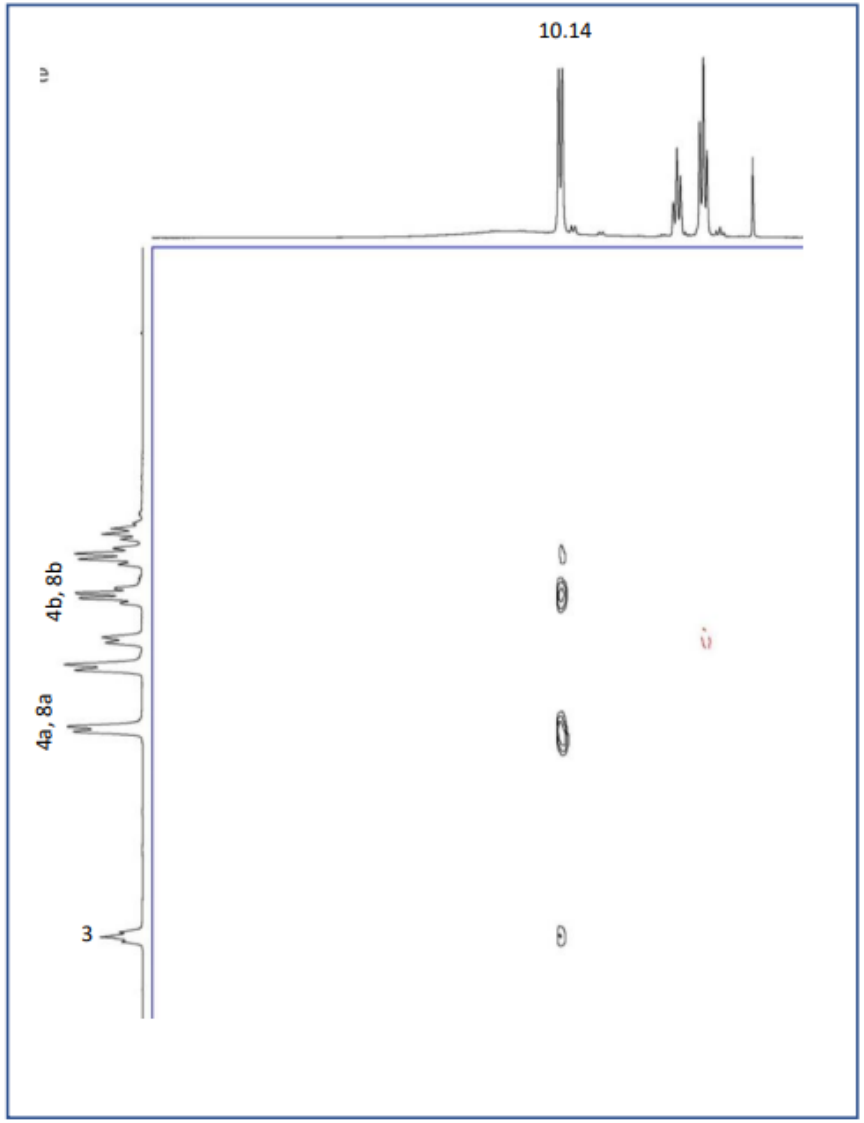

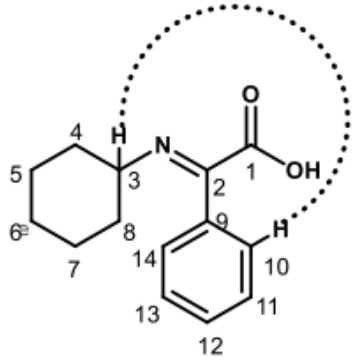

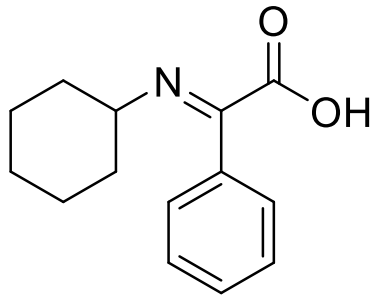

5.74

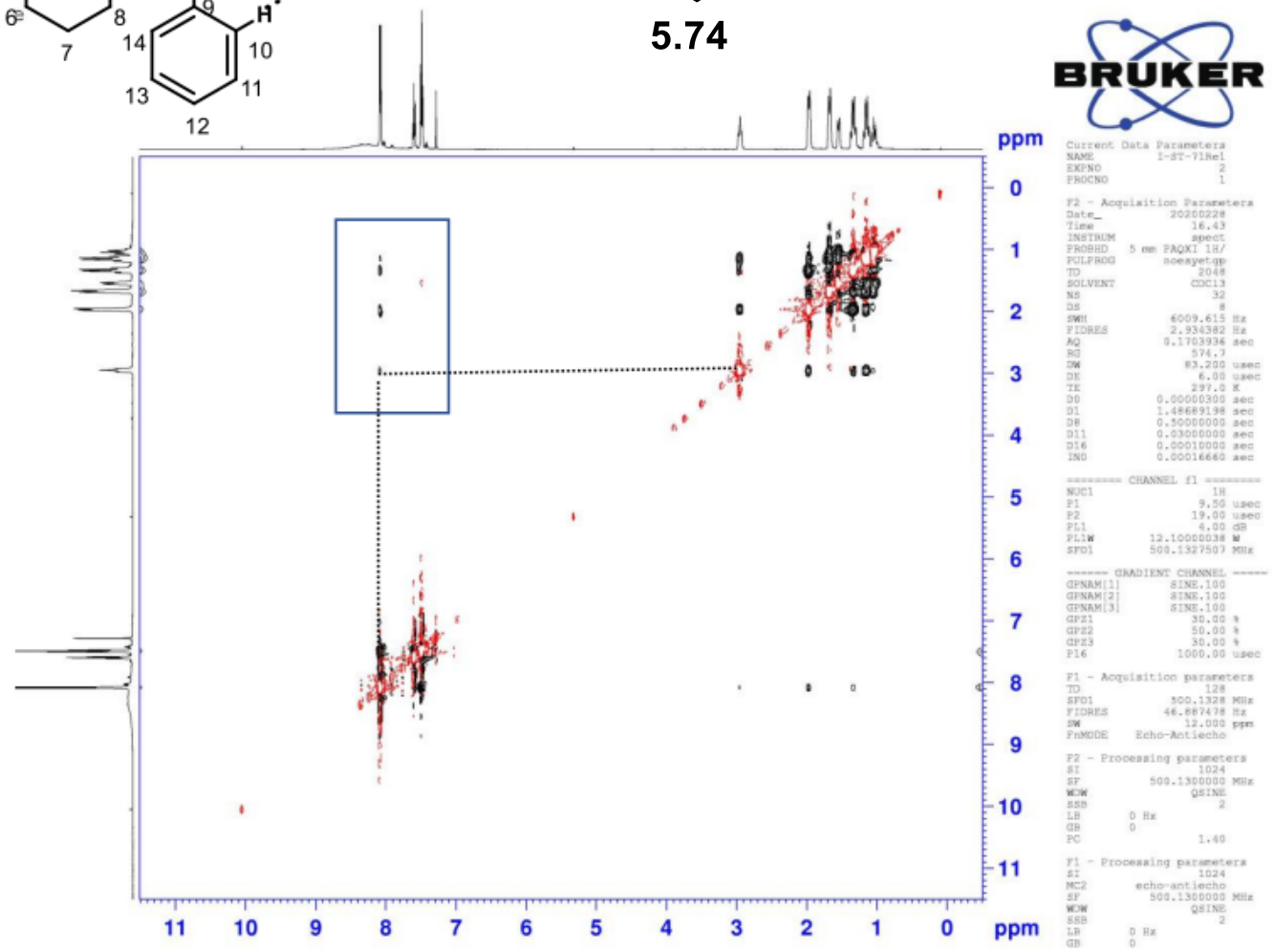

The NOESY correlation of H-14 with H-3, H-4 and H-8 confirms the geometry of structure as '*E*'-

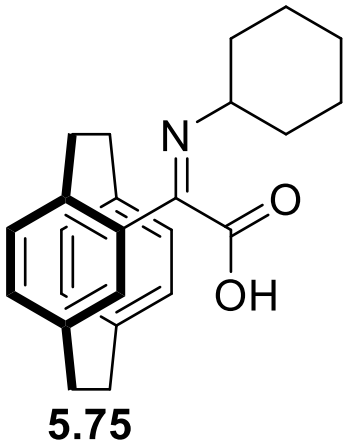

5.75

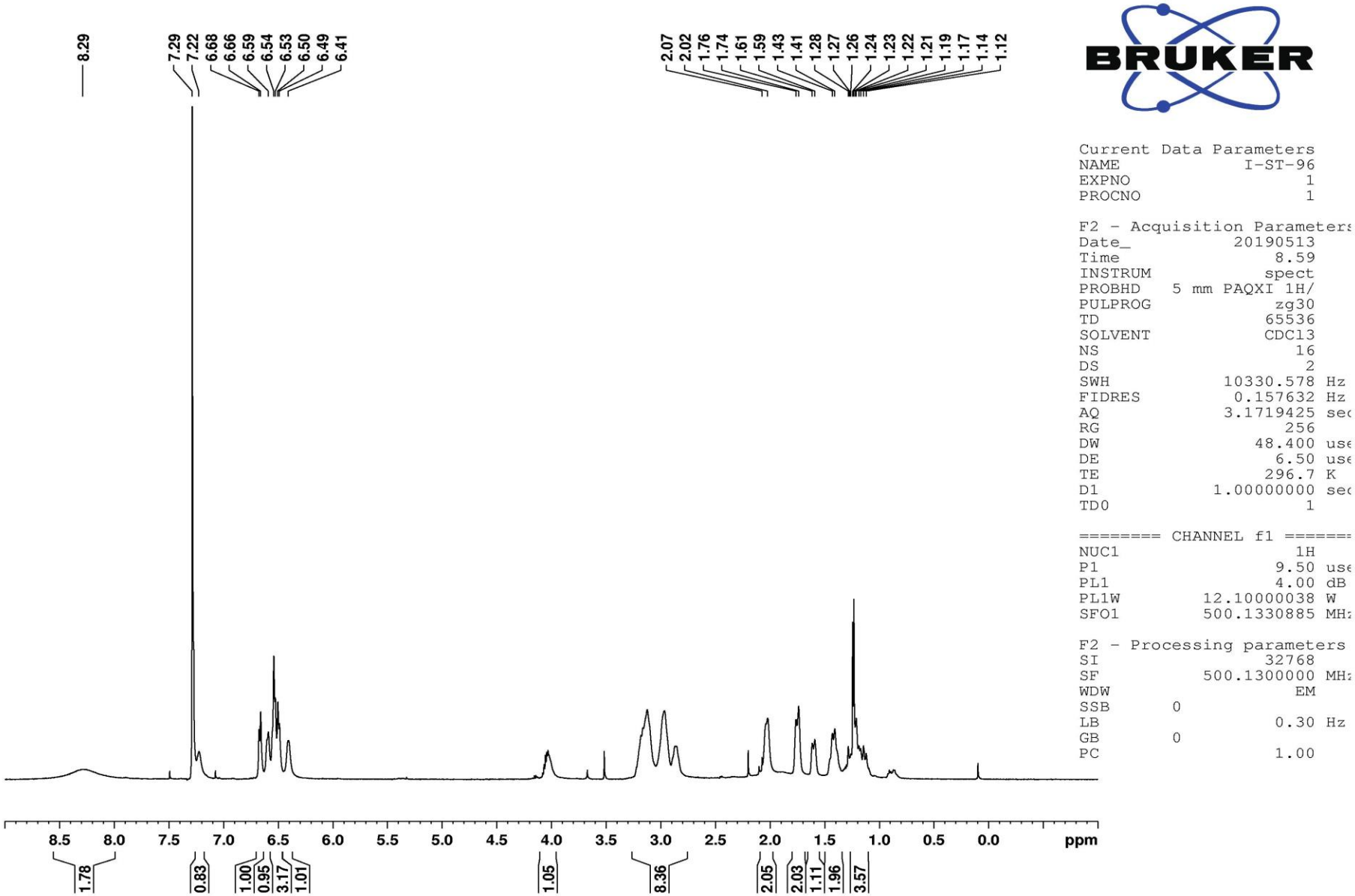

BRUKER

```
Current Data Parameters
NAME                  I-ST-96
EXPNO                       1
PROCNO                      1

F2 - Acquisition Parameters
Date_              20190513
Time                   8.59
INSTRUM               spect
PROBHD   5 mm PAQXI 1H/
PULPROG                zg30
TD                    65536
SOLVENT               CDCl3
NS                       16
DS                        2
SWH               10330.578 Hz
FIDRES             0.157632 Hz
AQ                3.1719425 sec
RG                      256
DW                   48.400 use
DE                    6.50 use
TE                   296.7 K
D1              1.00000000 sec
TD0                       1

======== CHANNEL f1 =======
NUC1                     1H
P1                    9.50 use
PL1                   4.00 dB
PL1W         12.10000038 W
SFO1         500.1330885 MHz

F2 - Processing parameters
SI                    32768
SF           500.1300000 MHz
WDW                      EM
SSB       0
LB                    0.30 Hz
GB        0
PC                    1.00
```

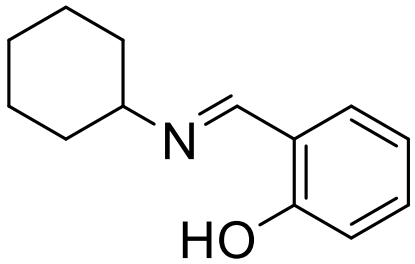

5.73

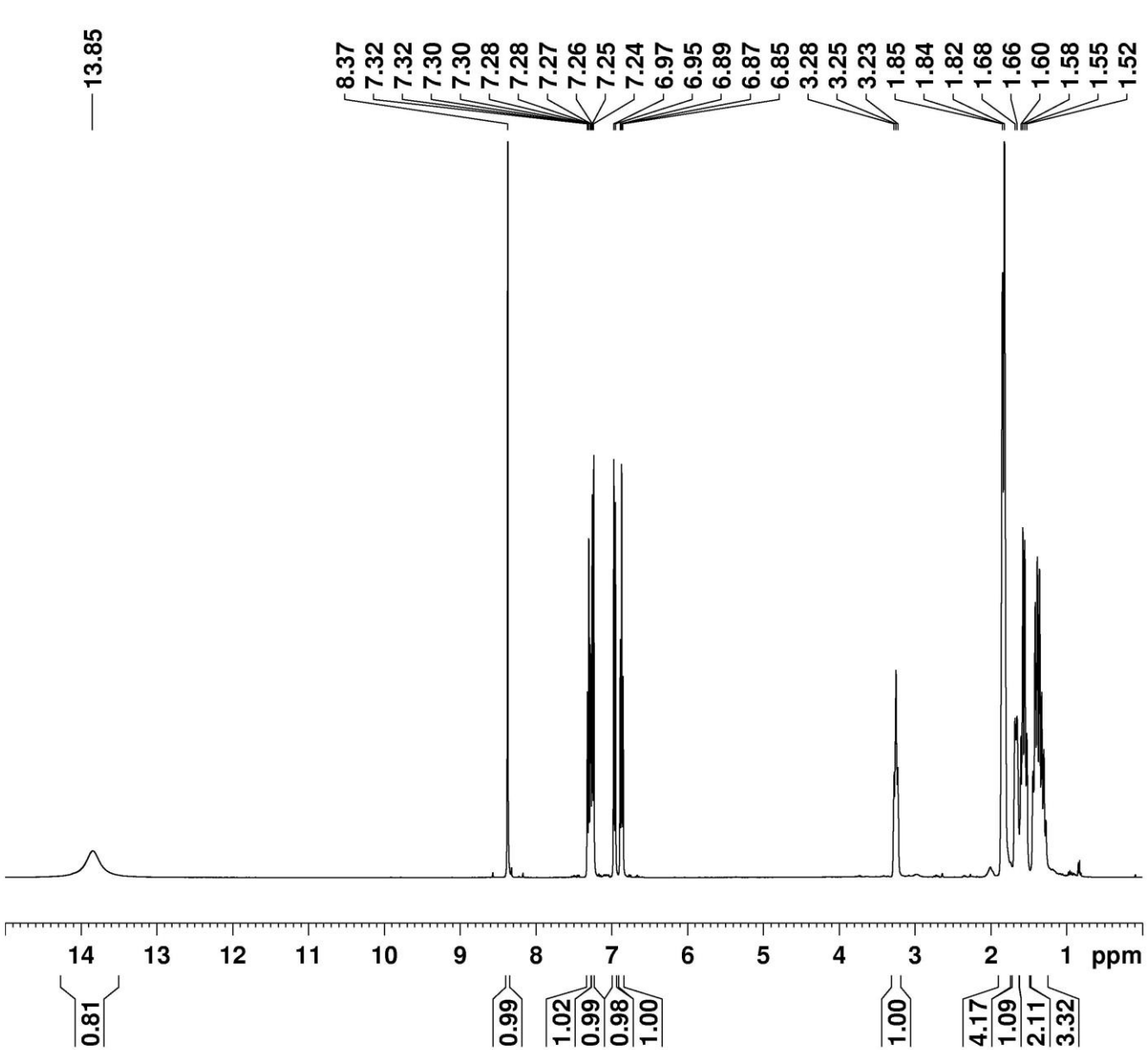

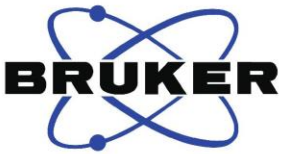


```
Current Data Parameters
NAME                  I-ST-111
EXPNO                        1
PROCNO                       1

F2 - Acquisition Parameters
Date_                 20190530
Time                     13.48
INSTRUM                  spect
PROBHD    5 mm Multinucl
PULPROG                  zg30
TD                      65536
SOLVENT                 CDCl3
NS                         32
DS                          2
SWH                  8278.146 Hz
FIDRES               0.126314 Hz
AQ                   3.9583745 sec
RG                        50.8
DW                      60.400 use
DE                       6.00 use
TE                      300.0 K
D1                 1.00000000 sec
TD0                          1

======== CHANNEL f1 =======
NUC1                        1H
P1                       10.00 use
PL1                       3.80 dB
SFO1              400.1324710 MHz

F2 - Processing parameters
SI                       32768
SF                400.1300000 MHz
WDW                         EM
SSB          0
LB                       0.30 Hz
GB           0
PC                       1.00
```

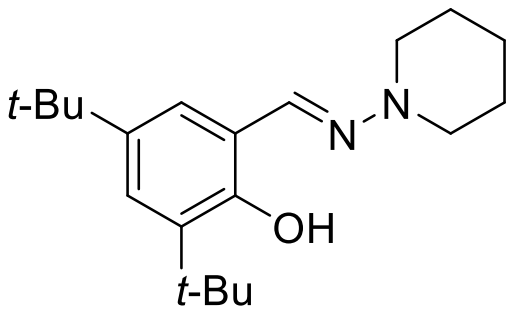

5.65

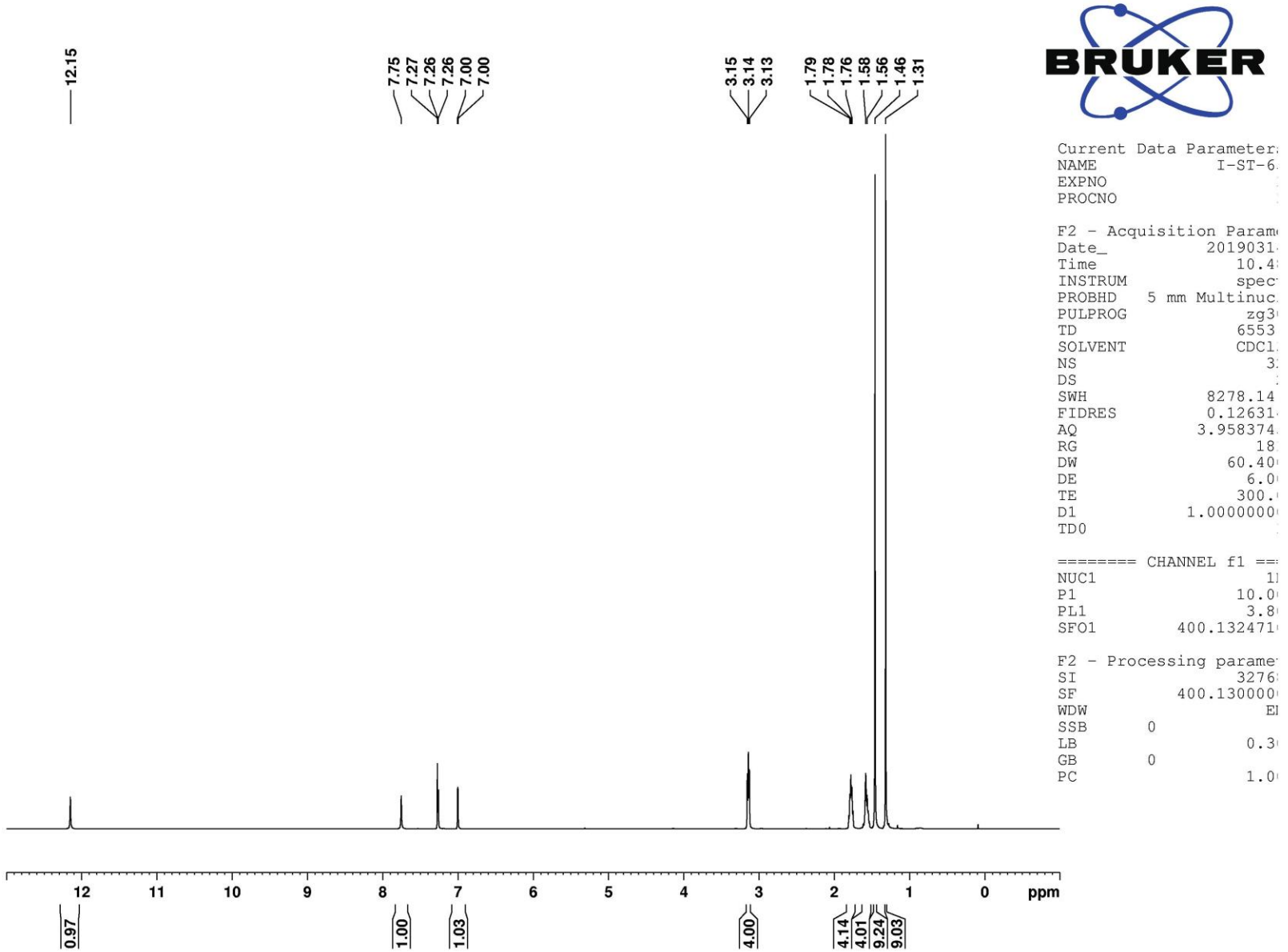


```
Current Data Parameter
NAME                 I-ST-6
EXPNO
PROCNO

F2 - Acquisition Param
Date_             2019031
Time                 10.4
INSTRUM              spec
PROBHD   5 mm Multinuc
PULPROG              zg3
TD                   6553
SOLVENT              CDCl
NS                      3
DS
SWH               8278.14
FIDRES            0.12631
AQ                3.958374
RG                     18
DW                  60.40
DE                    6.0
TE                  300.
D1             1.0000000
TD0

======== CHANNEL f1 ==
NUC1                   1
P1                  10.0
PL1                  3.8
SFO1          400.132471

F2 - Processing parame
SI                   3276
SF            400.130000
WDW                    EM
SSB       0
LB                   0.3
GB        0
PC                   1.0
```

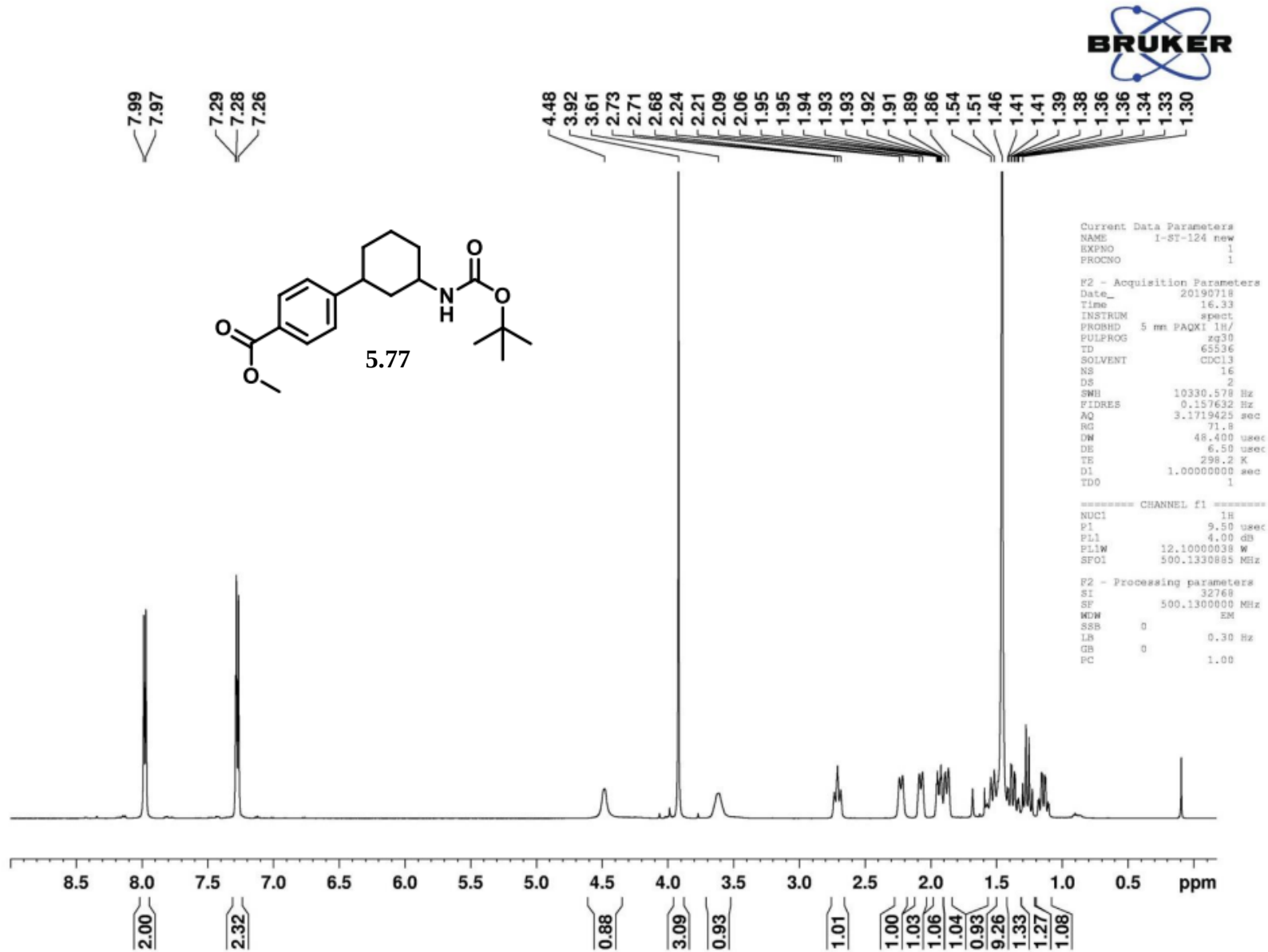
7.99
7.97
7.29
7.28
7.26
4.48
3.92
3.61
2.73
2.71
2.68
2.24
2.21
2.09
2.06
1.95
1.95
1.94
1.93
1.93
1.92
1.91
1.89
1.86
1.54
1.51
1.46
1.41
1.41
1.39
1.38
1.36
1.36
1.34
1.33
1.30
5.77
Current Data Parameters
NAME I-ST-124 new
EXPNO 1
PROCNO 1
F2 - Acquisition Parameters
Date_ 20190718
Time 16.33
INSTRUM spect
PROBHD 5 mm PAQXI 1H/
PULPROG zg30
TD 65536
SOLVENT CDCl3
NS 16
DS 2
SWH 10330.578 Hz
FIDRES 0.157632 Hz
AQ 3.1719425 sec
RG 71.8
DW 48.400 usec
DE 6.50 usec
TE 298.2 K
D1 1.00000000 sec
TD0 1
======== CHANNEL f1 ========
NUC1 1H
P1 9.50 usec
PL1 4.00 dB
PL1W 12.10000038 W
SFO1 500.1330885 MHz
F2 - Processing parameters
SI 32768
SF 500.1300000 MHz
WDW EM
SSB 0
LB 0.30 Hz
GB 0
PC 1.00
8.5
8.0
7.5
7.0
6.5
6.0
5.5
5.0
4.5
4.0
3.5
3.0
2.5
2.0
1.5
1.0
0.5
ppm
2.00
2.32
0.88
3.09
0.93
1.01
1.00
1.03
1.06
1.04
0.93
9.26
1.33
1.27
1.08

checkCIF/PLATON report

Structure factors have been supplied for datablock(s) vsp41

THIS REPORT IS FOR GUIDANCE ONLY. IF USED AS PART OF A REVIEW PROCEDURE FOR PUBLICATION, IT SHOULD NOT REPLACE THE EXPERTISE OF AN EXPERIENCED CRYSTALLOGRAPHIC REFEREE.

No syntax errors found. CIF dictionary Interpreting this report

Datablock: vsp41

Bond precision: C-C = 0.0053 A Wavelength=1.54178

Cell: a=21.0536(5) b=21.0536(5) c=8.1516(3)
alpha=90 beta=90 gamma=120
Temperature: 100 K

	Calculated	Reported
Volume	3129.15(19)	3129.15(19)
Space group	R 3	R 3
Hall group	R 3	R 3
Moiety formula	3(C17 H16 O2), C H4 O, H2 O	0.333(C3 H12 O3), 0.333(H6 O3), 3(C17 H16 O2)
Sum formula	C52 H54 O8	C52 H54 O8
Mr	806.95	806.95
Dx,g cm-3	1.285	1.285
Z	3	3
Mu (mm-1)	0.685	0.685
F000	1290.0	1290.0
F000’	1293.86	
h,k,lmax	26,26,10	26,26,10
Nref	2904[1452]	2862
Tmin,Tmax	0.921,0.947	0.635,0.754
Tmin’	0.921	

Correction method= # Reported T Limits: Tmin=0.635 Tmax=0.754
AbsCorr = MULTI-SCAN

Data completeness= 1.97/0.99 Theta(max)= 75.704

R(reflections)= 0.0446(2609) wR2(reflections)= 0.1178(2862)

S = 1.087 Npar= 188

The following ALERTS were generated. Each ALERT has the format
test-name_ALERT_alert-type_alert-level.
Click on the hyperlinks for more details of the test.

Alert level B

PLAT721_ALERT_1_B Bond Calc 0.87000, Rep 0.9(2) Dev... 0.03 Ang.
O1W -H1WA 1_555 2_665 ..... # 7 Check

Alert level C

PLAT230_ALERT_2_C Hirshfeld Test Diff for O1 --C17 . 6.0 s.u.
PLAT230_ALERT_2_C Hirshfeld Test Diff for O2 --C17 . 6.5 s.u.
PLAT340_ALERT_3_C Low Bond Precision on C-C Bonds ..... 0.00526 Ang.

Alert level G

PLAT007_ALERT_5_G Number of Unrefined Donor-H Atoms ..... 4 Report
PLAT042_ALERT_1_G Calc. and Reported Moiety Formula Strings Differ Please Check
PLAT300_ALERT_4_G Atom Site Occupancy of H3 Constrained at 0.3333 Check
PLAT300_ALERT_4_G Atom Site Occupancy of H18A Constrained at 0.3333 Check
PLAT300_ALERT_4_G Atom Site Occupancy of H18B Constrained at 0.3333 Check
PLAT300_ALERT_4_G Atom Site Occupancy of H18C Constrained at 0.3333 Check
PLAT300_ALERT_4_G Atom Site Occupancy of H1WA Constrained at 0.3333 Check
PLAT300_ALERT_4_G Atom Site Occupancy of H1WB Constrained at 0.3333 Check
PLAT417_ALERT_2_G Short Inter D-H..H-D H2 ..H3 . 2.07 Ang.
x,y,z = 1_555 Check
PLAT417_ALERT_2_G Short Inter D-H..H-D H2 ..H3 . 1.15 Ang.
1-y,1+x-y,z = 2_665 Check
PLAT720_ALERT_4_G Number of Unusual/Non-Standard Labels ..... 2 Note
PLAT779_ALERT_4_G Suspect or Irrelevant (Bond) Angle(s) in CIF ... 11.00 Deg.
H1WA -O1W -H1WB 1_555 1_555 3_565 ..... # 11 Check
PLAT779_ALERT_4_G Suspect or Irrelevant (Bond) Angle(s) in CIF ... 11.00 Deg.
H1WA -O1W -H1WB 3_565 1_555 2_665 ..... # 15 Check
PLAT779_ALERT_4_G Suspect or Irrelevant (Bond) Angle(s) in CIF ... 11.00 Deg.
H1WB -O1W -H1WA 1_555 1_555 2_665 ..... # 18 Check
PLAT789_ALERT_4_G Atoms with Negative _atom_site_disorder_group # 3 Check
PLAT912_ALERT_4_G Missing # of FCF Reflections Above STh/L= 0.600 5 Note
PLAT978_ALERT_2_G Number C-C Bonds with Positive Residual Density. 1 Info

---

0 **ALERT level A** = Most likely a serious problem - resolve or explain
1 **ALERT level B** = A potentially serious problem, consider carefully
3 **ALERT level C** = Check. Ensure it is not caused by an omission or oversight
17 **ALERT level G** = General information/check it is not something unexpected

2 ALERT type 1 CIF construction/syntax error, inconsistent or missing data
5 ALERT type 2 Indicator that the structure model may be wrong or deficient
1 ALERT type 3 Indicator that the structure quality may be low
12 ALERT type 4 Improvement, methodology, query or suggestion
1 ALERT type 5 Informative message, check

It is advisable to attempt to resolve as many as possible of the alerts in all categories. Often the minor alerts point to easily fixed oversights, errors and omissions in your CIF or refinement strategy, so attention to these fine details can be worthwhile. In order to resolve some of the more serious problems it may be necessary to carry out additional measurements or structure refinements. However, the purpose of your study may justify the reported deviations and the more serious of these should normally be commented upon in the discussion or experimental section of a paper or in the "special_details" fields of the CIF. checkCIF was carefully designed to identify outliers and unusual parameters, but every test has its limitations and alerts that are not important in a particular case may appear. Conversely, the absence of alerts does not guarantee there are no aspects of the results needing attention. It is up to the individual to critically assess their own results and, if necessary, seek expert advice.

Publication of your CIF in IUCr journals

A basic structural check has been run on your CIF. These basic checks will be run on all CIFs submitted for publication in IUCr journals (*Acta Crystallographica, Journal of Applied Crystallography, Journal of Synchrotron Radiation*); however, if you intend to submit to *Acta Crystallographica Section C* or *E* or *IUCrData*, you should make sure that full publication checks are run on the final version of your CIF prior to submission.

Publication of your CIF in other journals

Please refer to the *Notes for Authors* of the relevant journal for any special instructions relating to CIF submission.

PLATON version of 16/05/2021; check.def file version of 13/05/2021

Datablock vsp41 - ellipsoid plot

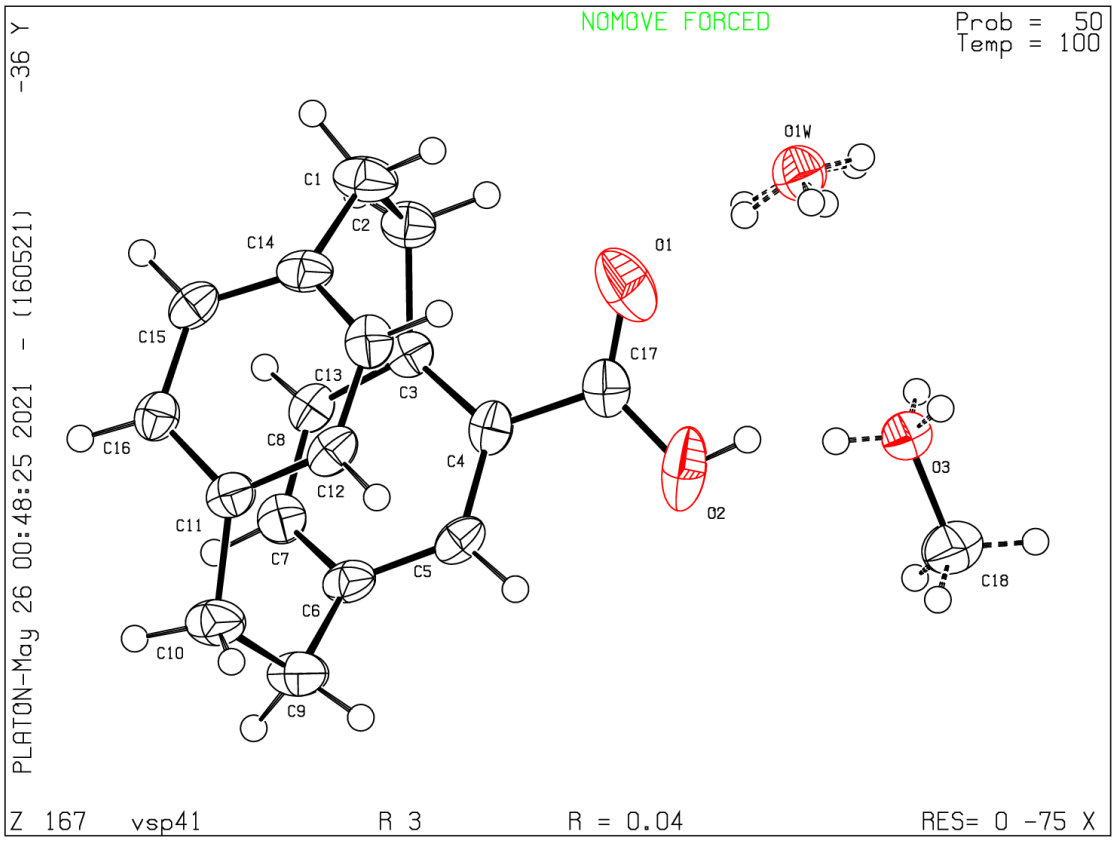

checkCIF/PLATON report

Structure factors have been supplied for datablock(s) vsp39

THIS REPORT IS FOR GUIDANCE ONLY. IF USED AS PART OF A REVIEW PROCEDURE FOR PUBLICATION, IT SHOULD NOT REPLACE THE EXPERTISE OF AN EXPERIENCED CRYSTALLOGRAPHIC REFEREE.

No syntax errors found. CIF dictionary Interpreting this report

Datablock: vsp39

Bond precision: C-C = 0.0030 A Wavelength=1.54178

Cell: a=8.0990(3) b=9.1760(4) c=19.4978(8)
alpha=90 beta=90 gamma=90
Temperature: 100 K

	Calculated	Reported
Volume	1449.01(10)	1449.01(10)
Space group	P 21 21 21	P 21 21 21
Hall group	P 2ac 2ab	P 2ac 2ab
Moiety formula	C18 H16 O4	C18 H16 O4
Sum formula	C18 H16 O4	C18 H16 O4
Mr	296.31	296.31
Dx,g cm-3	1.358	1.358
Z	4	4
Mu (mm-1)	0.785	0.785
F000	624.0	624.0
F000'	626.02	
h,k,lmax	10,11,24	10,11,24
Nref	3039[1766]	2990
Tmin,Tmax	0.910,0.969	0.630,0.754
Tmin'	0.910	

Correction method= # Reported T Limits: Tmin=0.630 Tmax=0.754
AbsCorr = MULTI-SCAN

Data completeness= 1.69/0.98 Theta(max)= 76.268

R(reflections)= 0.0348(2842) wR2(reflections)= 0.0917(2990)

S = 1.056 Npar= 264

The following ALERTS were generated. Each ALERT has the format
test-name_ALERT_alert-type_alert-level.
Click on the hyperlinks for more details of the test.

Alert level B

PLAT355_ALERT_3_B Long O-H (X0.82,N0.98A) O2 - H2 . 1.09 Ang.

Alert level C

PLAT089_ALERT_3_C Poor Data / Parameter Ratio (Zmax < 18) ..... 6.62 Note
PLAT222_ALERT_3_C NonSolvent Resd 1 H Uiso(max)/Uiso(min) Range 4.4 Ratio
PLAT355_ALERT_3_C Long O-H (X0.82,N0.98A) O4 - H4 . 1.06 Ang.
PLAT911_ALERT_3_C Missing FCF Refl Between Thmin & STh/L= 0.600 2 Report

Alert level G

PLAT912_ALERT_4_G Missing # of FCF Reflections Above STh/L= 0.600 18 Note
PLAT913_ALERT_3_G Missing # of Very Strong Reflections in FCF .... 2 Note
PLAT978_ALERT_2_G Number C-C Bonds with Positive Residual Density. 6 Info

0 **ALERT level A** = Most likely a serious problem - resolve or explain
1 **ALERT level B** = A potentially serious problem, consider carefully
4 **ALERT level C** = Check. Ensure it is not caused by an omission or oversight
3 **ALERT level G** = General information/check it is not something unexpected

0 ALERT type 1 CIF construction/syntax error, inconsistent or missing data
1 ALERT type 2 Indicator that the structure model may be wrong or deficient
6 ALERT type 3 Indicator that the structure quality may be low
1 ALERT type 4 Improvement, methodology, query or suggestion
0 ALERT type 5 Informative message, check

It is advisable to attempt to resolve as many as possible of the alerts in all categories. Often the minor alerts point to easily fixed oversights, errors and omissions in your CIF or refinement strategy, so attention to these fine details can be worthwhile. In order to resolve some of the more serious problems it may be necessary to carry out additional measurements or structure refinements. However, the purpose of your study may justify the reported deviations and the more serious of these should normally be commented upon in the discussion or experimental section of a paper or in the "special_details" fields of the CIF. checkCIF was carefully designed to identify outliers and unusual parameters, but every test has its limitations and alerts that are not important in a particular case may appear. Conversely, the absence of alerts does not guarantee there are no aspects of the results needing attention. It is up to the individual to critically assess their own results and, if necessary, seek expert advice.

Publication of your CIF in IUCr journals

A basic structural check has been run on your CIF. These basic checks will be run on all CIFs submitted for publication in IUCr journals (*Acta Crystallographica, Journal of Applied Crystallography, Journal of Synchrotron Radiation*); however, if you intend to submit to *Acta Crystallographica Section C* or *E* or *IUCrData*, you should make sure that full publication checks are run on the final version of your CIF prior to submission.

Publication of your CIF in other journals

Please refer to the *Notes for Authors* of the relevant journal for any special instructions relating to CIF submission.

PLATON version of 16/05/2021; check.def file version of 13/05/2021

Datablock vsp39 - ellipsoid plot

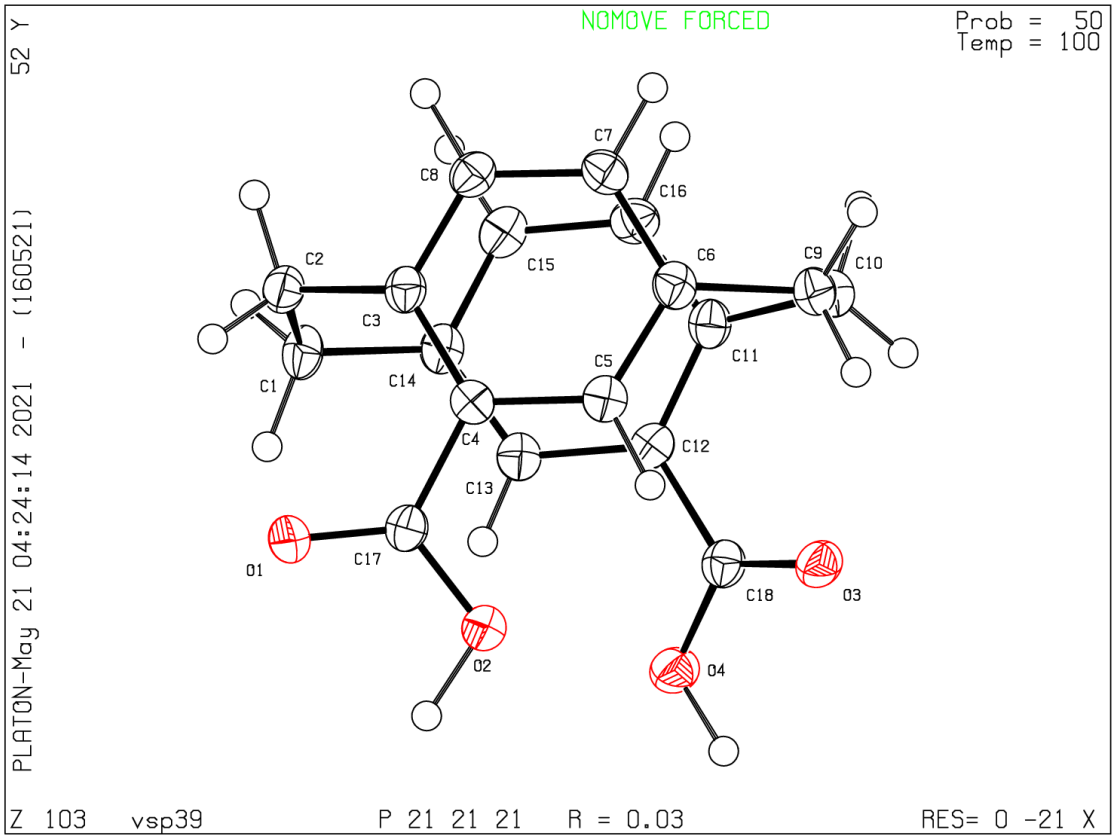

checkCIF/PLATON report

Structure factors have been supplied for datablock(s) ijs13

THIS REPORT IS FOR GUIDANCE ONLY. IF USED AS PART OF A REVIEW PROCEDURE FOR PUBLICATION, IT SHOULD NOT REPLACE THE EXPERTISE OF AN EXPERIENCED CRYSTALLOGRAPHIC REFEREE.

No syntax errors found. CIF dictionary Interpreting this report

Datablock: ijs13

```
Bond precision:   C-C = 0.0200 A           Wavelength=1.54178

Cell:             a=14.9325(13)     b=13.8504(10)       c=17.6365(15)
                  alpha=90          beta=112.056(5)     gamma=90
Temperature:      100 K
```

	Calculated	Reported
Volume	3380.7(5)	3380.7(5)
Space group	P 21/n	P 1 21/n 1
Hall group	-P 2yn	-P 2yn
Moiety formula	4(C26 H36 Au2 Cl2 N4), 3(C H2 Cl2), 4(H2 O) [+ solvent]	C26 H36 Au2 Cl2 N4, H2 O, 0.75(C H2 Cl2), 0.75[CH2CL2]
Sum formula	C107 H158 Au8 Cl14 N16 O4 [+ solvent]	C26.75 H39.50 Au2 Cl3.50 N4 O
Mr	3804.55	951.13
Dx,g cm-3	1.869	1.869
Z	1	4
Mu (mm-1)	18.821	18.821
F000	1814.0	1814.0
F000'	1787.21	
h,k,lmax		17,16,21
Nref		6168
Tmin,Tmax	0.048,0.041	0.467,0.754
Tmin'	0.008	

```
Correction method= # Reported T Limits: Tmin=0.467 Tmax=0.754
AbsCorr = MULTI-SCAN

Data completeness=                  Theta(max)= 68.236
```

R(reflections)= 0.0706(5304)

wR2(reflections)= 0.1784(6168)

S = 1.086 Npar= 351

The following ALERTS were generated. Each ALERT has the format
test-name_ALERT_alert-type_alert-level.
Click on the hyperlinks for more details of the test.

Alert level B

```
PLAT110_ALERT_2_B ADDSYM Detects Potential Lattice Translation ...          ? Check
PLAT112_ALERT_2_B ADDSYM Detects New (Pseudo) Symm. Elem         A         100 %Fit
PLAT113_ALERT_2_B ADDSYM Suggests Possible Pseudo/New  Space Group       C2/c Check
             Check Model Parameter Symmmetry for Reflection Data Support
PLAT417_ALERT_2_B Short Inter D-H..H-D       H1D      ..H3       .       1.98 Ang.
                                                  x,y,z  =      1_555 Check
PLAT971_ALERT_2_B Check Calcd Resid. Dens.  1.12Ang From Au2             2.64 eA-3
PLAT972_ALERT_2_B Check Calcd Resid. Dens.  0.88Ang From Au2            -2.88 eA-3
PLAT972_ALERT_2_B Check Calcd Resid. Dens.  0.95Ang From Au1            -2.84 eA-3
PLAT972_ALERT_2_B Check Calcd Resid. Dens.  0.84Ang From Au1            -2.55 eA-3
```

Alert level C

```
PLAT250_ALERT_2_C Large U3/U1 Ratio for Average U(i,j) Tensor ....        2.2 Note
PLAT342_ALERT_3_C Low Bond Precision on  C-C Bonds ..............    0.01995 Ang.
PLAT414_ALERT_2_C Short Intra D-H..H-X       H1       ..H20B     .       1.90 Ang.
                                                  x,y,z  =      1_555 Check
PLAT414_ALERT_2_C Short Intra D-H..H-X       H3       ..H25A     .       1.93 Ang.
                                                  x,y,z  =      1_555 Check
PLAT906_ALERT_3_C Large K Value in the Analysis of Variance ......      4.308 Check
PLAT911_ALERT_3_C Missing FCF Refl Between Thmin & STh/L=    0.600         18 Report
               0 16  0,  -2 16  1,  -1 16  1,   1  6  1,   1 16  1,  -8 12  4,
              -1 16  4,   0 16  4,   1 16  4,  -3 15  5,  -2 16  5,  -1 16  5,
               0 16  5,   1  0 19,  -2  0 20,  -6  1 21,  -5  0 21,  -5  1 21,
PLAT971_ALERT_2_C Check Calcd Resid. Dens.  1.39Ang From Au1             2.45 eA-3
PLAT971_ALERT_2_C Check Calcd Resid. Dens.  1.22Ang From Au2             2.43 eA-3
PLAT971_ALERT_2_C Check Calcd Resid. Dens.  1.24Ang From Au2             2.16 eA-3
PLAT971_ALERT_2_C Check Calcd Resid. Dens.  1.14Ang From Au2             2.03 eA-3
PLAT971_ALERT_2_C Check Calcd Resid. Dens.  1.52Ang From Au1             2.00 eA-3
PLAT971_ALERT_2_C Check Calcd Resid. Dens.  1.17Ang From Au1             1.94 eA-3
PLAT971_ALERT_2_C Check Calcd Resid. Dens.  1.21Ang From Au1             1.87 eA-3
PLAT971_ALERT_2_C Check Calcd Resid. Dens.  0.77Ang From C1A             1.56 eA-3
PLAT971_ALERT_2_C Check Calcd Resid. Dens.  1.28Ang From C22             1.55 eA-3
PLAT972_ALERT_2_C Check Calcd Resid. Dens.  0.88Ang From Au1            -2.19 eA-3
PLAT972_ALERT_2_C Check Calcd Resid. Dens.  0.88Ang From Au2            -2.18 eA-3
PLAT972_ALERT_2_C Check Calcd Resid. Dens.  1.00Ang From Au1            -2.12 eA-3
PLAT972_ALERT_2_C Check Calcd Resid. Dens.  1.41Ang From C14            -1.79 eA-3
PLAT972_ALERT_2_C Check Calcd Resid. Dens.  0.92Ang From Au2            -1.76 eA-3
PLAT972_ALERT_2_C Check Calcd Resid. Dens.  0.86Ang From Au2            -1.67 eA-3
PLAT972_ALERT_2_C Check Calcd Resid. Dens.  1.05Ang From Au2            -1.51 eA-3
PLAT976_ALERT_2_C Check Calcd Resid. Dens.  0.98Ang From O1      .      -1.08 eA-3
PLAT977_ALERT_2_C Check Negative Difference Density on H1        .      -0.43 eA-3
PLAT977_ALERT_2_C Check Negative Difference Density on H1D       .      -0.80 eA-3
PLAT977_ALERT_2_C Check Negative Difference Density on H2A       .      -0.38 eA-3
PLAT977_ALERT_2_C Check Negative Difference Density on H3        .      -0.46 eA-3
```

```
PLAT977_ALERT_2_C Check Negative Difference Density on H10A      .      -0.39 eA-3
PLAT977_ALERT_2_C Check Negative Difference Density on H10B      .      -0.34 eA-3
PLAT977_ALERT_2_C Check Negative Difference Density on H21C      .      -0.38 eA-3
PLAT977_ALERT_2_C Check Negative Difference Density on H24A      .      -0.53 eA-3
PLAT977_ALERT_2_C Check Negative Difference Density on H24B      .      -0.44 eA-3
```

Alert level G

```
FORMU01_ALERT_1_G  There is a discrepancy between the atom counts in the
           _chemical_formula_sum and _chemical_formula_moiety. This is
           usually due to the moiety formula being in the wrong format.
           Atom count from _chemical_formula_sum:   C26.75 H39.5 Au2 Cl3.5 N4 O1
           Atom count from _chemical_formula_moiety:C27.5 H41 Au2 Cl5 N4 O1
PLAT002_ALERT_2_G Number of Distance or Angle Restraints on AtSite         6 Note
PLAT003_ALERT_2_G Number of Uiso or Uij Restrained non-H Atoms ...         5 Report
PLAT007_ALERT_5_G Number of Unrefined Donor-H Atoms ..............         2 Report
             H1    H3
PLAT042_ALERT_1_G Calc. and Reported MoietyFormula Strings  Differ     Please Check
             Calc: 4(C26 H36 Au2 Cl2 N4), 3(C H2 Cl2), 4(H2 O)
             Rep.: C26 H36 Au2 Cl2 N4, H2 O, 0.75(C H2 Cl2), 0.75[CH2CL2]
PLAT045_ALERT_1_G Calculated and Reported Z Differ by a Factor ...      0.250 Check
PLAT083_ALERT_2_G SHELXL Second Parameter in WGHT  Unusually Large     167.47 Why ?
PLAT116_ALERT_2_G ADDSYM Included (Pseudo) Lattice Translation ...     Please Check
PLAT172_ALERT_4_G The CIF-Embedded .res File Contains DFIX Records          3 Report
PLAT173_ALERT_4_G The CIF-Embedded .res File Contains DANG Records          1 Report
PLAT178_ALERT_4_G The CIF-Embedded .res File Contains SIMU Records          1 Report
PLAT186_ALERT_4_G The CIF-Embedded .res File Contains ISOR Records          2 Report
PLAT187_ALERT_4_G The CIF-Embedded .res File Contains RIGU Records          1 Report
PLAT300_ALERT_4_G Atom Site Occupancy of Cl3        Constrained at       0.75 Check
PLAT300_ALERT_4_G Atom Site Occupancy of Cl4        Constrained at       0.75 Check
PLAT300_ALERT_4_G Atom Site Occupancy of C1A        Constrained at       0.75 Check
PLAT300_ALERT_4_G Atom Site Occupancy of H1AA       Constrained at       0.75 Check
PLAT300_ALERT_4_G Atom Site Occupancy of H1AB       Constrained at       0.75 Check
PLAT302_ALERT_4_G Anion/Solvent/Minor-Residue Disorder (Resd  2  )       100% Note
PLAT304_ALERT_4_G Non-Integer Number of Atoms in ..... (Resd  2  )       3.75 Check
PLAT605_ALERT_4_G Largest Solvent Accessible VOID in the Structure        179 A**3
PLAT720_ALERT_4_G Number of Unusual/Non-Standard Labels ..........          2 Note
             H1AA    H1AB
PLAT860_ALERT_3_G Number of Least-Squares Restraints .............         39 Note
PLAT868_ALERT_4_G ALERTS Due to the Use of _smtbx_masks Suppressed          ! Info
PLAT912_ALERT_4_G Missing # of FCF Reflections Above STh/L=  0.600          3 Note
PLAT978_ALERT_2_G Number C-C Bonds with Positive Residual Density.          0 Info
```

```
   0 ALERT level A = Most likely a serious problem - resolve or explain
   8 ALERT level B = A potentially serious problem, consider carefully
  32 ALERT level C = Check. Ensure it is not caused by an omission or oversight
  26 ALERT level G = General information/check it is not something unexpected

   3 ALERT type 1 CIF construction/syntax error, inconsistent or missing data
  42 ALERT type 2 Indicator that the structure model may be wrong or deficient
   4 ALERT type 3 Indicator that the structure quality may be low
  16 ALERT type 4 Improvement, methodology, query or suggestion
   1 ALERT type 5 Informative message, check
```

It is advisable to attempt to resolve as many as possible of the alerts in all categories. Often the minor alerts point to easily fixed oversights, errors and omissions in your CIF or refinement strategy, so attention to these fine details can be worthwhile. In order to resolve some of the more serious problems it may be necessary to carry out additional measurements or structure refinements. However, the purpose of your study may justify the reported deviations and the more serious of these should normally be commented upon in the discussion or experimental section of a paper or in the "special_details" fields of the CIF. checkCIF was carefully designed to identify outliers and unusual parameters, but every test has its limitations and alerts that are not important in a particular case may appear. Conversely, the absence of alerts does not guarantee there are no aspects of the results needing attention. It is up to the individual to critically assess their own results and, if necessary, seek expert advice.

Publication of your CIF in IUCr journals

A basic structural check has been run on your CIF. These basic checks will be run on all CIFs submitted for publication in IUCr journals (*Acta Crystallographica*, *Journal of Applied Crystallography*, *Journal of Synchrotron Radiation*); however, if you intend to submit to *Acta Crystallographica Section C* or *E* or *IUCrData*, you should make sure that full publication checks are run on the final version of your CIF prior to submission.

Publication of your CIF in other journals

Please refer to the *Notes for Authors* of the relevant journal for any special instructions relating to CIF submission.

PLATON version of 14/11/2023; check.def file version of 14/09/2023

Datablock ijs13 - ellipsoid plot

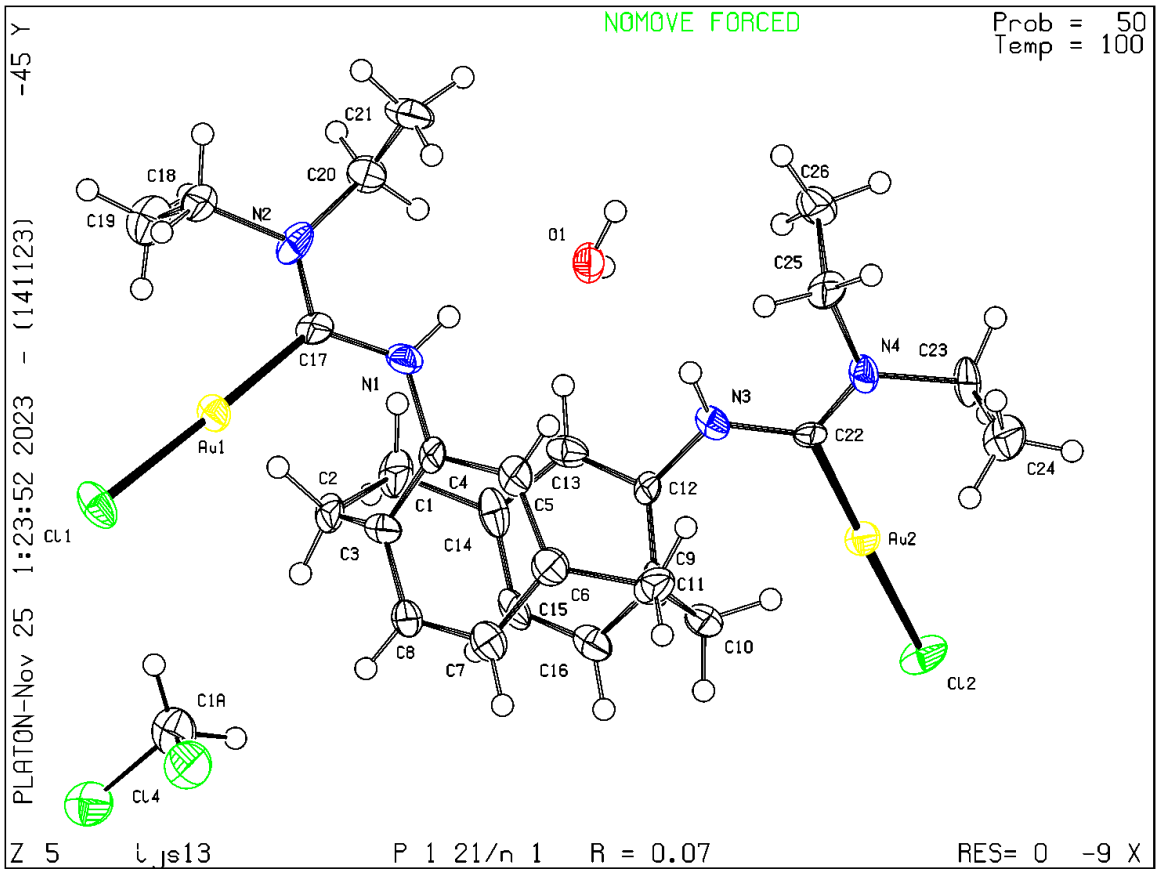

checkCIF/PLATON report

Structure factors have been supplied for datablock(s) spcc55

THIS REPORT IS FOR GUIDANCE ONLY. IF USED AS PART OF A REVIEW PROCEDURE FOR PUBLICATION, IT SHOULD NOT REPLACE THE EXPERTISE OF AN EXPERIENCED CRYSTALLOGRAPHIC REFEREE.

No syntax errors found. CIF dictionary Interpreting this report

Datablock: spcc55

```
Bond precision:   C-C = 0.0473 A          Wavelength=1.54178

Cell:           a=13.0158(8)      b=13.0566(9)     c=24.1653(17)
                alpha=98.948(4)   beta=92.740(4)   gamma=113.675(4)
Temperature:    100 K
```

	Calculated	Reported
Volume	3687.6(4)	3687.6(4)
Space group	P 1	P 1
Hall group	P 1	P 1
Moiety formula	C76 H72 Br4 O10 Rh2 [+ solvent]	C76 H72 Br4 O10 Rh2
Sum formula	C76 H72 Br4 O10 Rh2 [+ solvent]	C76 H72 Br4 O10 Rh2
Mr	1670.76	1670.79
Dx,g cm-3	1.505	1.505
Z	2	2
Mu (mm-1)	6.602	6.602
F000	1676.0	1676.0
F000'	1674.70	
h,k,lmax	15,15,28	15,15,28
Nref	25352[12676]	23872
Tmin,Tmax	0.439,0.768	0.533,0.753
Tmin'	0.354	

```
Correction method= # Reported T Limits: Tmin=0.533 Tmax=0.753
AbsCorr = MULTI-SCAN

Data completeness= 1.88/0.94        Theta(max)= 65.374
```

R(reflections)= 0.1026(22550)

wR2(reflections)= 0.2310(23872)

S = 1.184 Npar= 1622

The following ALERTS were generated. Each ALERT has the format
test-name_ALERT_alert-type_alert-level.
Click on the hyperlinks for more details of the test.

Alert level A

PLAT234_ALERT_4_A Large Hirshfeld Difference C028 --C80 . 0.32 Ang.
PLAT234_ALERT_4_A Large Hirshfeld Difference C00M --C041 . 0.35 Ang.
PLAT234_ALERT_4_A Large Hirshfeld Difference C16 --C19 . 0.37 Ang.

Alert level B

PLAT213_ALERT_2_B Atom C00X has ADP max/min Ratio ..... 4.8 prolat
PLAT234_ALERT_4_B Large Hirshfeld Difference C22 --C23A . 0.30 Ang.
PLAT234_ALERT_4_B Large Hirshfeld Difference C02K --C04Q . 0.28 Ang.
PLAT234_ALERT_4_B Large Hirshfeld Difference Br2 --C054 . 0.30 Ang.
PLAT234_ALERT_4_B Large Hirshfeld Difference C02T --C03D . 0.26 Ang.
PLAT241_ALERT_2_B High 'MainMol' Ueq as Compared to Neighbors of C22 Check
PLAT241_ALERT_2_B High 'MainMol' Ueq as Compared to Neighbors of C80 Check
PLAT241_ALERT_2_B High 'MainMol' Ueq as Compared to Neighbors of C041 Check
PLAT342_ALERT_3_B Low Bond Precision on C-C Bonds ..... 0.04732 Ang.
PLAT369_ALERT_2_B Long C(sp2)-C(sp2) Bond C019 - C01O . 1.57 Ang.
PLAT369_ALERT_2_B Long C(sp2)-C(sp2) Bond C01N - C036 . 1.59 Ang.
PLAT369_ALERT_2_B Long C(sp2)-C(sp2) Bond C03F - C04I . 1.58 Ang.
PLAT410_ALERT_2_B Short Intra H...H Contact H9B ..H03N . 1.82 Ang.
x,y,z = 1_555 Check
PLAT971_ALERT_2_B Check Calcd Resid. Dens. 0.70Ang From C23A 2.82 eA-3
PLAT971_ALERT_2_B Check Calcd Resid. Dens. 0.56Ang From C00M 2.53 eA-3

Alert level C

CRYSC01_ALERT_1_C The word below has not been recognised as a standard identifier.
greenish
THETM01_ALERT_3_C The value of sine(theta_max)/wavelength is less than 0.590
Calculated sin(theta_max)/wavelength = 0.5896
PLAT090_ALERT_3_C Poor Data / Parameter Ratio (Zmax > 18) ..... 7.71 Note
PLAT213_ALERT_2_C Atom O00H has ADP max/min Ratio ..... 3.7 oblate
PLAT213_ALERT_2_C Atom C02U has ADP max/min Ratio ..... 3.4 prolat
PLAT213_ALERT_2_C Atom C03M has ADP max/min Ratio ..... 3.4 prolat
PLAT213_ALERT_2_C Atom C04W has ADP max/min Ratio ..... 3.5 prolat
PLAT220_ALERT_2_C NonSolvent Resd 1 C Ueq(max)/Ueq(min) Range 5.1 Ratio
PLAT220_ALERT_2_C NonSolvent Resd 2 C Ueq(max)/Ueq(min) Range 4.9 Ratio
PLAT222_ALERT_3_C NonSolvent Resd 1 H Uiso(max)/Uiso(min) Range 4.5 Ratio
PLAT234_ALERT_4_C Large Hirshfeld Difference Br07 --C039 . 0.19 Ang.
PLAT234_ALERT_4_C Large Hirshfeld Difference Br00 --C02X . 0.23 Ang.
PLAT234_ALERT_4_C Large Hirshfeld Difference O00D --C00X . 0.18 Ang.
PLAT234_ALERT_4_C Large Hirshfeld Difference O00H --C010 . 0.17 Ang.
PLAT234_ALERT_4_C Large Hirshfeld Difference C014 --C01I . 0.18 Ang.
PLAT234_ALERT_4_C Large Hirshfeld Difference C014 --C01M . 0.20 Ang.
PLAT234_ALERT_4_C Large Hirshfeld Difference C014 --C03J . 0.21 Ang.

```
PLAT234_ALERT_4_C Large Hirshfeld Difference C02U     --C03J     .       0.22 Ang.
PLAT234_ALERT_4_C Large Hirshfeld Difference C039     --C03I     .       0.22 Ang.
PLAT234_ALERT_4_C Large Hirshfeld Difference Rh04     --O01R     .       0.18 Ang.
PLAT234_ALERT_4_C Large Hirshfeld Difference Br0A     --C046     .       0.19 Ang.
PLAT234_ALERT_4_C Large Hirshfeld Difference O00W     --C01P     .       0.23 Ang.
PLAT234_ALERT_4_C Large Hirshfeld Difference O01R     --C036     .       0.25 Ang.
PLAT234_ALERT_4_C Large Hirshfeld Difference C00M     --C012     .       0.20 Ang.
PLAT234_ALERT_4_C Large Hirshfeld Difference C018     --C01F     .       0.22 Ang.
PLAT234_ALERT_4_C Large Hirshfeld Difference C019     --C01O     .       0.19 Ang.
PLAT234_ALERT_4_C Large Hirshfeld Difference C01K     --C02W     .       0.24 Ang.
PLAT241_ALERT_2_C High   'MainMol' Ueq as Compared to Neighbors of         C2 Check
PLAT241_ALERT_2_C High   'MainMol' Ueq as Compared to Neighbors of         C7 Check
PLAT241_ALERT_2_C High   'MainMol' Ueq as Compared to Neighbors of        C13 Check
PLAT241_ALERT_2_C High   'MainMol' Ueq as Compared to Neighbors of       C02Z Check
PLAT241_ALERT_2_C High   'MainMol' Ueq as Compared to Neighbors of       C03L Check
PLAT241_ALERT_2_C High   'MainMol' Ueq as Compared to Neighbors of       C04Q Check
PLAT241_ALERT_2_C High   'MainMol' Ueq as Compared to Neighbors of         O2 Check
PLAT241_ALERT_2_C High   'MainMol' Ueq as Compared to Neighbors of         C5 Check
PLAT241_ALERT_2_C High   'MainMol' Ueq as Compared to Neighbors of         C9 Check
PLAT241_ALERT_2_C High   'MainMol' Ueq as Compared to Neighbors of        C19 Check
PLAT241_ALERT_2_C High   'MainMol' Ueq as Compared to Neighbors of        C20 Check
PLAT241_ALERT_2_C High   'MainMol' Ueq as Compared to Neighbors of        C21 Check
PLAT241_ALERT_2_C High   'MainMol' Ueq as Compared to Neighbors of       C02L Check
PLAT241_ALERT_2_C High   'MainMol' Ueq as Compared to Neighbors of       C03D Check
PLAT241_ALERT_2_C High   'MainMol' Ueq as Compared to Neighbors of       C03Y Check
PLAT241_ALERT_2_C High   'MainMol' Ueq as Compared to Neighbors of       C044 Check
PLAT241_ALERT_2_C High   'MainMol' Ueq as Compared to Neighbors of       C04W Check
PLAT242_ALERT_2_C Low    'MainMol' Ueq as Compared to Neighbors of       Rh01 Check
PLAT242_ALERT_2_C Low    'MainMol' Ueq as Compared to Neighbors of       C013 Check
PLAT242_ALERT_2_C Low    'MainMol' Ueq as Compared to Neighbors of       C014 Check
PLAT242_ALERT_2_C Low    'MainMol' Ueq as Compared to Neighbors of       C01D Check
PLAT242_ALERT_2_C Low    'MainMol' Ueq as Compared to Neighbors of       C23A Check
PLAT242_ALERT_2_C Low    'MainMol' Ueq as Compared to Neighbors of       C01X Check
PLAT242_ALERT_2_C Low    'MainMol' Ueq as Compared to Neighbors of       C028 Check
PLAT242_ALERT_2_C Low    'MainMol' Ueq as Compared to Neighbors of       C02K Check
PLAT242_ALERT_2_C Low    'MainMol' Ueq as Compared to Neighbors of       C02X Check
PLAT242_ALERT_2_C Low    'MainMol' Ueq as Compared to Neighbors of       C039 Check
PLAT242_ALERT_2_C Low    'MainMol' Ueq as Compared to Neighbors of       C051 Check
PLAT242_ALERT_2_C Low    'MainMol' Ueq as Compared to Neighbors of       Rh02 Check
PLAT242_ALERT_2_C Low    'MainMol' Ueq as Compared to Neighbors of       C00M Check
PLAT242_ALERT_2_C Low    'MainMol' Ueq as Compared to Neighbors of       C00Y Check
PLAT242_ALERT_2_C Low    'MainMol' Ueq as Compared to Neighbors of       C018 Check
PLAT242_ALERT_2_C Low    'MainMol' Ueq as Compared to Neighbors of        C16 Check
PLAT242_ALERT_2_C Low    'MainMol' Ueq as Compared to Neighbors of       C01N Check
PLAT242_ALERT_2_C Low    'MainMol' Ueq as Compared to Neighbors of        C44 Check
PLAT242_ALERT_2_C Low    'MainMol' Ueq as Compared to Neighbors of       C02H Check
PLAT242_ALERT_2_C Low    'MainMol' Ueq as Compared to Neighbors of       C02S Check
PLAT242_ALERT_2_C Low    'MainMol' Ueq as Compared to Neighbors of       C02V Check
PLAT242_ALERT_2_C Low    'MainMol' Ueq as Compared to Neighbors of       C03O Check
PLAT242_ALERT_2_C Low    'MainMol' Ueq as Compared to Neighbors of       C046 Check
PLAT242_ALERT_2_C Low    'MainMol' Ueq as Compared to Neighbors of       C054 Check
PLAT360_ALERT_2_C Short  C(sp3)-C(sp3) Bond  C20      - C28      .       1.40 Ang.
PLAT361_ALERT_2_C Long   C(sp3)-C(sp3) Bond  C21      - C04H     .       1.67 Ang.
PLAT362_ALERT_2_C Short  C(sp3)-C(sp2) Bond  C038     - C051     .       1.41 Ang.
PLAT362_ALERT_2_C Short  C(sp3)-C(sp2) Bond  C01U     - C03D     .       1.41 Ang.
PLAT363_ALERT_2_C Long   C(sp3)-C(sp2) Bond  C02W     - C04H     .       1.68 Ang.
PLAT363_ALERT_2_C Long   C(sp3)-C(sp2) Bond  C035     - C04W     .       1.66 Ang.
```

```
PLAT368_ALERT_2_C Short  C(sp2)-C(sp2) Bond  C020     - C039     .       1.23 Ang.
PLAT368_ALERT_2_C Short  C(sp2)-C(sp2) Bond  C01E     - C03F     .       1.21 Ang.
PLAT369_ALERT_2_C Long   C(sp2)-C(sp2) Bond  C00T     - C00U     .       1.53 Ang.
PLAT369_ALERT_2_C Long   C(sp2)-C(sp2) Bond  C00X     - C01M     .       1.55 Ang.
PLAT369_ALERT_2_C Long   C(sp2)-C(sp2) Bond  C00Z     - C02Q     .       1.56 Ang.
PLAT369_ALERT_2_C Long   C(sp2)-C(sp2) Bond  C010     - C03C     .       1.55 Ang.
PLAT369_ALERT_2_C Long   C(sp2)-C(sp2) Bond  C01P     - C01Y     .       1.53 Ang.
PLAT369_ALERT_2_C Long   C(sp2)-C(sp2) Bond  C03B     - C054     .       1.53 Ang.
PLAT410_ALERT_2_C Short Intra H...H Contact  H13B     ..H05C     .       1.92 Ang.
                                                      x,y,z  =      1_555 Check
PLAT411_ALERT_2_C Short Inter H...H Contact  H15A     ..H04C     .       2.06 Ang.
                                                    1+x,y,z  =      1_655 Check
PLAT411_ALERT_2_C Short Inter H...H Contact  H4A      ..H16B     .       2.08 Ang.
                                                   -1+x,y,z  =      1_455 Check
PLAT411_ALERT_2_C Short Inter H...H Contact  H10A     ..H04O     .       2.01 Ang.
                                                   x,-1+y,z  =      1_545 Check
PLAT721_ALERT_1_C Bond    Calc     1.52(5), Rep     1.53220 Dev...       0.01 Ang.
             C7       -C8              1_555   1_555 ........     #  317 Check
PLAT906_ALERT_3_C Large K Value in the Analysis of Variance ......     2.315 Check
PLAT911_ALERT_3_C Missing FCF Refl Between Thmin & STh/L=    0.590       177 Report
PLAT918_ALERT_3_C Reflection(s) with I(obs) much Smaller I(calc) .         2 Check
PLAT971_ALERT_2_C Check Calcd Resid. Dens.  0.66Ang From Br2            2.13 eA-3
PLAT971_ALERT_2_C Check Calcd Resid. Dens.  1.20Ang From Br0A           2.12 eA-3
PLAT971_ALERT_2_C Check Calcd Resid. Dens.  0.97Ang From Br2            1.51 eA-3
PLAT972_ALERT_2_C Check Calcd Resid. Dens.  0.21Ang From Br2           -1.67 eA-3
PLAT972_ALERT_2_C Check Calcd Resid. Dens.  0.61Ang From Br0A          -1.60 eA-3
PLAT972_ALERT_2_C Check Calcd Resid. Dens.  0.50Ang From Br0A          -1.53 eA-3
PLAT975_ALERT_2_C Check Calcd Resid. Dens.  0.91Ang From O00E    .      0.88 eA-3
PLAT977_ALERT_2_C Check Negative Difference Density on H1A       .     -0.31 eA-3
PLAT977_ALERT_2_C Check Negative Difference Density on H4A       .     -0.35 eA-3
PLAT977_ALERT_2_C Check Negative Difference Density on H15B      .     -0.45 eA-3
PLAT977_ALERT_2_C Check Negative Difference Density on H18B      .     -0.34 eA-3
PLAT977_ALERT_2_C Check Negative Difference Density on H19B      .     -0.40 eA-3
PLAT977_ALERT_2_C Check Negative Difference Density on H20A      .     -0.38 eA-3
PLAT977_ALERT_2_C Check Negative Difference Density on H03J      .     -0.43 eA-3
PLAT977_ALERT_2_C Check Negative Difference Density on H04F      .     -0.34 eA-3
PLAT977_ALERT_2_C Check Negative Difference Density on H04Q      .     -0.35 eA-3
PLAT977_ALERT_2_C Check Negative Difference Density on H05C      .     -0.43 eA-3
```

Alert level G

```
PLAT002_ALERT_2_G Number of Distance or Angle Restraints on AtSite        58 Note
PLAT003_ALERT_2_G Number of Uiso or Uij Restrained non-H Atoms ...       160 Report
PLAT033_ALERT_4_G Flack x Value Deviates > 3.0 * sigma from Zero .     0.055 Note
PLAT083_ALERT_2_G SHELXL Second Parameter in WGHT  Unusually Large     64.41 Why ?
PLAT154_ALERT_1_G The s.u.'s on the Cell Angles are Equal ..(Note)     0.004 Degree
PLAT172_ALERT_4_G The CIF-Embedded .res File Contains DFIX Records        29 Report
PLAT176_ALERT_4_G The CIF-Embedded .res File Contains SADI Records        16 Report
PLAT178_ALERT_4_G The CIF-Embedded .res File Contains SIMU Records         4 Report
PLAT186_ALERT_4_G The CIF-Embedded .res File Contains ISOR Records         3 Report
PLAT187_ALERT_4_G The CIF-Embedded .res File Contains RIGU Records         4 Report
PLAT335_ALERT_2_G Check Large C6 Ring C-C Range C014     -C03J          0.23 Ang.
PLAT335_ALERT_2_G Check Large C6 Ring C-C Range C01B     -C023          0.19 Ang.
PLAT335_ALERT_2_G Check Large C6 Ring C-C Range C020     -C039          0.26 Ang.
PLAT335_ALERT_2_G Check Large C6 Ring C-C Range C02I     -C04N          0.15 Ang.
PLAT335_ALERT_2_G Check Large C6 Ring C-C Range C14      -C04J          0.18 Ang.
PLAT335_ALERT_2_G Check Large C6 Ring C-C Range C018     -C01S          0.17 Ang.
```

```
PLAT335_ALERT_2_G Check Large C6 Ring C-C Range C01E     -C03F           0.37 Ang.
PLAT343_ALERT_2_G Unusual sp3      Angle Range in Main Residue for        C19 Check
PLAT606_ALERT_4_G Solvent Accessible VOID(S) in Structure .....          ! Info
PLAT720_ALERT_4_G Number of Unusual/Non-Standard Labels .....          245 Note
PLAT722_ALERT_1_G Angle   Calc      120.00, Rep      121.10 Dev...      1.10 Degree
             C02O    -C022    -H022       1_555  1_555  1_555     #  209 Check
PLAT722_ALERT_1_G Angle   Calc      107.00, Rep      108.10 Dev...      1.10 Degree
             H80A    -C80     -H80B       1_555  1_555  1_555     #  538 Check
PLAT722_ALERT_1_G Angle   Calc      121.00, Rep      119.80 Dev...      1.20 Degree
             C035    -C36     -H36        1_555  1_555  1_555     #  623 Check
PLAT722_ALERT_1_G Angle   Calc      106.00, Rep      107.10 Dev...      1.10 Degree
             C03B    -C28     -H28B       1_555  1_555  1_555     #  666 Check
PLAT860_ALERT_3_G Number of Least-Squares Restraints .............      1232 Note
PLAT909_ALERT_3_G Percentage of I>2sig(I) Data at Theta(Max) Still       90% Note
PLAT913_ALERT_3_G Missing # of Very Strong Reflections in FCF ....         3 Note
PLAT933_ALERT_2_G Number of HKL-OMIT Records in Embedded .res File         1 Note
PLAT978_ALERT_2_G Number C-C Bonds with Positive Residual Density.         0 Info
PLAT992_ALERT_5_G Repd & Actual _reflns_number_gt Values Differ by         2 Check
```

---

3 **ALERT level A** = Most likely a serious problem - resolve or explain
15 **ALERT level B** = A potentially serious problem, consider carefully
107 **ALERT level C** = Check. Ensure it is not caused by an omission or oversight
30 **ALERT level G** = General information/check it is not something unexpected

7 ALERT type 1 CIF construction/syntax error, inconsistent or missing data
105 ALERT type 2 Indicator that the structure model may be wrong or deficient
10 ALERT type 3 Indicator that the structure quality may be low
32 ALERT type 4 Improvement, methodology, query or suggestion
1 ALERT type 5 Informative message, check

It is advisable to attempt to resolve as many as possible of the alerts in all categories. Often the minor alerts point to easily fixed oversights, errors and omissions in your CIF or refinement strategy, so attention to these fine details can be worthwhile. In order to resolve some of the more serious problems it may be necessary to carry out additional measurements or structure refinements. However, the purpose of your study may justify the reported deviations and the more serious of these should normally be commented upon in the discussion or experimental section of a paper or in the "special_details" fields of the CIF. checkCIF was carefully designed to identify outliers and unusual parameters, but every test has its limitations and alerts that are not important in a particular case may appear. Conversely, the absence of alerts does not guarantee there are no aspects of the results needing attention. It is up to the individual to critically assess their own results and, if necessary, seek expert advice.

Publication of your CIF in IUCr journals

A basic structural check has been run on your CIF. These basic checks will be run on all CIFs submitted for publication in IUCr journals (*Acta Crystallographica*, *Journal of Applied Crystallography*, *Journal of Synchrotron Radiation*); however, if you intend to submit to *Acta Crystallographica Section C* or *E* or *IUCrData*, you should make sure that full publication checks are run on the final version of your CIF prior to submission.

Publication of your CIF in other journals

Please refer to the *Notes for Authors* of the relevant journal for any special instructions relating to CIF submission.

Validation response form

Please find below a validation response form (VRF) that can be filled in and pasted into your CIF.

```
# start Validation Reply Form
_vrf_PLAT234_spcc55
;
PROBLEM: Large Hirshfeld Difference C028     --C80      .       0.32 Ang.
RESPONSE: ...
;
# end Validation Reply Form
```

PLATON version of 18/05/2022; check.def file version of 17/05/2022

Datablock spcc55 - ellipsoid plot

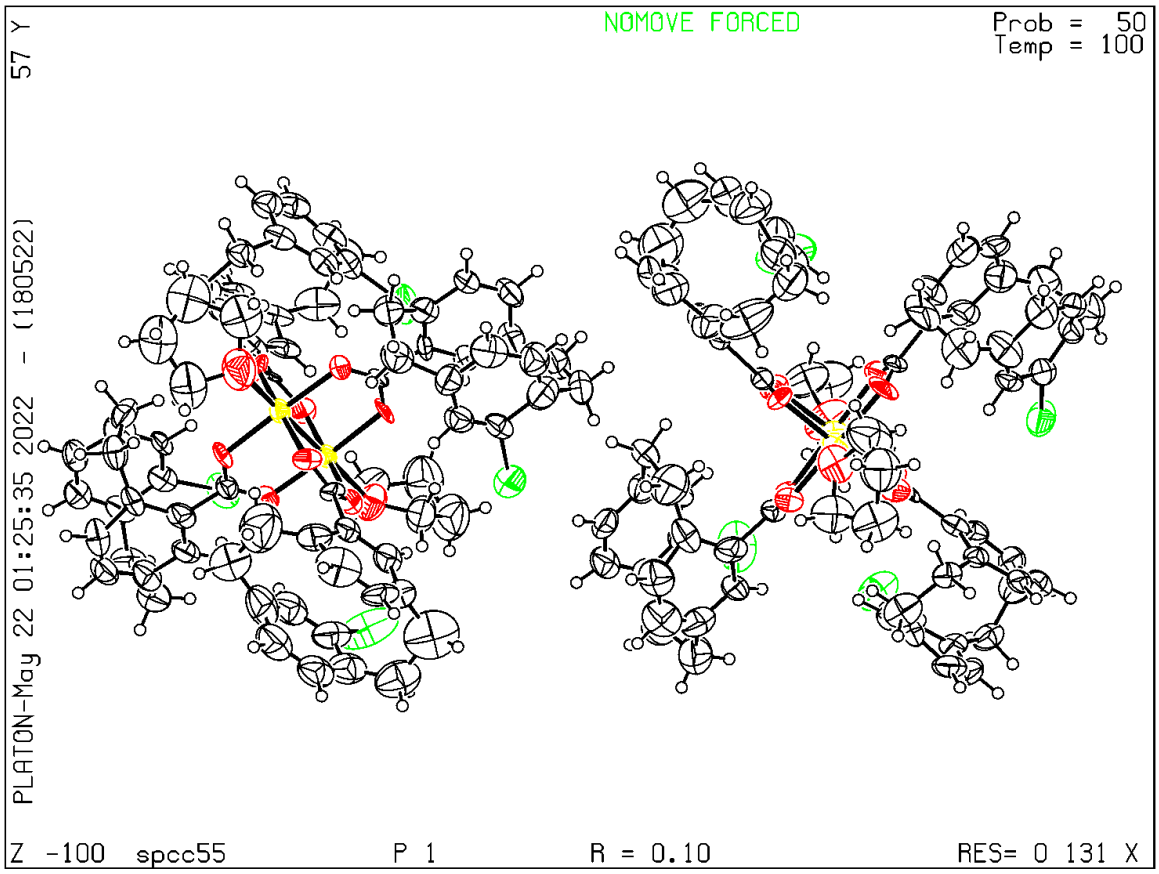

checkCIF/PLATON report

Structure factors have been supplied for datablock(s) vsp42

THIS REPORT IS FOR GUIDANCE ONLY. IF USED AS PART OF A REVIEW PROCEDURE FOR PUBLICATION, IT SHOULD NOT REPLACE THE EXPERTISE OF AN EXPERIENCED CRYSTALLOGRAPHIC REFEREE.

No syntax errors found. CIF dictionary Interpreting this report

Datablock: vsp42

Bond precision: C-C = 0.0075 A Wavelength=1.54178

Cell: a=21.0174(10) b=21.0174(10) c=8.1510(6)
alpha=90 beta=90 gamma=120
Temperature: 100 K

	Calculated	Reported
Volume	3118.2(4)	3118.2(4)
Space group	R 3	R 3
Hall group	R 3	R 3
Moiety formula	3(C17 H16 O2), C H4 O, H2 O	0.333(C3 H12 O3), 3(C17 H16 O2), 0.333(H6 O3)
Sum formula	C52 H54 O8	C52 H54 O8
Mr	806.95	806.95
Dx,g cm-3	1.289	1.289
Z	3	3
Mu (mm-1)	0.687	0.687
F000	1290.0	1290.0
F000’	1293.86	
h,k,lmax	26,26,10	26,25,9
Nref	2904[1452]	2652
Tmin,Tmax	0.921,0.934	0.536,0.754
Tmin’	0.866	

Correction method= # Reported T Limits: Tmin=0.536 Tmax=0.754
AbsCorr = MULTI-SCAN

Data completeness= 1.83/0.91 Theta(max)= 76.031

R(reflections)= 0.0573(2542) wR2(reflections)= 0.1542(2652)

S = 1.065 Npar= 184

The following ALERTS were generated. Each ALERT has the format
test-name_ALERT_alert-type_alert-level.
Click on the hyperlinks for more details of the test.

Alert level C

STRVA01_ALERT_4_C Flack parameter is too small
From the CIF: _refine_ls_abs_structure_Flack -0.500
From the CIF: _refine_ls_abs_structure_Flack_su 0.300
PLAT340_ALERT_3_C Low Bond Precision on C-C Bonds ..... 0.00747 Ang.
PLAT751_ALERT_4_C Bond Calc 0.85000, Rep 0.848(3) ..... Senseless s.u.
O2 -H2 1_555 1_555 ..... # 6 Check
PLAT752_ALERT_4_C Angle Calc 109.00, Rep 108.7(6) ..... Senseless s.u.
C17 -O2 -H2 1_555 1_555 1_555 # 7 Check
PLAT911_ALERT_3_C Missing FCF Refl Between Thmin & STh/L= 0.600 3 Report
PLAT977_ALERT_2_C Check Negative Difference Density on H2 -0.38 eA-3

Alert level G

PLAT002_ALERT_2_G Number of Distance or Angle Restraints on AtSite 2 Note
PLAT003_ALERT_2_G Number of Uiso or Uij Restrained non-H Atoms ... 2 Report
PLAT007_ALERT_5_G Number of Unrefined Donor-H Atoms ..... 4 Report
PLAT032_ALERT_4_G Std. Uncertainty on Flack Parameter Value High . 0.300 Report
PLAT042_ALERT_1_G Calc. and Reported Moiety Formula Strings Differ Please Check
PLAT083_ALERT_2_G SHELXL Second Parameter in WGHT Unusually Large 5.18 Why ?
PLAT172_ALERT_4_G The CIF-Embedded .res File Contains DFIX Records 2 Report
PLAT186_ALERT_4_G The CIF-Embedded .res File Contains ISOR Records 1 Report
PLAT300_ALERT_4_G Atom Site Occupancy of H3 Constrained at 0.3333 Check
PLAT300_ALERT_4_G Atom Site Occupancy of H18A Constrained at 0.3333 Check
PLAT300_ALERT_4_G Atom Site Occupancy of H18B Constrained at 0.3333 Check
PLAT300_ALERT_4_G Atom Site Occupancy of H18C Constrained at 0.3333 Check
PLAT300_ALERT_4_G Atom Site Occupancy of H1WA Constrained at 0.3333 Check
PLAT300_ALERT_4_G Atom Site Occupancy of H1WB Constrained at 0.3333 Check
PLAT417_ALERT_2_G Short Inter D-H..H-D H2 ..H3 . 1.08 Ang.
-x+y,1-x,z = 3_565 Check
PLAT720_ALERT_4_G Number of Unusual/Non-Standard Labels ..... 2 Note
PLAT789_ALERT_4_G Atoms with Negative _atom_site_disorder_group # 3 Check
PLAT860_ALERT_3_G Number of Least-Squares Restraints ..... 14 Note
PLAT912_ALERT_4_G Missing # of FCF Reflections Above STh/L= 0.600 6 Note
PLAT966_ALERT_5_G Note: Non-Standard (i.e. 2.0) OMIT Threshold of 2.0 Sig(I)
PLAT978_ALERT_2_G Number C-C Bonds with Positive Residual Density. 0 Info

---

0 **ALERT level A** = Most likely a serious problem - resolve or explain
0 **ALERT level B** = A potentially serious problem, consider carefully
6 **ALERT level C** = Check. Ensure it is not caused by an omission or oversight
21 **ALERT level G** = General information/check it is not something unexpected

1 ALERT type 1 CIF construction/syntax error, inconsistent or missing data
6 ALERT type 2 Indicator that the structure model may be wrong or deficient
3 ALERT type 3 Indicator that the structure quality may be low
15 ALERT type 4 Improvement, methodology, query or suggestion
2 ALERT type 5 Informative message, check

It is advisable to attempt to resolve as many as possible of the alerts in all categories. Often the minor alerts point to easily fixed oversights, errors and omissions in your CIF or refinement strategy, so attention to these fine details can be worthwhile. In order to resolve some of the more serious problems it may be necessary to carry out additional measurements or structure refinements. However, the purpose of your study may justify the reported deviations and the more serious of these should normally be commented upon in the discussion or experimental section of a paper or in the "special_details" fields of the CIF. checkCIF was carefully designed to identify outliers and unusual parameters, but every test has its limitations and alerts that are not important in a particular case may appear. Conversely, the absence of alerts does not guarantee there are no aspects of the results needing attention. It is up to the individual to critically assess their own results and, if necessary, seek expert advice.

Publication of your CIF in IUCr journals

A basic structural check has been run on your CIF. These basic checks will be run on all CIFs submitted for publication in IUCr journals (*Acta Crystallographica, Journal of Applied Crystallography, Journal of Synchrotron Radiation*); however, if you intend to submit to *Acta Crystallographica Section C* or *E* or *IUCrData*, you should make sure that full publication checks are run on the final version of your CIF prior to submission.

Publication of your CIF in other journals

Please refer to the *Notes for Authors* of the relevant journal for any special instructions relating to CIF submission.

PLATON version of 02/06/2021; check.def file version of 02/06/2021

Datablock vsp42 - ellipsoid plot

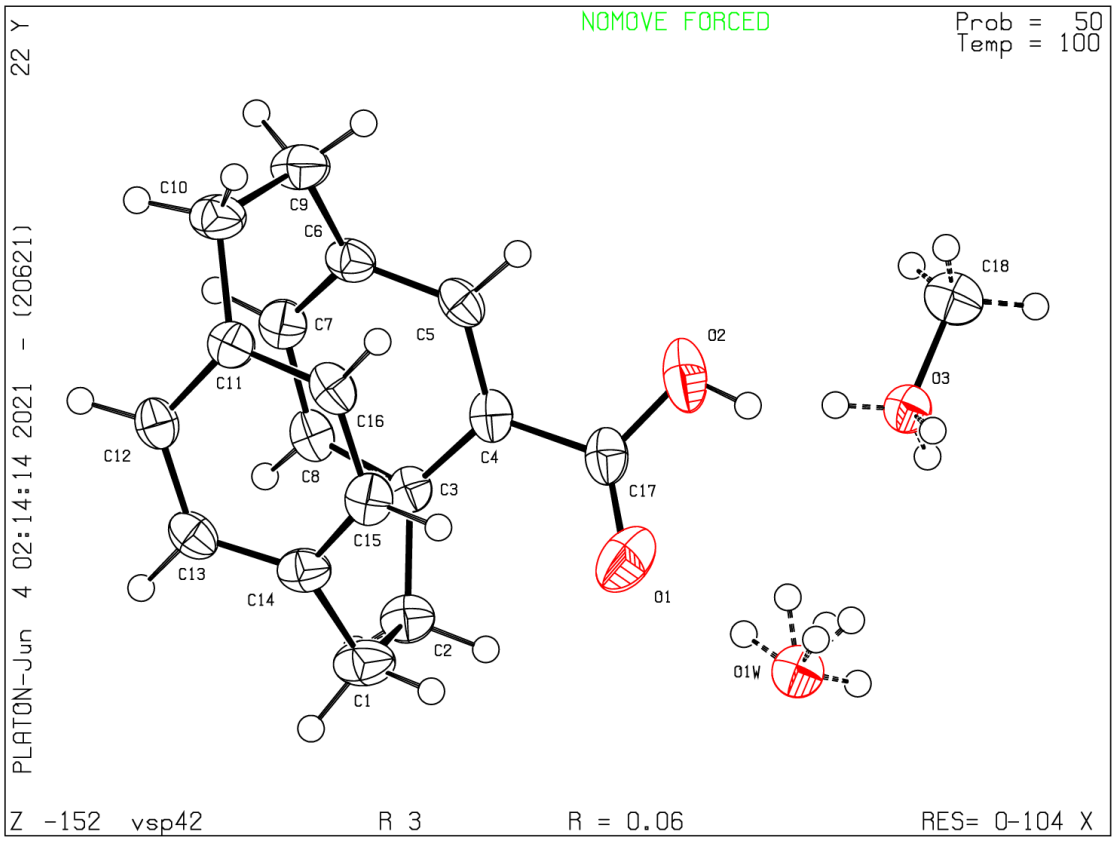

checkCIF/PLATON report

Structure factors have been supplied for datablock(s) vsp40

THIS REPORT IS FOR GUIDANCE ONLY. IF USED AS PART OF A REVIEW PROCEDURE FOR PUBLICATION, IT SHOULD NOT REPLACE THE EXPERTISE OF AN EXPERIENCED CRYSTALLOGRAPHIC REFEREE.

No syntax errors found. CIF dictionary Interpreting this report

Datablock: vsp40

```
Bond precision:  C-C = 0.0029 A          Wavelength=1.54178

Cell:             a=8.0930(3)     b=9.1709(3)     c=19.4808(7)
                  alpha=90        beta=90         gamma=90
Temperature:      100 K
```

	Calculated	Reported
Volume	1445.87(9)	1445.87(9)
Space group	P 21 21 21	P 21 21 21
Hall group	P 2ac 2ab	P 2ac 2ab
Moiety formula	C18 H16 O4	C18 H16 O4
Sum formula	C18 H16 O4	C18 H16 O4
Mr	296.31	296.31
Dx,g cm-3	1.361	1.361
Z	4	4
Mu (mm-1)	0.787	0.787
F000	624.0	624.0
F000’	626.02	
h,k,lmax	10,11,24	10,11,24
Nref	3032[1762]	2998
Tmin,Tmax	0.893,0.961	0.626,0.754
Tmin’	0.868	

```
Correction method= # Reported T Limits: Tmin=0.626 Tmax=0.754
AbsCorr = MULTI-SCAN

Data completeness= 1.70/0.99      Theta(max)= 76.265

R(reflections)= 0.0307( 2825)     wR2(reflections)= 0.0756( 2998)

S = 1.072                 Npar= 264
```

The following ALERTS were generated. Each ALERT has the format
test-name_ALERT_alert-type_alert-level.
Click on the hyperlinks for more details of the test.

Alert level C

PLAT089_ALERT_3_C Poor Data / Parameter Ratio (Zmax < 18) ..... 6.63 Note
PLAT355_ALERT_3_C Long O-H (X0.82,N0.98A) O2 - H2 . 1.06 Ang.
PLAT355_ALERT_3_C Long O-H (X0.82,N0.98A) O4 - H4 . 1.03 Ang.

Alert level G

PLAT912_ALERT_4_G Missing # of FCF Reflections Above STh/L= 0.600 13 Note
PLAT978_ALERT_2_G Number C-C Bonds with Positive Residual Density. 10 Info

0 **ALERT level A** = Most likely a serious problem - resolve or explain
0 **ALERT level B** = A potentially serious problem, consider carefully
3 **ALERT level C** = Check. Ensure it is not caused by an omission or oversight
2 **ALERT level G** = General information/check it is not something unexpected

0 ALERT type 1 CIF construction/syntax error, inconsistent or missing data
1 ALERT type 2 Indicator that the structure model may be wrong or deficient
3 ALERT type 3 Indicator that the structure quality may be low
1 ALERT type 4 Improvement, methodology, query or suggestion
0 ALERT type 5 Informative message, check

It is advisable to attempt to resolve as many as possible of the alerts in all categories. Often the minor alerts point to easily fixed oversights, errors and omissions in your CIF or refinement strategy, so attention to these fine details can be worthwhile. In order to resolve some of the more serious problems it may be necessary to carry out additional measurements or structure refinements. However, the purpose of your study may justify the reported deviations and the more serious of these should normally be commented upon in the discussion or experimental section of a paper or in the "special_details" fields of the CIF. checkCIF was carefully designed to identify outliers and unusual parameters, but every test has its limitations and alerts that are not important in a particular case may appear. Conversely, the absence of alerts does not guarantee there are no aspects of the results needing attention. It is up to the individual to critically assess their own results and, if necessary, seek expert advice.

Publication of your CIF in IUCr journals

A basic structural check has been run on your CIF. These basic checks will be run on all CIFs submitted for publication in IUCr journals (*Acta Crystallographica*, *Journal of Applied Crystallography*, *Journal of Synchrotron Radiation*); however, if you intend to submit to *Acta Crystallographica Section C* or *E* or *IUCrData*, you should make sure that full publication checks are run on the final version of your CIF prior to submission.

Publication of your CIF in other journals

Please refer to the *Notes for Authors* of the relevant journal for any special instructions relating to CIF submission.

PLATON version of 16/05/2021; check.def file version of 13/05/2021

Datablock vsp40 - ellipsoid plot